https://dspace.org/

Characterization and modeling of mercury speciation in industrially polluted areas due to energy production and mineral processing in south africa

Makiese, Julien Gilles Lusilao

2012-08-27
http://hdl.handle.net/10539/11829

Downloaded from a DSpace repository. https://dspace.org/

CHARACTERIZATION AND MODELING OF MERCURY SPECIATION IN INDUSTRIALLY POLLUTED AREAS DUE TO ENERGY PRODUCTION AND MINERAL PROCESSING IN SOUTH AFRICA

Julien Gilles Lusilao Makiese

A thesis submitted to the Faculty of Science, University of the Witwatersrand, Johannesburg,
in fulfillment of the requirements for the degree of
Doctor of Philosophy
Johannesburg 2012

Declaration

I declare that this thesis is my own, unaided work. It is being submitted for the Degree of Doctor of Philosophy to the University of the Witwatersrand, Johannesburg. It has not been submitted before for any degree or examination to any other University.

…… ……

(Signature of candidate)

10th day of April 2012

Abstract

Coal combustion is recognized as the primary source of anthropogenic mercury emission in South Africa followed by gold mining. Coal is also known to contain trace concentrations of mercury which is released to the environment during coal mining, beneficiation or combustion. Therefore, determining the mercury speciation in coal is of importance in order to understand its behavior and fate in the environment.

Mercury was also used, at a large extent, in the Witwatersrand Basin (South Africa) for gold recoveries until 1915 and is still used in illegal artisanal mining. Consequences of these activities are the release of mercury to the environment. Nowadays, gold (and uranium) is also recovered through the reprocessing of old waste dumps increasing the concern related to mercury pollution.

While much effort has been put in the northern hemisphere to understand and control problems related to anthropogenic mercury release and its fate to the ecosystem, risk assessment of mercury pollution in South Africa was based, until very recently, on total element concentrations only or on non systematic fragmental studies. It is necessary to evaluate mercury speciation under the country's semi arid conditions, which are different to environmental conditions that exist in the northern hemisphere, and characterize potential sources, pathways, receptors and sinks in order to implement mitigation strategies and minimize risk.

In this study, analytical methods and procedures have been developed and/or optimized for the determination of total mercury and the speciation of inorganic and organic forms of mercury in different sample matrices such as air, coal, sediment, water and biota.

The development of an efficient and cost effective method for total gaseous mercury (TGM) determination was achieved using nano-gold supported metal oxide (1% wt Au) sorbents and cold vapor atomic fluorescence spectrometry (CV-AFS). Analytical figures of merit and TGM concentrations obtained when using Au/TiO_2, as a mercury trap, were similar to those obtained with traditional sorbents.

The combination of isotope dilution with the hyphenated gas chromatography-inductively coupled plasma mass spectrometry (ID GC-ICP-MS) was also achieved and used successfully for the speciation analysis of mercury in solid, liquid and biological samples.

The developed, or optimized, methodologies were used to estimate the average mercury content and characterize the speciation of mercury in South African coals, and also to study the speciation of mercury in selected South African environmental compartments impacted by gold mining activities.

The obtained average mercury content in coals collected from the Highveld and Waterberg coalfields (0.20 ± 0.03 mg kg^{-1}) was close to the reported United States Geological Survey (USGS) average for South African coals. Speciated isotope dilution analyses and sequential extraction procedures revealed the occurrence of elemental mercury, inorganic and organo-mercury species, and also the association of mercury mainly to organic compounds and pyrite.

The environmental pollution assessment was conducted within the Witwatersrand Basin, at four gold mining sites selected mainly for their mining history and from geophysical information obtained through satellite images. This study showed a relatively important pollution in three of the four sites, namely the Vaal River west site near Klerksdorp, the West Wits site near Carletonville (both in the North-West Province) and the Randfontein site in the West Rand (Gauteng Province). Only one site, the closed Rietfontein landfill site in the East Rand (Gauteng Province) was found to be not impacted by mercury pollution.

The methylation of mercury was characterized in all sites and factors governing the mercury methylation process at the different study sites were also investigated.

Geochemical models were also used to explain the distribution, transport and fate of mercury in the study systems.

Dedication

To my wife Mireille K. Tshibwabwa and my daughter Jewel E. Lusilao

Acknowledgement

I would like to thank my supervisor, Prof. Ewa M. Cukrowska, for her valuable advice, guidance, and support throughout this long journey and for giving me the opportunity to improve my scientific knowledge through workshops, seminars, conferences and trainings abroad.

Special thanks to Drs David Amouroux, Emmanuel Tessier and the whole team of the CNRS-LCABIE-IPREM (Pau, France) research group for your scientific input in my research and for the French food and wine shared together.

Many thanks to Ms Isabel Weiersbye (APES, Wits University) for the valuable information provided, for her contribution during the different sampling campaigns and for the support. To David Furniss, your presence during the sampling and your knowledge of the GIS mapping were very helpful.

Thanks to the following institutions and companies: the National Research Foundation (NRF), THRIP and the University of the Witwatersrand for the financial support, AngloGold Ashanti Limited for supporting part of this project and for allowing us to access their mining sites for sampling, Eskom for providing the majority of the coal samples used in our work. Thanks to Jason McPherson (Mintek, Autek) for providing the nanogold sorbents.

To the environmental Analytical Chemistry group, especially to Dr Hlanganani Tutu and Prof Luke Chimuka, and to all my friends, thanks for making this journey less stressfull than it could actually be.

To Elysée Bakatula, you were always there like a real sister.

To my family, your encouraging calls and mails used to come at the right time. I just hope that i have managed to make you proud of being your blood.

Table of contents

Declaration ..... *ii*

Abstract ..... *iii*

Dedication ..... *v*

Acknowledgement ..... *vi*

List of figures ..... *xii*

List of tables ..... *xvi*

Abbreviations ..... *xviii*

Chapter 1 Introduction and problem statement *1*

1.1 Introduction 1

1.2 Statement of the problem 2
1.2.1 Gaseous mercury measurements 2
1.2.2 Mercury concentration and distribution in South African coal 5
1.2.3 Mercury pollution from gold mining operations in South Africa 8

Chapter 2 Literature review *16*

2.1 Introduction 16

2.2 Latest global mercury emission inventories 17

2.3 Major anthropogenic sources of mercury 22
2.3.1 Coal 22
2.3.1.1 Mercury in coal 25
2.3.1.2 Coal in South Africa 26
2.3.2 Mining 31
2.3.2.1 Important mining concepts 33
2.3.2.2 Mercury and gold mining 37
2.3.2.3 Impact of mining in mercury pollution 40

2.4 The biogeochemistry of mercury 44
2.4.1 Atmospheric cycling and chemistry of mercury 45
2.4.2 Aquatic biogeochemistry of mercury 49

2.5 Mercury methylation 51

2.6 Transport and deposition of mercury from gold mine drainage and tailings in watersheds 59

Chapter 3 A review of analytical procedures for mercury determination *63*

3.1 Introduction 63

3.2 Sampling and samples storage 63
3.2.1 Storage and preservation of samples 64
3.2.2 Water samples 65
3.2.3 Solid samples 66
3.2.4 Biological samples 67
3.2.5 Air samples 67

3.3 Analytical procedures for mercury determination 68
3.3.1 Total mercury determination 69
3.3.2 Mercury species analysis 71
3.3.3 Hyphenated techniques in speciation analysis 73
3.3.4 Element selective detection in gas chromatography 75
3.3.5 Advances in gas chromatography prior to element selective detection 78
3.3.6 Purge and trap using capillary cryofocussing 79
3.3.7 ICP MS detection in gas chromatography 80
3.3.8 Speciated isotope dilution analysis (SIDMS) 80
3.3.9 Liquid chromatography with ICP-MS detection 84

3.4 Sample preparation for mercury determination 86
3.4.1 Total mercury 87
3.4.2 Advances in sample preparation for GC-based hyphenated techniques 88
3.4.3 Derivatization techniques 89
3.4.4 Solid-phase micro-extraction 90

3.5. Analytical methods for inorganic constituents in coal 91
3.5.1 Analytical methods for elemental concentrations 92
3.5.1.1 Instrumental X-ray/g-ray techniques 94
3.5.1.2 Optical absorption/emission techniques 95
3.5.1.3 Miscellaneous methods 97
3.5.2 Determination of coal mineralogy 98

3.6 Specific methods for the determination of modes of occurrence of trace elements 99
3.6.1 Indirect methods 100
3.6.2 Direct microscopic methods 103

Chapter 4 Objectives of the study *106*

Chapter 5 Sampling procedures and optimization of analytical methods *109*

5.1 Introduction 109

5.2 Cleaning protocol 109

5.3 Sampling 110
5.3.1 Water sampling 110
5.3.2 Sediment sampling 112

5.3.3 Tailings sampling 113
5.3.4 Plants collection 114

5.3 Sample preparation 114
5.3.1 Total mercury determination 115
5.3.2 Analysis of mercury species 116

5.4 Optimization of analytical instruments for mercury determination 117

5.5 Figures of merit 121

5.6 Validation of analytical methods used for mercury determination 125

5.7 Determination of total metals concentration 127

5.8 Ion chromatography 130

5.9 CHNS analyser 132

5. 10 Computer modeling 133

5.11 Summary 133

Chapter 6 The use of nano-structured gold supported on metal oxides sorbents for the trapping and preconcentration of gaseous mercury *135*

6.1 Introduction 135

6.2 Sorbents origin 136

6.3 Analytical Method 136

6.4 Instrument setup 139

6.5 Analytical methodology 141

6.6 Air sampling for TGM determination 144

6.7 Optimization of sampling conditions 144

6.8 Performances of nano-gold materials as analytical traps 146

6.9 Quality control 152

6.10 TGM analysis 153

6.11 Conclusion 154

Chapter 7 Speciation of mercury in South African coal *156*

7.1 Samples origin 157

7.2 Analytical procedures 158
7.2.1 Chemicals 158
7.2.2 MAE for the determination of total mercury and mercury species 159
7.2.3 Isotopically enriched inorganic and monomethylmercury spikes 161
7.2.4 Derivatization procedures 162

7.2.5 Sequential extraction procedure 162

7.3 Methods validation 164
7.3.1 Total mercury in coal CRMs 164
7.3.2 Speciated isotope dilution (SIDMS) analysis of mercury in coal CRMs 165

7.4 Results and discussion 166
7.4.1 Total mercury concentration in studied coals 166
7.4.2 SIDMS analysis of coals 170
7.4.3 Mercury modes of occurrence in Highveld coals 173

7.5 Conclusion 186

Chapter 8 Mercury speciation in the Vaal River and West Wits mining operations... *188*

8.1 Scope of the study 188

8.2 General description of the Vaal River and West Wits operations 190
8.2.1 The Vaal River mining operations 192
8.2.2 The West Wits mining operations 194

8.3 Collection and description of samples 200
8.3.1 The Vaal River campaigns 200
8.3.2 The West Wits campaign 203

8.4 Mercury in the Vaal River West Region 205
8.4.1 Mercury in the Vaal River West waters 205
8.4.2 Mercury in Vaal River west sediments 208
8.4.3 Mercury distribution during the wet season sampling 211
8.4.4 Mercury methylation in the Vaal River West area 216
8.4.5 Impact of seasonal changes on mercury transport, distribution and fate 219
8.4.6 Mercury in plants at the Vaal River West area 227
8.4.7 TGM measurements at the old mine ventilation shaft 231

8.5 Mercury in the West Wits Region 234
8.5.1 Mercury in West Wits waters 234
8.5.2 Mercury in West Wits tailings and sediments 238
8.5.3 Mercury concentrations in West Wits plants 241
8.5.4 Summary 243

Chapter 9 The impact of post gold mining on mercury pollution in the West and East Rand regions 246

9.1 Introduction 246

9.2 Site description 251

9.3 Results and Discussion 257
9.3.1 Mercury in waters 257
9.3.2 Mercury methylation in the old water borehole 262
9.3.3 Mercury in soils and sediments 265

9.3.4 Mercury methylation in soils and sediments 270
9.3.5 Mercury in sediment profiles 272
9.3.6 Factors controlling the mercury methylation in sediments 276
9.3.7 Mercury in plants 277
9.3.8 Mercury fractionation and speciation modeling 281

9.4 Summary 290

Chapter 10 Conclusions *292*

References *297*

Appendix *335*

List of publications and conference presentations *343*

List of figures

Figure 1.1 Map of the Witwatersrand Basin in South Africa 10
Figure 2.1 Coalfields of South Africa..... 28
Figure 2.2.Schematic product and waste streams at a metal mine..... 34
Figure 2.3 TGM in the atmosphere at several locations 47
Figure 2.4 Summary of some of the important physical and chemical transformation of mercury in the atmosphere..... 48
Figure 2.5 Generalised view of mercury biogeochemistry in the aquatic environment. 50
Figure 2.6 Schematic diagram showing transport and fate of mercury and potentially contaminated sediments from hydraulic and drift mine environment through rivers, reservoirs, and the flood plain, and into an estuary 60
Figure 3.1. Schematic of a quadrupole ICP-MS 70
Figure 3.2. Analytical steps for speciation..... 72
Figure 3.3. General Scheme of analytical techniques used for speciation..... 74
Figure 3.4 Example of an hyphenated GC-ICP-MS 78
Figure 3.5 The isotope dilution principle..... 82
Figure 3.6 Scheme of the coupling between HPLC and ICP-MS..... 85
Figure 3.7 Closed and open microwave assisted extraction systems..... 88
Figure 3.8 Subdivision of analytical techniques for inorganics in coal 92
Figure 3.9 Comparison of sequential leaching schemes used in the IEA speciation study. 102
Figure 5.1 *In Situ* measurements of physico-chemical parameters of a water sample ... 111
Figure 5.2 Sediment core sampling and pre-conditioning steps 113
Figure 5.3 Sampling in bottom TSF with a PVC core 113
Figure 5.4 Collection of algae in a creek 114
Figure 5.5 The Multiwave 3000 MAE system and the vessel design..... 115
Figure 5.6 The CEM apparatus 116
Figure 5.7 Image of the ICP-MS used for Hg_{TOT} determination 118
Figure 5.8 Hyphenated GC-ICP-MS X-Series 2..... 1
Figure 5.9 ICP-MS calibration for different mercury isotopes..... 122
Figure 5.10 GC-ICP-MS chromatogram of IHg (1 μg L^{-1}) and MHg (0.1 μg L^{-1}) standards 1
Figure 5.11 Hg isotope peaks for a 0.1 μg L^{-1} MHg standard..... 1
Figure 5.13 Overlapped chromatograms of successive injections of MHg standards.... 124
Figure 5.12 GC-ICP-MS calibration of IHg and MHg species 1
Figure 5.14 Image of the ICP-OES instrument..... 127
Figure 5.15 ICP-OES scans of Fe (left) and Mg (right) 1
Figure 5.16 ICP-OES calibration of some elements at selected wavelengths 129
Figure 5.17 The compact IC system and its components within the separation center .. 130
Figure 5.18 IC chromatogram showing peaks of a 5 mg L^{-1} standard solution of F^-, Cl^-, NO_2^-, NO_3^-, PO_4^{3-} and SO_4^{2-} 131
Figure 5.19 Example of IC calibration curves of F^- (R^2 = 1.000), Cl^- (R^2 = 0.996), NO_2^- (R^2 = 0.999), NO_3^- (R^2 = 0.999), PO_4^{3-}(R^2 = 0.998), and SO_4^{2-} (R^2 = 0.999) 132
Figure 6.1 Au-Al_2O_3, Au-ZnO and Au-TiO_2 materials used in the study 136

Figure 6.2 The DA-CVAFS setup 137
Figure 6.3 Schematic of the DA-CVAFS system 138
Figure 6.4 SEM image of gold particles (small black dots) dispersed on TiO_2..... 139
Figure 6.6 Example of signal obtained with the injection of 10 µl of Hg^0 141
Figure 6.5 Schematic of the mercury trap..... 1
Figure 6.7 Source of Hg^0 standards 1
Figure 6.8 Calibration lines obtained with different syringes..... 142
Figure 6.9 Analytical protocols for mercury standards calibration and TGM analysis..... 1
Figure 6.11 Collection of air samples in the roof of the laboratory..... 145
Figure 6.10 Schematic of sampling setup 1
Figure 6.12 Concentrations of Hg^0 as a function of sample volume 1
Figure 6.13 AFS chromatograms of 20 µL Hg^0 desorbed from different traps..... 146
Figure 6.14 AFS Calibrations of Hg^0 standards at argon flow of 60 ml min^{-1} 147
Figure 6.15a Calibrations obtained with Au-TiO_2 at different Ar flows 149
Figure 6.15b Calibrations obtained with Au and Au-TiO_2 at Ar flow of 100 ml min^{-1}.. 149
Figure 6.16 Examples of baseline obtained after the desorption of mercury from the different traps 150
Figure 6.17 TGM in the laboratory ambient air where 154
Figure 7.1 Location of current and future coal-fired power plants in South Africa. 158
Figure 7.2 The automated mercury analyzer for direct solid introduction 160
Figure 7.3 Procedures for total mercury and speciation analyses..... 1
Figure 7.4 Schematic of the sequential extraction procedure used in this study 1
Figure 7.5 GC-ICP-MS chromatogram of SARM 20..... 165
Figure 7.6 Hg in Highveld coals measured with different methodologies 168
Figure 7.7 GC-ICP-MS chromatogram of “Duvha” sample..... 171
Figure 7.8 GC-ICP-MS chromatogram showing the presence of unknown Hg species 171
Figure 7.9 Example of GC-ICP-MS chromatograph obtained after propylation..... 172
Figure 7.10 Correlation between retention time and molecular weight for different Hg species 173
Figure 7.11. Leaching results for crushed (A) and raw (B) coals..... 176
Figure 7.12 Comparison between unleached Hg and the MeHg content in coals 177
Figure 7.13 SIDMS chromatograms of Tutuka coal (A) and ash (B) samples..... 178
Figure 7.14 Leaching results for crushed (A) and raw (B) coals..... 180
Figure 7.15 Correlation between unleached Hg and organic matter 182
Figure 7.16 Correlation between Hg leached by HNO_3 and the pyritic sulfur 182
Figure 7.17 Correlation between leached Hg and sulfate sulfur..... 183
Figure 7.18 Correlation between Hg in HCl fraction and the sulfur content in coals 1
Figure 7.19 Correlation between Hg in HCl and HNO_3 fractions 1
Figure 8.1 Geological settings of the major goldfields in the Witwatersrand Basin 189
Figure 8.2 Vaal River and West Wits operations in the regional context..... 191
Figure 8.3 Indicating the AGA area of responsibility of the Vaal River operations 192
Figure 8.4 Main watercourses and quaternary catchments in the Schoonspruit and Koekemoer Spruit catchment..... 194
Figure 8.5 Land in and around West Wits operations 195
Figure 8.6 West Wits Sub Catchments and Regional Flow..... 197
Figure 8.7 Map indicating the main working areas for Savuka TSF’s 198

Figure 8.8 West Wits Borrow Pits 199
Figure 8.9 Vaal River West sampling area 202
Figure 8.11 West Wits sampling area 204
Figure 8.10 View of the West Wits Old North sampling area 1
Figure 8.12 Example of GC-ICP-MS chromatogram of VR water 206
Figure 8.13 Mercury species in VR waters from the dry season sampling 207
Figure 8.14 Mercury speciation in VR sediments 210
Figure 8.15 Satellite picture of the VR West site 211
Figure 8.16 IHg and MHg in sediment profile WC1 214
Figure 8.17 Selected elements concentrations in the sediment profile WC1 214
Figure 8.18 Example of Hg species distribution in a sediment profile 1
Figure 8.19 Sulfur, sulfate, organic matter and iron trends in the profile WC1 218
Figure 8.20 Hg_{TOT} in VR surface and borehole waters from the wet season sampling.. 220
Figure 8.21 Impact of seasonal change in the Hg load in sediments adjacent the VR West Complex TSF and near the Schoonspruit 222
Figure 8.22 Hg species in sediment collected near Schoonspruit 223
Figure 8.23 Eh-pH diagram showing that study sediment samples speciated as Hg^0 224
Figure 8.24 Changes in the Hg load in Bokkamp Dam and its surrounding 225
Figure 8.25 Trends of Hg species from a sediment profile near the Bokkamp Dam 226
Figure 8.26 Example of metals concentrations in the profile adjacent to Bokkamp Dam 227
Figure 8.27 GC-ICP-MS chromatogram of VR plant 60B 228
Figure 8.28 Hg_{TOT} in selected VR plants 229
Figure 8.29 MHg in selected VR plants 231
Figure 8.30 Experimental set-up for Total Gaseous Mercury in air. 232
Figure 8.31 IHg and MHg in WW waters 235
Figure 8.32 Preliminary mapping of vegetation sub-units at West Wits operations 236
Figure 8.33 GC-ICP-MS chromatogram of WW water sample 21. 236
Figure 8.34 GC-ICP-MS chromatogram of tailings collected from the Old North TSF 239
Figure 8.35 Mercury in surface sediments within the WW Savuka mine area 239
Figure 8.36 IHg and MHg in sediment profile 19F 241
Figure 8.38 GC-ICP-MS chromatogram of WW plant 19B 242
Figure 9.1 Mines of the West Rand and West Wits Line Mining Areas 1
Figure 9.2 Location of the Rand Uranium and its neighboring mines 247
Figure 9.3 Location of study sites 1
Figure 9.4 Map of the study area in Randfontein (Source: Google) 1
Figure 9.5 The Randfontein sampling area 253
Figure 9.6 View of the land in the Randfontein site 253
Figure 9.7 The Randfontein sampling points 1
Figure 9.8 GIS image of the Rietfontein (“Scaw metals”) sampling site 1
Figure 9.9 View of the adit within the Rand Uranium site 1
Figure 9.10 Eh–pH relationships of all samples. 260
Figure 9.11 Mercury species in Randfontein surface water 262
Figure 9.12 Mercury species, Eh and pH trends in the old Randfontein borehole 1
Figure 9.13 Mercury in Rietfontein surface sediments 265
Figure 9.14 Example of GC-ICP-MS chromatogram of Randfontein sediments 1

Figure 9.15 Correlation between Hg concentrations in waters and corresponding soils 268
Figure 9.16 Mercury in the Randfontein site 1
Figure 9.17 Hg_{TOT} in Randfontein surface sediments from the mining area to the Krugersdorp Game Reserve 270
Figure 9.18 Mercury species in Randfontein surface sediments 271
Figure 9.19 Mercury and selected metals patterns in soil profile 93 1
Figure 9.20 Correlation between carbon content and total mercury in the soil profile 93 274
Figure 9.21 Example of mercury and selected metals pattern in soil profiles from the Randfontein site 275
Figure 9.22 Mercury species, organic matter (expressed as %C) and sulfate pattern in the sediment profile “93” 276
Figure 9.23 Mercury in Rietfontein (green) and Randfontein (yellow) plants 279
Figure 9.24 Mercury species in selected plants 281
Figure 9.25 Sequential extraction result of selected Randfontein soils 283
Figure 9.26 Fraction of mercury in different solvents 284
Figure 9.27 Predominant inorganic mercury species in Randfontein waters 287
Figure 9.28 pH-Cl diagram of water sample 91from the Randfontein creek in AMD... 288
Figure 9.29 pH-Cl diagram of water sample 94 from the game reserve..... 289
Figure A1 Schematic of different steps of the analytical protocol for the mercury speciation in sediments by ID GC-ICP-MS 335
Figure A2.1 Rietfontein and West Wits sites..... 337
Figure A2.2 Municipality warning notice at the Wonderfontein Spruit (West Wits) 338
Figure A2.3 The Kanana township near Schoonspruit where ASGM activities have been reported (VR site) 338
Figure A2.4 The closed ventilation shaft near Orkney and an example of the mrecury trap used during air collection 339
Figure A2.5 The Bokkamp Dam during the dry and wet season samplings..... 339
Figure A2.6 Water and vegetation conditions at the Rand Uranium adit, and conditions of the Randfontein creek from the mining site to the Game Reserve 342

List of tables

Table 2.1 Global mercury emissions by natural sources estimated for 2008 18
Table 2.2 Global mercury emissions from anthropogenic sources..... 19
Table 2.3 Global emissions of total mercury from major anthropogenic sources in Mg yr^{-1} 20
Table 2.4 Production of coal by country and year 24
Table 2.5 Proved recoverable coal reserves at end-2006 in million tonnes..... 25
Table 2.6 World production of selected non-fuel mineral commodities in l999and 2006 32
Table 2.7 Simplified mining activities whereby a resource is mined, processed and metallurgically treated 35
Table 2.8 Mine water terminology..... 37
Table 3.1 Summary of recommended bottle types, preservation, and storage for mercury species 65
Table 5.1 Microwave programme for sample extraction..... 116
Table 5.2 ICP-MS parameters..... 119
Table 5.3 Operating conditions of the hyphenated GC-ICP-MS 120
Table 5.4 ICP-MS calibration parameters 121
Table 5.5 Total mercury concentration in CRMs by ICP-MS 125
Table 5.6 IHg and MeHg in CRMs by ID GC-ICP-MS 126
Table 5.7 Optimized parameters of ICP-OES..... 128
Table 5.8 Example of calibration parameters obtained with the ICP-OES 129
Table 5.9 IC parameters for anions determination..... 131
Table 5.10 Standards calibration of the CHNS analyser 133
Table 6.1 Analytical parameters of studied materials..... 147
Table 6.2 Method Analytical performances..... 153
Table 7.1 Coal fired power stations and the types of coal and ash samples collected.... 157
Table 7.2 Hg_{TOT} in CRMs coal 164
Table 7.3 SIDMS results for different spiking methods….. …… . 165
Table 7.4 SIDMS results obtained after derivatization with $NaBEt_4$ and $NaBPr_4$ 166
Table 7.5 Hg_{TOT} (μg kg^{-1}) in coals measured with different analytical procedures..... 167
Table 7.6 Comparison of Hg concentrations in Highveld coals 168
Table 7.7 Hg_{TOT} in coals from the Waterberg Coalfield..... 168
Table 7.8 Comparison of Hg_{TOT} (mg kg^{-1}) in South African and global coals..... 169
Table 7.9 IHg and MeHg in Highveld coals 170
Table 7.10 Propylated mercury species and their corresponding molecular weight 173
Table 7.11 Concentration of mercury in coals and ashes leachates..... 174
Table 7.12 Mercury content (in %) from different fractions in crushed coals 175
Table 7.13 Mercury content (in %) from different fractions in raw coals..... 175
Table 7.14 Proximate and ultimate values of puleverized Highveld coals..... 181
Table 7.15 Total sulfur (S_T), pyrite sulfur (S_P), organic sulfur (S_O), qnd sulfate sulfur (S_S) in study coals (dry weight basis)..... 183
Table 7.16 Comparison between Hg leached in the HCl fraction from different studies185
Table 8.1 The VR dry season sampling details..... 201
Table 8.2 The VR wet season sampling details 203

Table 8.3 The WW sampling details 205
Table 8.4 IHg, MHg and field measurements in VR waters (n=3) 206
Table 8.5 Hg_{TOT}, IHg and MHg for Vaal River sediments for the dry season sampling 209
Table 8.6 Mercury concentration in sediments for the VR wet season sampling 212
Table 8.7 Total concentrations of selected metals in studied sediments and waters 215
Table 8.8 Hg concentrations in waters from VR wet season sampling 219
Table 8.9 Mercury and other selected elements in VR borehole waters from the wet season sampling 220
Table 8.10 Hg_{TOT} and Hg species concentration in selected VR plants 228
Table 8.11 TGM concentrations in air 233
Table 8.12 Mercury in West Wits waters 234
Table 8.13 Concentration of selected elements in WW waters 238
Table 8.14 Mercury in WW sediments and tailings 240
Table 8.15 Mercury concentration in selected WW plants 242
Table 9.1 Description of the Randfontein sampling 255
Table 9.2 Description of the Rietfontein landfill sampling 256
Table 9.3 Mercury concentration and field measurements of Rietfontein and Randfontein water samples 258
Table 9.4 Concentrations of selected elements and anions in Randfontein waters 261
Table 9.5 Mercury in Rietfontein sediments 265
Table 9.6 Mercury in Randfontein soils and sediments 266
Table 9.7 Carbon, Sulfur, Chloride and sulfate contents in selected sediment profiles from the Randfontein site 272
Table 9.8 Concentrations of selected elements in sediment cores from Randfontein 275
Table 9.9 Mercury in Rietfontein plants 277
Table 9.10 Mercury in Randfontein plants 278
Table 9.11 Calculated TC values for selected soils and plants 280
Table 9.12 Hg concentrations in different leachates of Randfontein soils 283
Table 9.13 Percentage of Hg leached with different solvents 284
Table 9.14 Species distribution in water sample 91 288
Table 9.15 Species distribution in water sample 94 289

Abbreviations

AAS: Atomic Absorption Spectrometry

ADL: Absolute Detection Limit

AFS: Atomic Fluorescence Spectrometry

AGA: AngloGold Ashanti Limited

AMD: Acid Mine Drainage

AMS: Accelerator Mass Spectrometry

ASGM (or AGM): Artisanal Scale Gold Mining

ASTM: American Society for Testing and Materials

ASV: Anodic Stripping Voltammetry

BC: Before Christ

BSE: Back-Scattered Electron

BSEI: Back-Scattered Electron Image

CAAA: The United States Clean Air Act Amendment

CGC: Capillary Gas Chromatography

CHNS: Carbon, Hydrogen, Nitrogen and Sulfur

CNRS-LCABIE-IPREM: Centre National pour la Recherche Scientifique-Laboratoire de Chimie Appliquée et Bio-Environment-Institut Pour la Rechereche de l'Environment et des Matériaux

CRG: Central Rand Group

CRM (or SRM): Certified (or Standard) Reference Material

CSIR: Council for Scientific and Industrial Research

CV: Coal Value

CVAAS: Cold Vapor Atomic Absorption Spectrometry

CVAFS: Cold Vapor Atomic Fluorescence Spectrometry

DA-CVAFS: Double Amalgamation Cold Vapor Atomic Fluorescence Spectrometry

DGM: Dissolved Gaseous Mercury

DOC: dissolved organic carbon

DOM: Dissolved Organic Matter

DPASV: Differential Pulse Anodic Stripping Voltammetry

DWAF: Department of Water Affairs and Forestry

EC (or CE): Electrochromatography (or Capillary Electrophoresis)

Ec: Electrical Conductivity

EDX: Energy-Dispersive X-ray

EtHg: Ethylmercury

EI-MS: Electron Impact Mass Spectrometry

FDHM: Full Duration at Half Maximum

FFF: Field Flow Fractionation

GC: Gas Chromatography

GC-AAS: Gas Chromatography Atomic Absorption Spectrometry

GC-AFS: Gas Chromatography Atomic Fluorescence Spectrometry

GC – EI-MS: Gas Chromatography Electron Impact Mass Spectrometry

GC – ICP-MS: Gas Chromatography Inductively Coupled Plasma Mass Spectrometry

GC – MIP-AED: Gas Chromatography Microwave Induced Plasma Atomic Emission

GDMS: Glow-Discharge Mass Spectrometry

GFAAS: Graphite Furnace Atomic Absorption Spectrometry

GIS: Geographic Information System

GPS: Global Positioning System

HAP(s): Hazardous Air Pollutant(s)

HG: Hydride Generation

$HgEt_2$: Diethylmercury

Hg_{TOT}: Total Mercury

HPLC: High Performance Liquid Chromatography

HTA: High-Temperature Ash

IAEA: International Atomic Energy Agency

IC: Ion Chromatography

ICP-MS: Inductively Coupled Plasma Mass Spectrometry

ICP-AES: Inductively Coupled Plasma Atomic Emission Spectrometry

ID GC – ICP-MS: Isotope Dilution Gas Chromatography Inductively Coupled Plasma Mass Spectrometry

IDMS: Isotope Dilution Mass Spectrometry

ID TIMS: Isotope Dilution thermal ionization Mass Spectrometry

IEA CCC: International Energy Agency Clean Coal Center

IHg: Inorganic Mercury

INAA: Instrumental Neutron Activation Analysis

IRMM: Institute for Reference Materials and Measurements

ISE: Ion Selective Electrode

ISO: International Organization for Standardization

IUPAC: International Union of Pure and Applied Chemistry

LA : Laser Ablation

LC: Liquid Chromatography

LOD (or DL): Limit Of Detection

LTA: Low-Temperature Ash

MAE: Microwave-Assisted Extraction

MC ICP-MS: Multicollector Inductively Coupled Plasma Mass Spectrometry

MC GC-ICP-MS: Multicapillary: Gas Chromatography Inductively Coupled Plasma Mass Spectrometry

MCL: Maximum Contaminant Level

MDL: Method Detection Limit

MEC: Mercury Emission from Coal

MeHg (MMHg or MHg): (mono)Methylmercury

MeEtHg (or MeHgEt): Methylethylmercury

MeHgH: Methylmercury Hydride

MLQ: Method Limit of Quantification

MW: Molecular Weight

NAA: Neutron Activation Analysis

$NaBEt_4$: Sodium Tetraethylborate

$NaBPr_4$: Sodium Tetrapropylborate

NIES: National Institute for Environmental Studies

NIST: National Institute of Standards and Technology

NRCC: National Research Council of Canada

ORP (or Eh): Redox Potential

PEL: Probable Effect Level

PFA: Perfluoroalkoxy

PIXE/PIGE: Particle Induced X-ray/γ-ray Emission

PMT: Photomultiplier Tube

POC: Particulate Organic Carbon

PP: Polypropylene

PTFE: Polytetrafluoroethylene (or Teflon®)

PVC: Polyvinylchloride

RGM: Reactive Gas Phase Mercury

RN: Removable Needles

RNAA: Radiochemical Neutron Activation Analysis

ROM: Run-Of-Mine

RSD: Relative Standard Deviation

SA: South Africa

SABS: South African Bureau of Standards

SAMA: South African Mercury Assessment program

SCI: Sasol Chemical Industries

SEM: Scanning Electron Microscope

SEM-EDX: Scanning Electron Microscope Energy-Dispersive X-ray

SEP: Sequential Extraction Procedure

SFE: Supercritical Fluid Extraction

SHE: Standard Hydrogen Electrode

SIDMS: Speciated Isotope Dilution Mass Spectrometry

SIMS: Secondary Ion Mass Spectrometry

SPME: Solid-Phase Micro Extraction

SRB: Sulfate Reducing Bacteria

SSF: Sasol Synthetic Fuels

SSMS: Spark-Source Mass Spectrometry

SXRF: Synchrotron X-ray Fluorescence

T: Temperature

TC: Transfer Coefficient

TEL: Threshold Effect Level

TET: Toxic Effect Threshold

TGM: Total Gaseous Mercury

TLC: Thin-Layer Chromatography

TMAH: Tetramethylammonium Hydroxide

TOF: Time-Of-Flight

TPM: Particulate Phase Mercury

TSF: Tailings Storage Facility

TST : Traitement des Signaux Transitoires

UNEP: United Nations Environment Program

USA: United States of America

USEPA: United States Environmental Protection Agency

USGS: The United States Geological Survey

VR: Vaal River

WHO GV: World Health Organization Guideline Value

WRG: West Rand Group

WW: West Wits

XAFS: X-ray Absorption Fine Structure

XRF: X-ray Fluorescence

Chapter 1
Introduction and problem statement

1.1 Introduction

Mercury is well known as one of the most hazardous contaminants that may be present in the environment. The growing global concern over the release of mercury to the environment has prompted the preparation of country-specific inventories that quantify mercury emissions from various sources (Leaner *et al.*, 2009). A global Mercury Program was recently created by the United Nations Environment Program (UNEP) Governing Council in order to raise awareness of the nature of mercury pollution problems. The main goals of this program consist on assisting Governments and other stakeholders to identify, understand, and implement actions to mitigate mercury problems in their countries (USEPA, 2008).

The mobilization and release of mercury by human activities is referred to as anthropogenic mercury emissions. In South Africa (SA), the largest point sources of mercury emissions are coal combustion followed by gold mining activities (reprocessing of old tailing dams and artisanal mining) (Naicker *et al.*, 2003; Lusilao, 2009; Telmer and Veiga, 2009) and the largest single combustion source is coal-fired power plants (Pacyna, *et al.*, 2006; Dabrowski *et al.*, 2008). The country is ranked among the top 10 producer and consumer of coal in the world and is also a primary producer of important and strategic metals such as gold, platinum, lead and zinc (Pirrone *et al.*, 2010). Although the production facilities of these minerals and materials are known for their contribution to mercury pollution, limited information is available for SA (and the rest of the African continent) in relation to emissions from anthropogenic sources and mercury content in products (Pirrone *et al.*, 2010).

In 2006, the Council for Scientific and Industrial Research (CSIR) hosted a meeting in Pretoria (SA) to discuss the way forward in establishing a mercury assessment for the country. The workshop focused on initiating a South African Mercury Assessment (SAMA) program, which aims to develop a framework for mercury research focusing initially on the sources, transport, fate and consequences of mercury from coal-fired power plants in SA (Leaner, 2006).

Some of the expectations from the participants at the workshop were to address the mercury biogeochemical cycle by addressing the whole chain of events in deposition and effects, and to develop methodologies for accurate and reliable measurements for mercury species, that includes date-to-date analysis and continuous monitoring. This focus area is important since it was recognized that mercury research in South(ern) Africa is practically inexistent (Leaner, 2006). Therefore, the development of mercury research will enable the collection of reliable data that can be used to address mercury pollution problems within the country, and on a larger scale, to the African continent.

A particular aspect of mercury is that it exists in the environment in a number of different chemical and physical forms with different behavior in terms of transport and environmental effects (Schroeder and Munthe, 1998). Among the different mercury species, monomethylmercury (MeHg, MMHg or MHg) is of particular interest due to its high toxicity and to its high capacity to bioaccumulate in food chains (USEPA, 1997a; Bloom and Watras, 1989; Brosset and Lord, 1995).

For toxicological and biogeochemical studies the total concentration of mercury is of little value without knowledge of its chemical forms. Thus, speciation of mercury is a critical determinant of its mobility, reactivity, and potential bioavailability in mercury-impacted regions. Understanding the movement and geochemistry of mercury from these regions is therefore necessary in order to predict the potential impacts and hazards associated with the mercury contamination.

1.2 Statement of the problem

1.2.1 Gaseous mercury measurements

An interest has aroused, during the last two decades, in studying the environmental turnover of mercury species, be it organic or inorganic, and large research efforts have been put into the identification and quantification of these species over the last (Stoichev *et al.*, 2006).

Currently, it is difficult to detect mercury at extremely low concentrations such as those found in water (μg m^{-3}) or air samples (ng m^{-3}) (Harris *et al.,* 2007). The available detection equipment is very strongly matrix dependent and cannot detect small amounts of the pollutant. Several methods/systems exist to monitor low concentration levels of mercury and generally provide limits of detection from ng m^{-3} (Stoichev *et al.,* 2006). Their sensitivity, however, is achieved at the expenses of elaborate and time-consuming sample preparation and pre-concentration procedures.

Analytical methods have also been developed within our research laboratory for the determination of inorganic and organomercury forms in different liquid and solid matrices. These methods were successfully tested on real environmental samples (Lusilao, 2009), though it was clearly emphasized that the developed methods had to be improved for ultra trace mercury determination.

In the past, investigations of atmospheric mercury have been done on gaseous species, and methodologies for accurate determination of gaseous mercury in ambient air are now well established (Xiao *et al.,* 1997; Tekran, 1998). Furthermore, recent advances in analytical instrumentation (better selectivity and sensitivity) and "trace metal-free" methodologies have made the determination of atmospheric levels of mercury (pg m^{-3} range) feasible, and have significantly advanced the knowledge of atmospheric behavior of mercury (Xiao *et al.,* 1997; Tekran, 1998). Nevertheless, high quality data are still scarce (especially for the southern hemisphere) and improved techniques and methods for sampling and analysis of gaseous mercury are still needed. The generated information, linked with other data can be used to assess the various pathways of human exposure to mercury.

Mercury occurs in the atmosphere in mainly three forms: elemental mercury vapor (Hg^0), reactive gas phase mercury (RGM) and particulate phase mercury (TPM). Of these three species, only Hg^0 has been tentatively identified with spectroscopic methods (Edner *et al.,* 1989) while the other two are operationally defined species, i.e. their chemical and physical structure cannot be exactly identified by experimental methods but are instead characterized by their properties and capability to be collected by different sampling equipment.

Sampling and analysis of atmospheric mercury is often made as total gaseous mercury (TGM) which is an operationally fraction defined as species passing through a 0:45 μm filter or some other simple filtration device such as quartz wool plugs and which are collected on gold, or other collection material. TGM is mainly composed of elemental mercury vapour with minor fractions of other volatile species such as $HgCl_2$; CH_3HgCl or $(CH_3)_2Hg$. At remote locations, where TPM concentrations are usually low, TGM makes up the main part (> 99%) of the total mercury concentration in air (Munthe *et al.*, 2001).
Number of methods have been developed to measure TGM, RGM and TPM at both urban and background levels (Lu *et al.*, 1998).
The different mercury species are ubiquitous in the atmosphere with ambient TGM concentrations averaging about 1.5 ng m^{-3} in the background air throughout the world (Iverfeldt, 1991). Higher concentrations are found in industrialized regions and close to emission sources. RGM and TPM vary substantially in concentration typically from 1 to 600 pg m^{-3}, depending on location (Keeler *et al.*, 1995; Stratton and Lindberg, 1995).

It is, therefore, clear that mercury measurement methods must be able to detect mercury at relatively low levels to be utilized for environmental gaseous samples. For example, mercury concentrations in coal combustion flue gas may range between 1 to 30 ng m^{-3}. Thus, in order to detect mercury in flue gas, the analytical method must be sensitive enough to accurately measure within 0.5 ng m^{-3} with no interferences from other flue gas constituents (Laudal *et al.*, 1998). This imperatively requires the use of preconcentration techniques.
Numerous methods (automated or manual) are used as a preconcentration step prior to the mercury analysis. These methods consist on a liquid or solid sorption system to collect volatile species. A variety of liquid and solid sorbents can be used to separate and preconcentrate mercury species. Solid sorbents offer several advantages relative to liquid sorbents such as greater stability and easier handling. Moreover, solid sorbents also can be used repeatedly and the mercury collected can be analyzed directly using sensitive techniques (Laudal *et al.*, 1998).
These advantages provide impetus for the development of solid sorption methods. Mercury can be selectively captured on solid sampling medium through adsorption,

amalgamation, diffusion, and ion exchange processes. The gold trap is one of the mostly used solid sorbents. Different techniques using gold (foil, chips, thin film, etc.) coating on a substrate are available (EMEP, 2002). As an example, the International Organization for Standardization (ISO) has developed a standard method of sampling mercury by amalgamation on gold/platinum alloy thread (ISO, 2003).

The general principle for those techniques consist on trapping mercury from the sample using the gold trap and after collection, the trap is heated to remove mercury species. The trap can be re-used many times after desorption and sensitive detection methods are used for the identification and quantification of desorbed mercury species.

On another hand, in developing and testing innovative and cost-effective mercury control technologies, there are two main approaches that have been studied for mercury vapor control at elevated temperatures. One involves direct capture of Hg^0 by injection of sorbents, usually powdered activated carbons (USEPA, 2003). The other approach focuses on the development of oxidation catalysts, such as noble metal catalysts, to transform Hg^0 to Hg^{2+} for removal during scrubbing processes (Presto and Granite, 2008). A recent trend in the development of these new "mercury traps" for low concentrations consists on the use of nanostructured materials which shows mercury removal up to 95% (Sjostrom and Chang, 2003; USPTO, 2006).

It is, therefore, believed that such materials can also be used as analytical traps for the preconcentration of low level mercury.

1.2.2 Mercury concentration and distribution in South African coal

Environmental legislation in the developed countries has had significant impact on coal utilization, especially coal combustion for power generation, in limiting emissions of potentially hazardous materials such as inorganic constituents in coal to the environment.

This legislation has led to significant development of new models for the behavior of inorganics in coal combustion and a complementary enhancement of many analytical methods for determining inorganics in coal (Huggins, 2002).

It has long been recognized that there are environmental consequences related to the use of coal for energy production. Extensive research has been conducted in the northern

hemisphere and reports written about the environmental problems associated with coal mining, processing, and combustion and related problems such as acid mine drainage, acid rain, smog, and greenhouse gas emissions (Finkelman et al., 2002).

In the United States, for example, the mercury concentration in coal has been a subject of wide-spread discussion since the passage of the 1990 clean air act amendment (CAAA) (Toole-O'Neil *et al.,* 1999). The CAAA specifies 189 potential hazardous air pollutants (HAPs) among these are trace elements, including mercury. The CAAA focuses on mercury for special consideration because of its potentially adverse impact on human health.

There appears to be considerable sources of mercury input in Southern Africa. Global human activities such as combustion of fossil fuels and the incineration of waste materials are estimated to account for 70% of the total mercury in the atmosphere. Unfortunately, the amount of mercury emissions in the region is unknown (Leaner, 2006).

It is known that the main variables affecting mercury emissions to the environment during coal combustion include the mercury content of the coal, the type and efficiency of control devices used to reduce gaseous and particulate emissions, and the total amount of coal combusted (Wagner and Hlatshwayo, 2005).

Recent studies conducted by Dabrowski *et al.* (2008) and Leaner *et al.* (2009), based on the total amount of coal burned in all power plants per year, the mercury content of South African coals and the emission control devices used in each power plant, suggested that mercury emitted from South African coal fired power stations was lower than previously reported by Pacyna *et al.* (2006). However, the authors also suggested that further research is required to validate and refine the results obtained from their studies.

Indeed, the mercury concentrations used for the above studies were based either on estimates of the average mercury content in South African coals (Leaner *et al.,* 2009) or on the few published data (Dabrowski *et al.,* 2008).

Watling and Watling (1982) have determined a mercury concentration of 0.33 mg kg^{-1} for South African coals whereas Wagner and Hlatshwayo (2005) reported a mean value of 0.15 ± 0.05 mg kg^{-1} (ranging between 0.04 and 0.27 mg kg^{-1}) in coal samples obtained from the Highveld coalfield. More recently, the United States Geological Survey (USGS)

reported an average mercury concentration of 0.16 mg kg^{-1} for forty South African coals collected at different coalfields (Kolker *et al.,* 2011).

Previous studies on the geochemistry of coal, including South African coal, have demonstrated a notable vertical variation in mercury concentration compared to horizontal variation, indicative of different depositional environments vertically and possibly of localized metamorphism (Watling and Watling, 1982; Sakulpitakphon *et al*., 2004). The variability of reported mercury concentrations of South African coals shows the need of more analysis of South African coals and the importance of sampling strategies, especially when it comes to mercury determination.

Further, mercury has the property of strong volatility at high temperature and tends to adsorb in many types of containers used for storage. Care must be taken to avoid loss of the analyte during sample preparation and storage (Stoichev *et al.,* 2006). Results presented by Wagner and Hlatshwayo (2005) for six Highveld coals were, at least, 20% lower compared to those reported by the USGS for five of the six analyzed samples. Besides, the mercury concentration of 0.19 mg kg^{-1} measured for the certified reference material (SARM 20) also was about 20% lower than the certified mean of 0.25 mg kg^{-1}. This shows that mercury was lost somewhere during the sample preparation, probably during the digestion, as mentioned by the authors. Therefore, the actual mercury concentration in the Highveld coal is presumed to be higher than reported.

On another hand, since the US Environmental Protection Agency (USEPA) issued a federal rule to reduce mercury emissions from coal-fired power plants (Hoffart *et al.,* 2006) there have been many studies about the removal of mercury after the combustion of coal. However, only a few studies have been done about the pre-combustion removal of mercury from coal (Iwashita *et al.,* 2004).

The intention of coal cleaning is to reduce the inorganic contaminants in the coal before it is crushed and introduced into the boiler for combustion. Conventional coal cleaning methods usually employ pyrite-attacking mechanisms (Dronen *et al.,* 2004) because some of the mercury in the coal is associated with the pyrite fraction. The greatest fraction of cleaned coal is bituminous varieties, due mainly to their high pyrite and sulfur content. A

much smaller fraction of the subbituminous coals are cleaned, while lignite coals are rarely cleaned (Hoffart *et al.,* 2006).

In general, low grade bituminous coal is used for combustion in South African's power plants and no coal washing (and potential removal of mercury) takes place prior to burning (Dabrowski *et al.,* 2008). The majority of power plants receive coal from mines situated in the Witbank and Highveld coalfields (see Chapter 2 for location map), while few of them receive coal from mines situated in the Sasolburg and Waterberg coalfields, (Chamber of Mines, 2004). Only few data are available on the specific mercury content of these coals.

In addition, Dvornikov (Toole-O'Neil *et al.,* 1999 and the reference therein) proposed, on the basis of extensive studies of Soviet coal, that mercury occurs as mercury sulfide, metallic mercury and organometallic compounds whereas Gao *et al.* (2008) have, more recently, demonstrated the occurrence of the toxic methylmercury in some China coals.

Unfortunately, while many studies in the world have been devoted to the problem of mercury in coal, such as its modes of occurrence and its emission behavior, little is known about the speciation of mercury in South African coals.

The quantification of mercury and the determination of its distribution in South African coals are therefore very important to understand mercury behavior during coal beneficiation, cleaning and combustion. This will also help in developing suitable cleaning procedures for South African coals prior to combustion.

In a summary, due to the complex chemical structure of coal matrices, it is important to define the speciation of mercury in coal in order to get a better understanding of its fate and effect in biological, geological and atmospheric ecosystems after mining and/or combustion and to determine which cleaning methods can be successfully used.

1.2.3 Mercury pollution from gold mining operations in South Africa

Mining activities are known to play a significant role in the economic development of SA. Up until a few years back, SA was the world's largest gold producer. China surpassed

SA as the world's largest producer in 2007. China continues to increase gold production and remained the leading gold-producing nation in 2009, followed by Australia, SA, and the United States (www.mbendi.com).

In 2008, SA was estimated, by the USGS, to have 6,000 metric tons of gold reserves (USGS, 2008), although a later study presented by Hartnady **(**2009) suggests that South African gold reserves are only about half of the USGS estimate i.e. 2,948 metric tons and places SA only fourth in world rank, after Australia (5,000 t), Peru (3,500 t) and Russia (3,000 t). Ninety five percents of SA's gold mines are underground operations, reaching depths of over 3.8 km. Coupled with declining grades, increased depth of mining and a slide in the gold price, costs have begun to rise, resulting in the steady fall in production. The future of the gold industry in SA therefore depends on increased productivity.

By far the most gold that has been mined in SA (98%) has come from the Witwatersrand goldfields (figure 1.1). SA does have other smaller gold producers outside of the Witwatersrand ("Wits"), in the form of Archaean greenstone belts. The main gold producing greenstone belts are the Barberton Greenstone Belt situated in the Mpumalanga province, just north of Swaziland and the Kraaipan greenstone belt located west of Johannesburg, near Kuruman. Other smaller belts exist in the Northern Province, but have been worked sporadically (www.mbendi.com).

The name "Witwatersrand" means "White Waters Ridge" and was derived from the white quartzite ridge which strikes parallel to the edge of the basin in which the sediment was deposited. The gold mines in this area are situated around an ancient sea (over 2700 million years old) where rivers deposited their sediments in the form of sand and gravel which became the conglomerate containing the gold. The Witwatersrand Basin is approximately 350 km long and 200 km wide. The gold mines in this area are possibly the deepest mines in the world (mining operations at 3600 m and exploration core-drilling up to 4600 m). Peak gold production occurred in 1970 when over 1000 metric tons were mined (Hartnady, 2009). However gold production has declined since 1980.

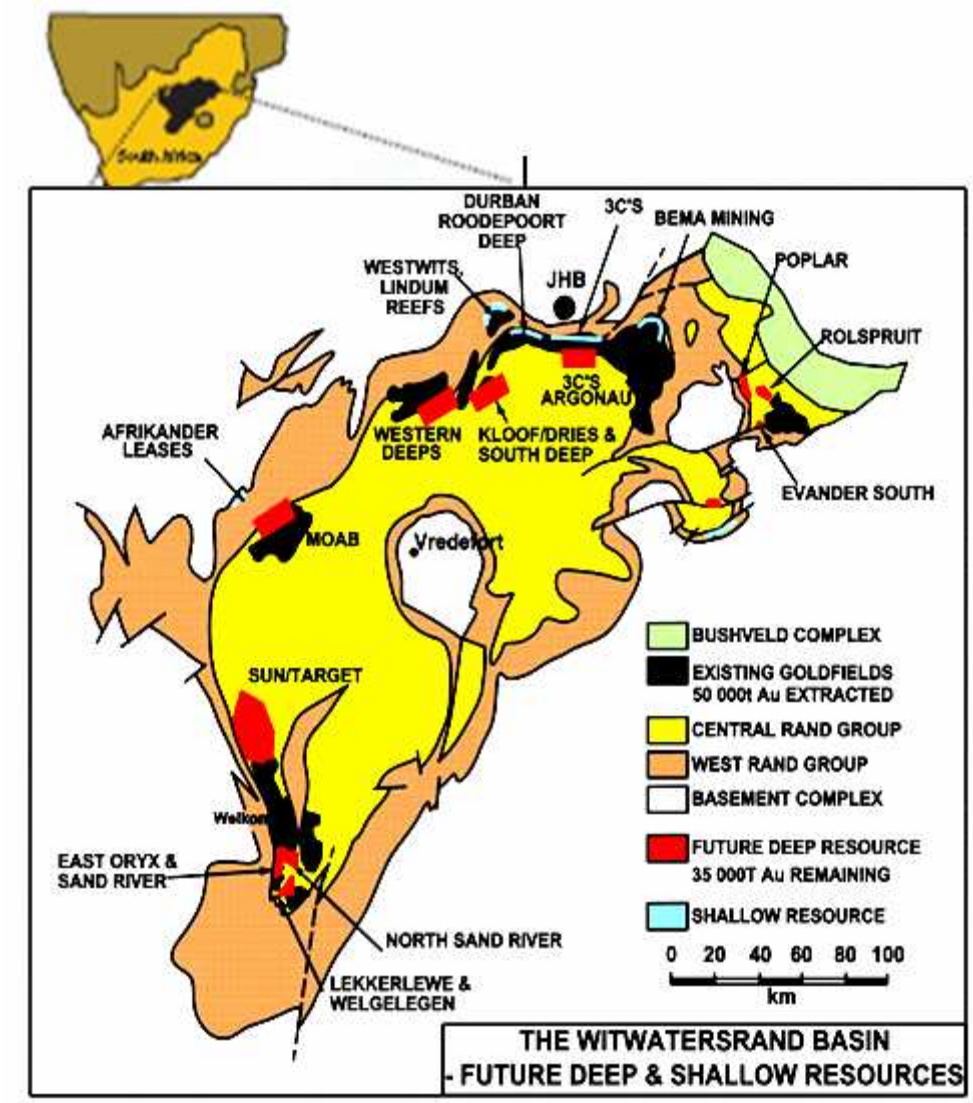

Figure 1.1 Map of the Witwatersrand Basin in South Africa (Modified after Tutu, 2006 and the reference therein)

The average recovery grade of the Witwatersrand gold mines has declined from 13.3 g t^{-1} in 1970 to 5.3 g t^{-1} in 1991 (Mphephu, 2004; wwwu.edu.uni-klu.ac.at) .

Over 100 mineral species have been reported from the gold-bearing reefs. Zircon, chromite and other "heavy minerals" occur throughout the Witwatersrand. The most common silicate minerals in the reefs are quartz, muscovite, pyrophyllite, chloritoid and chlorite (wwwu.edu.uni-klu.ac.at).

The sulphide minerals are the second most abundant minerals. A wide variety of nickel-cobalt-platinum sulpharsenides as well as copper sulphosalts and antimony-bearing

minerals are present. Included in this group are species such as cobalt-rich arsenopyrite, gersdorrite and cobaltite, and the platinum group minerals geversite, sperrylite, braggite and cooperite. Pyrite is present in a variety of habits and forms. The main uranium-bearing minerals are uraninite and brannerite with minor amounts of coffinite and uranothorite. Uranium (and gold) tends to be enriched when found in combination with carbon. In some places a "reef", the Carbon Leader, is developed and mined as the gold content is exceptionally high.

Most of the gold in the Witwatersrand is present as native gold which occurs in a variety of forms and habits, such as microscopic vein lets or overgrowths and is usually only visible under the microscope (the average gold particle ranges from 0.005mm to 0.5mm in diameter). There are however remarkable exceptions like those observed on the Randfontein Estates gold mine or in the City Deep Mine. In this latest, beautiful clear quartz crystals up to 10 cm long with small calcite crystals were found (wwwu.edu.uni-klu.ac.at).

Gold mining began on the Witwatersrand in 1886 across a broad arc some 60 km long, marking the outcrop of the Main Reef conglomerates. It soon became evident that the gold occurrence was of considerable significance, and prospectors and miners flocked to the area. Townships were established along the length of the outcrop to accommodate the growing workforce (McCarthy and Venter, 2006). Coal was discovered on the East Rand in the late 1880s, and by 1890 was being transported by rail along the Rand to supply the power needs of the growing industry (Jeffrey, 2005). Gold exploitation commenced in the Central Rand, followed by the West and East Rand (late 1890s) and continued to the West Wits area and Orange Free State Goldfields (1951) and after 1958 spread to the Eastern part of the Basin, the Evander Goldfield. This resulted to the creation of. a vast mining–industrial complex in the Witwatersrand Basin. The mining activity gave rise to a large conurbation centered on Johannesburg, which today accommodates millions of people (Forstner and Wittmann, 1976; Mc Carthy and Venter, 2006, Naicker et al., 2003). Since the gold-bearing conglomerate encountered in SA is always intimately associated with a matrix, crushing and grinding were therefore a prerequisite to the recovery of gold, whether by amalgamation, cyanidation, flotation or gravity concentration.

Gold was initially extracted using a mercury amalgam method. Ore mined underground was brought to the surface, where it was milled to a fine sand, during and after which it was exposed to a film of mercury spread on copper plates. These were periodically removed, and the mercury–gold amalgam scraped off and distilled to recover the gold. The tailings were transported to dumps near the extraction plant, producing the so called ‘‘sand dumps’’ (Naicker *et al.*, 2003).

Although cyanidation was introduced later on, to supplement amalgamation and has become the only method of treatment on several mines, Forstner and Wittmann (1976) observed that approximately 43% of the total South African gold output was still attained by amalgamation in the late 1970s. They estimated the consumption of mercury to fluctuate between 10 and 40 mg per ton of milled rock.

The success achieved by the cyanide process lies in the selective dissolution of gold by weak cyanide solutions from other ore constituents. Gold is precipitated from the cyanide solution by zinc dust and a 10% lead nitrate solution, and is recovered from the zinc precipitate by calcining the base metal constituents to the oxide form and by smelting with a borosilicate flux to eliminate the sulfur content. The tailings were pumped to large dumps, known as ‘‘slimes dumps’’.

Due to the high degree of extraction efficiency and more economic results achieved by direct cyanidation, practically no scope has been offered for the application of flotation methods to the recovery of gold in SA. The only exception is the recovery of uranium oxide as by-product from gold ores from 1952. Extraction of uranium oxide requires leaching of gold plant slime with concentrated sulfuric acid (Forstner and Wittmann, 1976).

The main residues from gold-mining operations consist of waste rocks, cyanided sand and slime, surplus mine water and discarded solutions such as waste sulfuric acid. The waste rock can be disposed of as concrete aggregate, rail-ballast, etc. and has commercial value.

Due to the high selectivity of both the mercury amalgamation and the cyanidation for gold, other ore minerals were unaffected during the extraction process, and hence reported to the tailings dumps (Naicker *et al.*, 2003). By the end of 1972, it was reported

that more than three millions metric tons of ore had been cumulatively mined (Forstner and Wittmann, 1976) and, in the late 1980s, approximately 240 tailings dams covering a surface area of 44 000 hectares were registered in the Witwatersrand Basin (Tutu, 2006). In the last two decades, many of these dumps have been and are being retreated to recover the remaining gold, and the tailings are pumped to disposal sites (Mpephu, 2004). Due to inadequate design, poor management and neglect, these tailings dams have been subjected to varying degrees of water and wind erosion which led to serious environmental damages such as the pollution of surrounding watersheds, as a result of acid mine drainage generated mainly from sulphides and heavy metals in the tailings dams, air pollution in the form of airborne dust from unrehabilitated, partially rehabilitated and reprocessed tailings dams, and the sterilization of appreciable tracts of land partly as a result of shallow undermining (Tutu, 2006).

Many studies also have reported the existence of acid mine drainage on the Witwatersrand (e.g. Wittmann and Forstner, 1976; Naicker *et al.*, 2003), and the presence of enhanced concentrations of heavy metals including mercury in surface waters and sediments (Naicker et al., 2003, McCarthy and Venter, 2006). The source was assumed to be from surface run-off from the main tailing dumps in the catchment as well as pumped water from mining operations (Marsden, 1986). Other studies showed that the dumps, particularly those consisting predominantly of sand sized tailings, were polluting the underlying ground water which in turn was entering the surface water environment via ground-water seeps (Mphephu, 2004).

The migration of pollutants such as mercury from these remote poorly-monitored mine sites can result in elevated mercury levels in more populated urban regions. Therefore, understanding the transport and bio-geochemistry of mercury from mines in the Witwatersrand Basin is necessary in order to predict ecological consequences associated with this form of contamination.

In soils and surface waters, mercury can exist in the mercuric (Hg^{+2}) and mercurous (Hg^{+1}) states as a number of complex ions with varying water solubilities. Mercuric mercury, present as complexes and chelates with ligands, is probably the predominant form of mercury present in surface waters (ATSDR, 1999). The transport and partitioning of mercury in surface waters and soils is influenced by the particular form of the

compound (speciation). Therefore, the speciation of mercury is a critical determinant of its mobility, reactivity, and potential bioavailability in gold-mine impacted regions. Net generation of methylmercury, for example, is important in investigations of the environmental effects of mercury contamination, because of its toxicity and also due the fact that methylmercury is the form of mercury that is concentrated by fish and aquatic food chains (USGS, 2003).

Mercury speciation in these complex natural systems is additionally influenced by a number of physical, geological, and anthropogenic variables (Kim *et al.*, 2004).

Sediments, on another hand, are important carriers for trace metals in the environment and reflect the current quality of the system. Analysis of the development of concentrations of metals along sediment cores therefore makes it possible to determine the history of metal contamination for a certain region (de Lacerda *et al.*, 1991). Harris et al. (2007) reported that methylmercury in sediment is a useful indicator to assess changes in mercury load, changes to the net bioaccessibility of inorganic mercury and changes in bacterial activity. Recent studies (Nsengimana, 2007; Lusilao, 2009) done on the Klip River basin in SA have also demonstrated that sediments and stream-water are a useful barometer of changes in mercury load. Because of the importance of sediments in mercury methylation, investigation of selected sediment environments from the Witwatersrand Basin could generate significant information regarding the relative impact of mercury contamination on the presence of methylmercury in reservoirs and wetlands.

Understanding conditions that regulate the formation and behavior of methylmercury in aquatic sediments is, therefore, essential for determining the modes of transfer of this contaminant to the water column and biota.

Unfortunately, as mentioned previously, mercury research in SA is practically non-existent and the few fragmented risk assessments of local mercury pollution is based on total mercury concentrations among other elements (Leaner, 2006). Due to the limited data available on the anthropogenic emission of mercury in SA, the level of mercury pollution and its consequences in terms of ecosystem services and human health appear to be highly underestimated in the country. In order to get a better assessment of the local

environmental impact of mercury pollution from gold mining sites, adequate information concerning its speciation is thus required.

Chapter 2
Literature review

2.1 Introduction

Interest in the impact of mercury released into the environment been driven by the human health concerns associated with mercury ingestion, mainly through the consumption of seafood (Grigal, 2002). Mercury (Hg) occurs in two oxidation states in environmental media: metallic (Hg^0 or Hg(0)) and mercuric (Hg^{2+} or Hg(II)). Under ordinary conditions, Hg^0 vaporizes readily and is easily transported in the atmosphere. Natural sources of mercury to the atmosphere include degassing of the earth's crust through volcanoes and diffusion from ore bodies (Nriagu, 1979). Human activities such as mining and associated smelting, burning of fossil fuels, and industrial uses of mercury in chloralkali plants, paints, batteries, medicine, and dentistry have significantly increased the global reservoir of atmospheric mercury since the beginning of the industrialized period (Fitzgerald *et al.*, 1998). The wide distribution of mercury via atmospheric processes and its deposition, from the atmosphere, to terrestrial and aquatic systems has led to the recognition of mercury as a toxic global pollutant (Fitzgerald *et al.*, 1998; Jackson, 1997).

There are various questions related to uncertainties of the relative importance of different mercury sources (natural and anthropogenic), processes controlling cycling and fate in the environment, and toxicological effects on humans and wildlife (Krabbenhoft *et al.*, 2005). The purpose of this chapter is to provide a general description of some of the latest understanding of the processes that affect the biogeochemical cycling of mercury in the environment. However, it is necessary, in order to put mercury cycling in the proper context, to present a brief history of human uses of mercury and an overview on the past and present mercury sources to the environment, and reasons for concern.

As early as 430 BC in Almadén, Spain, humans discovered how to extract mercury from geologically enriched deposits (Martínez-Cortizas *et al*., 1999). Over the past twenty-five centuries, mining operations around the globe have extracted more than 800,000 metric tons of mercury and dispersed it for industrial and commercial purposes (Ferrara, 1999).

This resulted not only in high levels of environmental contamination near processing areas, but also regional to global scale impacts through evasion of gaseous elemental mercury (Hg^0) and subsequent long-range transport and deposition.

The migration of mercury-enriched sediment into stream flow spreads the mercury from mine sites into surrounding watersheds. More than a century later, continued dispersion of this mercury contamination of streams, large rivers, reservoirs, and wetlands well downstream of the mines continues, and is a major topic of concern and research worldwide. Volatilization of Hg^0 from various mining operations (mercury or gold mining), or emissions from contaminated mine tailings, has resulted in regional-scale mercury contamination via atmospheric transport and deposition at locations as far as 1000 km away from sources (Schuster et al., 2002). The large-scale geographic spread of mercury from sites of use, its subsequent emission and transport to distant sites of deposition summarizes the modern view of the current global mercury problem.

2.2 Latest global mercury emission inventories

By the 1970s, researchers across the northern hemisphere generally concluded that atmospheric mercury concentrations, and corresponding deposition rates, had generally increased 3–5 fold over historical times, although considerable variation in historic/current flux ratio is seen among specific study sites and the variation appears to relate to proximity to emission sources (Krabbenhoft *et al.*, 2005).

These sources can be broadly classified as combustion sources (principally coal-fired utility boilers, municipal waste combustors, commercial/ industrial boilers, medical waste incinerators), and manufacturing sources (principally heavy-metal processing, chlor-alkali, cement, and pulp and paper manufacturing) (USEPA, 1997a). Unlike most other widespread contamination issues, the mercury problem also has a natural-source component that, according to Mason *et al*. (1994), comprises about a third of the global mercury emission budget. Table 2.1 presents an estimate of the global mercury emission from natural sources.

Table 2.1 Global mercury emissions by natural sources estimated for 2008
(After Pirrone *et al.*, 2010)

Source	Hg (Mg yr^{-1})	Contribution (%)
Oceans	2682	52
Lakes	96	2
Forest	342	7
Tundra/Grassland/Savannah/Prairie/Chaparral	448	9
Desert/Metalliferous/Non-vegetated Zones	546	10
Agricultural areas	128	2
Evasion after mercury deposition events	200	4
Biomass burning	675	13
Volcanoes and geothermal areas	90	2
Total	5207	100

Quantifying the total contribution of natural mercury sources to the global mercury budget is critically important for evaluating what environmental response might be expected from proposals or regulatory actions to reduce mercury emissions.

Natural emissions are, as mentioned above, principally derived from crustal degassing, volcanoes, and volatilization from geologically-enriched materials (Rasmussen, 1994; Gustin *et al.*, 2000; Rytuba, 2005). Another major class of "naturally appearing" mercury sources is emissions from forest fires, soils and oceans (Mason *et al.*, 1994; Friedli *et al.*, 2003). However, the majority of these mercury fluxes are actually re-emissions of mercury originally released from anthropogenic sources and deposited after long-range transport (Mason *et al.*, 1994; Fitzgerald et al., 1998; Ebinghaus *et al.*, 1999).

This emission and re-emission phenomenon is one example of the biogeochemical cycles that control the distribution and fate of mercury in the environment.

.

Earlier studies of global mercury emissions were aimed primarily to assess the contributions from anthropogenic sources (Nriagu and Pacyna, 1988; Pirrone *et al.*, 1996; Pacyna *et al.*, 2006), particularly from coal, oil and wood combustion as well as from solid waste incineration and pyrometallurgical processes. Several studies have estimated global emissions from volcanoes (Ferrara *et al.*, 2000; Pyle and Mather, 2003), artisanal small scale gold mining (Lacerda, 1995; Veiga *et al.*, 2006), re-emission from oceans and surface waters (Mason and Sheu, 2002), top soil and vegetation (Gustin *et al.*, 2000) and forest fires (Friedli *et al.*, 2003; Ebinghaus et al., 2007). Recent assessments of mercury

emissions to the global atmosphere have included the contribution of the most important anthropogenic and natural sources (AMAP/UNEP, 2008; Pacyna *et al.*, 2009; Pirrone *et al.*, 2010). Table 2.2 summarizes the global contribution of the most important anthropogenic sources.

Table 2.2 Global mercury emissions from anthropogenic sources (Pirrone *et al.*, 2010)

Source category	Hg emission (Mg yr^{-1})
Coal and oil combustion	810
Non-ferrous metal production	310
Pig iron and steel production	43
Cement production	236
Caustic soda production	163
Mercury production	50
Artisanal gold mining production	400
Waste disposal	197
Coal bed fires	32
Vinyl chloride monomer production	24
Other	65
Total	2320

In the last decades a considerable amount of research has been done to improve mercury emission inventories at country level (Pirrone *et al.*, 2010), including those countries with economies in transition (Feng *et al.*, 2009; Streets *et al.*, 2009).

In Europe, mercury emissions from anthropogenic sources in the year 2005 (table 2.3) were near 145 Mg, with the highest contribution from stationary combustion sources (52%). The total anthropogenic mercury emission from North America is estimated to be 153 Mg yr^{-1}. The major sources are known to be coal combustion and the incineration of solid waste for the United States (USEPA, 2005), and smelters for non-ferrous metal production for Canada and Mexico (CEC, 2001; Environment Canada, 2008).

For Russia, the total anthropogenic emissions are estimated to be 70 Mg yr^{-1}, with 77% being the contribution from processes where mercury is mobilized as an impurity (ACAP, 2005).

Table 2.3 Global emissions of total mercury from major anthropogenic sources in Mg yr^{-1} (after Pirrone *et al.*, 2010). The South African contribution is shown in bold

	SC[a]	NFMP	PISP	CP	CSP	MP	GP	WD	O	T	Ref. year
S. Africa	**32.6**	**0.3**	**1..3**	**3.8**	**0.0**	**0.0**	**0.3**	**0.6**	**1.3**	**40.2**	**2004**
China	268.0	203.0	8.9	35.0	0.0	27.5	44.7	14.1	7.6	609.1	2003
India	124.6	15.5	4.6	4.7	6.2	0.0	0.5	77.4	7.5	240.9	2004
Australia	2.2	11.6	0.8	0.9	0.0	0.0	0.3	0.2	0.6	16.6	2005
Europe	76.6	18.7	0.0	18.8	6.3	0.0	0.0	10.1	14.7	145.2	2005
Russia	46.0	5.2	2.6	3.9	2.8	0.0	4.3	3.5	1.5	69.8	2005
N. America	65.2	34.7	12.8	15.1	10.3	0.0	0.0	13.0	1.7	152.8	2005
S. America	8.0	13.6	1.8	6.4	2.2	0.0	16.2	0.0	1.5	49.7	2005
Total	623.2	302.2	32.8	88.6	27.8	27.5	66.3	118.9	36.4	1324.3	
Others[b]	186.8	7.1	10.4	147.1	135.1	22.5	333.7	68.5	28.2	939.4	2006
Total	**810.0**	**310.0**	**43.2**	**235.7**	**162.9**	**50.0**	**400.4**	**187.4**	**64.6**	**2319.7**[c]	

[a] SC: Stationary combustion; NFMP: Non-ferrous metal production; PISP: Pig iron and steel production; CP: Cement production; CSP: Caustic soda production; MP: Mercury production; GP: Gold production; WD: Waste disposal; CB: Coal-bed fires; VCM: Vinyl chloride monomer production; O: Other; T: Total
[b] Others: Rest of the world
[c] This sum considers also CB and VCM estimates, which account for 32.0 Mg yr^{-1} and 24 $Mgyr^{-1}$, respectively. Totals for countries do not include these values.

Mercury emissions in China were estimated to be 609 Mg in 2003, with a large fraction (44%) due to coal combustion, which in China includes three major subcategories: coal-fired power plants, industrial boilers and residential uses. As China is the largest coal producer and consumer in the world, mercury emissions in China have been increasing rapidly in recent years and are receiving increasing attention (Streets *et al.*, 2009; Wang *et al.*, 2009). By 2007, coal consumption by power generation in China increased to 1.49 billion tons, indicating an even higher annual growth rate of 5.9% during 2004–2007 (Wu *et al.*, 2006).

In India, The highest contributing source categories are coal combustion (52%) and waste disposal through incineration (32%). Industrial mercury emissions in India have decreased from 321 Mg in 2000 to 241 Mg in 2004. The Ministry of Environment and Forests in New Delhi has stated that 86% of mercury-cell chlorine plants have been converted to membrane technology (Mukherjee et al., 2009). This change suggests that mercury emissions from this sector have decreased from 132 Mg in 2000 to 6.2 Mg in 2004.

In Brazil, the amount of mercury entering the environment was estimated to be about 200 Mg yr^{-1} (Pirrone et al., 2010). The major source of mercury pollution in this country is known to be gold production, especially artisanal scale gold mining (Telmer and Veiga,

2009). This case will be discussed with more details in the following section. An estimate done in the Alta Floresta area (Brazil) showed that a typical month's production of 230 kg of gold emitted 240 kg of mercury to the atmosphere as Hg^0 and 60 kg of mercury into rivers. In addition, emissions of mercury from coal fired power plants is about 5.6 Mg yr^{-1} (emission factor 0.2 mg kg^{-1}) with a coal consumption of about 28 Tg yr^{-1} (Mukherjee et al., 2009).

In Australia, the total mercury emission from anthropogenic sources is 16.6 Mg yr^{-1} with coal fired power plants (2.2 Mg yr^{-1}) and non-ferrous metal smelters (11.6 Mg yr^{-1}) representing the major emission sources (Nelson, 2007).

There is limited information available for SA (and other African countries) in terms of emission sources. Nevertheless most mercury released to the environment originates from coal combustion and gold mining activities (Pacyna *et al.,* 2006; Dabrowski *et al.,* 2008; Telmer and Veiga, 2009). Leaner *et al.* (2009) critically revised previous estimates (Pacyna *et al.,* 2006), giving an estimate for the country of 40.2 Mg yr^{-1}. Most of the mercury emissions are related to electric power generation facilities that account for 81% of the total national emission (Dabrowski *et al.,* 2008). The coal gasification process accounts for 4% of the total, whereas coal combustion in cement kilns and producing clinker is the major source of mercury in cement production, representing 9% of the total emission. It is of importance to notice, here, that there is a specific concern about the uncertainty of anthropogenic emission estimates from regions that are inadequately described in terms of point sources, such as Africa and South America, or from regions that exhibit unusually large uncertainties, as it is the case for Asia. These uncertainties affect model development, environmental policy and human welfare (Pirrone *et al.,* 2010).

Estimates presented in table 2.3 show that summing up the contributions from anthropogenic sources nearly 2320 Mg of mercury is released annually to the global atmosphere (31% GEb). A comparison of the above estimates with those previously reported in the literature suggests that Europe and North America are reducing their contribution to the global mercury burden, whereas emissions in Asia are increasing, the latter is primarily driven by the upward trend of energy demand that in the last decade has grown at a rate of 6 to 10% per year (Pirrone *et al.,* 2010).

The improvement of the mercury emission inventory on a global scale, with special attention to fossil fuel fired power plants in countries characterized by fast economic growth (i.e. China, India) is in agreement with recommendations and requirements of major international conventions and programs aimed to reduce the impact of human activities on ecosystems and human health (Pirrone *et al.*, 2010).

2.3 Major anthropogenic sources of mercury

Mercury is released to the atmosphere from a large number of man-made sources, which include fossil-fuel fired power plants, ferrous and non-ferrous metals manufacturing facilities, caustic soda production plants, ore processing facilities, incinerators for urban, medical and industrial wastes, cement plants and chemicals production facilities.

The current global atmospheric budget (table 2.2) shows that the majority of mercury emissions originate from combustion of fossil fuels (11% GEb), followed by artisanal small scale gold mining (5% GEb). Coal combustion and gold production are also believed, by many authors (e.g. Pacyna *et al.*, 2006; Dabrowski *et al.*, 2008; Pirrone *et al.*, 2010), to be the major contributors of mercury pollution in SA. That is the reason why a particular attention is given in this section to these pollution sources.

2.3.1 Coal

Coal is a fossil fuel formed in ecosystems where plant remains were preserved by water and mud from oxidization and biodegradation, thus sequestering atmospheric carbon. Coal is a readily combustible black or brownish-black rock. It is a sedimentary rock, but the harder forms, such as anthracite coal, can be regarded as metamorphic rock because of later exposure to elevated temperature and pressure. It is composed primarily of carbon and hydrogen along with small quantities of other elements, notably sulfur. Coal is extracted from the ground by coal mining, either underground mining or open pit mining (surface mining) (www.Wikipedia.org; Kroschwitz and Grant, 1993; Selsbo, 1996). Coal is the largest source of fuel for the generation of electricity world-wide, as well as the

largest world-wide source of carbon dioxide emissions, slightly ahead of petroleum and about double that of natural gas.

Coal is classified into four main types or ranks (lignite, subbituminous, bituminous, anthracite), depending on the amounts and types of carbon it contains and on the amount of heat energy it can produce. The rank of a deposit of coal depends on the pressure and heat acting on the plant debris as it sank deeper and deeper over millions of years. For the most part, the higher ranks of coal contain more heat-producing energy (EIA, 2008; Kroschwitz and Grant, 1993).

- *Lignite*: is the lowest rank of coal with the lowest energy content. Lignite coal deposits tend to be relatively young coal deposits that were not subjected to extreme heat or pressure. Lignite is crumbly and has high moisture content. It is used almost exclusively as fuel for electric power generation.

- *Subbituminous*: coal has a higher heating value than lignite. Subbituminous coal typically contains 35-45% carbon, compared to 25-35% for lignite. Its properties range from those of lignite to those of bituminous coal and are used primarily as fuel for steam-electric power generation. Additionally, it is an important source of light aromatic hydrocarbons for the chemical synthesis industry.

- *Bituminous coal*: contains 45-86% carbon, and has two to three times the heating value of lignite. Bituminous coal was formed under high heat and pressure. It is used primarily as fuel in steam-electric power generation, with substantial quantities also used for heat and power applications in manufacturing and to make coke.

- *Anthracite*: contains 86-97% carbon, and has a heating value slightly lower than bituminous coal. It is used primarily for residential and commercial space heating.

World coal consumption in 2006 was 6.118 billions tons (Pirrone *et al.*, 2010), representing the primary fuel used in electrical power generation facilities (42%) and accounts for about the 27% of world's energy consumption (EIA, 2009). Table 2.4 shows the trend of coal production in different countries from 2003 to 2006.

Table 2.4 Production of Coal by Country and year (million tonnes) (www.Wikipedia.org)

Country	2003	2004	2005	2006	Share
PR China	1722.0	1992.3	2204.7	2380.0	.384
United States	972.3	1008.9	1026.5	1053.6	.170
India	375.4	407.7	428.4	447.3	.072
Australia	351.5	366.1	378.8	373.8	.060
Russian Federation	276.7	281.7	298.5	309.2	.050
South Africa	**237.9**	**243.4**	**244.4**	**256.9**	**.041**
Germany	204.9	207.8	202.8	197.2	.032
Indonesia	114.3	132.4	146.9	195.0	.031
Poland	163.8	162.4	159.5	156.1	.025
Total World	**5187.6**	**5585.3**	**5886.7**	**6195.1**	**1**

When coal is used for electricity generation, it is usually pulverized and then burned in a furnace with a boiler. The furnace heat converts boiler water to steam, which is then used to spin turbines which turn generators and create electricity. The thermodynamic efficiency of this process has been improved over time. "Standard" steam turbines have topped out with some of the most advanced reaching about 35% thermodynamic efficiency for the entire process, which means 65% of the coal energy is waste heat released into the surrounding environment (www.Wikipedia.org).

The total known deposits recoverable by current technologies, including highly polluting, low energy content types of coal (i.e., lignite, bituminous), might be sufficient for 300 years' use at current consumption levels, although maximal production could be reached within decades (EIA, 2007).

At the end of 2006 the recoverable coal reserves amounted around 800 or 900 gigatons. The US Energy Information Administration gives world reserves as 998 billion short tons (= 905 gigatons), approximately half of it being hard coal (See also Table 2.5). At the current production rate, this would last 164 years. At the current global total energy consumption of 15 terawatt, there is enough coal to provide the entire planet with all of its energy for 57 years (EIA, 2007).

Table 2.5 Proved recoverable coal reserves at end-2006 in million tonnes (teragrams) (www.Wikipedia.org)

Country	Bituminous and anthracite	SubBituminous and lignite	TOTAL	Share
USA	111,338	135,305	246,643	27.1
Russia	49,088	107,922	157,010	17.3
China	62,200	52,300	114,500	12.6
India	90,085	2,360	92,445	10.2
Australia	38,600	39,900	78,500	8.6
South Africa	**48,750**	**0**	**48,750**	**5.4**
Ukraine	16,274	17,879	34,153	3.8
Kazakhstan	28,151	3,128	31,279	3.4
Poland	14,000	0	14,000	1.5
Brazil	0	10,113	10,113	1.1
Germany	183	6,556	6,739	0.7
Colombia	6,230	381	6,611	0.7
Canada	3,471	3,107	6,578	0.7
Czech Republic	2,094	3,458	5,552	0.6
Indonesia	740	4,228	4,968	0.5
Turkey	278	3,908	4,186	0.5
Greece	0	3,900	3,900	0.4
Hungary	198	3,159	3,357	0.4
Pakistan	0	3,050	3,050	0.3
Bulgaria	4	2,183	2,187	0.2
Thailand	0	1,354	1,354	0.1
North Korea	300	300	600	0.1
New Zealand	33	538	571	0.1
Spain	200	330	530	0.1
Zimbabwe	502	0	502	0.1
Romania	22	472	494	0.1
Venezuela	479	0	479	0.1
TOTAL	**478,771**	**430,293**	**909,064**	**100.0**

2.3.1.1 Mercury in coal

Depending on the source and quality of the coal, any number of naturally occurring elements can be found. For instance, Huggins (2002) reported up to 79 elements in US coals among these are the 11 inorganic elements listed by the U.S. Clean Air Act Amendments as potentially hazardous air pollutants: antimony, arsenic, beryllium,

cadmium, chromium, cobalt, lead, manganese, mercury, nickel and selenium (Finkelman, 1994). Among these metals, mercury is the most concerned health issues resulting from its emission because the element is quite volatile, so that 30–75% of mercury in coal will be released to air when coal is burned in coal-fired power plant (Iwashita *et al.,* 2004). Therefore, many studies have been devoted to the problem of mercury in coal such as its occurrence in coal, its emission behavior, and the reduction of mercury emission (Feng and Hong, 1999; Hoffart *et al.,* 2006; Toole-O'Neil *et al.,* 1999).

Although it is very difficult to generalize the mercury concentration in coal, the literature indicates that the mercury content in coal varies between 0.01 and 1.5 mg kg^{-1} (Toole-O'Neil *et al.,* 1999; Pirrone *et al.,* 2010). The concentration of mercury is somewhat lower in lignite coals than in bituminous and sub-bituminous coals. However, the lower heating values of lignite coals relative to bituminous and sub-bituminous coals suggest that the amount of lignite burned per megawatt of energy produced is higher compared to other coal types (Tewalt and Finkelman, 2001). Moreover, concentrations of mercury within the same mining field may vary by one order of magnitude or more (Mukherjee *et al.,* 2009).

2.3.1.2 Coal in South Africa

Coal is found in SA in 19 coalfields (figure2.1), located mainly in KwaZulu-Natal, Mpumalanga, Limpopo, and the Free State, with lesser amounts in Gauteng, the North West Province and the Eastern Cape.

The main coal mining areas are presently in the Witbank-Middelburg, Ermelo and Standerton-Secunda areas of Mpumalanga, around Sasolburg-Vereeniging in the Free State/Gauteng and in northwestern KwaZulu- Natal where smaller operations are found.

Single, although large, collieries are found near Ellisras and Tshipise (Jeffrey, 2005).

The South African coal resource and reserve estimates vary widely since each value of the reserves was estimated under a different set of circumstances (e.g. depth, seam thickness and grade cut-offs), different classification systems and at different times with different sets of economic constraints using different criteria. Recent studies suggest that the total remaining recoverable reserves are estimated at 49 billion tons (table 2.5).

The Waterberg, Highveld and the Witbank coalfields contain above 70% of the total reserves. The Witbank coalfield is nearing depletion and additional sources for coal supply must soon be identified if the coal industry is to continue into the 21st century. The Waterberg coalfield is a likely replacement of the Witbank coalfield, simply because it has the potential to contain the vast majority of the country's remaining *in situ* virgin coal resources. The Highveld coalfield reserves are important to the long-term life of Sasol's Sasol Synthetic Fuels (SSF) and Sasol Chemical Industries (SCI), which requires 40 million tons a year. It is likely that production will continue for a considerable number of years.

The Sasolburg-Vereeniging coalfield is also a supplier to SSF and SCI, as well as supplying coal to Lethabo power station. The remaining coal reserves of the Free State coalfield are low-grade coal suitable for power generation and possible liquid fuel production, while the remaining reserves in the South Rand Coalfield are classified as lowgrade bituminous coal with a CV of less than 25.5 MJ kg^{-1} (Bredell**,** 1987). The Limpopo (Tuli) coalfield is reported to contain between 349–517 Mt of mineable *in situ* raw bituminous coal with the potential to provide, after washing, between 125–243 Mt of metallurgical coal. South Africa currently produces less than 0.5 Mt of saleable coking coal (Spalding**,** 2003) per annum and therefore the Limpopo (Tuli) coalfield will remain a potentially valuable coking coal resource for the future.

The Highveld coalfield of SA (figure 2.1) is part of the Lower Permian Vryheid Formation (~280 Ma) in the Karoo Supergroup (Roberts, 2008). It is located mainly in Mpumalanga Province, approximately 130 km southeast of Johannesburg and 100 km south of Witbank (Hagelskamp *et al.*, 1988). There are five coal seams (No. 1 – No. 5) associated with this formation, however only the No. 2 and No. 4 seams are economically mined over much of the area. The bituminous coal seams were deposited under cool, wet conditions with water originating from retreating glacial activity to the north (Hagelskamp *et al.*, 1988; Hodgson and Krantz, 1998; Wagner and Hlatshwayo, 2005).

Coal quality increases from west to east, increasing in vitrinite content and overall rank (Sullivan, 1995). Coal in Gauteng, for instance, tends to occur in thick, shallow deposits and is of poorer quality than seams in Kwazulu Natal, which are deeper and thinner.

The Highveld Coalfield is the next most productive coalfield, after the Witbank coalfield, with ten operating collieries. In 2001, it accounted for about 73.65 million tons (24.92 %) of the total run-of-mine (ROM) production (Jeffrey, 2005). Mining was largely initiated by the development of the coal-fired Kriel and Matla power stations with collieries established to feed these power stations. Since then, the five Sasol mines around the Secunda area were developed. All the Sasol mines are dedicated coal suppliers to the SSF and SCI where the coal is used as a feedstock in the production of liquid fuels and chemicals (Jeffrey, 2005).

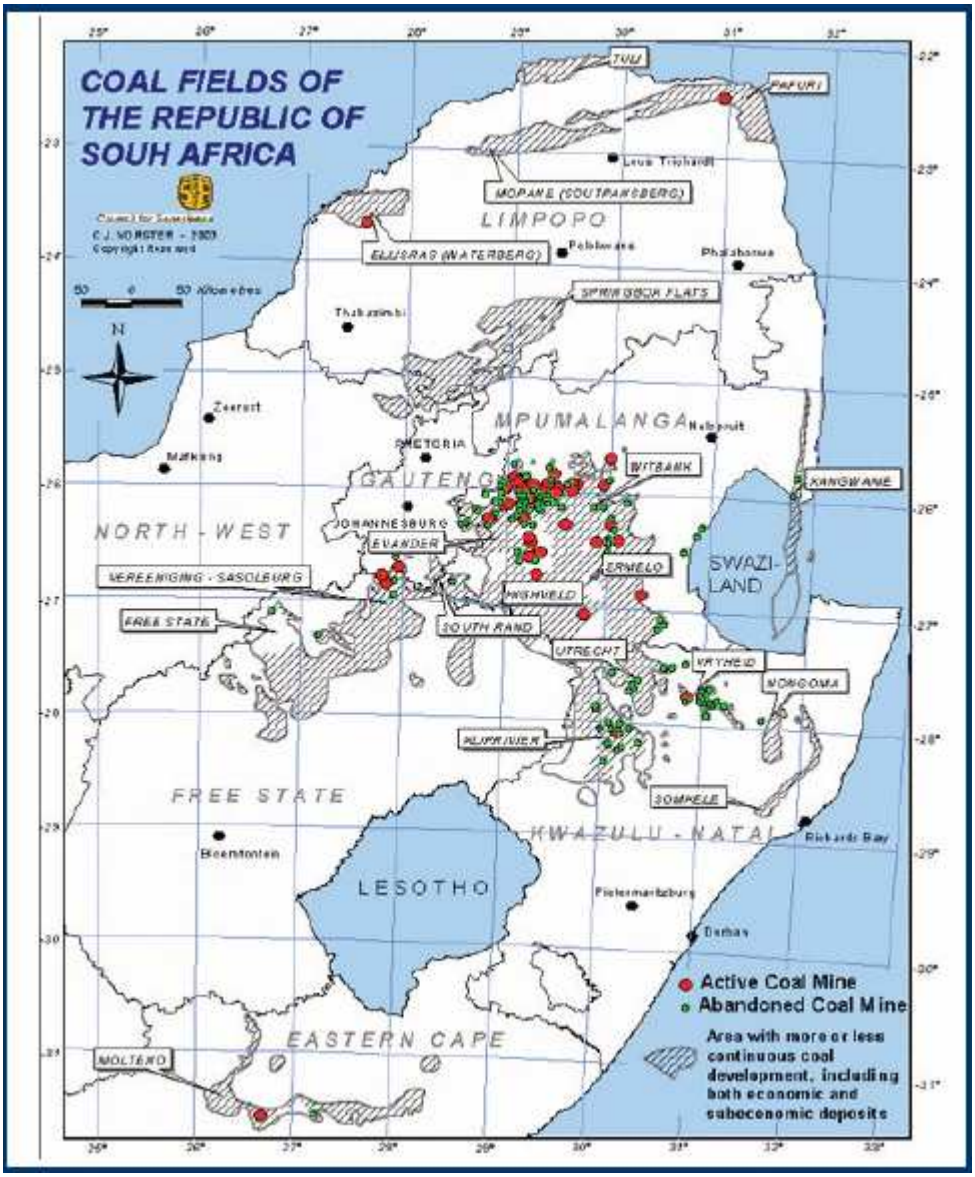

Figure 2.1 Coalfields of South Africa (After Fourie et al., 2008)

The coal produced at Forzando and Dorstfontein Collieries is exported, whereas New Denmark Colliery is a dedicated supplier of coal to Eskom's Tutuka power station.

South African coals, generally categorized as low rank bituminous with high ash content (Wagner and Hlatshwayo, 2005), have a heating value of 23,000-30,000 btu kg^{-1}, relatively low sulfur content, and when combusted, produce a low lime (CaO) ash which does not cement easily with water. Most of the trace metals are found in the non-coal interlayers (also known as partings or middlings) that are mined and combusted along with viable ore, resulting in incomplete combustion and increased ash production. Nonvolatile trace metals end up in the fly ash or bottom ash, which are then disposed of in an ash dump (dry) or dam (wet) (Swaine, 2000; Goodarzi *et al.*, 2008).

Coal is the leading fuel produced and consumed in SA, where reserves rank fifth, with production being sixth in the world as shown in table2.4 (McCarthy and Rubidge, 2005). SA houses the vast majority of recoverable coal reserves in Africa (Table 2.5). Coal mining in the Highveld region began in the 1890's and by the end of the century, there were 4 collieries in the Middleburg-Witbank district which produced coal (~2000 kilotons per year) almost exclusively to support the bustling goldfields in Johannesburg (Roberts, 2008). Production and export increased in 1907 due to the installment of a rail line and continued to increase steadily into the 1970s, at which point a steep demand for electricity forced the expansion of operations in both coal mining and power station construction (Lang, 1995). Since then, demand has continued to increase. In 2002, 245.3 million tons (Mt) of coal was produced, with 171.6 Mt of that consumed within SA. The balance was exported to the European Union and East Asia, making SA the third largest coal exporter for that year (EIA, 2005). Eskom, one of the world's largest utility companies, remains almost completely responsible for providing electricity to SA and exports power to Botswana, Lesotho, Mozambique, Namibia, Swaziland and Zimbabwe (Roberts, 2008). Coal-fired power stations produce 90% of SA's electricity, consuming over 90 Mt of coal per year. The most economical coal mining takes place in Mpumalanga Province where several power stations typically have dedicated coal mines

(Dabrowski *et al.,* 2008). Coal use by Sasol is also significant, accounting for approximately 25 % of the total coal consumption in SA (Dabrowski, 2010).

Coal is transported from the mine to the power station on conveyor belts where it is crushed to a fine powder and burned in modern boilers to produce high-pressure steam. This steam turns turbines which results in the production of electricity. Smoke from the boilers is filtered to remove all possible emissions, but gases (sulfur dioxide, carbon dioxide, and nitrogen oxides), extremely fine particulates, and highly volatile heavy metals such as mercury and selenium escape (Goodarzi *et al.,* 2008). The remaining ash, containing most of the naturally-occurring heavy metals present in the coal is "returned to the ground and isolated from the environment" (Roberts, 2008) in long-term storage dumps or dams.

Mercury emissions via coal combustion are particularly relevant in the South African context. Considering the world-wide importance of power stations as a source of mercury to the atmosphere, it is likely that the electricity generation sector may be an important source of emissions in SA. This was highlighted by a paper that listed SA as the second highest source of mercury emissions to the atmosphere on a global scale (Pacyna *et al.,* 2006).

Few studies are available on the mercury content of coal used in South African power stations. Mercury levels in South African coals indicate an average concentration that is equivalent to the global average value of ~0.2 mg kg^{-1}. Previous studies reported an average mercury content of 0.327 mg kg^{-1} (Watling and Watling, 1982) for South African coals, while a more recent study (Wagner and Hlatshwayo, 2005) performed on highveld coals, reported an average mercury content of 0.15 mg kg^{-1}. A critical discussion of these figures was presented in chapter 1. While, the mercury content of South African coal seems to be relatively low, the large quantities of coal burned every year potentially results in high annual mercury emissions. In 2004, approximately 110 million tonnes of coal was consumed for electricity production. A more recent estimate for 2007 indicates an increase to approximately 125 million tonnes. Based on coal consumption data, emission control devices fitted in the stacks of the power stations and estimates of the mercury content of coal (using an assumed concentration of 0.2 mg kg^{-1}), it has been estimated that SA emits about 10 tonnes (ranging between 2.6 and 17.6 tonnes) of

mercury to the atmosphere per year (Dabrowski *et al.*, 2008). The range in estimates is associated with the uncertainty in the actual mercury content of the coal used and in the efficiency of the emission control devices in trapping mercury. While this estimate is considerably lower than the 50 tonnes estimated in other studies (Pacyna *et al.*, 2006), when expressed as a ratio of the total population in South Africa, the per capita mercury emissions (0.24 g per person per year) are relatively higher than other leading industrialized nations such as Canada (0.15), China (0.13), Russia (0.16) and the USA (0.2) (Dabrowski *et al.*, 2010). This would seem to suggest, that while total mercury emissions could be lower than previously expected in South Africa, the country still appears to emit high levels in relation to the local population, suggesting that the potential for exposure to humans and the environment is relatively high.

South African mercury emissions are not likely to decrease in the future. In fact, the exact opposite is true. South Africa has experienced a steady growth in demand for electricity on the back of increased economic development over the last decade. This demand has put South Africa's power generation under increased pressure, leading to the recent energy crisis (2009) experienced across the country. Consequently, demand currently exceeds available capacity and development of increased power generation infrastructure is essential. South Africa's coal reserves are estimated at about 50 billion tons, and, based on the current production rate, are sufficient to last another 200 years. The current energy crisis in combination with the lack of development of alternative energy sources (such as nuclear, hydroelectric, wind and solar energy) indicates that the country's future primary energy needs will continue to be provided by coal (Dabrowski *et al.*, 2010).

Eskom's expansion programme will result in the consumption of approximately 200 million tons of coal by 2018, which is an increase of 60 % over current usage. Therefore, mercury emissions arising from this source can be expected to increase significantly to almost double the current emissions.

2.3.2 Mining

Mining has been and still is a continuing source of environmental heavy metals contamination. The modern mining industry is of considerable importance to the world

economy as it provides a great diversity of mineral products for industrial and household consumers (table 2.6). The consequence of the large size of the mining and mineral processing industry is not only the large volume of materials processed but also the large volume of wastes produced. The exploitation of mineral resources results in the production of large volumes of waste rocks as they have to be removed to access the resource (Lottermoser, 2010).

Table 2.6 World production of selected non-fuel mineral commodities in l999and 2006 (Lottermoser, 2010 and references therein)

Mineral	Production 1999	Production 2006
Antimony	0.122 Mt	0.134 Mt
Arsenic trioxide	38800 t	52700t
Bauxite	127 Mt	178 Mt
Beryl	6210 t	4480 t
Chromite	14 Mt	19.7 Mt
Cobalt	29900 t	67500 t
Copper	12.6 Mt	15.1 Mt
Gold	2540 t	2460 t
Iron ore	990 Mt	1800 Mt
Lead	3.02 Mt	3.47 Mt
Manganese ore	20.4 Mt	33.4 Mt
Mercury	1800 t	1480 t
Molybdenum	0.123 Mt	0.185 Mt
Nickel	1.12 Mt	1.58 Mt
Niobium-tantalum concentrate	57100 t	67700 t
Platinum-group elements	379 t	518 t
Silver	17700 t	20200 t
Tin	0.198 Mt	0.304 Mt
Titanium concentrates	4.17 Mt	6.7 Mt
Tungsten	31000 t	90800 t
Vanadium	42200 t	56300 t
Zinc	8.04 Mt	10 Mt

For example, only a very small valuable component is extracted from metalliferous ores during processing and metallurgical extraction. The great majority of the total mined material is gangue which is generally rejected as processing and metallurgical waste. Therefore, mining operations result in the production of a high volume of unwanted material.

2.3.2.1 Important mining concepts

To understand the environmental impact of mining activities it is of importance to explain technical concepts of the principal mining operations. Definitions presented in this section were obtained from Lottermoser (2010), unless stated otherwise.

Industrial mining operations include mining, mineral processing, and metallurgical extraction. Mining is defined as the extraction of material from the ground in order to recover one or more component parts of the mined material. Mineral processing or beneficiation aims to physically separate and concentrate the ore mineral(s), whereas "metallurgical extraction" aims to destroy the crystallographic bonds in the ore mineral in order to recover the sought after element or compound.

At mine sites, mining is always associated with mineral processing of some form (e.g. crushing; grinding; gravity, magnetic or electrostatic separation; dotation). It is sometimes accompanied by the metallurgical extraction of commodities such as gold, copper, nickel, uranium or phosphate (e.g. in situ leaching).

All three principal mining activities produce wastes. Mine wastes are defined herein as solid, liquid or gaseous by-products of mining operations. They are unwanted, have no current economic value and accumulate at mine sites. Many mine wastes, especially those of the metal mining industry, contain metals and/or metalloids at elevated concentrations.

In most metal ores, the metals are found in chemical combination with other elements forming metal-bearing ore minerals such as oxides or sulfides. Ore minerals are defined as minerals from which elements can be extracted at a reasonable profit.

In contrast, industrial minerals are defined as any rock or mineral of economic value excluding metallic ores, mineral fuels, and gemstones. Thus, ore is a rock, soil or sediment that contains economically recoverable levels of metals or minerals. Mining results in the extraction of ore/industrial minerals and gangue minerals. Mineral processing enriches the ore/industrial mineral and rejects unwanted gangue minerals. Finally, metallurgical extraction destroys the crystallographic bonds of minerals and rejects unwanted elements.

Mine wastes can be classified as solid mining, processing and metallurgical wastes and mine waters (table 2.7 and figure 2.2).

Mining wastes either do not contain ore minerals, industrial minerals, metals, coal or mineral fuels, or the concentration of the minerals, metals, coal or mineral fuels is subeconomic. Mining wastes are heterogeneous geological materials and may consist of sedimentary, metamorphic or igneous rocks, soils, and loose sediments. Nearly all mining operations generate wastes, often in very large amounts.

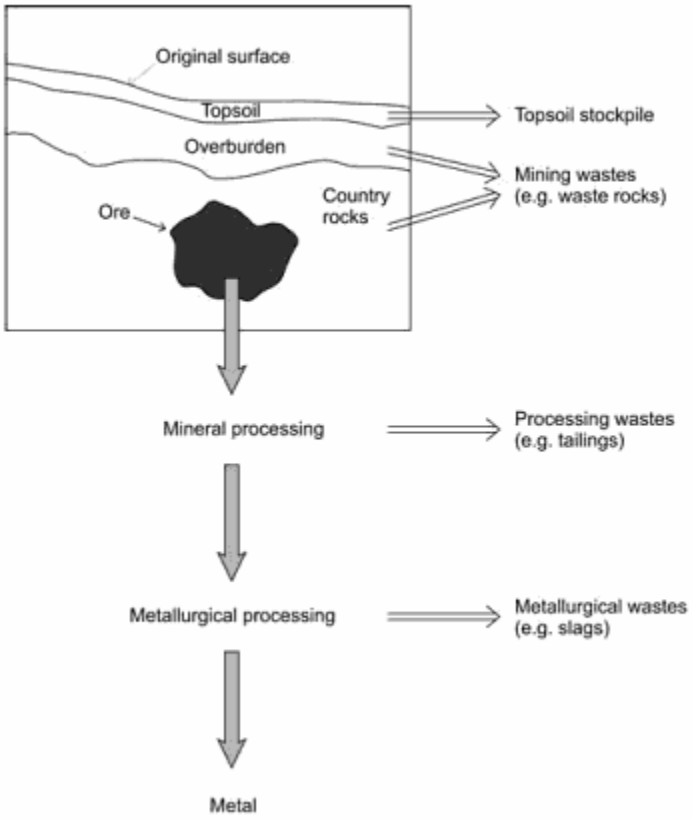

Figure 2.2 Schematic product and waste streams at a metal mine (Lottermoser, 2010)

Table 2.7 Simplified mining activities whereby a resource is mined, processed and metallurgically treated (After Lottermoser, 2010)

Activity generating the mine waste	Mine wastes
Open pit mining, underground mining	Mining waste (e.g; waste rocks, overburden, spoils, mining water, atmospheric emissions)
Mineral processing, coal washing, mineral fuel processing	Processing wastes (e.g. tailings, sludges, mill water, atmospheric emissions)
Pyrometallurgy, hydrometallurgy, electrometallurgy	Metallurgical wastes (e.g. slags, roasted ores, flue dusts, ashes, leached ores, process water, atmospheric emissions)

Processing wastes are defined herein as the portions of the crushed, milled, ground, washed or treated resource deemed too poor to be treated further. The definition thereby includes tailings, sludges and waste water from mineral processing, coal washing, and mineral fuel processing. Tailings are defined as the processing waste from a mill, washery or concentrator that removed the economic metals, minerals, mineral fuels or coal from the mined resource.

The physical and chemical characteristics of processing wastes vary according to the mineralogy and geochemistry of the treated resource, type of processing technology, particle size of the crushed material, and the type of process chemicals. The particle size for processing wastes can range in size from colloidal size to fairly coarse, gravel size particles. Processing wastes can be used for backfilling mine workings or for reclamation and rehabilitation of mined areas, but an alternative method of disposal must be found for most of them. Usually, this disposal simply involves dumping the wastes at the surface next to the mine workings. Most processing wastes accumulate in solution or as a sediment slurry. These tailings are generally deposited in a tailings dam or pond which has been constructed using mining or processing wastes or other earth materials available on or near the mine site.

Processing of metal and industrial ores produces an intermediate product, a mineral concentrate, which is the input to extractive metallurgy. Extractive metallurgy is largely based on hydrometallurgy (e.g. Au, U, Ni) and pyrometallurgy (e.g. Cu, Pb, Sn, Fe), and to a lesser degree on electrometallurgy (e.g. Al, Zn) (Ripley *et al.*, 1996; Warhurst, 2000).

Hydrometallurgy involves the use of solvents to dissolve the element of interest (e.g. leaching of the ore at gold mines with a cyanide solution). In contrast, pyrometallurgy is based on the breakdown of the crystalline structure of the ore mineral by heat whereas electrometallurgy uses electricity. These metallurgical processes destroy the chemical combination of elements and result in the production of various waste products including atmospheric emissions.

Metallurgical wastes are defined as the residues of the leached or smelted resource deemed too poor to be treated further. Hydrometallurgical extraction is performed at many gold, uranium or phosphate mines, and wastes accumulate on site. In contrast, electro- and pyrometallurgical processes and their wastes are generally not found at modern mine sites, unless there is cheap fuel or readily available energy for these extractive processes. At many historical metal mines, the ore or ore mineral concentrate was smelted or roasted in order to remove sulfur and to produce a purer marketable product. Consequently, roasted ore, slag, ash, and flue dust are frequently found at historical metal mine sites.

In addition to the removal, processing of rock and the production/disposal of solid wastes, mining operations also involve the production, use and disposal of mine water. The term mine water is collective and includes any water at a mine site including surface water and subsurface ground water (Morin and Hutt, 1997 and table 2.8).

Water is needed at a mine site for dust suppression, mineral processing, coal washing, and hydrometallurgical extraction. Mine water commonly contains process chemicals and it is generated and disposed of at various stages during mining activities. Water of poor quality requires remediation as its uncontrolled discharge. Drainage or seepage from the mine site may be associated with the release of heat, suspended solids, bases, acids, and dissolved solids including process chemicals, metals, metalloids, radioactive substances or salts. Such a release could result in a pronounced negative impact on the environment surrounding the mine site (Lottermoser, 2010).

Table 2.8 Mine water terminology (Lottermoser, 2010)

Term	Definition
Type of mine water	
Mine water	Any surface water or ground water present at a mine site
Mining water	Water that had contact with any of the mine workings
Mill water	Water that is used to crush and size the ore
Process water	Water that is used to process the ore using hydrometallurgical extraction techniques; it commonly contains process chemicals
Leachate	Mine water that has percolated through or out of solid mine wastes
Effluent	Mining, mill or process water that is discharged into surface waters
Mine drainage water	Surface or ground water that actually or potentially flows from the mine site into surrounding areas
Acid mine drainage (AMD) water	Low pH surface or ground water that formed from the oxidation of sulfide minerals and that actually or potentially flows from the mine site into surrounding areas
Type of process	
Mine seepage	Slow flow of ground water to the surface at pit faces, underground workings, waste dumps, tailing dams, and heap leach piles
Mine drainage	Process of water discharge at a mine
Acid mine drainage (AMD)	Process whereby low pH mine water is formed from the oxidation of sulfide minerals

2.3.2.2 Mercury and gold mining

Mercury has been mined for more than 2,000 years and most of the mercury used historically by man has been produced through the mining of ore. Mercury can be highly enriched in certain rocks called ore deposits. The most common mineral containing mercury in ore deposits is cinnabar, or mercury sulfide (HgS), but naturally occurring

elemental mercury, or quicksilver (Hg^0), is also found in some mercury deposits (USGS, 2003). Both cinnabar and elemental mercury are distinctive, making their identification relatively easy. Elemental mercury is a silver-colored liquid at room temperature; cinnabar is a distinctive red mineral. Roasting the ore in a furnace easily converts cinnabar to elemental mercury; this ease of conversion is another reason why mercury has been mined for such a long time. Elemental mercury is the final product obtained through mining of cinnabar.

Historically, the largest mercury mines have been those in Spain, Italy, Slovenia, Peru, China, the former U.S.S.R., Algeria, Mexico, Turkey, and the United States (USGS, 2003), but many other mercury mines are found throughout the world. Most mercury mines are presently closed owing to low demand and low prices for mercury worldwide, primarily as a result of environmental and health concerns surrounding mercury.

Although few mercury mines in the world are presently operating, closed and inactive mercury mines are sites of some of the highest mercury concentrations on Earth.

One of the significant mining uses of mercury worldwide is the amalgamation of gold by mercury, a technique used for the extraction of precious metals in many mines. The first known usage of amalgamation in gold mining occurred in Spain as early as 700 BC and the process was subsequently used extensively by the Romans around 50 BC. The Spanish also experienced the first documented case of mercury pollution (Lacerda and Salomons, 1998).

In the U.S., Miners used Hg^0 to recover gold at both placer (alluvial) and hardrock mines (Hunerlach and Alpers, 2003). In placer mine operations, loss of Hg^0 during gold recovery was reported to be as much as 30 percent or higher, depending upon the efficiency of the gold recovery apparatus (Hunerlach and Alpers, 2003). More than 100,000 t of mercury was produced in California since 1850, of which more than 10,000 t was used to extract gold by amalgamation from the gold-bearing gravels (Churchill, 1999). The South African gold mining case and the related mercury concern was introduced in the section that stated the reasons of the current study (See section 1.2.3)

As a result of the extensive use of mercury for amalgamation during gold recovery and its subsequent loss, Hg^0 is commonly present in riverbanks, soils, and drainages throughout

the region of historic gold mining operations. Mercury concentrations in sediments are generally higher in areas of large-scale gold mining and processing activities. In sluice boxes, where gold was recovered, and in areas where mining debris is continually reworked by seasonal runoff, total mercury concentrations can be as much as 1,000 mg kg^{-1} in tailings. In general, total mercury concentrations tend to increase with the amount of fine-grained material because the amount of surface area available for adsorption increases with an increase in the amount of fine-grained material (Hunerlach and Alpers, 2003).

From the late 19th century onwards, mercury was no longer used since cyanide leaching was invented which allowed large-scale gold mining operations. Although this practice is not generally used in developed countries, in the 1970s, the mercury process was reintroduced in countries like Brazil, Bolivia, Venezuela, Peru, Ecuador, Colombia, French Guyana, Indonesia, Ghana, and the Philippines (Lacerda and Salomons, 1998; Veiga, 1997).

Since 1980, artisanal scale gold mining (AGM or ASGM) activities have been increasing steadily. The term artisanal mining is preferred to be used as a simple way to encompass all small, medium, large, informal, legal and illegal mining activities that use rudimentary processes to extract gold from secondary and primary ore bodies (Veiga, 1997). ASGM is believed to account for one-quarter of the world's gold output and continues to play an important economic role and provides livelihood for a large number of people. However, research findings from the Brazilian Amazon demonstrate that the threatening potential consequence of the modern Amazon "gold rush" is the uncontrolled use of mercury (Donkor et al., 2006).

Mercury amalgamation is used in ASGM because the technique is cheap, simple, fast, independent, and reliable. And so in many settings, it is hard to beat (Telmer and Veiga, 2009; Lacerda and Salomons 1998).

Significant liquid mercury is lost to streams and rivers surrounding many gold mining areas throughout the world as a result of amalgamation practices. In some of these areas, liquid mercury that was used decades ago remains in these rivers as a potential environmental problem (USGS, 2003).

2.3.2.3 Impact of mining in mercury pollution

Major impacts of mining on land can occur before, during and after operation and may include: vegetation clearance; construction of access roads, infrastructure, survey lines, drill sites, and exploration tracks; creation of large voids, piles of wastes, and tailings dams; surface subsidence; excessive use of water; destruction or disturbance of natural habitats or sites of cultural significance; emission of heat, radioactivity, and noise; and the accidental or deliberate release of solid, liquid or gaseous contaminants into the surrounding ecosystems (Lottermoser, 2010).

The major factor that influences contaminant release is the geology of the mined resource. Climate and topography as well as the applied mining and mineral processing activities also play their role in the type and magnitude of contaminant release from a specific mine site or waste repository (Lottermoser, 2010). The geology of a deposit may influence, for example, the chemistry of local ground and surface waters and the properties of soils. Also, local soils, sediments and waters can be naturally burdened with trace elements. This is especially the case where weathering and erosion have exposed metallic mineral deposits and have led to the mobilization of trace elements into the environment. At such sites, soils, sediments and waters are naturally enriched in metals and metalloids (Kelley and Hudson, 2007).

The natural occurrence of elements varies between different ore deposit and rock types. Thus, rocks and ores with particular element enrichments cause environmental signatures in receiving streams, soils and sediments, and these enrichments may even bring about adverse effects on local and regional ecosystems. The environmental signatures and impacts of mineral deposits may occur naturally or can be caused by improper mining and mine waste disposal practices (Lottermoser, 2010).

Much of the environmental impacts of mining are associated with the release of harmful elements from mine wastes. Mine wastes pose a problem because some of them may impact on local ecosystems. Anthropogenic inputs of metals and metalloids to atmospheric, terrestrial and aquatic ecosystems as a result of mining have been estimated to be at several million kilograms per year (Nriagu and Pacyna, 1988; Smith and Huyck, 1999).

However, many metals are essential for cellular functions and are required by organisms at low concentrations (Smith and Huyck, 1999). It is only when the bioavailable (i.e. available for uptake into the organism) concentrations of these metals are excessively high that they have a negative impact on the health of the organism and toxicity might be seen. Processes that cause toxicity, disrupt ecological processes, inflict damage to infrastructure, or pose a hazard to human health are referred to as pollution (Thornton *et al.*, 1995). In contrast, contamination refers to processes which do not cause harmful effects (Thornton *et al.*, 1995).

Environmental contamination as a result of mining is not new to the industrialized world and the knowledge that mining and smelting may lead to environmental impacts is not new to modern science either. The concern for the health of miners has evolved in parallel with mining development, particularly in respect to the exposure of humans to mercury and arsenic. Mercury deposits in the Mediterranean were first worked by the Phoenicians, Carthaginians, Etruscans and Romans, who used the ore as a red pigment for paint and cosmetics (Ferrara, 1999). During the Middle Ages, metal contamination of soils and sediments around mine sites became common (e.g. Hurkamp *et al.*, 2009) and in 1540, Biringuccio wrote a book on metallurgy and documented the poisonous effect of arsenic, mercury, zinc and sulfur (Biringuccio, 1540).

Today, mines wastes are produced around the world in nearly all countries. In many developing countries, the exploitation of mineral resources is of considerable importance for economic growth, employment and infrastructure development. Many of the world's poorest countries and communities are affected by artisanal mining and the associated uncontrolled release of mine wastes.

Artisanal mining is highly labor intensive and employs 10-15 million people worldwide, and up to 100 million people are estimated to depend on small-scale mining for their livelihood (Lottermoser, 2010). The largely unregulated mining practices and associated uncontrolled release of mine wastes cause environmental harm. One example is mercury which has been used for nearly 3000 years to concentrate and extract gold and silver from geological ores (Lacerda and Salomons, 1998). The use of mercury in gold mining is associated with significant releases of mercury into the environment and with an uptake

of mercury by humans during the mining and roasting processes (Lacerda and Salomons, 1998). Around 2100 years ago, Roman authorities were importing mercury from Spain to be used in gold mining in Italy. Curiously, after less than 100 years, the use of mercury in gold mining was forbidden in mainland Italy and continued in the occupied territories. It is quite possible that this prohibition was already a response to environmental health problems caused by the mercury process (Lacerda and Salomons, 1998).

The unregulated mining practices have caused mercury contamination of rivers such as the Amazon on a massive scale (Lottermoser, 2010). In fact, artisanal gold mining is one of the most significant sources of mercury releases into the global environment (See table 2.2).

Mercury is released to the environment during artisanal gold mining in a variety of ways. When it is used to amalgamate gold, some escapes directly into water bodies as Hg^0 droplets or as coatings of mercury adsorbed onto sediment grains (Telmer and Veiga, 2009). The mercury that forms the amalgam with gold is emitted to the atmosphere when the amalgam is heated – if a fume hood or retort is not used. As well naturally occurring mercury in soils and sediments that are eroded by sluicing and dredging becomes remobilized and bioavailable in receiving waters. Finally, where a combination of cyanide and mercury are used, the formation of water soluble cyano-mercuric complexes enhances transport and bio-availability. Even though the fate of mercury in any of these processes is poorly understood, the interactions of cyanide and mercury are the least understood at this time (Telmer and Veiga, 2009).

The use cyanide during gold extraction dissolves not only gold but also mercury, forming cyano-mercury complexes wich are easily mobilized by rain and often, due to poor containment practices, quick reach stream waters. The water-soluble mercury cyanide is expected to be either more bioavailable or easier biomethylated than Hg^0. Therefore, mercury from ASGM is first released into surface water and soils and later emitted (latent emissions) to the atmosphere, or exposed in products.

The following processes are used during mercury amalgamation with gold (Telmer and Veiga, 2009):

- The “whole ore amalgamation” is the process of bringing mercury into contact with 100% of the material being mined. This process uses mercury very inefficiently (3 and 50 units of mercury are consumed to produce one unit of gold) and most of the mercury loss during the process initially occurs into the solid tailings which are often discharged directly into receiving waters and soils. Importantly, this mercury continues to evade into the environment for centuries. It is also certain that mercury in tailings that are subsequently leached with cyanide to recover more gold, a growing trend also observed in SA (Tutu, 2006), undergoes enhanced aqueous transport and emission to the atmosphere. This is because of the complexation of mercury by cyanide since mercury and cyanide, like gold and cyanide, readily form soluble complexes, and that when cyano-mercury complexes degrade, mercury readily volatilizes.

Immediate emissions to the atmosphere during whole ore amalgamation occur when the recovered amalgam is heated to produce the gold and are therefore, in the simplest case, roughly equal to the amount of gold produced.

- In case when only a “gravity concentrate” is amalgamated, losses are normally about 1 to 2 units of mercury for each unit of gold produced, but can be significantly lower if a mercury capturing system (e.g. retorts or fume hoods) is used when the amalgam is burnt.

Sometimes the tailings are rich in valuable minerals and will therefore be further processed. During reprocessing the tailings are often amalgamated a second time to recover any residual gold, and further processed to produce a high grade heavy mineral concentrate which is contaminated in mercury and a waste which is discarded.

Another cause of Hg pollution is the “dirty mercury” which is the mercury used 3 to 4 times for amalgamation and becomes much less effective and, therefore, discarded (Telmer and Veiga, 2009).

The widespread application of amalgamation techniques has resulted in mercury contamination of many streams around the world. Such contamination has been caused by historic gold mining operations in the United States (USGS, 2003), Russia (Laperdina, 2002), South America (Lacerda and Salomons, 1998), Asia (Feng *et al.*, 2009), Europe (Covelli *et al.*, 2001), and Australia (Churchill *et al.*, 2004).

Much of the mercury used in the gold mining process ends up in the rivers. The elemental mercury after reaching the rivers is transformed partly to the highly toxic methylmercury form, which process is described in details in the following section. A major proportion of the mercury is also lost to the atmosphere, as mentioned above, through burning of the gold-mercury amalgam or through degassing of metallic mercury from tailings, soils, sediments, and rivers (de Lacerda and Marins, 1997; Pfeiffer *et al.*, 1993). Nearly 3000 t of mercury have been released into the Amazon environment in the last 15 years. The annual emission of mercury to the atmosphere in the Brazilian Amazon has been estimated to be greater than the total annual emission of mercury from industry in the United Kingdom (Lottermoser, 2010).

Uncontrolled gold mining in the Amazon not only results in mercury contamination of air, soils, sediments, rivers, fish and plants but also in the destruction of rainforests, increased erosion of riverbanks, and the exposure of miners, gold dealers, fishermen and residents to toxic mercury concentrations. The miners show symptoms of mercury poisoning also known as Mad Hatter's or “Minamata Disease” (see section 2.4). They burn off the gold-mercury amalgam in an open pan or closed retort to distill the mercury and to concentrate the gold. Roasting of the amalgam commonly takes place in a hut and on the same fire used to cook food. Miners - eager to see how much gold will remain once the mercury is burned off - will stand directly over the amalgam as it is burned. The gold miners end up inhaling the mercury vapor and as a result, many have been poisoned (Telmer and Veiga, 2009).

2.4 The biogeochemistry of mercury

There are three prominent processes that release mercury of mixed natural and anthropogenic origin to the atmosphere. These three include biomass burning (deliberate and natural) and the evasion of mercury from soils and the ocean. The general factors controlling emission of mercury from these sources have been discussed by Fitzgerald and Lamborg (2003).

Due to the chalcophilic nature of its associations, mercury is found in higher abundances in intrusive magmatic rocks and locations of subaerial and submarine volcanism with

peak concentrations as high as several percent in ore-grade minerals (e.g., 35% mercury in sphalerite; Ozerova, 1996). Thus, mercury concentrations in soils weathered from this material can be very high as well (Gustin *et al.,* 2000) and represent a potentially significant source of mercury to the atmosphere through low-temperature volatilization.

As with soils, biomass burning and oceanic evasion also mobilize both natural and anthropogenic mercury and represent sources of mixed origin. In this way, these media act to recycle mercury in the environment, extending the residence time of mercury at the Earth's surface.

On another hand, watersheds are known to be major sources of mercury to the aquatic environment. However, and similar to biomass burning and evasion, the mercury released from watersheds is of mixed origin with a fairly long residence time (Fitzegerald and Lamborg, 2003).

2.4.1 Atmospheric cycling and chemistry of mercury

Mercury exists in the atmosphere in primarily four forms: gaseous elemental mercury vapor (Hg^0) or metallic or zero valent mercury; gaseous divalent mercury Hg_2^{2+} (mercurous) or Hg^{2+} (mercuric-Hg (II)); particulate-bound mercury (Hg_p or particulate phase mercury-TPM), both Hg^0 and Hg^{2+}; and organic mercury (mainly methylmercury (MeHg) (USEPA, 1997a). The vapor pressure of mercury is strongly dependent on temperature, and it vaporizes readily under ambient conditions. Consequently, elemental mercury (Hg^0) is not found in nature as a pure, confined liquid, but instead exists as a vapor in the atmosphere. It is insoluble in water and is less chemically active than other forms of mercury. As a result, its removal rate is slow and thus can be transported in the atmosphere thousand of miles from emission sources. Consequently, gaseous elemental mercury vapor (Hg°) is the major component of the global circulation of atmospheric mercury (Schroeder and Munthe, 1998).

Gaseous mono and divalent mercury (Hg_2^{2+} and Hg^{2+}), also called reactive gaseous mercury (RGM), can form many inorganic and organic chemical compounds; however, mercurous mercury (Hg_2^{2+}) is very unstable under ordinary environmental conditions and therefore is generally not found in the atmosphere. Mercuric mercury (Hg^{2+}) is less

volatile than Hg_2^{2+} and more water-soluble than Hg^0. Mercuric mercury may be found in the gas phase or bound to airborne particles (TPM). Both gas-phase and particulate Hg^{2+} are readily removed from the atmosphere by precipitation. Oxidation processes in the atmosphere and in-cloud water can also convert elemental mercury to Hg^{2+}. Because of its high solubility, gas-phase Hg^{2+} may be removed from the atmosphere within a few tens to a few hundred kilometers from its source. Particular-phase mercury may be deposited at intermediate distances from the source depending on the size of the aerosol (Schroeder and Munthe, 1998). Elemental mercury on the other hand has a relatively long lifetime of 0.5 to 2 years due to its low solubility in water and slow removal rate from the atmosphere via deposition and transformation to water-soluble species (Munthe *et al.*, 2001).

Although a small fraction of the mercury in atmospheric deposition is in the form of organomercury species such as mono and dimethylmercury, the dominant source of these species to most aquatic systems is *in situ* formation, or formation within the watershed (Waldron *et al.*, 2000).

Fitzgerald and Lamborg (2003) reported that concentrations of total gaseous mercury (TGM), which includes elemental, ionic and gaseous alkylated forms, in remote areas are typically in the range of 1-2 ng m^{-3} (figure 2.3). Concentrations below 1 ng m^{-3} are to be found under certain conditions and higher values are often observed in urban/suburban locations.

Basic processes involved in the atmospheric fate and transport of mercury include:

- emissions to the atmosphere,
- transformation and transport in the atmosphere,
- deposition from the air, and
- re-emission to the atmosphere.

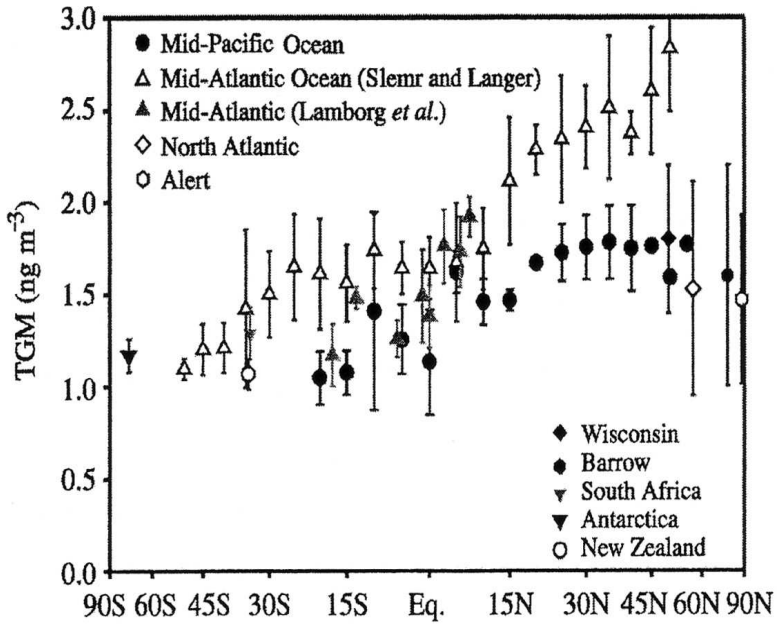

Figure 2.3 TGM in the atmosphere at several locations (Lamborg *et al.*, 2002)

In a summary, elemental mercury vapour is not thought to be susceptible to any major process of direct deposition to the earth`s surface. There is an indirect pathway, by which $Hg^0$ released into the atmosphere may be removed and deposited to the earth`s surface (figure 2.4).

It was quickly realized that the mercury species to be found in greatest abundance in precipitation was ionic mercury (e.g. Fogg and Fitzgerald, 1979). The discrepancy between the dominant gas (Hg^0) and precipitation phase species (Hg^{2+}) implied a process of oxidation of elemental mercury in the atmosphere and its subsequent scavenging as being a major component of the mercury cycle.

Many mechanisms for elemental mercury oxidation in the atmosphere have been proposed and a few have been studied in detail through laboratory experiments (Fitzgerald and Lamborg, 2003 and the references therein). Some of the proposed mechanisms are shown in figure 2.4.

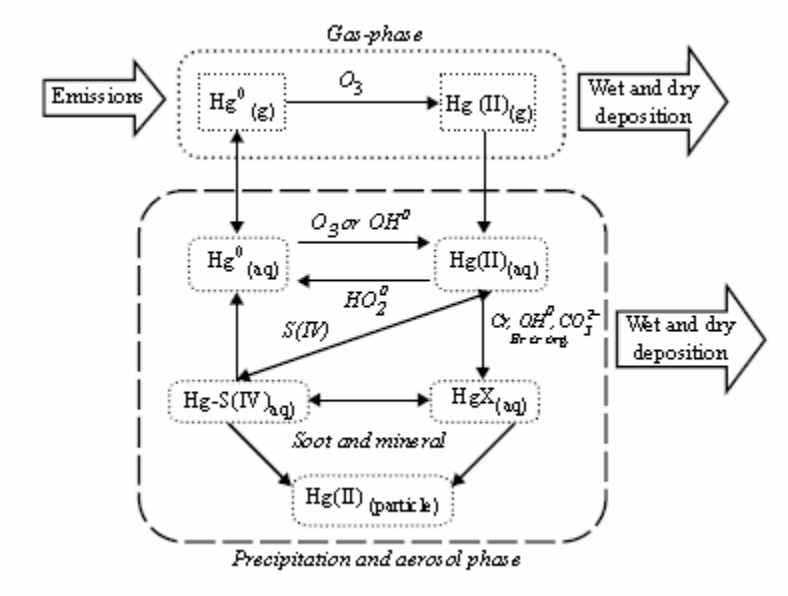

Figure 2.4 Summary of some of the important physical and chemical transformation of mercury in the atmosphere (from Fitzgerald and Lamborg, 2003 and the references therein)

Chemical reactions are thought to occur in the aquatic phase (cloud droplets) that both oxidize Hg^0 to divalent mercury, Hg(II), and reduce Hg(II) to Hg^0 (Lindqvist *et al.*, 1991):

$Hg^0(g) \rightarrow Hg^0(aq)$ (2.1)

$Hg^0(aq) + O_3(aq) \rightarrow Hg(II)(aq)$ (2.2)

$Hg(II)(aq)$ + soot/possible evaporation $\rightarrow Hg(II)(p)$ (2.3)

$Hg(II)(aq) + SO_3^{2-}(aq) \rightarrow Hg^0(aq)$ (2.4)

With (g) = gas phase molecule; (aq) = aqueous phase molecule and (p) = particulate phase molecule.

The Hg(II) produced would then be susceptible to atmospheric removal via wet deposition.

There is still an inconsistency between experiments related to the mechanisms for mercury removal. Many lab, field, and model efforts indicate that the lifetime of mercury in the atmosphere must be one to two years (Fitzgerald and Lamborg, 2003), but there is a number of plausible removal mechanisms that suggest the flux from the atmosphere is more consistent with lifetimes that are less than a year. The likely resolution of this problem lies in the observation that majority of the Earth's surface is covered by areas

that are not temperate or boreal forests, including the open ocean and tropical regions (Fitzgerald and Lamborg, 2003).

2.4.2 Aquatic biogeochemistry of mercury

There is an interesting mechanistic scheme that was derived from the Mercury Cycling Model developed by Hudson and colleagues (1994) which summarizes the biogeochemistry of mercury in the aquatic environment (figure 2.5).

Although organic and inorganic ligands and organisms differ in fresh and salty environments, it is believed that much of the biogeochemical processing and movement of mercury are expected to be similar to the model above mentioned (Fitzgerald and Lamborg, 2003).

Based on existing distribution and speciation data for mercury in natural waters, important features associated with mercury cycling in natural waters are highlighted in the following summary:

(i) The speciation of mercury in water is dependent on a number of factors such as the dissolved solid phase partition coefficient (K_D) for mercury in water (Hurley *et al.,* 1994; Babiarz et al., 2001), the pH, pE and composition of the water matrix (Lusilao, 2009 and the references therein).

(ii) The total mercury (Hg_{TOT}) in water, which is defined as the BrCl oxidized fraction of mercury, can be partition into dissolved (filter passing) and particulate phases (Harris *et al.,* 2007).

(iii) For the dissolved phase, current analytical procedures only allow for the measurement of total mercury, methylated mercury and elemental mercury (e.g. Watras *et al.,* 1994; Fitzgerald *et al.,* 1991). The latter two mercury species generally account for up to a few percent of the dissolved total mercury in water (Wiener *et al.,* 2003).

Therefore, most researchers currently rely on thermodynamic modeling in order to provide insights into the speciation of the majority of the mercury in aquatic environments, and to relate speciation to important considerations like cycling and bioavailability (Benoit *et al*. 2003).

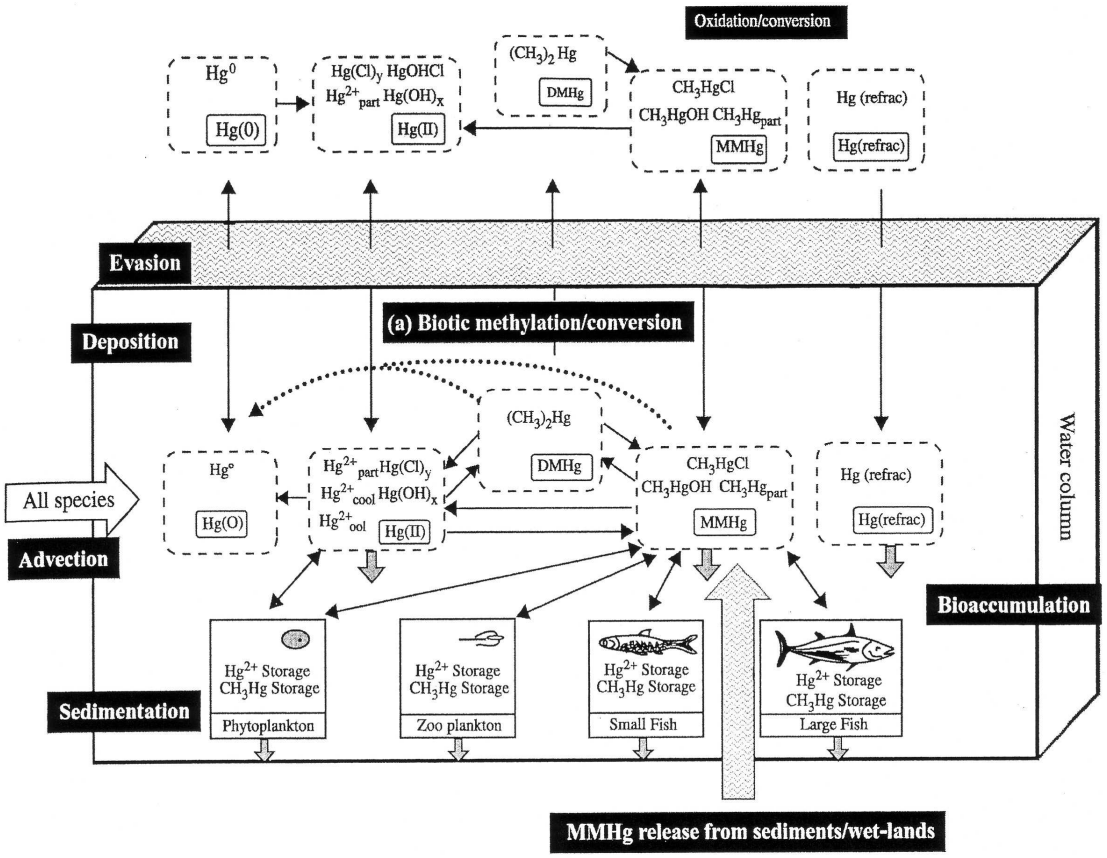

Figure 2.5 Generalised view of mercury biogeochemistry in the aquatic environment. (Hudson *et al.*, 1994)

(iv) In aerobic natural waters, the most important inorganic ligands are Cl^- and OH^- while dissolved organic carbon (DOC) is the most important organic ligand.

(v) In freshwater, where concentrations from 3 to 30 mg L^{-1} are common, DOC is the most important ligand for mercury. Simple organic ligands such as carboxylic acid have weak binding constants for mercury, whereas thiols have very strong binding constants and will dominate the inorganic mercury species distribution under most environmental conditions (Haitzer *et al.*, 2002).

(vi) In anoxic waters, reduced sulfur species (most notably sulfide) are the strongest inorganic ligands for mercury. As sulfide concentrations increase, HgS is favored followed by $HgHS^{2-}$ then HgS_2^{2-} and finally $Hg(HS)_2$ (Benoit *et al*. 1999a).

The formation of a neutral HgS complex is dominant at low concentrations of sulfide (Benoit *et al.* 1999b). However, at low sulfide levels, thiols may then become competitive for mercury binding.

Moreover, in discussing the various reactions of mercury, another important process that needs to be addressed is the issue of photochemistry. Once deposited in natural waters, mercury undergoes an aquatic redox cycling between oxidized Hg^{2+}, dissolved gaseous Hg^0 (DGM), and methylmercury. Diel changes of DGM that track solar radiation (typically, highest DGM levels around noon and lowest during night) have been observed in natural freshwaters. These findings implicate an intrinsic role of sunlight in controlling aquatic DGM dynamics. This is of significance for aquatic mercury biogeochemical cycling and its environmental impacts because the competition of this sunlight-driven pathway for Hg^{2+} substrate with the methylation pathway would reduce mercury toxic hazards in local aquatic ecosystems through removal of Hg^{2+} as a result of its reduction to Hg^0 and its subsequent evasion (Zhang and Lindberg, 2001). Yet, mechanistic understanding of the phenomena has remained limited.

2.5 Mercury methylation

While inorganic mercury (Hg^{2+} or IHg) is the major source of mercury to most aquatic systems, it is methylmercury (CH_3Hg^+, MHg, MMHg or MeHg) that bioconcentrates in aquatic food webs and is the source of health advisories worldwide that caution against the consumption of fish containing elevated MHg (Benoit *et al.*, 2003; Lindqvist *et al.*, 1991; USEPA, 1997).

Two large-scale poisonings, in Minamata, Japan and in Iraq, between 1950 and 1975, focused attention on the health risks associated with mercury consumption, especially in its methylated form (Mason and Benoit, 2003 and the references therein). In Minamata, MHg from a vinyl chloride-acetic acid plant was the source of contamination (Fujiki and Tajima, 1992). IHg, used as a catalyst, was primarily methylated to MHg within the plant and subsequently discharged in the wastewater. Historically, fish levels as high as 20 mg kg^{-1} and sediment levels above 500 mg kg^{-1} of mercury were reported (Fujiki and Tajima, 1992).

Patient hair concentrations were similarly elevated (as high as 700 mg kg^{-1} Hg). More than 1000 people have died, and mercury poisoning is now often referred to as “Minamata disease”.

The poisoning incident in Iraq was the result of the consumption of seed grain preserved with MHg, a commonly used preservative at the time (Mason and Benoit, 2003 and the reference therein).

In many direct discharge incidents, contrary to Minamata, elevated levels of mercury in fish, as MHg, have resulted from methylation of the mercury in the aquatic environment.

Although a small fraction of the mercury in atmospheric deposition is MHg, the dominant source of MHg to most aquatic systems is *in situ* formation, or formation within the watershed (Krabbenhoft *et al.,* 1995).The current consensus, based mainly on temperature-dependency of mercury methylation and its response to biological substrates (Compeau and Bartha, 1985; Berman and Bartha, 1986), is that biological methylation of IHg to MHg is more important than abiotic processes in natural systems. Biological methylation was first demonstrated by Jensen and Jernelov (1969) and it is now generally accepted that sulfate reducing bacteria (SRB) are the key mercury methylators (Compeau and Bartha, 1985; Gilmour and Riedel, 1995), although a number of organisms besides SRBs have been shown to produce MHg in pure culture from added IHg (Robinson and Tuovinen, 1984). It is generally accepted that MHg is produced in an accidental side reaction of a metabolic pathway involving methylcobalamin (Choi *et al.,* 1994), although this pathway has only been demonstrated in one SRB.

The ability of methylcobalamin to spontaneously methylate mercury *in vitro* (Compeau and Bartha, 1983) prompted investigations into the methyl carrier in sulfate reducers. Berman et al. (1990) suggested, based on the selective inhibition of mercury methylation in *D. desulfuricans* LS, that methylation was mediated by a cobalt porphyrin compound in this organism. Their continued work (Choi and Bartha, 1993) identified this corrinoid to be cobalamin (vitamin B-12), and they suggested that mercury methylation is an enzymatically catalyzed process *in vivo*.

The following sequence and reaction have been proposed (Rodriguez Martin-Doimeadios *et al.,* 2004) to explain the mercury methylation:

$$Hg^0 \rightarrow Hg^{2+} \rightarrow CH_3Hg^+ \rightarrow (CH_3)_2Hg \qquad (2.5)$$

$$HgCl_2 + CH_3CoB_{12} \rightarrow CH_3HgCl + CoB_{12}Cl \qquad (2.6)$$

Cobalamin also has been identified in some acetogens and methanogens (Stupperich *et al.,* 1990). Therefore, not all organisms that contain cobalamin are capable of methylating mercury. Diffusion across the cell membrane has been proposed as the important uptake mechanism (Benoit *et al.,* 1999a). This hypothesis is consistent with studies that have demonstrated diffusion of neutral mercury complexes (chloride complexes) across artificial membranes and into diatom cells (Mason *et al.,* 1995 and 1996).

It has also been noted in many field studies that the rate of mercury methylation, and the MeHg concentration in sediments, decrease as the sediment sulfide concentration increases (Benoit et al., 1999a, Choi and Bartha, 1994).

A number of mercury complexes exist in solution in the presence of dissolved sulfide, including HgS^0, $Hg(SH)_2^0$, $Hg(SH)^+$, HgS_2^{2-} and $HgHS_2^-$ (Benoit *et al.,* 2003) and it is possible that inorganic mercury uptake by SRB occurs via diffusion of the dissolved neutral mercury complexes, such as HgS^0. If so, then the bioavailability of mercury to the bacteria would be a function of sulfide levels, as this is the ligand controlling mercury speciation in solution in low oxygen zones where SRB are active. It has been shown through chemical complexation modeling that the speciation of mercury tends to shift toward charged complexes as sulfide levels increase (Benoit *et al.,* 1999b), decreasing the fraction of mercury as uncharged complexes, and, as a result, the bioavailability of mercury to methylating bacteria.

The primary site of methylation is just below the oxic/anoxic interface, which is often near the sediment surface in aquatic systems (Krabbenhoft *et al.,* 1995; Korthals and Winfrey, 1987). It should be noted, however, that MHg can be produced in environments where sulfate reduction is low, such as upland soils, where other bacteria and fungi may be important methylators. However, studies have focused on environments within aquatic ecosystems where the MHg produced has greatest likelihood of entering the aquatic food chain, and where sulfate reduction is a dominant degradation pathway for organic matter in sediments.

One obvious mediator of mercury methylation rate is the concentration of IHg substrate, and its chemical form. Although there is a significant relationship between mercury and MHg across ecosystems, mercury does not appear to be largest source of variability in MHg production among ecosystems. The relationship between mercury and MHg

concentrations in surface lake, river and estuary sediments and wetland soils across many ecosystems is weak but there is, on average, about 1% of the total mercury (Hg_{TOT}) as MHg for the lower concentration (<500 ng g^{-1}) sites, which represent the range in mercury concentration of natural, unimpacted environments. The measured concentration at any time point is an integration of the impact of all the processes influencing MHg, such as differing loading rates (Allan and Heyes, 1998; Allan *et al.,* 2001) and methylation and demethylation rates (Korthals and Winfrey, 1987), which vary spatially and temporarily (with season and temperature).

Overall, within single rivers or wetlands, or even clusters of similar ecosystems, significant relationships can exist, but the relationships currently have no predictive power, given the importance of other parameters, discussed below, in influencing methylation rate by controlling the availability of mercury to, and activity of, the methylating bacteria, and given our current level of understanding.

Effective regulation of mercury pollution requires the ability to predict the relationship between mercury and MHg among ecosystems, a goal that researchers and modelers seem to be slowly approaching. Clearly, while many other factors influence mercury methylation, the supply and availability of mercury is a key parameter.

In addition to the effect of sulfide, other chemical factors influencing methylation include the supply of labile carbon (Miskimmin, 1991) although the role of dissolved organic carbon (DOC) is complex. The distribution of methylation activity is tied to the distribution of biodegradable organic matter but complexation of mercury by DOC may influence mercury bioavailability. Maximal net methylation is often observed in surface sediments (Korthals and Winfrey, 1987) where microbial activity is greatest due to the input of fresh organic matter. As a result, systems with high levels of organic matter production, such as wetlands, recently flooded reservoirs, or periodically flooded river plains, may exhibit extremely high rates of methylmercury production (Benoit *et al.,* 2003).

The impact of organic content on mercury methylation appears to be complex (Korthals and Winfrey, 1987; Miskimmin, 1991). While mercury binds strongly to DOC, laboratory complexation studies using DOC suggest that this binding is not sufficient for Hg-DOC complexation to be important in systems where sulfide is present (Benoit *et al.,* 2001;

Reddy *et al.,* 2000). Thus, while DOC has been shown to be the most important complexing ligand in surface waters in the absence of sulfide (Reddy *et al.,* 2000), it is likely to be unimportant in mercury complexation in sediment porewaters under typical DOC concentrations and >0.01 μM sulfide (Benoit *et al.,* 2001; Reddy *et al.,* 2000).

However, binding of mercury to organic matter is important in the solid phase. Laboratory studies suggest that in oxic regions, organic complexation is much more important than binding of mercury to metal oxide phases in all except very low organic matter sediments (Miller and Mason, 2001).

It has been suggested that Fe-S formation scavenges mercury in anoxic regions of the sediment (Mikac *et al.,* 1989) and that mercury binds strongly to pyrite such that, even when only small amounts are present, it is the dominant solid phase binding mercury in sediments (Huerta-Diaz and Morse, 1992). These studies focused on regions of low organic content and, in contrast, sediment sequential extraction studies done by Benoit et al. (Miller and Mason, 2001) show that mercury is associated with the organic fraction even in the presence of significant solid sulfide phases. Furthermore, it has been shown that the sediment particle-dissolved distribution coefficient (Kd) is a strong function of organic carbon (Bloom *et al.,* 1999). In the environment, concentrations of iron, sulfur and carbon typically co-vary in sediments, and all often correlate with mercury, and it is therefore difficult to ascertain from field data which is the ultimate controlling phase (Mason and Lawrence, 1999). Laboratory and field studies (Miller and Mason, 2001) suggest that the binding of mercury to organic matter involves interaction with the thiol groups of the organic molecules and thus, in a sense, the complexation of mercury to inorganic sulfide phases or to organic matter are comparable as both involve the interaction between mercury and a reduced sulfur species.

The conflicting influences of sulfate and sulfide on the extent of mercury methylation are well illustrated by the studies in the Florida Everglades (Gilmour *et al.,* 1998) which showed that the highest methylation rates, and the highest %MHg in the sediment, were at sites of intermediate sulfate-reduction rates and sulfide concentration.

As the sulfide concentration decreases, the relative concentration of predicted HgS^0 concentration increases. The peak in methylation rate results from the combination of the

increasing availability of mercury to the SRB coupled with the decreasing sulfate reduction rate. These results confirm the importance of both mercury speciation, and bacterial activity, in controlling mercury methylation rate. Overall, the sites with the highest mercury methylation are those that also have the highest fish MeHg concentrations (Mason et Benoit, 2003), confirming the direct link between the extent of mercury methylation and fish MeHg levels.

Experiments performed in Everglades sediments incubated with sulfate or sulfide showed that in cores taken from a relatively low sulfate site, addition of sulfate stimulated methylation, and sulfate reduction, even though sulfide levels increased slightly whereas the addition of sulfide alone resulted in inhibition of methylation. This demonstrates that inhibition occurs at low μM sulfide concentrations in Everglades sediments. However, high rates of mercury methylation have been demonstrated in highly sulfidic saltmarsh sediments (King *et al.,* 2000). Benoit *et al.* (2003) suggested that the high rates of sulfate-reduction in these sediments could make up for the very low percentage of dissolved mercury that would exist as neutral species. For Everglades sites with higher ambient sulfate, addition of sulfate did not increase methylation but addition of more sulfide led to an inhibition of mercury methylation.

Overall, the results of the field and laboratory studies show that the balance between sulfate availability, which controls SRB activity, and sulfide production and accumulation, which control mercury bioavailability, are critical in modeling methylation rates.

Since the complexation of mercury with sulfide and thiols involves acid-base chemistry, the role of pH needs to be considered. An inverse correlation between lake water pH and mercury in fish tissues has been observed in a number of studies (Benoit et al., 2003 and references therein) suggesting that pH influences methylation and demethylation in aquatic ecosystems. In some freshwater studies, methylation was reduced with decreasing pH (Winfrey and Rudd, 1990) while the impact on demethylation was small. In other studies, increasing rates of mercury methylation in epilimnetic lake waters and at the sediment surface were found with lowered pH (Miskimmin *et al.,* 1992; Ramlal *et al.,* 1985; Xun *et al.,* 1987). Winfrey and Rudd (1990) reviewed potential mechanisms for low pH effects on mercury methylation and suggested that changes in mercury binding

could account for the seemingly conflicting results seen in all of these studies. They pointed out that lowering pH may lead to increased association of mercury with solid phases, decreased dissolved pore water mercury, and (presumably) to lower availability of IHg to bacteria. Considering the reaction of mercury with the solid phase ($RSH + Hg^{2+} = RSHg^{+} + H^{+}$), and the dissolved speciation, the following overall reaction can be postulated (Mason et Benoit, 2003):

$$RSHg^{+} + H_2O + HS^{-} = HgS^{0} + RSH + H^{+} \qquad (2.7)$$

In the pH range of 7-10 (pKa_1 ~7 for H_2S and assuming the pK for RSH is around 10), an increase in pH, at constant sulfide, will result in an increase in HgS^0 relative to $RSHg^+$ ($[HS^-]/[RSH]$ is essentially constant) and thus methylation should increase with pH. Below a pH of 7, decreasing pH (increasing $[H^+]$) leads to decreasing $[HS^-]$, and as a result, HgS^0 will decrease relative to $RSHg^+$ with pH i.e., methylation rate should decrease (Mason et Benoit, 2003). This theoretical consideration supports the notions put forward by Winfrey and Rudd (1990) and suggests that a decrease in pH will lead to a decrease in methylation rate in sediments because of changes in the concentration of bioavailable mercury in porewaters. The magnitude of the effect will depend on the pH range as the impact of pH is more marked at low pH. Overall, these considerations suggest that sulfide concentration will have the most significant impact on mercury bioavailability in porewater but that other factors such as organic matter content, pH, temperature and the presence or absence of inorganic sulfide phases all play a role in controlling mercury bioavailability to methylating bacteria.

Temperature is another important variable as the temperature responses of methylation and demethylation have been reported to differ (Korthals and Winfrey, 1987). However, seasonal changes in mercury complexation that affect methylation and demethylation differently could account for these observations.

Demethylation of MeHg can occur via a number of mechanisms, including microbial demethylation and reduction by *mer* operon-mediated pathways, and by .oxidative demethylation processes (Marvin-Dipasquale and Oremland, 1998; Marvin-DiPasquale et al., 2000). Microbial degradation of MeHg occurs through the cleavage of the carbon-

mercury bond by the enzyme organomercurial lyase followed by reduction of Hg^{2+} by mercuric reductase to yield methane and Hg^0 (Robinson and Tuovinen, 1984).

As many as half of the bacteria from mercury contaminated sites may contain the *mer* operon (Liebert.et al., 1999). However, another mechanism also appears to mediate MeHg degradation. While methane and Hg^0 are the primary products of *mer*-mediated mercury demethylation, CO_2 has also been observed as a major MeHg demethylation product by Marvin-Dipasquale and co-workers (Marvin-Dipasquale and Oremland, 1998; Marvin-DiPasquale *et al.,* 2000). These authors suggested that MeHg degradation can occur through biochemical pathways used to derive energy from single carbon substrates, and they termed this process "oxidative demethylation", i.e.:

$$4CH_3Hg^+ + 2H_2O + 4H^+ = 3CH_4 + CO_2 + 4Hg^{2+} + 4H_2 \qquad (2.8)$$

A variety of aerobes and anaerobes (including sulfate reducers and methanogens) have been implicated in carrying out oxidative demethylation, and oxidative demethylation has been observed in freshwater, estuarine and alkaline-hypersaline sediments (Marvin-Dipasquale and Oremland, 1998;). However, the identity of the organisms responsible for oxidative demethylation in the environment remains poorly understood. Further, no organism has been isolated that carries out this pathway.

In addition, photochemical MHg degradation in the water column has been demonstrated (Sellers *et al.,* 1996). The *mer*-based pathway is an inducible detoxification mechanism, while oxidative demethylation is thought to be a type of C1 metabolism. Numerous researches suggest that oxidative demethylation is the dominant process in uncontaminated surface sediments (Marvin-Dipasquale and Oremland, 1998; Marvin-DiPasquale *et al.,* 2000) whereas in highly contaminated environments, the *mer* operon is more prevalent among the microbial community, and Hg^{2+} reduction activity is enhanced (Liebert.*et al.,* 1999).

2.6 Transport and deposition of mercury from gold mine drainage and tailings in watersheds

The fate of mercury in water, sediments and soils in gold mining areas has been studied mostly in large surveys at a great number of mining sites such as the Amazon region, Mindanao Island in the Philippines and a few last century USA gold rush sites (Lacerda and Salomons, 1998).

The different mining processes using mercury amalgamation result in different wastes, mercury dispersal mechanisms, degree of mercury mobility, and biological availability in terrestrial and aquatic ecosystems. Figure 2.6 describes the transport and fate of mercury in environments impacted by gold mining.

In areas where gold is mined from active bottom sediments from rivers, mercury is lost to the environment as elemental Hg^0 directly into rivers whereas while the mining operation involves grinding of gold-rich soils, Hg^0 is concentrated in tailings and can eventually be mobilized through leaching and particle transport during rains. The insoluble and practically unreactive Hg^0 remains present in most surface environments, at least for many decades (Fitzgerald *et al.*, 1991) and also displays very low availability to biological uptake (Taysayev, 1991).

Moreover, while fluvial transport can move mercury from river mining operations at considerable distances in a few years, mercury dispersal from tailings, on another hand, can be a very slow process, sometimes involving the transport of the tailings themselves through erosion (Miller *et al.*, 1993) and migration through groundwater (Prokopovich, 1984). These releasing processes may last through time, posing an environmental contamination risk even after mining activity has ceased for centuries (Fuge *et al.*, 1992).

In both mining situations, an important proportion of mercury is lost to the atmosphere either through burning of the Au-Hg amalgam or through volatilization of Hg^0 from soils, sediments and rivers.

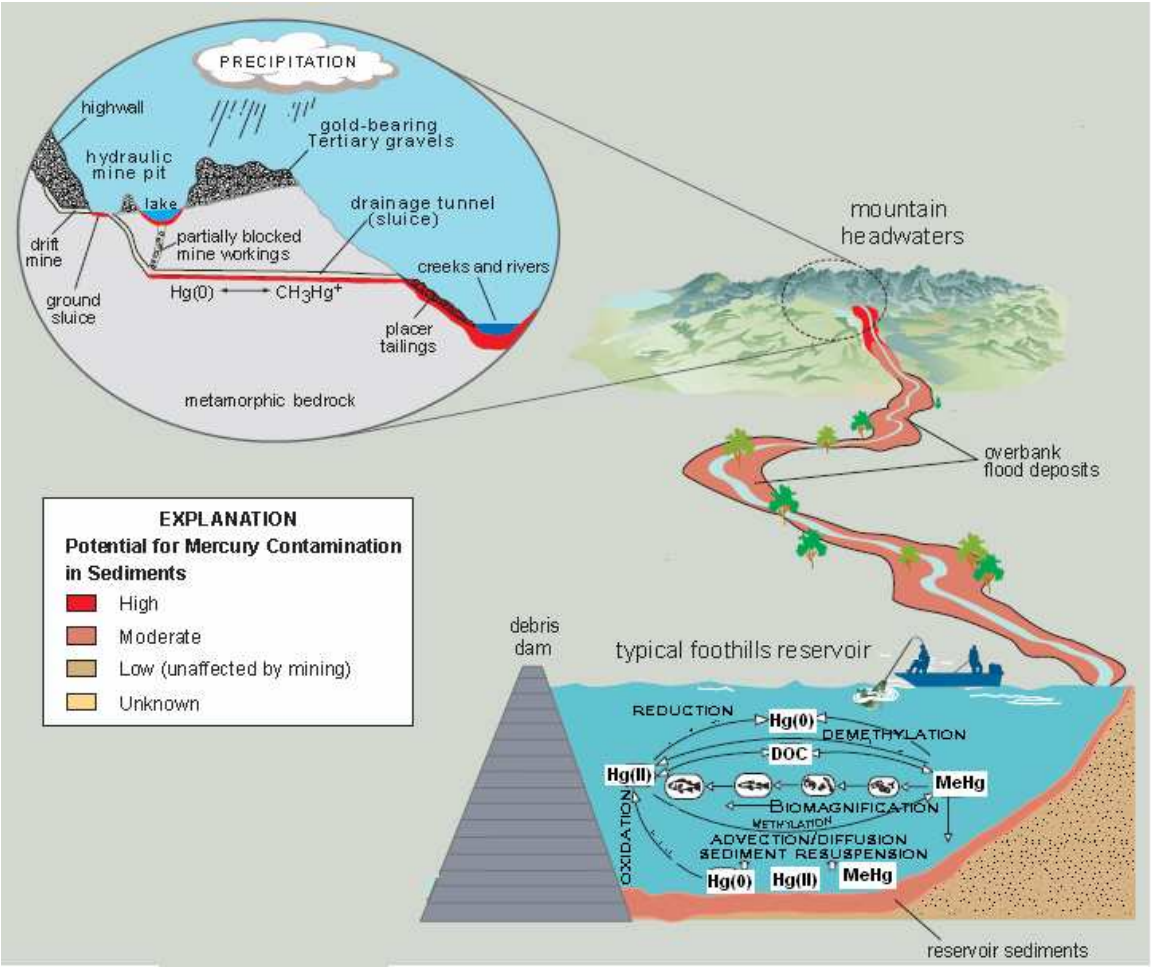

Figure 2.6 Schematic diagram showing transport and fate of mercury and potentially contaminated sediments from hydraulic and drift mine environment through rivers, reservoirs, and the flood plain, and into an estuary. A simplified mercury cycle is shown (Modified after Hunerlach and Alpers, 2003)

The fate of mercury once introduced into the aquatic environment will depend on the characteristics (limnology) of the receiving waters and mercury will be transformed (partly) into the highly toxic methylmercury form, as described in the previous section.

Limnological classification divides tropical rivers into the following classes based on their major hydrochemical properties (Lacerda *et al.*, 1990; Furch *et al.*, 1982): “white”, “black” and “clean” rivers.

• White Water rivers, which are rich in suspended matter (>200 mg l^{-1}) have a neutral pH and moderate electric conductivity (>40 µS cm^{-1}), and mean dissolved element concentrations similar to the mean of world rivers. The Amazon River is a typical representative of this class of rivers.

• "Black water" rivers, which drain weathered, sandy tropical soils and floodplains, are rich in dissolved organic substances, are acidic (pH < 5.0) and have low concentrations of dissolved constituents (electric conductivity < 10 μS cm^{-1}). Many rivers of the Congo basin fit into this category.

• "Clear water" rivers present acidic to neutral pH, low organic and inorganic dissolved constituents and are relatively rich in iron oxides from weathered laterite soils where they originate.

Attempts have been made to study the influence of the different tropical river types upon the distribution of mercury, since such river types (white, black and clear water rivers) present different hydrochemistries which strongly influence various other constituents of river systems in the tropics, including sediment geochemistry, trace metal distribution and aquatic biota (Furch *et al.,* 1982; Lacerda *et al.,* 1990).

Preliminary results obtained from the study done on the distribution of mercury in the sediments of ten rivers of the Madeira River basin, belonging to the three different classes mentioned above (Lacerda *et al.,* 1990) showed that black water rivers are enriched with mercury when compared to other river classes. The enrichment of mercury in black water rivers may be related to the high organic matter content typical of this river class and to their acidity. Mercury would form relatively refractory compounds with organic matter, facilitating its accumulation in river sediments. Also, acidity would accelerate the oxidation of Hg° to Hg^{2+}, enhancing the possibility of mercury binding to organic matter (Lindqvist *et al.,* 1984; see also figure 2.6). Similar results have been found for other trace metals in the same rivers and were also associated with the higher organic matter content of black water river sediments.

Moreover, it was suggested that mercury could also be transported associated with particulate organic carbon (POC) derived from the decomposition of plant litter brought into tropical rivers during the flooding period (Lacerda *et al.,* 1990). Researchers also demonstrated experimentally the increasing solubility and decreasing adsorption onto sediments of Hg^0 in the presence of humic acids in waters draining tailings in central Brazil (Lacerda *et al.,* 1998 and the reference therein).

Another study done in five remote lakes located within Brazilian gold mining areas (Lacerda *et al.*, 1991) also demonstrated a significant positive relationship between mercury and organic matter in surface sediments ($r = 0.82$; $P < 0.01$) which shows that organic matter content of sediments may also control mercury accumulation in freshwater sediments. These findings seem to corroborate those found in black water rivers in the Madeira River basin described above.

However, the relationship between mercury and organic matter has not been detected in partitioning studies of white water river sediments receiving Hg^0 directly from dredges (Pfeiffer *et al.*, 1993) or in rivers receiving elemental Hg^0 from riverbank mining. Therefore, organic matter seems to be an important substrate for mercury only in sediments receiving indirect input of mercury as Hg^{2+}, either from leaching of tailings or from the atmosphere.

Another important factor that needs to be highlighted concerning the mercury transport and fate is that the mercury dispersal mechanisms should vary according to the season, either through intensive erosion during the rainy season or through the effect of dilution on the existing mercury content in rivers (Lacerda *et al.*, 1998).

Finally, the difference in mining procedure seems to be a key factor controlling mercury dispersal. In areas where gold is mined from soil or rocks, during the rainy season the leaching and erosion of contaminated particles result in higher total mercury concentrations in rivers, while in areas where mercury is mined from river bottom sediments, mercury concentrations in water are lower during the rainy season owing to dilution and the decrease in the mining activity itself (Lacerda *et al.*, 1998).

Chapter 3
A review of analytical procedures for mercury determination

3.1 Introduction

Technology capable of highly precise analysis of low-level mercury and its species are of importance in order to conduct proper risk assessment. Obtaining reliable analytical data for mercury requires the following: appropriate sample collection; pre-treatment for analysis; the selection of a measurement method and preparation method for sample test solutions suited to the samples; experience in their use; and confirmation of the reliability of one's own analytical data (Suzuki *et al.*, 2004).

On another hand, there is an increase attention that has been paid to mercury and other trace elements in coal due to their toxicity and also to the fact that these hazardous trace elements are released to the environment during coal beneficiation and combustion resulting in serious environmental and healthy concerns (Zheng *et al.*, 2008a and references therein). Therefore, methods have been developed in order to study the occurrence of these elements and understand their behavior during industrial processes.

This chapter will first provide an overview of sampling and analytical methods for total mercury and mercury species (especially inorganic and methylmercury) determination for specific target samples and will briefly discuss some important **a**nalytical methods used for the determination of inorganic constituents in coal.

3.2 Sampling and samples storage

Sampling, the first step in trace element analysis, must ensure the representativity of the sample in the context studied. For this reason also, it represents the most potential source of errors. If the sampling is not based on the use of appropriate tools with particular cautions, both systematic and random errors may occur, attaining in some cases several orders of magnitude (Hoenig, 2001). In addition, when performing a mercury analysis, one must regularly pay attention to preventing contamination of the samples by keeping the laboratory clean; providing appropriate ventilation; and adequately washing

glassware, tools, and containers. Therefore, number of works were dedicated on the topic (e.g. Suzuki *et al.,* 2004; Parker and Bloom, 2005 and Stoichev *et al.,* 2006) and a discussion on sampling and samples storage conditions for mercury analysis was presented in our previous work (Lusilao, 2009).That is why the following section only presents a summary of the current knowledge on sampling techniques and appropriate storage conditions for mercury analysis.

3.2.1 Storage and preservation of samples

Most experienced researchers recognize the following: (1) low-level mercury samples should not be stored in polyethylene bottles (Bothner and Robertson, 1975; Bloom, 1994); (2) methylated species are degraded by light (Sellers *et al.,* 1996); (3) volatile mercury speciation is too unstable to preserve, thus volatile species must be separated in the field (Fitzgerald, 1986; Mason and Fitzgerald, 1991); (4) Teflon® bottles are best for low-level mercury samples, and lids must be wrenched on tightly (Gill and Fitzgerald, 1985; Stoichev *et al.,* 2006); (5) freezing/thawing preserves monomethylmercury (MHg), but may alter the inorganic mercury (IHg) speciation (Parker and Bloom, 2005); and (6) hydrochloric acid is a superior preservative to nitric acid because the chloride helps to complex the Hg^{2+} (Parker and Bloom, 2005).

Table 3.1 provides a summary of recommended storage conditions for mercury species. Mercury may be lost to the walls regardless of acidification; therefore, it is necessary to add an oxidizer to the original sample bottle prior to analysis for total mercury determination (Parker and Bloom, 2005).

Rigorous cleaning procedures must be used for all laboratory ware and other equipment that comes into contact with samples. There are different cleaning procedures, but usually cleaning for several days in acid baths is included (Jackson, 1988).

After such treatments, the material is usually rinsed with mercury free deionized water or double distilled water and stored in mercury free area, preferably sealed in clean plastic bags. Some authors recommend storage of laboratory ware in dilute nitric or hydrochloric acids until use (Stojchev *et al.,* 2006).

Table 3.1 Summary of recommended bottle types, preservation, and storage for mercury species (Parker and Bloom, 2005)

Species	Bottle type	Preservation	Storage	Estimated stability
Total mercury	Glass (with Teflon-lined lid) or Teflon	BrCl in original bottle	not critical	>1 year
Methylmercury	Glass (with Teflon-lined lid) or Teflon	0.4% HCl freshwater, 0.2% H_2SO_4 seawater	refrigerate, dark	6–12 months
Hg^0	Glass (with Teflon-lined lid)	no headspace	refrigerate, dark	1 day
Dimethylmercury	Glass (with Teflon-lined lid)	no headspace	refrigerate, dark	1 day
Hg(II)	Glass (with Teflon-lined lid)	none	refrigerate, dark	2–5 days
Dissolved/suspended ratio	Glass (with Teflon-lined lid) or Teflon	none	refrigerate, dark	2–5 days

3.2.2 Water samples

To adopt a sampling strategy it is necessary to consider the nature of the studied sites and the heterogeneity due to mixing of different water masses (Quevauviller, 2001).

The sampling and storage bottles have to be rinsed with the site water immediately before sampling. Surface waters can be sampled with pumps using polytetrafluoroethylene (PTFE or Teflon®) tubes but in many cases surface waters are taken “by hand” directly in the sampling bottle using long polyethylene gloves. The bottle has to be opened and closed under water to avoid mixing with the surface microlayer or oxidation of the sample (Stojchev *et al.*, 2006).

The porewaters are collected by direct filtration of the wet sediments or centrifugation of the samples followed by filtration (Gilmour et al., 1998; Bloom et al., 1999). After sampling, the porewaters are treated in the same manner as the surface waters (Baeyens, 1992).

For the analysis of volatile mercury forms (Hg^0 and $(CH_3)_2Hg$), large volume of samples are recommended (10 to 20 L) and the samples should not be acidified to avoid the oxidation of the volatile species. If samples cannot be purged and trapped in the field,

they should be collected in completely full glass bottles with Teflon-lined caps, as those species are lost rapidly from Teflon and polyethylene bottles (Parker and Bloom, 2005).
When only total mercury is of interest, a simple procedure may be employed that allows long-term storage with full recovery and little risk of contamination. The sample should be collected into a Teflon or glass bottle with Teflon-lined lid and then preserved with a strong oxidizer such as acidic bromine monochloride (BrCl) or chromic acid. Nitric acid is not oxidizing under dilute conditions and so allows a considerable equilibrium of Hg^0 concentration in solution. BrCl is preferred, owing to its lower mercury blanks and lower degree of toxicity for waste disposal. This approach destroys all speciation information, but also disaggregates organic matter sufficiently to eliminate wall losses.
If speciation information is desired, then the samples must be preserved less aggressively, at least until all other species have been determined. Once the other species have been determined, BrCl can then be added to the original sample bottle to ensure that any Hg on the walls is resolubilized prior to analysis (Parker and Bloom, 2005).

In brief, the choice of material is critical to preserve the speciation of mercury in water samples. Several studies investigated the stability of mercury species in standard solutions depending on the storage material and it was found that the solutions of MHg are stable in glass bottles at 4^0C but the best storage material is PTFE. It is giving the lowest contamination. This fact is very important at extremely low concentrations found in real samples. For the determination of mercury forms the best choice is “on-site” analysis to preserve the speciation. If it is not possible to analyze the sample immediately it has to be stored at special conditions. The water samples are stored normally at 4^0C in the dark after the addition of a small volume of ultra pure concentrated acid (0.1 to 1% v/v). The losses depend on the sample matrix and need further investigation (Parker and Bloom, 2005).

3.2.3 Solid samples

The contamination risk for sediments is less important than for waters but the technical problems can be very complicated. The sampling strategy depends on the objective of the

study. For the investigation of the temporal variations it is necessary to collect the samples from the same site using Global Positioning System (GPS). For stratigraphic studies it is obligatory not to mix sedimentary layers (Stojchev *et al.,* 2006).

The sediments can be sieved with Nylon® sieves to eliminate stones and other gross particles. They are transferred in acid-cleaned vials and immediately frozen (-20 ^{0}C) to increase the stability of MHg (Parker and Bloom, 2005). Later in the laboratory the sediments can be dried either with clean air flux (Rodriguez Martin-Doimeadios *et al.,* 2000) or freeze-dried (Varekamp *et al.,* 2000).

3.2.4 Biological samples

To adopt a sampling strategy for biological samples it is necessary to consider the trophic level of the studied organisms (Zooplankton, plants, benthic organisms, macroorganisms, etc.) (Horvat *et al.,* 1999; Heller and Weber, 1998).

In general, the samples are frozen immediately after the preliminary treatment. Later in the laboratory they are analyzed directly or after freeze-drying (Stojchev *et al.,* 2006). The biotissues should be stored in the dark to avoid photodegradation (Yu and Yan, 2003).

3.2.5 Air samples

Sampling for mercury from air can be difficult because of the normally low ambient concentrations and the potential for contamination artifacts. Advances in sampling and measurement techniques have led to more reliable mercury data in recent years. There are currently two basic approaches for sampling of mercury vapor from air: (1) use of a pump to pass a known volume of air through a trap designed for collection of mercury, and (2) passive diffusive sampling onto a gold film or Hopcalite adsorbent (Brumbaugh *et al.,* 2000 and references therein). Passive methods are generally limited to the sampling of gaseous Hg^0 whereas pump methods can utilize various trapping approaches in order to differentiate among particulate-sorbed and gaseous mercury species. For pump and trap methods, the analysis can be performed in a semi-continuous manner (on site) or by a

static sampling approach whereby the trapped mercury is taken to a laboratory for analysis. With either approach, the trapped mercury is typically thermally desorbed and then quantified by spectrometric methods. Commercial on-site mercury vapor analyzers which contain the pump, trap, and analyzer in one integrated unit are also available (Amyot *et al.*, 1997).

Although the pump and trap approach is generally more precise and allows for sampling integration of relatively short time intervals, passive sampling is useful for screening applications and longer-term integrative sampling (weeks to months). It may also be more practical in certain instances, such as for the determination of mercury at remote locations or for the monitoring of time-averaged occupational exposure.

3.3 Analytical procedures for mercury determination

A number of methods can be employed to determine mercury concentrations in environmental media. The concentrations of total mercury, elemental mercury, organic mercury compounds (especially methylmercury) and chemical properties of various mercuric compounds can be measured, although speciation among mercuric compounds is not usually attempted. In addition, while it is possible to speciate the mercuric fraction further into reactive, non-reactive and particle-bound components (Munthe *et al.*, 2001), it is generally not possible to determine which mercuric species (e.g. HgS or $HgCl_2$) is present in environmental media.

The purpose of this section is to describe the analytical methods that are available for detecting, and/or measuring mercury. Rather than provide an exhaustive list of analytical methods, the intention here is to identify well-established methods that are used as the standard methods of analysis. A more detailed discussion on the subject was also presented in our work on the development and optimization of analytical methods for mercury speciation (Lusilao, 2009).

Many of the analytical methods used for environmental samples are those approved by organizations such as the USEPA. Other methods are those that are developed by research groups or are modified versions of previously used methods in order to obtain lower detection limits, and/or to improve accuracy and precision.

3.3.1 Total mercury determination

One of the significant advances in mercury analytical methods has been in the accurate detection of mercury at low levels (less than 1 mg kg^{-1}). Over the past four decades mercury determinations have progressed from detection of microgram levels of total mercury (Hg_{TOT}) to picogram (Horvat *et al.,* 1993) or even femtogram levels (Stoichev *et al.,* 2006) of particular mercury species. In the last decade, investigations of mercury in natural waters have established that concentrations of mercury species are in the level of ng L^{-1} (Stoichev *et al.,* 2006). Clearly, sensitive techniques avoiding any memory effect or carry over problems are required to analyze mercury at these low concentrations. Mercury contamination of samples has been shown to be a significant problem in the precedent section. The use of ultra-clean sampling techniques is critical for the more precise measurements required for detection of low levels of mercury.

Analytical techniques mostly employed for Hg_{TOT} determination in natural waters at picogram levels are based on Cold Vapor Atomic Absorption Spectrometry (CVAAS), Inductively Coupled Plasma Mass Spectrometry (ICP-MS), Plasma Atomic Emission Spectrometry (ICP-AES) and Cold Vapor Atomic Fluorescence Spectrometry (CVAFS) detection, after decomposition of all mercury species into Hg^{2+}. After a digestion step, reduction of the sample with $SnCl_2$ or $NaBH_4$ is usually employed (Logar *et al.,* 2002). Other methods such as Anodic Stripping Voltammetry (ASV) and Neutron Activation Analysis (NAA) have been used to determine mercury levels in aqueous media (ATSDR, 1999).

Mercury levels have been determined in numerous environmental matrices, including air, water (surface water, drinking water, groundwater, sea water, and industrial effluents), soils and sediments, fish and shellfish, hair, blood, foods, pharmaceuticals, and pesticides (ATSDR, 1999).

The advantage of ICP-AES and ICP-MS over other analytical techniques is undoubtedly their multi-element capability and the potential of coupling to various separation and sample preparation techniques. There is a common perception that, while ICP-AES is reliable, robust and suitable for routine analysis, ICP-MS is superior in terms of detection limit and therefore a more appropriate research tool. ICP-MS is routinely used in many

diverse research fields such as earth, environmental, life and forensic sciences and in food, material, chemical, semiconductor and nuclear industries (Linge, 2006). The high ion density and the high temperatures in the plasma make it an ideal atomizer and element ionizer (figure 3.1) for all types of samples and matrices introduced by a variety of specialized devices. Outstanding properties such as high sensitivity (with LOD as low as 10^{-6} to 10^{-9} mg L^{-1}), relative salt tolerance, compound-independent element response and highest quantization accuracy lead to the unchallenged performance of ICP-MS in efficiently detecting, identifying and reliably quantifying trace elements (Montaser, 1998; Lusilao, 2009). ICP-MS is also capable of correcting the artifacts during analysis. The main inconveniences are the high instrumental and operational costs.

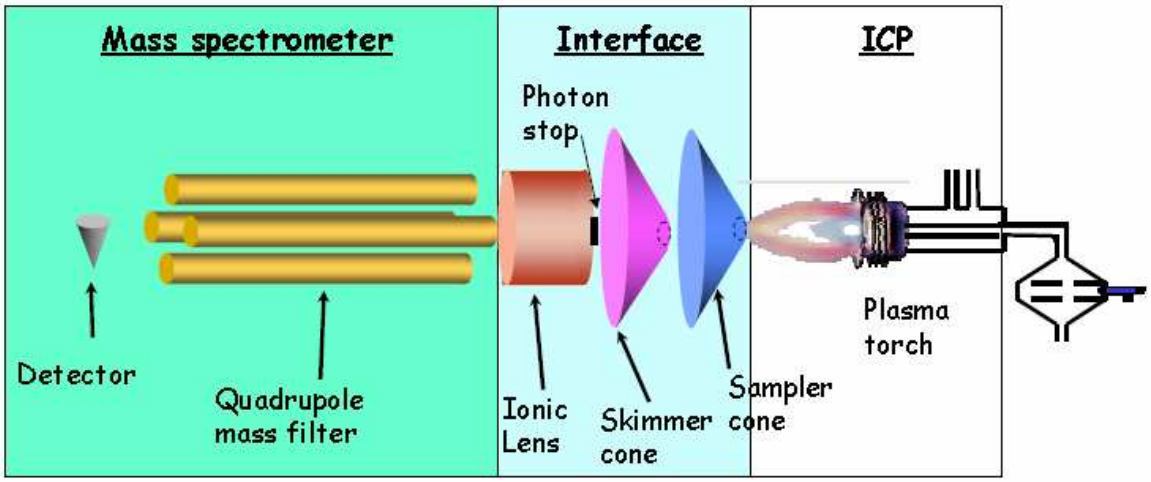

Figure 3.1 Schematic of a quadrupole ICP-MS. A nebulized sample is atomized in a high temperature plasma (~10,000K) and the ion beam is focused, through the cones and ionic lenses, to the quadrupole where the target isotopes are selected, or "filtered", according to their mass to charge ratio and quantified by an appropriate detector

On the other hand, it is very desirable to take advantage of the unique capabilities of the ICP-MS detector. Only this technique allows the measurement of individual isotopes of mercury with sufficient sensitivity, which is essential if one wants to apply enriched mercury isotopes in any kind of stable isotope tracing experiment or carry out isotope dilution analyses. Several methods using ICP-MS as a detector are developed to accomplish this goal. Different approaches also exist to achieve the ultra low levels of detection necessary for determining mercury species in pristine environments.

The AFS detector is also very sensitive for mercury, simple and much lower priced. Coupled systems with AFS could be used in situ to overcome the sample storage problems. The limitations are scatter and background levels of impurities. Atomic absorption, on the other hand, although it has been extensively used, suffers from the fact that it is non-linear and measurements at lower levels are extremely difficult (Stockwell, and Corns, 1993). CVAAS is an alternative of choice for mercury determination in water. This method is very sensitive and has been proven to be reliable. Water samples generally do not require digestion, but mercury in the samples is usually reduced to the elemental state and preconcentrated prior to analysis (Logar *et al.*, 2002).

Electrochemical techniques, in particular differential pulse anodic stripping voltammetry (DPASV), are also extensively used for metal ion analysis (Zejli *et al.*, 2005). Many papers on trace determination of mercury by ASV, using different types of working electrode, have been published. This method has found a wide application in trace analysis because it requires inexpensive instrumentation and it is possible to determine trace elements in various matrices such as water, sediment or even biological samples with very low detection limits (Diederich *et al.*, 1994). The main inconvenient of this method is that it is time consuming.

Spectrophotometry has often been used to determine mercury in aqueous matrices. Sample preparation methods vary and have included separation by thin-layer chromatography (TLC) or column chromatography, selective extraction, and ligand formation. While recoveries were good, spectrophotometry is not as sensitive as techniques mentioned above (ATSDR, 1999).

3.3.2 Mercury species analysis

As it was mentioned previously, mercury exists in a large number of different chemical and physical forms with a wide range of properties, and its ecological and toxicological effects are strongly dependent on the chemical form present. Inorganic mercury species may be transformed by biotic and/or abiotic processes to much more toxic organic, methylated forms, such as methylmercury. Therefore, the total concentration of mercury alone is of little value for toxicological and biogeochemical studies without knowledge of its chemical forms.

The recognition of the fact that, in environmental chemistry, occupational health, nutrition and medicine, the chemical, biological and toxicological properties of an element are critically dependent on the form in which the element occurs in the sample has spurred a rapid development of an area of analytical chemistry referred to as speciation analysis (Templeton *et al.,* 2000). The International Union of Pure and Applied Chemistry (IUPAC) defines a chemical species as a specific and unique molecular, electronic, or nuclear structure of an element (Templeton *et al.,* 2000). Speciation of an individual element refers to its occurrence in or distribution among different species. Speciation analysis is the analytical activity of identifying and quantifying one or more chemical species of an element present in a sample (Templeton *et al.,* 2000).

A succession of analytical stages is required for speciation analysis (figure 3.2). The main steps to "speciated" mercury, particularly inorganic and methylmercury are extraction, preconcentration, separation and specific detection (Stoichev *et al.,* 2006).

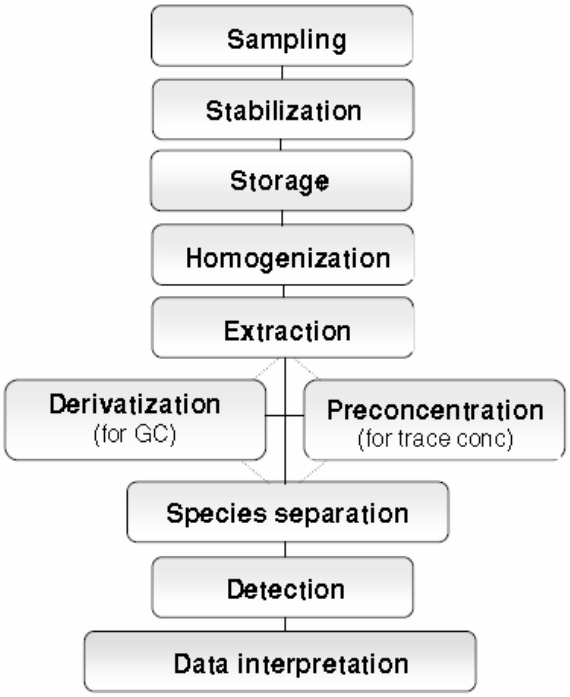

Figure 3.2 Analytical steps for speciation (After Stoichev *et al.,* 2006)

The combination of a chromatographic separation technique, that ensures that the analyte compound leaves the column unaccompanied by other species of the analyte element, with atomic spectrometry, permitting a sensitive and specific detection of the target element, has become a fundamental tool for speciation analysis, as discussed in many review (e.g. Caruso *et al.*, 2000; Cornelis *et al.*, 2003).

Recent advances in the application of these hyphenated (coupled) techniques allow the species-selective determination of volatile organometallic (Sn, Hg, Pb) contaminants, non-volatile organometalloid (As, Se) compounds and heavy metal complexes in environmental matrices.

3.3.3 Hyphenated techniques in speciation analysis

A suitable analytical technique for speciation analysis should mainly address the following issues:

(i) Selectivity of the separation technique allowing the target analyte species to reach the detector well separated from potential matrix interferents and from each other,

(ii) Sensitivity of the element or molecular selective detection technique since the already low concentrations of trace elements in environmental samples are usually distributed among several species,

(iii) Species identification. Retention time matching usually employed requires the availability of standards. When standards are non available, the use of a molecule-specific detection technique is mandatory.

The above challenges can be addressed by hyphenated techniques such as those schematically shown in figure 3.3. In the most frequent case a separation technique using chromatography (gas or liquid) (Stojchev *et al.*, 2006), electrochromatography or capillary electrophoresis (EC or CE) (Kuban *et al.*, 2007; Ali *et al.*, 2005).is combined with ICP MS. The coupling is realized directly (for GC), via a nebulizer (for column liquid separation techniques) or by laser ablation (for planar techniques). A review of application papers highlights trends in elemental speciation analysis using ICP-MS since 2000 and describes developments in speciation using GC, LC, CE and field flow fractionation (FFF) (Linge, 2006 and references therein).

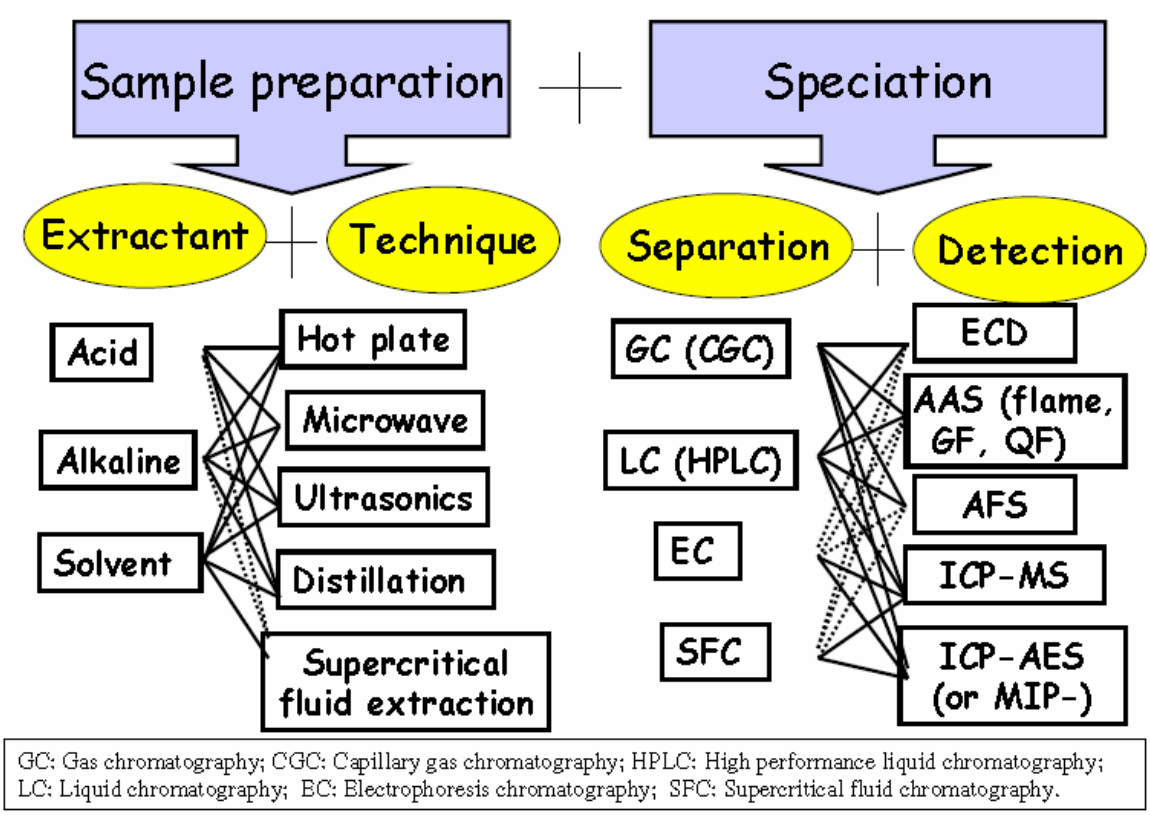

Figure 3.3 General Scheme of analytical techniques used for speciation (Amouroux, 2007)

The separation component of the coupled system becomes of particular concern when the targeted species have similar physicochemical properties. Gas chromatography should be chosen wherever possible because of the high separation efficiency and the very low achievable detection limits because of the absence of the condensed mobile phase (Liu and Lee, 1999). For non-volatile species column liquid phase separation techniques, such as HPLC and CE, are the usual choice because of the ease of on-line coupling and the variety of separation mechanisms and mobile phases available allowing the preservation of the species identity.

For element-specific detection in gas chromatography, a number of dedicated spectrometric detection techniques can be used (see figure3.3), for example, quartz furnace atomic absorption or atomic fluorescence for mercury, microwave induced plasma atomic emission for lead or tin, but it is ICP-MS that has been establishing its position as the versatile detector of choice. ICP-MS is virtually the only technique

capable of coping, in on-line mode, with the trace element concentrations even in LC and CE effluents. The femtogram level absolute detection limits may turn out to be insufficient if an element present at the ng ml^{-1} level is split into a number of species, or when the actual sample amount analyzed is limited to several nanolitres as in the case for CE.

The isotope specificity of ICP-MS offers a still underexploited potential for tracer studies and for improved accuracy in quantification via the use of isotope dilution techniques which are discussed further.

3.3.4 Element selective detection in gas chromatography

The practical applications to volatile organometallic species are dominated by the three techniques GC – MIP-AED, GC – ICP-MS and GC – EI-MS, the only exception being the determination of methylmercury in the environment where the position of GC-AAS and GC-AFS (Liang *et al.,* 2004 and references therein) is still remarkably strong. An AFS detector coupled with a gas chromatograph is a commercially available hyphenated system allowing speciation of mercury (Armstrong *et al.,* 1999). GC-AFS is a convenient method for mercury speciation in environmental matrices but the risk of artefacts due to the presence of hydrocarbons prevents this technique to be successfully used for more complex matrices.

Flame AAS initially used was quickly abandoned because of insufficient sensitivity preventing applications to real-world samples and an electrothermally heated silica tube is usually used as the atomization cell (Forsyth, and Marshall, 1985; Diederich *et al.,* 1994).

Mass spectrometry of molecular ions, which is a common detection technique in GC of organic compounds, is relatively seldom used in speciation analysis. For quantitative analysis the widest popularity was enjoyed by electron impact mass spectrometers (EI-MS) operated in the single ion monitoring mode for which detection limits are two orders of magnitude lower than in the full scan mode for structure elucidation. For most organometallic compounds detection limits at the low picograrn level can be achieved in the single ion monitoring mode (Fish, 1983).

Plasma detectors compare favorably with spectrometers listed above. The use of different plasmas for element-specific detection in GC effluents was critically reviewed (Lobinski and Adams, l997). The practical significance of these studies in terms of applications is almost non existent with the exception of the microwave induced plasma.

The coupling of GC – MIP-AED has been extremely popular in speciation analysis of anthropogenic environmental contaminants and products of their degradation with detection limits that could be matched only by ICP MS (Lobinski and Adams, l997). Another factor contributing considerably to the popularity of GC – MIP-AED has been the commercial availability of an instrument.

GC - MIP AED offers sufficiently attractive figures of merit to be applied on a routine basis to speciation of organotin and organolead compounds in the environment and methylmercury in biological tissues. It is being gradually replaced by GC – ICP-MS whose lower detection limits allow a simpler sample preparation procedure, work with more dilute extracts, and especially a sensitive speciation analysis of complex matrices. The position of ICP-MS has recently become stronger owing to the availability of the commercial interface and this detection technique is discussed in section 3.2.7.

The combination of capillary GC (CGC) with ICP-MS has become an ideal methodology for speciation analysis for organometallic compounds in complex environmental and industrial samples because of the high resolving power of GC and the sensitivity and specificity of ICP-MS. Indeed, the features of ICP-MS such as low detection limits reaching the one femtograrn (1 fg) level, high matrix tolerance allowing the direct analysis of complex samples, such as gas condensates, or the capability of the measurement of isotope ratios enabling accurate quantification by isotope dilution, position ICP-MS at the lead of the GC element specific detectors.

The ICP quadrupole MS ((Q) ICP-MS), which is schematically shown in figure 3.1, is undergoing a constant improvement leading to a wider availability of more sensitive, less interference prone, smaller in size and cheaper instruments which favors their use as chromatographic detectors. The introduction of ICP time-of-flight (TOF) MS increased the speed of data acquisition allowing multiisotope measurement of millisecond-wide chromatographic peaks and improving precision of isotope ratios determination (Heisterkamp and Adams, 2001; Haas *et al.*, 2001). An even better precision was reported

for magnetic sector multicollector (MC ICP-MS) instruments used as on-line GC detectors (Krupp *et al.*, 2001a). These instrumental developments go in parallel with the miniaturization of GC hardware, allowing the time-resolved introduction of gaseous analytes into an ICP, based on microcolumn multicapillary GC, and sample preparation methods including microwave-assisted, solid phase micro extraction or purge and capillary trap automated sample introduction systems (Lobinski *et al.*, 1998).

The basic requirement for an interface is that the analytes should be maintained in the gaseous form during transport from the GC column to the ICP, in a way that any condensation is prevented. This can be achieved either by an efficient heating of the transferline avoiding the cold spots, or by using an aerosol carrier. This results in two basic types of designs of the GC – ICP-MS interface (figure 3.4):

(I) The "dry plasma" which is based on the direct connection of the transferline to the torch (Rodriguez *et al.*, 1999) and where the spray chamber is removed and the transferline inserted part of the way up the central channel of the torch;

(II) The "wet plasma" which is based on mixing the GC effluent with the aqueous aerosol in the spray chamber prior to introduction into the plasma detectors and allows, therefore, the mass bias correction via internal standards (Krupp *et al.*, 2001a).

Regardless of the type of the interface an addition of oxygen to the plasma gas is essential to prevent carbon deposition (and sometimes metal entrapment) and to reduce the solvent peak.

Nowadays, GC – ICP-MS interfaces are commercially available, having proven the recognition of the maturity of this coupling by the analytical instrumentation industry.

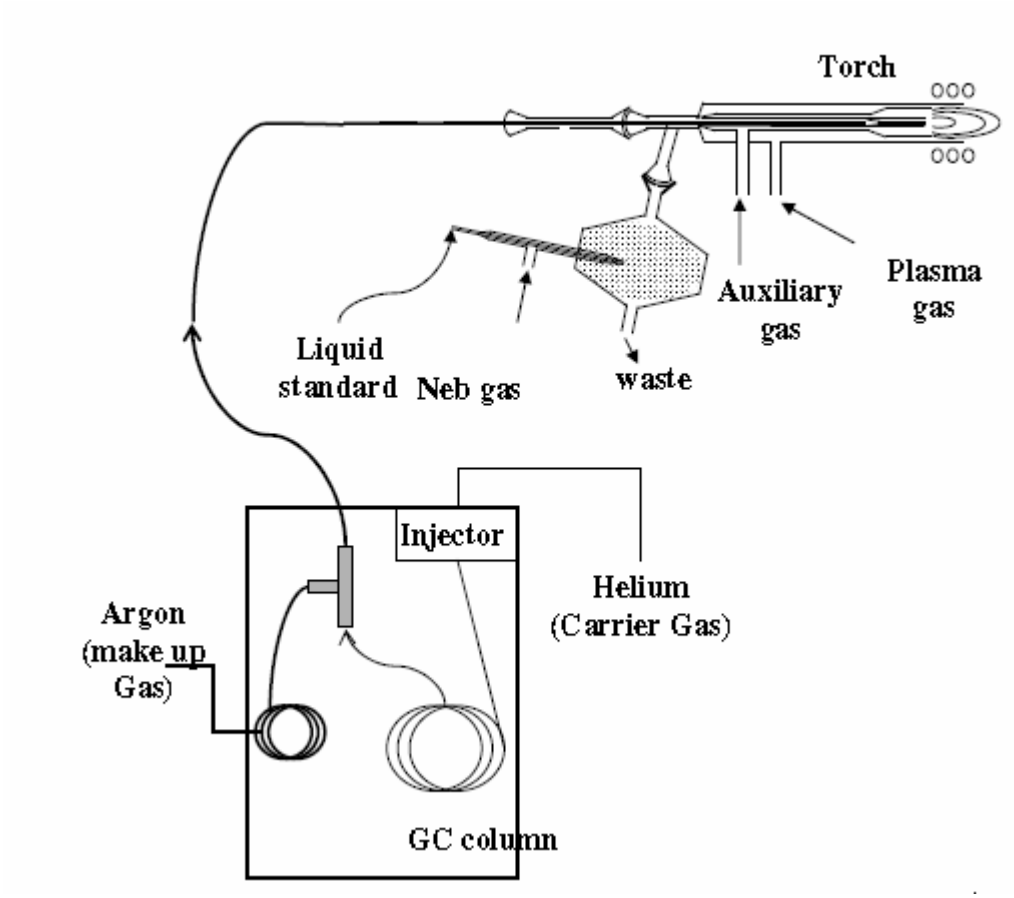

Figure 3.4 Example of an hyphenated GC-ICP-MS with the possibility of working in dry or wet plasma

3.3.5 Advances in gas chromatography prior to element selective detection

Packed column GC used in the early studies on GC – ICP-MS coupling (Vanloon *et al.*, 1986) has practically given way to capillary GC and the coupling of the latter to ICP-MS was first described by Kim *et al.* (1992).

Although packed columns can, by design, handle high flow rates and large sample sizes, their efficiency and resolution properties are compromised because of the high dispersion of the analytes on the column. The large column volume negatively affects the sensitivity in the peak height mode and the detection limits. The packing itself may be chemically active toward many organometallic species, which makes silanization necessary and worsens the reliability of results. It should be noted, however, that still a considerable number of works, especially those using hydride generation purge and trap are carried out

with packed column chromatography because of easier handling of highly volatile species at temperatures below 100°C (Amouroux *et al.,* 1998).

Capillary GC offers improved resolving power over packed column GC – ICP-MS which is of importance for the separation of complex mixtures of organometallic compounds found in many environmental samples. Capillary GC can cope with the co-elution of the solvent and the volatile compounds, such as $(CH_3)_2Hg$, and thus to avoid or to minimize the plasma quenching. A drawback in the use of capillary GC is the loss of sensitivity due to the reduced sample size and the high dilution factor with the detector's makeup gas necessary to match the spectrometer's optimum flow rate.

Number of papers has also appeared on multicapillary (MC) GC which employs columns that consist of a bundle of 900 - 2000 capillaries of a small (20-40 μm) internal diameter (for a review see Lobinski *et al.,* 1999). Multicapillary GC features high flow rates which minimize the dilution factor and facilitate the transport of the analytes to the plasma. The hyphenation of MC GC with ICP-MS using a non-heated interface offered 0.08 pg detection limits for mercury speciation (Slaets *et al.,* 1999).

3.3.6 Purge and trap using capillary cryofocussing

A semi-automated compact interface for time-resolved introduction of gaseous analytes from aqueous solutions into an ICP MS without the need for a full-size GC-oven was described (Wasik *et al.,* 1998). The working principle was based on purging the gaseous analytes with an inert gas, drying the gas stream using a 30 cm tubular Nation membrane and trapping the compounds in a thick film-coated capillary tube followed by their isothermal separation on a multicapillary column. Routine detection limits of 0.5 ± 10 pg (as metal) for water samples were achieved for the selected alkyl-metal(loid) species of arsenic, germanium, mercury and tin (Tseng *et al.,* 2000). Recoveries were reported to be quantitative up to a volume of 50 ml (Wasik *et al.,* 1998).

3.3.7 ICP MS detection in gas chromatography

Quadrupole mass analyzers have predominantly been used since their sensitivity has improved by a factor of 10 during the past two decades. Of other types of analyzers, TOF-MS has been extensively studied as a GC detector during the last decade (Hasterkamp and Adams, 2001). Applications of sector-field analyzers, also with multicollectors, have appeared (Krupp *et al.*, 2001a and b).

The use of enriched isotopes with ICP-MS detectors has been of benefit for the development of speciation methodology. The isotopic specificity of ICP-MS opens the way to the use of stable isotopes or stable isotope enriched species for studies of transformations and of artifact formation during extraction and derivatization processes and for the wider implementation of the isotope dilution quantification. The latter had until recently been limited by the non-availability of organometallic species with the isotopically enriched element. However, standards for the isotopically enriched CH_3Hg^{201} (Demuth and Heumann, 2001), mono, di and tributyltin (Encinar *et al.*, 2001) have been synthesized and applications are being developed. The prerequisite of the use of stable dilution techniques is the precise and accurate measurement of the isotopic ratios.

In GC- ICP-MS the isotope ratio determinations are more precise if the intensities of the isotopes are integrated over the whole chromatographic peak instead of only measuring the isotope ratio at a single point of the peak (Heumann *et al.*, 1998). A precision of 1% was reported for the mercury isotope ratios determined for methylethylmercury (MeEtHg) eluted from a packed column by GC – ICP-MS (Hintelrnann *et al.*, 1995).

3.3.8 Speciated isotope dilution analysis (SIDMS)

Isotope dilution (ID) MS is a method of proven high accuracy. The sources of systematic errors are well understood and can be controlled which makes IDMS accepted as a definitive method of analysis.

Isotope dilution is based on the addition of a known amount of enriched isotope to a sample. Equilibration of the spike isotope with the natural element, molecule or species in the sample alters the isotope ratio that is measured. With the known isotopic abundance

of both spike and sample, the amount of the spike added to the known amount of sample, concentration of the spike added, and the altered isotope ratio, the concentration of the element/molecule/species in the sample can be calculated (USEPA, 2007a).

IDMS has proven to be a technique of high accuracy for the determination of total metals in various matrices (Fasset and Paulsen, 1989; Bowers Jr et al., 1993; Moore et al., 1984). IDMS has several advantages over conventional calibration methodologies, namely external calibration and standards addition, because partial loss of the analyte, after equilibration of the spike and the sample, will not influence the accuracy of the determination. Fewer physical and chemical interferences influence the determination as they have similar effects on each isotope of the same element. The isotope ratio to be measured for quantification in IDMS can be measured with very high precision, typically RSD ≤0.25% (USEPA, 2007a). Quantification is a direct mathematical calculation from determined isotopic ratios and known constants and does not depend on a calibration curve or sample recovery. An example of calculation for the determination of ^{202}Hg using an enriched spike of ^{200}Hg is given below:

$$C_{sample} = C_x M_x \qquad (3.1)$$

$$C_s = C_{spike}/M_s \qquad (3.2)$$

$$C_x = \frac{C_s W_s}{W_x}\left(\frac{{}^{200}A_s - R_{200/202}\,{}^{202}A_s}{R_{200/202}\,{}^{202}A_x - {}^{200}A_x}\right) \qquad (3.3)$$

where, C_S and C_X are the concentrations of the isotope-enriched spike and the sample in μmole g^{-1}, respectively. M_S and M_X are the average atomic weights of the isotope enriched spike and the sample in g $mole^{-1}$, respectively. $^{200}A_S$ and $^{200}A_X$ are the atomic fractions of ^{200}Hg for the isotope-enriched spike and sample, respectively. $^{202}A_S$ and $^{202}A_X$ are the atomic fractions of ^{202}Hg for the isotope-enriched spike and sample, respectively. Cspike is the concentration of the isotope-enriched spike in μg g^{-1}. $R_{200/202}$ is the isotope ratio (^{200}Hg / ^{202}Hg).

SIDMS takes a unique approach to speciated analysis that differs from traditional methods. Traditional speciation methods attempt to hold each species static while making the measurement. Unfortunately, speciation extraction and analysis methods inherently measure the species after species conversions have occurred. SIDMS has been developed to address the correction for the species conversions (USEPA, 2007a). In SIDMS (figure 3.5), each species is "labeled" with a different isotope-enriched spike in the corresponding species form. Thus, the interconversions that occur after spiking are traceable and can be corrected. While SIDMS maintains the advantages of IDMS, it is capable of correcting for the degradation of the species or the interconversion between the species (Kingston, 1995; Huo and Kingston, 2000; Kingston *et al.*, 1998; Meija *et al.*, 2006). SIDMS is also a diagnostic tool that permits the evaluation of species-altering procedures and permits evaluation and validation of other more traditional speciation analysis methods. SIDMS is applicable to be used in conjunction with other methods when knowledge of species concentration, conversion and stability is necessary.

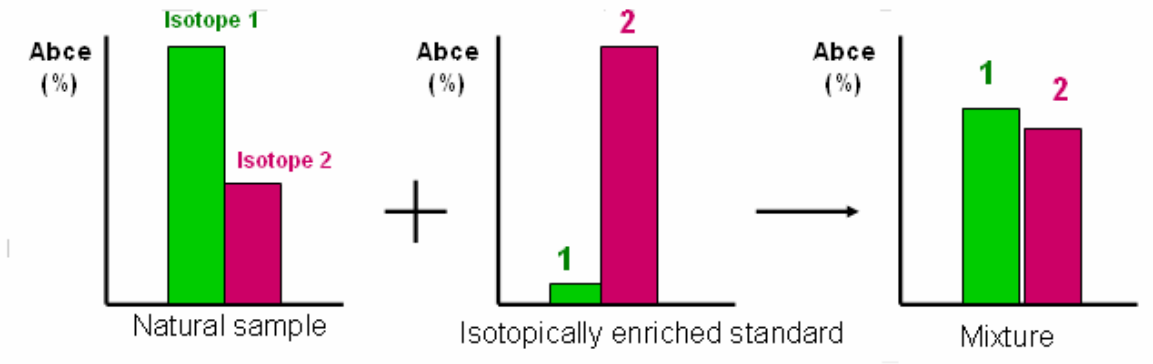

Figure 3.5 The isotope dilution principle: a known amount of the analyte containing an "abnormal" isotopic composition (Isotope 2) is added to the sample

Fundamentals of ID GC – ICP-MS for species-specific analysis were extensively discussed by Gallus and Heuman (1996). They were illustrated by the determination of Se(IV) in water after conversion of the analyte species into piazselenol. In ID GC – ICP-MS (or more generally SIDMS) the sample is spiked with the species to be determined in which one of the isotopes of the metal or metalloid was enriched (e.g. $CH_3{}^{201}Hg^+$ or $^{199}Hg^{2+}$; see also figure 3.5). After equilibration of the spike, the sample preparation procedure, GC – ICP-MS is run and the isotopic ratio of the metal(loid) in the species of

interest is measured. The analysis principle is identical as in classical ID ICP-MS; however, some fundamental differences occur.

Both IDMS and SIDMS require the equilibration of the spike isotope(s) and the natural isotope(s). For IDMS, the spike and sample can be in different chemical forms; only total elemental concentrations will result. In general, IDMS equilibration of the spike and sample isotopes occurs as a result of decomposition, which also destroys all species-specific information when the isotopes of an element are all oxidized or reduced to the same oxidation state. For SIDMS, spikes and samples must be in the same speciated form. This requires the chemical conversion of the elements in spikes to be in the same molecular form as those in the sample.

For solution or liquid samples, spiking and equilibration procedures can be as simple as mixing the known amount of the sample and the spikes prior to analysis. Efforts are taken to keep the species in their original species forms after spiking. Aqueous samples such as drinking water, ground water, and others may be directly spiked and analyzed.

Solid samples such as soils, sludges, sediments, biota and other samples containing solid matrices require spiking before or after extraction/digestion in order to solubilize and equilibrate the species prior to introduction to the mass spectrometer.

This method has also been used to certify reference materials and for environmental forensic analysis (USEPA, 2007a). The inconvenience is that usually a long time is needed for equilibration between the sample and the spikes.

The speciated isotope dilution analysis is only possible for element species well defined in their structure and composition. The species must not undergo intercoversion and isotope exchange prior to separation. The equilibration of the spike and analyte, attainable in classical ID thermal ionization MS (ID TIMS) cannot be guaranteed to be achieved for speciated ID analysis in solid samples. Consequently, the prerequisite of the ID method, that the spike is added in the identical form as the analyte, is extremely difficult, not to say impossible, to attain. Nevertheless, some advantages, such as the inherent corrections for the loss of analyte during sample preparation, for the incomplete derivatization yield, and for the intensity suppression/enhancement in the plasma are evident. In particular, ID quantification seems to be attractive in speciation analysis of

complex matrices when the different organic constituents of the sample modify continuously the conditions in the plasma and thus the sensitivity (Snell *et al.,* 2000).

Isotopically enriched species should represent the ultimate means for specific accurate and precise instrumental calibration. Not only they are useful for routine determination by speeding analysis, but they also assist in the testing and diagnostics of new analytical methods and techniques.

The determination of dibutyltin in sediment was carried out by ID analysis using an ^{118}Sn-enriched spike. No recovery corrections for aqueous ethylation or extraction into hexane were necessary and no rearrangement reactions were evident from the isotope ratios (Encinar *et al.,* 2000). A mixed spike containing ^{119}Sn enriched mono-, di- and tributyltin was prepared by direct butylation of ^{119}Sn metal and characterized by reversed isotope dilution analysis by means of natural mono-, di- and tnbutyltm standards. The spike characterized in this way was used for the simultaneous determination of the three butyltin compounds in sediment certified reference materials (Encinar *et al.,* 2001). Isotopically labelled $(CH_3)_2Hg$, CH_3HgCl and $HgCl_2$ species were prepared and used for the determination of the relevant species in gas condensates with detection limits in the low pg range (Snell *et al.,* 2000). The use of SIDMS has proven to be a powerful tool to check whether any interconversion is taking place between Hg(II) and MeHg (methylation/demethylation) and to discover the error of the specific steps of sample preparation and their contribution to the overall transformations of a known species (Hintelmann, 1999; Monperrus *et al.,* 2003).

3.3.9 Liquid chromatography with ICP-MS detection

Many element species of interest in environmental speciation analysis are non volatile and cannot be converted into such by means of derivatization. They include virtually all the coordination complexes of trace metals but also many truly organometallic (containing a covalently bound metal or metalloid) compounds. For all these species HPLC is the principal separation technique prior to element selective detection.

The various possibilities of on-line coupling a separation technique with an element (species) specific detector for species-selective analysis of metallo compounds of

biological origin include different modes of HPLC or electrophoresis in terms of separation, and atomic spectrometry (or molecular MS) in terms of detection. The presence of a metal bound to the biomacromolecule in a sample is considered to be the prerequisite of using an element-specific detector.

The choice of the detector component becomes crucial when the amount of analyte species is very small and a high sensitivity is necessary. That is the reason why ICP-MS is the most popular. An important problem is often the interface between chromatography and spectrometry (figure 3.6) as the separation conditions may be not compatible in terms of flow rate and mobile phase composition with those required by the detector.

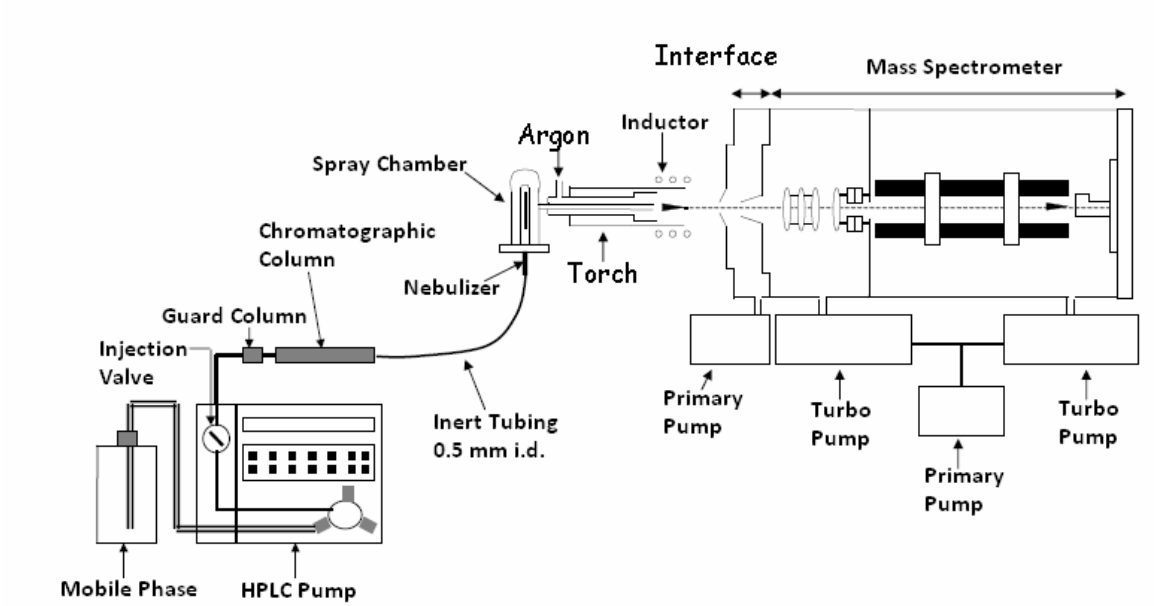

Figure 3.6 Scheme of the coupling between HPLC and ICP-MS

For the analysis of mercury forms in natural waters using HPLC for separation, it is necessary to preconcentrate them before the injection in the chromatographic column (Shade and Hudson, 2005). Direct coupling of HPLC with the detector is not sensitive enough to analyze real water samples. For this reason, post-column vapor generation is used to improve the sensitivity and decrease the matrix effects (Shade and Hudson, 2005). However, generation of cold vapor from organomercury species requires an extra step for conversion to Hg^{2+}; otherwise, the efficiency of cold vapor generation depends on the species present. The conversion is usually performed online by different approaches such as chemical oxidation with $K_2Cr_2O_7$ at ambient temperature which

requires a long reaction time for efficient conversion (Wu, 1991). Thus, UV radiation, microwave heating, or an external heating source is used to facilitate the decomposition of organomercury species (Falter and Scholer, 1994).

In brief, gas chromatography with ICP-MS detection has reached maturity as the analytical technique for speciation of organometallic species in a variety of matrices. It shows comparable figures of merit with that of GC – MIP-AED for standard applications including speciation of organomercury, organolead and organotin in the environment but offers a number of advantages in cases where extremely low sensitivity, multielemental screening, precise isotope ratios measurements or the analysis of complex matrices are required.

3.4 Sample preparation for mercury determination

The sample preparation varies with the complexity of the matrix, but most complex samples require decomposition of the matrix and reduction of the mercury to its elemental form. It should be noted that, for mercury analysis in different sample matrices a careful quality control/quality assurance of the obtained data should be practice in order to validate the result which should include simultaneous determination of suitable certified reference materials (CRMs).

Currently, the CRMs prepared for the quality control/quality assurance of analytical values for mercury as well as methylmercury in various biological and environmental matrices are commercially available from several organizations, including the IAEA (International Atomic Energy Agency, Analytical Quality Control Services) (IAEA, 2003), NIST (National Institute of Standards and Technology, Office of Standard Reference Materials, USA) (Klobes *et al.*, 2006), NRCC (National Research Council of Canada) (Barcelo, 1993) NIES (National Institute for Environmental Studies, Japan) (Suzuki *et al.*, 2004), IRMM (Institute for Reference Materials and Measurements, European Commission) (IRMM, 2010) and SABS (South African Bureau of Standards) (www.sabs.ro). These CRMs may be used as needed.

3.4.1 Total mercury

The reactive mercury in water samples is determined by selective reduction with tin chloride ($SnCl_2$), which forms Hg^0. The stable complexes of Hg(II) and the organomercurials are not reduced (Stoichev *et al.*, 2006). For measuring Hg_{TOT} by this method it is necessary to oxidize all chemical forms of mercury in the water before the reduction step. The oxidation can be done in acid media with permanganate or bromate (Logar *et al.*, 2001). If preconcentration of Hg^0 is used, lower LODs are obtained (Puk and Weber, 1994).

Environmental solid samples are generally made into a solution with wet digestion methods and analyzed by compatible instrumental techniques.

Most of the conventional digestion procedures are not only laborious and time-consuming, but also lack sufficient efficiency and reliability. Other extraction methods, such as sonication, distillation or soxhlet extraction, also have the above drawbacks, even though reliable results are usually achieved (Tseng *et al.*, 1998).

Innovative techniques such as supercritical fluid extraction (SFE) and microwave-assisted extraction (MAE) have been developed and are a substantial advance. However, SFE potentially has technological limitations and shows insufficient extraction efficiency, usually depending on sample matrix and analyte polarity (Tseng *et al.*, 1998). Besides, the expensive equipment required increases the cost of the analysis.

Two different approaches in microwave extraction procedures are the use of a closed system (pressurized with a closed vessel) or an open system (non-pressurized with an open vessel) (Stoichev *et al.*, 2006, also see figure 3.7). They have different characteristics and application. The main advantages of the MAE technique are absence of inertia, rapidity of heating, reduction of extraction time, better reproducibility and reliability, ease of automation, and good ability for selective leaching and total digestion in a wide array of sample matrices. Thus, the application of this technique to sample preparation has been widely investigated in various fields of the environmental and analytical chemistry (Tseng *et al.*, 1998).

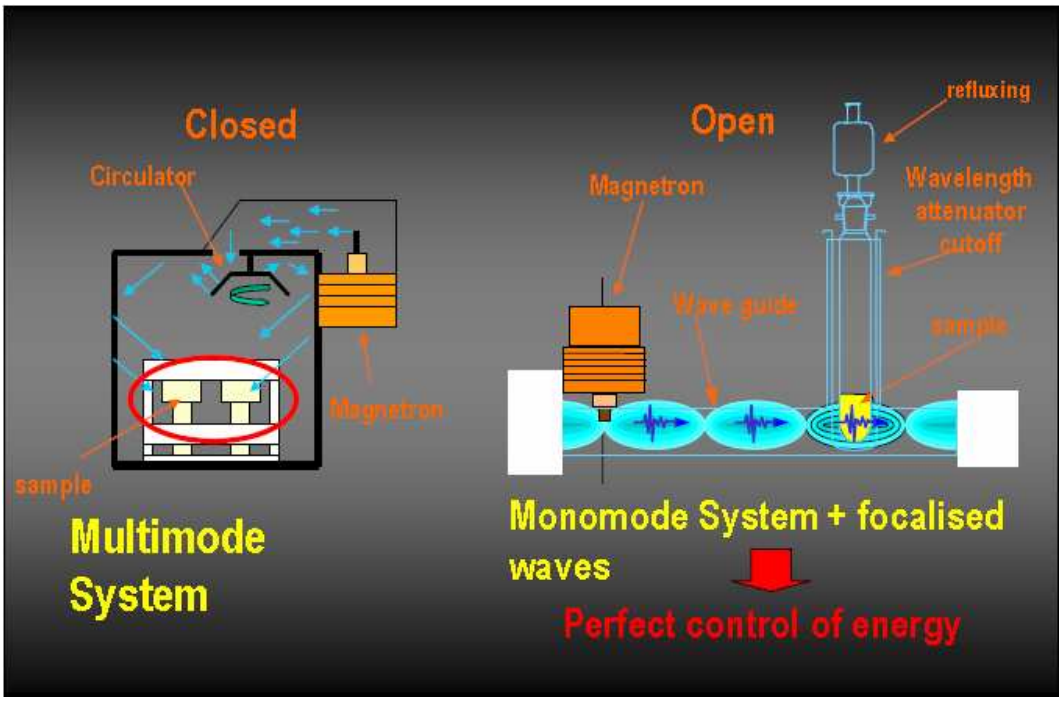

Figure 3.7 Closed and open microwave assisted extraction systems (Amouroux, 2007)

The extraction of Hg_{TOT} from sediments is performed with concentrated HNO_3 or acid mixtures under efficient reflux or bomb decomposition. Sometimes additional oxidants are added, such as H_2O_2, $KMnO_4$, etc. (Varekamp *et al.*, 2000).

3.4.2 Advances in sample preparation for GC-based hyphenated techniques

In order to extract the mercury species intact, several types of milder are used, such as citrate buffer and extraction with dithizone/chloroform, $KBr/CuSO_4/H_2SO_4$ (Lambertsson *et al.*, 2001), HCl/HNO_3 mixtures (Stoichev *et al.*, 2006), etc.

Solid sample preparation by acid or alkaline extraction with different heating sources (sonication, stream distillation, etc.) requires from 2 to 24 hours for complete recovery of mercury species whereas the microwave extraction of the mercury species is an extremely fast method (2-10 min) (Rodriguez Martin-Doimeadios *et al.*, 2003). Both open and closed systems are used for alkaline or acid extractions of mercury species from the sediments. This method should, however, be used with caution since it may also suffer, as for other techniques such as distillation-based methods, from artifact formation of CH_3Hg^+ (Stoichev *et al.*, 2006; Bloom *et al.*, 1997); Liang *et al.*, 2004).

The increased use of microwave-assisted extraction techniques in speciation analysis has been also reflected with regard to GC –ICP-MS (Lobinski *et al.,* 1998; Slaets *et al.,* 1999).

Volatile forms such as Hg^0 and Me_2Hg can be directly analyzed after fast desorption from the sampling traps (gold trap, carbotrap or Tenax) and preconcentration without derivatization. But, in most of the cases, it is necessary to derivatize the ionic mercury species in order to convert them to volatile forms, which are then separated by GC and detected by specific atomic detectors.

During the hydride generation (HG) with sodium borohydride ($NaBH_4$), the Hg^{2+} is transformed to Hg^0, while MeHg forms MeHgH. The derivatization should be applied in inert atmosphere and should start at pH 1-2 because otherwise MeHg is reduced to Hg^0. The HG can therefore be directly applied for sea and estuarine waters (Tseng et al., 1998).

The most important recent advances in sample preparation included the introduction of $NaBPr_4$ for the derivatization of organometallic species (De Smaele *et al.,* 1998), and the use of headspace solid-phase micro extraction (SPME) (De Smaele *et al.,* 1999; Aguerre *et al.,* 2000; Mester *et al.,* 2001), stir bar sorptive extraction (Vercauteren *et al.,* 2001) and purge and capillary trapping for analyte recovery and preconcentration (Wasik *et al.,* 1998).

3.4.3 Derivatization techniques

The position of tetraalkylborates allowing the derivatization in the aqueous phase, such as sodium tetraethylborate ($NaBEt_4$), for organomercury and organotin speciation analysis and the latest introduced sodium tetrapropylborate ($NaBPr_4$) for organolead has been well established. Synthesis of $NaBPr_4$ was described in detail and the possibility of the simultaneous determination of Sn, Hg and Pb following the propylation was demonstrated (De Smaele *et al.,* 1998).

Two careful comparison studies are worth-noting. In one of them three derivatization approaches, namely anhydrous butylation using a Grignard reagent, aqueous butylation by means of $NaBEt_4$ and aqueous propylation with $NaBPr_4$ were compared for mercury

speciation (Kotrebai *et al.,* 1999). The absence of transmethylation during the sample preparation was checked using a 97% enriched ^{202}Hg inorganic standard (Fernandez *et al.,* 2000).

During the ethylation with $NaBEt_4$ the Hg^{2+} is transformed to $HgEt_2$, while MeHg forms MeHgEt as follow:.

$$Hg^{2+} + 2NaB(C_2H_5)_4 \rightarrow Hg(C_2H_5)_2 + 2Na^+ + 2\text{"}B(C_2H_5)_3\text{"} \quad (3.4)$$

$$CH_3Hg^+ + NaB(C_2H_5)_4 \rightarrow CH_3HgC_2H_5 + Na^+ + \text{"}B(C_2H_5)_3\text{"} \quad (3.5)$$

The ethylation is motivated by the higher stability of MeHgEt compared to MeHgH. In salty water one part of MeHg is reduced to Hg^0 during the ethylation. Thus, this procedure can be directly applied only to fresh waters (Ceulemans and Adams, 1996). As mentioned above, isotope dilution ICP-MS is a new powerful approach to solve the problems with the matrix and non-quantitative derivatization. A drawback of the ethylation procedure is the impossibility to distinguish between Hg^{2+} and $EtHg^+$, both species that often coexist in the environment (Cai *et al.,* 1997). An alternative is the use of the propylation as a derivatization technique with $NaBPr_4$ as derivatizing agent which is more tolerant to interferences from chlorides (Demuth and Heumann, 2001). However, it was found that the propylation of extracts from soil samples suffers also from artifact formation of MeHg and especially of ethylmercury during the derivatization (Huang, 2005). Derivatization techniques for GC were reviewed (Liu and Lee, 1999).

3.4.4 Solid-phase micro-extraction

Solid-phase micro-extraction (SPME) is a preconcentration technique based on the sorption of analytes present in a liquid phase or, more often, in a headspace gaseous phase, on a microfiber coated with a chromatographic sorbent and incorporated in a microsyringe. The analytes sorbed in the coating is transferred to a GC injector for thermal desorption. SPME is an emerging analytical tool for elemental speciation in environmental and biological samples (Mester *et al.,* 2001). This solvent-free technique

offers numerous advantages such as simplicity, the use of a small amount of liquid phase, low cost and the compatibility with an on-line analytical procedure.

SPME is based on the equilibrium between the analyte concentrations in the headspace and in the solid phase fiber coating. Low extraction efficiencies are hence sufficient for quantification but the amount of the analyte available may be very small. Therefore, it is of interest to combine SPME with the high sensitivity of GC – ICP-MS.

The first work SPME - GC – ICP-MS concerned speciation of organomercury, -lead and -tin compounds ethylated in-situ with $NaBEt_4$ and sorbed from the headspace on a poly(dimethylsiloxane)-coated fused silica fiber (Moens *et al.*, 1997).

A detection limit of 2 pg l^{-1} was reported for an aqueous standard but a value of 125 pg l^{-1} was given for the sample extract corresponding to a DL in the low ng g^{-1} range (dry weight) (Vercauteren *et al.*, 2000).

3.5. Analytical methods for inorganic constituents in coal

Most technical and environmental problems associated with coal utilization arise because of the mostly non-combustible, inorganic components in coal. But, since the organic and inorganic fractions are intimately associated in coal, a complete separation of these components cannot be achieved and even a well-cleaned coal will contain a significant fraction of inorganics. Consequently, in order to minimize environmental problems related to coal-utilization it is important to understand the behavior of its inorganic components (Huggins, 2002).

Moreover, the determination of elemental concentrations alone is not enough to understand how a particular inorganic component will behave. Thus, it has been recognized that the mode of occurrence and the association of an element are often as important as its concentration in determining its behavior during coal cleaning, coal combustion, and other coal utilization processes (Raask, 1985; Swaine, 1990; Finkelman, 1994).

Methods for analysis of inorganic components in coal can be divided into the following categories (figure 3.8): (i) methods that measure elemental concentrations in the coal (or ash); (ii) methods that determine mineralogical components; and (iii) methods that

determine elemental modes of occurrence. These categories are briefly described in the following sections. Each of these three types of analysis provides different information about inorganic components in coal and to understand fully the behavior of a specific entity in coal utilization may require data from each type of analysis.

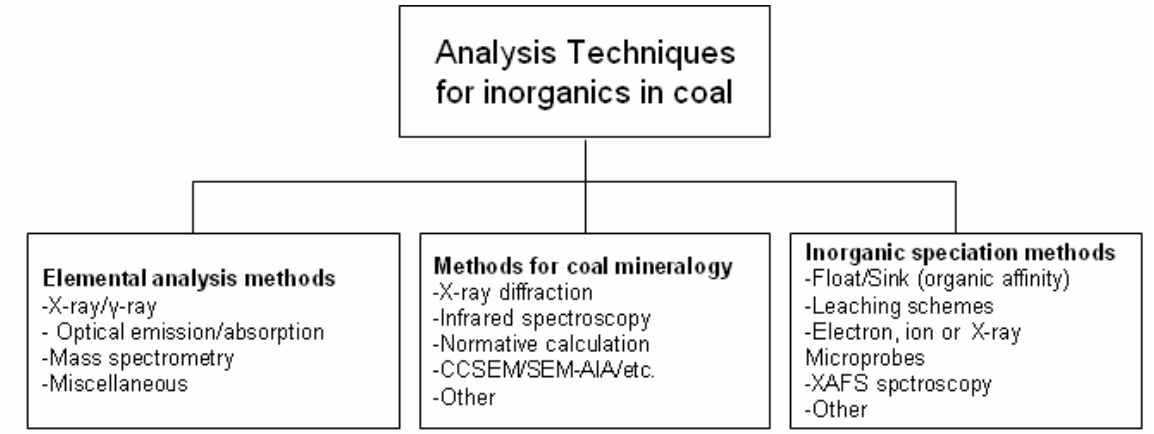

Figure 3.8 Subdivision of analytical techniques for inorganics in coal
(After Huggins, 2002)

It should be noted, although this is not within the scope of this section, that many other methods exist for determining specific entities in coal that could be considered to be in the inorganic realm (See, for example, ASTM, 2000). These methods include wt.% ash in coal, forms-of-sulfur analysis, total sulfur in coal, total chlorine in coal and SO_3 in ash from coal (Huggins, 2002 and references therein).

3.5.1 Analytical methods for elemental concentrations

There are many methods available for determining the concentrations of major and trace inorganic elements in coal. Such methods vary from those that are applicable to just one element in a particular matrix to instrumental techniques that are, in principle, capable of determining all elements in the periodic table in any matrix. Elemental analytical techniques can be divided into four broad groups (Huggins, 2002):

- Instrumental x-ray/γ-ray techniques: Instrumental Neutron Activation Analysis (INAA), Radiochemical Neutron Activation Analysis (RNAA), X-ray

Fluorescence (XRF), Synchrotron XRF (SXRF) and Particle Induced X-ray/γ-ray Emission (PIXE/PIGE).

- Optical absorption/emission techniques: AAS, OES and ICP-OES.
- Mass spectrometric (MS) methods: Glow-Discharge MS (GDMS), Spark-Source MS (SSMS), ICP-MS, etc.
- Miscellaneous techniques: such techniques generally determine one or a few elements that, for one reason or another, cannot be adequately determined by other more general methods; such techniques include wet chemical and various electroanalytical methods such as Ion Selective Electrode (ISE) and Ion Chromatography (IC).

In this section, emphasis will be given to determinations of the more critical trace elements, such as the 15 trace elements (As, Cd, Cr, Hg, Ni, Pb, Se, Be, Co, Mn, Sb, F, Cl, Th and U) defined as hazardous air pollutants (HAPs) by the US CAAA, (U.S. Congress, 1990). This list of elements includes all eight of the elements of ‘‘prime environmental interest’’ defined by Swaine (1990), such as mercury, and also most of the 14 others listed by him ‘‘that could be of environmental interest’’.

The elemental analysis methods described in this section can be performed on the whole coal directly or may be done on high-temperature ash (HTA), prepared by controlled combustion at a temperature between 400 and 800ºC, or on low-temperature ash (LTA), prepared by oxidizing away the carbonaceous matter under an oxygen plasma at temperatures that normally do not exceed 200ºC (Gluskoter, 1965; Shirazi and Lindqvist, 1993).

Generally, working directly on the coal allows a quicker and simpler sample preparation and one that is least likely to result in loss of volatile elements, such as As, Se, Hg, B, halogens, etc. However, whether working with ash or coal, most techniques yield their best results on samples that are finely pulverized and well homogenized.

The advantage of ashing is that it can significantly improve the sensitivity and precision of the determination of a trace element, although the matrix corrections required by some techniques (e.g., XRF) are also significantly larger for ash than for coal, which can somewhat offset the advantage. Furthermore, high-temperature ashing will cause easily volatilized trace elements to be released from the sample and completely lost for the

analysis. Sample preparation by low-temperature ashing (Gluskoter, 1965; Shirazi and Lindqvist, 1993) offers a good compromise between working on coal or HTA for trace element determinations, but unfortunately is less routinely practiced. One further advantage of the ashing is the easier dissolution of the inorganics.

Spectrometric techniques discussed in the previous sections (AAS, ICP-AES and ICP-MS) offer better performance and quantitative precision when the elements are introduced into these instruments in solution or liquid form, rather than in solid form. Hence, ashing is often considered a necessary step in preparing suitable analytes for these techniques. However, in the last decade or more, direct coal digestion has been explored as a means of preparing suitable liquids for these techniques, while at the same time avoiding both LTA and HTA. Such digestion methods enable a solution of coal and its components to be obtained that is suitable for analysis by techniques such as AAS, ICP-AES or ICP-MS. Methods for direct digestion of coal include microwave-oven acid digestion (Fadda *et al.,* 1995; Laban and Atkin, 1999), and a two-step acid digestion in a PFA bomb (Querol *et al.,* 2001). These coal digestion methods have been shown to yield analytical results that agree well with data for standard reference coals obtained by more conventional methods (Querol *et al.,* 2001).

3.5.1.1 Instrumental X-ray/g-ray techniques

INAA and XRF became accepted for elemental analysis of coal in the late 1960s (Kiss, 1966) and early 1970s (Kuhn *et al.,* 1975).

Major advantages of INAA are (Huggins, 2002): (i) sample preparation and, therefore, potential for contamination are minimized; (ii) up to 40 elements can be determined simultaneously; (iii) capability of determining some elements at sub-mg kg^{-1} concentrations; and (iv) the adjustment for matrix effects is generally much less critical than for the other techniques in this group.

Major disadvantages of the technique are (Huggins, 2002): (i) for best precision, a neutron reactor should be used as the source of the thermal neutron flux, which of course is a serious limitation on the availability of the technique; (ii) some elements, notably B, Be, Cd, Cu, F, Hg, Mo, Ni, Pb and Tl, are not easily analyzed by INAA because their

cross-sections for thermal neutron capture are low and hence, these elements have relatively large detection limits; and (iii) the technique tends to have a long turnaround time because it is typical practice to perform γ-ray counting immediately after irradiation and then again some weeks or months later so that interferences from short-lived radioactive species are eliminated and better precision can be obtained on longer-lived species. Despite these limitations, it is likely that INAA has been the most widely used method for obtaining concentration data on trace elements in coal and other fossil fuel materials (Bettinelli *et al.*, 1992).

XRF methods have been used for chemical analysis of major elements in geological materials, including coals and other fossil fuels, for many years (e.g., Kiss, 1966). Subsequently, XRF techniques have been extended to determinations of trace elements in coal as well (e.g. Kuhn *et al.*, 1975; Evans *et al.*, 1990).

The major advantages of XRF are: (i) it is widely available; (ii) modern instruments are often fully automated for unattended operation with up to 50 samples; (iii) sample preparation is relatively easy and usually involves no more than pulverization and pelletization; (iv) it covers the concentration range from <1 mg kg^{-1} to 100 wt.% (Huggins, 2002).

The main disadvantages appear to be: (i) its sensitivity to trace elements is comparatively low and hence detection limits and the precision and accuracy of the technique are not as good as for other methods; (ii) matrix corrections, although generally predictable, are needed for the best precision; and (iii) the escape depth for the fluorescent radiation is variable from less than 5 Am to as much as 200 Am, depending on the energy of the radiation (Huggins, 2002)..

3.5.1.2 Optical absorption/emission techniques

These techniques were the first multi-element techniques applied to trace element determinations in fossil fuels (see, for example, Brown and Swaine, 1964).

ICP-AES is the technique that is largely superseding other OES techniques because of the superior properties of an ICP as an excitation source (Swaine, 1990).

The latest developments with ICP and trace element analysis of coal appear to be moving in the direction of combining ICP with mass spectrometry (See section 3.2).

The main disadvantage of optical absorption/emission techniques for elemental determination in coal is that the analysis is best done on solutions of coal ash or on acid-digested coal rather than on coal directly. However, efforts have been made to introduce coal directly into a graphite furnace (GFAAS), and aqueous suspensions of finely ground coal, in particular, have been tried with limited success (O'Reilly and Hicks, 1979). Ikavalko *et al.* (1999) have successfully developed microwave-assisted acid digestion of coal as a means of introducing solubilized coal directly into the AA spectrometer. Standard solutions for each element to be determined are a necessity for development of in-house calibration curves for the most precise determinations; however, the use of reference standard materials, such as NIST SRMs, is generally not necessary as matrix effects are negligible (Huggins, 2002)..

Mercury was determined by the cold-vapor AAS procedures (Doughten and Gillison, 1990) and amalgamation of mercury on gold followed by flameless AAS has also been developed for the determination of mercury (Swaine, 1990).

A related method that is in use in some laboratories, as an alternative to AAS techniques, for the determination of arsenic, mercury and selenium is atomic fluorescence spectroscopy (Swaine, 1990; Querol *et al.*, 2001).

Mass spectrometric (MS) detection is being investigated and appended to many different volatilization methods for elemental analysis. For fossil fuel analysis, ICP-MS appears to be the most promising "new" technique; however, there are other promising MS techniques, such as Secondary Ion Mass Spectrometry (SIMS), and Accelerator Mass Spectrometry (AMS), both of which have not been applied extensively to fossil fuels (Huggins, 2002 and references therein)..

As for other MS techniques used for trace-element analysis, an important question to be addressed is whether or not such techniques can be developed for direct measurements on the coal rather than ash, so that the problem of loss of volatile elements during ashing may be avoided. One attempt to address this problem involves combining laser ablation (LA) processes on coal with an ICP-MS system (Lichte, 1992). The LA process forms

very fine particles that are then swept by an argon stream into the ICP, where they are vaporized and ionized for the MS determination.

Other methods have been reported which vary from that described by Lichte (1992) in the means used to prepare the coal prior to its introduction into the ICP by using a microwave oven acid digestion (Fadda *et al.,* 1995), a solution nebulization and laser ablation (Rodushkin *et al.,* 2000), or a two-step acid digestion in a PFA-bomb (Querol *et al.,* 2001). Up to 67 elements, ranging from lithium to uranium, and including such major elements as carbon, can be analyzed by ICP-MS (Conrad and Krofcheck, 1992) with detection limits for in the range of 5–100 ng g^{-1}. Accuracy and precision appear to be limited principally by sample homogenization as typically less than 5 mg of coal is consumed in the analysis (Lachas *et al.,* 1999). However, the precision, typically of the order of ±20% for a single scan, can be improved by combining multiple determinations as a single determination generally takes less than a minute.

The ICP-MS variations described above appear to constitute a powerful new technique for quantitative trace element determinations in fossil fuels.

3.5.1.3 Miscellaneous methods

For certain of the HAP trace elements, notably the halogens, none of the techniques discussed above is sufficiently sensitive for an accurate determination and/or the element is highly volatile so that it cannot be trapped efficiently by ashing and, hence, can only be determined on a whole coal basis. For these elements, various individualized analytical methods have been developed. These methods include electroanalytical methods, such as ion-selective electrode (ISE) and ion chromatography (IC), and chemical analysis methods.

ISE methods are generally applied to those elements that form stable anions in aqueous solutions, e.g. F^-, Cl^-, where an anion selective electrode can be used to determine the concentration of the desired anionic species. Generally, pretreatment techniques are used to separate and/or concentrate the anionic species of interest prior to the determination. Such methods include alkali fusion, oxygen bomb digestion, and pyrohydrolysis (Huggins, 2002 and references therein).

On another hand**,** the field of IC was established by efforts to couple a conductivity detector to separations performed on an ion-exchange chromatographic column and this technique has become the method of choice for the determination of anions in a wide range of samples (Cox *et al.,* 1992). As alternatives to conductivity detectors, amperometric and indirect photometric detectors have also been used with IC. For determinations of anionic species in coal, the major problem is to ensure complete extraction of all the anionic species from the coal, and total coal digestion methods are generally preferred. Fluorine, chlorine, and sulfur can be readily determined by IC methods after oxygen bomb digestion (Cox *et al.,* 1992) and other additional species, namely bromine, phosphorus, and nitrogen, may also be determined by this method (Huggins, 2002).

3.5.2 Determination of coal mineralogy

The determination of the mineralogy of a coal provides valuable information about the inorganics in coal that cannot be obtained from a chemical analysis alone. For example, geologists interested in following the origin and depositional history of coal forming peats and transformations of such peats into coal (coalification), can gain much information from the mineralogical and geochemical assemblages present in coal (e.g., Rimmer and Davis, 1986). In addition, researchers interested in how critical elements behave during coal combustion and cleaning processes need to know what minerals are present in the coal, what their size distributions might be, and how such minerals control or interact with critical elements during utilization. In order to do this, there is a need of obtaining as complete a mineralogical description of the coal as possible.

Unfortunately, it is not as easy to determine the mineralogy of coal as of other geological materials. Traditional petrographic methods are made more difficult because of the intimate admixture of inorganic matter and macerals in coal (Huggins, 2002). It is, therefore, of interest to develop new methods that will allow the accurate and reliable determination of mineral matter. Such methods should preferably be used without separation of the mineral matter from the coal so that association of minerals with macerals and of minerals with other minerals might also be determined.

The following four methods can be used for determining the mineral matter in coal (Jenkins and Walker, 1978): (i) X-ray diffraction (XRD); (ii) infrared (IR) spectroscopy; (iii) chemical analysis (normative calculation); and (iv) optical and scanning electron microscopy (SEM) methods.

3.6 Specific methods for the determination of modes of occurrence of trace elements

Concentration is not the only factor of importance that needs to be considered when assessing the behavior of trace elements in coal utilization and related environmental concerns. Another factor of equal and, sometimes, of more importance that should also be included in such assessments is information on the occurrence of trace elements in coal or ash. Numerous indirect methods have been tried for the determination of trace-element modes of occurrence in coal. The concept of organic affinities, defined by how a trace element partitions among float and sink gravity fractions, has been used to classify trace element occurrences in coal (Gluskoter *et al.,* 1977) with some success. More recent variations on these procedures have also been presented (e.g. Querol *et al.,* 2001).
However, questions regarding the association of the element, meaning whether an element is present in solid solution in a major mineral or forms its own mineral, are usually not answered by this indirect method. More recently, attention has shifted away from float-sink methods to leaching methods as the prime indirect method of determining elemental modes of occurrence. However, leaching schemes are based on an assumed limited set of elemental occurrences. There is no provision in such tests for unanticipated occurrences. Consequently, there remains considerable uncertainty regarding the validity of the data obtained in such tests, unless they are verified by direct observational methods (Finkelman, 1994).

Various electron and ion probe techniques have been used to examine trace element modes of occurrence directly on coal. Scanning electron microscopic and micro-X-ray diffraction techniques have been used to directly investigate the occurrence and association of many trace elements in coals (Finkelman and Stanton, 1978 and Finkelman, 1981; 1982; 1988). However, such observational microscopic techniques are

very time-consuming, even for semi-quantitative information, and tend to favor the occurrences of trace elements in discrete mineral forms rather than the dispersed occurrences of the element in macerals in the coal (Huggins, 2002).

Another direct approach is to establish spectral ‘‘fingerprints’’ for some standard occurrences of an element and then employ the same spectroscopic technique to measure the spectra from the element in a coal or coal fraction. Hence, by comparing the spectrum from the coal with spectra in the database of standards and employing spectra deconvolution or simulation methods where needed, it is possible to determine the major modes of occurrence of an element in a particular coal (Huggins, 2002). One spectroscopic technique that has been extensively employed for investigating the forms of occurrence of trace elements in coal and ash is X-ray absorption fine structure (XAFS) spectroscopy.

Microscopic and/or spectroscopic methods can be combined with indirect methods of determining modes of occurrence, such as float-sink methods (Huggins *et al.,* 1997) or sequential leaching methods (Kolker *et al.,* 2000) and the net result is better understanding of both the modes of occurrence of the elements and of the assumptions inherent in the indirect methods.

3.6.1 Indirect methods

The organic affinity of the element can be determined by performing float/sink tests at different specific gravities and then determining the trace element contents in the different fractions. The higher the organic affinity the more the element reports to light specific gravity fractions, and hence, the more it is associated with the organic fraction of the coal. This method was exhaustively used in the major trace element study performed by Gluskoter *et al.* (1977).

The efficiency of float/sink processes with respect to a given trace element in a specific form may vary greatly from coal to coal, merely as a consequence of how the host mineral or maceral distributes between the float/sink fractions. These different pieces of information cannot be separated. Hence, different values of organic affinity for a given element among different coals have little or no significance. In addition, the knowledge

that the effective organic affinity for a trace element in a coal is low still does not provide any insight into whether the trace element is dispersed in a major mineral or forms its own mineral (Huggins, 2002).

Despite these limitations, however, the concept of organic affinity may still be a useful parameter in the absence of other information.

Leaching methods have a major advantage over float-sink methods in that specific elemental forms are anticipated to be either present or absent in different fractions depending on their solubility behavior in the various reagents used for the different leaching stages. A number of sequential leaching methods have also been proposed for understanding elemental modes of occurrence and basically each laboratory has their own leaching scheme. Davidson (2000) compares methods and data from sequential leaching schemes developed in three research laboratories located in the United States, in the United Kingdom and in Australia. These three schemes are compared and contrasted in figure3.9.

In all three schemes, the idea is to leach specific groups of inorganics or minerals progressively from the coal. After each stage of the leaching scheme, a multi-element chemical analysis is performed on the residue and/or the leachate to determine the amounts of trace elements removed by that particular leaching reagent. The different fractions of an element removed by the various leaching reagents are then assumed to have occurred in the coal in different forms, as indicated in figure 3.9.

The main problem with sequential leaching protocols is that the classification is principally based on the expectation of how certain minerals will behave in a suite of increasingly stronger reagents and there is little accommodation of any variation in leaching behavior due to variations in composition, grain-size, association, etc.

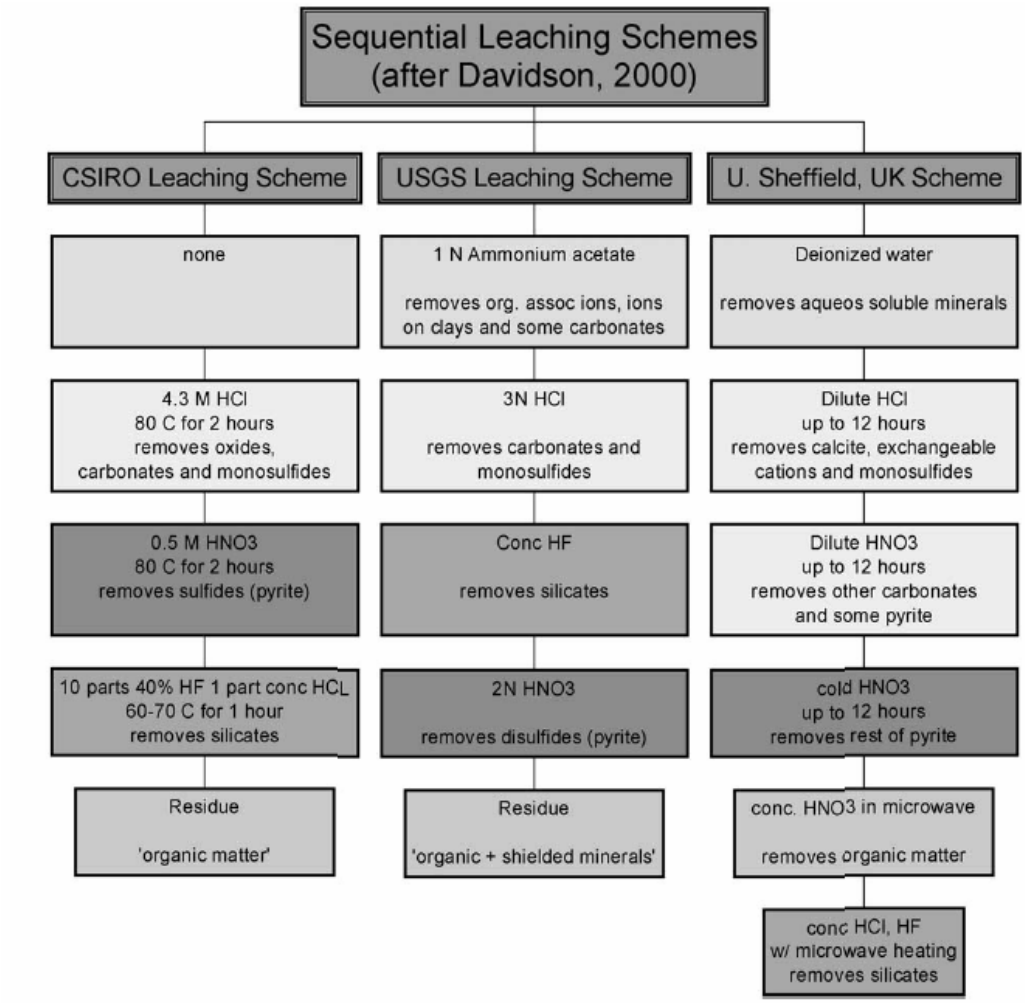

Figure 3.9 Comparison of sequential leaching schemes used in the IEA speciation study (Huggins, 2002 and the reference therein)

For example, ‘‘carbonate minerals’’ are expected to dissolve in HCl, but depending on the strength of the solution, the solution temperature, the grain-sizes of the carbonate minerals, and the time of exposure of the coal to the leachant, such procedures may be effective for calcite, but less effective or even ineffective for other, less-common carbonates, such as siderite, magnesite, rhodochroisite, or dolomite (Huggins, 2002).

Querol *et al.* (2001) list a number of other specific deficiencies of leaching methods. It must also be re-emphasized that leaching protocols will never identify an unusual or unexpected elemental occurrence.

Both sequential leaching and float/sink separations have difficulty dealing with fine mineral matter that is highly dispersed and encapsulated in macerals by organic matter.

For float/sink methods, the highly dispersed nature of such fine mineral matter generally causes them to be associated with the lightest specific gravity fractions; consequently, such inorganic components are typically referred to as ‘‘organically associated’’. For leaching methods, the encapsulation of inorganics by organic matter can make them impregnable to attack by the leaching agents and hence such inorganics are always incorrectly assigned.

There are ways to avoid this complication An alternative approach might be to conduct sequential leaching schemes on low-temperature ash, in which all the encapsulating organic matter has been oxidized away. Such an approach does not appear to have been explored significantly (Huggins, 2002).

In order to establish better trace element occurrences, various approaches have been attempted that combine two indirect methods. For example, Finkelman *et al.* (1990) employed sequential leaching complemented by data on element volatility from sequential combustion (ashing) tests at different temperatures. Querol *et al.* (2001) used results from both sequential leaching and float-sink separation. However, the results obtained by these indirect techniques, even when combined, still often remain inconclusive and they need to be complemented and confirmed by data from more direct methods.

3.6.2 Direct microscopic methods

A scanning electron microscope (SEM), equipped with an energy-dispersive X-ray (EDX) detector and a back-scattered electron (BSE) detector, can be used to determine trace element occurrences in polished or fracture surfaces of coal specimens. The reason why the SEM is capable of finding many trace element occurrences is because the brightness of the backscattered electron image (BSEI) is determined in large part by the average atomic number of the material under the electron beam (Huggins, 2002). As a result, phases rich in heavy trace elements appear much brighter than normal silicate and sulfide minerals in the coal and can be readily located for standard EDX analysis in the SEM. The main advantage of the SEM-EDX technique is that information is obtained on the chemical association of the trace element, from which the mineral occurrence can

often be deduced. On occasion, the individual mineral grain containing the trace element can sometimes be removed and subjected to micro-Xray diffraction to confirm its mineralogical identity.

Unfortunately, as mentioned previously, the method is very time-consuming and demanding of the microscopist. SEM-EDX is also not as powerful for determining trace element occurrences that are dispersed at low abundance levels, either in major minerals or in macerals in the coal.

Further, the lower the atomic number of the trace element, the more difficult it becomes to locate, regardless of whether it is present in discrete or dispersed form. Therefore, this technique is likely to be biased towards the discrete and exotic forms of occurrence of heavy trace elements, unless the investigator is extremely systematic in his sampling (Huggins, 2002).

XAFS spectroscopy, on the other hand, appears to be the only spectroscopic method, currently available, that is capable of obtaining significant information on trace element forms of occurrence in fossil fuels and related materials. Unlike the microscopic methods described above, the XAFS spectrum derived from a given element is a weighted average of all forms of occurrence of the element in the coal or coal fraction, regardless of whether the element forms a discrete mineral or is dispersed in major minerals or macerals. Indeed, if there is a bias with this technique, it is likely to be towards dispersed forms-of-occurrence rather than discrete mineral occurrences of a trace element, as has been demonstrated for the major element, sulfur (Huggins *et al.,* 1992). Moreover, in addition to being a direct probe of an element's mode of occurrence in coal or ash, the technique is also nondestructive.

The major inconveniences of the XAFS are that it can only be performed at a synchrotron source and, consequently, the availability of the method is limited; and only a single spectrum is obtained that is a weighted average of the spectra of the different forms of occurrence of the element in the coal or ash (Huggins, 2002).

In theory, XAFS spectroscopy is applicable to virtually all elements in the periodic table. In practice, however, the technique is currently limited experimentally to trace elements

with atomic numbers above 20 that occur in coal in excess of about 5 mg kg^{-1} (Huggins, 2002).

In conclusion, environmental issues associated with coal utilization, especially the release of particulate matter and HAPs to the atmosphere from coal combustion, are placing increased emphasis on accurate and reliable analytical methods for inorganics in coal. At the current time, it would appear that elemental concentrations can be reliably determined using techniques such as X-ray fluorescence for the major inorganics in coal and a combination of various methods (e.g., INAA, PIXE/PIGE or polarized XRF combined with ICP-MS or ICP-AES and AAS methods) for the 15 or so trace elements listed as HAPs in the 1990 Amendments to the Clean Air Act.

Various methods for determining the mode of occurrence of trace elements in coal were presented. There appears to be a significant need here for the combined application of both direct and indirect methods for elemental speciation. Data based solely on inferences from indirect methods are fraught with uncertainty because such methods are based on unverified assumptions. Use of electron or ion probe methods to obtain information on the elemental associations of the trace element will help resolve such uncertainties. Similarly, although XAFS spectroscopy can be used to determine elemental modes of occurrence directly, this method suffers a high detection limit and would appear to be more powerful when combined with leaching or other indirect speciation methods, because it can also test the assumptions and help, where possible, resolve the uncertainties inherent in the indirect methods.

Finally, as summarized by Davidson (2000), agreement among the methods for element speciation may vary from reasonable (e.g. for Mn, Cu, Cd, Se, and Hg) to poor (e.g. Co, Ni, Be, Sb), with the remainder intermediate (e.g. Se, Pb).

Chapter 4
Objectives of the study

Based on the different aspects highlighted in the problem statement, namely the need of the development of analytical techniques for gaseous mercury measurements, the limited data on the mercury content in South African coals, including the lack of information on its chemical and physical associations, and also on the need of a better assessment of mercury pollution and fate in the country ecosystems (biological, geological and atmospheric systems) impacted by gold mining operations, the main objectives of this project were divided into three different sections as follows:

- The development and optimization of procedures for the sampling and determination of gaseous mercury;
- The determination of total mercury and the characterization of its speciation in South African coals and;
- The quantitative assessment of mercury pollution and the determination of the mercury distribution, transformation, transport and fate in some selected goldfield areas within the Witwatersrand Basin.

The following questions were addressed in order to achieve this aim:

- How can locally made materials contribute in developing a simple and cost effective trapping technique for the sampling and determination of ultratrace mercury and how can their performance be compared to conventional traps?
- What is the average mercury concentration of South African coals that can be used for reliable inventories of the atmospheric mercury emission from local coal fired power stations?
- What are the modes of occurrence of mercury in South African coals and what is the efficiency of solvents extraction procedures in reducing the mercury content in the study coals? Does the toxic methylmercury naturally occur in South African coals and at which extent?

- What is the impact of current as well as historic gold mining activities in terms of mercury pollution in the local environmental systems?
- What are the biogeochemical interactions (i.e. bioavailability, distribution, mobility and fate) of mercury in the South African semi arid environment?
- What are the principal factors that control the mercury speciation in the study systems?
- How do climatic and seasonal changes affect the terrestrial mercury cycling?

To answer these questions, the following specific objectives were addressed:

- To use nano-structured gold supported on metal oxides materials for the preconcentration of mercury in its gaseous form and to optimize analytical parameters of the nanogold traps using atomic fluorescence spectrometry.
- To apply the developed and optimized methodologies to environmental samples.
- To characterize coal and ash samples collected from some South African coal-fired power stations and/or coalfields, to determine the total mercury content in these samples and compare the average concentration with the literature data for local and world coals.
- To identify and quantify inorganic and organic mercury species in local coals using speciation techniques and also to provide information on modes of occurrence of mercury in the study coals using sequential extraction procedures.
- To identify potential sources of mercury pollution in goldfields and to make quantitative assessments of geochemical parameters, important anions, total mercury and other heavy metals through field sampling and laboratory analysis by using a wide range of analytical techniques including spectroscopic, and electroanalytical measurements and to use this data for geochemical modeling.
- To study the speciation and distribution of mercury by the coupling of gas chromatography and inductively coupled plasma mass spectrometry (GC-ICP-MS) in water systems distal and proximate to mining Tailings storage facilities (TSFs) and to map the trends using GIS techniques.
- To assess the impact of long term pollution and seasonal changes on the spread of mercury in watersheds.

- To determine factors controlling the methylation of mercury in the study waters and sediment profiles by correlating analytical data from spectrometric and electroanalytical measurements with geochemical (field) data such as pH and redox measurements.
- To determine the bioavailability of mercury and the extent of its accumulation in plants (that is, biological systems).

Chapter 5
Sampling procedures and optimization of analytical methods

5.1 Introduction

This chapter focuses on the sampling techniques, the sample preparation procedures and the analytical techniques used. Details about the analytical methodologies and instrumental parameters used before their application to real environmental samples are provided. Further details for the various sampling sites are given in each case study.

5.2 Cleaning protocol

Working under clean conditions is one of the most important considerations for successful analysis at very low concentration levels. Special attention was paid to the procedure for cleaning all vessels used for sampling and sample preparation. The aim of the rigorous cleaning procedure used was to ensure that analysis will be performed with a minimum risk of contamination. The following cleaning protocol, adapted after Monperrus *et al.* (2005), was used for all experiments in this study:

- All vessels were first cleaned with a biocide detergent (1 or 2% in hot tap water) and stored for half an hour, rinsed thoroughly with tap water and then with deionized water with an electrical resistivity of 18.2 MΩ cm (Millipore, USA).
- All vessels were then soaked in a 10% (v/v) HNO_3 analytical grade (Merck) solution for 3 days (or for an hour in ultrasonic bath). Bottles were then rinsed with deionized water.
- All vessels were finally soaked in 10% (v/v) HCl analytical grade (Merck) solution as described above for HNO_3. Bottles were then dried in a laminar flow hood or in an oven after being rinsed with copious amount of de-ionised water and stored in double sealed polyethylene bags until use.

5.3 Sampling

The different sampling techniques used for waters, sediments, tailings and plants collection are presented below including their pre-treatment and storage conditions prior sample preparation steps. *In situ* measurements conditions are also discussed.

5.3.1 Water sampling

The water samples were collected according to commonly accepted sampling procedures (Tutu, 2004 and references therein; USEPA, 2007b; Quevauviller, 2001). Water samples were collected as duplicate samples at each site into acid-washed and conditioned polypropylene (PP) one litre bottles. The recommended "clean hands–dirty hands" procedure was used during sampling in order to discriminate the contamination risk (Montgomery *et al.,* 1995).

Surface waters were collected in dams and wetlands "by hand" directly in the sampling bottle using nitrile gloves. The bottle had to be opened and closed under water to avoid mixing with the surface microlayer or oxidation of sample (Stoichev *et al.,* 2006). In streams, samples were taken in the main stream flow away from the banks and a point sampler consisting of an aluminium rod and a PP cup was used to collect the sample.

The sampling bottles were rinsed with the site water immediately before sampling and the rinsed water was discarded away from the sampling point. The goal of this procedure was to condition or equilibrate the sampling equipment to the sample environment and to help ensure that all cleaning-solution residues had been removed before sampling (Tutu, 2006; Stoichev *et al.,* 2006).

The PP bottles were filled with water leaving no air space and the field parameters such as temperature (T), pH, electrical conductivity (Ec) and redox potential (Eh) were measured *in situ* before tightly closing the containers to prevent any leakage (figure 5.1). Each bottle was then marked with the date of sampling and sample description, placed into cooler boxes and transported to the laboratory. Global Positioning System (GPS) coordinates were also taken at each sampling point and were used for mapping with the

Geographic Information System (GIS) software (ArcGIS 9.x, USA). Quality control, or blank, samples were used to assess the level of contamination and to quantify any background concentrations.

Field parameters measurements were carried out with a portable kit (WTW multi-parameter instrument pH/Cond 340i and ORP, Germany) equipped with a pH electrode, an integrated temperature probe, a standard conductivity cell and an oxidation-reduction potential probe. The meters were calibrated and tested prior to sampling using standard buffer solutions according to the manufacturer's instructions.

Redox potentials were obtained from Pt electrodes versus Ag/AgCl and all reported potentials were corrected relative to the standard hydrogen electrode (SHE).

Figure 5.1 *In Situ* measurements of physico-chemical parameters of a water sample

Once in the laboratory, each sample was divided into two parts: the one was filtered under vacuum with 0.45 µm filter papers (Millipore) and used for the anions (Cl^-, F^-, NO_3^-, NO_2^-, PO_4^{3-} and SO_4^{2-}) determination by ion chromatography; the other was unfiltered and acidified with 1% (v/v) HCl suprapure (37%, Sigma Aldrich) and then analysed for mercury and other metals using ICP techniques. The samples were transferred in PTFE (or Teflon®) bottles or in borosilicate bottles with PTFE-lined caps and stored at 4°C until analysis.

5.3.2 Sediment sampling

Sediment (surficial and bulk) samples were collected from adjacent to gold tailings facilities, and from dams, streams and wetlands. Background samples were also collected in order to determine the contrast between background mercury concentrations and contamination.

For stratigraphic (profile) studies, piston corer (auger) or Polyvinylchloride (PVC) cores of 50 cm height were used for sample collection. In a few cases, pits were excavated to a maximum depth of 3 m and samples were collected at 20 cm depth intervals after scrapping off the outer layers of the sediment profile. Geochemical (field) parameters of the sediments were also determined, mainly by inserting the appropriate probe into the slurry *in situ*. Where the slurry was not immediately available, it was made by mixing a portion of the sediment (about 50 g) to about 50 ml of deionised water and the measurements taken of the resulting slurry (Tutu, 2006). The GPS coordinates of the sampling points were also measured. Collected samples were then stored in double plastic bags in the dark within cold boxes.

In the laboratory, samples were first frozen at -18°C to increase the stability of $MeHg^+$ (Parker and Bloom, 2005) and PVC cores were sliced into portions of 2 to 5 cm thickness using a saw equipped with a clean stainless steel blade. The sediments were sieved, when necessary, with Nylon sieves to eliminate stones and other gross particles. After homogenization, a representative portion of each sample was freeze-dried (Varekamp et al., 2000) in a lyophilizer (Labconco, USA) at -40°C for 24 to 48 hours and the dried samples were pulverised with acid-washed pestles and mortars and then stored at 4°C in acid-cleaned polystyrene bottles for further preparation (figure 5.2).

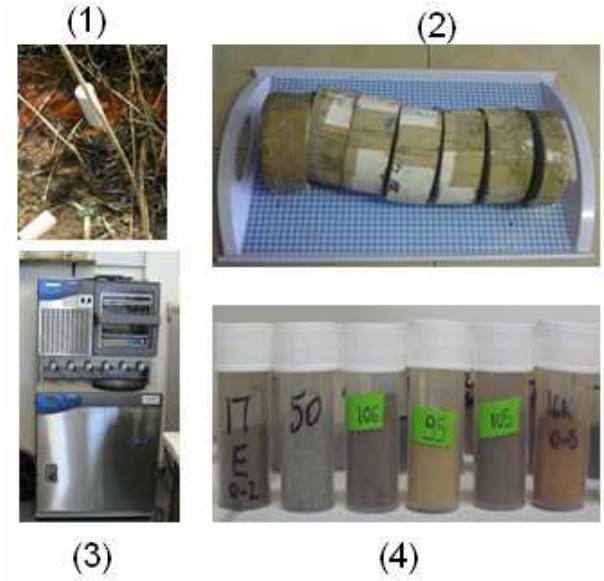

Figure 5.2 Sediment core sampling (1) and pre-conditioning steps which included: dissection of the PVC core (2), sample drying in a lyophilizer (3) and storage in acid-washed polystyrene bottles (4)

.

5.3.3 Tailings sampling

Tailings samples were collected both vertically and laterally. Near surface samples were collected by means of shovels (after scrapping off the oxidised layers) while the subsurface samples were collected by means of PVC cores (figure 5.3). The methods used depended largely on the accessibility of the sampling points. The samples were then treated in the same way as for sediments.

Figure 5.3 Sampling in bottom TSF with a PVC core

5.3.4 Plants collection

Samples of plant tissues (algaes, twigs and leaves) were collected randomly from wetlands, creeks, ponds or from plants growing on the tailings dumps and tailings footprints for phytoremediation purposes. To minimize the risk of contamination, plastic gloves were used to collect the samples (figure 5.4) and hand separation of the plant tissues from other material. Samples were rinsed with deionized water to remove eventual metals attached at the surface and were kept in polyethylene plastic bag, then frozen and dry-frozen at -40°C (Cabanero *et al.,* 2002) within hours of collection. After being ground to a homogeneous powder with the help of liquid nitrogen (Heller and Weber, 1998), the samples were stored in the dark, to avoid photodegradation, cleaned polystyrene bottles (Yu and Yan, 2003).

Figure 5.4 Collection of algae in a creek

5.3 Sample preparation

Sample preparation procedures for mercury analysis was not only matrix dependent but also depended whether total mercury or mercury species analysis had to be performed. An analytical balance (Precisa 180A, Switzerland), with a precision of 10^{-4} g, was used for all the weightings.

5.3.1 Total mercury determination

The procedure used for the sediment samples treatment was adapted from an existing method developed by the US Environmental Protection Agency (USEPA, 1996; Mangum, 2009).

Briefly, 0.1 ± 0.005 g of sediment was digested in a closed microwave assisted extraction (MAE) system (Multiwave 3000, Anton Paar) equipped with PTFE-TFM liners (figure 5.5) at 800 W and for 45 minutes using 6 ml HNO_3 (Merck), 2 ml HCl (Merck), 1 ml HF (Merck) and 1 ml H_2O_2 (Merck). The average temperature within the extracting vessels was about 170^0C.

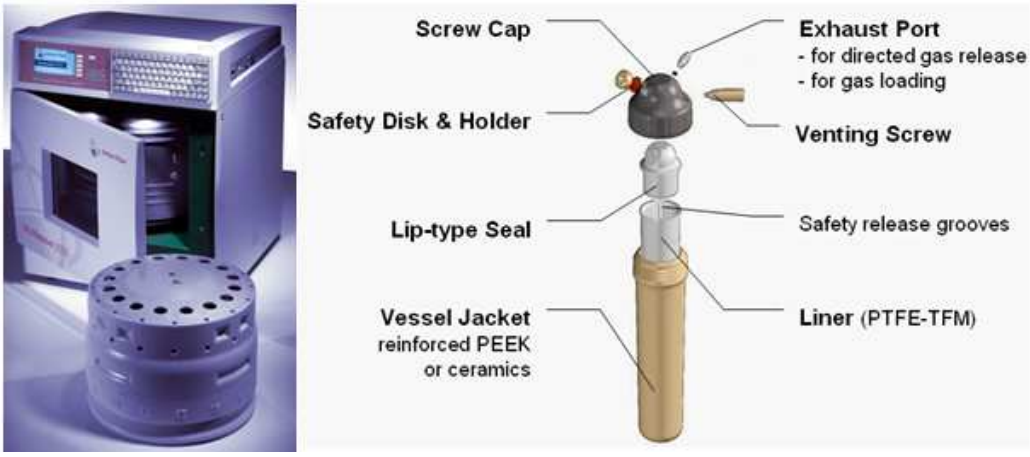

Figure 5.5 The Multiwave 3000 MAE system and the vessel design

The microwave programme is presented in the table 5.1 below. Six millilitres of concentrated H_3BO_3 (Merck) were added to each sample to neutralize the damaging effect of HF for glass made materials such as the ICP torch. The digested samples were then diluted with deionized water and kept at 4°C in Teflon bottles until analysis.

Table 5.1 Microwave programme for sample extraction

Phase	Power (W)	Ramp (min)	Hold (min)	Fan
1	800	10:00	20:00	1
2	0	5:00	10:00	3

Sample weight: 0.1g; Reagent: HNO_3 (6ml); HCl (2ml); HF (1ml); H_2O_2 (1 ml)

5.3.2 Analysis of mercury species

For the extraction of Hg^{2+} (IHg) and CH_3Hg^+ (MHg) species in solid samples (Dietz et al., 2001; Tseng et al., 1997a) an aliquot of 0.25 g of dry sample was placed in the extraction tube of an open-microwave (figure 5.6) oven (CEM, USA) and 5 ml of 6M HNO_3 (Sigma Aldrich) for sediments or 25% tetramethylammonium hydroxide (TMAH, Sigma Aldrich) for plants were added and then exposed to microwave radiation at 70 W for 4 min.

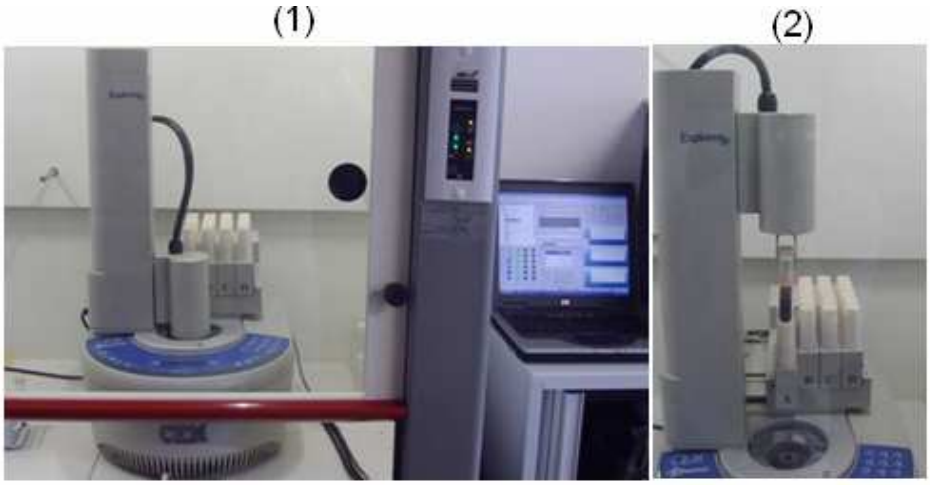

Figure 5.6 The CEM apparatus (1) with an automated vessel introduction system into the microwave oven (2)

The extraction of mercury compounds in plants by microwave systems has been performed using TMAH since this reagent was found by Tseng *et al.* (1997b) to allow complete alkaline hydrolysis of biomaterials (i.e., proteins, lipids, and sugars). Extraction using TMAH appeared to be efficient for mercury species in biological tissues.

After centrifugation, the extract was transferred into a 22-ml Pyrex vial with Teflon-lined cap and, in the case of isotope dilution (ID) analysis, all the extracts were spiked prior to derivatization with a specific amount of isotopically enriched standard solutions of Hg^{2+} (Hg^{199}) and CH_3Hg^+ (CH_3Hg^{201}) obtained from CNRS-LCABIE-IPREM (France). The spiking step was not necessary when the analysis was performed by external calibration. During the derivatization of mercury compounds for GC-ICP-MS analysis, mixed standards solutions of different mercury compounds, plant and sediment extracts were buffered to pH 3.9 - 4.1 with 5 ml of a 0.1 M CH_3COOH-CH_3COONa buffer. The pH was adjusted, when needed, by addition of suprapure HCl or NH_3 (Sigma Aldrich). Then, 0.2 ml of 1% (w/w) high purity $NaBEt_4$ (Sigma Aldrich) was added together with 1 to 2 ml of isooctane (2,2,4-Trimethylpentane, CHROMASOLV® Plus, 99.5%, Sigma Aldrich) to derivatize and extract the alkylated compounds formed. After 5 min of manual shaking and 5 min of further centrifugation (2500 rpm), the organic layer was transferred to a glass vial and stored at -18°C until measurements. All samples were measured on the day of their derivatization.

In the case of water analysis, 100 ml of sample accurately weighed in a flask were directly submitted to the spiking (for ID analysis) followed by derivatization with $NaBPr_4$ (instead of $NaBEt_4$) in order to see the eventual occurrence of ethylmercury species but also to minimize the effect of chloride content that affects the ethylation procedure, as demonstrated by Monperrus *et al.* (2005).

5.4 Optimization of analytical instruments for mercury determination

An ICP-MS (SPECTROMASS 2000, Germany) instrument, shown in figure 5.7, was used for Hg_{TOT} determination. Acid-washed torch and spray chamber were used in order to minimize contamination. The nebulizer was also rinsed with deionized water and silicosteell tubings (Restek) were used to reduce mercury adsorption in the sample introduction system.

Figure 5.7 Image of the ICP-MS used for Hg_{TOT} determination

ICP-MS parameters such as ion optics voltages, mass scan, time scan, pump speed, argon flow were optimized for a better resolution and analyte-background intensity ratio. An example of optimized instrument conditions is presented in table 5.2. The software used for data analysis was Smart analyzer provided by SPECTRO.

A range of mercury standards in 5% HNO_3 were prepared on a day of analysis from a stock solution of 10 mg L^{-1} (De Bruyn Spectroscopic Solutions, SA) for the instrument calibration and analyses were performed on triplicates. Results were reported as means of 7 measurements.

GC-ICP-MS coupling was achieved using the X-Series 2 ICP-MS (Thermo Scientific, USA) and all electrical and analytical connections were established using the Thermo Scientific GC-ICP-MS Coupling Pack (figure 5.8).

Table 5.2 ICP-MS parameters

Instrument Parameters	SPECTROMASS 2000
RF power	1350 W
Nebulizer gas flow	1000 ml min^{-1}
Coolant gas flow	3 scale units
Auxiliairy gas flow	1 scale units
Pump speed	2
Nebulizer step	1
Default dwell time	1s
Isotope monitored	^{199}Hg, ^{201}Hg, ^{202}Hg
Sampler	Nickel
Skimmer	Nickel
p Interface	2.013 mbar
p Quadrupole	5.46 x 10^{-6} mbar
Detection mode	SEM

The X-Series 2 ICP-MS is configured with a dual mode sample introduction system to enable simultaneous introduction and analysis of liquid and gaseous samples.

Figure 5.8 Hyphenated GC-ICP-MS X-Series 2

The GC, equipped with an automatic injector, is then connected to the X-Series 2 using the temperature controlled GC Transfer Line and Power Supply Unit. The key components of this sample introduction system include the facility for simultaneous

connection of both the temperature controlled GC transfer line and the nebulizer/impact bead spray chamber configuration.

The dual mode sample introduction system allows analysis of aqueous multielement solutions for X-Series 2 tuning and optimization whilst operating in the GC-ICP-MS configuration.

This configuration enabled continuous aspiration of internal standard (10 μg L^{-1} of ^{205}Tl) and allowed optimization of the instrument performance and simultaneous measurement of ^{205}Tl (Sigma Aldrich) for mass bias correction during the chromatographic run. Operating conditions and instrumentation are listed in table 5.3.

Table 5.3 Operating conditions of the hyphenated GC-ICP-MS

GC conditions	
Column	MXT Silicosteel 30 m; i.d. 0.53 mm; d.f. 1 μm
Injection port	Splitless
Injection port temperature	250°C
Injection volume	1 μl
Carrier gas flow	He 25 ml min^{-1}
Make-up gas flow	Ar 300 ml min^{-1}
Oven program	
Initial temperature	60°C
Final temperature	250°C
Ramp time	60°C min^{-1}
Transfer line	
Temperature	280°C
Length	0.5 m
Inner	Silicosteel i.d. 0.28 mm; o.d. 0.53 mm
Outer	Silicosteel i.d. 1.0 mm; O.d. 1/16 inch
ICP-MS conditions	
Rf power	1250 W
Plasma gas flow	15 L min^{-1}
Auxillary gas flow	0.9 L min^{-1}
Nebulizer flow	0.6 L min^{-1}
Isotopes/Dwell times	Hg (202, 201, 200, 199, 198)/30 ms; Tl (205)/5 ms

GC separation parameters (temperature program and gas flow) were optimized in order to obtain symmetrical peaks and to minimize peak integration errors. The raw data of the transient isotope signals for the different species were further processed using "Traitement des Signaux Transitoires" (TST) software developed by the CNRS-LCABIE research unit (France) in order to obtain the peak areas and the corresponding isotope ratios.

Working standard solutions of inorganic and methylmercury (IHg and MHg) were prepared on the day of analyses by appropriate dilution of the stock standard solutions of $HgCl_2$ (Sigma Aldrich) in 1% HNO_3 and CH_3HgCl (Sigma Aldrich) in 1% CH_3OH (Merck) respectively and then stored in the refrigerator. Enriched standards abundances (IHg^{199} and MHg^{201}) were determined experimentally and concentrations of spiked enriched standards were determined by reverse dilution.

5.5 Figures of merit

An excellent linearity was obtained with the ICP-MS instrument for Hg_{TOT} standards and the calibration range was about 0.1 to 50 ng ml^{-1} for all the isotopes analyzed as it is shown in table 5.4 and figure 5.9. The limit of detection (LOD) for ^{202}Hg isotope was then 0.06 μg L^{-1}.

Table 5.4 ICP-MS calibration parameters

Parameter	^{199}Hg	^{201}Hg	^{202}Hg
Range (μg L^{-1})	0.093 - 50.000	0.107 - 50.000	0.067 - 50.000
LOD (μg L^{-1})	0.093	0.107	0.067
Correlation coefficient	0.998	0.998	0.999

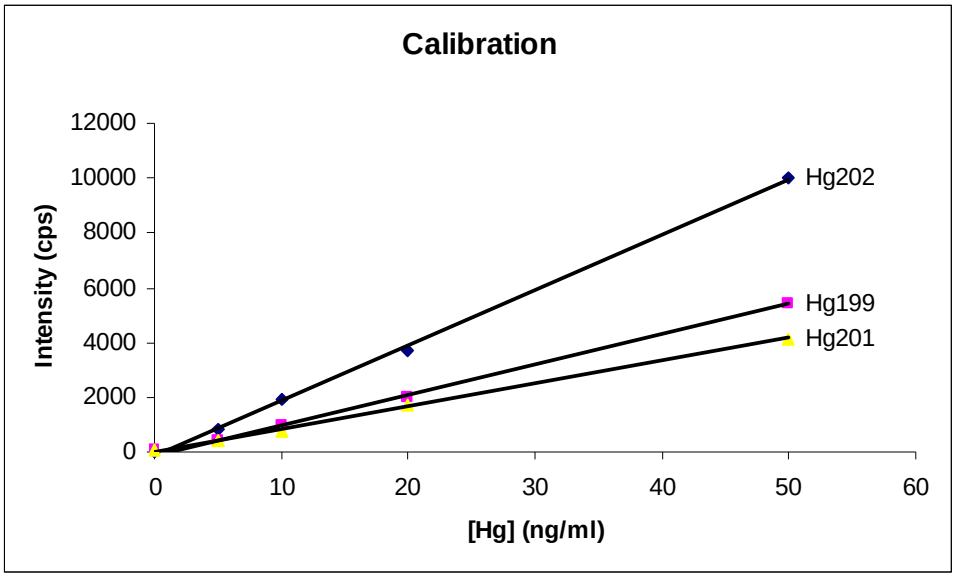

Figure 5.9 ICP-MS calibration for different mercury isotopes

The capillary column chromatograms were obtained by use of the settings given in table 5.3 above. An example of chromatogram obtained under optimal GC-ICP-MS conditions for IHg/MeHg standard solution is presented in figure 5.10.

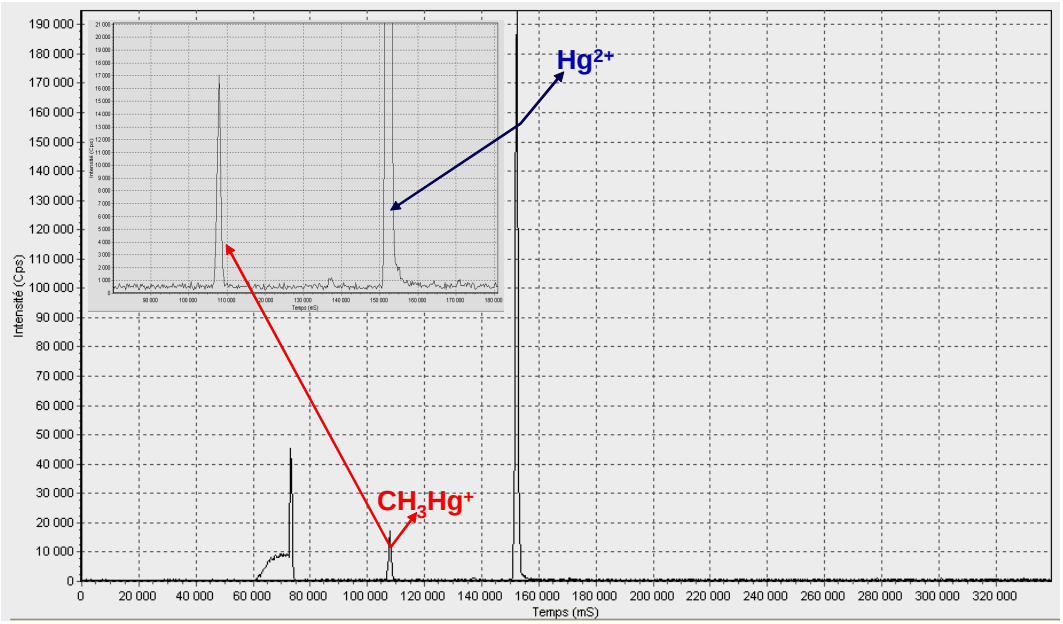

Figure 5.10 GC-ICP-MS chromatogram of IHg (1 µg L^{-1}) and MHg (0.1 µg L^{-1}) standards

It can be seen from this chromatogram that a clear separation of the different species has been achieved and good peaks were obtained. Measurements of mass separation (isotope specific detection) were also successfully achieved (figure 5.11) which allowed the use of ID technique.

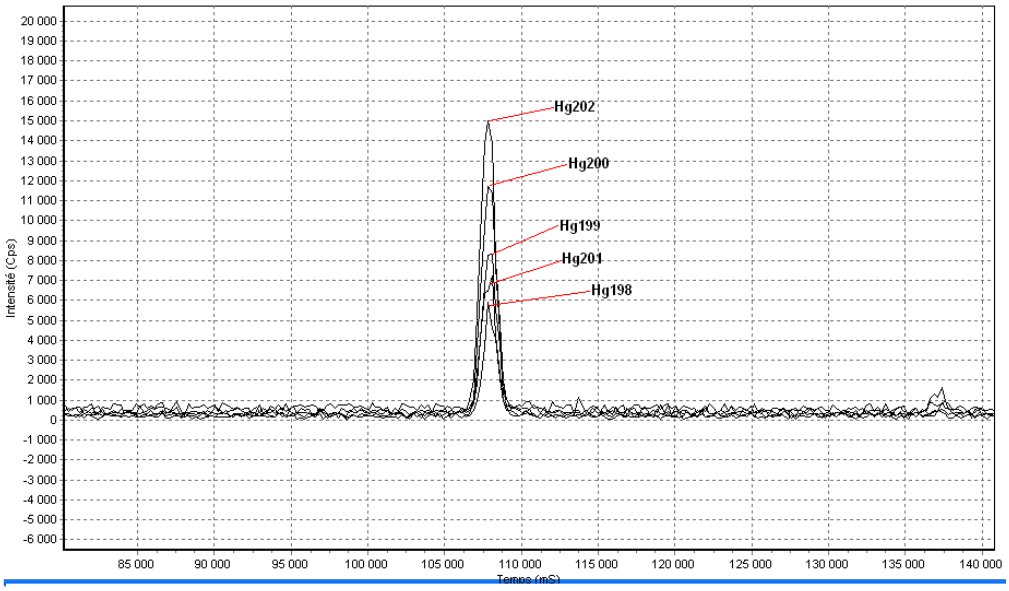

Figure 5.11 Hg isotope peaks for a 0.1 µg L^{-1} MHg standard

Figure 5.12 presents the result of the external standard calibration obtained for both IHg and MHg species. It shows the excellent linearity of the GC-ICP-MS coupling system over a range of more than 3 orders of magnitude. An excellent repeatability was also obtained for the retention time as shown in figure 5.13 with MHg peaks always appearing after 107.5 ± 0.5 s (RSD = 0.5%) and IHg coming after 152.4 ± 0.2 s (RSD = 0.1%).

The peaks obtained during the calibration correspond to concentrations in the ng and sub-ng ranges. The instrumental detection limits were estimated as 3 times the standard deviation of 6 blanks (deionized water) measurement. These limits depend only to a small extent on the individual species.

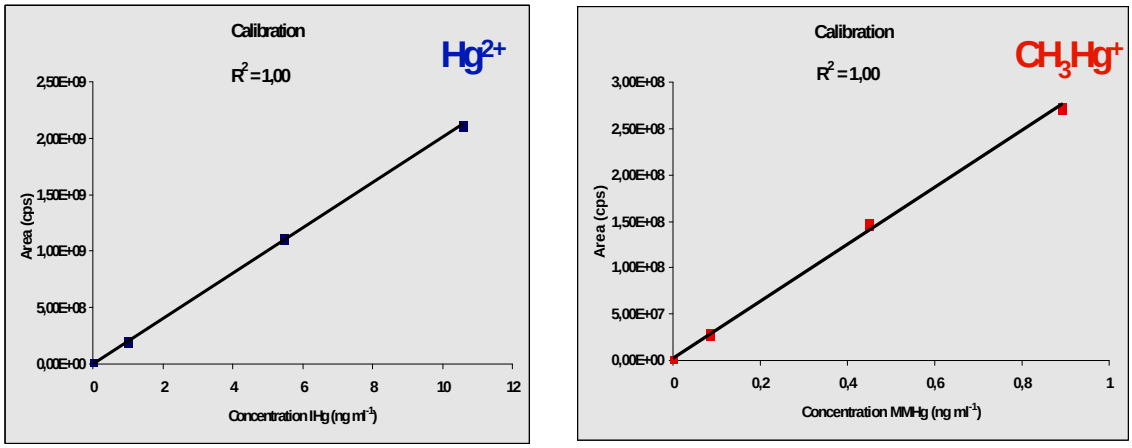

Figure 5.12 GC-ICP-MS calibration of IHg and MHg species

The detection limit was 0.039 (0.017 in SIDMS) ng L^{-1} for IHg and 0.0094 (0.0069 in SIDMS) ng L^{-1} for MHg which makes the method suitable for the quantification of mercury species in natural water systems.

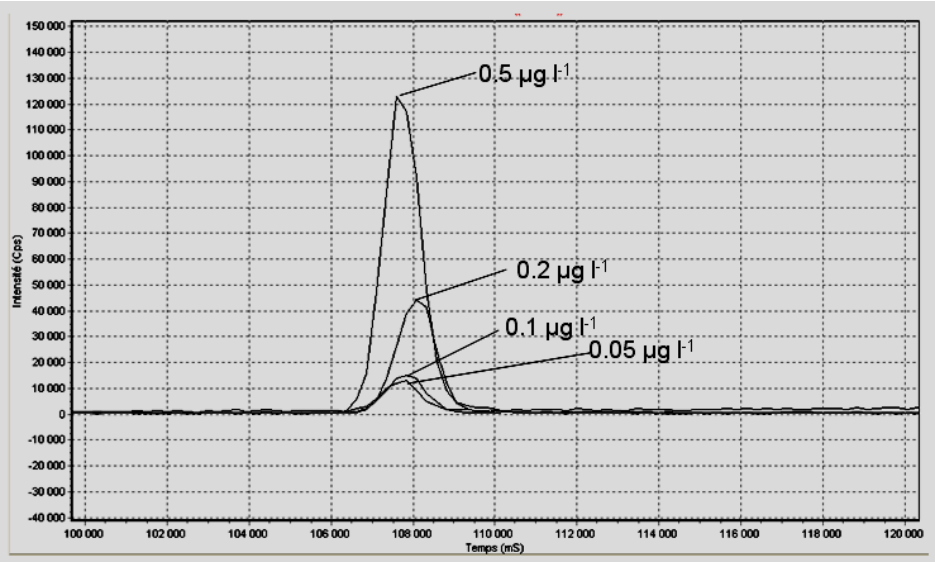

Figure 5.13 Overlapped chromatograms of successive injections of MHg standards

5.6 Validation of analytical methods used for mercury determination

Reference materials (CRMs) of sediment (RTC015-050 and IAEA 405) and fish (BCR 463 and 464 Tuna fish) certified for Hg_{TOT}, IHg and MHg were analyzed in order to validate the methodologies used in this study. Each CRM was prepared in triplicate following exactly the above mentioned sample preparation procedures. Blanks were also prepared in the same way as for CRMs to verify if contamination occurred during sample preparation and/or analysis.

Results obtained for total mercury analysis of CRMs are presented in table 5.5.

Table 5.5 Total mercury concentration in CRMs by ICP-MS

CRM		Certified	Measured		
Type	Name	Hg_{TOT} (µg kg^{-1})	Hg_{TOT} ± SD (n=3; µg kg^{-1})	RSD (%)	Recovery (%)
Sediment	RTC015-050	100 ± 20	99 ± 7	7.1	99
Tuna Fish	BCR 463	2850 ± 160	2874 ± 152	5.3	101

Concentrations of mercury species obtained with the isotope dilution technique were calculated using the equation below:

$$C_s = C_{sp} \frac{m_{sp}}{m_s} \frac{M_s}{M_{sp}} \frac{R_m A_{sp}^b - A_{sp}^a}{A_s^a - R_m A_s^b} \qquad (5.1)$$

Where:

C_s is the concentration of mercury in the sample in µg l^{-1},

C_{sp} is the concentration of mercury in the spike determined by reverse isotope dilution in µg l^{-1},

m_s is the mass of the sample in µg,

m_{sp} is the mass of the spike in µg,

M_s is the atomic weight of the sample,

M_{sp} is the atomic weight of the spike,

$\mathbf{A^a_s}$ and $\mathbf{A^b_s}$ are the isotopic abundance (in %) of isotopes a and b in the sample, respectively,

$\mathbf{A^a_{sp}}$ and $\mathbf{A^b_{sp}}$ are the isotopic abundance (in %) of isotopes a and b in the spike, respectively, and

$\mathbf{R_m}$ is the isotopic ratio of isotopes "a" and "b".

The isotopic abundance was calculated as follow:

$$\mathbf{A_i\ (\%) = (X_i/\sum X) \times 100} \qquad (5.2)$$

Where:

A_i is the isotopic abundance of the isotope "i" in the standard, X_i is the peak area of the isotope i and $\sum X$ the sum of peak areas of all the analyzed isotopes.

Concentration of stock solutions of "natural" standards used for the reverse isotope dilution analysis were determined every time analyses had to be performed in order to minimize errors related to analyte loss or degradation during storage.

The measured concentrations for IHg and MHg species in CRMs are reported in table 5.6.

Table 5.6 IHg and MeHg in CRMs by ID GC-ICP-MS

CRM		Certified (μg kg^{-1})		Measured ± SD (n=3; μg kg^{-1})				
Type	Name	IHg	MHg	IHg	RSD (%)	MHg	RSD (%)	Recovery (%)(*)
Sediment	IAEA 405	810 ± 140	5.5 ± 0.5	820 ± 25	3.0	5.5 ± 0.4	7.3	101
Tuna Fish	BCR 464	120 ± 60	5120 ± 160	177 ± 4	2.3	4953 ± 20	0.4	98

(*) The recovery is calculated for IHg + MHg

It can be seen from the above tables that excellent precision and accuracy were obtained for both total mercury and mercury species determination since all the measurements fell within certified ranges with relative standard deviations (RSD) always below 10% and a percentage recovery close to 100%. These results not only confirmed the performance of

the used analytical techniques but also demonstrated the efficiency of sample preparation procedures since no important loss or contamination of mercury was observed. Speciation analysis also has shown no significant interconversion between IHg and MHg species.
The ID technique for speciation analysis appears to be an analytical approach of choice especially for the precise quantification of the low level of mercury species in natural environmental systems.

5.7 Determination of total metals concentration

Total metal concentrations in water and digested sediment samples were obtained by ICP-OES (Spectro Genesis, Germany). The instrumental conditions were optimized to obtain sufficient sensitivity and precision. A photographic image of the instrument is shown in figure 5.14.

Figure 5.14 Image of the ICP-OES instrument

The parameters such as those presented in table 5.7 were used and each element was determined at various wavelengths. Wavelengths that represent a good compromise between maximum sensitivity and the ability to encompass a large range of concentrations are selected.

Table 5.7 Optimized parameters of ICP-OES

Parameter	Value
Plasma power	1400 W
Coolant flow	14 ml min^{-1}
Auxiliary flow	1 ml min^{-1}
Nebulizer flow	1 ml min^{-1}
Total preflush time	45 s
Measure time	45 s

Figure 5.15 shows selected scans for iron and magnesium at 259.941 nm and 279.553 nm, respectively which exhibited good sensitivity (high peak intensity for a given concentration) and signal-background ratio i.e. better detection limit.

Sometimes a different wavelength from that which is normally used may be used particularly in instances where self-absorption occurs, for example, when analyzing very concentrated samples.

Results were reported for the wavelength that showed the best reproducibility compared to CRM certified concentrations. Multielemental standards of 10 mg L^{-1} in 1% HNO_3 (De Bruyn Spectroscopic Solutions, SA) were diluted to make daily working standards of 0.1 to 1 mg L^{-1} for the instrument calibration.

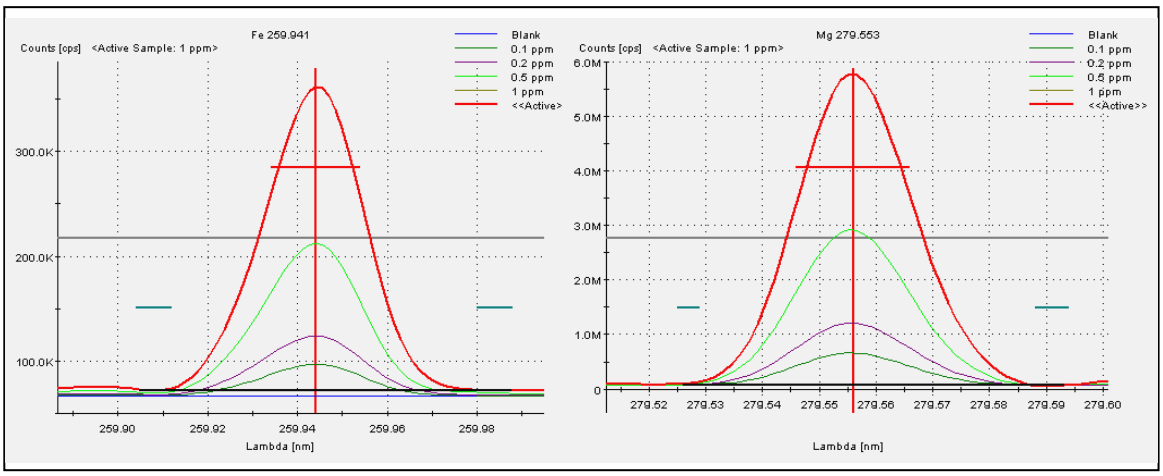

Figure 5.15 ICP-OES scans of Fe (left) and Mg (right)

The instrumental limit of detection (LOD) was calculated for each analyte using results from standard calibrations. An example of calibration curves for some metals at specific wavelengths is given in figure 5.16

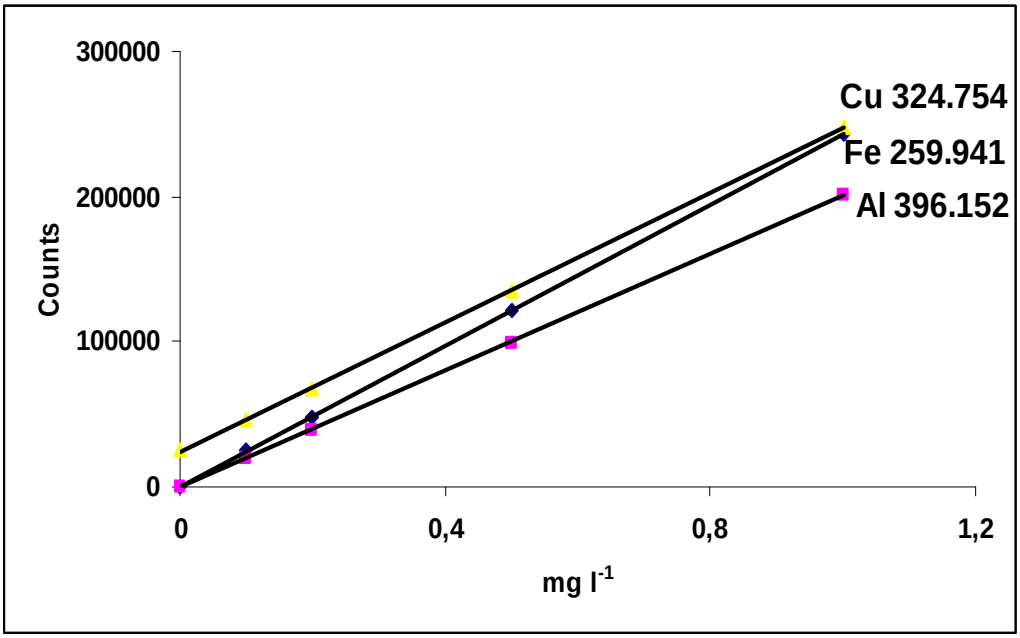

Figure 5.16 ICP-OES calibration of some elements at selected wavelengths

Calibration parameters obtained for some selected metals are shown in table 5.8.

Table 5.8 Example of calibration parameters obtained with the ICP-OES

Element	Al	Cu	Fe	Mg	Mn
Wavelength (nm)	396.152	324.754	259.941	279.553	257.611
Range (mg l^{-1})	0.0030 - 1.2000	0.0030 - 1.2000	0.0020 - 1.2000	8.86 E-06 - 1.2000	0.0004 - 1.2000
LOD (mg l^{-1})	0.0030	0.0030	0.0020	8.86 E-06	0.0004
Regression coefficient	0.999	1.000	1.000	1.000	0.999

5.8 Ion chromatography

Anions in water and leachate samples were analysed by ion chromatography (IC), as shown in figure 5.17, using a compact IC system (Metrohm, Switzerland) equipped with a separation center (733 IC), a detector (732 IC), an interface (762 IC), a suppressor module (753 IC) and a pump (709 IC). Data were treated using IC Net 2.3 software (Metrohm). Analyses were performed using the parameters presented in table 5.9.

The eluent was a solution of 1.0 mM $NaHCO_3$ and 3.2 mM Na_2CO_3. The solution was sonicated and filtrated under vacuum through a 0.45 µm filter paper. A 50 mM solution of H_2SO_4 was used as a conductivity suppressor regenerant solution (USEPA, 2007c). A 5 ml syringe equipped with a male pressure fitting was used for sample injection.

A 1000 mg l^{-1} standard stock solution of F^-, Cl^-, NO_2^-, NO_3^-, PO_4^{3-}, and SO_4^{2-} was prepared by diluting an accurately weighed amount of their corresponding salts, namely NaF (Merck), NaCl (Merck), $NaNO_2$ (Merck), $NaNO_3$ (Merck), KH_2PO_4 (Merck), and Na_2SO_4 (Merck), respectively in 1 L of deionized water (Millipore, USA). The stock solution was then filtered with a 0.45 µm filter paper and kept at 4°C.

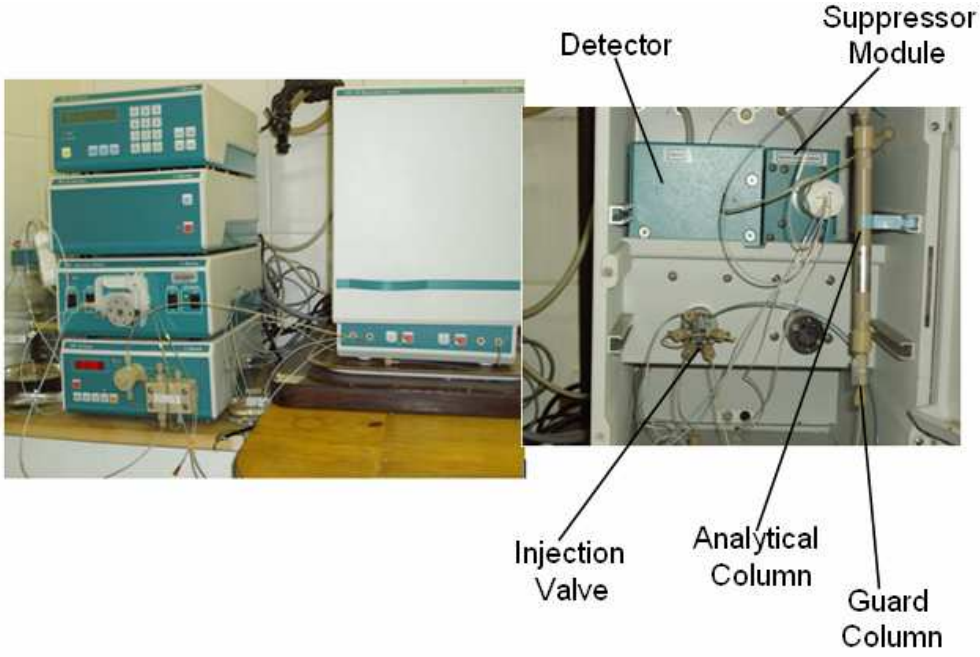

Figure 5.17 The compact IC system and its components within the separation center

Table 5.9 IC parameters for anions determination

Guard column	Metrosep A suppA/5 (6 1006 500) (Metrohm)
Analytical column	Metrosep A supp 5 (6 1006 520) 150/4.0 mm (Metrohm)
Flow rate	0.7 ml min^{-1}
Temperature	±25°C
Injection volume	±50µl
System back pressure	12 MPa
Run time	17 min

Working standards of 1, 5 and 10 and 20 mg l^{-1} were prepared from the stock solution on the day of analysis and used for calibrating the instrument. Environmental samples (water or leachate) were first filtered as for the stock solution to avoid the clogging of the working column and diluted before analysis in order to fit them in the calibration curve and to avoid detector saturation. Figure 5.18 shows chromatogram peaks obtained with a standard solution whereas an example of calibration curves obtained for the different anions is shown in figure 5.19.

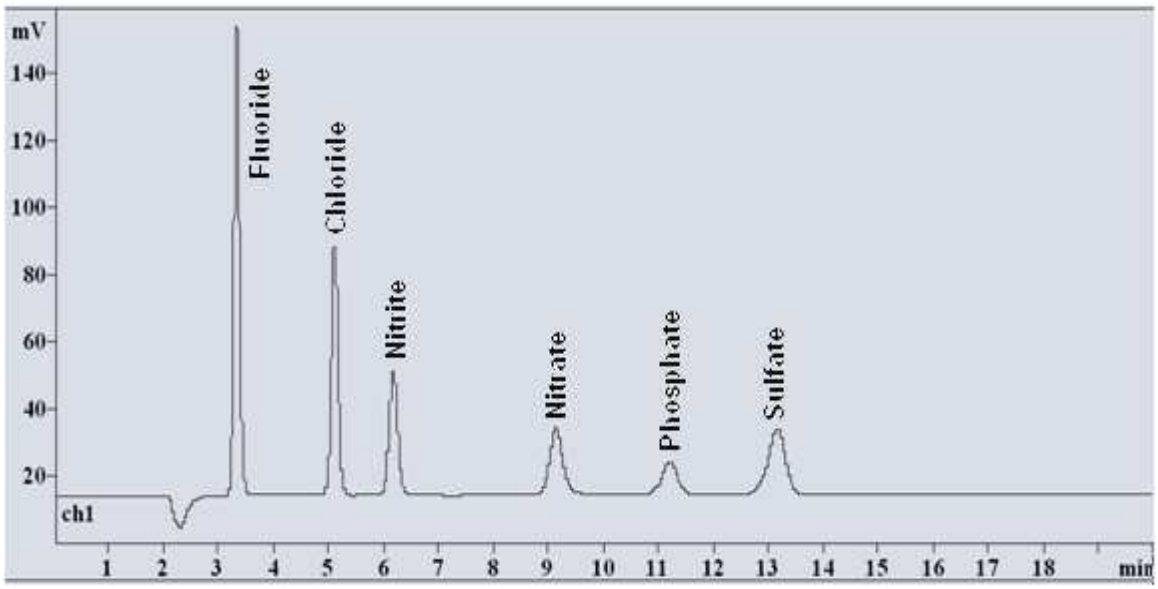

Figure 5.18 IC chromatogram showing peaks of a 5 mg L^{-1} standard solution of F^-, Cl^-, NO_2^-, NO_3^-, PO_4^{3-} and SO_4^{2-}

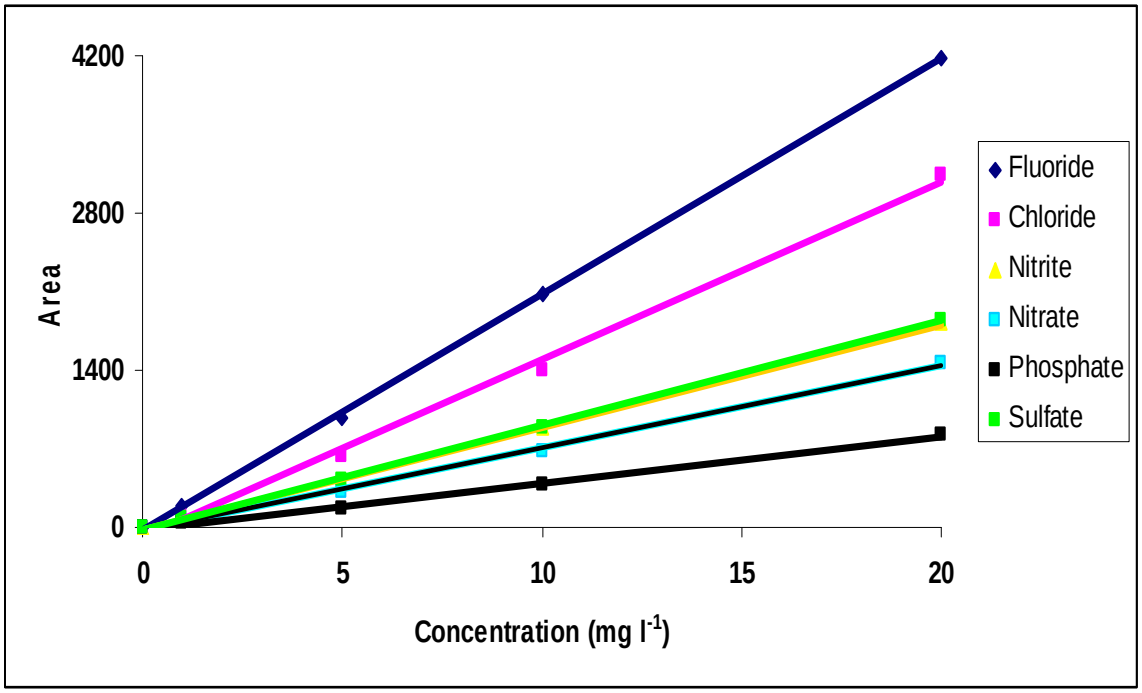

Figure 5.19 Example of IC calibration curves of F^- (R^2 = 1.000), Cl^- (R^2 = 0.996), NO_2^- (R^2 = 0.999), NO_3^- (R^2 = 0.999), PO_4^{3-}(R^2 = 0.998), and SO_4^{2-} (R^2 = 0.999)

5.9 CHNS analyser

The CHNS analyser (Leco-932, USA) used in this study was calibrated with standards of Sulfamethazine and Corn Gluten (Leco) and the results are given in table 5.10. A Sartorius CP2P micro balance (Gottingen, Germany) with a precision of 10^{-6} g was used to weigh samples. The samples were weighed into silver capsules and introduced into the oxidation furnace by means of a carousel.

The above standards were chosen because their certified values are reported for all 4 elements (carbon, hydrogen, nitrogen and sulfur) although our components of interest for the study were only carbon and sulfur.

Table 5.10 Standards calibration of the CHNS analyser

Standard	Carbon %	Hydrogen %	Nitrogen%	Sulphur %
Sulfamethazine	51.78	5.07	20.13	11.52
Measured (n = 3)	**51.69 ± 0.32**	**4.94 ± 0.15**	**20,03 ± 0.10**	**11,52 ± 0.05**
Corn Gluten	52.29 ± 0.39	7.13 ± 0.07	11.35 ± 0.07	0.933 ± 0.041
Measured (n = 3)	**52.17 ± 0.28**	**7.21 ± 0.03**	**11.74 ± 0.47**	**0.969 ± 0.110**

5. 10 Computer modeling

Computer modeling techniques are widely used in environmental sciences to represent, explain, predict or estimate natural phenomena.

Quantitative models, for instance, are used to determine contaminant migration from mine tailings and toxic waste sites (Tutu, 2006). Such models are based on the premise that they follow the laws of chemistry, physics and biology.

The transport, mobility, bioavailability and toxicity of metals in fresh water can depend to a large extent upon their chemical speciation; it is therefore desirable to have a model that can predict metal speciation in natural systems.

A geochemical assessment model for environmental systems, namely the USEPA Visual Minteq version 2.32, was used in this work to calculate the equilibrium concentrations of dissolved and solid mercury species for the study systems. Chemical equilibrium diagrams were also established using the Medusa 32 model or based on existing Eh-pH diagrams for mercury species. The models were useful to understand the distribution and availability of mercury, and to explain its migration and fate in the study environmental compartments.

5.11 Summary

Sampling protocols, samples conditioning and storage conditions were followed with care in order to minimize loss or contamination and also to preserve the integrity of target species within the collected samples. Analytical methodologies were optimized for total

mercury and mercury species determination for different sample matrices using an ICP-MS and the coupling of GC with ICP-MS. The optimized methodologies were sensitive and specific enough even for the identification and quantification of mercury species at ng L^{-1}. A sample preparation procedure was also developed demonstrating the efficiency of the microwave assisted extraction technique (close and open) with recovery close to 100% for reference materials.

In brief, the analytical procedures used in this study were suitable for a fast, sensitive, accurate, and precise Hg_{TOT} determination and simultaneous determination of mercury species in water, sediment and biota. These procedures can be used for background mercury species determination. The procedures also offered the possibility of reducing sample preparation time, especially for speciation analysis since only 4 minutes were required for sample extraction with a low-power focused microwave field.

A significant improvement in the precision of mercury species determination was obtained using the isotope dilution technique which also contributed in minimizing analytical errors related to analyte loss or artifact methylation/demethylation of mercury that might occur during sample preparation.

Finally, Field measurements together with total metals concentration, anions determination and CHNS results were obtained from calibrated meters and optimized instruments, and were later used as comparative data for a better understanding of the mercury chemistry in the different environmental studies.

Chapter 6
The use of nano-structured gold supported on metal oxides sorbents for the trapping and preconcentration of gaseous mercury

6.1 Introduction

One of the most important environmental concerns of mercury is not only its toxicity but also its persistence and long-life in the atmosphere. Mercury from point source emissions may remain localized in the environment, or may be transported regionally and even globally (USEPA, 1997) Thus, simple, rapid, sensitive, and selective detection of atmospheric mercury is of great significance for environmental science and medicine for reliable mercury emission estimations and in order to achieve the goal of assessing the potential human health risks from exposure to mercury (Jiang *et al.*, 2009).

It was previously mentioned (see chapter 3) that sampling and analysis of atmospheric mercury is mostly made as total gaseous mercury (TGM) which mainly consists of Hg^0 (Schroeder and Munthe, 1998) and which is collected on gold, or other collection material (Munthe *et al.*, 2001). Gold and other precious metals are well known for their high efficiency in trapping mercury traces from gases by forming amalgams. Therefore, gold based collectors play an important role in the preconcentration and separation of mercury species from, for example, air, stack gas and gas condensate4 prior to detection (Zierhut *et al.*, 2009 and references therein).

Many commercially available mercury detection systems use gold in different forms such as sand, wool, gauze, foil, wire or deposits on different supports and packed into quartz tubes (e.g. Schroeder et al., 1995a and b; Labatzke and Schlemmer, 2004). In recent years, the catalytic properties of finely dispersed gold particles on oxide support materials have attracted much attention. Gold was recently recognized to be an extremely unique and highly active metal when prepared as supported nano-particles (Bond and Thompson, 1999; Gong and Mullins, 2009). This is mainly due to the reduced dimensions of the gold particles and a strong interaction with the support (Zhou *et al.*, 2004; Risse et al., 2008). Gold catalysts are, therefore, believed to exhibit potential applications of both industrial and environmental importance.

In this chapter, three nano-structured gold supported metal oxides materials, namely Au-TiO_2, Au-ZnO and Au-Al_2O_3 were used for the preconcentration and determination of gaseous mercury and their respective analytical performance were compared to the one of commercially available pure gold wool trap. The most performing "nano-trap" was later on used as a sampling trap and its performance was compared with the one obtained with the traditionally used gold-coated sand sorbent.

6.2 Sorbents origin

Nano-gold sorbents were provided by Project AuTEK (figure 6.1) which is a joint venture formed between Mintek, a science council based in South Africa, and the three major South African gold mining houses, namely Anglogold Ashanti, Gold Fields and Harmony Gold Mining Company Ltd. The main focus of Project AuTEK is to research and develop novel industrial applications for gold which involves research in the fields of catalysis, nanotechnology and biomedical science (www.mintek.co.za).
Details concerning the synthesis conditions of the materials were not provided except that each sorbent was reported to contain only 1% (w/w) of gold.

Figure 6.1 Au-Al_2O_3, Au-ZnO and Au-TiO_2 materials used in the study

6.3 Analytical Method

Gaseous mercury analysis was performed by double amalgamation cold vapor atomic fluorescence spectrometry (DA-CVAFS) which is shown in figure 6.2.

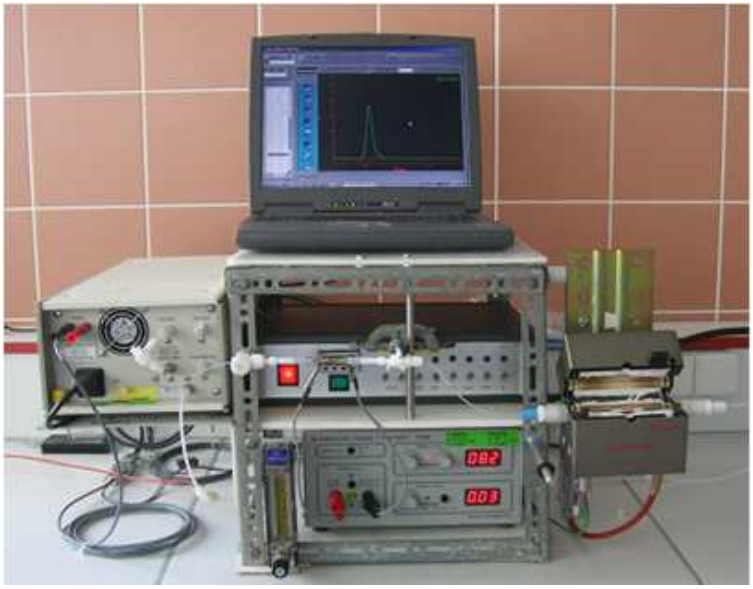

Figure 6.2 The DA-CVAFS setup

Mercury is an ideal element for determination by fluorescence because it is atomic at room temperature and also absorbs and fluoresces at the same wavelength (Stockwell and Corns, 1993). The double amalgamation technique, as developed by Bloom (Bloom. and Crecelius, 1983), consists on trapping gaseous mercury species in a first trap called sampling column and desorbing them by heating the trap at 550-600°C to a second trap known as the analytical column (figure 6.3).

This latest usually contains pure gold that allows a more efficient thermal desorption (900°C) of the analyte to the detector. A transient signal is obtained with an increased signal/noise ratio which lowers the detection limit and, therefore, improves the sensitivity of the method. Another advantage of the double amalgamation is also in the preconcentration that occurs in the second trap and in the reduction of interferences such as water vapor and organic compounds during the first thermal desorption.

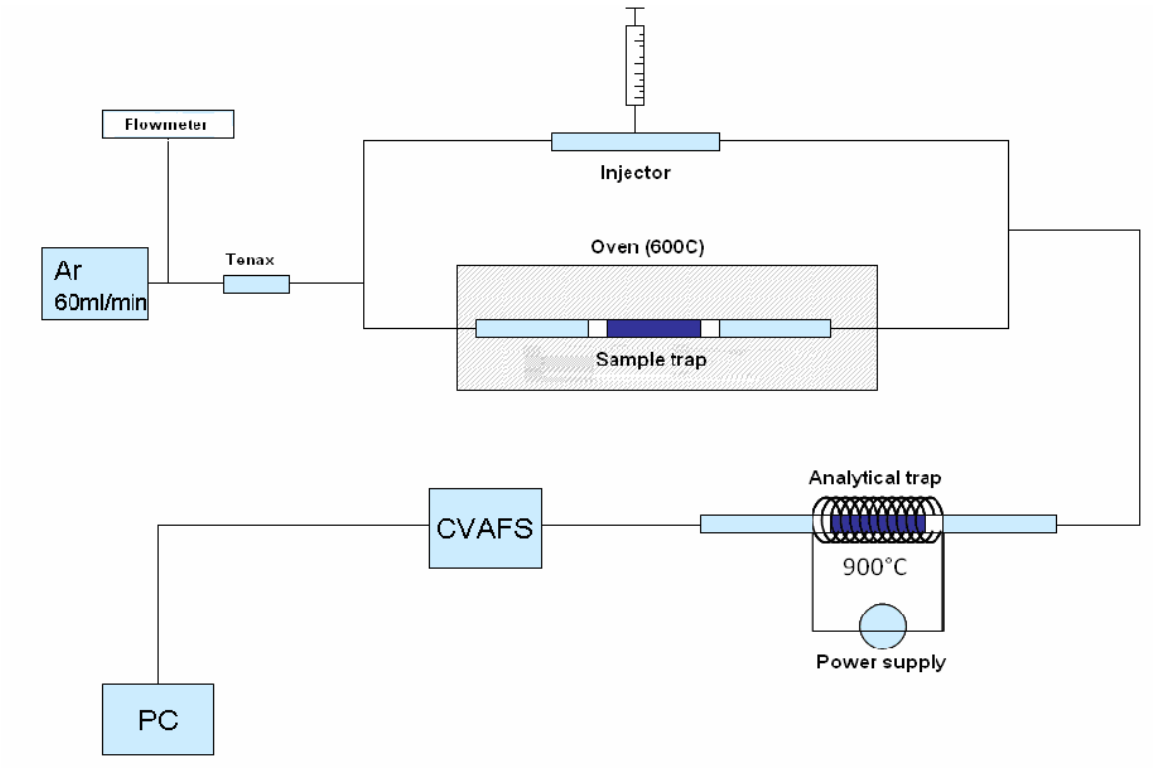

Figure 6.3 Schematic of the DA-CVAFS system

The CVAFS detector used in this study was a Tekran 2500 (USA) which is very sensitive and specific for mercury. Ultra pure argon (99.999% purity) was used as a carrier gas which allowed detection limits in the pg range. The sample was carried through a flow of argon into a quartz cell irradiated with a low vapor pressure mercury lamp at a wavelength of 253.7 nm. Elemental mercury atoms were, therefore, excited and fluoresced in all directions and the emitted photons were then detected by a photomultiplier tube (PMT) which is positioned at right-angle to the fluorescence lamp.

A signal measuring the emitted radiation (in mV) versus time was obtained which intensity was directly proportional to the amount of absorbing mercury atoms i.e. to the concentration of injected mercury vapor.

It has to be noticed that AFS detectors can be sensitive to negative or positive interferences which cause the diminution or enhancement of the analytical signal, respectively. Negative interferences are mainly due to the phenomenon known as quenching i.e. the collision between excited atoms and other molecules in the atomization sources (Cai, 2000). To avoid this problem, the use of argon as carrier gas is

recommended instead of nitrogen, oxygen or air, which are reported to decrease the instrument sensitivity (Cai, 200).

Positive interferences are due to the presence of moisture and organic solvents. Very broad peaks with high baseline are mostly observed in this case.

6.4 Instrument setup

Columns used in this study were quartz tubes of 12 cm length each with an internal diameter of 6 mm. The analytical columns were filled either with approximately 0.1 g of pure gold or with the same amount of the above mentioned nano-gold (1% wt Au) supported on metals oxide (figure 6.4) and the trapping material was held securely with quartz wool, as shown in figure 6.5.

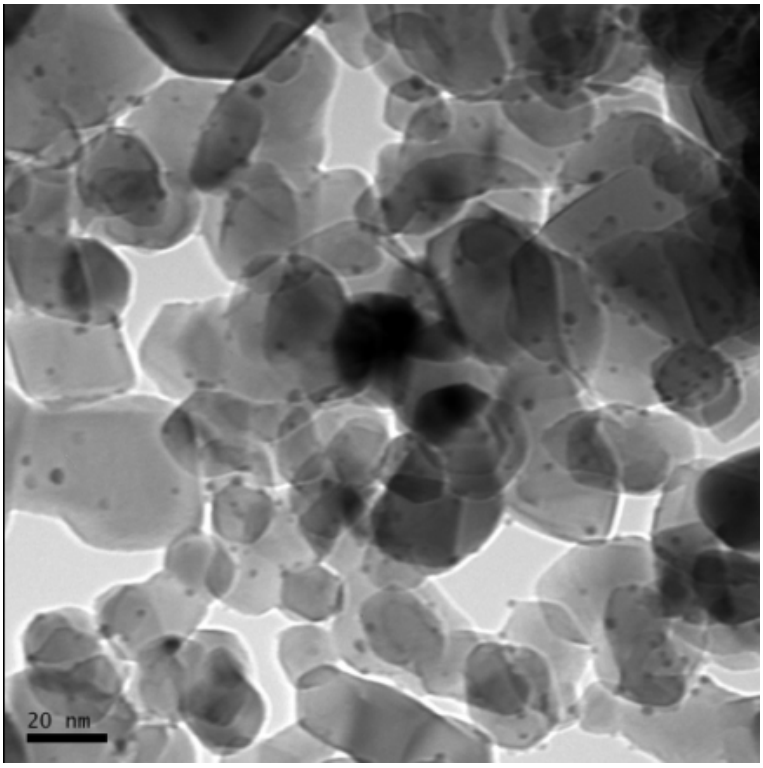

Figure 6.4 SEM image of gold particles (small black dots) dispersed on TiO_2

The sampling column, on another hand, was filled with 0.1 g of the commercial gold coated sand (Brooks Rand, USA) or with 0.1 g of Au/TiO_2. The choice of Au/TiO_2 as sampling trap will be discussed further.

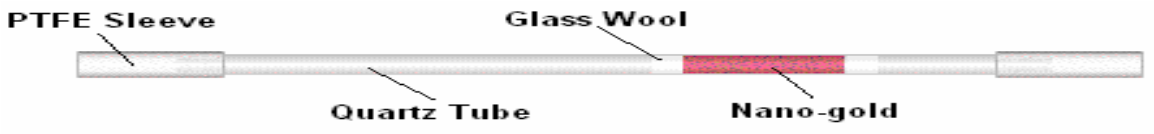

Figure 6.5 Schematic of the mercury trap

and were hermetically sealed until use. Both columns (analytical and sampling) were mounted in series and connected by Teflon tubes. Tubes were chosen with the smallest diameter possible to minimize the dead volume of the system, especially between the detector and the analytical trap. All connections and Teflon tubes were decontaminated in acid baths, rinsed with deionized water and dried under a laminar flow hood. An optimized argon flow of 60 ml min^{-1} was used to carry the analyte to the detector. The argon flow was frequently controlled by connecting a flowmeter at the exit of the analytical column. The optimized flow allowed an ideal residential time of the gas flow in the measuring cell and a maximum sensitivity of the instrument.

The thermal desorption of the sampling column was performed at 600°C within a temperature controlled ceramic oven. The analytical trap was heated with a Nickel/Chromium coil of resistance (Gilphy RW 80), supplied with a current of 5.5 A and a potential of 7 V. This setup allowed the temperature to increase to 900°C within 30 seconds. The measured signal was transmitted to a computer (figure 6.6) and the transient signals were treated as chromatographic peaks using the AZUR software (Jasco, France).

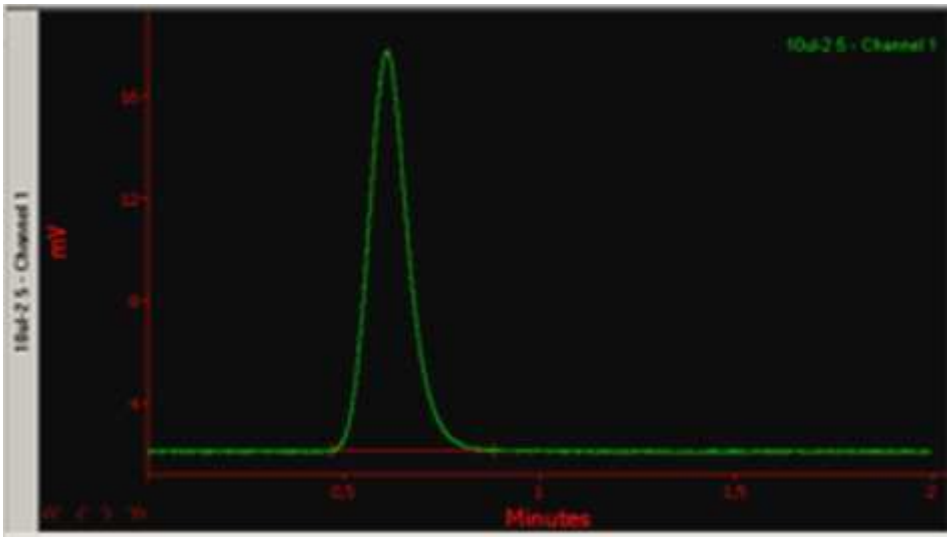

Figure 6.6 Example of signal obtained with the injection of 10 µl of Hg^0

6.5 Analytical methodology

The calibration was done by injecting gaseous mercury (Hg^0) standards directly to the analytical trap (gold wool or nano-gold traps). The source of Hg^0 was a drop of liquid mercury contained in a headspace bottle (figure 6.7).

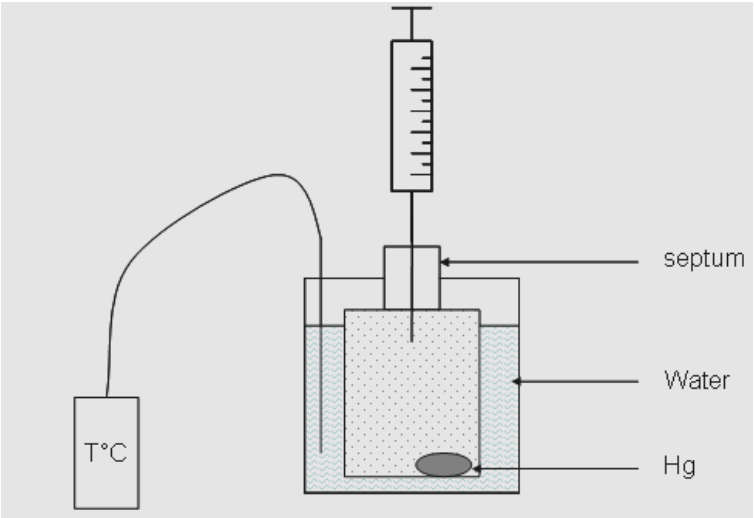

Figure 6.7 Source of Hg^0 standards

The mercury drop was then in equilibrium with the gaseous phase. A known volume of gas was collected with a syringe through a septum. The concentration of Hg^0 at the equilibrium was, therefore, temperature dependent only and was measured with a thermocouple. The relationship between the vapor pressure of Hg^0 and the temperature is available in the literature (e.g. CRC Handbook of Chemistry and Physics, 2005). Thus, the amount of injected mercury could be accurately determined.

Repeated injections of known amounts of Hg^0 allowed the obtention of a calibration line. Due to the high volatility of Hg^0, care was taken during the successive injections to obtain measurements with good repeatability. Syringes with removable needles (RN) and of different capacity (i.e; 10, 50 and 100 µl, respectively) were used during the optimization. It was found that the 100 µl, RN syringe exhibited the best calibration line in terms of regression coefficient and slope (figure 6.8). For this reason, this syringe was used for all standards injections.

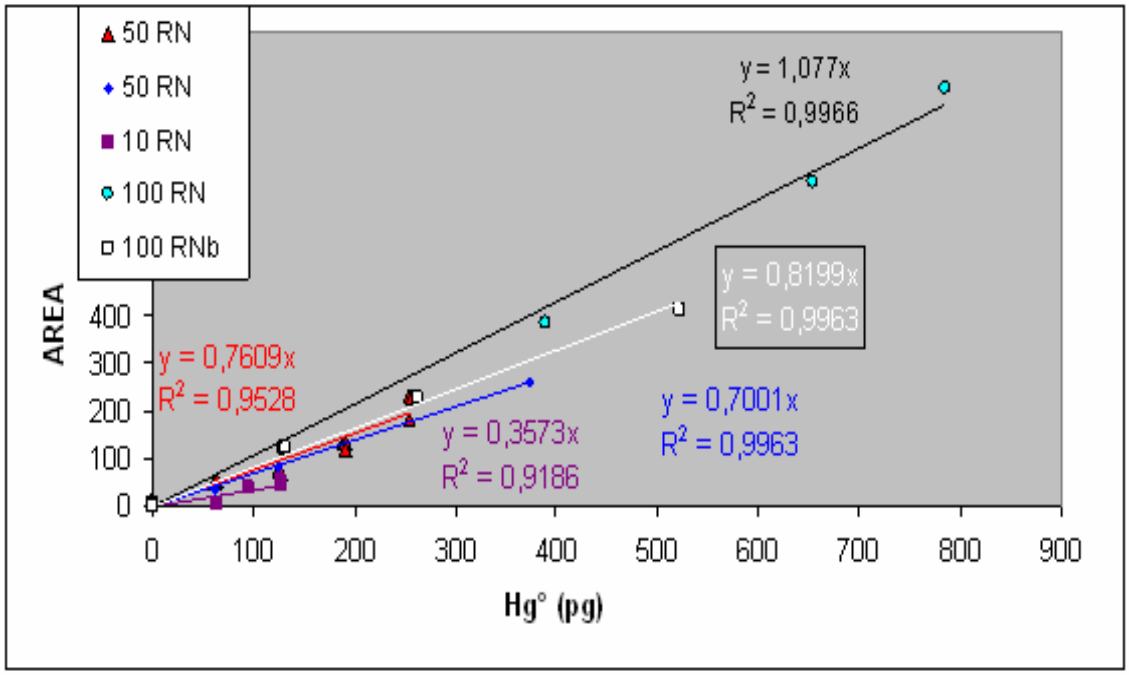

Figure 6.8 Calibration lines obtained with different syringes

Analytical performances of nano-gold materials were first evaluated by injecting Hg^0 standards and by comparing the obtained instrumental calibration lines to the one obtained with pure gold. The most performing nano-gold material (Au/TiO_2) was, later

on, used for the collection of TGM at different locations in our research laboratory (LCABIE-IPREM Pau, France). The TGM determination was also performed by DA-CVAFS and the performance of nano-traps was compared to the one of commercial gold-coated sand traps. A summary of the analytical steps followed for both experiments is illustrated in figure 6.9.

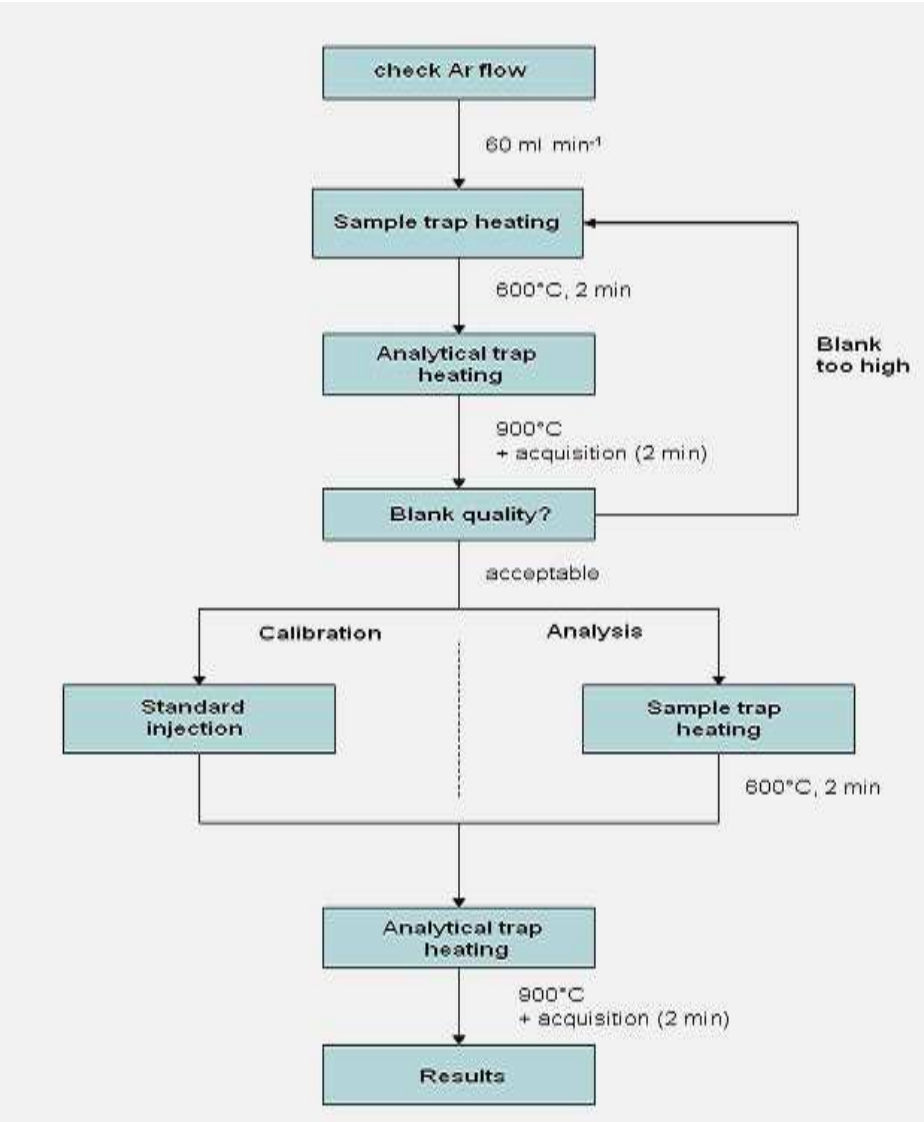

Figure 6.9 Analytical protocols for mercury standards calibration and TGM analysis

6.6 Air sampling for TGM determination

Simultaneous collection of air for TGM measurements was done, as described in figure 6.10, with Au/TiO_2 and gold-coated sand traps in different laboratory compartments using a peristaltic pump (ASF THOMAS, Germany).

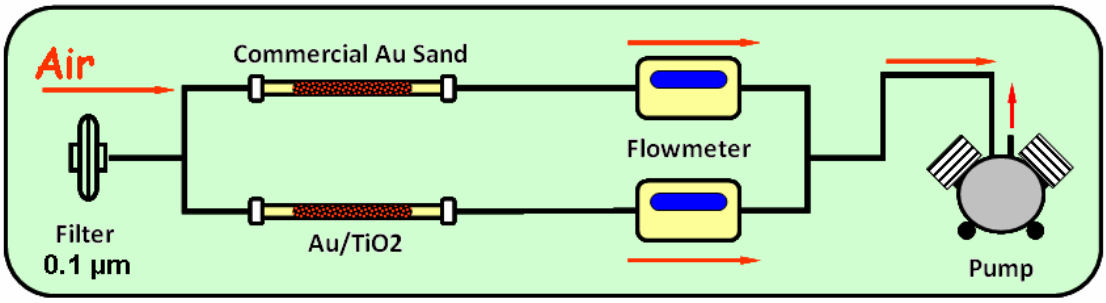

Figure 6.10 Schematic of sampling setup

The flow was controlled with a flowmeter (Bronkorst HiTech B.V. E-7000, Netherland) in order to get an accurate measurement of the sample volume. Two parallel sampling lines were used with an air sampling flow of 600 ml min^{-1}. A 0.1 µm quartz filter (Whatman) was used to prevent the introduction of dust and aerosols in the traps.

6.7 Optimization of sampling conditions

Air samples were collected at the ground floor (L1), first floor (L2), second floor (L3), and from the roof (R) of the laboratory building (see example in figure 6.11).

A volume gradient was established in order to optimize the sampling time (i.e. the sample volume) and, therefore, to ensure samples representativity.

Figure 6.11 Collection of air samples in the roof of the laboratory. The simultaneous sampling setup with both commercial and nano-traps is shown in the right picture

Short collection times of 10, 20 and 40 minutes were used at a flow of 600 ml min^{-1} which corresponded to sample volumes of 6, 12 and 24 L, respectively (figure 6.12).

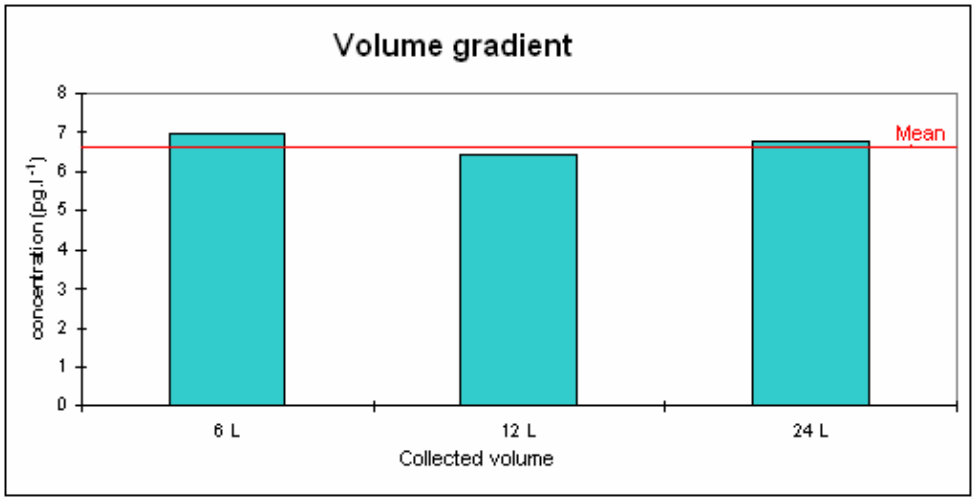

Figure 6.12 Concentrations of Hg^0 as a function of sample volume

The obtained mercury concentrations (mean value: 6.5 ± 0.5 ng m^{-3}) were all beyond the method detection limits (see section 6.8 below). Due to sample variability caused by the air circulation in the building, the difference in mercury concentration (± 8%) for the different sampling volumes was not significant. The optimized sampling time were, thus,

chosen to be 20 minutes i.e. 12 L in volume. Everyday, early in the morning, the sampler was conditioned, prior sampling, by sucking the air for about twenty minutes in order to stabilize it and to minimize mercury adsorption on the walls. After sampling, all traps were hermetically sealed, stored in a double plastic bag and immediately analyzed in the laboratory.

6.8 Performances of nano-gold materials as analytical traps

An example of analytical signals obtained with the commercial gold trap and the different nano-structured gold sorbents is shown in the figure 6.13 below.

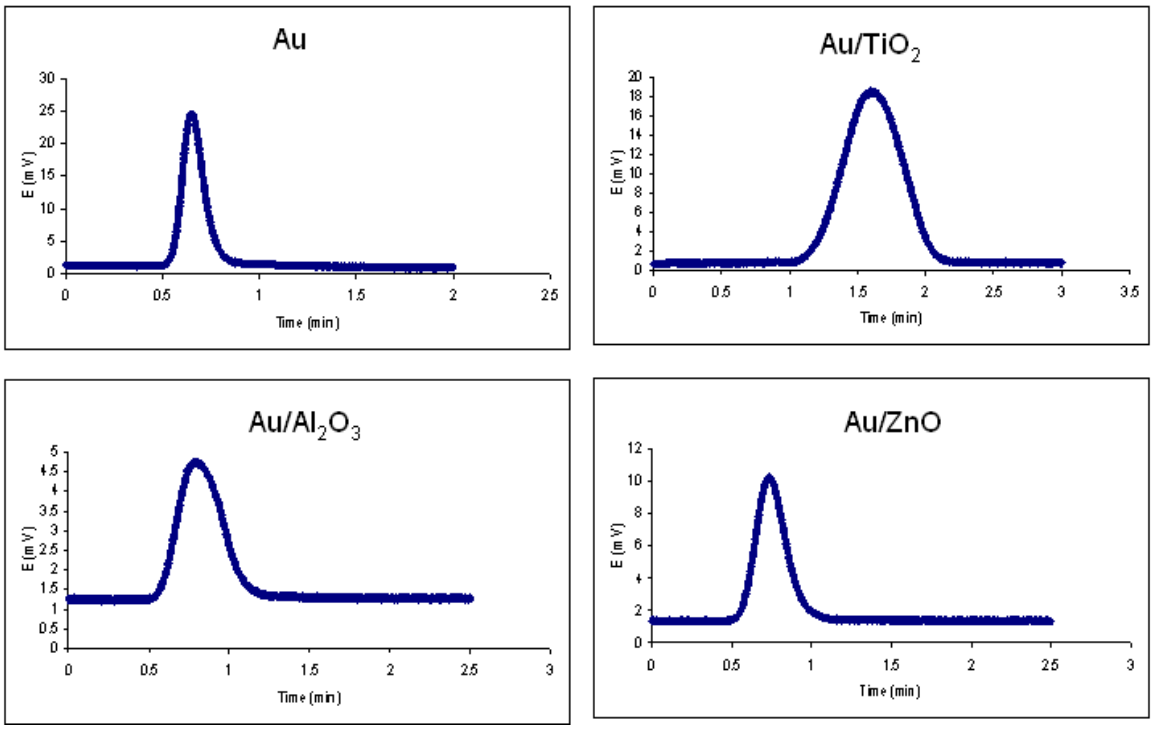

Figure 6.13 AFS chromatograms of 20 µL Hg^0 desorbed from different traps

Good linearity and repeatability were obtained with the three nano-gold materials in the volume range of 10 – 60 µL Hg^0, which corresponds to a concentration range of 132-778 pg Hg^0 at an argon flow of 60 mL min^{-1} (figure 6.14).

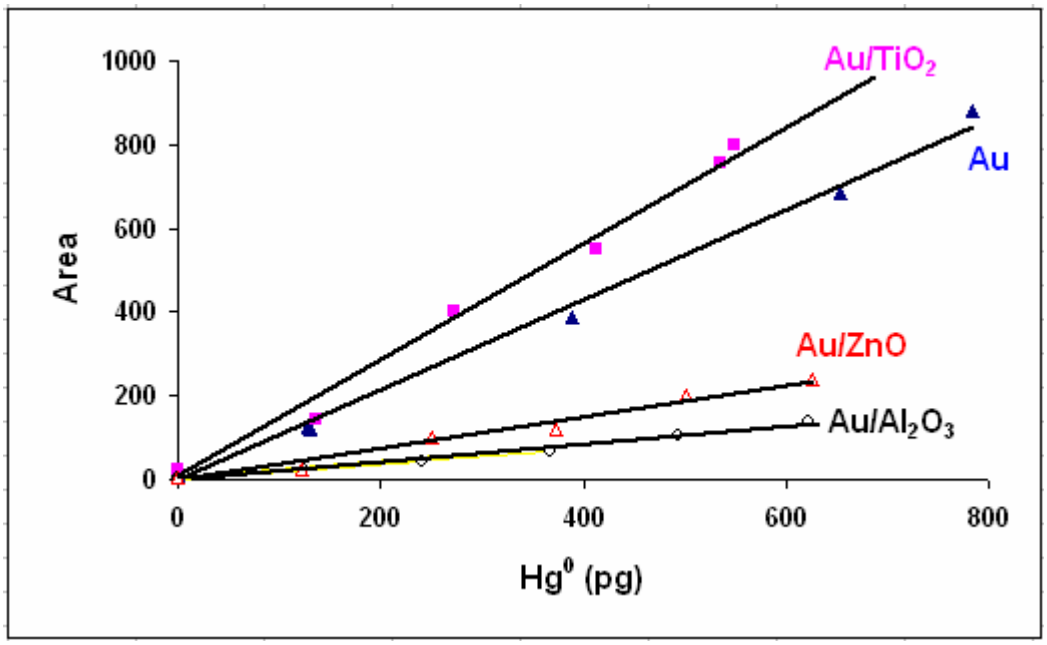

Figure 6.14 AFS Calibrations of Hg^0 standards at argon flow of 60 ml min^{-1}

Parameters such as the retention time, the number of theoretical plates, and the full duration at half maximum (FDHM) height also have been studied and are presented in table 6.1.

Table 6.1 Analytical parameters of studied materials

Parameters	Au	Au/TiO_2	Au/Al_2O_3	Au/ZnO
Retention time (min)	0.71 ± 0.05	0.83 ± 0.03	0.80 ± 0.01	0.73 ± 0.01
Slope (ua pg^{-1})	1.07	1.39	0.21	0.38
Regression coefficient	0.997	0.995	0.988	0.986
FDHM (min)	0.15 ± 0.01	0.43 ± 0.06	0.33 ± 0.03	0.20 ± 0.01
Theoretical plates	136 ± 7	36 ± 2	33 ± 5	69 ± 3

The following observations were made from the obtained results:

- The commercial Au trap presented better characteristics compared to the other materials with the highest number of theoretical plates (i.e. greater efficiency) allowing the obtention of sharper peaks. This trap also showed the best regression coefficient (0.997) for the above mentioned volume range and argon flow.

- TiO_2/Au showed broader peaks than the other materials with one of the smallest number of theoretical plates denoting retention of mercury during desorption.

- The obtained correlation coefficients (R^2) between the injected amount of Hg° and the obtained peak area were satisfying for all the nano-gold columns. These columns can, therefore, be used for a quantitative analysis of gaseous mercury.

- The higher the calibration slope, the better the analytical response from the detector (i.e. better sensitivity). The slope obtained with Au/TiO_2 was 1.39 ua pg^{-1}. This column exhibited the best sensitivity under the above mentioned conditions compared to the commercial gold (1.07 ua pg^{-1}) and the other nano-traps ((0.21 ua pg^{-1} for Au/Al_2O_3 and 0.38 ua pg^{-1} for Au/ZnO). The linearity range of Au/TiO_2 was even improved by increasing the carrier gas flow to 100 mL min^{-1}. Calibrations with Au/TiO_2 trap also exhibited a much better slope (0.908) under the new conditions compared to the one obtained with gold wool (0.423) as shown in figures 6.15a and b. Therefore, it is believed that Au/TiO_2 could replace the commercial gold wool as a reliable analytical trap for the quantification of gaseous mercury, although the commercial gold still presents the advantage of a complete and fast desorption of the trapped mercury. This allowed a faster clean-up of the sorbent (i.e. faster obtention of blanks) and a reduction of the overall analytical time. For this reason, the commercial gold was retained as the analytical trap for TGM determination.

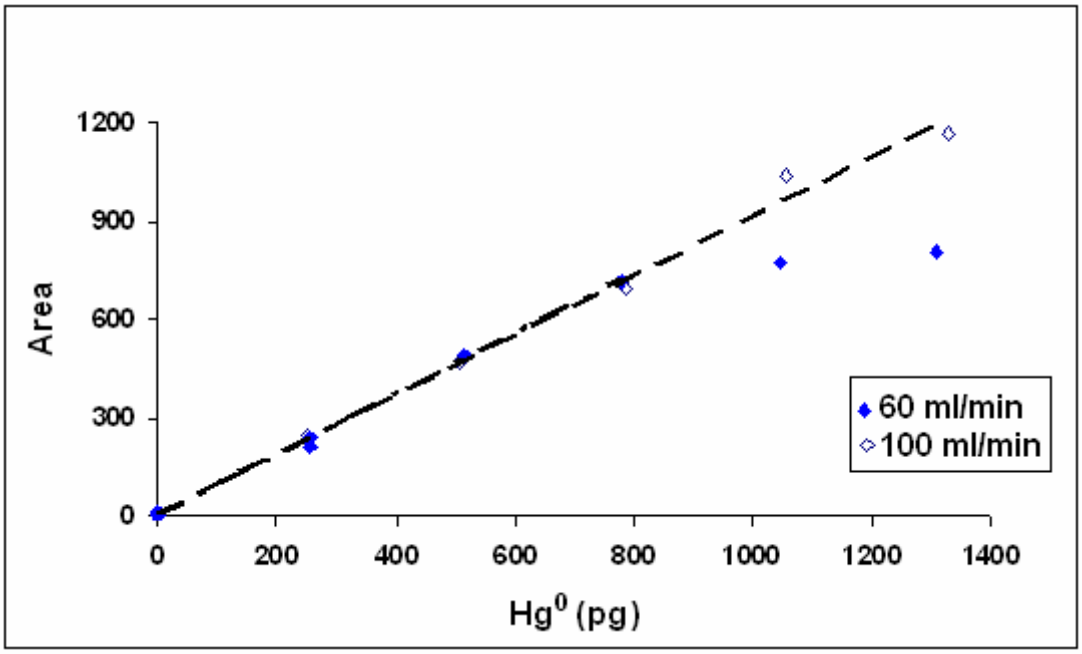

Figure 6.15a Calibrations obtained with Au-TiO_2 at different Ar flows

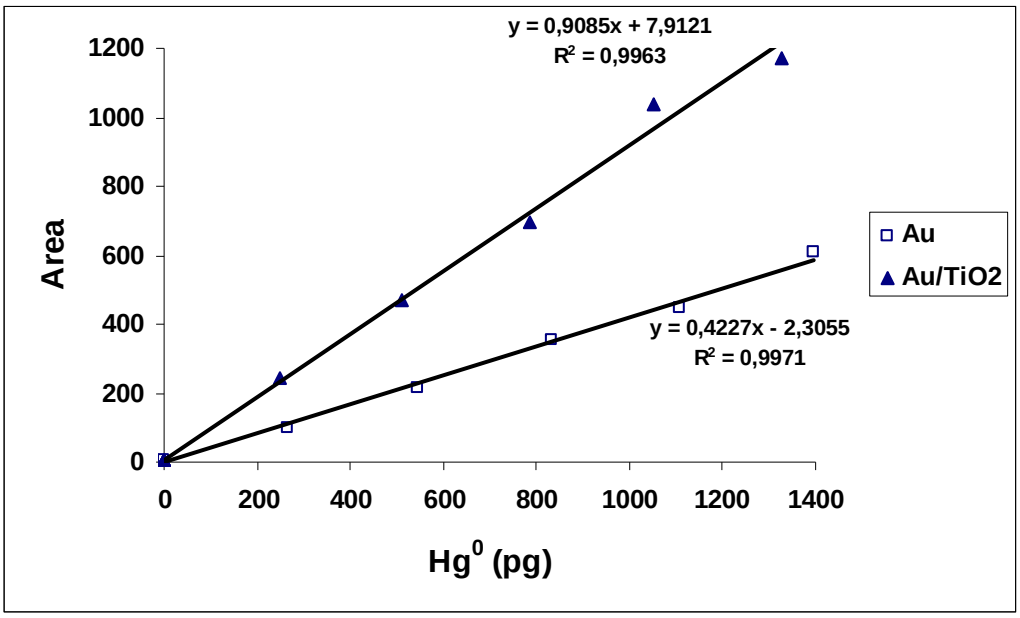

Figure 6.15b Calibrations obtained with Au and Au-TiO_2 at Ar flow of 100 ml min^{-1}

- It is important to notice that, although chromatograms obtained with Au/ZnO and Au/Al_2O_3 had retention times similar to the one for Au wool, these materials showed lower linearity range compared to Au/TiO_2 with lower slopes (figure 6.14

and table 6.1). They also have demonstrated poor baseline recovery after mercury desorption figure 6.16). This implies a greater retention of mercury vapor in the sorbents compared to Au/TiO_2.

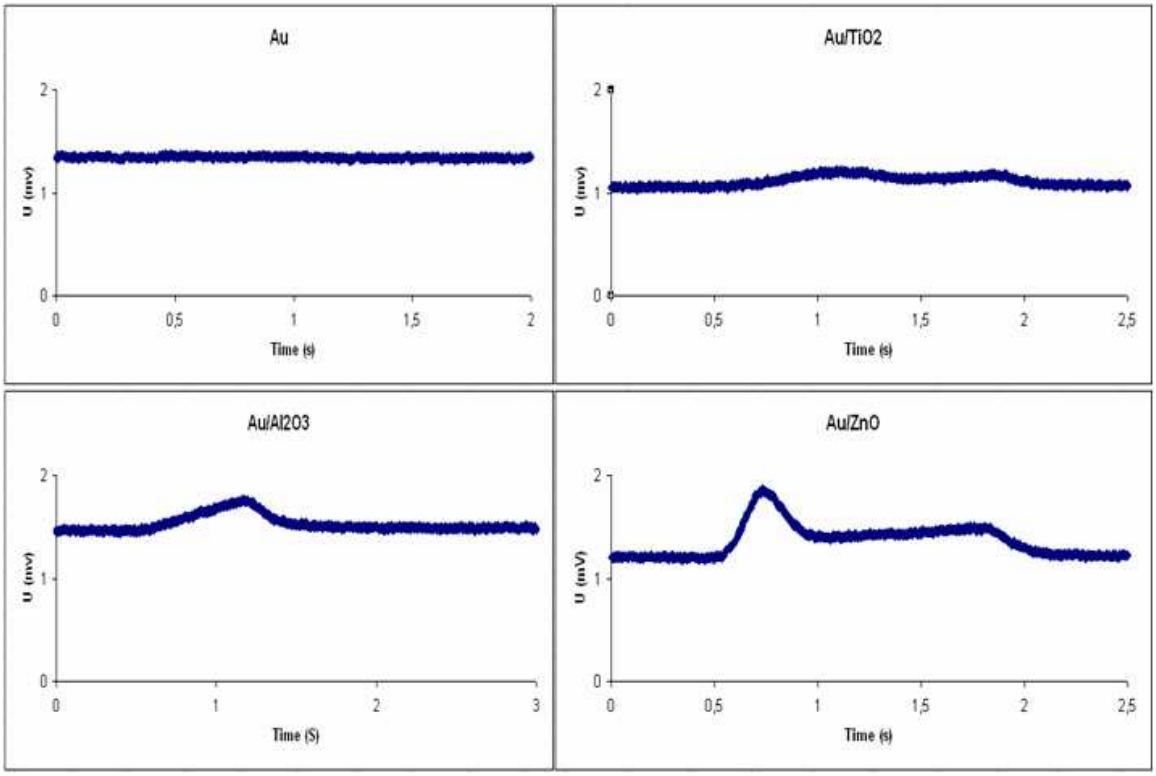

Figure 6.16 Examples of baseline obtained after the desorption of mercury from the different traps

- Au/ZnO sorbents have shown different analytical responses (poor reproducibility) when the materials were roughly or finely grinded whereas Au/Al_2O_3 exhibited some hygroscopic properties (i.e. retention of water vapor during column preparation) which probably explain the broad mercury peak and the high baseline level (positive interferences) observed in chromatograms obtained with this trap. A deeper characterization of these materials is of importance in order to improve their performance.

The difference in analytical performances observed between the nano-sorbents could be explained by the inner structure of the materials used. Although details concerning the preparation of the different nano-gold sorbents were not provided, numerous experimental and theoretical studies aimed at a better understanding of the properties of

gold in the nanometer size regime have suggested that adsorption properties of gold catalysts are deeply influenced by the pore size and specific surface area of the material. The pore size and specific surface area vary with gold loading (Peter *et al.,* unpublished). Gold can be present as individual particles in the catalyst or can form agglomerations or clusters. The size and the shape of the gold aggregates depend on the temperature and can be metastable once formed at low temperatures (Risse *et al.,* 2009). These factors directly affect electronic, optical, and chemical characteristics of nano-gold catalysts. Additives are often used to improve catalytic performances of commercial catalysts. These additives may act as either promoters, for example, to improve parameters such as the selectivity, the activity and the lifetime of the catalyst or they can act as inhibitors of unwanted reactions (Ntho, 2007).

In the case of the ultrathin oxide films, it was shown that the metal substrate lying underneath the film may affect the properties of gold particles, thus leading to an adsorption behavior that depends on the oxide thickness (Risse *et al.,* 2009). This could explain the fact that different adsorption capacities were observed with some sorbents (e.g. Au/ZnO), depending on the physical pretreatment. On another hand, Zhang and Huang (2010) in their study on the functional surface modification of natural cellulose substances for colorimetric detection and adsorption of Hg^{2+} in aqueous media, have demonstrated, using solid UV–vis spectra of TiO_2 alone and TiO_2 coated with cellulose nanofibre, that TiO_2 does not retain mercury. This suggests that the retention of mercury in the metal oxide support can be excluded as a potential factor responsible of the increase of mercury adsorption capacity in the nano-structured materials. It was suggested that the plausible role of the oxide support is to stabilize particular atomic configurations, charge states, or electronic properties of the ultrasmall gold aggregates, which are in turn responsible for a distinct chemical behavior (Risse *et al.,* 2008).

Finally, studies have also shown that water strongly interacts with oxygen atoms in gold supported metal oxides to make a water-oxygen complex or hydroxyls (Lazaga *et al.,* 1993; Kim et al., 2006; Gong et al., 2007), although Quiller and colleagues (2008) have suggested that isolated stable hydroxyls may not be formed and could be more transient in character. The susceptibility of nano-gold supported metal oxides materials to act as a

Brønsted base or a nucleophilic base (Outka and Madix, 1987), due to the presence of oxygen atoms, could explain the "wetting" observed with the Au/Al_2O_3 sorbent.

It can therefore be seen from the above observations that Au/TiO_2 has demonstrated better analytical performances compared to Au/Al_2O_3 and Au/ZnO. This is the reason why Au/TiO_2 was selected to be tested as a sampling trap under real environmental conditions.

6.9 Quality control

TGM determination is known to be a delicate analysis because mercury is ubiquitous, persistent and can adsorb in different types of materials. Minimizing contamination problems is one of the biggest challenges in trace mercury analysis which requires the decontamination of all the materials and the skillful handling of "ultratrace" techniques during sampling and analysis. It is, therefore, of importance to proceed to number of blanks determinations in order to trace eventual sources of contamination during sampling, storage and/or analysis and to ensure the good quality of measurements. Blanks determinations were performed before and after each measurement in order to ensure a complete desorption of mercury in the trap and to clean the analytical line.

It was also necessary to proceed to a quality control before TGM analysis to minimize any effect that could affect the mercury determination at such a low level (memory effect, contamination, etc.). The absolute detection limit (ADL) of the DA-CVAFS technique was determined using the instrument background signal (noise) of twenty measurements and was found to be 0.04 pg of Hg^0. The method detection limit (MDL) and the method limit of quantification (MLQ) were also determined using a mean volume of 12 L for both Au-coated sand and Au/TiO_2. Finally, a global method detection limit (sampling and analysis) was determined by replacing Whatman filters with gold-coated sand traps: the air passing through the columns was assumed to be "mercury free". The sampling columns (Au-coated sand and Au/TiO2) were then submitted to the same analytical protocol used for TGM determination. The different analytical performances obtained are presented in table 6.2.

Table 6.2 Method Analytical performances

	n	MDL (ng m^{-3}) (*)		MLQ (ng m^{-3})	
		Au	TiO_2/Au	Au	TiO_2/Au
DA/CVAFS	10	0.07	0.10	0.22	0.33
Sampling	5	0.15	0.19	0.52	0.62

(*)The MDL is calculated for a sample volume of 12 L

Detection limit values were excellent and suitable for the detection of Hg^0 at background level. It has to be recalled that TGM levels for background continental areas were reported to be in the range of 1.0 to 4.0 ng m^{-3} (Fitzgerald *et al.*, 1984; Lindqvist and Rodhe, 1985).

6.10 TGM analysis

Results of the TGM measurements performed on the collected air samples from the laboratory environment are presented in figure 6.17.

The TGM in collected samples ranged between 6 - 10 ng m^{-3} for the Au/TiO_2 trap, and 6 - 9 ng m^{-3} for the commercial gold sand. Due to the level of TGM measured and the variability in samples (air recirculation in the building, weather changes and activities in the laboratory), the obtained values were not considered to be significantly different. Indoor (L1, L2, L3) and outdoor (R) concentrations were almost similar, although the variability in R was higher than in L samples. This is probably due to changes in environmental conditions during sampling (wind direction and speed, air temperature, point sources, etc).

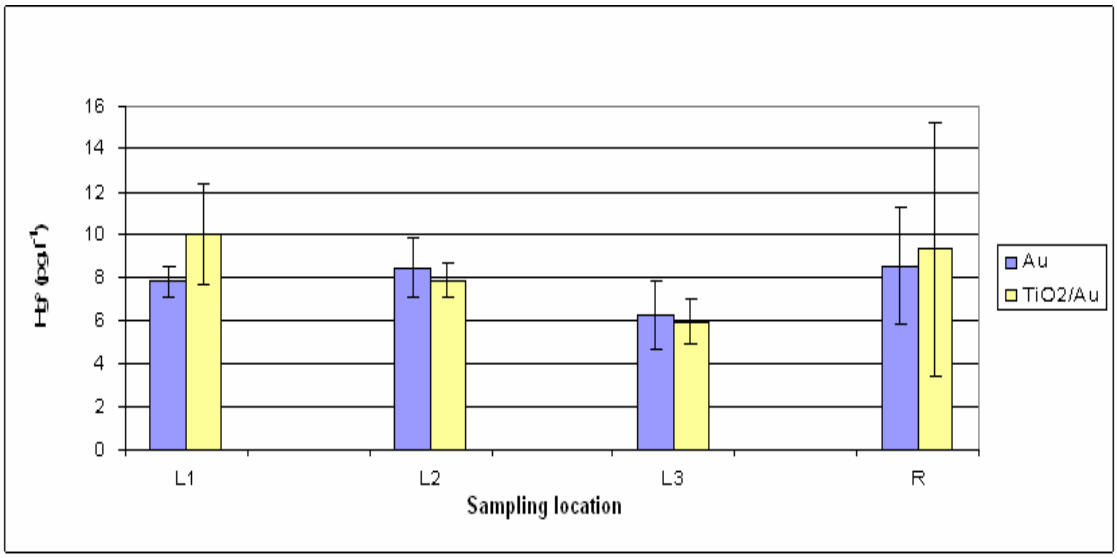

Figure 6.17 TGM in the laboratory ambient air where "Au" stands for gold coated sand

TGM is known to exhibit an important diurnal variability with, generally, a maximum peak at midday (Amouroux *et al.*, 1999). Au/TiO_2 and gold-coated sand have shown similar average of TGM level confirming the successful application of the nano-gold trap in real environmental conditions. The average TGM level in the study environment was about 7.6 ± 1.5 ng m^{-3} which represents the average range obtained in urban areas (Ebinghaus *et al.*, 1995; Pécheyran *et al.*, 2000).

Au/TiO_2 has demonstrated a consistent response after being used for more than 3 months on a daily basis depending on storage conditions. A degradation of the adsorption efficiency was observed when the sorbents were stored at room temperature and/or exposed to the light for several hours.

6.11 Conclusion

This study has demonstrated the successful application of nano-structured gold supported in metal oxide materials for the trapping and preconcentration of mercury directly from the gaseous phase. Au/TiO_2 has shown better analytical performances compared to Au/ZnO and Au/Al_2O_3, although it has also exhibited some retention problems. The superior performance of Au/TiO_2 may relate to the grain morphology of TiO_2, dispersion of gold particles, and the architecture of metal/oxide junctions. A deeper characterization

of the inner structure of the studied materials is crucial to understand the different behaviors observed and to improve, where necessary, the performance of the materials.

The development of an analytical procedure for TGM determination using Au/TiO_2 sorbents was achieved in a performant and cost effective way compared to current methods since only 1% (w/w) of gold was required for the preparation of the materials. The excellent MDL obtained with Au/TiO_2 makes it suitable for background TGM determination and environmental measurements of TGM with Au/TiO_2 were similar to those obtained with traditional gold traps.

Finally, the nano-sorbents will be tested in a near future for the trapping of mercury in water samples and in flue gas released from power stations as they can provide an interesting alternative to existing sorbents.

Chapter 7

Speciation of mercury in South African coal

The mercury concentration in South African coal is currently a subject of ongoing discussions involving local and international scientists (e.g. Wagner and Hlatshwayo, 2005; Leaner *et al.*, 2009; Kolker *et al.*, 2011). Recently, the International Energy Agency Clean Coal Center (IEA CCC) has organized, in collaboration with the South African department of environmental affairs, the 8th workshop on Mercury Emission from Coal (MEC 8) (Kruger Park, SA) where a number of local and international organizations, university research groups, private and public companies, have presented their latest knowledge on coal emission related research with an emphasis on South African coal. The special consideration given to SA coal is due to the big amount burned annually in power plants which places coal combustion as the biggest mercury pollution source in the country.

Reducing mercury emissions from SA coal-fired power plants may help minimize or avoid health problems caused by exposure to excess mercury.

The US Geological Survey (USGS, 2001) has presented several ways in which this reduction can be accomplished which include the use of high-rank coals, the selective mining of coal (avoiding parts of a coal bed that are higher in mercury content), the use of coal washing techniques (to reduce the amount of mercury in the coal delivered to the power plants), switching from coal to natural gas, and the use of post-combustion removal of mercury from the power plant stack emissions.

Therefore, information on the abundance, distribution, and forms of mercury in coal may be helpful not only in selecting the most efficient and cost-effective options for mercury reduction but also in predicting mercury distribution in a coal deposit, and its behavior during coal mining, preparation and combustion.

The focus of the study discussed in this chapter is to (1) determine mercury concentrations in collected South African coals and compare the average value with the published averages of local and world coals, (2) perform speciation analysis in order to identify some of the mercury species (Hg^0, Hg^{2+} and CH_3Hg^+, etc) that might be present

in coals, (3) provide information on modes of occurrence of mercury in SA coals using sequential extraction procedures.

7.1 Samples origin

Not all samples, used in this study, were collected by our research team. Most coal and ash samples were supplied by local power stations (Highveld coals and Waterberg coals). Twelve coal (six raw and six pulverized) and two ash samples were obtained from six power stations located mainly in the Mpumalanga Province (Highveld Region) and five other coal samples were collected from the Waterberg Coalfield located in the Limpopo Province. Little was revealed by samples suppliers about samples sources and sampling conditions. A map describing the different location of South African's coal-fired power stations is presented in figure 7.1. Waterberg samples were collected at different (unspecified) seams and were only used for the determination of total mercury concentration. Table 7.1 presents a brief description of the study samples.

Table 7.1 Coal fired power stations and the types of coal and ash samples collected

Sample ID	Description
AIT	Older ash from Tutuka power station
FAT	Fresher ash from Tutuka power station
TRC	Raw coal from Tutuka power station
TPC	Pulverized coal from Tutuka power station
DRC	Raw coal from Duvha power station
DPC	Pulverized coal from Duvha power station
KCC	Pulverized coal from Kriel power station
KUC	Raw coal from Kriel power station
LRC	Raw coal from Lethabo power station
LPC	Pulverized coal from Lethabo power station
MRC	Raw coal from Majuba power station
MPC	Pulverized coal from Majuba power station
RCC	Raw coal from Camden power station
CCC	Pulverized coal from Camden power station

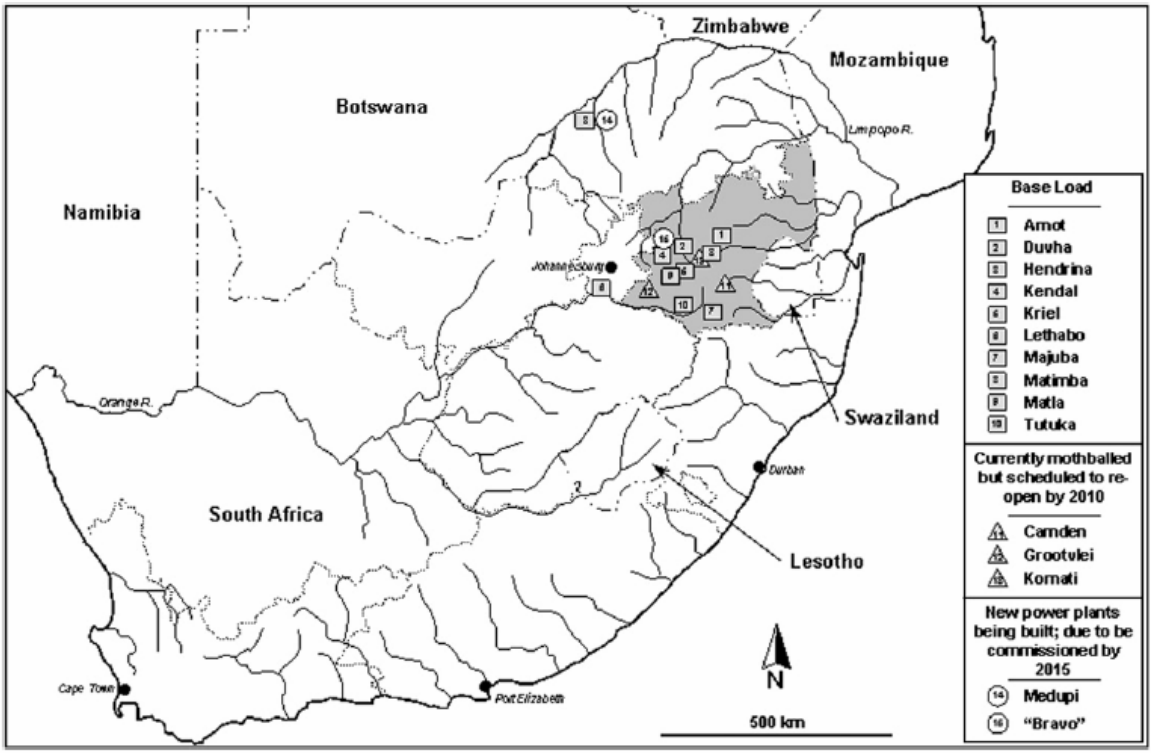

Figure 7.1 Location of current and future coal-fired power plants in South Africa. The Mpumalanga Province is shaded to highlight the presence of major power plants within this province (Dabrowski *et al.*, 2008).

7.2 Analytical procedures

7.2.1 Chemicals

All chemicals were analytical grade reagents and solutions were prepared in deionized water 18.3 MΩ cm (MILLIPORE). Concentrated nitric (55%), hydrochloric (32%), hydrofluoric (40%) (Merck), boric acid (99.5%) (M&B), ammonia (25%) and acetic acid (99%) (Merck) were used to prepare an ammonium acetate solution. All these reagents were used for the sample extraction and digestion. A stock solution of 10 ± 0.3 mg L^{-1} mercury in 10% HNO_3 (De Bruyn Spectroscopic Solutions, SA) was also used for the preparation of standards.

Reagents used for SIDMS analysis were the same as described in chapter 5.

7.2.2 MAE for the determination of total mercury and mercury species

Microwave digestion was used for the determination of Hg_{TOT}. Coal samples were first grinded to finer particles using acid cleaned mortars and pestles. The procedure used for the sample treatment was adapted from an existing method developed by CEM (www.cem.com).

Coal and ash samples, including coal reference materials (SARM20 and NIST 2685b), were digested prior to analysis using a closed microwave system (Multiwave 3000, Anton Paar). The following program was used for the digestion:

Sample mass: ±0.20 g Reagents: HNO_3 (10ml); HF (2ml); HCl (1ml)

Step	Power (W)	Ramp (min)	Hold (min)	Fan
1	400	15	25	1
2	0	5	5	3

The concentrated HF was later neutralized with H_3BO_3 to minimize the damaging effect of HF to glass made materials, and all the samples were then diluted with de-ionized water (Millipore). Blanks were also prepared using the same methodology as for the samples. The digested samples were finally kept in a fridge until Hg_{TOT} determination by ICP-MS (SPECTRO, 2000).

Total mercury in coals was also determined, for comparative analysis, by a direct sample introduction technique using an automated mercury analyzer (AMA254, Leco). The AMA254 (figure 7.2) technique of direct combustion features a combustion/catalyst tube that decomposes the sample in an oxygen-rich environment and removes interfering elements.

A gold amalgamator trap collects all mercury from the evolved gases and a dual-path length cuvette/spectrophotomer specifically determines mercury over a wide dynamic range. The method was approved by the EPA and ASTM and offers a fast, cost effective alternative to conventional CVAAS or ICP. This system combusts various matrices without sample pre-treatment or concentration step. The instrument requires no chemicals, providing a mercury determination in approximately five minutes.

Figure 7.2 The automated mercury analyzer for direct solid introduction

The instrument is able to determine trace amounts of mercury in various materials including coal, combustion residues, soils, biological samples, and other solid/liquid samples. The instrument detection system is based on a standard AAS at a specific wavelength (253.7 nm).

The extraction of mercury species in coal and ash samples, for SIDMS analysis, was performed by an open microwave-assisted extraction instrument (CEM, USA). The technique was previously described in the literature by Rodrıguez Martın-Doimeadios *et al.* (2003) and was also discussed in chapter 5. Briefly, 0.2 g of finely pulverized coal was suspended in 5 mL HNO_3 (6 N) and exposed to microwave irradiation at a power of 75 W for 5 min. The supernatant solution was separated after centrifugation at 3000 rpm for 5 min, poured into 22-ml Pyrex vials with Teflon caps, and stored in a refrigerator until analysis.

7.2.3 Isotopically enriched inorganic and monomethylmercury spikes

Two spiking procedures were tested in order to optimize the equilibrium between the analyte and spikes (figure 7.3):

- *Direct spike to the solid in aqueous slurry before extraction (Method 1):* Approximately 1.0 g of sample was spiked with a known amount of enriched $^{199}Hg^{2+}$ and $^{201}CH_3Hg^+$ solutions, the concentration of which had been determined beforehand by reversed speciated isotope dilution. 30 ml of water was added, and the resultant slurry was placed in a vortex for 5 minutes. The remaining solvent was evaporated overnight at ambient temperature in the dark in a laminar flux hood. The dry sample was subsequently subjected to the microwave-extraction procedure.

- *Spike to the acid extract after microwave heating (Method 2):* Spikes were added to the leachate after acid leaching and the removal of remaining coal particles.

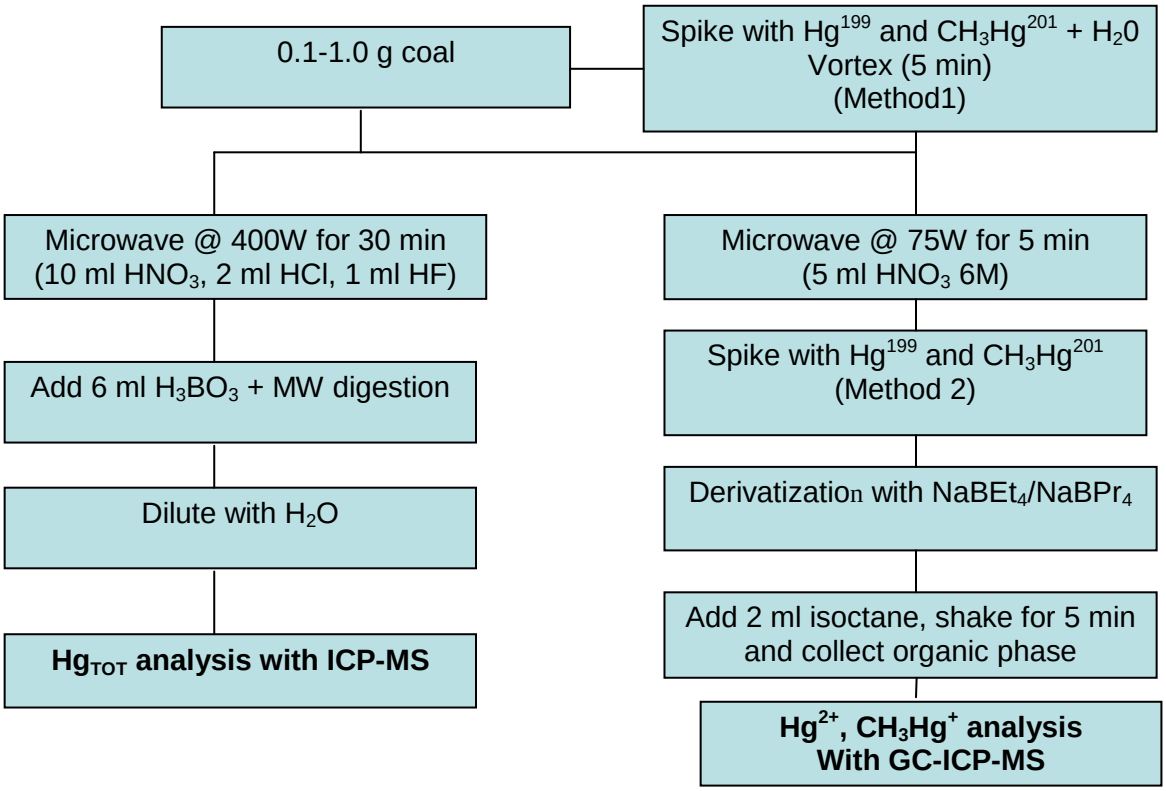

Figure 7.3 Procedures for total mercury and speciation analyses

7.2.4 Derivatization procedures

Two different derivatization procedures were used to identify the mercury species (figure 7.3):

- *Ethylation:* Mixed standard solutions of different mercury compounds together with coal and ash extracts were all buffered to pH 3.9 with 5 ml of a 0.1 M acetic acid-sodium acetate buffer. The pH was adjusted, where necessary, to 3.9 by addition of concentrated NH_3 or HCl (suprapure). A specific volume (1 – 2 ml) of a 1 to 2% sodium $NaBEt_4$ solution was added as derivatization reagent and 2 ml of isooctane was also added to extract the alkyl compounds formed. After 5 min of manual shaking and 5 min of further centrifugation (3000 rpm), the organic layer was transferred to a glass vial and stored in freezer until measurement.
- *Propylation:* This procedure was used in order to identify the possible occurrence of ethylmercury in coal as this latest cannot be identified with the ethylation due to the presence of Hg^{2+} which forms, as for ethylmercury, diethylmercury compounds during the derivatization with $NaBEt_4$.

The same derivatization procedure was followed as for the ethylation. The only difference was in the use of $NaBPr_4$ as the derivatizing agent instead of $NaBEt_4$.

During the analysis, 1 µl of the sample was injected to the GC for mercury species separation and the detection was performed with an ICP-MS (X-serie7, Thermo Fischer). The instrument parameters were similar to those previously described in chapter 5.

7.2.5 Sequential extraction procedure

The leaching procedure carried out is based on the USGS procedure however modified and consists of a five consecutive leaching steps involving five different solvents (figure 7.4).

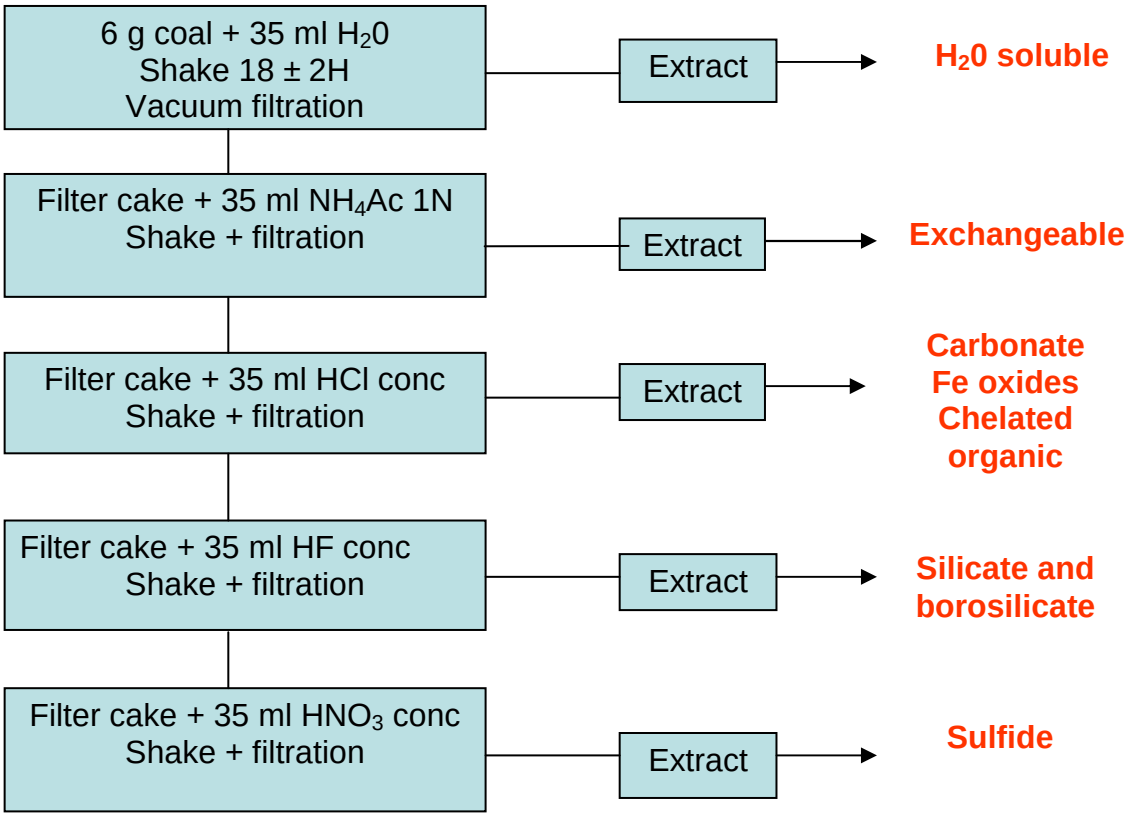

Figure 7.4 Schematic of the sequential extraction procedure used in this study

Initially, a measured sample of around 6 g of each of the grinded coals as well as two ash samples was placed into separate 60 ml Teflon bottles with a leak-proof screw closure. The sequential extraction then involved adding 35-ml of milli-Q water which is used to remove water soluble mercury and the bottles were then placed in a shaker for 18H (±2H). Subsequent to this procedure, the water was then removed from the coal by using a 0.45-micron cellulose nitrate membrane filter (Millipore) in a vacuum filtration system. The leachate was stored in a fridge until analysis while a mass of approximately 1 g was removed from the recovered filter cake for acid digestion and the rest transferred back to the Teflon bottle for further leaching. To this a 35-mL aliquot of 1.0 N ammonium acetate (NH_4–Ac) was added. The NH_4–Ac solvent was used to remove mercury associated with exchangeable sites. The coal slurry was then placed in a shaker and allowed to process for 18H (±2H). The leachate was stored for mercury analysis. From the filter cake recovered, a 1-g sample was isolated for acid digestion and mercury

analysis while the remainder of the filter cake was returned to a Teflon bottle for the next step of leaching. The same procedure was applied for concentrated HCl (to remove any mercury bound to carbonates, iron oxides, and certain chelated organic compounds), concentrated HF (to remove silicates and borosilicates) and 2.0N HNO_3 to ensure that disulfide bound mercury, mainly from the pyrite fraction is leached. Any unleached mercury is assumed to be organically bound.

7.3 Methods validation

Analytical procedures used in this study were validated with to CRMs of coals, SARM 20 (SABS, SA) and NIST 2685b (NIST, USA), both only certified in total mercury. Unfortunately, a reference material of coal certified in MHg was unavailable when this study was carried out. The validation for speciation analysis was therefore done by comparing results from the different analytical procedures used.

7.3.1 Total mercury in coal CRMs

Measured total mercury concentrations in CRMs were all within the certified range (table 7.2) with recoveries beyond 90%. Statistical "t" tests have shown that the measured Hg_{TOT} were not significantly different to certified values at 95% confidence level. This was a better result compared to the one reported by Wagner and Hlatshwayo (2005) which showed a loss of about 20% of Hg_{TOT}, for SARM 20, suggesting a non efficient sample preparation probably during the microwave assisted extraction. Excellent RSDs were also obtained demonstrating a good repeatability of the measurements. The methods were therefore selected for total mercury determination in coals.

Table 7.2 Hg_{TOT} in CRMs coal

CRM	Instrument	Measured Hg ($\mu g\ kg^{-1}$) ± SD	RSD (%)	Certified Hg ($\mu g\ kg^{-1}$)	Recovery (%)
SARM 20	AMA254	232.4 ± 12.4	5.4	250	93
	ICP-MS	240.2 ± 8.4	3.5	(180-270)	96
NIST 2685b	ICP-MS	135.5 ± 4.8	3.5	146.2 ± 10.6	93

7.3.2 Speciated isotope dilution (SIDMS) analysis of mercury in coal CRMs

Results obtained with the direct slurry spiking (method 1) and the acid extract spiking (method 2) for SIDMS analysis of SARM 20 were compared and are presented in table 7.3. An example of chromatogram obtained from the speciation analysis performed on SARM 20 is shown in figure 7.5. A good resolution was obtained for both Hg^{2+} (IHg) and CH_3Hg^+ (MHg) with an excellent signal/background ratio for the low level MHg. The detection limits were 0.36 ng kg^{-1} for IHg and 0.09 ng kg^{-1} for MHg.

No significant difference was observed in IHg and MHg concentrations when both methods were used, although the spiking after the microwave extraction (method 2) appeared to give slightly higher concentration than the slurry spiking (method 1).

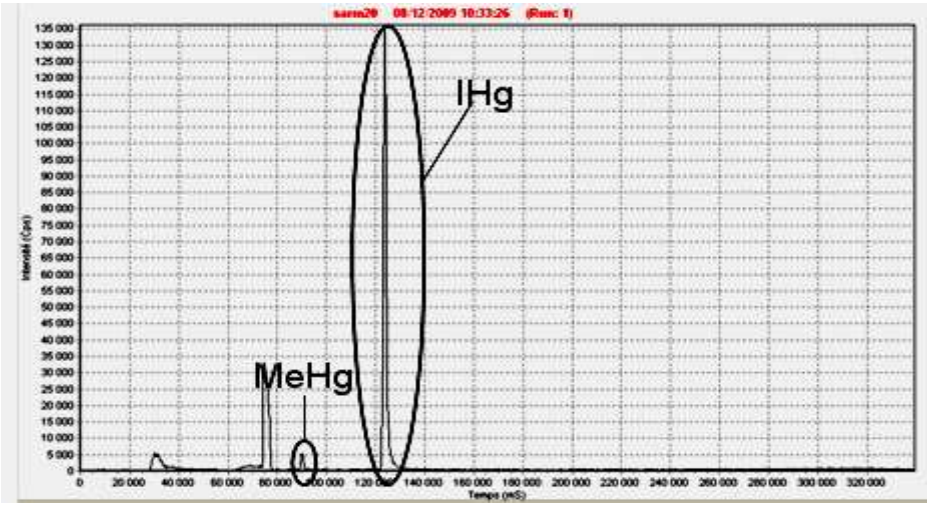

Figure 7.5 GC-ICP-MS chromatogram of SARM 20

Besides, method 2 was time consuming due to the need of an overnight evaporation of the added water. For these reasons, method 1 was selected for the analysis of study coals.

Table 7.3 SIDMS results from different spiking methods

	Method 1		Method 2	
CRM	IHg	MHg	IHg	MHg
(n=7)	(µg kg^{-1})	(µg kg^{-1})	(µg kg^{-1})	(µg kg^{-1})
SARM 20	221.2 ± 4.3	0.42 ± 0.03	225.2 ± 6.5	0.57 ± 0.06

IHg and MHg values obtained after propylation with $NaBPr_4$ matched the results obtained after ethylation with $NaBEt_4$ (table 7.4). No apparent artifact methylation was observed. Therefore, both derivatization procedures were considered valid for IHg and MHg speciation of coal samples.

Table 7.4 SIDMS results obtained after derivatization with $NaBEt_4$ and $NaBPr_4$

	Ethylation		Propylation	
CRM (n=7)	IHg ($\mu g\ kg^{-1}$)	MHg ($\mu g\ kg^{-1}$	IHg ($\mu g\ kg^{-1}$)	MHg ($\mu g\ kg^{-1}$)
SARM 20	221.2 ± 4.3	0.42 ± 0.03	226.4 ± 2.39	0.45 ± 0.05

On another hand, it was found that the concentration of mercury obtained after summing individual species concentration (i.e. IHg + MHg ~ 225 $\mu g\ kg^{-1}$) was lower than the Hg_{TOT} of 240 $\mu g\ kg^{-1}$ (i.e. about 94% recovery). This suggests that either mercury was not fully extracted from coal during the microwave extraction or there were some unidentified and, therefore, not quantified mercury species in the CRM. This recovery problem and the implied existence of unknown mercury species in coal are discussed further.

7.4 Results and discussion

7.4.1 Total mercury concentration in studied coals

Hg_{TOT} was measured in raw and pulverized Highveld coals using both direct solid introduction technique (AMA 254) and ICPMS (SPECTRO 2000) after microwave digestion. Results are presented in table 7.5.

Significant discrepancies were observed between data obtained from raw and pulverized coals with, generally, higher mercury content in pulverized coals. This can be attributed to a sample uniformity problem as it needs to be recalled that information about sampling conditions were not given by samples suppliers.

Table 7.5 Hg_{TOT} (µg kg^{-1}) in coals measured with different analytical procedures

Sample (n = 3)	Crushed Coal AMA 254	Crushed Coal ICP-MS	Raw Coal AMA 254	Raw Coal ICP-MS
Kriel	243.2 ± 25.7	167.0 ± 4.8	86.94 ± 12.5	218.9 ± 10.6
Lethabo	214.3 ± 30.0	185.9 ± 8.8	306.7 ± 76.4	250.4 ± 29.8
Majuba	336.3 ± 55.8	303.3 ± 23.6	166.0 ± 17.3	244.2 ± 35.9
Duvha	250.9 ± 40.6	225.7 ± 17.1	281.8 ± 51.1	309.6 ± 38.1
Camden	160.0 ± 23.9	172.0 ± 24.0	98.4 ± 19.3	102.6 ± 8.2
Tutuka	289.1 ± 28.0	262.5 ± 18.8	124.3 ± 19.6	178.0 ± 6.4
Mean ± SD	249.0 ± 60.7	219.4 ± 54.9	177.4 ± 94.9	217.3 ± 70.8

However, previous studies have also demonstrated that mercury (or metals) concentrations in coals might seriously differ from one stock pile to another. Other studies on the geochemistry of coal, including South African coal, have shown a notable vertical variation in mercury concentration compare to horizontal variation, indicative of different depositional environments vertically and possibly of localized metamorphism (Watling and Watling, 1982; Sakulpitakphon *et al*., 2004). These studies show the importance of sampling strategies for trace elements determination, especially when it comes to mercury.

Nevertheless, mercury concentrations measured from both analytical methods were closer in the pulverized coals than in the raw coals (see also figure 7.6) with a better repeatability obtained with the ICP-MS analysis. That is why Hg_{TOT} of pulverized coals performed with the ICP-MS (mean Hg: 219.4 ± 54.9 µg kg^{-1}) was used in further discussion.

The results obtained in this study were compared to published data (table 7.6) and, with the exception of Kriel and Lethabo, our data were similar to those found in the literature. No clear explanation could be found for the discrepancy observed on the above mentioned samples. Details on analytical procedures used for the published data used in this comparison were also not found.

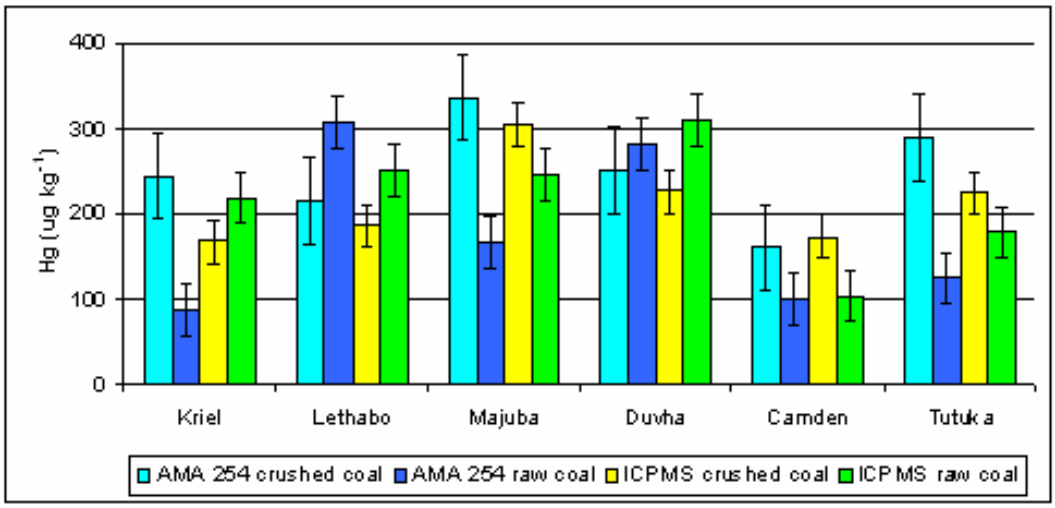

Figure 7.6 Hg in Highveld coals measured with different methodologies

Table 7.6 Comparison of Hg concentrations in Highveld coals

Coal ID	Reported Hg [(a)] (mg kg^{-1})	This study (mg kg^{-1}[(b)])
Duvha	0.23	0.23 ± 0.02
Kriel	0.34	0.17 ± 0.00
Lethabo	0.36	0.19 ± 0.00
Majuba	0.29	0.30 ± 0.02
Tutuka	0.29	0.26 ± 0.02
Mean	0.30 ± 0.05	0.23 ± 0.05

[a]Leaner et al. (2009) and the reference therein: reported data were measured in coal use at SA's power stations in 2001; [b]Results are presented in mg kg^{-1} to be consistent with published data

As mentioned previously, Hg_{TOT} was also performed in five coal samples collected from the Waterberg Coalfield. Obtained results are presented in table 7.7.

Table 7.7 Hg_{TOT} in coals from the Waterberg Coalfield

Coal samples	Hg (µg kg^{-1})
SA	183.4 ± 3.5
SB	230.4 ± 3.6
SC	190.9 ± 6.0
SD	143.9 ± 5.7
SE	155.5 ± 3.7
Mean	180.8 ± 33.8

The overall average concentration of mercury in coals from the Highveld region (mean: 219.4 ± 54.9 μg kg^{-1}) and the Waterberg Coalfield (mean: 180.8 ± 33.8 μg kg^{-1}) was 199.1 ± 25.9 μg kg^{-1} (0.20 ± 0.03 mg kg^{-1}).

The average mercury concentration in South African coals obtained in this study matched perfectly the USGS average value for Highveld coals of 0.20 mg kg^{-1} (table 7.8), although it was slightly higher than the mean reported by Wagner and Hlatshwayo (2005) (average 0.15 ± 0.05 mg kg^{-1}) for Highveld coals and the average of 0.16 mg kg^{-1} reported by the USGS for 40 South African's coals (Kolker *et al.*, 2011).

It needs to be recalled that Wagner and co-worker could not obtained the certified value for some metals, such as mercury, in SARM 20 and attributed the low recovery to the loss (~20% of Hg) that could occur during the opening of the digestion vessels after the microwave digestion and/or to the dilution factor since the analysis was performed with an ICP-OES instrument which is known to be less performing for low level metals concentration.

Table 7.8 Comparison of Hg_{TOT} (mg kg^{-1}) in South African and global coals

SA coals (This study)	SA coals (Watling and Watling, 1982)	SA coals (Wagner and Hlatshwayo, 2005)	SA coals (Leaner et al., 2009)	SA coals/ USGS (Wagner and Hlatshwayo, 2005)	SA coals/ USGS (Kolker et al., 2011)	Global average (Zhang et al., 2004)
0.20 ± 0.03	**0.327**	**0.15 ± 0.05**	**0.29 ± 0.10**	**0.20**	**0.16**	**0.12**

The authors even suggested that ICP-MS may be a better tool to use rather than ICP-OES (Wagner and Hlatshwayo, 2005). For this reason, the mercury concentration in Highveld coals is presumed to be higher than reported by these authors.

It appears, from the gathered data on the mercury content in South African coals, that a global average value of 0.2 mg kg^{-1} is more reliable to use in order to estimate mercury emissions from South African coal-fired power stations. But, more samples with proper sampling procedures are still required to improve the current database.

7.4.2 SIDMS analysis of coals

Six coal samples mainly from the Highveld region were analyzed by the above described procedure (section 7.2). The analytical results of the samples are listed in table 7.9. MHg was detected in all six samples with concentrations at the sub-ng level.

Table 7.9 IHg and MeHg in Highveld coals

Coal	IHg (μg kg^{-1})	MHg (μg kg^{-1})
Tutuka	261.1 ± 4.9	0.2 ± 0.1
Duvha	210.2 ± 3.6	0.3 ± 0.0
Kriel	142.9 ± 0.5	0.2 ± 0.1
Lethabo	184.3 ± 5.5	0.1 ± 0.0
Majuba	280.5 ± 0.1	0.4 ± 0.1
Camden	135.8 ± 0.2	0.1 ± 0.0
Average	202.5 ± 59.9	0.2 ± 0.1

The average MHg concentration was 0.2 μg kg^{-1} (range: 0.1-0.4 μg kg^{-1}) with the highest concentration for Majuba coal. This average value was lower than the one of 0.45 μg kg^{-1} (range: 0- 1.26 μg kg^{-1}) reported by Gao *et al.* (2008) for China coals.

GC-ICP-MS chromatogram allowed the identification of the following mercury species (figure 7.7): Hg^0, Hg^{2+} and CH_3Hg^+. This observation is in agreement with Dvornikov studies on soviet coal (Finkelman, 1994; Toole-O'Neil *et al.*, 1999 and references therein) who proposed that mercury occurs as mercury sulfide, metallic mercury and organomercury compounds.

Here, it is important to notice that a considerable amount of elemental mercury was probably oxidized by the 6M HNO_3 used during the microwave extraction and, therefore, IHg does not express only the concentration of naturally occurring Hg^{2+} forms in coals.

Other additional peaks than Hg^0, Hg^{2+} and CH_3Hg^+ were also obtained (figure 7.8) suggesting the existence of other forms of organomercurials in SA coals than MeHg.

This probably explains the reason why the sum of IHg and MHg could not match Hg_{TOT}, in most of the samples, except for Tutuka which show a recovery of almost 100%. The average recovery obtained with the used procedure was about 92%. The same situation was observed with SARM 20 and Gao *et al.* (2008) also mentioned the occurrence of other organomercury species in China coals.

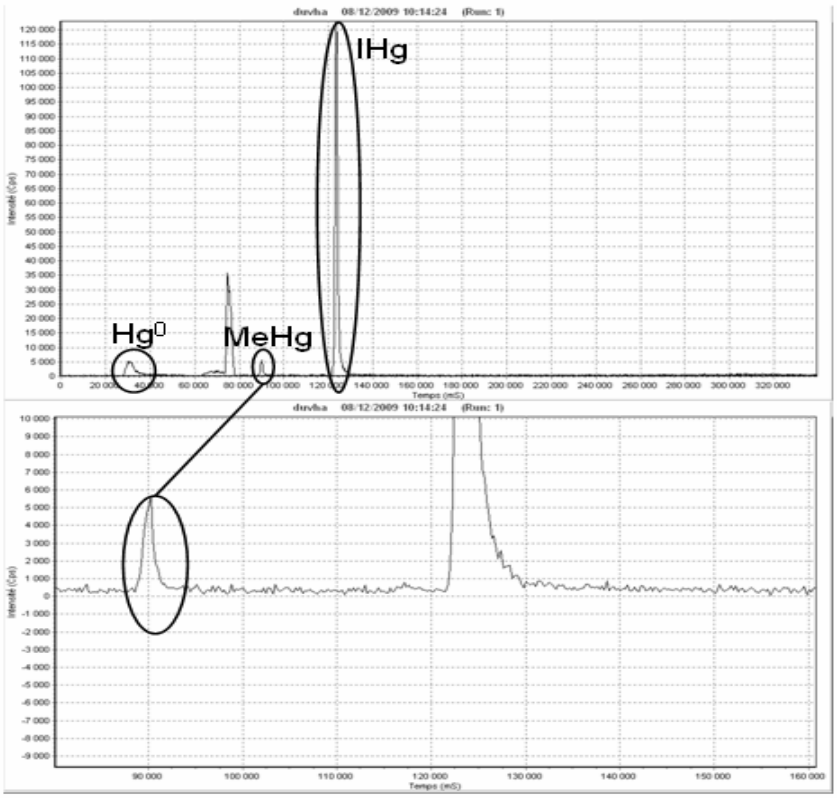

Figure 7.7 GC-ICP-MS chromatogram of “Duvha” sample showing the presence of 3 different Hg species (MHg appears more clearly in the magnified chromatogram)

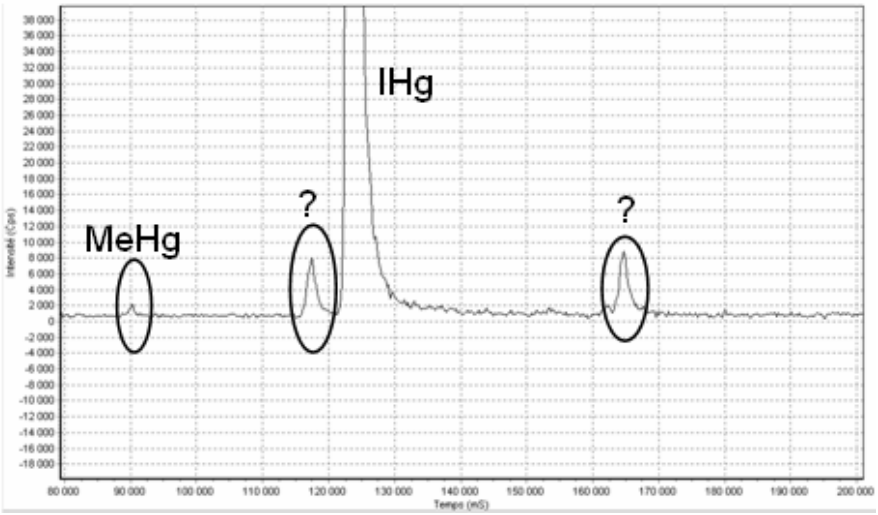

Figure 7.8 GC-ICP-MS chromatogram showing the presence of unknown Hg species

In their study on the speciation of mercury in selected China coals, Gao and colleagues (2008) have also identified ethylmercury (EtHg) in one sample at a concentration of 0.71

μg kg^{-1}. Due to the lack of standard, EtHg was not possible to be directly identified during our study. However, a theoretical approach was used in order to verify if one of the unknown peaks could be EtHg. In order to identify this species, a propylation of mercury species was of importance, prior to analysis, to avoid the artifact ethylation of IHg when $NaBEt_4$ is used. Figure 7.9 presents an example of chromatogram obtained after propylation with an unknown peak between MeHg and IHg. This peak was thought to be for the propylated ethylmercury i.e. ethylpropyl mercury ($CH_3CH_2Hg(CH_2)_2CH_3$ or EtHgPr).

The theoretical approach consisted of plotting a graph of peak retention time versus molecular weight (MW) and to compare the experimental MW for EtHgPr with the one in the literature (table 7.10).

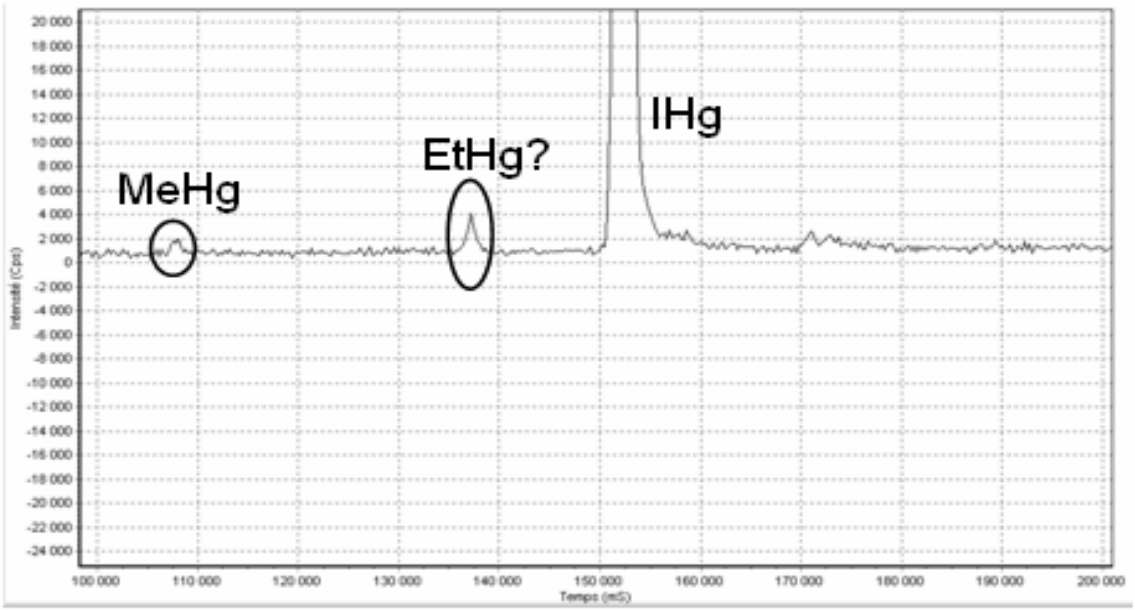

Figure 7.9 Example of GC-ICP-MS chromatograph obtained after propylation

A linear curve was obtained (figure 7.10) where the unknown peak corresponded to a MW of about 277. This value is closed to the actual MW of EtHgPr (MW = 272) which is the form of EtHg obtained after derivatization with $NaBPr_4$. This suggests that the unknown peak could be identified as EtHg, although a proper identification with a standard is still required.

Table 7.10 Propylated mercury species and their corresponding molecular weight

Species (after propylation)	GC-ICP-MS Peak time (S)	Molecular Weight
Hg^0	30	201
$CH_3HgCH_2CH_2CH_3$ (MeHgPr)	108	260
$CH_3CH_2CH_2HgCH_2CH_2CH_3$ (Pr_2Hg)	155	287
Unknown	138	277*

*Deduced from the experimental graph

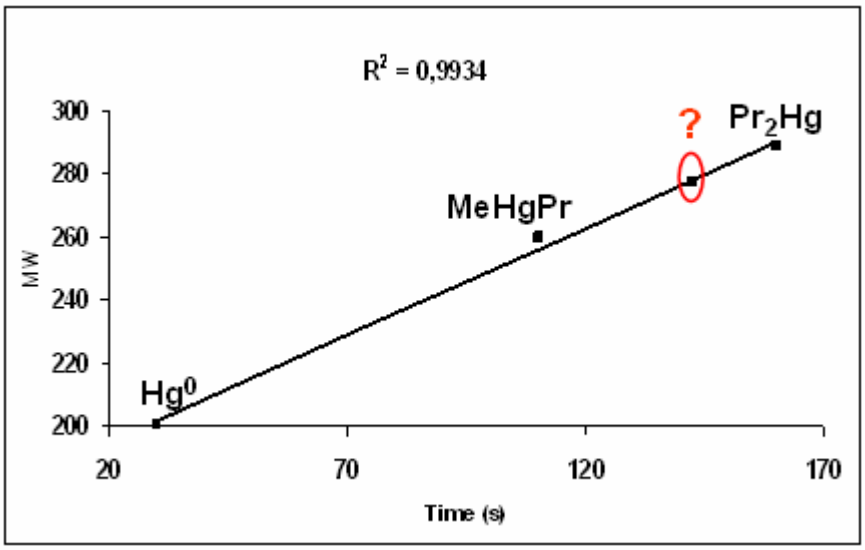

Figure 7.10 Correlation between retention time and molecular weight for different Hg species

7.4.3 Mercury modes of occurrence in Highveld coals

The sequential extraction procedures were performed on the 12 coal (raw and crushed) and 2 ash samples provided. The obtained results are presented in table 7.11. Concentrations reported as zero were below the method detection limit and the mean values are reported only for the 12 coal samples (i.e. except samples AIT and FAT).

Table 7.11 Concentration of mercury in coals and ashes leachates

Sample	H_2O	CH_3COONH_4	HCl	Hg ($\mu g\ kg^{-1}$) HF	HNO_3	Total leached	Hg_{TOT}	%leached
AIT[(*)]	2.6	0.3	87.7	10.7	87.8	189.1	168.2	112.5
FAT	1.9	0.3	84.1	6.7	133.7	226.7	239.1	94.8
TRC	1.4	2.0	24.9	0.0	155.5	183.7	178.0	103.2
TPC	3.1	0.6	39.6	23.0	126.8	193.0	262.5	73.5
DRC	9.9	0.6	36.4	10.6	60.8	118.2	309.6	38.2
DPC	6.6	0.7	52.7	22.0	37.7	119.6	225.7	53.0
KCC	6.4	1.2	10.5	6.6	65.6	90.2	167.0	54.0
KUC	2.9	1.2	26.1	37.8	60.7	128.7	218.9	58.8
LRC	3.5	1.2	22.5	0.0	74.5	101.7	250.4	40.6
LPC	2.9	1.2	36.5	16.5	87.5	144.6	185.9	77.8
MRC	3.0	0.7	40.1	5.2	49.6	98.6	244.2	40.4
MPC	2.9	0.6	56.6	13.5	91.2	164.7	303.3	54.3
RCC	2.4	0.6	27.4	0.0	50.2	80.5	102.6	78.5
CCC	2.3	0.8	36.6	0.0	68.3	108.0	172.0	62.8
Mean ± SD	3.9 ± 2.4	0.9 ± 0.4	34.1 ± 12.9	11.3 ± 11.9	77.4 ± 34.0	127.6 ± 36.6	218.3 ± 60.4	61.3 ± 19.2

[(*)]Highlighted data are for ash samples and are not included in reported means

The percentages of mercury in different fractions are listed in tables 7.12 and 7.13.

Table 7.12 Mercury content (in %) from different fractions in crushed coals

Sample	H_2O	CH_3COONH_4	HCl	HF	HNO_3	Total leached	Total unleached
Tutuka	1.2	0.2	15.1	8.8	48.3	73.5	26.5
Duvha	2.9	0.3	23.3	9.7	16.7	53.0	47.0
Kriel	3.8	0.7	6.3	3.9	39.3	54.0	46.0
Lethabo	1.6	0.6	19.6	8.9	47.1	77.8	22.2
Majuba	1.0	0.2	18.7	4.4	30.1	54.3	45.7
Camden	1.3	0.4	21.3	0.0	39.7	62.8	37.2
Mean ± SD	2.0 ± 1.1	0.4 ± 0.2	17.4 ± 6.0	6.0 ± 3.8	36.8 ± 11.8	62.6 ± 10.8	37.4 ± 10.8

Table 7.13 Mercury content (in %) from different fractions in raw coals

Sample	H_2O	CH_3COONH_4	HCl	HF	HNO_3	Total leached	Total unleached
Tutuka	0.8	1.1	14.0	0.0	87.4	103.2	0.0
Duvha	3.2	0.2	11.7	3.4	19.6	38.2	61.8
Kriel	1.3	0.5	11.9	17.3	27.7	58.8	41.2
Lethabo	1.4	0.5	9.0	0.0	29.8	40.6	59.4
Majuba	1.2	0.3	16.4	2.1	20.3	40.4	59.6
Camden	2.3	0.6	26.7	0.0	48.9	78.5	21.5
Mean ± SD	1.7 ± 0.9	0.5 ± 0.3	14.9 ± 6.3	3.8 ± 6.7	39.0 ± 26.0	59.9 ± 26.3	40.1 ± 26.3

Results were in excellent agreement with general trends observed in coal samples (Toole-O'Neil *et al*., 1999; Feng and Hong, 1999; Hoffart *et al*., 2006; Zheng *et al*., 2008b) with the lowest mercury concentrations in the ion-exchangeable (mean: 0.5%; range: 0.2 - 1.1%) and water leachable (mean: 1.8%; range: 0.8 - 3.8%) fractions which are extracted by NH_4-Ac and H_2O, respectively and the highest mercury concentration as sulfide-bound mercury (mean: 37.9%; range: 16.7 - 87.4%) extracted with HNO_3. In between, depending on the coal, there are carbonate (mean: 16.2%; range: 6.3 - 26.7%) and silicate-bound (mean: 4.9%; range: 0.0 - 17.3%) species extracted with HCl and HF, respectively. The remaining mercury is assumed to be organically bound and represents aproximately 39% (mean: 38.7%; range: 0.0 - 59.6%) of the total mercury content in analyzed coals. It has to be noticed that 2 samples (AIT and TRC) have shown abnormal leaching percentages of more than 100% (112.5 and 103.2%, respectively). Such results were also reported by Feng and Hong (1999) in their study on the modes of occurrence of mercury in coals from Guizhou (China) with the highest percentage in leachate of about

123%. The difference obtained in this study between the total mercury in leachates and Hg_{TOT} for the two samples can be atributed to analytical errors. But the magnitude of the difference was thought not to affect the quality of the result, except for the sample AIT which was already excluded in the reported mean (table 7.11) since it was an ash sample.. Figure 7.11 compares the percentage of mercury leached in raw and pulverized coals. Pulverized samples exhibited a slightly better leaching efficiency (mean Hg leached: 62.6%) compared to raw coal (mean Hg leached: 59.9%).

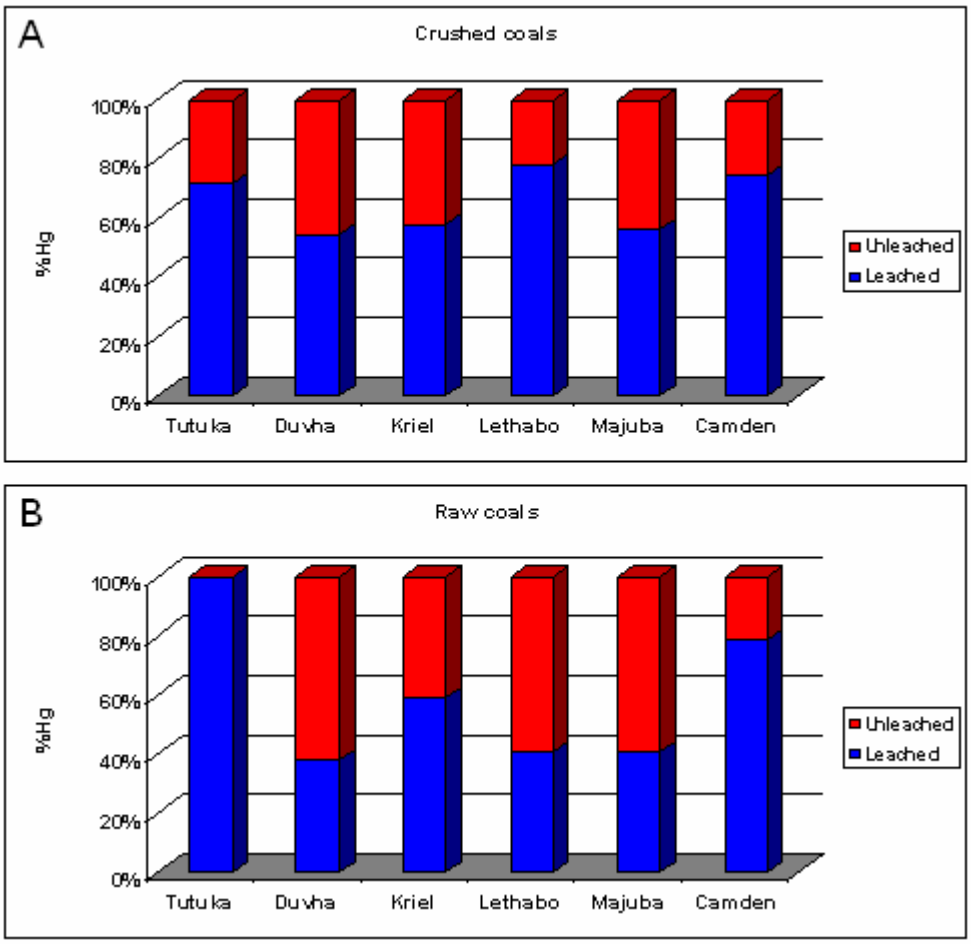

Figure 7.11. Leaching results for crushed (A) and raw (B) coals

The leaching efficiency also showed smaller variability with the pulverized samples (range: 53.0 - 77.8%) compared to raw coals (range: 38.2 – 103.2%). In addition, the percentage of mercury leached was always beyond 50% for pulverized coals whereas 3 of the 6 raw coals exhibited a percentage leached near 40%. Here again, as it was already

observed with total mercury measurements, results obtained with pulverized coals were more consistent than for raw coals.

A comparison was also made between the percentage of unleached mercury and the MHg concentration in pulverized coals (figure 7.12) in order to assess the impact of organic content on solvents leaching efficiency since MHg was the only oraganomercury that was formally identified in the study coals.

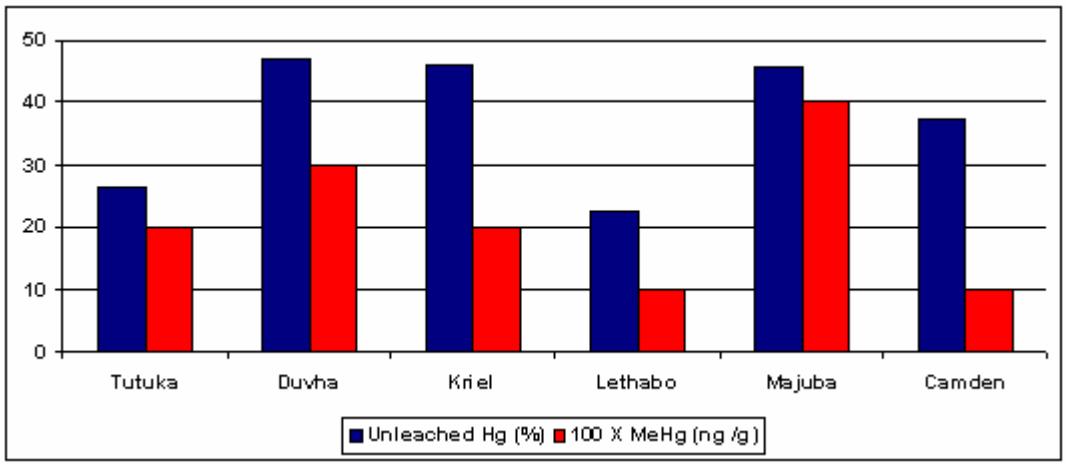

Figure 7.12 Comparison between unleached Hg and the MeHg content in coals

Although a weak correlation was obtained (R^2: 0.43), it appeared that samples with the highest MeHg content (Majuba, Duvha and Kriel, respectively) also had the highest percentage of unleached mercury after sequential exctration and the sample with the lowest MeHg content (Lethabo) had lowest percentage of unleached mercury.

Hoffart et al. (2006) have discussed the limited accessibility by solvents to the basic sites of coals where compounds may be present and Toole-O'Neil *et al.* (1999) have reported difficulties encountered with conventional cleaning methods in removing mercury from samples in which mercury is either organically bound or present in fine-grained minerals disseminated through the organic fraction of the coal.

The effect of organically bound mercury in reducing solvents leaching efficiency can also be seen when compared the leaching performance obtained between coal and ash samples. For example, samples TPC and FAT are pulverized coal and ash samples, respectively, obtainted from Tutuka power station. FAT exhibited a mercury removal of 95% whereas the corresponding coal showed about 74% of mercury leached. A

significant amount of mercury was found in the HCl fraction for FAT (35%) compared to TPC (15%) suggesting an increase of the HCl leachabale fraction in the ash sample which is presumed to be the result of coal combustion. Nitric acid also leached more mercury in ash (56%) than in coal (48%). SIDMS analysis of Tutuka fly ash (figure 7.13) showed only two mercury peaks (IHg and Hg^0) confirming the total absence of organomercurials in the sample whereas the corresponding coal presented a number of organomercury species together with IHg and Hg^0.

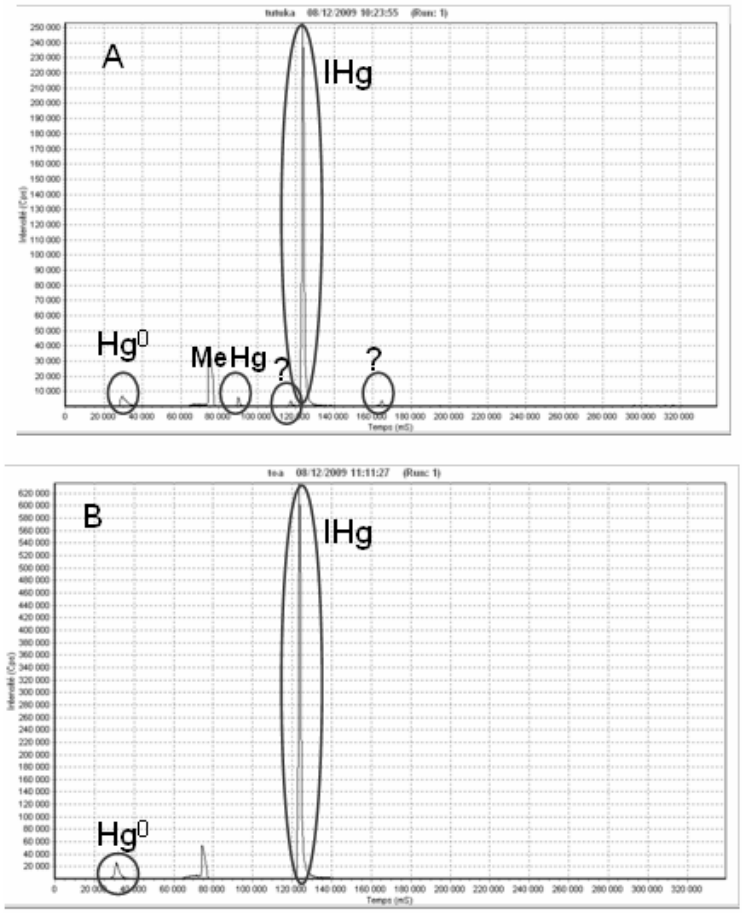

Figure 7.13 SIDMS chromatograms of Tutuka coal (A) and ash (B) samples

Wang *et al.* (2003) also observed that chromium, vanadium, cobalt and nickel in the ashes were more largely dissolved in both HCl and HNO_3 than those from the raw coal and they have deduced an organic association of these trace elements in their coal.

Palmer and colleagues (cited by Toole-O'Neil *et al.,* 1999) have presented a 35–75% (mean: 60%) mercury removal from 10 US bituminous coals using nitric acid. More recently, Hoffart *et al.* (2006) demonstrated a 50 - 70% mercury leaching efficiency in butiminous coals.

The overal mean values obtained in our study for the percentage of mercury leached in raw and pulverized coals were very closed (about 60 and 63%, respectively) giving a global average of 61.3 ± 19.2% (range: 38.2 – 78.5%, excluding Tutuka raw coal). Therefore, results obtained in this work agree with those mentioned above and authorize the adoption of the used sequential extraction procedure for the investigation of mercury removal in coals.

On another hand, when compared the fraction of mercury leached by different solvents used (figure 7.14), it appears that the modes of occurrence of mercury are variable in studied coals and the pyrite-HgS (38%), together with the organic-bound mercury (39%) seem to be the dominant forms. It is important to recall that previous studies done on modes of occurrence of mercury in coals have also shown results greatly depending on the nature of the coal (e.g. Feng and Hong, 1999; Iwashita *et al*., 2004; Hoffart *et al*., 2006; Zheng *et al*., 2008b)

The trend obtained in this study generally agreed with the observation made by Palmer et al. (1997) who reported that mercury has two dominant modes of occurrence with 25 to 65% of the mercury leached by HNO_3 indicating a pyritic assoiation. In addition, 5 to 35% (16% in this study) is leached by HCl . The HCl-leachable mercury may also, according to these authors, be associated with oxidized pyrite or HCl soluble sulfides, although Hoffart *et al.* (2006) stated that, due to the low solubility of HgS in HCl, the HCl-leachable fraction cannot represent the mono-sulfide associated fraction for mercury. Palmer and co-workers (1997) also proposed that the residual mercury (<35%) may be due to shielded pyrite and/or organic association. However, these authors also reported that there are some indications that mercury behaves slightly differently than other elements associated with pyrite and some mercury may be absorbed to the surfaces of organic rich particles. Dronen *et al.* (2004) also suggested that a significant fraction of the mercury is maintained in loose organic associations within the coal.

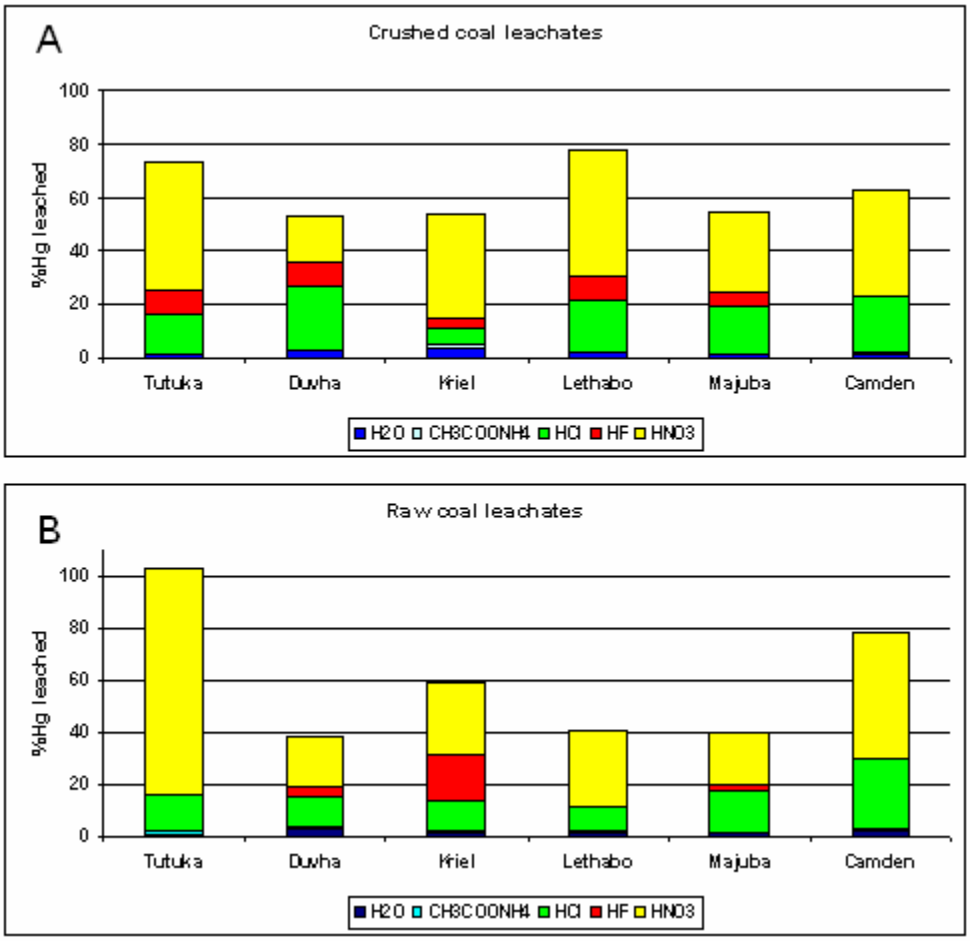

Figure 7.14. Leaching results for crushed (A) and raw (B) coals

Ruch *et al.* (1971) examined the distribution of mercury in specific gravity fractions of one coal. They found that a significant proportion of the mercury in this sample was associated with the pyrite and the remainder of the mercury (up to 50%) was in the lightest specific gravity fraction. These authors suggested that a part of the mercury in the light specific gravity fraction may have an organic association and also cautioned against making generalizations about the mode of occurrence of mercury in coal.

The complexity of the mercury modes of occurrence in coals was also highlighted by Swaine (1975) who cited two earlier studies of Soviet coal. In one study, mercury was found in pyrite and in the other study mercury was considered to be mainly organically bound, but, also to be present in sulfides and as a metallic mercury. Porritt and Swaine (1976) found that the correlation between mercury and pyrite in Australian coal did not

follow any clear pattern. They concluded that some of the mercury is associated with pyrite and some is associated with the organic matter.

An attempt was made, for a better understanding of our results, to correlate sequential extractions results with the ultimate and proximate data obtained for the study coals (table 7.14). Only pulverized samples were taken into account for this purpose since these samples showed a more consistent trend compared to raw coals.

Table 7.14 Proximate and ultimate values of puleverized Highveld coals

Sample	%moisture[a]	%ash[a]	%OM[a]	%C[b]	%H[b]	%N[b]	%S[b]
Tutuka	2.1	32.6	67.4	30.5	2.9	1.1	0.8
Duvha	0.9	32.5	67.5	35.3	3.0	1.1	1.1
Kriel	1.3	26.5	73.5	45.1	3.0	1.3	1.3
Lethabo	6.0	45.7	54.3	36.7	2.7	1.1	0.4
Majuba	3.3	26.0	74.0	38.5	3.2	1.2	1.0
Camden	2.0	29.9	70.1	38.9	3.0	1.1	2.1

[a]: Organic matter content determined after ASTM D 2974
[b]: determined with a CHNS analyzer (Leco)

An interesting correlation (R^2: 0.62) was found between the percentage of unleached mercury and the organic matter (figure7.15). This confirms the suggestion made previously that the unleached mercury is probably contained in the organic-bound fraction. A negative correlation was found between mercury in HNO_3 leached fraction and the pyritic sulfur (R^2: 0.68), as it is shown in figure 7.16. It has been reported that the correlation between the mercury content and the pyrite is not so strong (Iwashita *et al.*, 2004).

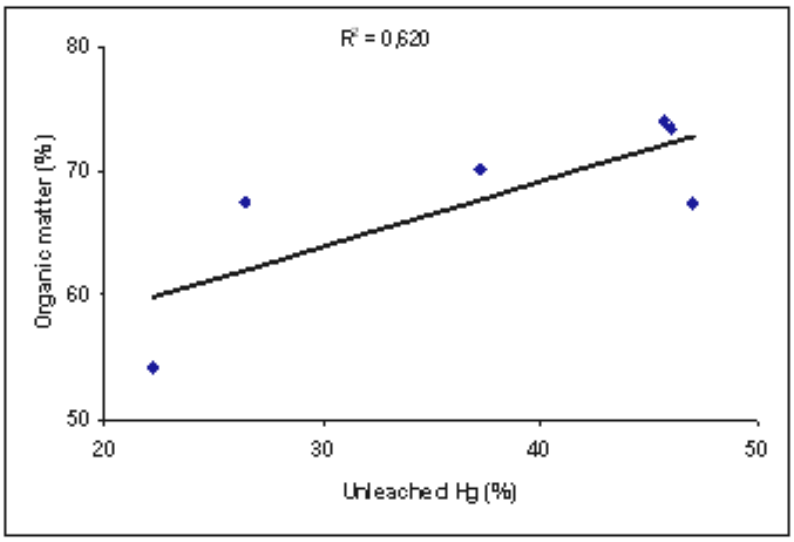

Figure 7.15 Correlation between unleached Hg and organic matter

Ruch *et al.* (1971) who reported a pyritic association in their studied coals also noted that the coal sample in which they found the highest mercury concentration contained only a trace of pyritic sulfur.

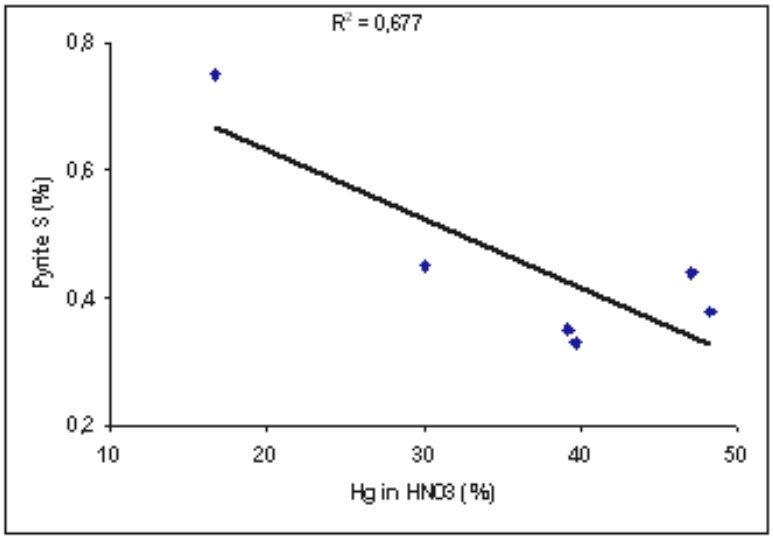

Figure 7.16.Correlation between Hg leached by HNO_3 and the pyritic sulfur

A correlation analysis was also performed between the mercury leached from the six highveld coals and the different sulfur forms (table 7.15), namely total sulfur (S_T), pyrite

sulfur (S_P), organic sulfur (S_O), and sulfate sulfur (S_S) which were determined using ASTM methods 2492 and 3177 (ASTM, 2007 a and b).

Surprisingly, it was found that the leached mercury had a significant correlation (R^2: 0.70) with sulfate sulfur (figure 7.17) and the correlation between mercury and forms of sulfur decreased in the following order: $S_S>S_P>S_T>S_O$.

Table 7.15 Total sulfur (S_T), pyrite sulfur (S_P), organic sulfur (S_O), qnd sulfate sulfur (S_S) in study coals (dry weight basis)

ID	$\%S_S$	$\%S_P$	$\%S_O$	$\%S_T$
Tutuka	0.08	0.38	0.40	0.87
Duvha	0.06	0.75	0.34	1.15
Kriel	0.03	0.35	0.64	1.02
Lethabo	0.09	0.44	0.12	0.50
Majuba	0.06	0.45	0.42	0.84
Camden	0.06	0.33	0.25	0.65

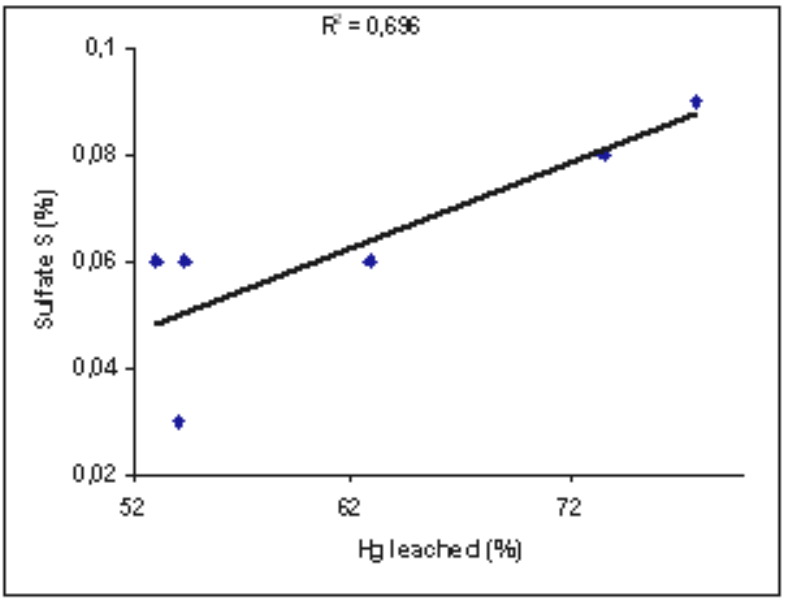

Figure 7.17 Correlation between leached Hg and sulfate sulfur

Luo *et al.* (2000) also found a strong affinity between mercury and sulfate sulfur in coals from the Weibei area in China and proposed the following sequence: $S_P>S_S>S_T>S_O$. They indicated that mercury occurred mostly as HgS in their coals. Further investigations are needed in order to understand the observation made in this study.

Finally, mercury in the HCl fraction correlated with total sulfur content (figure7.18) in coals (R^2: 0.59) which implies, as proposed by Palmer *et al.* (1997), that mercury in this fraction could also be associated with oxidized pyrite or HCl soluble sulfides, although a weak correlation (R^2: 0.30) was found between mercury in HCl and pyrite sulfur.

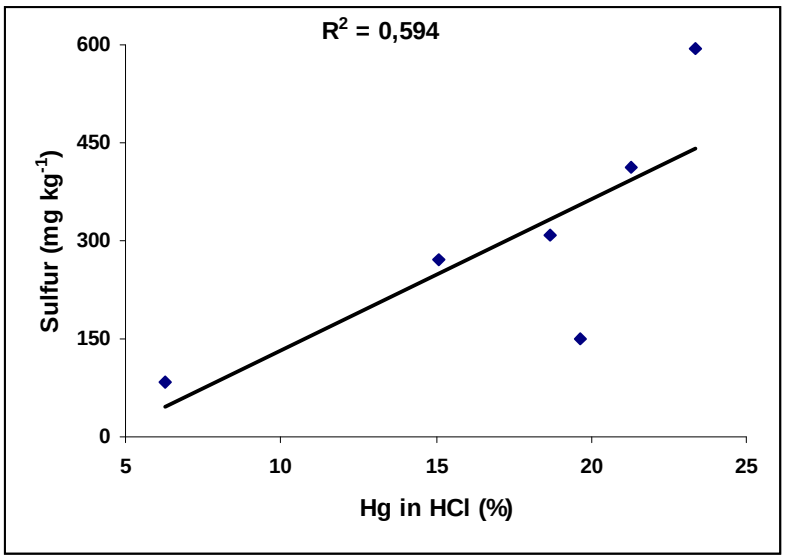

Figure 7.18 Correlation between Hg in HCl fraction and the sulfur content in coals

Moreover, when the mercury in HCl fraction was plotted against the mercury leached by HNO_3 (figure 7.19), a strong negative correlation (R^2: 0.81) was obtained. In their study on a two-step acid mercury removal process for pulverized coal, Hoffart and co-workers (2006) proposed that increasing the concentration and/or the temperature of the HCl solvent greatly increases the removal of mercury in the HCl leaching step. Subsequently, because HNO_3 is such a strong oxidant, it leached the compounds that were “missed” by the HCl leach.

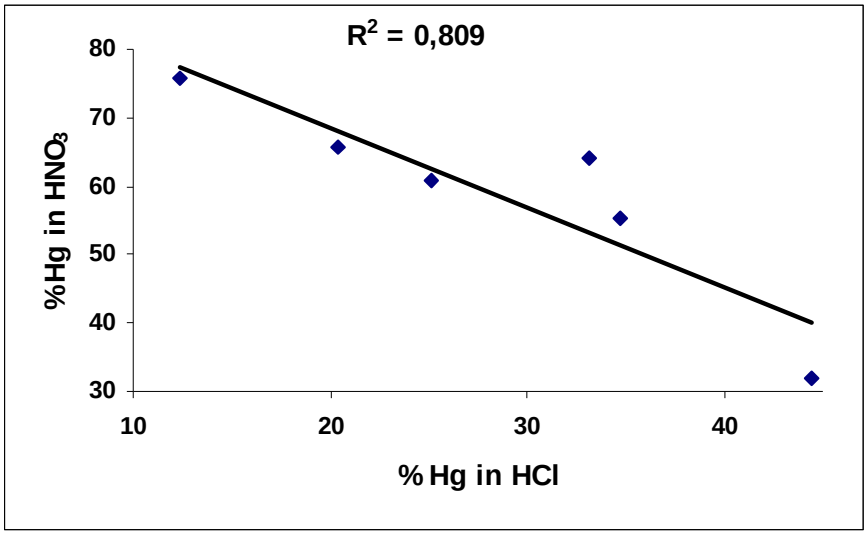

Figure 7.19 Correlation between Hg in HCl and HNO_3 fractions

It is important to note that most of the studies described above presented a small percentage of mercury in the HCl fraction with an average of approximately 5% (see examples presented in table 7.16). This is probably due to the use of dilute HCl instead of a concentrated one. The average of 16.2% obtained with the present study agrees, therefore, with the suggestion made by Hoffart and colleagues.

Table 7.16 Comparison between Hg leached in the HCl fraction from different studies

	36% HCl (This study)	0.5% HCl (Zheng *et al.*,2008b)	3.0 N HCl USGS procedure (Kolker *et al.*, 2002)
Mean Hg leached (%)	16.2	5.4	4

Moreover, results obtained in this study suggest that 61% of the mercury in Highveld coals is either in the elemental form or is inorganically bound. Filby *et al.* (1977) estimated that 47% of the mercury in their coal sample was inorganically bound and, more recently, studies carried out on some US lignite and bituminous coals have suggested mercury percentages between 54 and 90% in the inorganic fraction (Kolker *et*

al., 2002; Hoffart *et al.*, 2006). Here again, a good agreement is observed between data obtained from South African coals and studies performed in other coals.

7.5 Conclusion

Analytical procedures presented in this study were successfully used in determining total mercury, inorganic and methylmercury in coals. Obtained results were accurate, and exhibited good repeatability and reproducibility, although a material certified for speciation is not available.

The mercury concentration in studied coals varied between samples denoting a problem of sample uniformity. The average mercury concentration in the analyzed (pulverized) coals was 0.20 ± 0.03 mg kg^{-1}. This value was higher than the global average (0.12 mg kg^{-1}) and the average reported by the USGS for 40 SA coals (0.16 mg kg^{-1}) but matched the mean value obtained by the USGS for Highveld coals. More samples are still needed, that must be collected systematically and with care, to get a better average of mercury in SA coals. From the result obtained in this study and those currently available in the literature, we recommend the use of 0.2 mg kg^{-1} as the average of mercury content in SA coals to be used in estimations of mercury emissions from SA's coal-fired power stations.

SIDMS analysis has allowed the direct identification of Hg^0, Hg^{2+}, CH_3Hg^+ and the indirect identification of $CH_3CH_2Hg^+$. The occurrence of other mercury species were also observed which are thought to be organomercurials, although their identification was not possible with the used methodology.

Methylmercury concentrations of organomercuries in studied coals were relatively low, but the high toxicity of these species and the huge amount of coal consumed every year in SA may lead to serious environmental concerns during coal mining and beneficiation. This problem should be paid more attention to.

The mercury modes of occurrence varied strongly between coals. However, when sequential extraction results are combined together with correlations data, there is strong circumstantial evidence to indicate that a substantial proportion of mercury in studied coals is associated with organic constituents and pyrite. Some of the mercury in coal may be associated with other minerals such as iron oxides, carbonates and silicates.

The sequential extraction procedure used exhibited a 61% mercury leaching efficiency which is within the range of commonly used solvents leaching procedures.

The fairly wide range of effectiveness of mercury removal obtained in this work (38 – 79%) could be caused in part by differences in the modes of occurrence of mercury in coal. For samples in which mercury is either organically bound or present in fine-grained minerals disseminated through the organic fraction of the coal, the method was less efficient compared to cases where mercury was preferably bound to the inorganic fraction. Nevertheless, the procedure can be successfully used to assess the mercury removal from coals prior to combustion.

This study is believed to make an important contribution to the current knowledge on the mercury content and speciation in South African coals, although a lot has still to be done since experimental data on mercury in the country coal are still scarce.

Chapter 8
Mercury speciation in the Vaal River and West Wits mining operations

8.1 Scope of the study

The gold and uranium deposits of the Witwatersrand Basin form one of the great metallogenic provinces of the world. The accumulated sediments within the basin are collectively known as the Witwatersrand Supergroup and are made up of the West Rand Group (WRG) and the Central Rand Group (CRG) (McCarthy and Rubidge, 2005). The Far West Rand goldfields fall within a prominent semi-circular band of Transvaal Supergroup rocks, which commence south of Johannesburg and pass beyond Carletonville to Orkney (near Klerksdorp) in the West (figure 8.1).

One of the most important aquifers in South Africa is the dolomitic aquifer of the West Rand and Far West Rand area. Due to the anthropogenic influences from both mining and industrial sources, this aquifer is increasingly under threat of becoming a vast unexploitable reserve of no use as a groundwater resource (www.deepbio.princeton.edu).

Gold mining is the principle economic activity in the West Rand and Far West Rand regions. This industry is the basis of the economy and socio-economic development of the region. Gold mining on the West Wits Line contains of the biggest and richest mines in the entire Witwatersrand Basin (Robb *et al.*, 1998). Unfortunately, associated with all the economic and social benefits arising from gold mining there are several negative impacts on the environment.

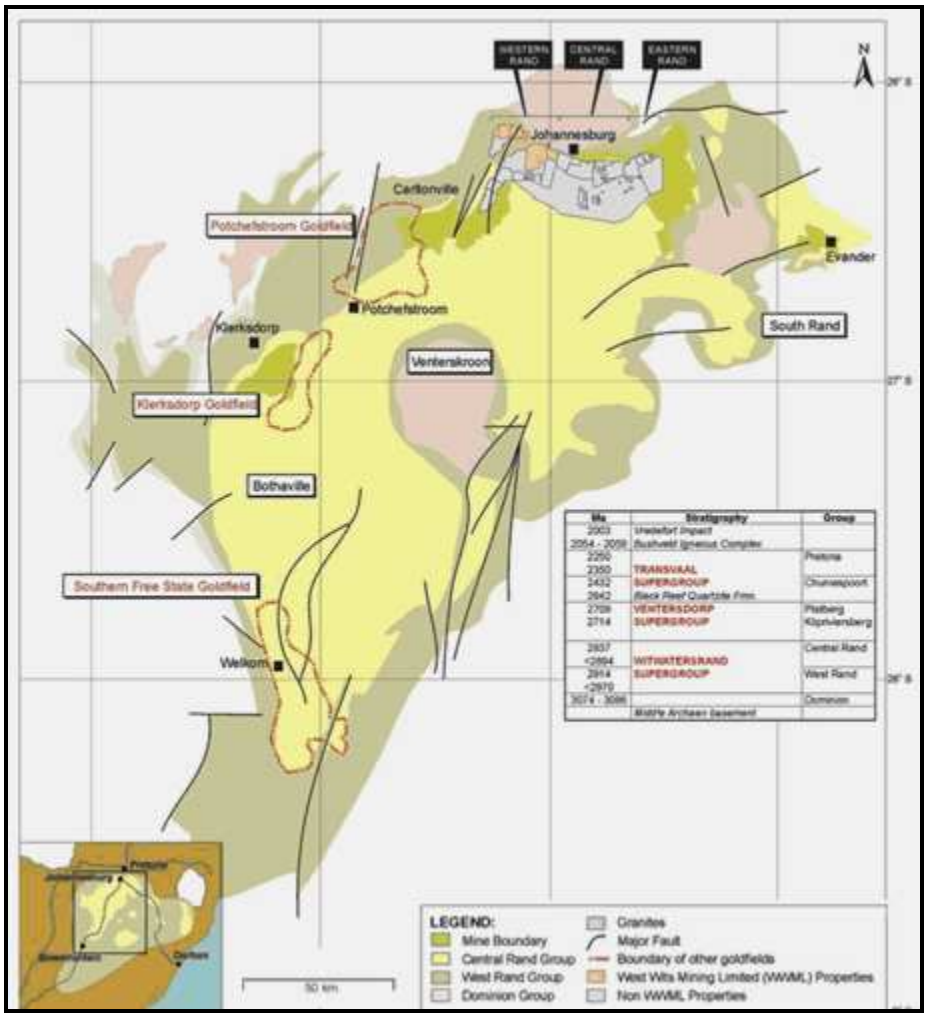

Figure 8.1 Geological settings of the major goldfields in the Witwatersrand Basin

The metal campaign initiated in 2009 and overseen by the Environmental Analytical Chemistry Research Group together with the School of Animal, Plant and Environmental Sciences, both at the University of the Witwatersrand (Johannesburg, SA), focuses on the biogeochemical speciation and risk of metals (e.g. mercury), metalloids (e.g. arsenic) and naturally-occurring radionuclides (e.g. uranium and it's daughters) on gold and uranium mining properties. The study is also of value in determining the magnitude and risk of off-site mining impacts.

In the present work, the main regions that were studied for are (i) the Varkenslaagte at West Wits, (ii) the Vaal River West and Kanana sub-catchments. Two additional sites were evaluated to achieve the assigned objective of characterizing the mercury speciation and place gold mine properties in a regional context on the Witwatersrand Basin (a) on

the West Rand - the decanting JCI Anglo American shafts and boreholes (now Harmony/Rand Uranium), and the receiving stream, wetlands and dams through the Krugersdorp game reserve to the Cradle of Mankind, (b) on the East Rand - an old mine property, partially cleaned Ergo TSF footprint, and adjacent Scaw Metals H:h Rietfontein B landfill (Rand Scrap Iron) which contains mine tailings from Ergo and mixed mining and metals waste.

The first two regions are active mining sites whereas the last two comprise closed or partially closed mining operations. For this reason, the study is presented in two separate chapters.

The present chapter will discuss the environmental risk assessment of the mercury pollution from active mines at the Vaal River West and the West Wits (Varkenslaagte) sites.

8.2 General description of the Vaal River and West Wits operations

The Southern African Division of AngloGold Ashanti Limited (AGA), one of the leading global gold mining companies, comprises several mining operations in South Africa and one in Namibia. South Africa operations are grouped into the Vaal River and West Wits regions (figure 8.2).

The Vaal River and West Wits operations comprise mainly of seven deep level gold mines and supporting infrastructures such as metallurgical plants (where gold is produced), chemical laboratories, tailings storage facilities (TSF), waste rock dumps and supporting services such as land management, mine services, commercial services and sustainable development (AGA, 2009a).

The main environmental concerns for the Vaal River (VR) and West Wits (WW) operations identified through environmental impact assessment processes are (AGA, 2009b):

- Seepage of contaminated water from TSF, trenches and pollution control dams
- Historical off-site impacts
- Seepage of contaminated water from waste rock dump

- Uncontrolled release of process water from pollution control dams
- On-site secondary sources, spillages and footprints (ore and mineral waste)
- Emission of dust from TSF and transport of hazardous substances such as yellow cake, acids, cyanide
- Uncontrolled release of process water from metallurgical plants and shafts impact.

The result of the above uncontrolled or poorly managed emission, release, seepage and waste, is a severe contamination of lands, surface water and groundwater with a potential health impact.

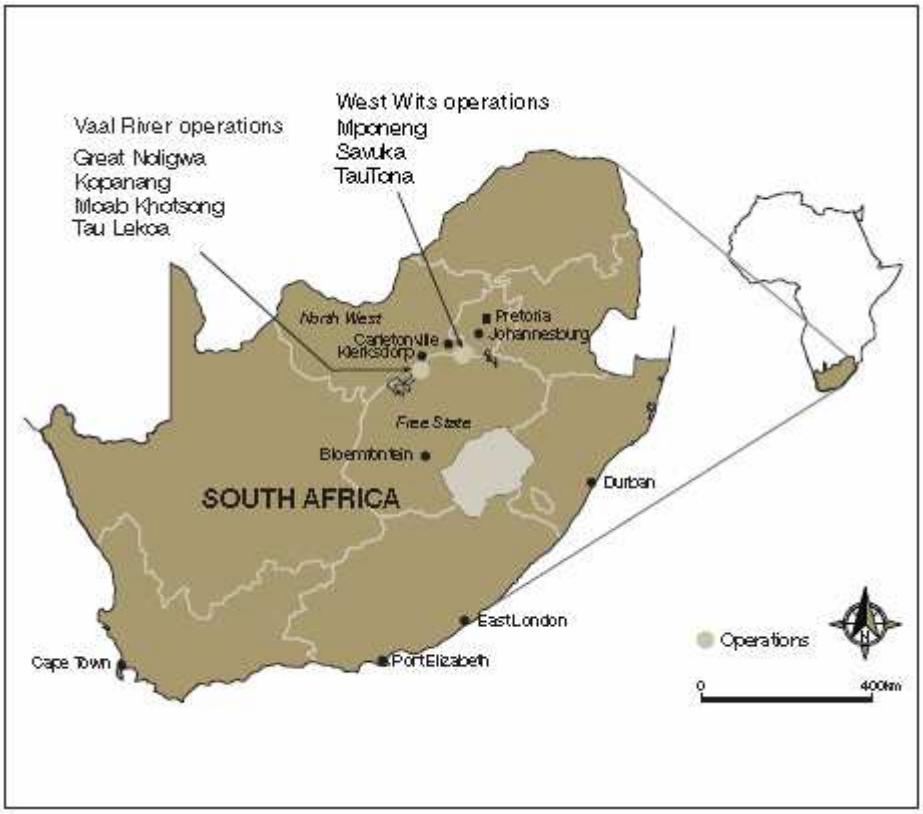

Figure 8.2 Vaal River and West Wits operations in the regional context (AGA, 2008c)

8.2.1 The Vaal River mining operations

The VR operations are located at the boundary between the North-West and the Free State provinces (figure 8.2). The map shown in figure 8.3 indicates the AGA areas of responsibility for VR.

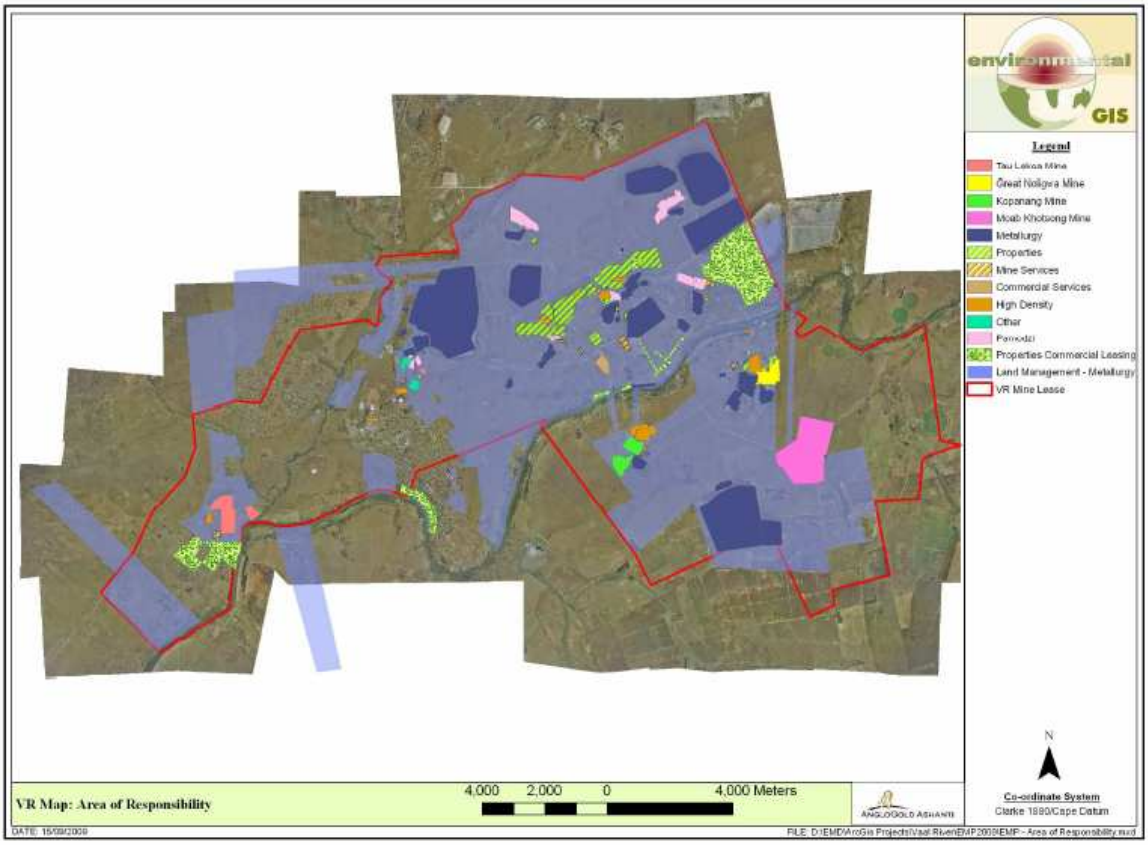

Figure 8.3 Indicating the AGA area of responsibility of the Vaal River operations

The VR operations lie in close proximity to the following towns:

- Orkney - which is surrounded by the VR operations;
- Klerksdorp - located 18 kilometres (km) to the North-west;
- Potchefstroom- located 50 km to the East;
- Bothaville – located 45 km to the South; and
- Leeudoringstad – located 56 km to the South-west.

The total mining lease area of the VR operations is approximately 18 274 hectares. The VR complex has four gold plants (Great Noligwa, Kopanang, Moab Khotsong and Tau Lekoa), one uranium plant and one sulphuric acid plant (AGA, 2008a).

Mining operations in the VR region commenced on shallow reefs in the late 19th century, and used amalgamation techniques. Sampling sites were identified from historical aerial photographs (post-1948), which show there had been extensive shallow mining of the Black Reef, and large spillages from old mine tailings facilities. Since then, some old tailings facilities have been re-worked. Few, if any, of the current gold mining companies utilize mercury, and deep-level mining is being undertaken alongside reprocessing of old tailings to recover gold left-over by previous extraction methods. However, environmental degradation from mining operations is widespread in the region, and there are anecdotal reports of artisanal mining using mercury amalgamation. These practices may have resulted in a long period of contamination.

The Vaal River is the primary surface water body within AGA VR operations. The Schoonspruit is the secondary surface water body. The topography of the mine area slopes towards the Vaal River basin. Surface run-off will therefore flow towards the Vaal River via natural flow paths. A portion of the western area slopes towards the Schoonspruit.

Landscape geomorphology and drainage has been influenced by the southerly flow of the Vaal River and the local geology. There are three major catenas in the area (figure 8.4): towards the Vaal River from north and south; towards the Schoonspruit in the North West; and towards the Koekemoerspruit in the north east. In the western part of the study area the Black Reef Formation forms an elongated ridge, which constitutes much of the watershed between the Schoonspruit and the Vaal River.

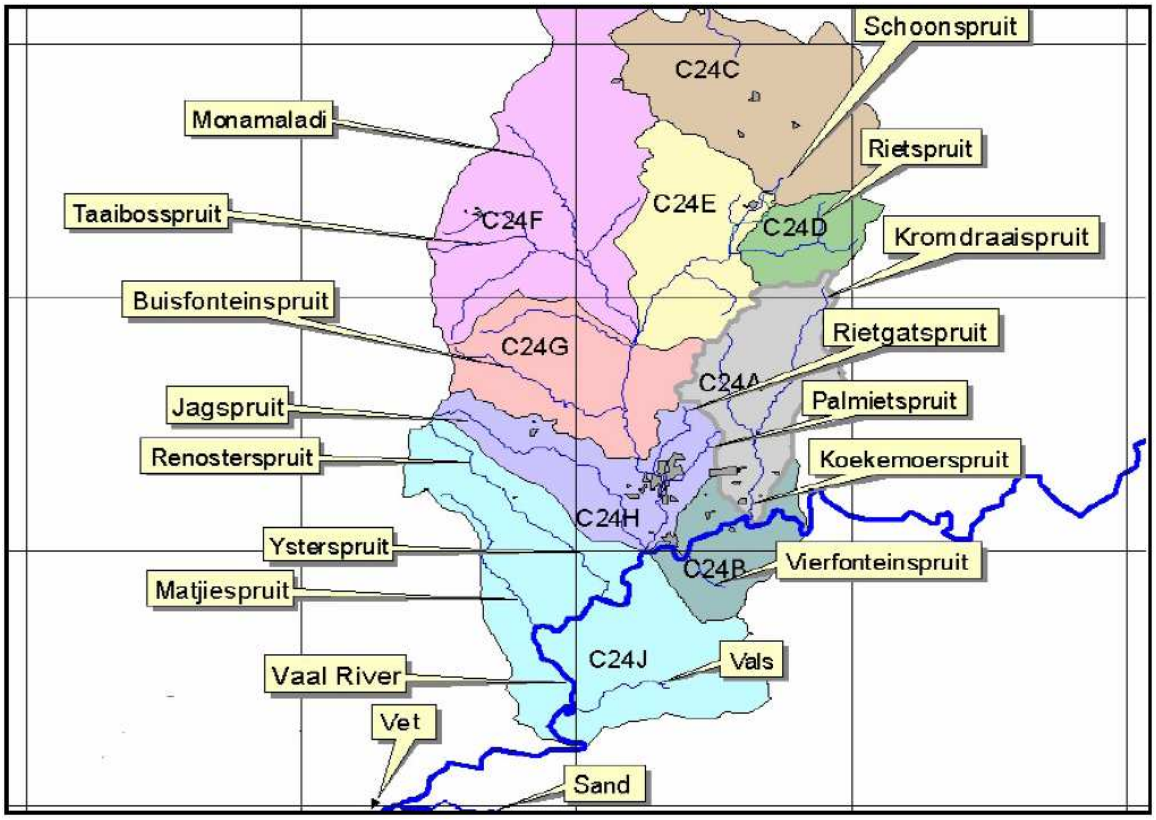

Figure 8.4 Main watercourses and quaternary catchments in the Schoonspruit and Koekemoer Spruit catchment

The major tributaries of the Schoonspruit are the Taaibosspruit, Jagspruit, Buisfonteinspruit and the Rietspruit. The groundwater recharge point of the Schoonspruit (the Ventersdorp eye), ensures that the Schoonspruit flows all year round. The eye water is mainly used for irrigation before it passes through the Klerksdorp city and mining areas. The Schoonspruit has its confluence with the Vaal River to the west of Orkney.

Artificial catchments comprise TSFs. Run-off and seepage from the TSFs flows in the soil and weathered zones.

8.2.2 The West Wits mining operations

The Mponeng, Savuka and TauTona mines are situated on the West Wits Line and are part of the West Wits (WW) operations (AGA, 2008b). These mines are located approximately 75 km west of Johannesburg within the Gauteng Province. The WW site is approximately 7 km south of Carletonville (figure 8.2). Other neighbouring towns are

Fochville and Potchefstroom, which are situated 12 km and 50 km respectively to the south and west of the mine (AGA, 2009a).

The land occupied by the WW operations (figure 8.5) is approximately 4176 hectares which straddle the boundary between Gauteng and the North West Provinces.

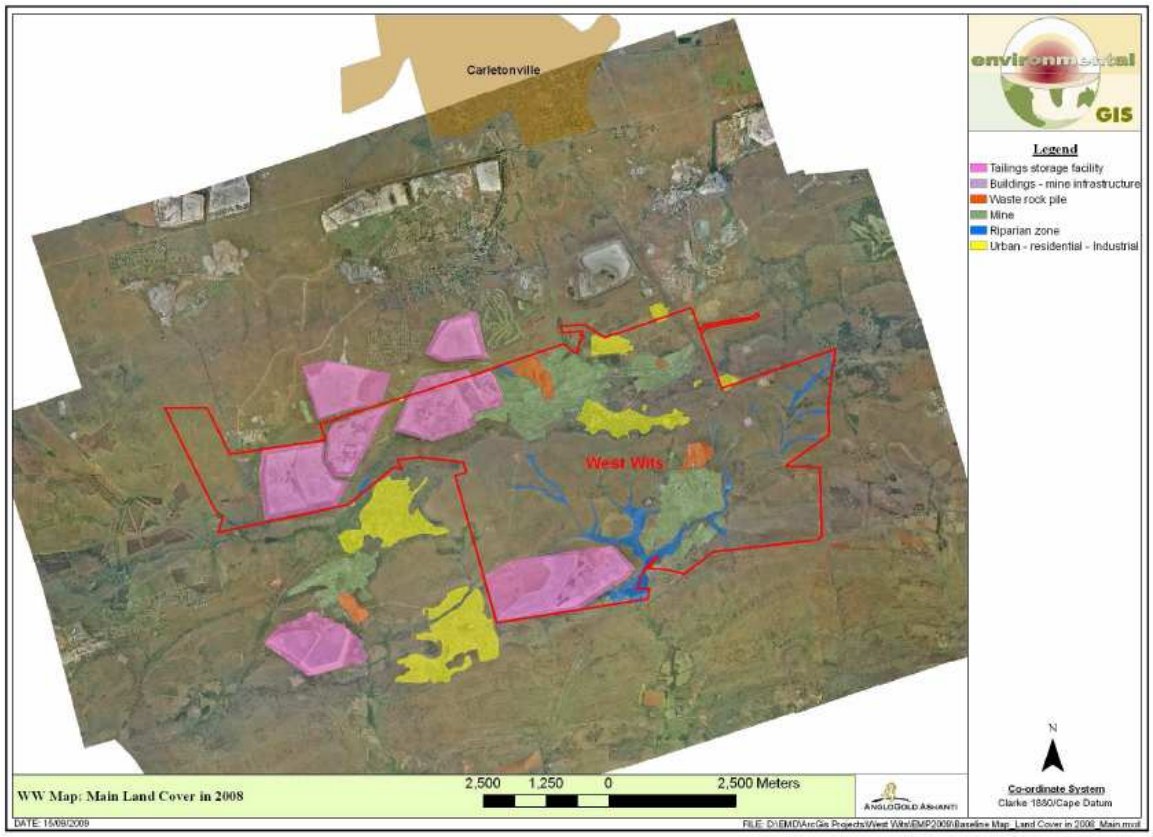

Figure 8.5 Land in and around West Wits operations

The WW operations are located within the Kromdraai Catchment of the Upper Vaal Water Management Area. The operational area can be divided into three surface water sub-catchments; two of which are situated on the northern side of the Gatsrand ridge watershed and one to the south. The north-western subcatchment drains to the northwest via the Varkenslaagte Spruit, a historical tributary of the Wonderfontein Spruit but which now drains into the dewatered Turffontein Dolomite Compartment. The sub catchments are illustrated in figure 8.6.

The north-eastern sub-catchment drains in a northerly direction to the Wonderfontein Spruit via a pipeline and lined canal system, which replaced the natural drainage because of the threat of sinkholes above the dewatered Oberholzer Dolomite Compartment.

The southern sub-catchment drains via a number of small streams, two of which are perennial: the van Eedens' spring, situated just to the north of the Mponeng Tailings Storage Facility, and the Elandsfontein South farmers' spring. The latter spring is registered via servitude in favour of the farm owners of South Elandsfontein. Water from this spring is discharged via the Aquatic Dam into the Elandsfonteinspruit. Both these springs discharge water of good quality (potable standards) into the Elandsfonteinspruit, which in turn is a tributary of the Loopspruit.

Both the Wonderfontein Spruit and the Loopspruit are tributaries of the Mooiriver, which flows into the Vaal River. The Wonderfontein Spruit has its confluence to the north (i.e. upstream) of the Boskop Dam (which is the source of potable water for the city of Potchefstroom), while the Loopspruit has its confluence to the south (i.e. downstream) of Potchefstroom.

Part of the water from the North Savuka Complex TSF drains to the West Boundary Dam, which in turn flows into the Varkenslaagte Stream. This stream does not form a tributary of any river as the water infiltrates into dolomites outside of the mine area.

Metallurgy within the WW operations manages both the active and inactive TSF's (North Old Complex). The two active TSF's are Savuka and Mponeng.

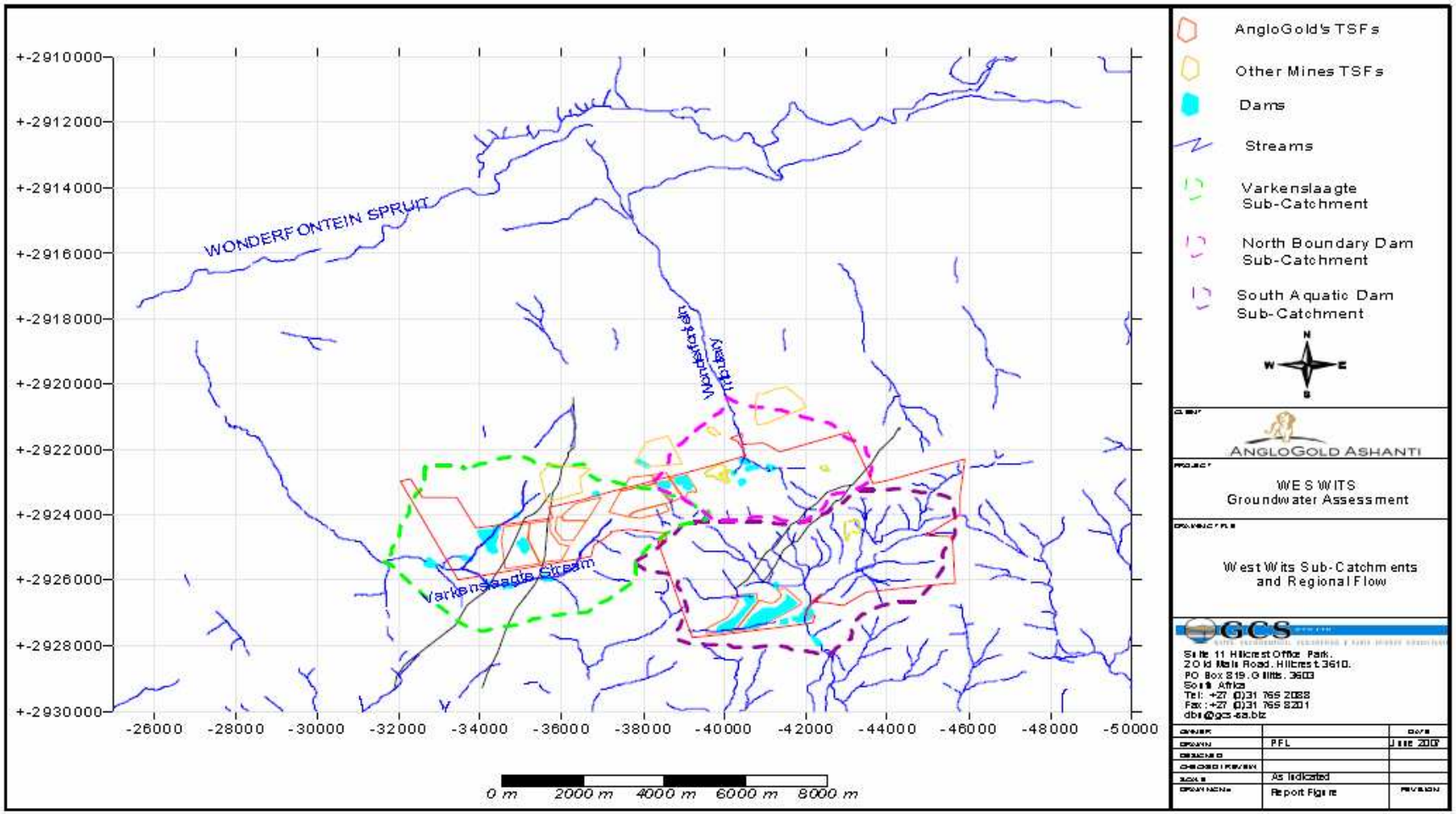

Figure 8.6 West Wits Sub Catchments and Regional Flow

The Savuka TSF comprises of 4 compartments (5A, 5B, 7A and 7B). Final treated pulp residue from Savuka Gold Plant is pumped to the Savuka (New North) TSF where the solid particles settle out on to the dam. Water is decanted using the penstocks at the centre of the facility and is piped into the return water dams. The water in the return water dam is pumped back to the plant as process water. The delivery pipelines to the tailings dam are open-end discharge and the tipping area is controlled by manual operation of the discharge valves. The pump house contains pumps used to pump water back to the plant and all other pumps being maintained. Figure 8.7 is a map indicating the main working areas for Savuka TSF which also was the main area of investigation during the present study.

Figure 8.7 Map indicating the main working areas for Savuka TSF's

During the early years of mining in the West Wits area there were no environmental protection requirements specified in regulations and waste materials consisting of inter

alia: ash, iron oxide, pyrite, slag, mine residue spillage, mine waste rock, steel, rubber, scales from gold and uranium plants and domestic waste were disposed of in borrow pits (figure 8.8) on the mine property (AGA, 2009a). Remediation works occurring currently in the site typically involve removal of the offending or gold-bearing material followed by backfilling and profiling with alternative inert material, placement of soil over the disturbed site where appropriate and the establishment of a vegetation cover.

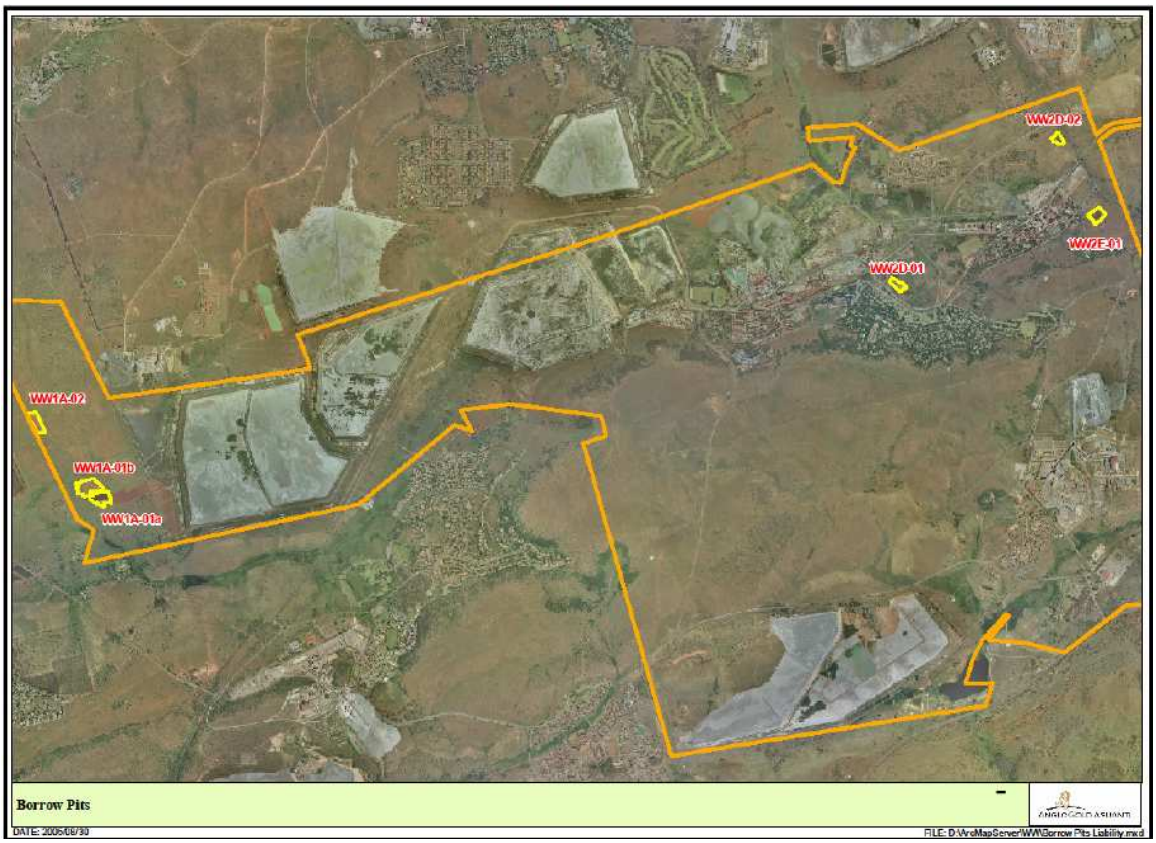

Figure 8.8 West Wits Borrow Pits (in yellow)

The majority of the Varkenslaagte sub-catchment groundwater contamination lies within a 500 m radius of the No 5 and 7 Compartments of the new Savuka TSF and the Old North TSF. Approximately 70% of the mass originates from the existing (old and new) TSF's (AGA WW EMP, 2009). This result in pollution plumes which are dominated by sulfate (almost 55%). These plumes are restricted to the local surface drainage paths which act as groundwater boundaries (which is mainly the Varkenslaagte drainage stream

in this case). However, there is a certain degree of uncertainty by making this statement which requires further investigation to confirm this aspect.

8.3 Collection and description of samples

8.3.1 The Vaal River campaigns

Two sampling campaigns were conducted in the VR West Complex during the late dry season and wet season (tables 8.1 and 8.2) to illustrate mercury behaviour and fate in the region. Water samples, surficial and bulk soil/sediment, tailing particles and plant samples were collected from adjacent to the West Complex North TSF, from a licensed pollution control dam known as the Bokkamp Dam which receives `dirty water' discharges from tailings facilities and recycles these back to the metallurgical process, and from the Schoonspruit stream which is known to have received spillages (pre-1940's) from tailings facilities and drainage from other sources in the catchment such as industries, graveyards and artisinal mining activities practiced by the local community mainly based in Kanana (figure 8.9).

The wet season sampling was motivated by the need of understanding the seasonal impact on the mercury transport and distribution in the site. Sampling points were selected based on data obtained from the dry season sampling.

Table 8.1 The VR dry season sampling details

Vaal River dry season sampling		
Sample ID	Description	GPS
33	Sediment from Vertelatan Shaft	S26°59.174' E026°39.945'
34A-C	Soil collected at different layers from an old ash heap	S26°59.390' E026°39.914'
36-37	Composite sample from the old mine working sites.	S26°59.390' E026°39.821'
38A & B	Water samples from Vaal River	S26°59.579' E026°39.823'
39	Sediment from Vaal River	
40A,B,C	Algaes from Vaal River	
41	Soil core from Vaal River	S26°59.574' E026°39.823'
42	Sediment from Vaal River	S26°59.564' E026°39.802'
43	Soil core from Vaal River	S26°59.566' E026°39.798'
44A,B,C	Water Hyacinth from Vaal River	
45	Old Wall Ash from infrastructure. ~50m to North	S26°59.548' E026°39.801'
46A & B	Water from Schoonspruit	S26°59.824' E026°38.842'
46D	Sediments from Schoonspruit	
47A,B,C	Water Hyacinth from Schoonspruit	
48	Algae from Schoonspruit	
49	Sediment from Schoonspruit	S26°57.823' E026°38.841'
50A-C	Sediment core from Auger in Schoonspruit	S26°57.517' E026°38.825'
52A & B	Water from Kanana canal near wetland	S26°57.497' E026°38.842'
52C & D	Sediments from Kanana canal	
53A-C	Composite from piles of sed. Cleared out of canal	S26°57.496' E026°38.842'
54A & B	Water from upper Kanana canal in wetland	S26°57.431' E026°38.868'
54C & D	Sediment from upper Kanana canal in wetland	S26°57.431' E026°38.868'
59A-F	Soil core on wetland from West Complex of Schoonspruit	S26°56.614' E026°39.831'
61A & B	Water samples Schoonspruit below West complex	S26°56.606' E026°39.804'
64A-C	Willow leaves from Schoonspruit below West complex	
65A	Water from creek near West complex North TSF	S26°55.782' E026°41.142'
65B	Sediment near West complex North TSF	
68A	Water sample from Bokkamp Dam	S26°57.720' E026°42.220'
68B	Sediment from Bokkamp Dam	S26°57.720' E026°42.220'
70A	Water from Vaal River near the Dam	S26°58.227' E026°43.389'
70B	Sediment from Vaal River near the Dam	

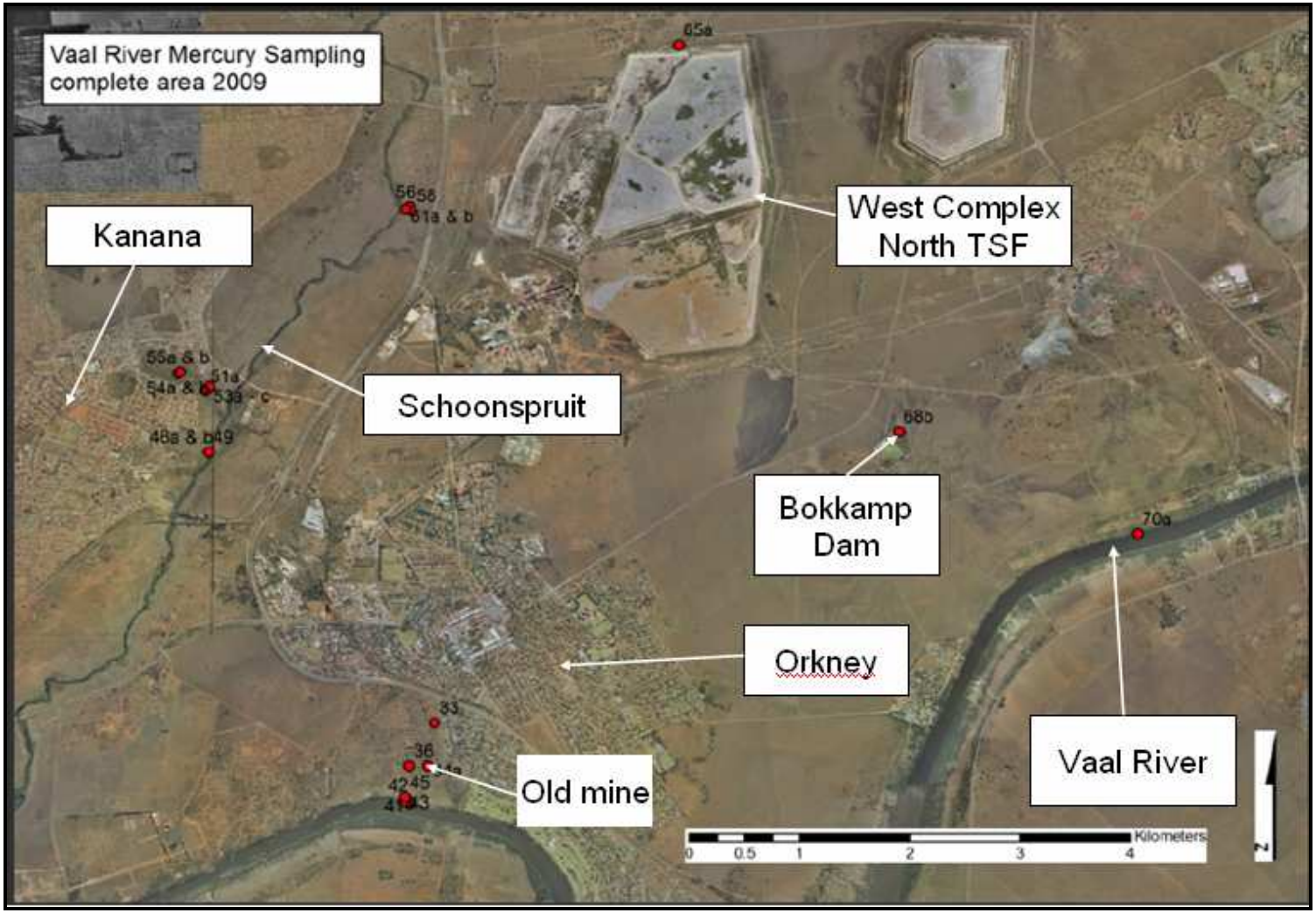

Figure 8.9 Vaal River West sampling area (red dots are for sampling points)

Table 8.2 The VR wet season sampling details

Sample ID	Description
WC Dig	Surface dry sediment collected adjacent to the West complex North (WC) TSF
WC Wash	Surface wet soil adjacent to the WC TSF
WC 1, 2 and 3	Sediment profiles collected near WC TSF
Bok Dam	Surface sediment within Bokkamp Dam
Bok Cpsite	Composite sediment within the dam
Bok upper, middle and bottom	Sediment profile from Bokkamp dam
PH	Sediment collected near pump house
Sch	Sediment profile near Schoonspruit
Bok W1 and W2	Water samples collected from the dam
SchW	Water from Schoonspruit

8.3.2 The West Wits campaign

West Wits soil, sediment, tailings, plant and water samples (table 8.3) were collected from TSFs, borrow pits, dams, and wetlands within the West wits Old North Complex (Savuka lease) as shown in figure 8.10.

In order to assess the off-site impact of WW operations the sampling campaign was extended following the path of the Vaarkenslaagte canal, via the Welverdened Road, to the Wonderfontein Spruit located about 5 km to the Carltonville-Potchefstrom Road (figure 8.11). The overall distance from the initial sampling point to the Wonderfontein Spruit was approximately 22 km.

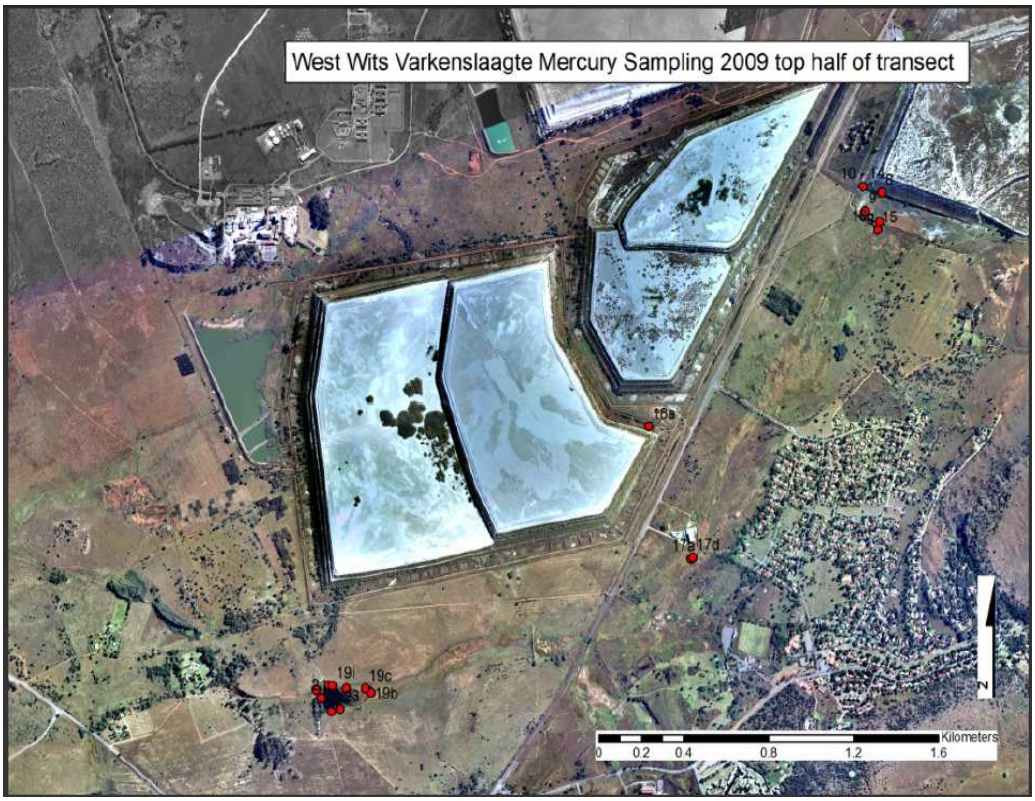

Figure 8.10 View of the West Wits Old North sampling area

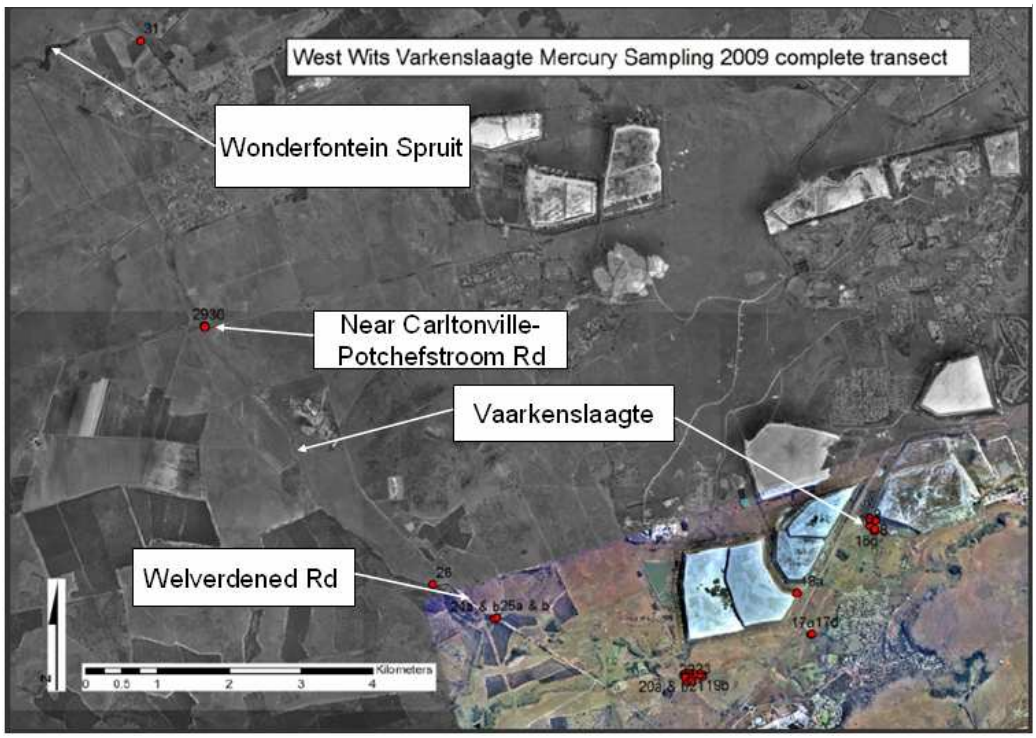

Figure 8.11 West Wits sampling area (the Old North Complex is brightened)

Table 8.3 The WW sampling details

Sample ID	Description	GPS
8	Soil core from Old North TSF	S26°25.638' E027°22.337'
15A-B	Water sample from Vaarkenslaagte canal (Top of canal below TSF)	S26°25.725' E027°22.376'
16G	Core from Old Reed Bed	S26°25.706' E027°22.380'
16K	Core from V. canal	
16L	Core from Reeds near V. canal	
16W,X,Y	Phragmites from V. canal	
17A-B	Water samples below Buldens Warehouse	S26°26.492' E027°21.847'
17C	Typha below Buldens Warehouse	S26°26.492' E027°21.847'
17E	Soil core below Buldens Warehouse	
18A	Soil core Tamarak Slope N North TSF	S26°26.183' E027°21.728'
19A	Water from Dam	S26°26.790' E027°20.822'
19B	Willow	S26°26.808' E027°20.943'
19F	Soil core	S26°26.798' E027°20.872'
19H	Algae	
20A-B	Water samples downstream from dam	S26°26.801' E027°20.787'
21	Water sample from dam	S26°26.820' E027°20.800'
23	Soil core	S26°26.846' E027°20.855'
24A-B	Water samples	S26°26.832' E027°19.190'
24c	Sediment Stream under Welverdened Rd	
25A-B	Stream before flows under Welverdened Rd	S26°26.373' E027°19.216'
25c	Sediment from Stream on Welv. Rd (Before bridge)	
26	Water sample (Farmer's land)	S26°26.124' E027°18.679'
27	Sediment (Farmer's land)	
29	Water near Carltonville-Potchefstrom Rd (NB. Fe pipe in centre of stream)	S26°24.187' E027°16.760'
30	Soil core	S26°24.192' E027°16.763'
31	Water sample	S26°22.035' E027°16.216'
32	Algae from Wonderfontein Spruit	

8.4 Mercury in the Vaal River West Region

8.4.1 Mercury in the Vaal River West waters

Field measurements and mercury concentrations determined in VR waters from the dry season sampling are presented in table 8.4. An Example of chromatograms obtained from the speciation analyses of VR waters by ID GC-ICP-MS is shown in figure 8.12.

The pH of water samples ranged from neutral to slightly alkaline (i.e. 6.9 to 8.9) and the redox potential from 210 to 446 mV. The electrical conductivity was generally moderate except in areas near pollution source such as the creek near the TSF (sample 65A) and the pollution control dam (68A) where values of several mS cm^{-1} were measured.

Table 8.4 IHg, MHg and field measurements in VR waters (n=3)

Sample	T (°C)	pH	Eh (mV)	Ec (mS cm^{-1})	IHg (ng L^{-1})	%RSD	MHg (ng L^{-1})	%RSD	%MHg
38A	21.0	8.2	400	0.93	0.344	9.1	bdl	-	0.0
46B	21.4	7.5	446	1.16	0.665	3.7	0.071	6.7	9.6
52A	21.8	8.0	399	0.66	0.048	6.5	0.268	4.0	84.7
54A	23.0	7.6	330	0.62	0.043	9.2	bdl	-	0.0
61A	22.0	7.3	279	1.15	bdl (*)	-	bdl	-	0.0
65A	23.5	6.9	210	5.86	1.004	9.1	0.004	4.7	0.4
68A	21.5	7.8	335	3.41	5.260	4.6	0.222	1.0	4.1
70A	21.1	8.9	320	0.81	0.006	7.9	0.086	10.3	93.2

(*)bdl: below detection limit

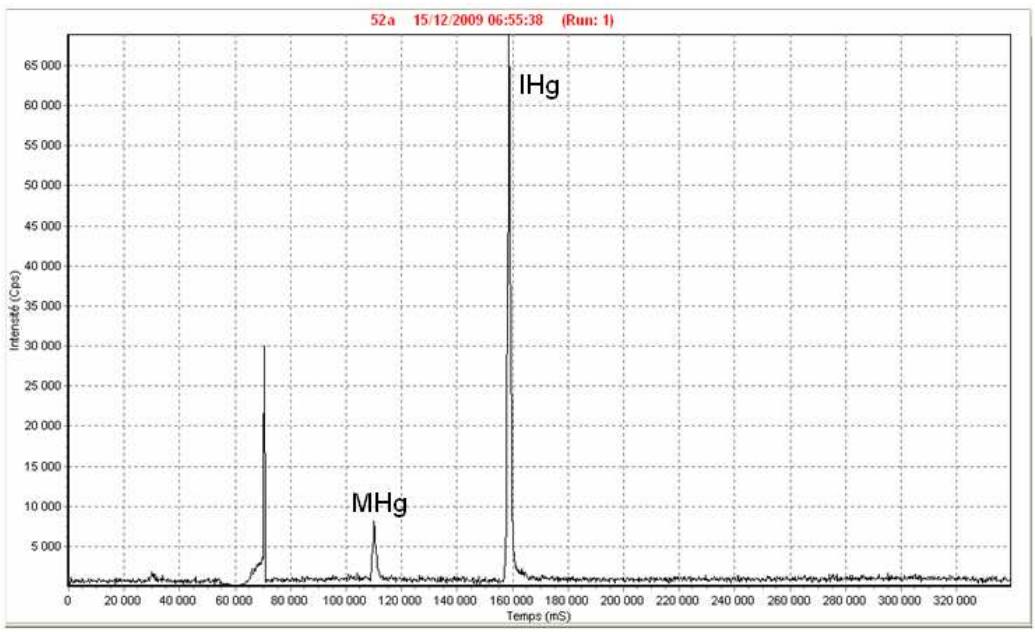

Figure 8.12 Example of GC-ICP-MS chromatogram of VR water

Total mercury concentrations in surface waters (unfiltered) varied from 0.043 to 5.483 ng L^{-1} with MHg ranging between 0.004 and 0.268 ng L^{-1}. Methylmercury values for most of the VR studied waters fall within the range seen elsewhere (e.g. Domagalski, 1998;

Domagalski *et al.*, 2000; Ashley *et al.*, 2002) meaning that between 1 and 10 percent of total mercury was MHg. Therefore, it can be say that MHg in VR waters was within the range of values commonly measured in relatively uncontaminated surface waters with normal methylation potential (see e.g., Kelly *et al.*, 1995). Proportions of methylmercury were high in samples 52A (85%) and 70A (93%) collected from Kanana Canal near a wetland and from the Vaal River near the Bokkamp Dam, respectively (see table 8.4 and figure 8.13). The presence of decaying organic matter in the corresponding watersheds could explain the high methylation rate observed. The corresponding sediment for sample 52A, which is sample 52D (table 8.5), also showed the highest methylmercury proportion among all analyzed surface sediments.

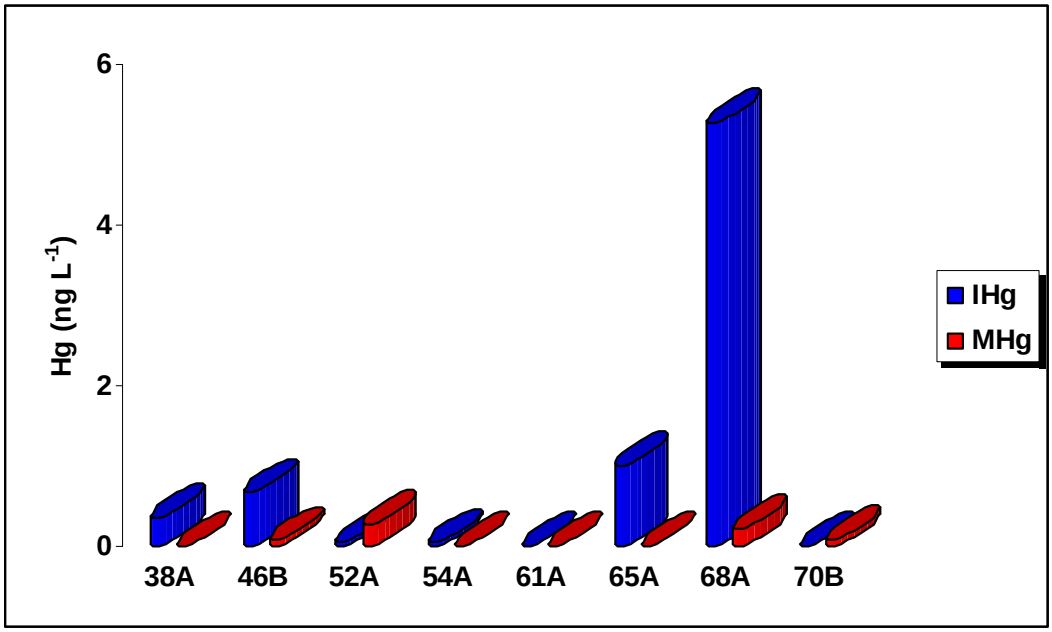

Figure 8.13 Mercury species in VR waters from the dry season sampling

Although no specific correlation was observed between field measurements and mercury species concentration, it was found that the highest methylation rates occurred at elevated pH (pH 8.0 and 8.9, respectively).

The most elevated mercury values were observed in the water collected from Schoonspruit (sample 46B: 0.735 ng Hg L^{-1}), located approximately 3 km from the West Complex North TSF, and also in the creek near the TSF (sample 65A: 1.008 ng Hg L^{-1})

which drains into Schoonspruit. It is believed that migration of leached mercury from the TSF or the surrounding polluted soil through runoff could explain the observed contamination. This will be further discussed when the above observations will be compared to measurements obtained from the wet season sampling. Sediments collected from Schoonspruit (sample 46D) and near the TSF (sample 65B) also showed some of the most elevated mercury values in sediments with total mercury concentrations of 749 and 940 µg kg^{-1}, respectively.

The highest mercury value in water was found in the Bokkamp Dam (sample 68A) with mercury concentration of 5.483 ng L^{-1} and 4% of the total mercury (i.e. 0.222 ng L^{-1}) as MHg. Sediments collected within the Dam exhibited the highest mercury value of the whole campaign with Hg_{TOT} of 10245 µg kg^{-1}. The impact of this polluted Dam in its surroundings will be examined further.

Existing aquatic life criteria for total mercury in water covers a wide range. As is the case with the criterion for sediment, the Threshold Effect Level (TEL) is the concentration above which there is evidence of potential for observable effects in biota, not necessarily including bioaccumulation and biomagnification. The lowest proposed criterion for chronic effects in fresh-water aquatic life is 12 ng L^{-1} of total recoverable mercury (Barkow, 1999). The California Water Quality Standard proposed the value of 50 ng L^{-1} and later, the U.S. EPA issued a guideline of 770 ng L^{-1} (dissolved mercury) for chronic effects in fresh-water aquatic life (Ashley *et al.*, 2002). Mercury values in all the waters collected during the dry season sampling were below the above threshold level, but low values are generally anticipated during the low-flow late-dry season conditions under which we obtained the samples (Ashley *et al.*, 2002).

8.4.2 Mercury in Vaal River west sediments

Due to the fact that only about 3% of Hg_{TOT} in sediments is in the form of MHg (Harris *et al.*, 2007), most of the sediment samples with low Hg_{TOT} were not analyzed for speciation. Results for the VR dry season sampling are shown in table 8.5.

Table 8.5 Hg_{TOT}, IHg and MHg for Vaal River sediments for the dry season sampling

Sample	Hg_{TOT} ($\mu g\ kg^{-1}$)	IHg ± SD (n = 3; $\mu g\ kg^{-1}$)	%RSD	MHg ± SD (n =3; $\mu g\ kg^{-1}$)	%RSD	%MHg
34A	217.31	nd (*)		n/a		
34D	323.14	258.09 ± 0.34	0.13	2.71 ± 0.30	11.1	1.0
36	140.28	nd		n/a		
37	166.47	123.71± 0.26	0.21	1.68 ± 0.76	4.5	1.3
39	37.26	nd		nd		
41	24.35	nd		nd		
42	11.67	nd		nd		
43	9.56	nd		nd		
45	68.55	nd		nd		
46D	749.31	660.72 ± 19.66	5.45	7.07 ± 0.64	9.0	1.1
49	333.11	274.32 ± 6.03	2.20	8.85 ± 4.59	5.2	3.1
50	53.56	nd		nd		
51A	200.95	173.74 ± 9.54	5.49	1.43 ± 0.77	5.4	0.8
52D	94.89	97.85 ± 1.42	1.45	6.42 ± 0.97	1.5	6.2
54C	104.31	96.98 ± 3.48	3.59	bdl		0.0
54D	62.74	50.82 ± 2.59	5.09	bdl		0.0
55A	118.65	85.51 ± 6.06	7.09	5.59 ± 0.65	11.6	6.1
59A	83.62	70.32 ± 1.49	2.12	bdl		0.0
59B	nd	34.24 ± 0.25	0.74	1.16 ± 0.01	1.0	3.3
59C	nd	40.94 ± 0.55	1.34	2.23 ± 0.50	2.2	5.2
59D	nd	35.53 ± 0.15	0.42	1.99 ± 0.28	1.4	5.3
59E	nd	37.69 ± 1.31	3.46	0.54 ± 0.21	4.0	1.4
59F	nd	37.56 ± 0.12	0.33	0.68 ± 0.12	7.7	1.8
62A	103.42	119.51 ± 6.56	5.49	2.06 ± 0.14	6.9	1.7
62B	94.45	73.54 ± 3.52	4.79	1.61 ± 0.29	2.0	2.1
65B	939.83	768.02 ± 12.60	1.64	3.19 ± 0.19	6.0	0.4
68B	10245.64	8478.81 ± 64.47	0.76	12.88 ± 0.81	6.3	0.2
70B	12.67	nd		nd		
72	63.54	32.24 ± 0.40	1.23	0.33 ± 0.02	7.1	1.0
73	53.2	nd		nd		

(*)nd = not determined

Background mercury values in the uncontaminated areas were relatively low, in the range of 10 to 80 $\mu g\ kg^{-1}$ which agrees with background values of 60 $\mu g\ kg^{-1}$ reported by Hornberger and others (1999).

Mercury concentrations were variable in sediments, with total Hg_{TOT} ranging from 10 to 10245 $\mu g\ kg^{-1}$. Various criteria have also been proposed for evaluating mercury levels in bulk sediments (USEPA, 1997b). The lowest of these is the USEPA TEL at 174 $\mu g\ kg^{-1}$ (MacDonald *et al.*, 2000). This is a proposed lower limit for effects on biota, above

which there is potential for observable effects such as bioaccumulation and biomagnification.

Most of sediments that exhibited Hg_{TOT} beyond the TEL were collected near pollution source such as the old mine working site near Klerksdorp (e.g. 34D: 323 µg Hg kg^{-1}), the West Complex North TSF (e.g. 65B: 939 µg Hg kg^{-1}) and the Bokkamp Dam (e.g. 68B: 10245 µg Hg kg^{-1}). Elevated mercury observed in some sediments from Kanana canal (e.g. 51A: 201 µg Hg kg^{-1}) and Schoonspruit (e.g. 46D: 749 µg Hg kg^{-1}) are believed to be the consequence of the drainage of contaminated particles from pollution sources.

MHg in surface sediments ranged between 0 and 13 µg kg^{-1}, with the highest proportion (i.e 6% of Hg_{TOT}) found in sample 55A collected from the upper Kanana canal, in a wetland (figure 8.14).

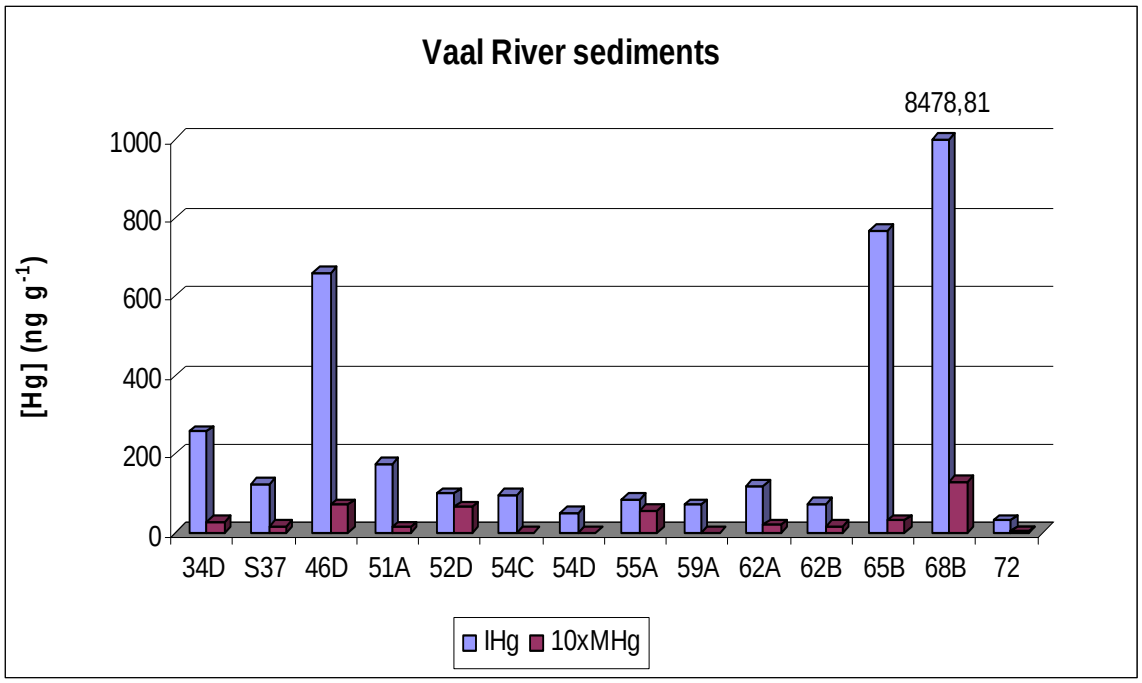

Figure 8.14 Mercury speciation in VR sediments (MHg was multiply 10 times due its low occurrence compare to IHg)

8.4.3 Mercury distribution during the wet season sampling

A different trend was observed after the late wet season sampling. Figure 8.15 highlights the points where the sampling was repeated in wet season, whereas table 8.6 presents different mercury concentrations obtained in surface sediments and sediment profiles together with field measurements.

As mentioned earlier, the selection of the wet season sampling points was based on the observations made during the previous sampling. Therefore, The West Complex North TSF, the Bokkamp Dam and the Schoonspruit were the main target in order to understand seasonal variations of the mercury load in the site and the impact of pollution sources in surrounding sediments and watersheds.

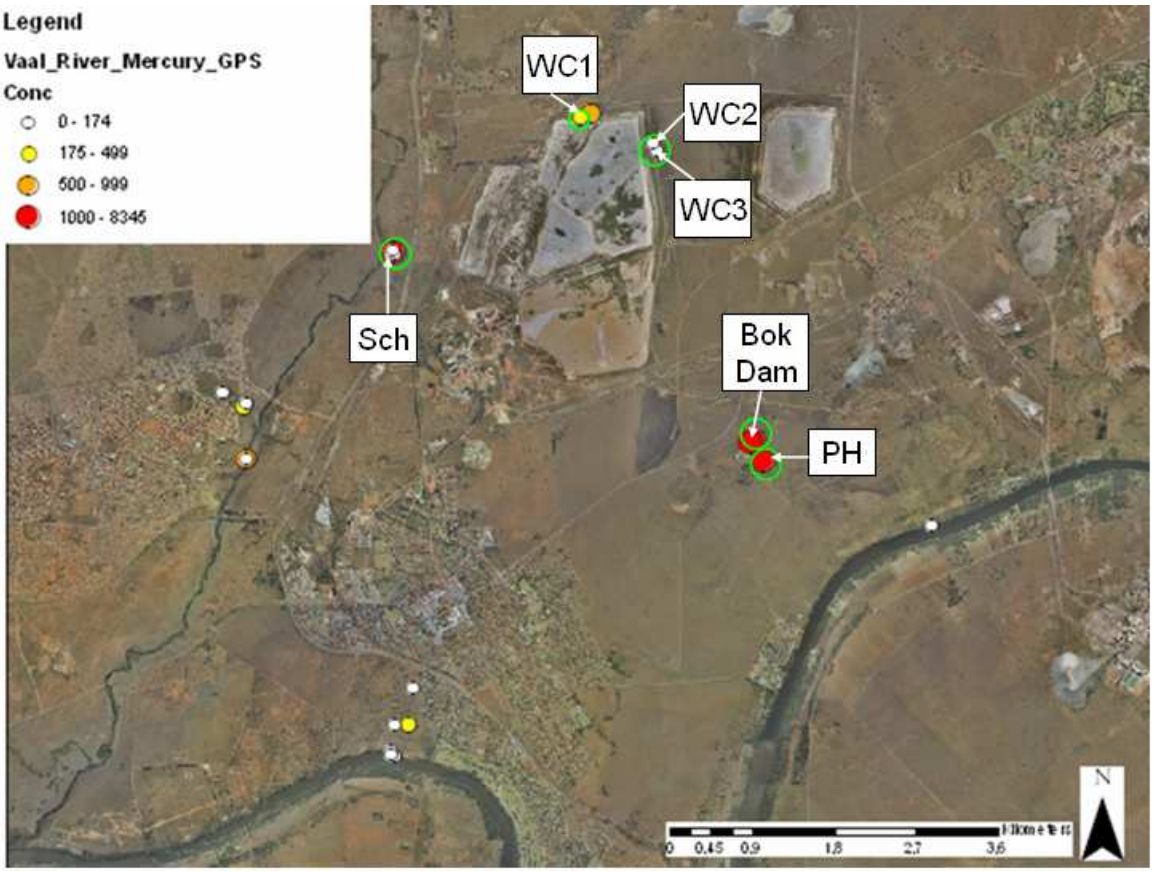

Figure 8.15 Satellite picture of the VR West site. Wet season sampling points are circled (in green)

Table 8.6 Mercury concentration in sediments for the VR wet season sampling

Sample	pH	Eh (mV)	Ec (mS cm^{-1})	Hg_{TOT} (µg kg^{-1})	%RSD	IHg (µg kg^{-1})	MHg (µg kg^{-1})	%MHg
WC1 Dig	5.83	409.6	2.39	353.24	8.79	nd	nd	
WC1 wash	3.95	406.3	3.01	373.67	2.19	nd	nd	
WC1 0-20(*)	4.80	322.3	0.85	216.60	5.65	282.71	8.27	2.8
WC1 20-40	4.45	324.7	0.14	165.91	1.87	158.2	bdl	0.0
WC1 40-60	5.61	332.5	2.98	187.23	7.21	213.36	6.04	2.8
WC1 60-80	5.71	349.2	4.22	462.35	0.80	446.81	2.03	0.5
WC1 80-100	5.93	206.1	6.14	1103.09	3.12	959.42	13.76	1.4
WC1 100-120	5.94	277	5.23	1272.57	0.57	1007.59	8.86	0.9
WC1 120-140	6.51	137	11.22	862.82	1.37	801.59	3.29	0.4
WC1 140-160	5.67	214	0.26	83.19	5.02	175.71	6.9	3.8
WC2 0-20	6.98	405.2	7.95	82.65	3.12	nd	nd	
WC2 20-40	7.15	393	3.83	67.68	8.24	nd	nd	
WC2 40-60	7.36	399.6	4.93	1637.44	0.26	nd	nd	
WC2 60-80	7.33	403.1	7.92	50.17	8.59	nd	nd	
WC2 80-90	7.37	409.1	9.04	92.22	2.58	nd	nd	
WC3 0-20	6.98	414.7	5.10	93.02	1.19	nd	nd	
WC3 20-40	7.02	416.6	3.06	20.96	4.16	nd	nd	
WC3 40-60	6.8	417.5	1.83	68.50	1.81	nd	nd	
WC3 60-80	7.04	414.8	1.40	113.96	2.32	nd	nd	
WC3 80-100	7.20	355.2	2.00	43.49	13.02	nd	nd	
PH 0-20	6.27	418	1.03	4286.82	1.09	4114.28	13	0.3
PH 20-40	6.54	397	1.88	125.87	5.42	110.44	9.5	7.9
PH 40-60	6.58	407	0.98	59.59	7.85	103.76	6.17	5.6
PH 60-80	6.82	421.5	0.94	56.25	6.02	147.55	3.84	2.5
PH 80-100	6.81	428.9	1.07	76.40	3.18	48.01	2.35	4.7
PH 100-120	6.83	366	1.48	89.06	1.07	60.57	3.67	5.7
PH 120-150	6.89	410	1.25	45.24	4.91	86.98	1.39	1.6
Bok Cpsite	7.23	373.8	2.34	1432.22	1.51	nd	nd	
Bok upper	4.58	398.6	1.22	1301.75	1.37	nd	nd	
Bok middle	6.56	364	1.59	396.26	3.02	nd	nd	
Bok bottom	3.87	392.8	1.01	60.74	2.70	nd	nd	
Bok Dam	6.00	385.5	1.05	179.06	2.89	nd	nd	
Sch 0-20	7.35	373.2	3.19	1004.11	1.26	872	17.14	1.9
Sch 20-40	7.36	376.1	1.91	347.30	2.68	219.78	bdl	0.0
Sch 40-60	7.33	332.9	2.19	5482.81	0.98	3099.81	140.48	4.3
Sch 60-80	7.65	350.1	2.11	481.48	1.95	302.71	37.79	11.1
Sch 80-100	7.66	371.5	1.85	177.19	5.40	129.91	22.81	14.9

(*): Figures in the sample column represent depth values (in cm) for the corresponding profile.

Field measurements were variable in the site. The pH of sediment samples ranged from 3.87 to 7.66 and the redox potential from 137 to 417 mV. The electrical conductivity reached values as high as 11 mS cm^{-1} in bulk sediment, suggesting an important presence

of ionic compounds. According to the AGA environmental management programme presented in 2009 (AGA VR EMP, 2009), the expected pH of the soil within the VR area should vary between 5.5 and 6.4. Lower pH values (3.9 for sample WC1-wash and 4.8 for sample WC1) observed in surface sediments near the TSF could be the evidence of the acidification of the area through probable pyrite oxidation. Elevated concentrations of iron (20465 mg kg^{-1}) and sulfate (20779 mg kg^{-1}) were measured in sample WC1-wash.

Total mercury concentration in surface sediments (0-20 cm depth) ranged from 83 to approximately 4300 µg kg^{-1}. Among all surface sediments, only sample WC3 exhibited total mercury below TEL. Nearly one quarter of the analyzed sediments fell within the mercury Probable Effect Level (PEL) of 486 µg kg^{-1} representing the concentration above which adverse effects are expected to occur frequently, and 15% of samples falling into the Toxic Effect Threshold (TET) concentration of 1000 µg kg^{-1} where sediments are considered to be heavily polluted (MacDonald *et al.*, 2000 and references therein).

At all sites, where bulk material was analyzed, it was enriched in mercury relative to probable background values, and values for the top 20 cm fraction were lower than the bulk values (except for sample PH). Enrichment in Hg_{TOT} was evident in deeper, saturated soils adjacent to tailings facilities, reaching concentrations at mg kg^{-1} level in a few cases (e.g. figure 8.16). The speciation analysis of mercury has shown the same trend as for total mercury and most of the analyzed metals have also shown the same pattern as described above with enrichment at about the same depth in the profile (see table 8.7 and figure 8.17).

The enrichment of mercury at deeper levels in sediments adjacent to the old tailings facilities might be due to historical loads of mercury in tailings and seepage from the facilities.

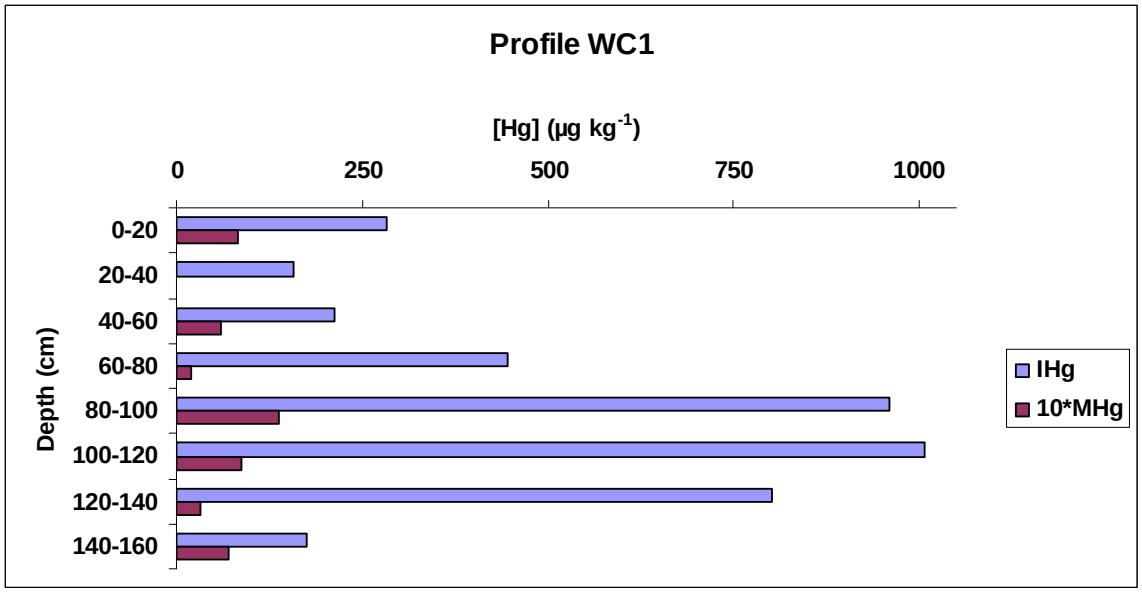

Figure 8.16 IHg and MHg in sediment profile WC1

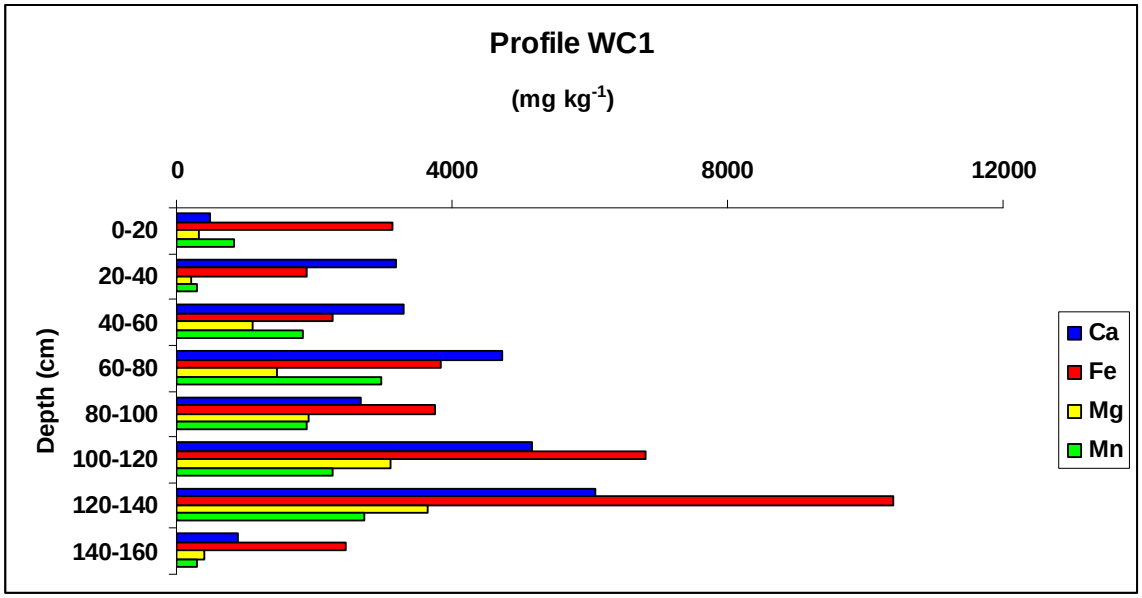

Figure 8.17 Selected elements concentrations in the sediment profile WC1

Table 8.7 Total concentrations of selected metals(*) in studied sediments (mg kg^{-1}) and waters (mg L^{-1})

Sample	Al	Au	Ba	Ca	Cd	Co	Cr	Cs	Cu	Fe	Ga	Ge	K	Li	Mg	Mn	Ni	Pb	U	V	Zn
WC1 Dig	1041,8	7,4	17,5	2725,6	1,5	23,4	15,3	17,7	31,3	5152,3	2,3	4,8	180,3	3,7	994,6	1721,6	47,5	4,1	6,0	2,8	31,5
WC1 Wash	3771,6	7,6	18,4	4470,1	2,8	23,6	26,8	18,6	38,4	20464,7	3,7	3,2	523,8	5,6	4016,1	2165,2	51,3	1,5	1,6	0,1	1,0
WC1 0-20	583,2	5,8	10,3	488,6	0,9	12,0	9,2	10,4	14,6	3123,9	1,2	2,1	82,9	1,4	325,8	850,8	19,9	0,2	0,3	0,1	0,4
WC1 20-40	408,7	3,6	6,9	3179,2	0,5	7,4	6,4	7,1	15,2	1905,2	0,8	0,9	45,1	1,4	219,8	284,7	12,3	1,0	0,5	0,0	0,3
WC1 40-60	581,0	6,8	12,0	3301,8	1,3	25,0	6,8	12,2	18,1	2275,0	1,0	4,2	135,2	1,8	1115,9	1843,6	51,8	0,4	0,6	0,1	1,0
WC1 60-80	772,3	7,1	14,5	4730,9	1,4	18,9	8,3	14,7	25,7	3837,0	1,4	6,6	164,2	2,9	1471,6	2970,5	42,6	0,5	0,7	0,0	1,4
WC1 80-100	718,4	3,5	15,5	2686,3	2,0	27,3	13,4	15,7	34,6	3760,9	2,4	7,4	142,8	3,7	1918,8	1888,1	30,7	0,8	0,5	0,0	0,5
WC1 100-120	1161,7	4,0	17,3	5154,5	1,9	15,1	13,8	17,5	36,7	6820,7	2,2	5,1	194,7	3,5	3098,9	2258,0	35,8	0,8	0,7	0,0	1,2
WC1 120-140	1362,3	3,3	16,5	6080,0	2,7	38,3	13,8	16,7	65,7	10418,2	3,0	5,7	185,7	3,3	3648,0	2727,8	46,0	1,2	0,6	0,1	0,8
WC1 140-160	735,0	3,3	12,6	891,2	0,6	5,5	10,5	12,8	6,0	2450,1	1,1	0,7	129,0	0,8	398,3	296,6	6,3	24,4	0,7	0,1	0,2
pH 0-20	7029,1	23,7	186,5	3740,5	28,3	566,6	53,9	200,8	74846,1	24530,3	16,7	286,9	487,7	15,3	3199,0	114438,8	3984,4	168,6	997,0	1,4	1900,7
pH 20-40	1297,9	5,9	76,6	11034,3	3,4	53,0	10,8	82,5	506,8	9575,8	3,3	31,6	381,6	4,3	503,8	18120,4	331,5	5,5	85,4	7,0	162,1
pH 40-60	2194,7	25,0	15,0	9665,9	2,0	10,2	15,0	75,2	1202,6	10628,0	3,2	17,8	496,1	2,8	721,6	11950,8	55,1	2,6	63,9	6,8	105,2
pH 60-80	1550,5	2,6	61,1	3500,2	2,1	7,9	15,6	68,5	168,3	8579,3	3,4	16,1	342,6	2,9	625,6	7789,9	38,7	2,8	51,8	7,7	10,4
pH 80-100	1844,0	7,9	65,4	6651,9	2,6	10,9	18,4	71,8	339,8	9475,4	4,0	25,4	427,5	5,0	840,7	11820,3	89,3	3,4	47,9	6,4	19,9
pH 100-120	1756,8	4,3	60,6	8006,6	2,0	5,8	15,3	66,9	141,5	7540,1	3,4	17,8	317,2	3,6	948,3	7991,0	32,6	2,2	43,0	6,2	7,0
pH 120-150	1032,0	2,6	39,7	5572,8	2,2	4,0	18,4	46,0	17,4	4001,0	3,6	18,2	322,3	3,3	1548,0	4175,6	61,9	1,4	69,9	6,8	5,1
Bok Dam	312,7	2,7	25,8	2435,7	0,7	2,7	4,0	25,9	2,7	2351,5	1,1	4,0	90,2	0,4	300,7	1473,4	4,9	1,0	17,2	3,6	0,7
Bok upper	3740,6	3,8	39,6	9064,5	10,8	90,5	25,7	39,8	9302,0	8272,8	4,7	44,7	138,5	6,3	1266,7	18406,1	1959,4	68,8	229,6	3,4	1326,0
Bok middle	759,6	4,0	9,1	1275,0	2,4	1,0	11,9	9,3	24,1	10146,1	4,4	0,7	108,5	2,4	569,7	27,1	7,9	64,6	85,6	4,3	7,2
Bok low	1323,6	3,5	71,2	1337,9	2,8	18,6	10,3	150,4	697,4	8952,3	4,9	27,7	85,4	4,2	242,0	9891,6	58,9	4,1	62,3	10,2	56,9
Bok cpsite	25421,8	3,8	46,2	101295,7	12,4	646,3	31,4	46,5	133983,7	98475,4	5,5	665,9	2193,6	7,6	18880,3	210543,1	14689,1	75,8	2056,5	58,8	10478,2
WC2 0-20	864,9	14,1	55,8	5526,2	1,7	7,9	11,3	56,1	19,3	6332,5	2,9	8,3	190,6	1,1	776,9	3239,5	17,9	4,5	56,9	8,5	13,3
WC2 20-40	5546,8	16,5	417,6	36178,2	1,3	5,4	5,8	469,8	6,4	52074,7	2,2	7,1	1970,7	0,7	5181,4	28230,0	14,1	1,9	35,9	6,6	5,0
WC2 40-60	3838,6	20,7	27,9	24213,9	0,9	3,3	5,3	28,1	4,2	32670,0	1,5	5,0	1251,7	0,7	3616,1	19137,5	6,5	1,3	22,9	4,5	1,8
WC2 60-80	177,4	2,4	17,9	1253,7	0,3	1,6	2,7	18,1	2,9	1162,0	0,5	2,3	30,6	0,5	156,0	773,6	2,8	0,2	9,5	2,3	1,1
WC2 80-90	5227,8	3,8	429,5	31100,1	0,9	4,9	5,0	488,7	7,1	29323,0	1,4	8,9	1406,9	0,9	6294,1	36875,8	8,2	1,3	18,0	3,5	2,5
SchW	0,1	0,2	0,1	5,1	0,0	0,0	0,0	0,1	0,0	0,1	0,0	0,0	1,9	0,0	2,7	0,0	0,0	0,0	0,0	0,0	0,0
Bok W1	0,1	0,2	0,1	51,6	0,0	0,1	0,0	0,1	0,5	0,1	0,0	0,0	3,9	0,0	7,0	1,0	0,2	0,1	0,0	0,0	0,1
Bok W2	0,1	0,1	0,1	49,8	0,0	0,1	0,0	0,0	0,5	0,0	0,0	0,0	3,7	0,0	6,7	1,0	0,1	0,3	0,0	0,0	0,0

(*): Concentration reported as “zero” were below the ICP-OES detection limit of 0.1 mg kg^{-1} (or mg L^{-1})

8.4.4 Mercury methylation in the Vaal River West area

The percentage of MHg in sediment samples ranged from 0.4% to almost 15%. Studies have shown that MHg usually represents less than 5% of the Hg_{TOT} in sediment (Harris *et al.*, 2007). The highest methylation rates were observed in sediments from the Schoonspruit stream.

It was reported that the mercury methylation is generally affected by factors that control availability of IHg (e.g. temperature, pH and redox potential) and also by factors that control the activity of mercury methylating agents (SRBs) such as the organic matter and sulfur (sulfide/sulfate) contents (see chapter 2).

In order to understand the main factors that control the mercury methylation process in the VR site, results of speciation analysis were compared with field measurements data and also with the organic matter and sulfur (or sulfate) contents determined in different sediment profiles.

It appeared from comparative data that most sediment profiles showed enrichment in MHg concentration near or at the layer corresponding to the lowest redox potential and the highest IHg concentration, as shown in figure 8.18 for the profile collected near Schoonspruit.

This trend was also observed by Hines and colleagues (2004). They concluded that redox potential, advective transport, or higher temperatures stimulating microbial sulfate reduction should explain the trend. Furthermore, Harris *et al.* (2007) reported maximum MHg concentrations where the inorganic pool of mercury in sediments was the most bioavailable to methylation processes. Metal ions adsorbed in acid media increase with pH, until the threshold value required for partial dissolution of solid and formation of soluble metal-humic complexes is exceeded (Lacerda *et al.*, 1998). Surficial sediments had lower pH than deeper sediments, and increases in Hg_{TOT} were correlated with pH. It is probable that methylation occurs in deep sediments at high pH but, due to its mobility, MHg migrates to shallow levels.

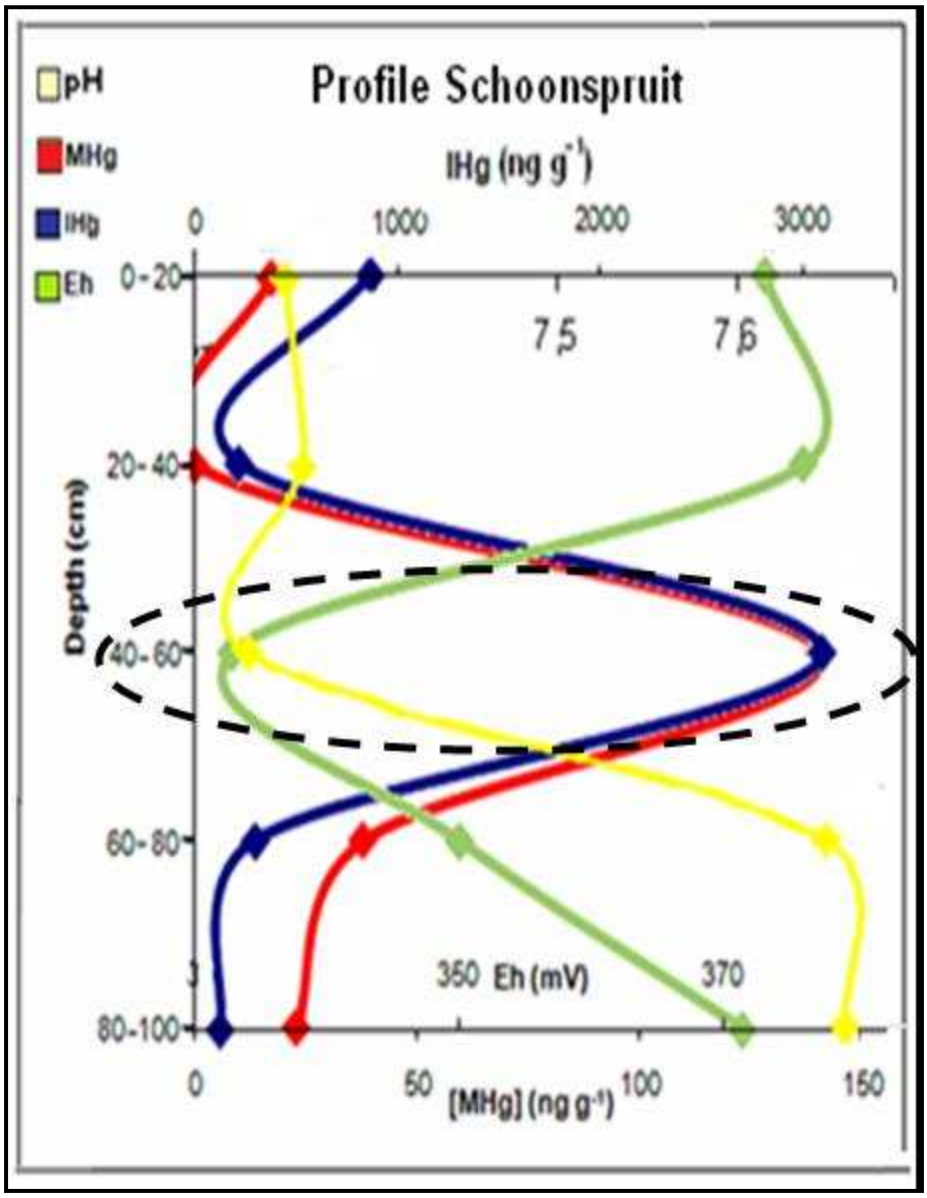

Figure 8.18 Example of Hg species distribution in a sediment profile
(The dashed area is the presumed region of MHg production)

In addition, an interesting correlation was found between methylmercury production in sediment profiles and other factors such as the organic matter, sulfur (or sulfate) and iron contents. The profile WC1, for example showed MHg enrichment at about 100 to 120 cm depth (figure 8.16). This region also corresponded to an important enrichment of the above mentioned factors (figure 8.19).

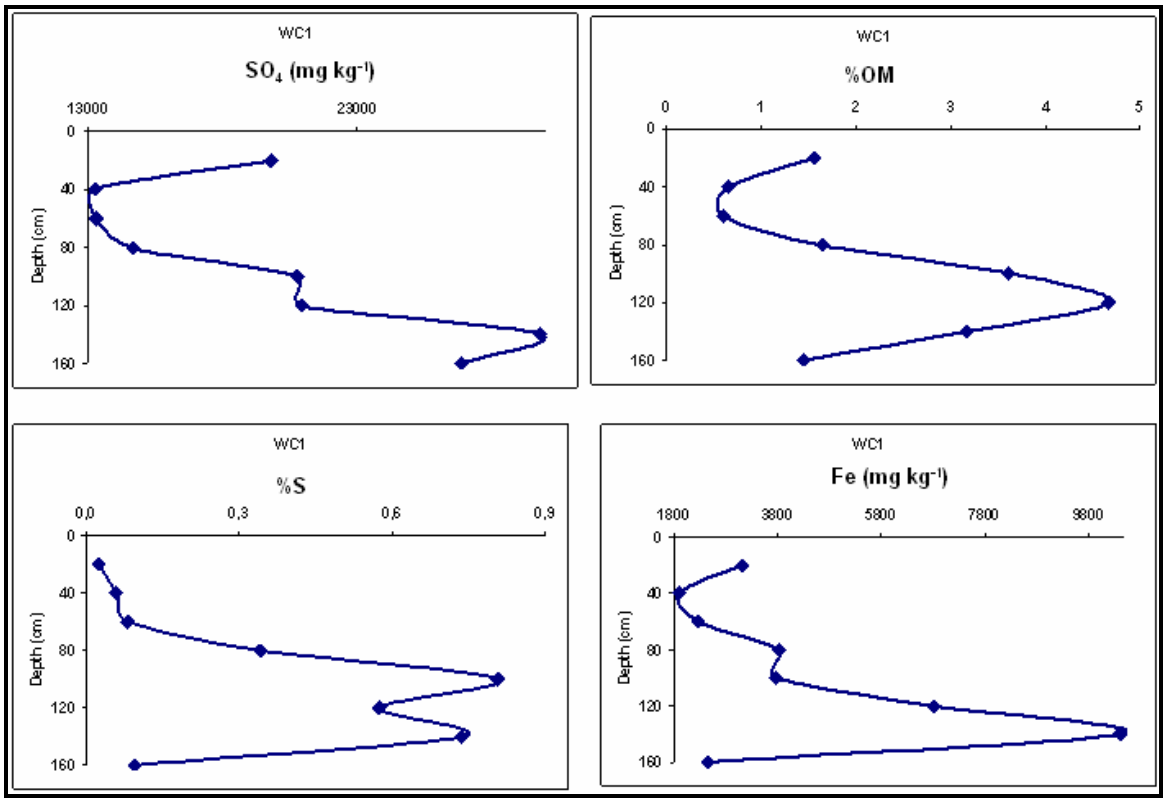

Figure 8.19 Sulfur, sulfate, organic matter (OM) and iron trends in the profile WC1

Studies of MHg levels in bulk surface sediment (e.g. Gilmour *et al.*, 1998; Krabbenhoft *et al.*, 1999; Mason and Lawrence, 1999; see also chapter 3) have demonstrated dependencies on inorganic mercury, organic matter, and sulfide suggesting that factors other than mercury concentration are also important in the control of the methylation. These studies proposed that sulfate additions can stimulate methylation by increasing microbial (SRB) activity (Benoit *et al.*, 2003).

It was also found that the presence of higher iron concentrations in sediments results in the removal of porewater sulfide by Fe–S precipitation. Therefore, as elevated sulfide levels can inhibit mercury methylation (Benoit *et al.*, 1999b), the Fe–S sequestration of sulfide, and other factors influencing sediment chemistry, results in more methylation of mercury.

Moreover, the interaction between heavy metals and soil colloids (clay, organic matter, or combination) has been described as ion exchange, surface adsorption, and chelation reactions (Mortensen, 1963; Nand Ram and Raman, 1983). The capability of humic substances to form complexes with heavy metals is attributed to their high content of

oxygen-containing functional groups such as carboxyl (COOH), hydroxyl (OH), and carbonyl (C=0) (Piccolo and Stevenson, 1982). Many studies have been carried out to evaluate the ability of clay minerals, organic matter (humic substances) or clay-humic-substances mixtures to adsorb heavy metals or to form complexes with heavy metals. The results of these studies suggested that the extent of heavy metal retention by mixtures of geologic or soil colloids has been found to vary with ionic strength, pH, type of clay minerals, organic functional groups and type of competing cations.

The above suggestions are in perfect agreement with the different trends observed in this study.

8.4.5 Impact of seasonal changes on mercury transport, distribution and fate

The mean concentration of Hg_{TOT} in waters of the pollution control dam (Bokkamp Dam) was above 1 µg L^{-1} (i.e. 1000 ng L^{-1}) at the wet season sampling with nearly 50% in the form of MHg (table 8.8). Harris *et al.* (2007) stated that concentrations of Hg_{TOT} in unfiltered water samples from lakes and streams lacking local anthropogenic or geologic sources are usually in the range of 0.3 to 8 ng L^{-1} whereas surface waters with high dissolved organic matter (DOM) contents often have "elevated" (5 to 20 ng L^{-1}) Hg_{TOT} concentrations. These authors also mentioned that streams draining areas with concentrated geologic sources of mercury or with large accumulation of Hg-contaminating tailings from mercury or gold mining can exceed 0.1 or even 1 µg L^{-1}(i.e. 100 or 1000 ng L^{-1}).

Table 8.8 Hg concentrations in waters from VR wet season sampling

Sample	pH	Eh (mV)	Ec (mS cm^{-1})	Hg_{TOT} (ng L^{-1})	%RSD	IHg (ng L^{-1})	MHg (ng L^{-1})	%MHg
Bok W1	7.41	452	4.4	1940	1.2	651	605	48.2
Bok W2	7.60	454	4.39	1040	6.0	478	461	49.5
SchW	7.49	482	0.8	82	7.8	46	26	36.1

Samples were also collected from five boreholes to assess the ground water pollution within the West Complex site (table 8.9).

Table 8.9 Mercury (µg L^{-1}) and other selected elements (mg L^{-1}) in VR borehole waters from the wet season sampling

Sample ID	T (°C)	pH	Eh (mV)	Ec (mS cm^{-1})	Hg	Ca	Fe	Mg	Mn	S
VRO3	15.0	7.6	85.0	3.8	1.01	100.48	20.18	276.00	31.76	362.50
VRO4	15.5	6.8	330.5	3.4	2.09	347.30	0.28	252.65	0.59	516.96
VRM16	16.2	6.8	199.2	3.4	2.21	358.40	14.07	312.29	0.38	680.28
VRM28	16.0	7.0	271.4	4.4	1.56	32.57	0.44	103.50	0.94	539.20
VRM38	16.1	4.6	474.5	5.3	3.31	73.01	35.00	764.50	332.00	1128.74

Total mercury concentrations were very high in these boreholes ranging between 1.0 to 3.3 µg L^{-1}. The highest Hg_{TOT} was recorded in sample VRM38 (figure 8.20) located at several hundreds km to the West Complex North TSF, near the sampling point WC1.
The pH at this point (as for WC1) was acidic (4.6) with high Eh (0.47 V) and Ec (5.3 mS cm^{-1}), denoting the existence of AMD in the area which could explain the release of mercury and others metals into the water.

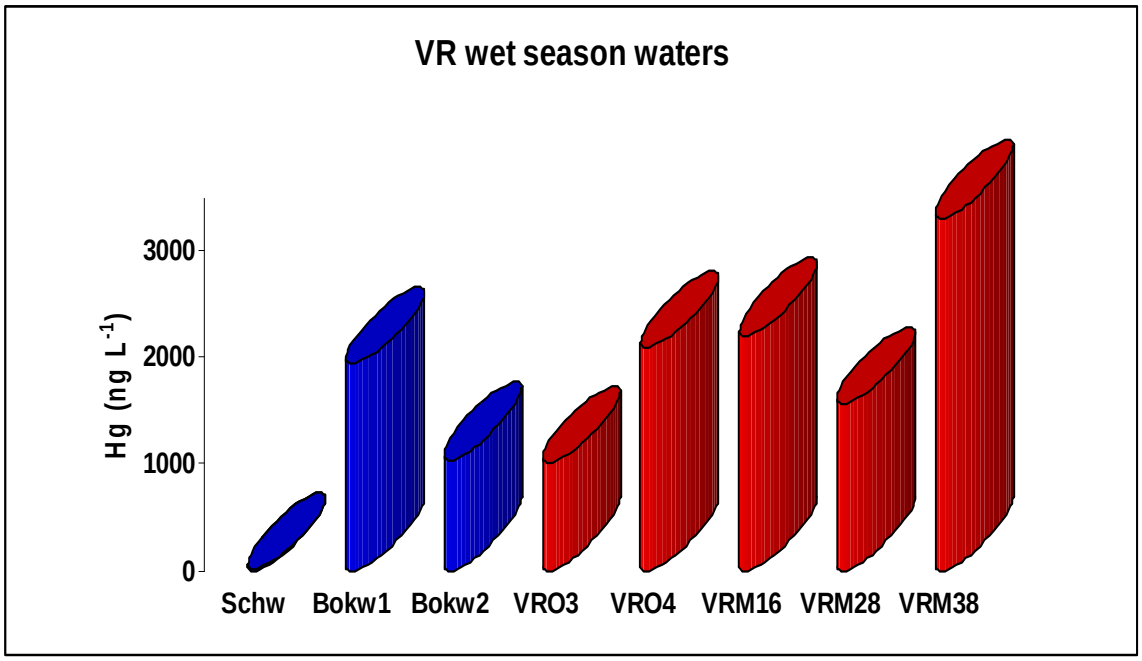

Figure 8.20 Hg_{TOT} in VR surface (blue) and borehole (red) waters from the wet season sampling

High sulfur (874 µg kg^{-1}), iron (37 µg kg^{-1}) and manganese (370 µg kg^{-1}) values were also measured at this point.

It is of importance to mention that all mercury concentrations measured in both surface and borehole waters were, except for the water collected from Schoonspruit (sample schw), exceeded national and international criteria for mercury in water, such as the World Health Organization Guideline Value (WHO GV) for drinkable water of 1 µg L^{-1} (WHO, 1993) which is also the recognized value by the South African Department of Water Affairs and Forestry (DWAF) (SAWQG, 1996). Three boreholes out of five (60%) had Hg_{TOT} exceeding the USEPA Maximum Contaminant Level of mercury in drinking water (MCL) of 2 µg L^{-1} (USEPA, 2009). Although the water fro Schoonspruit had a lower concentration than the rest of the samples (82 ng L^{-1}), the mercury level was still higher than the threshold level of 12 ng L^{-1}. The EPA recommends analyzing edible portions of fish, when the stream-water concentrations of mercury exceed the TEL, in order to determine if there has been any adverse effect (Gray *et al.*, 2000).

A study carried out in the Ankobra River Basin (Ghana) which is also seriously affected by gold mining (Kortatsi, 2006) showed concentrations of mercury in boreholes between 0.01 and 133 µg L^{-1} with median value of 41 µg L^{-1}. These values were observed in the boreholes only in the rainy period. In the dry season mercury concentrations were largely below detection (not reported). The study correlated mercury concentration in the wells to the recharge regimes of polluted surface water mentioning that this was likely to occur during the wet season than in the dry season. The author of the study concluded that the occurrence of mercury in the groundwater bodies was largely due to contamination from surface sources, perhaps, as result of the indiscriminate use of mercury for gold processing in the Ankobra basin.

The same observation was made in the VR West area. Trends in mercury concentrations differed from dry to rainy season with only up to 5 ng L^{-1} in water during the dry season despite mercury concentrations in the corresponding bottom sediment of 10500 µg kg^{-1}.

In areas where gold mining operations involve milling of Au-bearing ores and tailings deposition, metallic mercury can eventually be mobilized through particle transport and leaching (Lacerda and Salomons, 1998).

Although mercury leaching from tailings seems to be a slow process, over the years the bulk migration of spilled tailings and seasonal leaching from tailings and polluted soils may be important dispersal mechanisms for mercury. Seasonal migration of mercury could explain the patterns we observed in the stream bank sediments. In the rainy season (figure 8.21), mercury concentrations in surface sediment were 10 times higher than in the dry season (i.e. increased from approximately 103 to 1004 µg kg^{-1}). It was not possible to evaluate mercury in the bulk tailings which spilled into this stream. as this occurred in the first half of the 20th century. However, concentrations of mercury in surface sediments near the later TSF (which commenced construction in the 1940s and is still in operation) decreased from about 950 to 320 µg kg^{-1} (figure 8.21).

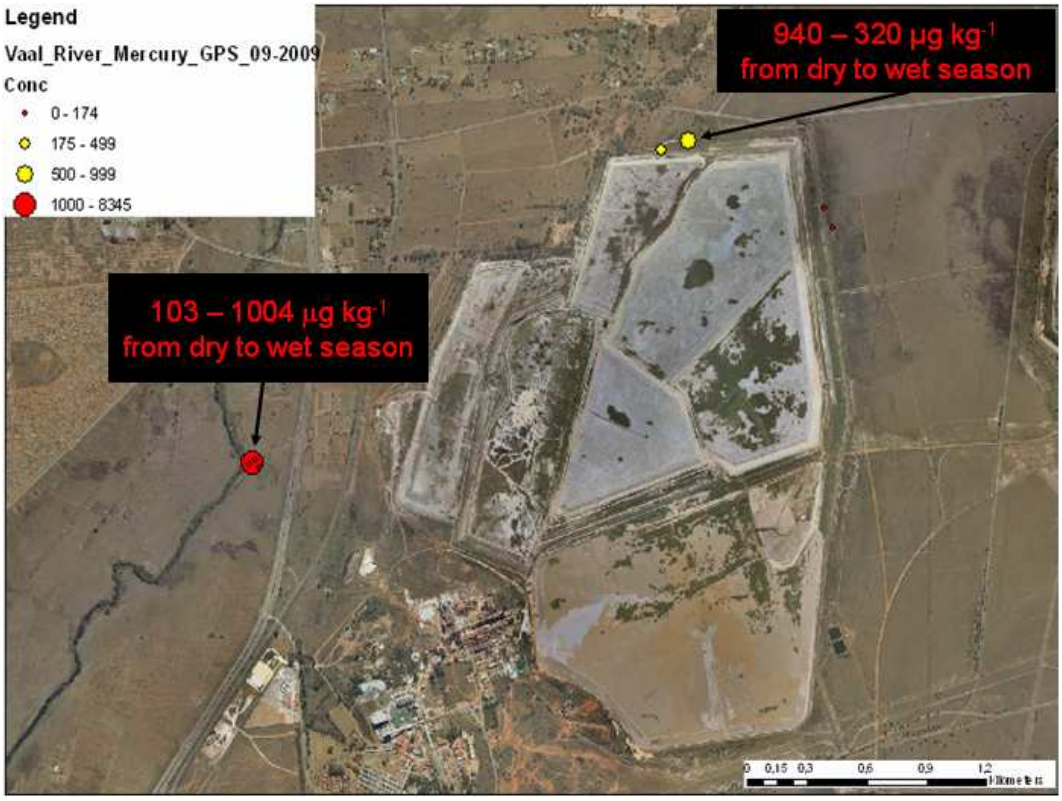

Figure 8.21 Impact of seasonal change in the Hg load in sediments adjacent the VR West Complex TSF and near the Schoonspruit

The contamination observed in the bank of Schoonspruit is a potential risk for the stream since MHg can be leached from the sediment and migrate to the water system where it

can be transported, later on, into the Vaal River which is located several kilometers downstream (see figure 8.15).

Moreover, there is also a risk for the important MHg content observed in the sediment profile from Schoonspruit (figure 8.22) to enter the food web through the aquatic system where it could biomagnify and bioaccumulate in fishes.

It has to be mentioned that fishing activities have been observed in the Vaal River (near Klerksdorp) at the time of the sampling.

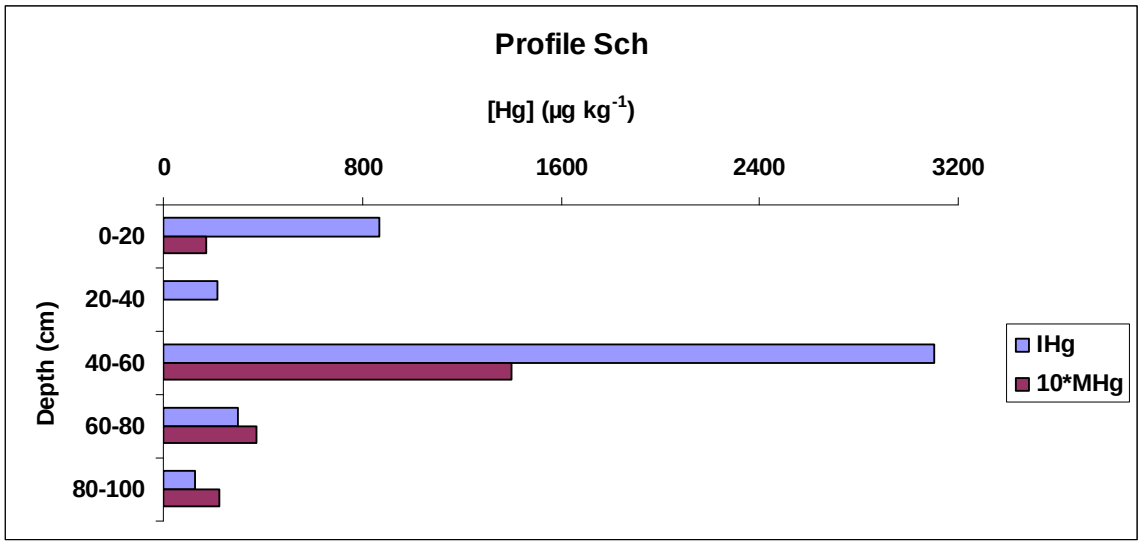

Figure 8.22 Hg species in sediment collected near Schoonspruit. Note the elevated MHg at 40-60 cm depth (about 147 µg kg^{-1})

On the Eh-pH diagram of mercury species (figure 8.23), elemental mercury is likely to be the predominant species of Vaal River West sediments.

Mercury is present primarily in its elemental form in tailings and bottom sediments between Carson City and Dayton (Lechler *et al.*, 1997). USGS research suggested that as these tailings and sediment move, the elemental mercury is absorbed onto clays, organic matter, and iron and manganese coatings (Lawrence, 2003). In the bank of Schoonspruit, methylmercury concentrations in sediments are as much as 147 µg kg^{-1}, which is significantly higher than in sediments collected elsewhere (table 8.6). These high methylmercury concentrations are probably related to the oxidation of elemental mercury

and high organic-carbon contents, which are favorable for mercury methylation (Lawrence, 2003).

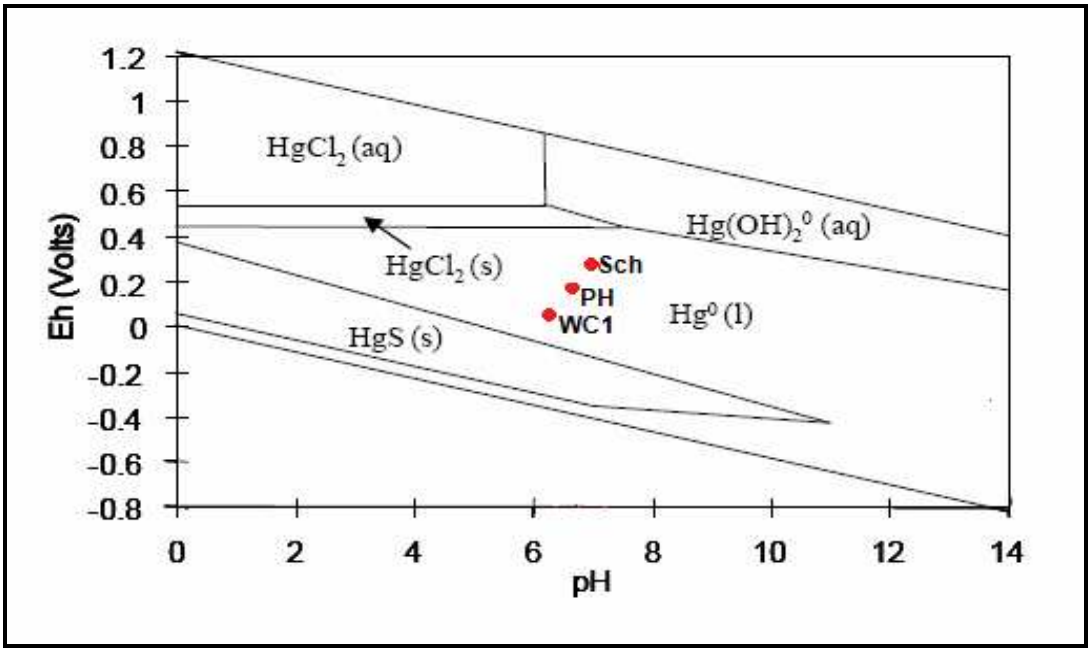

Figure 8.23 Eh-pH diagram showing that study sediment samples speciated as Hg^0

On another hand, Lacerda and Salomons (1998) studied changes in mercury concentrations in water and suspended particles, as well as in major physico-chemical parameters in streams receiving drainage from tailings during storm events, and found a drastic increase in the redox potential and in mercury concentrations in suspended particles. In the present study, pH in the pollution control dam decreased from the dry to the rainy season (from 7.8 to 7.5) and redox potential increased (from 335 to 450 mV), with a concomitant increase in mercury concentration in the (unfiltered) water. These results suggest that rain erodes fine particles enriched with mercury from contaminant sources, followed by mercury transport along with suspended particles. The relationship between mercury dispersion, erosion and transport of suspended particles, supports a seasonal dispersal mechanism, with rainfall also diluting the existing mercury in water bodies. We suggest that Hg-contaminated particles from tailings and secondary sources are transported during rains and deposited in sediments along drainage pathways. After this, remobilization of contaminated particles from sediment surfaces may take place,

resulting in a decrease in mercury concentrations in the drainage bottom sediments and exportation to areas away from mining sites (Lacerda and Salomons, 1998 and the reference therein). This process could explain the high mercury concentration of about 4300 µg kg^{-1} measured during the rainy season in the upper layer (0-20 cm) of sediments (sample "PH") in receipt of run-off from the pollution control dam (figure 8.24).

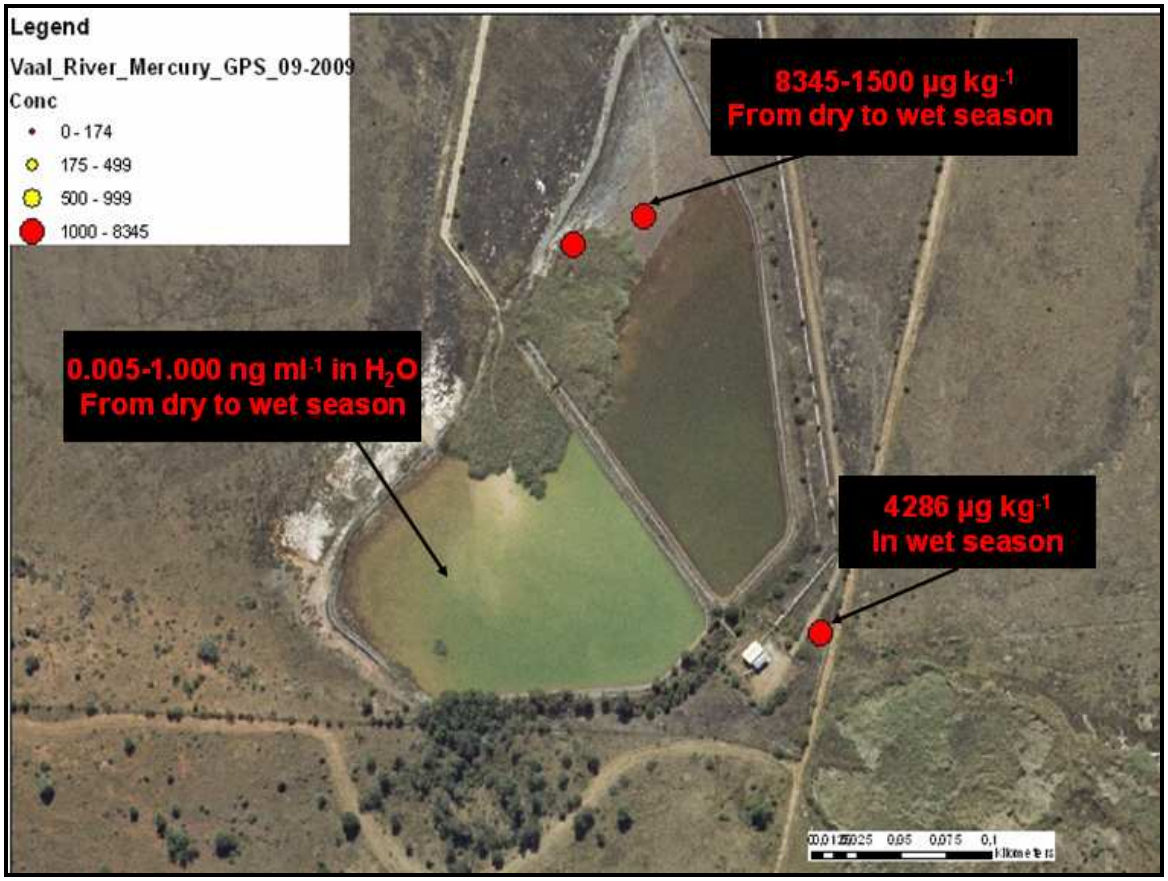

Figure 8.24 Changes in the Hg load in Bokkamp Dam and its surrounding

The decrease in mercury concentration within the control dam sediments (8500 down to 1500 µg kg^{-1} from dry to wet season), and in the depth profile of the directly adjacent sediment (from 4286 µg kg^{-1}at 0-20 cm to 126 µg kg^{-1} at 20-40 cm; figure 8.25), suggests that the localized surface accumulation of mercury is from recently deposited particles and leached mercury from the dam. In contrast, the enrichment of mercury at deeper levels in sediments adjacent to the old tailings facilities (e.g. sample WC1 in figure8.16), might be due to historical loads of mercury in tailings and seepage from the facilities.

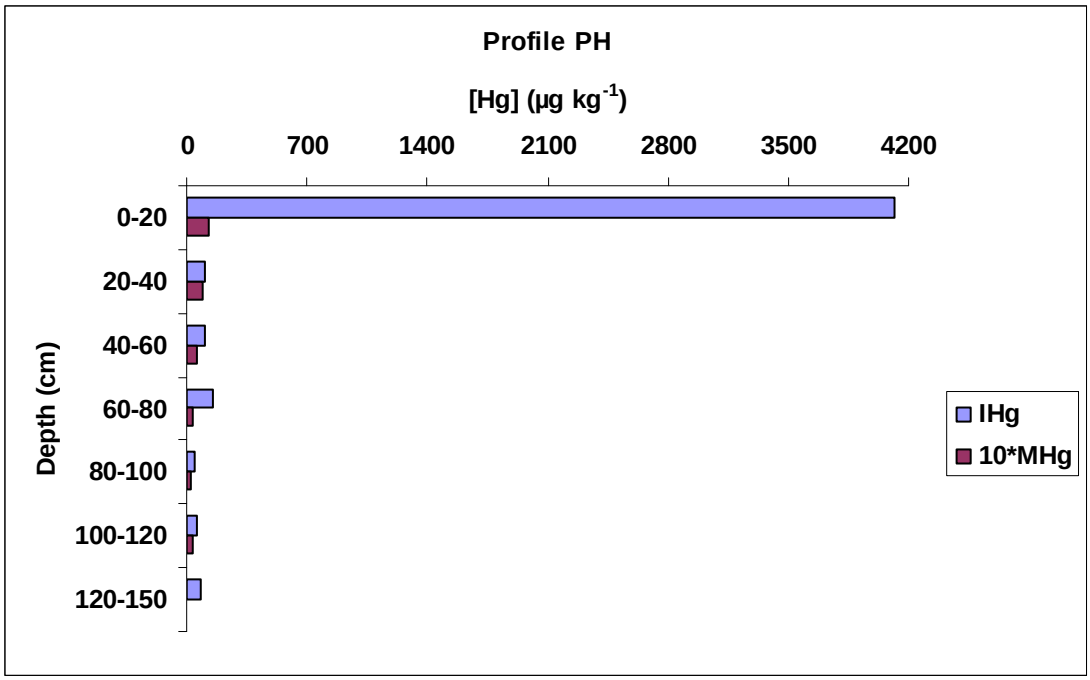

Figure 8.25 Trends of Hg species from a sediment profile near the Bokkamp Dam

An unusually high rainfall season preceded the wet season sampling with reported cases of overflows from the Dam. For example, AGA reported that few months after the dry season sampling the Bokkamp dam overflowed after receiving 74 mm of rain, releasing 6.000 kL of water (AGA, 2010). It has to be recalled that the dam was built with waste rocks and tailings. The intensive rainfalls that occurred after the dry season sampling and the subsequent overflows from the dam could explain the remobilization of mercury-bearing tailings and bottom sediments. and its dispersion away from the dam.

Total metals analysis of the same sediment profile (sample PH) also showed the same pattern as for mercury with extremely high concentration at the surface (0-20 cm) and a consequent drop at 20-40 cm depth. An example is shown in figure8.26 where the surface concentration of iron, cupper and manganese reached the percentage level i.e. 2.4, 7.5 and 11.4%, respectively (see also table 8.7).

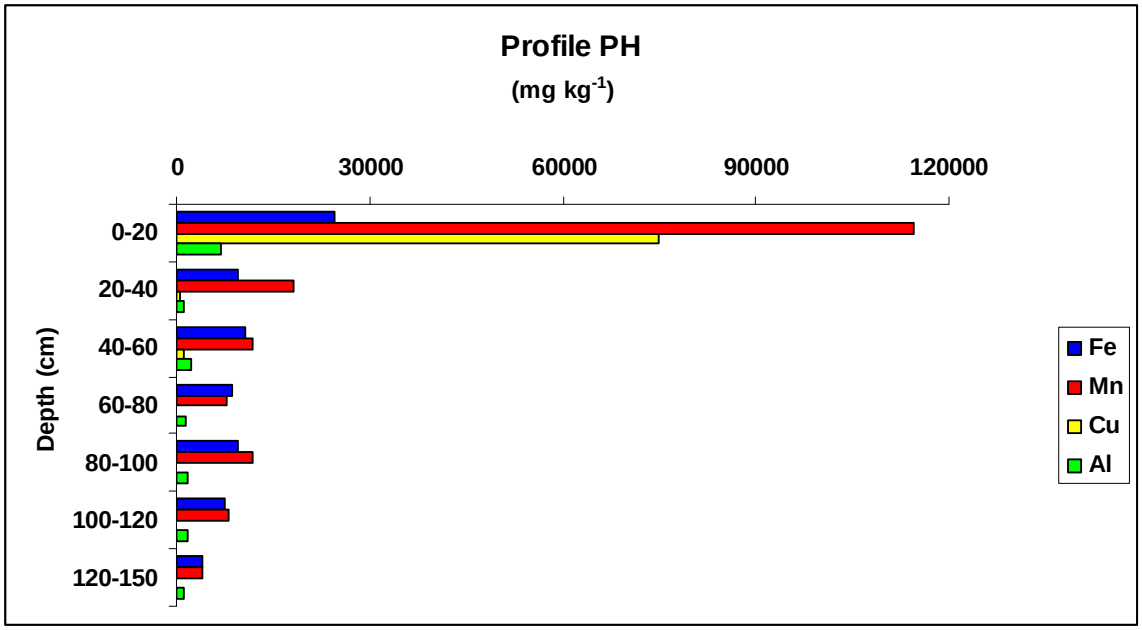

Figure 8.26 Example of metals concentrations in the profile adjacent to Bokkamp Dam

8.4.6 Mercury in plants at the Vaal River West area

Plants are known for their ability in accumulating mercury from a variety of sources such as dry and wet atmospheric deposition, water contained in the soil, and the available mercury released through mineral weathering (Huckabee and Janzen, 1975). Factors that may affect concentrations of mercury found in plants include the mercury sources, its chemical form and the physiology of the plant species. There may also be differences in the amount on IHg and MHg in different plant tissues. Therefore, concentrations of mercury in plants reflect the environmental exposure to mercury and ecological niche (Moore *et al.*, 1995).

.Moreover, as plant tissues decompose in the soil, the mercury released can either be retained by the soil or transformed into more mobile forms (such as MHg), which may be leached to other soil and aquatic systems where it may enter the food chain (e.g. Driscoll *et al.*, 1994). Veiga and co-workers (1994) have suggested that elevated concentrations of mercury in fish and humans in the Amazon may be related to deforestation activities, as well as mining operations.

Plants samples were randomly collected throughout the site and the concentration of selected plants are presented in table 8.10. An example of GC-ICP-MS chromatograms obtained during plants speciation analysis is shown in figure 8.27.

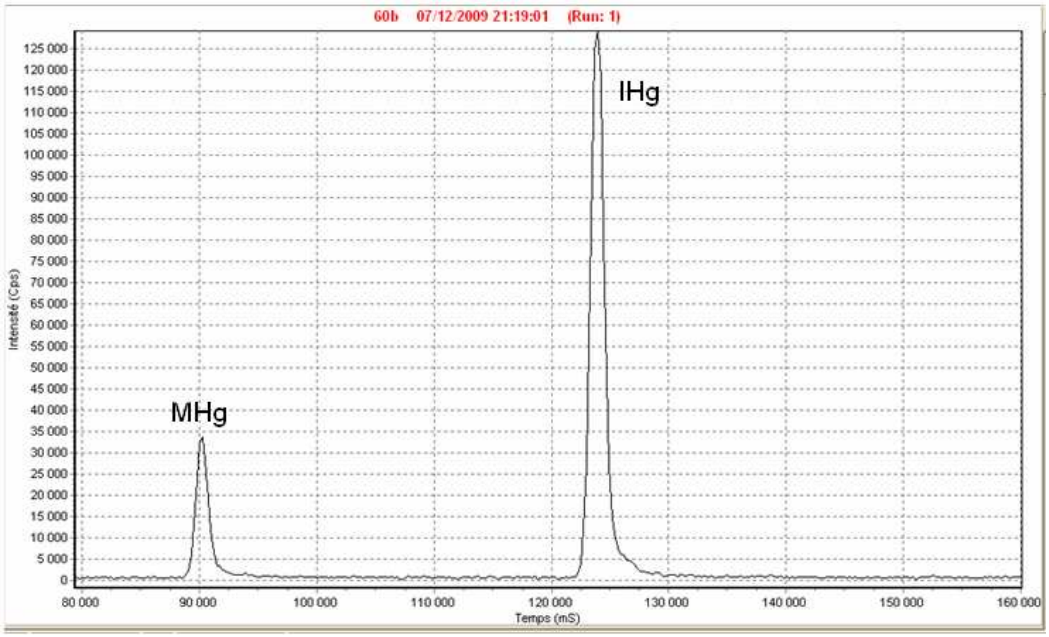

Figure 8.27 GC-ICP-MS chromatogram of VR plant 60B

Table 8.10 Hg_{TOT} and Hg species concentration in selected VR plants

Sample	Type	Hg_{TOT} ($\mu g\ kg^{-1}$)	IHg ± SD (n=3; $\mu g\ kg^{-1}$)	MHg ± SD (n=3; $\mu g\ kg^{-1}$)	%MHg
40A	Algae	70.7	nd	nd	
40B	Algae	93.8	63.1 ± 1.4	35.4 ± 2.6	35.9
47	Hyacinth	85.0	74.9 ± 0.2	0.3 ± 0.0	0.4
60B	Reed Typha	59.9	45.5 ± 0.3	8.1 ± 0.1	15.2
63	Algae	15.7	nd	nd	
64A	Willow leaves	17.8	nd	nd	
66B	Phragmites	24.9	nd	nd	
69A	Phragmites	247.3	244.4 ± 0.2	2.6 ± 0.2	1.1
74	Enterromorphe	85.1	nd	nd	
75	Myrophyllum	27.2	nd	nd	

Hg_{TOT} in VR plants varied between 17 and 207 $\mu g\ kg^{-1}$ whereas speciation analysis of selected samples showed MHg concentrations between 0.3 to 35.4 $\mu g\ kg^{-1}$, which correspond to 0.4 to 35.9 % of the Hg_{TOT} present as MHg.

Information on mercury concentrations in plant tissues obtained from the literature (Moore *et al.*, 1995) suggest concentrations range from below 10 to more than 10000 µg Hg kg^{-1}, with most of the large concentrations measured in samples collected from areas that are exposed to high levels of mercury, such as around chlor-alkali plants, cinnabar-containing mines and volcanoes, and Hg-rich rocks (Moore *et al.*, 1995 and references therein). Therefore, excluding these samples in areas of point-source mercury pollution, most samples contain between 10 and 300 µg Hg kg^{-1} and, when separated into groups, they form the following general sequence of medians (in µg Hg kg^{-1}): Grasses and herbs (20) < Tree and shrub leaves (29) < Aquatic macrophytes (40) < Sphagnum mosses (69) < Lichens (170) < Fungi (280).

Results obtained in the present study fell within the above range and also reveal major variations in terms of the amounts and ratio between species (figure 8.28) as well as within the tissue (table 8.10).

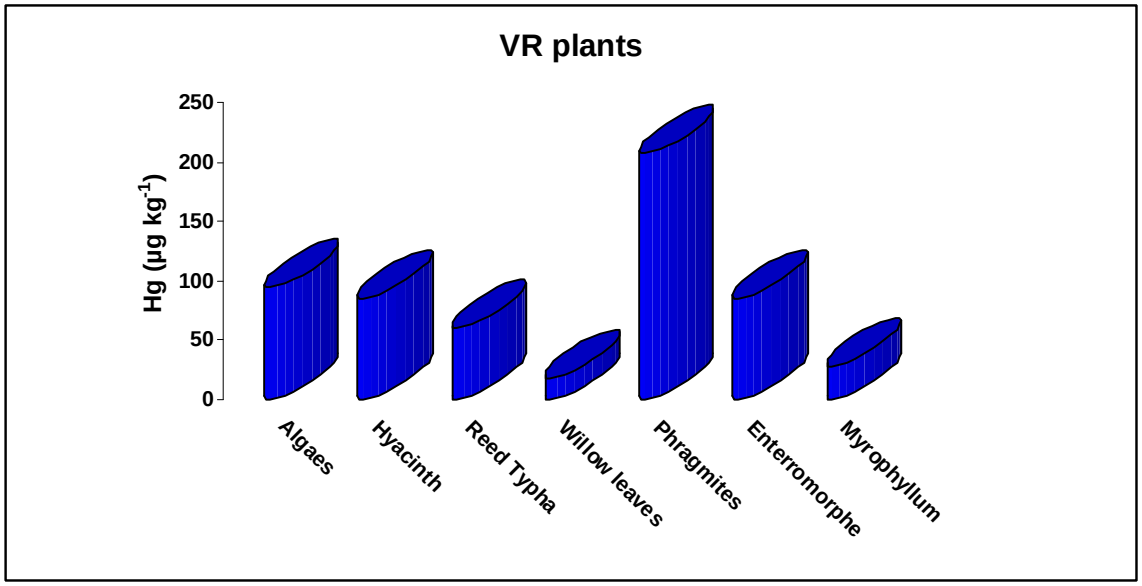

Figure 8.28 Hg_{TOT} in selected VR plants

Rasmussen (1995) mentioned that there can be considerable variations in total mercury concentrations in plant tissues of the same species collected from one site: the average coefficient of variation of Hg_{TOT} concentration in samples collected from the same site

was 18%. The relative standard deviation obtained for two algaes collected in the Vaal River (samples 40A and 40B) was 20%. However, the author recommends, for geochemical exploration purposes, the collection of three samples of each tissue type per site. The small number of samples analyzed in the present study and the large variation in concentrations within samples collected from the same species prevent drawing firm conclusions, although several trends are suggested that are worthy of further study.

Cappon (1987) reported Hg_{TOT} concentrations in vegetables from 3 to 139 µg kg^{-1} and MHg concentrations from 0.3 to 30 µg kg^{-1}, equivalent to 0 to 23% of the Hg_{TOT} concentration. Moore and colleagues (1995) measured concentrations of mercury in the plant tissues from 4 to 160 µg Hg_{TOT} kg^{-1} and 0.1 to 139 µg MeHg kg^{-1}. The proportion of Hg_{TOT} occurring as MeHg in their study ranged from 0.2 to 100%, with the highest percentages generally in those species with the largest Hg_{TOT} concentrations.

These authors also noticed that increasing concentrations of the two forms of mercury (IHg and MHg), and increasing percentages of Hg_{TOT} occurring as MHg (0.5 - 30%). were found in plants growing under wet conditions.

Nsengimana (2007), in his study of the speciation of mercury in the Klip River (SA) found much lower concentration of MHg (0.5 to 4.9 µg MHg kg^{-1}) which corresponded to 0.7 to 4.9% of total mercury.

Results obtained in the present study are in agreement with mercury concentrations found in plants where the mercury contamination in the area can be classified between a modest to a severe type of pollution (Moore *et al.*. 1995 and references therein). Total mercury concentration of 247 µg kg^{-1} was found in phragmites collected from the Bokkamp Dam. It is believed that this high value can be correlated to the elevated mercury concentration found in the dam (10245 µg kg^{-1}). Mercury in the phragmites was approximately 2.5% of the concentration found in the corresponding sediment. The same observation was made with phragmites collected near the West Complex TSF (Sample 66B) which also showed about 2.5% (25 µg kg^{-1}) of the mercury content in the adjacent sediment (sample 65B: 983 µg kg^{-1}).

As MHg is the form most easily absorbed within the food chain, the occurrence of substantial concentrations of MHg in the studied plants is of interest. The highest

proportion of MHg in VR plants (figure 8.29) were also found in samples growing under wet conditions i.e. in the Vaal River (sample 40B: 35 µg MHg kg^{-1}) and in the Schoonspruit (sample 60B: 8 µg MHg kg^{-1}).

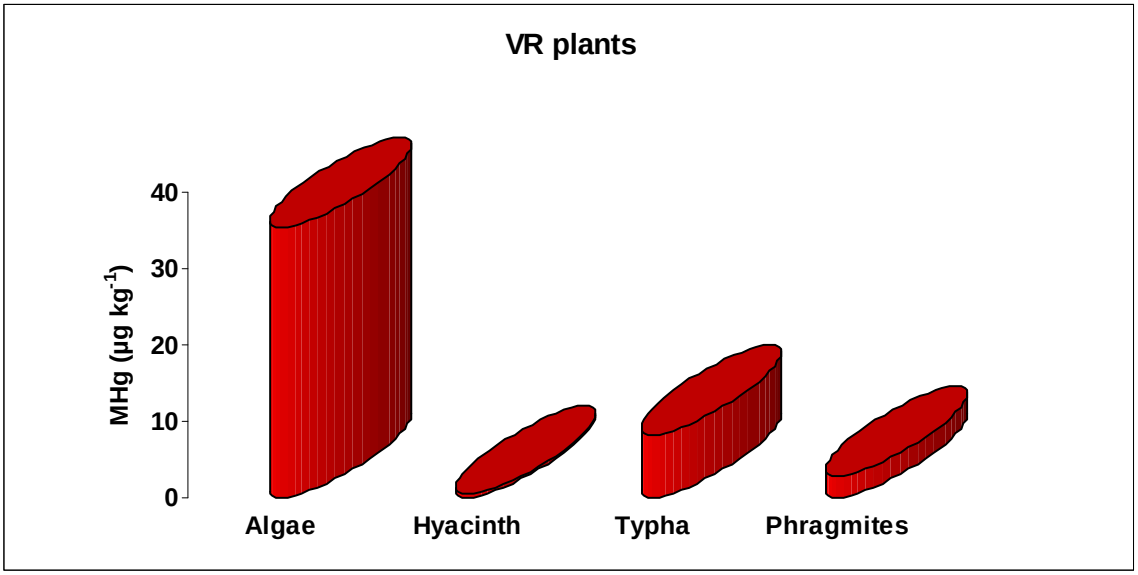

Figure 8.29 MHg in selected VR plants

It was not possible to determine from this study if the observed concentrations of MHg in plants resulted from its uptake from the soil and soil water, or from intrinsic methylation processes in plants.

It is of importance to note that widespread increases in the atmospheric deposition of mercury (Lucotte *et al.*, 1995) may also result in increased concentrations of mercury in plant tissues, which in turn may contribute to elevated bioaccumulation of mercury.

8.4.7 TGM measurements at the old mine ventilation shaft

No attempt has been made in this study to evaluate atmospheric deposition of mercury, which could add to total mercury in sediments and tailings in the area (Fitzgerald *et al.*, 1998). Notable increases in mercury concentrations in soils and sediments from atmospheric deposition, however, are likely to be restricted to within a few centimeters of the surface (e.g. Rood *et al.*, 1995). Also we have not yet attempted to evaluate gaseous mercury emission and redeposition, which could reduce or redistribute mercury.

However, a pilot study was carried out in order to determine TGM at the outlet of a ventilation shaft connecting several old gold mines near Orkney (figure 8.9). Air samples were collected at 1.5 m height above the ground using gold traps, as described in chapter 6. Air was pumped for 10 minutes with a vacuum cylinder through a Teflon tubing line (I.D. 1.6 mm; length 1.5 m) to the gaseous mercury trapping device. Air pumping flow rate was adjusted at 0.5 L min^{-1} and continuously controlled during the sampling period by a calibrated gas flowmeter (figure 8.30).

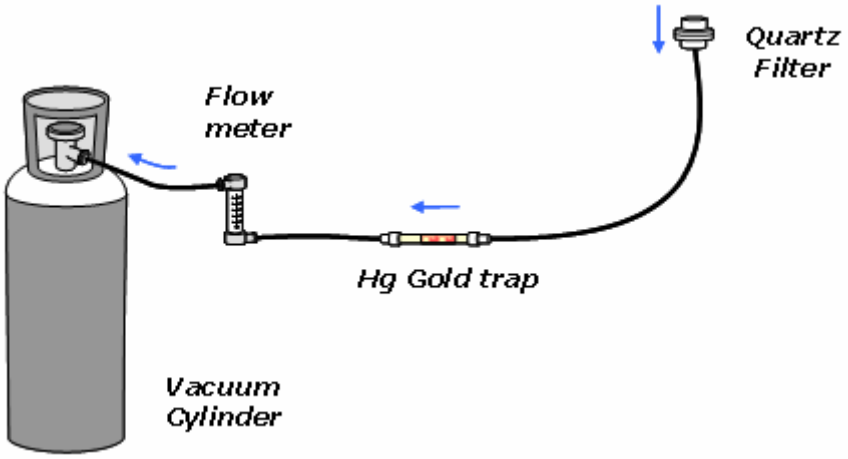

Figure 8.30 Experimental set-up for Total Gaseous Mercury in air

Due to the low capacity of the vacuum cylinder, it was not possible to achieve the equilibration step of the air sampler with ambient air. Prior to the sample collection, the sampler is usually run during an hour in order to equilibrate the sampling line with the air sample. This procedure aims to minimize or avoid any adsorption/desorption of gaseous mercury on/from the sampling line walls and thus to improve the accuracy of the TGM measurement.

Thus, only three air sample replicates of 2.8, 5.0 and 1.5 liters have been performed. The TGM concentrations measured at the outlet of the ventilation shaft are presented in Table 8.11.

Table 8.11 TGM concentrations in air

ID	Sampling flow (ml min^{-1})	Volume (L)	TGM (ng m^{-3})
A1	500	2.8	49.2
A2	500	5.0	21.8
A3	350	1.5	31.4

The measured TGM concentrations at the outlet of the ventilation shaft were significantly higher than typical background concentrations measured in pristine and open areas, where TGM contents usually range between 1 to 4 ng m^{-3} (Baker *et al.*, 2002; *et al.*, 2003; Gabriel *et al.*, 2005; Wangberg *et al.*, 2001). Within urban areas, concentrations are found higher and more variable reaching up to 15-25 n gm^{-3} (Pécheyran *et al.*, 2000; Gabriel *et al.*, 2005; Wang *et al.*, 2007).

TGM concentration in the first sample (A1) could be attributed to a contamination from the non equilibrated sampling line. Nevertheless, the sampling line used for the present work was quite short (1.5 m) and the mercury retention or contamination on/from its walls can be expected to be low. Although A1 shows a higher TGM content than the last two samples, the concentrations remain in the same range for the three samples and are likely to trace an underground gaseous mercury source from the old mines.

These results have to be compared with background atmospheric TGM contents in this peri-urban area surrounded by old mines. Further air sampling in both shafts and open sites is needed to confirm these preliminary results.

8.5 Mercury in the West Wits Region

8.5.1 Mercury in West Wits waters

Analytical data for WW waters together with field measurements are shown in table 8.12.

Table 8.12 Mercury in West Wits waters

Sample	T (°C)	pH	Eh (mV)	Ec (mS cm^{-1})	IHg (ng L^{-1})	%RSD	MHg (ng L^{-1})	%RSD	%MHg
15A	19.8	5.92	387.7	3.82	0.004	6.5	0.292	25.8	98.5
17A	20.4	6.67	482.9	3.88	0.330	2.0	7.835	6.3	96.0
19A	20.0	7.51	452	3.64	13.055	2.9	6.547	4.8	33.4
20A	20.0	7.74	445	3.55	0.195	2.4	3.436	6.6	94.6
21	20.0	7.8	442	3.53	0.009	15.9	2.680	1.1	99.7
24B	20.3	8.95	415	2.03	0.099	6.6	0.007	32.2	6.7
25B	19.3	8.97	384	2.02	0.003	9.4	bdl		0
26	21.2	8.3	409	2.24	0.558	6.2	bdl		0
29	20.9	8.29	417	2.23	0.048	3.1	5.305	12.8	99.1
31	22.4	8.04	443	0.88	0.006	4.5	0.054	2.8	89.9

Except for water sample 19A (19.6 ng Hg_{TOT} L^{-1}), collected from a water dam near the TSF compartment 7B (figures 8.10 and 8.31) which showed Hg_{TOT} beyond the TEL level of 12 ng L^{-1}, mercury values were generally low, and similar to values for waters obtained in the Vaal River region. This result could be anticipated, as WW waters were collected at the same period with the VR dry season waters.

Figure 8.x shows amounts of methylmercury versus total mercury (i.e. IHg + MHg) for unfiltered waters. In these waters, only 30% (3 samples out of 10) have shown MHg concentration below 10% of Hg_{TOT} (range: 0 to 7%), which is the range of values commonly seen in relatively uncontaminated surface waters with normal methylation potential (see e.g. Kelly *et al.*, 1995).

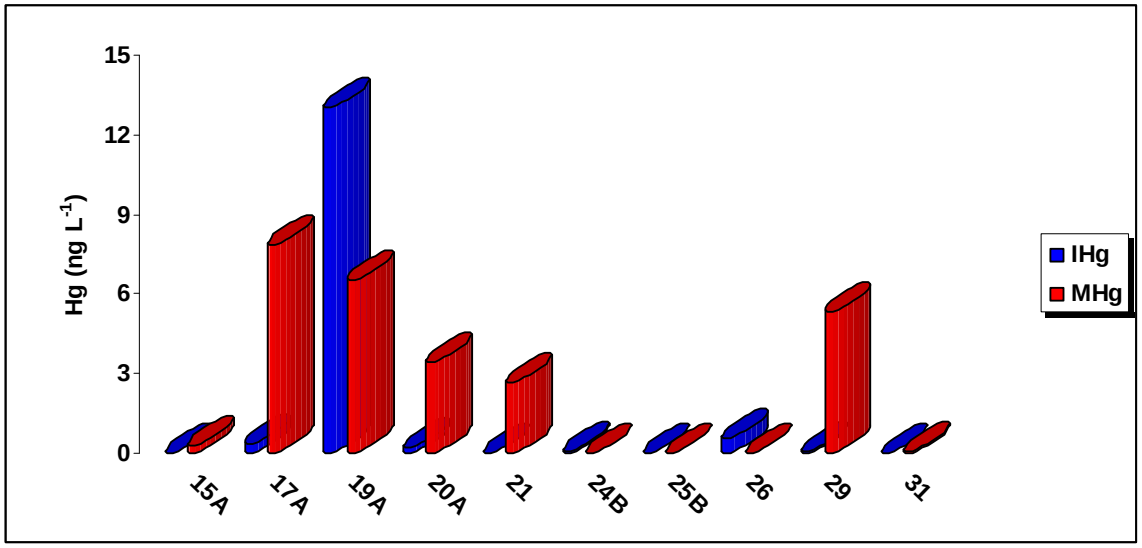

Figure 8.31 IHg and MHg in WW waters

Proportions of MHg were high in dams (e.g 19A), creeks (e.g. 17A) and streams (e.g. 29) (range: 33 to 99% of Hg_{TOT}), producing absolute values (0.007 to 7.835 µg MHg kg^{-1}) higher than those reported for the VR region. The high proportions of MHg are particularly significant, as it shows that conditions within the West Wits Old North sampling area may favor methylation of mercury.

It needs to be noticed that the vegetation in the area is characterized by a consistent number of grasslands, wetlands and woodlands (figure 8.32) with an important presence of decaying plants providing ideal conditions for mercury methylation.

Some of the GC-ICP-MS chromatograms of WW water samples exhibited a considerable presence of organomercury species with few of them showing unknown peaks (figure 8.33) similar to those detected in Highveld coals (see chapter 7).

This could be an evidence of the occurrence of ethylmercury in the site, although little is found in the literature to discuss the natural occurrence of this species in water systems (see for example Mao *et al.*. 2008).

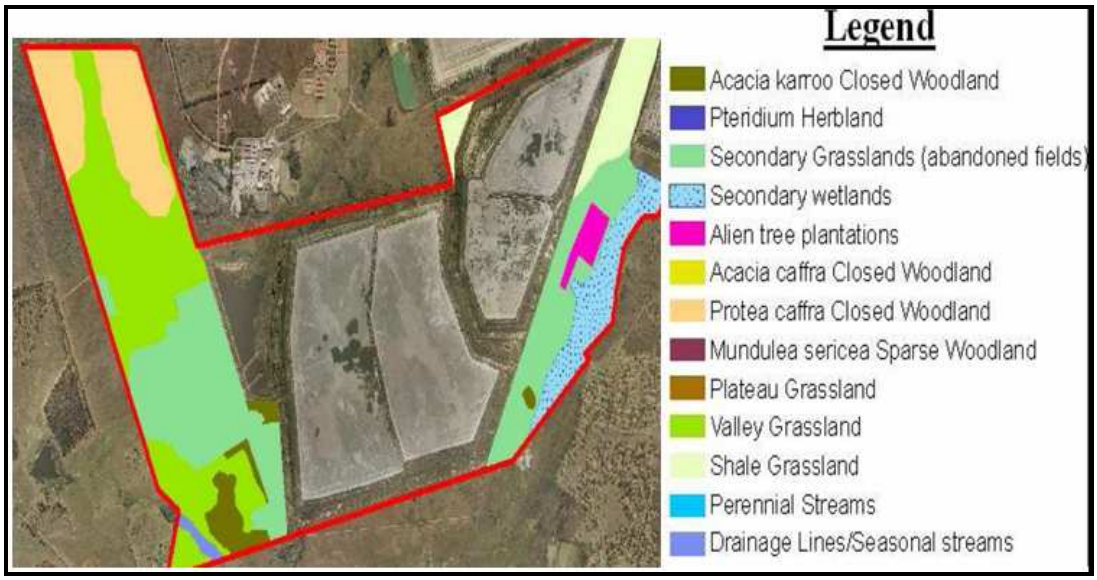

Figure 8.32 Preliminary mapping of vegetation sub-units at West Wits operations (AGA, 2009a)

However, studies have shown that derivatization processes (especially the ethylation) of water samples and the extraction of mercury species can be affected by elevated chloride content (Stoichev *et al.*, 2006; Yin *et al.*, 2010) and an important presence of humic acid (Yin *et al.*, 2010).

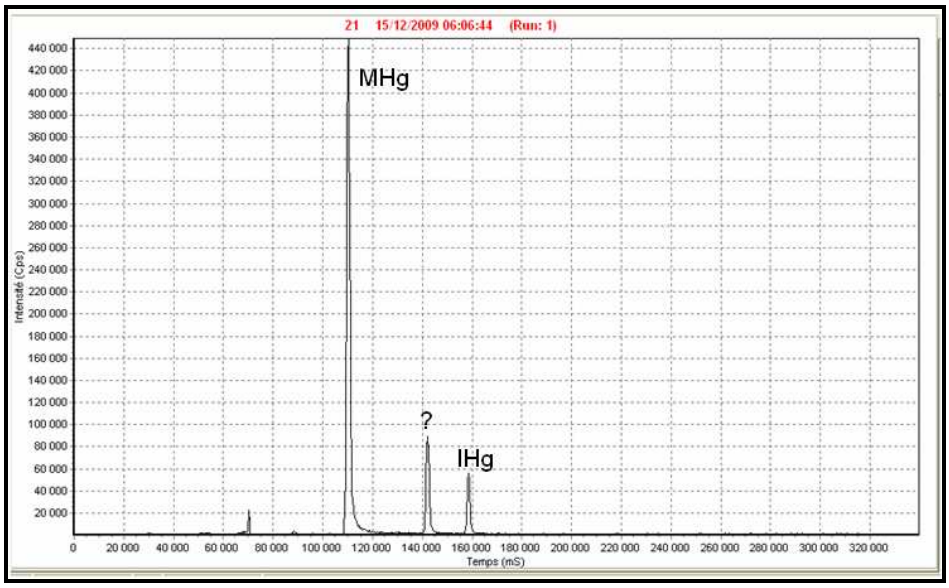

Figure 8.33 GC-ICP-MS chromatogram of WW water sample 21.
Note the presence of an important unknown peak at about140 seconds

Selected West Wits waters samples demonstrated an important salinity with sulfate (e.g. sample 17A: 1981 mg kg^{-1}) and chloride (e.g. 24A: 194 mg kg^{-1}) concentrations higher than those reported for some cases of water pollution (e.g. Ashley *et al.,* 2002) and the electrical conductivity was always at the mS cm^{-1} level (except in Wonderfonteinspruit). This reveals an important ion activity in the watersheds probably from the acid mine drainage generated in the Vaarkenslaagte canal by the oxidized pyrites from TSFs. The presence of elevated chloride concentrations and considerable organic matter content in WW waters could also affect the derivatization of mercury species and lead to a wrong estimation of their occurrence. Nevertheless, Jia and co-workers (2011) have study the effects of common coexisting ions (K^+, Ca^{2+}, Mg^{2+}, Cl^-, SO_4^{2-}, etc.) in real seawater samples on the recoveries of IHg, MeHg and EtHg using, for example, 10.000 µg L^{-1} for Cl^- and they obtained recoveries in the range of 89.7%–103.6% for the 3 species. They concluded that the interference from coexisting ions was negligible and could, therefore, be ignored. In addition, in order to minimize the matrix related concern of the ethylation, all the water samples were propylated with $NaBPr_4$, which is reported to provide low detection limit for organomercurials (Geerdink, 2007). However, aqueous $NaBPr_4$ solution is also unstable and the propylation reaction suffers from matrix effects when dealing with seawater (Schubert *et al..* 2000; Bravo-Sanchez *et al.,* 2004). Depending on the purity of the derivatization agent used, artifact formation of EtHg during aqueous propylation is sometimes a problem. For example, a previous study reported a conversion of up to 2.9% Hg^{2+} to EtHg during the propylation reaction (Huang, 2005). Although the $NaBPr_4$ used in the present study was of high purity (99.999%), a quality control analysis with appropriate standard materials is still of importance to confirm the occurrence of EtHg, and its magnitude in WW waters.

Elevated sulfur concentrations were also measured in West Wits waters, especially in the sample collected from the Vaarkenslaagte canal (15A: 4210 mg sulfur kg^{-1}) where the evidence of pyrite oxidation was observed (table 8.13).

Table 8.13 Concentration of selected elements (mg kg^{-1}) in WW waters

Sample	Al	Ba	Ca	Co	Fe	Ir	K	Li	Mg	Mn	Ni	S
15 A	0.69	0.02	428.5	0.59	27.8	22.1	78.4	0.03	110.6	44.4	0.03	4209.9
17 A	0.01	0.03	289.2	0.07	0.31	1.24	17.0	0.02	325.4	2.4	bdl	1929.2
19 A	1.00	0.06	457.9	0.06	0.04	0.64	47.6	0.17	92.6	1.2	0.03	2650.8
21	Bdl	0.05	175	0.06	0.05	0.62	40.1	0.16	35.6	1.2	0.04	1726.8
22	Bdl	0.05	420	0.06	0.04	0.67	39.3	0.16	85.2	1.3	0.03	1173.7
24 B	0.33	0.03	247.4	0.02	0.34	0.12	18.9	0.14	89.6	0.22	0.08	144.1
25 B	0.02	0.03	bdl	0.02	0.01	bdl	18.5	0.14	27.1	bdl	0.05	174.7
26	0.08	0.03	218.9	0.02	0.24	0.6	25.0	1.30	84.8	0.22	0.06	198.3
29	0.48	0.03	237.2	0.01	0.52	0.07	17.9	0.12	90.7	0.13	0.03	622.0
31	1.14	0.02	75.9	0.01	0.75	0.05	16.1	0.03	41.3	0.12	0.01	607.6

The pH measured at this point was the lowest (pH 5.9) of all the studied WW watersheds and with elevated iron and manganese contents (28 and 44 mg kg^{-1}, respectively). Oxidizing pyrites in nearby TSF are a possible source for iron, as well as sulfate in the canal which is tributary to the Wonderfonteinspruit. This could explain the important sulfur of 608 mg kg^{-1} content measured in sample 31 collected from the Wonderfontein stream.

8.5.2 Mercury in West Wits tailings and sediments

Concentrations of mercury and its species in collected tailings and sediments are presented in table 8.14, and figure 8.34 is an example of GC-ICP-MS chromatogram obtained from the mercury speciation in tailings.

From the obtained results, the background mercury concentration in the site was estimate to be about 35 to 50 µg kg^{-1}. Total mercury concentration in sediments from the WW region was lower than concentrations obtained in the VR region with Hg_{TOT} in surface sediment ranging between 36 and 628 µg kg^{-1}. Only four surface sediment samples were beyond the TEL value of 174 µg kg^{-1} with the highest concentrations measured from sediments collected near the old North TSF (sample S/A 10: 414 µg Hg kg^{-1}) and from the dam (sample 19F: 628 µg Hg kg^{-1}) as shown in figure 8.35.

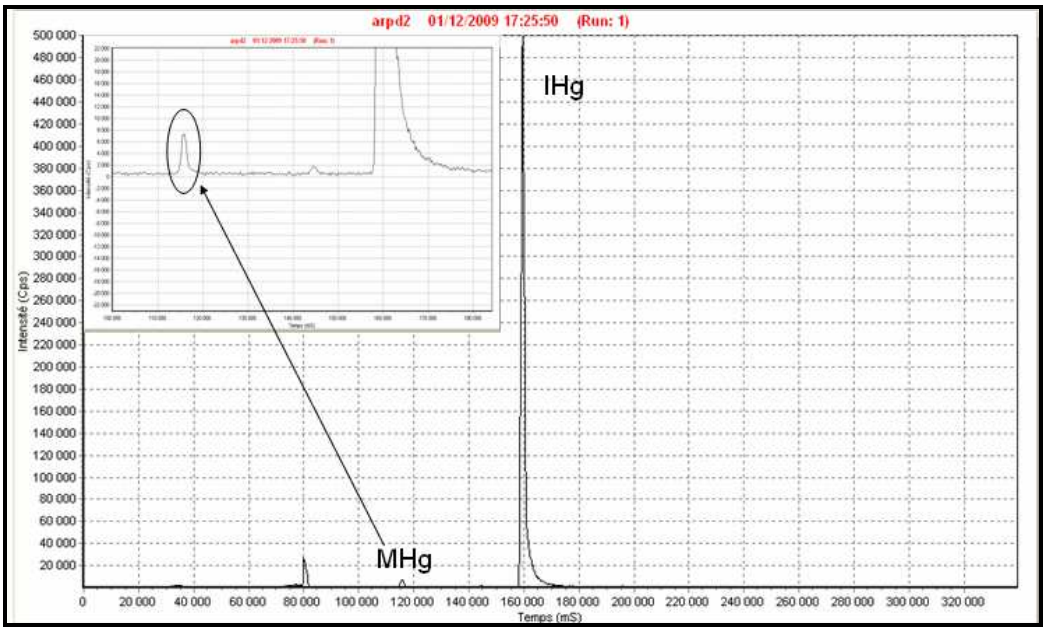

Figure 8.34 GC-ICP-MS chromatogram of tailings collected from the Old North TSF

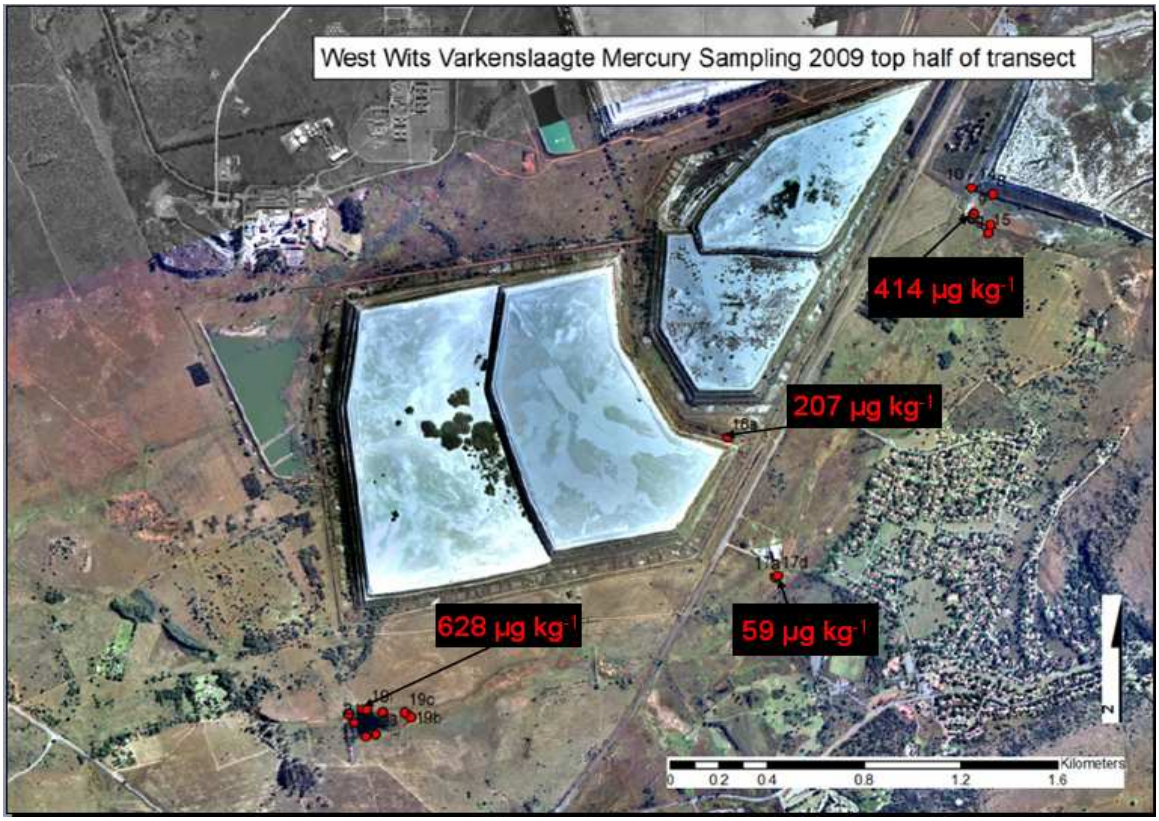

Figure 8.35 Mercury in surface sediments within the WW Savuka mine area

Table 8.14 Mercury in WW sediments and tailings

Sample (n =3)	Hg_{TOT} (µg kg^{-1})	IHg (µg kg^{-1})	%RSD	MHg (µg kg^{-1})	%RSD	%MHg
8	267.0 ± 20.7	290.9 ± 3.6	1.3	1.9 ± 0.2	8.7	0.6
S/A10(0-5)	414.4 ± 41.3	343.4 ± 31.3	9.1	4.3 ± 0.0	0.9	1.2
S/A10(5-10)	nd	229.7 ± 2.0	0.1	6.6 ± 0.4	6.1	2.8
S/A10(10-15)	nd	59.7 ± 3.0	5.0	1.9 ± 0.2	10.5	3.1
S/A10(15-20)	nd	33.4 ± 0.7	2.1	bdl		0.0
S/A10(20-25)	nd	25.9 ± 5.5	21.3	bdl		0.0
S/A10(25-30)	nd	20.0 ± 1.5	7.4	bdl		0.0
S/A10(30-35)	nd	15.2 ± 1.7	11.4	bdl		0.0
S/A10(35-40)	nd	14.6 ± 0.7	4.5	bdl		0.0
S/A10(40-45)	nd	11.6 ± 2.1	18.0	bdl		0.0
S/A10(45-50)	nd	9.4 ± 0.5	5.0	bdl		0.0
16G(0-2)	49.3 ± 1.9	nd		nd		
ARPD2	265.3 ± 17.6	226.7 ± 5.7	2.5	3.8 ± 0.9	25.3	1.6
16K(0-5)	38.9 ± 2.1	nd		nd		
16L(0-5)	344.2 ± 13.1	331.8 ± 5.0	1.5	1.9 ± 0.5	26.2	0.6
16L(5-10)	nd	205.0 ± 0.8	0.4	bdl		0.0
16L(10-15)	nd	57.8 ± 1.0	1.7	bdl		0.0
16L(15-20)	nd	55.3 ± 3.2	5.7	bdl		0.0
16L(20-25)	nd	274.7 ± 9.6	3.5	bdl		0.0
16L(25-30)	nd	192.4 ± 2.3	1.2	bdl		0.0
17E(0-2)	58.5 ± 3.0	nd		nd		
18A(0-2)	206.5 ± 15.6	164.6 ± 2.6	1.6	0.8 ± 0.1	9.2	0.5
19F(0-2)	628.4 ± 7.6	505.2 ± 1.4	2.3	8.8 ± 0.5	5.8	1.7
19F(2-4)	nd	420.4 ± 2.0	0.5	4.7 ± 0.1	2.1	1.1
19F(4-6)	nd	336.9 ± 16.7	4.9	8.1 ± 2.1	26.6	2.3
19F(6-10)	nd	565.4 ± 15.0	2.6	11.3 ± 1.0	8.7	2.0
19fF(10-15)	nd	76.0 ± 1.8	2.4	bdl		0.0
19F(15-20)	nd	51.4 ± 2.4	4.7	3.0 ± 0.0	0.4	5.4
23(0-2)	124.9 ± 6.5	119.6 ± 4.7	3.9	bdl		0.0
30(0-5)	35.9 ± 3.3	nd		nd		

The mean concentration found in tailings was about 265 µg kg^{-1} (samples 8 and ARPD2). Although the relationship between mercury concentrations in tailings and grain size has not been characterized in this study, it was reported that the finest tailings particles (< 2 mm), such as silt-clay (which is the case in the present study) can be enriched in mercury and exhibit concentrations around 200 µg kg^{-1} (Ashley *et al.*, 2002).

MHg values for tailings ranged between 1.9 to 3.8 µg kg^{-1}, indicating that there are conditions favorable for methylation of mercury occur in these materials in the area.

MHg also was identified in all surface sediments with concentrations ranging from 0.8 to 4.3 µg kg^{-1}, corresponding to 0.6 to 1.2% of Hg_{TOT}. As it was the case with water samples, the sediment profile collected in the dam (sample 19F) exhibited the highest proportion of MHg in bulk sediment with an enrichment observed at 6-10 cm depth (11 µg kg^{-1}) corresponding to a proportion of 2% of the Hg_{TOT}. But the highest MHg proportion occurred at deeper layer (15-20 cm) with more than 5% of Hg_{TOT} in the form of MHg (figure8.36). This suggests an important microbial activity occurring within the dam. It still needs to be recalled that the overall methylation rate observed in WW sediments falls into the average value of 1 to 3% reported in the literature.

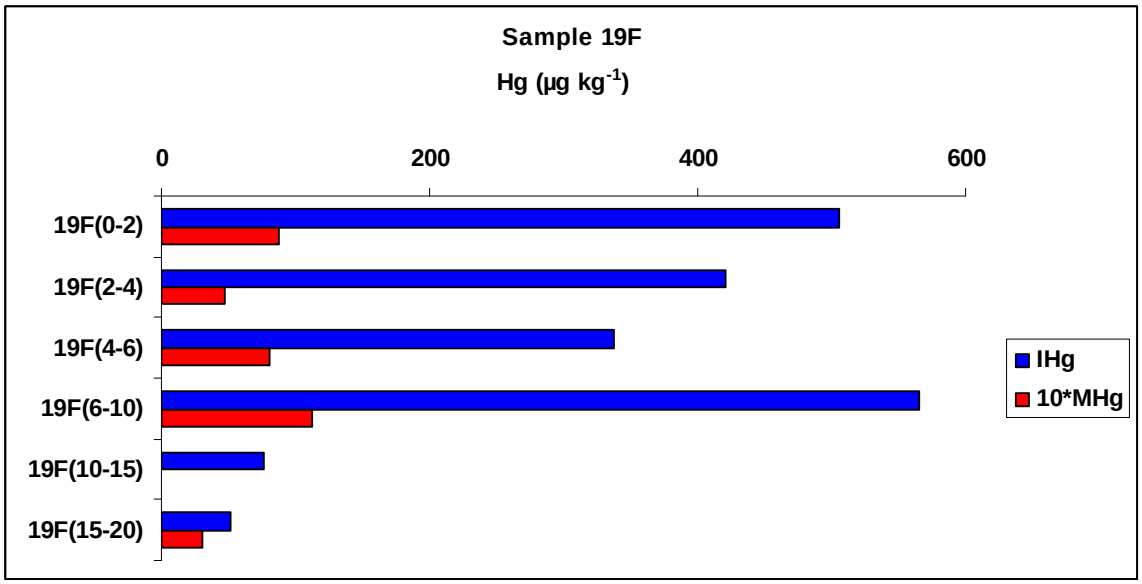

Figure 8.36 IHg and MHg in sediment profile 19F (figures in brackets are depth in cm)

8.5.3 Mercury concentrations in West Wits plants

Concentrations found in plants (table 8.15) were also lower (21 to 55 µg Hg kg^{-1}) compare to VR plants (16 to 247 µg Hg kg^{-1}). Here again the sample collected within the dam (19B) had the highest concentration of Hg_{TOT} with a MHg proportion of 7%. Figure 8.37 shows the chromatogram obtained during speciation analysis of the plant sample 19B by GC-ICP-MS.

Table 8.15 Mercury concentration in selected WW plants

Sample	Type	Hg_{TOT} ($\mu g\ kg^{-1}$)	IHg ± SD ($\mu g\ kg^{-1}$)	MHg ± SD ($\mu g\ kg^{-1}$)	%MHg
16Y	Phragmites	37.8	nd	nd	
17C	Typha	31.9	nd	nd	
19B	Willow	55.0	44.7 ± 2.9	3.5 ± 0.5	7.2
19H	Algae	20.7	nd	nd	
32	Algae	42.3	nd	nd	

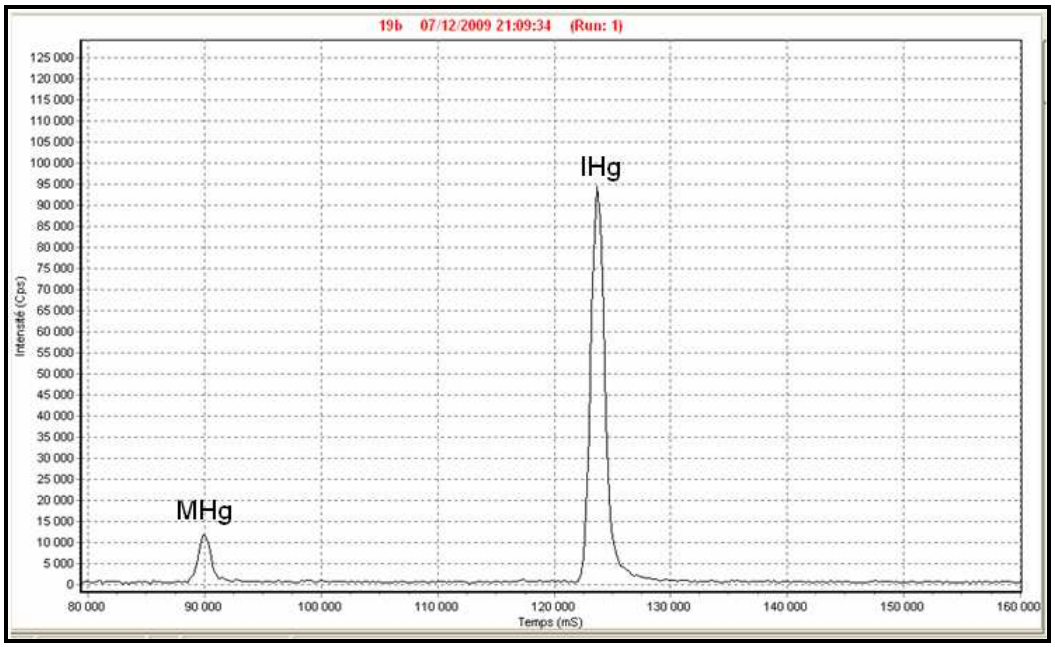

Figure 8.38 GC-ICP-MS chromatogram of WW plant 19B

It was not possible to draw a proper conclusion concerning the mercury uptake in WW plants due to the small number of analyzed samples.

Finally, a general trend was observed from the above results in the WW region which consisted on a decrease in mercury concentration (in waters, sediments and plants) following the path of the Vaarkenslaagte canal from the old North TSF area to the Wonderfonteinspruit, with the highest mercury load, and a consequent MHg production occurring in the dam close to the TSF compartment 7B.

8.5.4 Summary

The assessment of mercury contamination and the characterization of its distribution and transport in the Vaal River West and West Wits regions, as presented in this study, allowed us to draw the following conclusions:

- Mercury contamination from the mining and recovery of gold during the late 19th and early 20th centuries is widespread in environmental compartments near historic gold mines in the Vaal River West region. Mining operations has led to severe contamination of the bottom sediments of reservoirs downstream of the mines (Schoonspruit).
- Both IHg and MHg, which are potential risks to human health and to surrounding ecosystems, have been detected at considerable levels in the watersheds where mining was widespread. High levels of mercury accumulation found from mine sites, receiving waters, and even sediments downstream of mines indicate that a large part of the mercury used in gold ore processing was lost to the environment. The most elevated total mercury concentrations in waters, sediments and plants were found in the Bokkamp Dam and near the pump house behind the dam, respectively. Remobilization of mercury from the bottom sediment at the dam and its drainage by runoff during rainy season seems to be the cause of contamination of the sediment near the pump house.
- Mercury was found at concentrations beyond acceptable values from national and international criteria in borehole waters, especially in the one located near the West Complex North TSF, confirming a severe groundwater contamination. It is believed that the contaminations originates from surface activities, probably from the leaching of mercury polluted soil and tailings.
- Enhancement of mercury methylation occurred mainly in bulk sediments at regions corresponding to the lowest redox potential, higher pH and enrichment of inorganic mercury. A positive correlation was also found between the methylmercury, sulfate, organic matter and iron patterns in sediment profiles, demonstrating that other factors than the presence of IHg are also influencing the methylation process in the site.

- The pilot study carried out on the closed ventilation shaft near Klerksdorp presented TGM values much higher than those reported for background level and even higher than levels obtained within industrial zones. This suggests an important underground source of mercury vapour which needs to be investigated more extensively.
- Although the mercury found in waters, sediments and plants in the West Wits region was lower than in the Vaal River West, elevated concentrations, considering the background level, were found near TSFs with a considerable methylation rate. The study was carried out during the dry season only and, therefore, no particular conclusion could be drawn concerning seasonal transportation of mercury. Nevertheless, the decrease of mercury level from the Savuka Mine area to areas away from the mining site suggests that mining operations are probable responsible of the mercury contamination found on the site.
- Important concentrations of heavy metals and sulfur were found in the Vaarkenslaagte, suggesting a probable impact of acid mine drainage which seems to affect, to a certain extent, the Wonderfontein stream located about 20 km downstream.
- The highest mercury level found in plants, at both study sites, were measured in samples collected from areas where the highest mercury concentrations in sediments were also obtained. This confirms that the mercury level in plants can be a good indication of the magnitude of mercury contamination for a given site.
- Finally, the occurrence of methylmercury on both sites is of concern due to the possibility for this toxic species to enter the food web and bioaccumulate in fishes.

Results obtained in this study recommend further investigations in both sites, which should include: more gaseous mercury measurements, the determination of dissolved and particulates mercury in water, the analysis of a wider range of plants and also of fish samples from affected water systems. In addition, a continuous monitoring of the sites as well as the analysis of human materials such as blood, urine or hair, from the nearby

population, will contribute to a better characterization of the overall biogeochemical cycle of mercury in these areas and also to a better assessment of the ecosystem impacts resulting from both historic and current mining operations.

Chapter 9
The impact of post gold mining on mercury pollution in the West and East Rand regions

9.1 Introduction

In the late nineteenth century, soon after the discovery of gold in South Africa, mines have developed in the West Rand area (figure 9.1) located about 50 kilometers west of Johannesburg. Mining is still developing in the region since the youngest gold-mines in South Africa are found in this area (www.deepbio.princeton.edu).

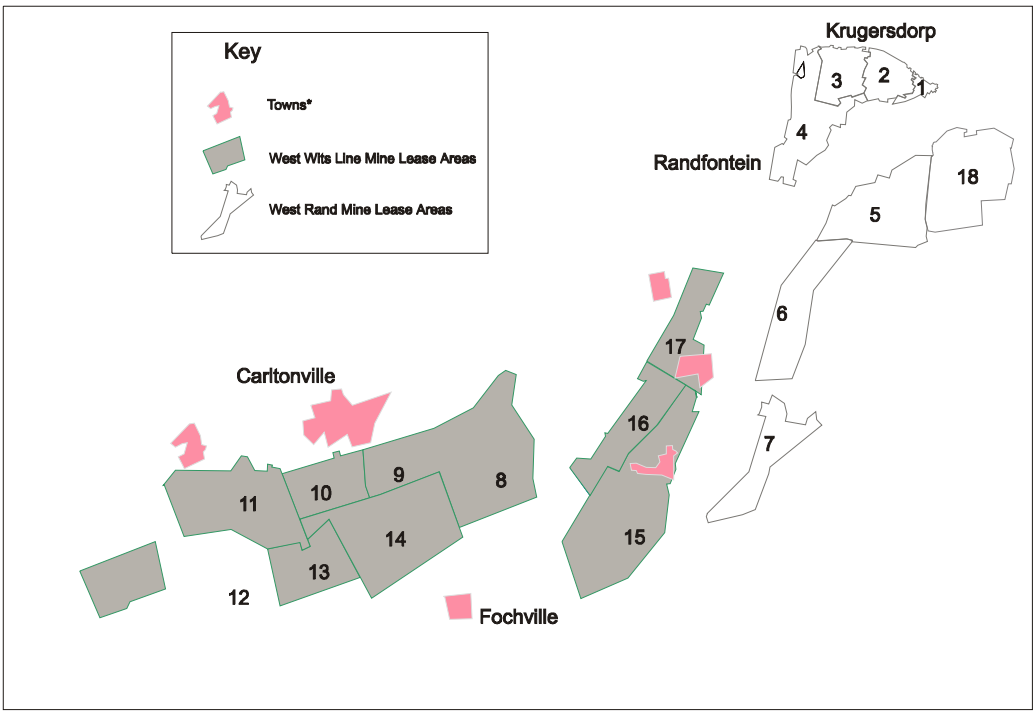

Figure 9.1 Mines of the West Rand and West Wits Line Mining Areas

Some of the mines have closed down whereas others have changed owners. Underground and opencast mining operations as well as the reclamation of sand and slimes dams are done in these mines. The gold-bearing reefs contain an array of minerals such as native gold, uranium oxides, traces of platinum and an array of sulfide minerals with pyrite being the most abundant. Most of the mines have produced uranium together with gold.

Among the mining companies operating in the West Rand area there is Rand Uranium which operations are located just 30 km from the heart of Johannesburg, near Randfontein, as shown in figure 9.2.

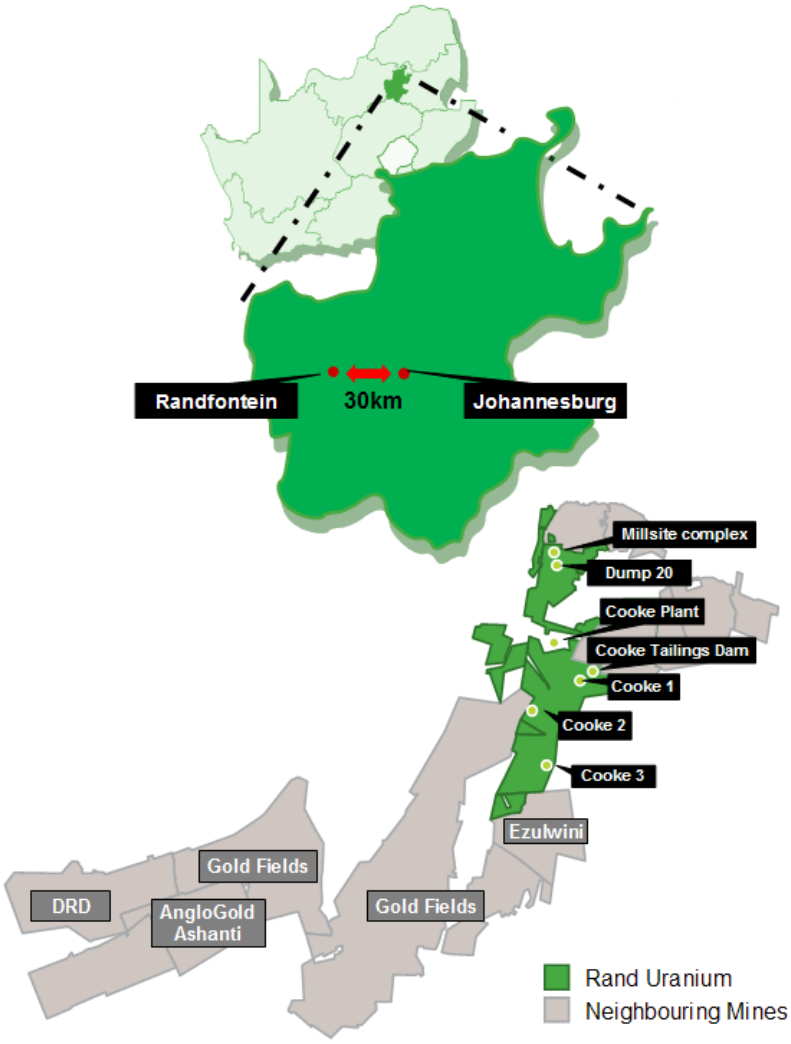

Figure 9.2 Location of the Rand Uranium and its neighboring mines
(Source: www.randuranium.co.za)

In 2008, Rand Uranium bought part of the cooke shafts and associated uranium assets that used to belong to Randfontein Estates Limited, a wholly owned subsidiary of Harmony Gold Mining Company Limited. The assets acquired included 3 cooke shafts;

one cooke Plant and some uranium and gold tailings dumps such as Dump 20, as represented in figure 9.2 (www.harmony.co.za (a and b); www.prf1.com).

The Millsite Gold Plant (figure 9.2) was commissioned in 1911 and, as a result of the milling and processing technology of the day, could not fine grind the ore to extract the contained gold, creating the Sand Dump (Dump 20) with a relatively high residual gold grade (0.46 g t^{-1}) (www.randuranium.co.za) and, therefore, the interest of reprocessing the tailings to recover the remaining gold.

Lang (2007) reported that, in 2002, acidic water began decanting out of a disused mine on Randfontein Estates about 42 kilometres south-west of Johannesburg, a property belonging at that time to Harmony Gold. While some of this acidic water was produced by Harmony's own operations, a large proportion was generated by its competitors.

The author also reported that the water coming out of the disused mine in Randfontein could not simply be channelled into the nearest river because it was far too acidic and could have had serious consequences for the environment.

As an emergency measure, Harmony fed the water into Robinson Lake, at that time a popular recreational area where fishing was a favourite pastime. Today the lake has very high levels of uranium and a pH level of 2.2 which makes it completely incapable of sustaining any life forms.

The mining company claimed in its 'Sustainable Development Report 2007' that it "treats the water to acceptable standards given the current treatment technologies available" and Lang (2007) to conclude said:” What Harmony finds acceptable, however, may be less so to environmentalists”.

The main difficulties encountered when investigating the post-mining influences of mining areas in South Africa, especially in relationship with closed and abandoned mines, are as follow (www.deepbio.princeton.edu):

- The mine was abandoned, thus there is no traceable responsible authority.
- The mine is listed as abandoned, but has actually been amalgamated into a larger company, sections of which are still active. For this reason, the holding company does not consider the mine to be closed.

- Many of the mines listed as “closed” have changed ownership and are still operating, perhaps mining different reefs or doing reclamation work under a new name, as it is the case with the Rand Uranium.
- The holding company is unwilling to submit information. There may be numerous reasons for this; the most probable being the effort required is seen as unprofitable.
- The access to the mining area is not easily granted or is limited to areas under the supervision of the holding company.

Concern has grown in recent years that acidic water flooding abandoned mine tunnels under Johannesburg will soon spill over into the watertable of the surrounding Witwatersrand Basin, threatening the health of millions of residents (Feuilherade, 2010).
A large portion of this mining area has been influenced by mining activity and some of these influences include:

- The aquifers have been subjected to extreme dewatering stresses.
- Mining and industrial development are extensive.
- Mining, industrial and human wastes have been disposed of in this area. These have created surface and groundwater pollution sources and related problems. Unfortunately, the extent of the problem remains obscure.
- There has been no overall monitoring program and much of what is feared about pollution in the area relates to individual perceptions, for example fears about refuse sites which may be polluting. Many of the mines are in the process of establishing such monitoring networks.
- The mines are dewatering. This causes local, deep cones of depression and draws groundwater into the mine, thus the subsurface water pathways have been altered and may be complicated, making it even more difficult for a reliable monitoring program to be established.

While it is of common knowledge that gold extraction in these mines has been initially processed using mercury amalgamation, no particular information could be found in the

literature that has specifically dealt with the ecological impact of historical use of mercury in the area.

That is why, in the present chapter, an attempt was made to assess the long-term post-operative legacy of gold mining in terms of mercury pollution and fate in the Randfontein area (West Rand). Metals associated with mines located in this area have been reported to travel hundreds of kilometers and impact downstream ecosystems (www.deepbio.princeton.edu). This study is also an initial step toward identifying mercury sources to this environmental compartment.

In addition, mining companies extracting ore in the Witwatersrand area, to the west as well as east of Johannesburg, have created a 300 km labyrinth of interlinking passage (www.deepbio.princeton.edu).

Therefore, as mentioned previously, in order to place our work in a regional context on the Witwatersrand Basin, a study was also carried out on the East Rand (Ekurhuleni) near Johannesburg (figure 9.3), in an old mine property which contains a partially cleaned TSF footprint, and in the adjacent Scaw Metals Rietfontein B landfill, an old clay quarry which contains mine tailings from Ergo and mixed mining and metals waste.

Scaw Metals, a metallurgical group belonging to Anglo American, has reported to restoring the Rietfontein landfill site and, following a pilot study, the site was fully planted in 2006 with trees and plants specially selected for their tolerance to adverse conditions and ability to remove pollutants from land, waste and water (www.angloamerican.com).

The company has mentioned that researchers from a number of universities such as the University of the Witwatersrand (SA) and Tel Aviv University (Israel) have collaborated on the project and, using aerial survey and monitoring work, including geo-hydrological studies, these researchers have found no mineral contamination of the planted areas around the site. The project was reported to complete planting at the site in early 2008 (www.angloamerican.com).

Figure 9.3 Location of study sites

Thus, it was found worth it to determine the current level of mercury on the site sediments and plants in order to assess the impact of phytoremediation works performed on the site.

9.2 Site description

This study investigated the speciation and fate of mercury in the decanting JCI Anglo American shafts and boreholes (now Harmony/Rand Uranium), and the receiving creek, wetlands and dams. The creek drains within a very old gold mining area located in Randfontein near Krugersdorp and receives both acidic water discharged from subsurface mine tunnels (acid mine drainage, AMD) and runoff from surrounding surface mine waste piles (slimes dam) (figure 9.4).

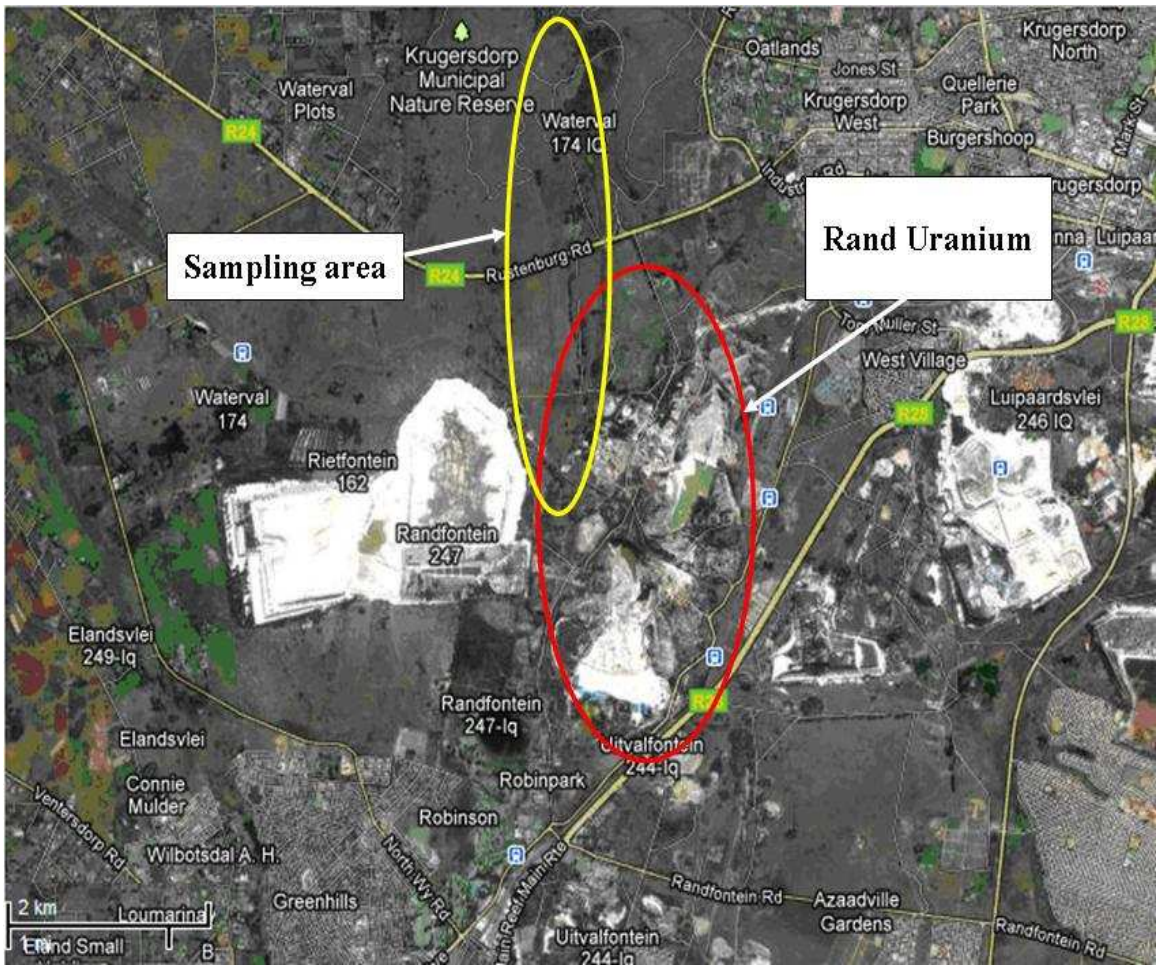

Figure 9.4 Map of the study area in Randfontein (Source: Google)

This creek also drains to the Krugersdorp Game Reserve wetlands. The game reserve is separated to the mining site by the Rustenberg road or R24 (figure 9.5).

The headwater of the drainage lies in an area in which there is an important and old slimes dam (figure 9.5). The creek is susceptible to flooding during summer rainfalls but discharge in the creek during the dry season is sustained by groundwater through inflow from seepage zones.

Figure 9.5 The Randfontein sampling area

The area is characterized by the presence of a bright red crust (figure 9.6), typical of iron oxide ores (Naicker *et al.*, 2003).

Figure 9.6 View of the land in the Randfontein site

Samples were collected during dry season, following the protocols presented in chapter 5, from boreholes, wetlands, dams and along the creek over a distance of approximately 10 km downstream of the mining area to the Krugersdorp Game Reserve (figure 9.7). In addition, water samples were taken in an adit that drains within the formal Rand Uranium and discharges into the creek.

Figure 9.7 The Randfontein sampling points

A description of collected samples and the corresponding GPS location are presented in table 9.1.

Table 9.1 Description of the Randfontein sampling

Sample ID	Description	GPS
78A-E	Water samples at different depths (1, 10, 20, 30 and 50m) from a borehole (“17 winds”) sunk before 1st world war	S26°07.295' E027°43.279'
80A	Sludge/sediment near the “17 winds”	S26°06.914' E027°43.382'
80B	Water near the “17 winds”	S26°06.914' E027°43.382'
	West Rand, Rand Uranium	
81A,B,C	Algae	
82A-C	Typha	
83A	Water sample clearest (“18 winds”)	S26°06.896' E027°43.484'
83B	Water: dirty section "near sack weir"	S26°06.898' E027°43.488'
	Wetland	
86A	Soil and algae	S26°06.712' E027°43.380'
86B	Typha	
87	Sediment	S26°06.712' E027°43.350'
88	Water upstream of sediment	S26°06.712' E027°43.350'
89A	Algae	
90	Water in reeds downstream from 87 & 88	
91	Water from borehole	
92	Soil core	S26°06.712' E027°43.350'
93	Soil core	
	Krugersdorp Nature Reserve	
94	Water sample Hippo pool	S26°05.954' E027°43.262'
95	Sediment hippo pool	S26°05.977' E027°43.207'
	Lion camp Dam	
97	Sediment	
98	Soil core	S26°05.128' E027°42.560'
99	Soil core	S26°05.117' E027°42.531'
100	Sediment	S26°05.977' E027°42.207'
103	“Clean” water	S26°04.615' E027°41.956'
105	Sediment	
106	Sediment	

The sampling campaigns for the Rietfontein site was also organized in late winter and, due the dry conditions found in the site during the sampling, only one water sample was collected from a sump. The sampling details are presented in table 9.2.

Table 9.2 Description of the Rietfontein landfill sampling

Sample ID	Description	GPS
Sump1	Landfill leachate from sump	-
2a	Sediment core	S26°18.104'; E028°25.170'
2b	Sediment core	S26°18.104'; E028°25.169'
3 scaw	Sediment core	S26°18.106'; E028°25.170'
4 scaw	Sediment core	S26°18.109'; E028°25.169'
5 scaw	Dry sediment crust in dam	S26°18.107'; E028°25.170'
5 adit (0-20 cm)	Surface soil next to adit entrance	S26°18.195'; E028°25.627'
6 adit (0-20 cm)	Surface soil midway between rock dump and shaft	S26°18.205'; E028°25.619'
7	Waste rock	-
	Trees on landfill	
Rp1	Rhos pendolina (deciduous)	S26°18.128'; E028°25.186'
Rp2	Rhos pendolina (deciduous)	S26°18.130'; E028°25.203'
Rl1	Rhos lancea (evergreen)	S26°18.133'; E028°25.183'
Rl2	Rhos lancea (evergreen)	S26°18.132'; E028°25.199'
C1	Combretum erythrophyllum (deciduous)	S26°18.134'; E028°25.200'
C2	Combretum erythrophyllum (deciduous)	S26°18.138'; E028°25.212'
T1	Tamarix usneoides (evergreen)	S26°18.134'; E028°25.188'
T2	Tamarix usneoides (evergreen)	S26°18.138'; E028°25.206'
1-6 Typha	Typha capensis (a reed)	-
Phragmites australis (a reed)	In small dam	-
1-6 Schoenopledus	Schoenopledus sp (a sedge) in small dam	-
ε1	Eucalyptus sp (leaves + bask)	S26°18.193'; E028°25.626'
ε2	Eucalyptus sp (leaves + bask)	S26°18.194'; E028°25.626'
ε3	Eucalyptus sp (leaves + bask)	S26°18.212'; E028°25.621'

Sediments were collected from a dry pond and near a waste rock pile site. Leaves were also taken from phytoremediation trees mainly from the oldest planting site and also near the waste rock pile (figure 9.8).

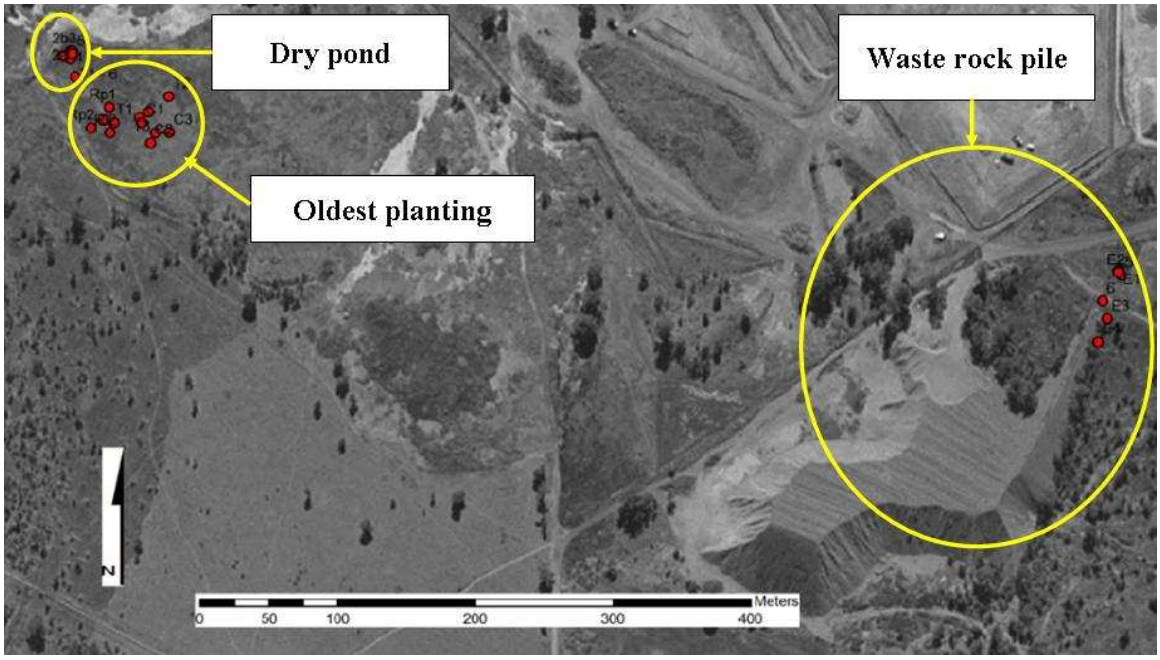

Figure 9.8 GIS image of the Rietfontein ("Scaw metals") sampling site

9.3 Results and Discussion

9.3.1 Mercury in waters

Mercury concentrations determined in waters collected from both sites and the ancillary data are presented in table 9.3.

At the Randfontein site, all analyzed waters were acidic with pH ranging between 2.9 and 5.0 (table 9.3), except for sample 94 collected from the game reserve which showed a pH value of 7.8. It has to be mentioned that at the boundary between the mining site and the game reserve, the pH is increased by the company that owns the mine in order to precipitate soluble metals and therefore, minimize the contamination in the water draining to the natural reserve.

The total mercury concentrations (i.e. IHg + MHg) measured in unfiltered surface waters at the Randfontein site varied from 0.01 to 222.76 ng L^{-1} and averaged 52.38 ng L^{-1}. Mercury concentrations in 4 samples (samples 88, 90, 91 and 94) nearly reached or

exceeded the 12 ng Hg L^{-1} that the EPA indicates may result in chronic effects to aquatic life (US EPA, 1992).

Table 9.3 Mercury concentration and field measurements of Rietfontein (in red) and Randfontein water samples

Sample	pH	T (°C)	Eh (mV)	Ec (mS cm^{-1})	HgT (ng L^{-1})	IHg (ng L^{-1})	% RSD	MHg (ng L^{-1})	% RSD	% MHg
Sump1	7.43	20.0	153	3.40	0.174	0.122	2.7	0.052	5.4	29.6
78A	4.77	20.5	349	3.88	0.237	0.144	5.9	0.093	7.8	39.3
78B	4.73	20.2	354	3.92	0.110	0.043	32.3	0.067	8.3	61.0
78C	4.66	20.2	345	3.93	0.530	0.481	1.3	0.049	52.6	9.3
78D	4.74	20.6	311	3.90	1.986	1.897	14.7	0.088	10.3	4.5
78E	4.63	20.3	305	3.93	0.897	0.837	27.3	0.059	79.3	6.6
83A	4.96	20.9	282	5.28	3.290	1.766	51.0	1.524	4.5	46.3
83B	4.9	20.9	309	5.26	0.010	0.010	3.2	bdl	-	0.0
88	3.09	21.0	560	5.20	159.012	158.975	1.4	0.038	1.8	0.0
90	2.91	20.0	620	5.20	11.839	11.800	3.5	0.039	1.2	0.3
91	3.06	21.1	550	5.19	222.754	220.636	3.5	2.118	35.2	1.0
94	7.76	17.9	374	4.05	17.637	17.578	2.9	0.059	12.0	0.3

Mercury concentration in waters was variable within the site and the highest mercury levels were found in the creek draining from the mining area, which has a history of more than a century in gold extraction, to the game reserve.

It has to be noted that sample 94 which also showed mercury beyond the threshold value of 12 ng L^{-1} was collected within the game reserve which shows that, although liming is performed to reduce the metal content in water, mercury is still found at a considerable level within the game reserve.

Mercury values in Randfontein waters were lower than in some areas affected by gold mining with amalgamation and mercury mining, such as in some China provinces (Dai *et al.*, 2004). However, these values were obviously higher than what measured in natural waters (e.g. Leermakers *et al.*, 2001). This showed that the mining area has been affected to a certain extent by mercury pollution obviously due to the long period of gold mining activities.

AMD discharges from the adit at the Rand Uranium to the creek and forms a tributary that flows few hundred meters through the inoperative mine site.

A hard orange precipitate covers the bed of the tributary (figure 9.9). The acidic water from the Rand Uranium enters a pond before mixing with the mine creek and, at this point of discharge from the adit, the water was clear with a pH of approximately 5.0. Hg_{TOT} at this point was about 3.3 ng L^{-1} (sample 83A), which was similar to the mercury level measured upstream (sample 80B: 4.3 ng Hg L^{-1}), as shown in table9.3.

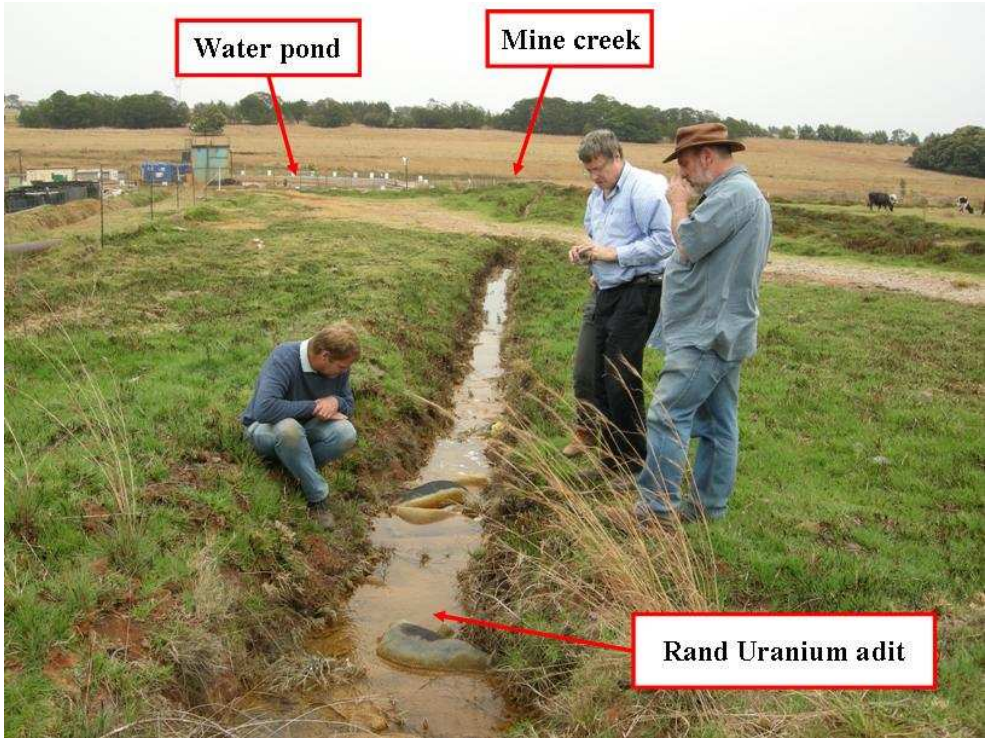

Figure 9.9 View of the adit within the Rand Uranium site

Physico-chemical properties of the AMD from the creek adjacent to the pond were different from AMD at the adit. The Hg_{TOT} within the creek ranged from 11.8 to 159.0 ng L^{-1}, which is substantially greater than values measured in the adit. The pH dropped to 2.9 and the redox potential increased to values as high as 620 mV (samples 88 and 90 in table 9.3). The drop in pH from 5.0 in the pond to 2.9 within the creek and increase of Eh from 0.28 to 0.62 V (figure 9.10) may be a result of enhanced pyrite oxidation of the slimes dam materials which enter the creek, as it was also observed by Ganguli and colleagues (2000).

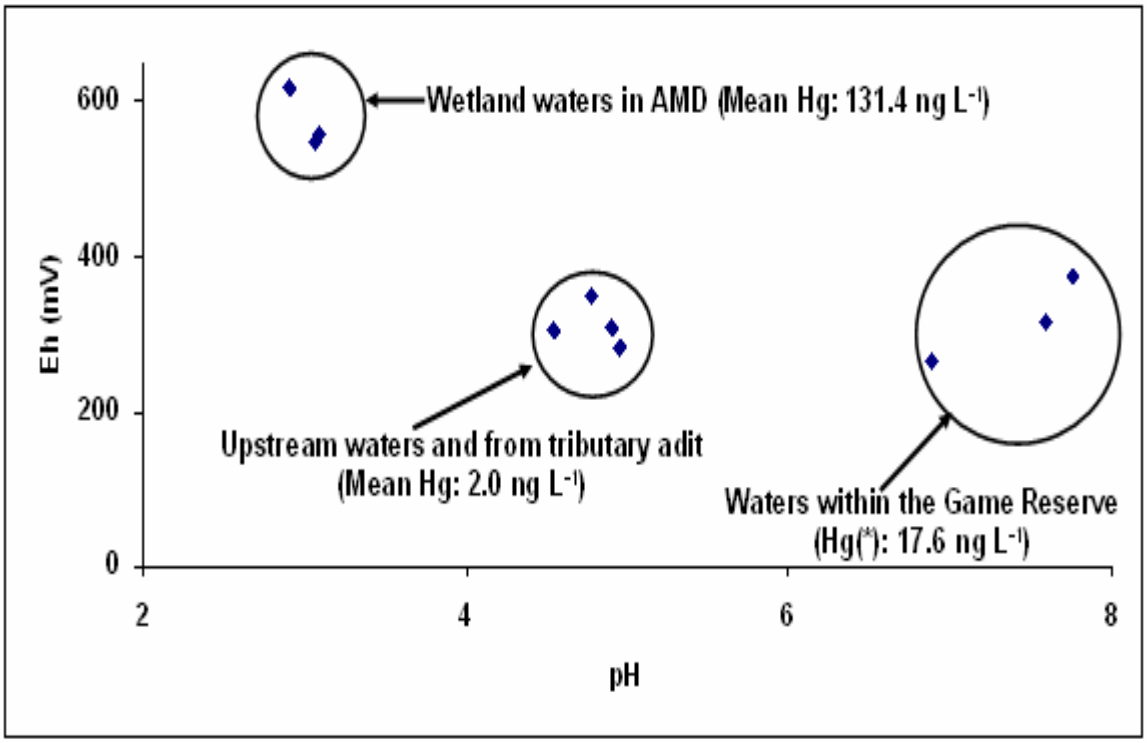

Figure 9.10 Eh–pH relationships of all samples.
(*) The Hg value reported for the game reserve is for one sample only

Because the mine was in almost continuous operation for about a century (this takes into account the reprocessing of tailings), the generated waste likely contains readily mobilized forms of mercury which will be discuss further. Waste materials (tailings) are therefore a potentially large reservoir of labile mercury and, therefore, the high downstream mercury concentrations in the mine creek may be attributed to leaching of materials exposed to surface weathering conditions.

Groundwater conditions within the mining area is very acidic, as measrured from boreholes (samples 78A-E and 91) with an average pH of 3.9, and has high sulfate and heavy metal concentrations (tables 9.3 and 9.4). Seepage water in the mining area is also characterized by high sulfate and heavy metal concentration, and the pH is relatively lower that the groundwater. This is the result of iron oxidation as the groundwater emerges at the surface, which further lowers the pH (Naicker *et al.*, 2003).

Table 9.4 Concentrations (mg kg^{-1}) of selected elements and anions in Randfontein waters

Sample	Al	Bi	Ca	Co	Cu	Fe	Li	Mg	Mn	Ni	Cl^-	$S0_4^{2-}$
78 A	18.0	0.4	738.0	5.0	0.4	1012.0	0.3	325.0	87.0	5.0	13.8	770.2
78 B	35.0	0.3	738.0	6.0	0.4	1202.0	0.3	34.7	164.0	10.0	21.0	840.4
78 C	26.0	0.3	475.0	4.0	0.4	804.0	0.3	223.0	69.0	5.1	18.0	595.7
78 D	58.0	0.5	350.0	9.0	0.6	710.0	0.3	545.0	171.0	16.0	30.0	535.1
78 E	23.0	0.4	523.0	4.0	0.5	921.0	0.3	245.0	77.0	6.0	66.0	674.1
80 B	28.0	0.6	1569.0	14.0	0.8	3463.0	0.4	720.0	292.0	25.0	110.0	2267.0
83 A	12.1	0.5	816.0	10.0	0.8	1720.0	0.4	361.0	111.0	12.0	21.8	1201.2
83 B	9.9	0.5	859.0	8.0	0.8	1650.0	0.4	382.0	115.0	11.0	20.1	1240.8
88	44.3	2.8	381.0	3.8	0.8	362.0	1.0	172.0	276.0	11.0	82.0	298.4
90	37.0	2.8	534.0	4.0	0.7	423.0	1.0	233.0	386.0	11.0	129.0	305.1
91	70.0	2.5	938.0	7.0	0.8	935.0	0.9	403.0	630.0	19.0	23.0	682.8
94	bdl	bdl	856.5	0.1	bdl	0.4	0.5	138.6	9.1	0.1	12.4	301.8
96	bdl	0.1	587.8	0.1	bdl	0.5	0.3	86.7	9.9	0.1	12.8	322.5
102	bdl	0.1	631.2	bdl	bdl	bdl	0.4	94.1	8.0	0.1	15.6	289.3
103	0.3	bdl	22.4	bdl	bdl	0.5	bdl	140.0	0.4	bdl	1.0	3.4
104	0.3	bdl	23.4	bdl	0.1	0.5	bdl	14.7	0.4	bdl	0.8	3.6

As mentioned previously, the pH within the mining area is low, ranging between 2.9 and 5.0. Heavy metals and sulfide (or sulfate) concentrations are dramatically high, due to the inflow of acidic ground water. In the north of the mining area i.e. within the game reserve, the pH rises (6.9 to 7.8) and metals concentrations decrease considerably going, in some cases, below methods detection limit (See samples 94 to 104 in tables 9.3 and 9.4). The pH increase and the subsequent metals reduction within the game reserve can be attributed to the liming performed at the boundary between the mining area and the game reserve and also to the dilution from tributaries draining within the reserve.

On another hand, the MHg concentrations in Randfontein waters were relatively uniform (figure 9.11), ranging between 0.04 to 1.52 ng L^{-1}, except for the sample 91 (2.12 ng MHg L^{-1}) which was collected in a borehole near wetland and which also showed the highest Hg_{TOT} (222.76 ng L^{-1}). The uniform MHg concentrations measured in the water may be a result of a balance between microbial methylation and demethylation as suggested by Ganguli and colleagues (2000) in their study on the mercury speciation in drainage from the New Idria Mercury Mine (USA). The high MHg value observed in the borehole may be attributed to the considerable availability of IHg (220.64 ng L^{-1}), caused by the high Eh and low pH conditions, whereas the elevated MHg of 1.52 ng L^{-1}, and

corresponding proportion of 46.3% to the total mercury, observed in the pond (sample 83A) may be the consequence of bacterial activities under the reducive condition (Eh = 0.28V) observed in the pond (table 9.3). The high iron load measured at this point (see table 9.4) could also be an important contributor to the mercury methylation.

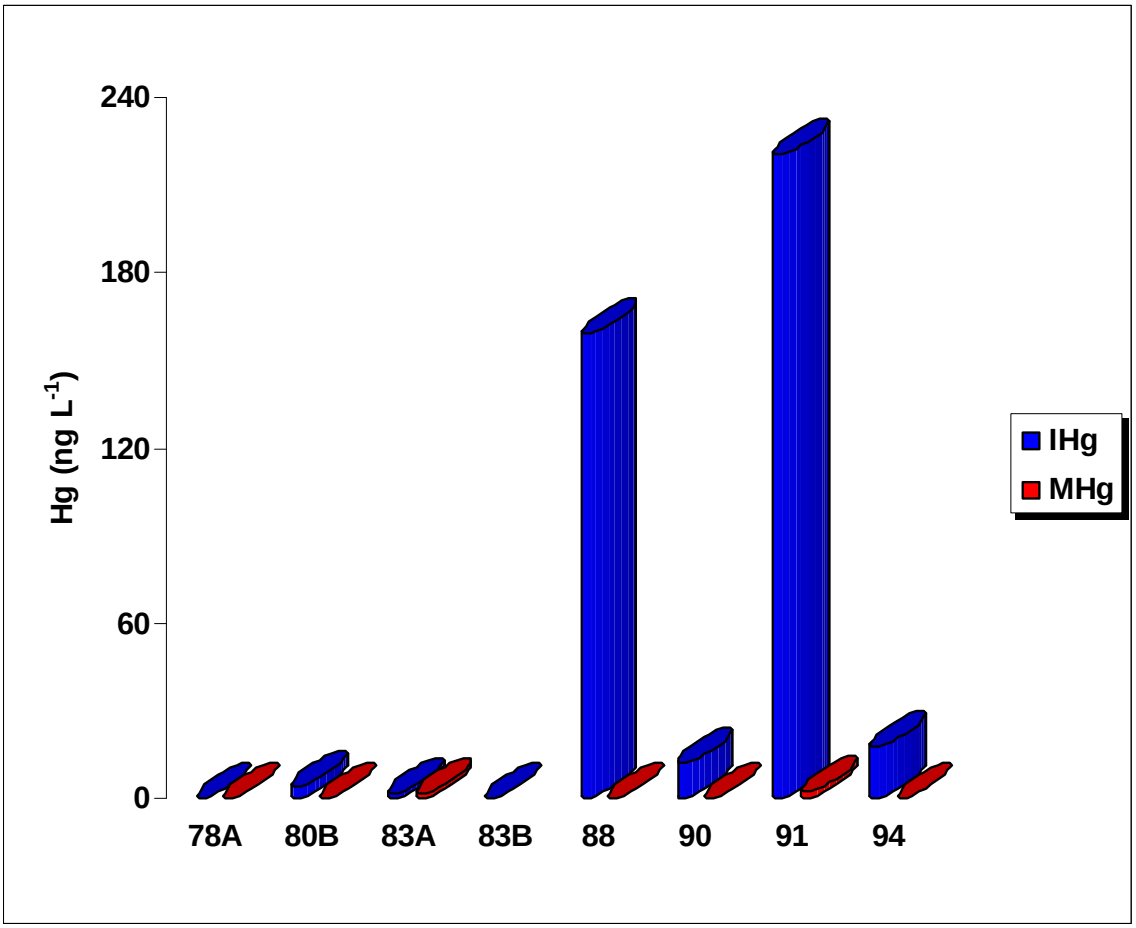

Figure 9.11 Mercury species in Randfontein surface water

9.3.2 Mercury methylation in the old water borehole

Factors that favor the mercury methylation in Randfontein water have been investigated in the case of a profile from an old borehole (figure 9.12) sunk before the 1st World War and which is located not far from the Dump 20 of the Rand Uranium. Samples were collected from the surface to 50 meters depth at 10 meters interval each. Figure 9.12 presents different patterns obtained for Eh, pH, IHg and MHg in the profile.

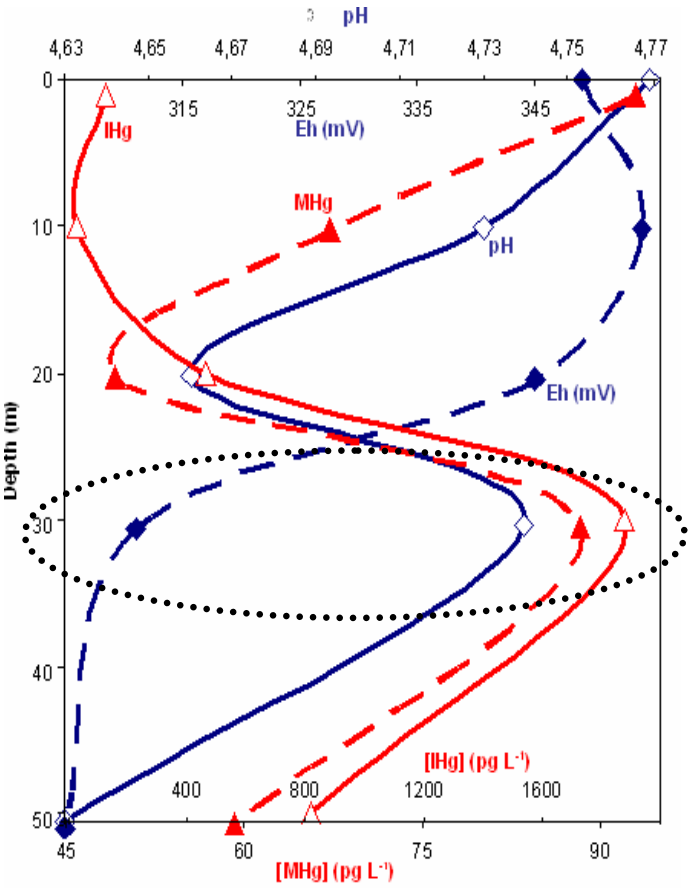

Figure 9.12 Mercury species, Eh and pH trends in the old Randfontein borehole (The dashed area corresponds to the probable region of MHg production)

It can be seen from the above figure that the highest MHg value (0.093 ng L^{-1}) was at the surface water. MHg decreased with depth but increased again at about 30 m depth (0.088 ng L^{-1}). In this zone, the IHg was at its highest value (1.897 ng L^{-1}) and the Eh was low (311 mV). Although the pH did not vary much in the profile, the value obtained at this point (pH 4.74) was close to the highest one measured at the surface (pH 4.77). The same trend was also observed in Vaal River sediment at the Schoonspruit (see chapter 8). Therefore, the mercury methylation within the old borehole may occur in deep water under the most reducive conditions but, due to its mobility, MHg migrates to shallow levels.

It is important here to recall that the borehole water may also be a subject of continuous methylation and demethylation processes which probably affects the overall methylation rate in the study system. Further investigations need to be done to explain this mechanism.

The water sample collected in the sump at the Rietfontein site (sample "sump1") exhibited similar trend as the surface water from the Randfontein old borehole (table 9.3), except for the pH which was much higher (pH 7.43) in Rietfontein than in the acidic water at the Randfontein site. Therefore, the low Eh (153 mV), the IHg content (0.122 ng L^{-1}), and of course the pH could be factors controlling the methylation in the sump. The MHg (0.052 ng L^{-1}) proportion to Hg_{TOT} at this point was about 30% and was in the same range than the proportion found at the surface of the Randfontein old borehole of 39%.

Both IHg and MHg were identify in the Rietfontein water at concentrations corresponding to values measured in waters from non impacted area, which implies that no mercury contamination was observed in the Rietfontein water, although this has to be taken with caution since only one water sample was analyzed from the site due to the dry conditions mentioned earlier. A sampling during rain season will be important for more conclusive results.

On another hand, it was surprising to find low mercury level in the Randfontein old borehole (0.237 ng Hg L^{-1} at the surface) since it is located near AMD and close to old dumps which are known to contain wastes from historic gold mining operation and, therefore, mercury waste from amalgamation processes. Volatilization of mercury to the atmosphere during the dry season may explain the above observation. Here again, a wet season sampling will provide interesting data for a more complete discussion of the mercury occurrence in the Randfontein site.

9.3.3 Mercury in soils and sediments

Mercury concentrations in Rietfontein surface sediments are shown in table 9.5.

Table 9.5 Mercury in Rietfontein sediments

Sample (n = 3)	Hg_{TOT} ($\mu g\ kg^{-1}$)	IHg ($\mu g\ kg^{-1}$)	%RSD	MHg ($\mu g\ kg^{-1}$)	%RSD	%MHg
2A scaw	62.8 ± 6.4	n/a		n/a		
2Bscaw	87.1 ± 9.2	78.3	4.3	6.4	1.5	7.6
3scaw	72.9 ± 5.4	n/a		n/a		
4scaw	68.7 ± 7.6	n/a		n/a		
Adit5	68.4 ± 4.2	n/a		n/a		
Adit6	125.0 ± 8.2	64.5	2.1	bdl	0.0	0

Total mercury values in Rietfontein ranged between 63 and 125 $\mu g\ kg^{-1}$ (figure9.13) with an arithmetic mean of 81 $\mu g\ kg^{-1}$.

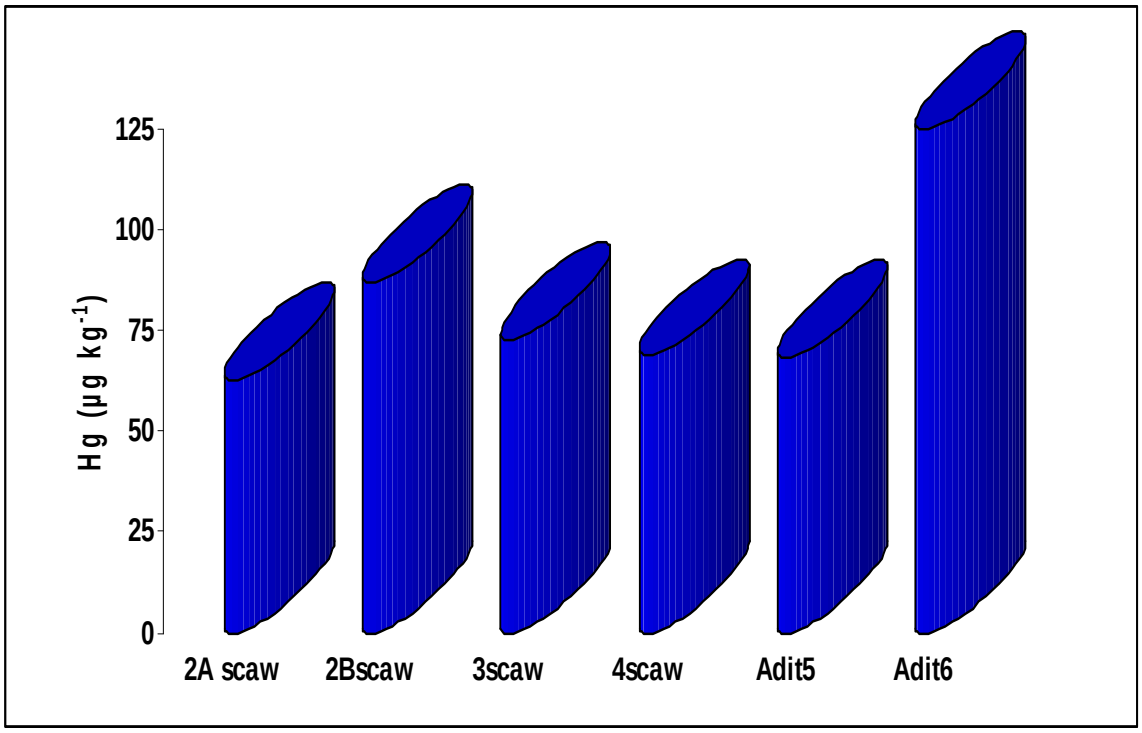

Figure 9.13 Mercury in Rietfontein surface sediments

These concentrations are closed to background values obtained in Vaal River sediment and confirm, as it was the case for the water sample, that no particular contamination was observed in the Rietfontein site. The highest mercury value was measured in a sample collected near the waste rock pile (sample “adit6”). This “high” value, which is still

below the EPA threshold level of 174 µg kg^{-1}, could also be due to the fine grain size of the material around the waste pile.

Results of sediments and soils analyses from the Randfontein site are presented in table 9.6 and figure 9.14 shows an example of GC-ICP-MS chromatogram of a soil sample. Total mercury values in the Randfontein surface sediments (or soils) ranged from 46 to 2207 µg kg^{-1}, with an average of 972 µg kg^{-1}.

Table 9.6 Mercury in Randfontein soils and sediments

Sample (n = 3)	Hg_{TOT} (µg kg^{-1})	IHg (µg kg^{-1})	%RSD	MHg (µg kg^{-1})	%RSD	%MHg
80A	87.6 ± 6.7	n/a		n/a		
86A	2316.3 ± 163.5	2090.2	1.5	5.9	9.1	0.3
87	2206.8 ± 131.0	1318.8	1.8	8.0	6.4	0.6
92 (0-2)	1982.9 ± 145.8	1397.5	1.2	1.9	14.6	0.1
92 (2-4)	n/a	1256.6	0.4	1.6	15.5	0.1
92 (4-6)	n/a	978.9	3.2	1.8	16.7	0.2
92 (6-8)	n/a	1244.9	3.5	0.9	13.3	0.1
92 (8-10)	n/a	1782.1	7.8	2.5	4.8	0.1
92 (10-15)	n/a	941.7	6.3	2.8	6.8	0.3
92 (15-20)	n/a	962.9	1.3	4.1	9.7	0.4
93 (0-2)	2580.6 ± 103.8	1734.4	0.9	10.4	5.3	0.6
93 (2-4)	n/a	1268.8	1.7	3.0	1.8	0.2
93 (4-6)	n/a	1255.9	0.3	3.2	4.5	0.3
93 (6-8)	n/a	1211.6	3.9	2.9	3.0	0.2
93 (8-10)	n/a	1319.8	0.1	4.3	2.5	0.3
93 (10-15)	n/a	1864.0	0.8	49.0	3.1	2.6
93 (15-20)	n/a	3901.7	0.0	81.5	5.8	2.1
95	47.7 ± 3.5	n/a		n/a		
97	390.6 ± 22.3	286.4	0.4	6.5	1.1	2.2
98 (0-2)	756.9 ± 38.8	653.2	1.9	3.7	5.6	0.6
98 (2-4)	n/a	641.4	2.8	11.3	3.5	1.7
98 (4-6)	n/a	655.3	1.2	29.1	3.8	4.3
98 (6-10)	n/a	442.8	2.1	10.3	2.3	2.3
98 (10-15)	n/a	324.1	4.9	1.0	17.1	0.3
98 (15-20)	n/a	283.6	1.9	1.6	16.5	0.6
98 (20-25)	n/a	140.2	1.1	0.9	20.4	0.63
100	220.7 ± 17.4	192.5	3.9	5.7	1.9	2.9
105	60.5 ± 4.3	n/a		n/a		
106	45.7 ± 2.2	n/a		n/a		

In many cases these values significantly exceeded the soil mercury background concentration in this area (i.e. about 45 µg kg^{-1}). Here, the average value was more than 10 times higher than the mercury mean value for Rietfontein sediments. The mercury concentration in wetland soils (i.e. samples 87, 92, 93 and 98) was found higher than elsewhere. This can be attributed to the known retention capacity of metals in wetlands.Dixon (1997) in his study on background concentrations of metals in wetland soils has reported a mean background value below 36 µg kg^{-1} for mercury (range: <11.50 to 300 µg kg^{-1}). Concentrations obtained in the present study were significantly higher (range: 1983 to 2316 µg kg^{-1}) than the background level reported by Dixon, which confirms the contamination from historical mining operations in the area.

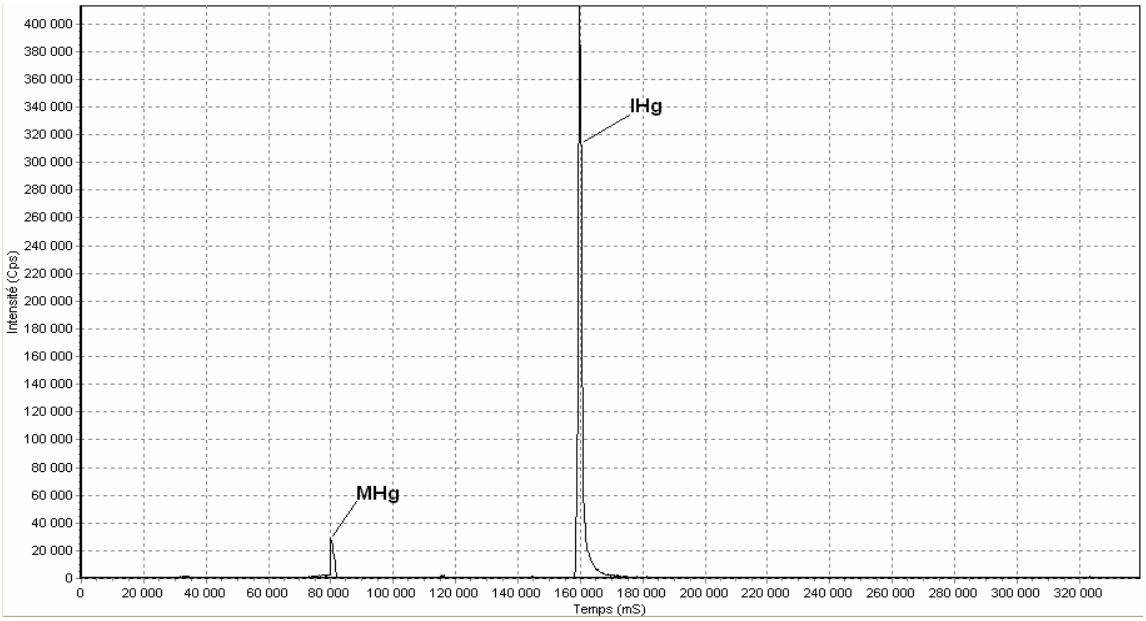

Figure 9.14 Example of GC-ICP-MS chromatogram of Randfontein sediments

Generally speaking, mercury in soils is the source of the mercury found in waters. Soils are also considered as the sink of mercury from waters through precipitation or adsorption processes. In this study, correlation analyses have shown that mercury concentration in soils was positively correlated to mercury from waters with a regression coefficient of 0.54 (figure 9.15).

This shows that the change in mercury content of Randfontein waters is also decided, among other factors such as atmospheric volatilization, by the exchange between soil and water.

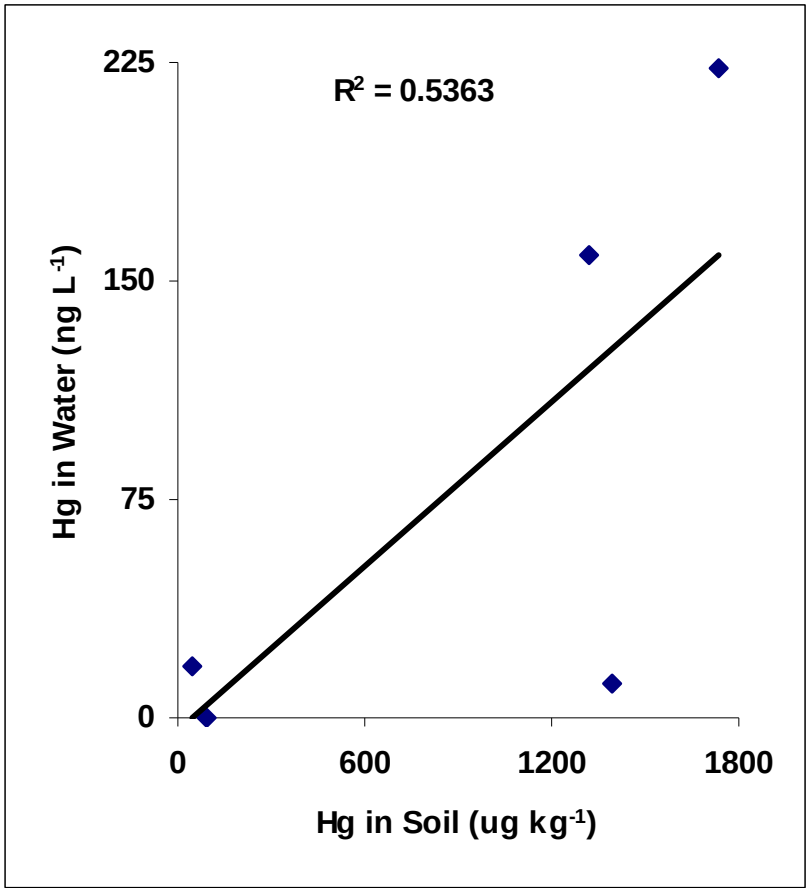

Figure 9.15 Correlation between Hg concentrations in waters and corresponding soils

Remarkably, total mercury concentrations in the Randfontein site increased first, and then decreased from upstream to downstream (figure 9.16), mostly due, as mentioned earlier, to dilution of tributary downstream or water treatment occurring at the boundary between the mining area and the game reserve.

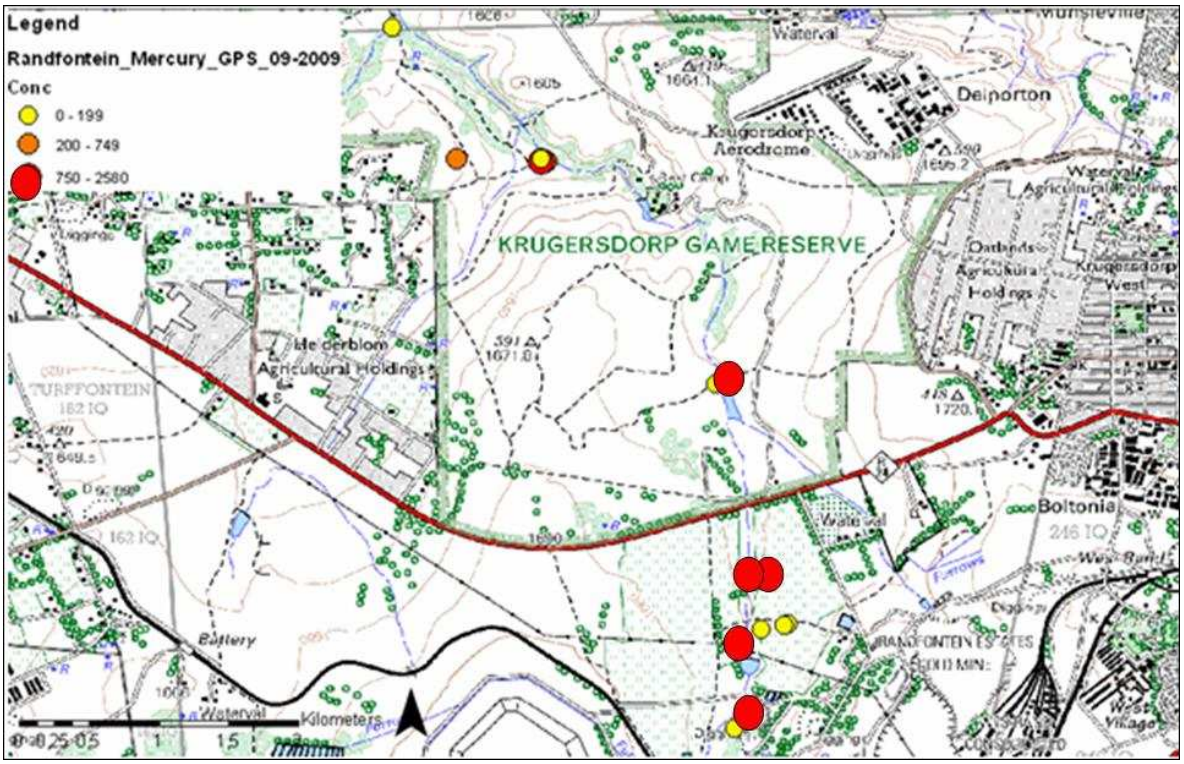

Figure 9.16 Mercury in the Randfontein site.
Note the number of red dots (i.e. Hg ≥ 750 µg kg^{-1}) within the mining site compared to the game reserve

This may explain the significant decrease of mercury level observed in sediments going from the mining site to the game reserve (figure 9.17) and also confirms that mining operations are the main source of pollution in the area.

These results agree with those derived from some Brazilian gold mining areas (Pestana *et al.*, 2000 and the reference herein), where a pattern of highly contaminated sediments near gold mine wastes and lower concentrations away from these sites was observed. The existence of a relationship between mercury contents in soil and distance with respect to the source was also recently observed by Santos-Francés and colleagues (2011) in the Cuyuni River basin (Venezuela). The mercury contents in their study varied according to the distance from the source and, as the distance from the source of pollution increase a gradual decrease in the mercury concentration was observed. These authors also mentioned that dispersion halos are not very extensive and are influenced by the

intensity, turbulence and dominant direction of the wind, soil texture, topography, and rainfall runoff.

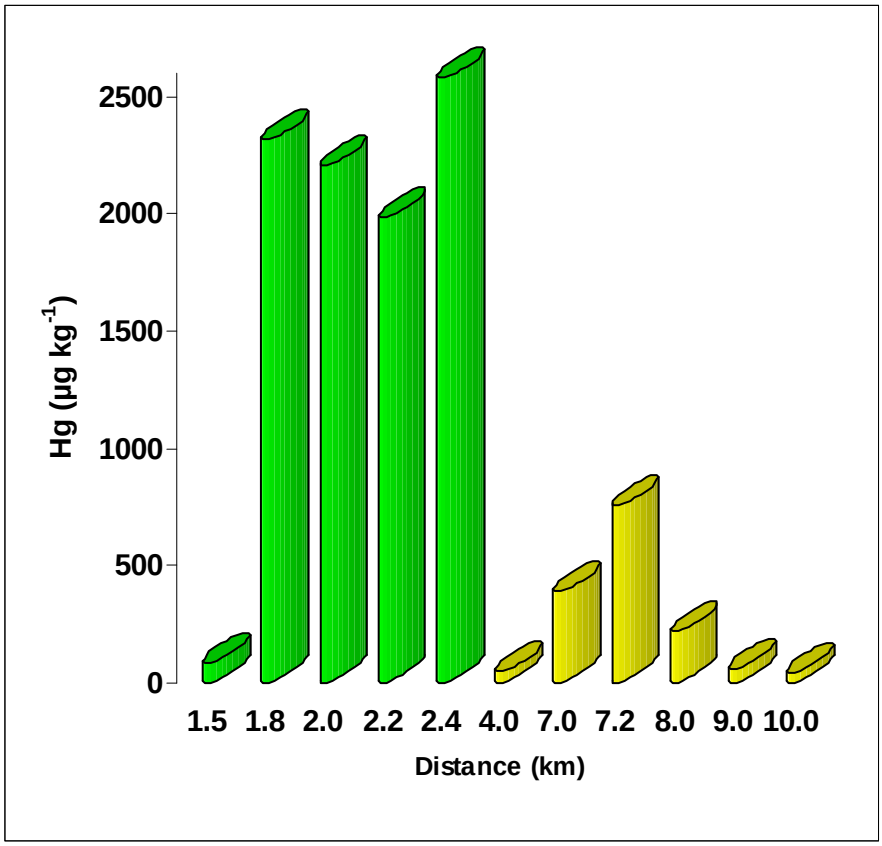

Figure 9.17 Hg_{TOT} in Randfontein surface sediments from the mining area (green) to the Krugersdorp Game Reserve (yellow).
Distances are estimated departing from the headwater

9.3.4 Mercury methylation in soils and sediments

Methylmercury concentrations in Randfontein surface sediments/soils were between 0.9 to 10.4 µg kg^{-1} with a mean of 5.4 µg kg^{-1} (table9.6 and figure9.18). The corresponding percentage MHg ranged between 0.1 and 2.2%.

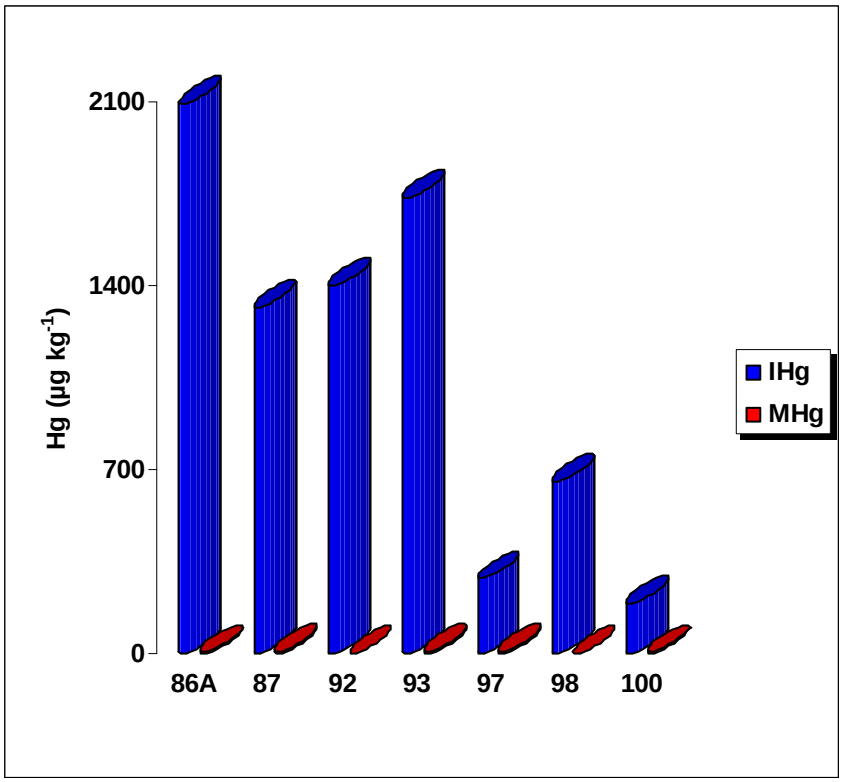

Figure 9.18 Mercury species in Randfontein surface sediments

The highest MHg proportions were found in sediments from the game reserve. This is understandable since a natural reserve is expected to contain high level of organic matters which is, by the way, confirmed by the high percentage of carbon found in the sediment profile 98, collected within the reserve, compared to percentages always below 1 of sample profile 93 taken from the mining area (table 9.7).

Moreover, the percentage of MHg to the total mercury concentration can be a useful index to describe the degree of pollution of a given water system. Usually, MHg concentrations in bottom sediments vary between 1 and 1.5% whereas in non-polluted areas this index takes values lower than 1 (Boszke *et al.*, 2003; Kannan and Falandysz, 1998). Methylmercury proportions obtained in the present study, in particular from samples within the natural reserve, are proof that active mercury methylation processes are occurring in the creek sediment in the Randfontein site which needs to be monitored carefully due to the possibility of MHg accumulation in the aquatic food chain at the natural reserve.

Table 9.7 Carbon, Sulfur, Chloride and sulfate contents in selected sediment profiles from the Randfontein site

Sample	C (%)	S (%)	Cl (mg kg^{-1})	SO_4 (mg kg^{-1})
93 (0-2)	0.21	0.44	29.8	7399.1
93 (2-4)	0.17	0.38	24.2	6428.7
93 (4-6)	0.17	0.35	18.5	5159.0
93 (6-8)	0.22	0.36	15.2	4389.9
93 (8-10)	0.37	0.43	16.4	5032.1
93 (10-15)	0.41	0.54	24.9	6431.5
93 (15-20)	0.60	0.75	31.2	7088.7
98 (0-2)	5.58	0.04	38.7	9155.5
98 (2-4)	5.89	0.05	21.6	3889.5
98 (4-6)	5.37	0.08	17.7	2915.7
98 (6-10)	4.00	0.01	13.9	1804.6
98 (10-15)	2.32	0.00	10.2	1371.9
98 (15-20)	1.73	0.01	7.9	1308.8
98 (20-25)	1.25	0.00	9.8	1091.9

9.3.5 Mercury in sediment profiles

Boszke and co-workers (2003) have reported that the natural Hg_{TOT} in the bottom sediments can vary from 10 to 200 µg kg^{-1} of dry mass, which is of the same order of magnitude as noted in non-polluted soils. These authors also mentioned that very high concentrations of mercury can be found in the sediments from highly polluted areas reaching values as high as several hundreds mg kg^{-1} of dry mass. The above statements agreed perfectly with our findings since Hg_{TOT} in bottom sediments from the less impacted area, i.e. at the game reserve, was about 757 µg kg^{-1} (sample 98) whereas mercury values from the mine bottom sediment samples reached values as high as 2581 µg kg^{-1} (sample 93). This shows the importance of the pollution at the mining site.

Moreover, while soil profiles in the area generally showed increasing mercury concentrations toward the surface, with the highest concentration found in the top 2-10 cm of the profiles, the soil profile of sample 93 collected from the wetland in AMD had a different pattern (figure 9.19), with a substantial mercury enrichment at 15-20 cm depth.

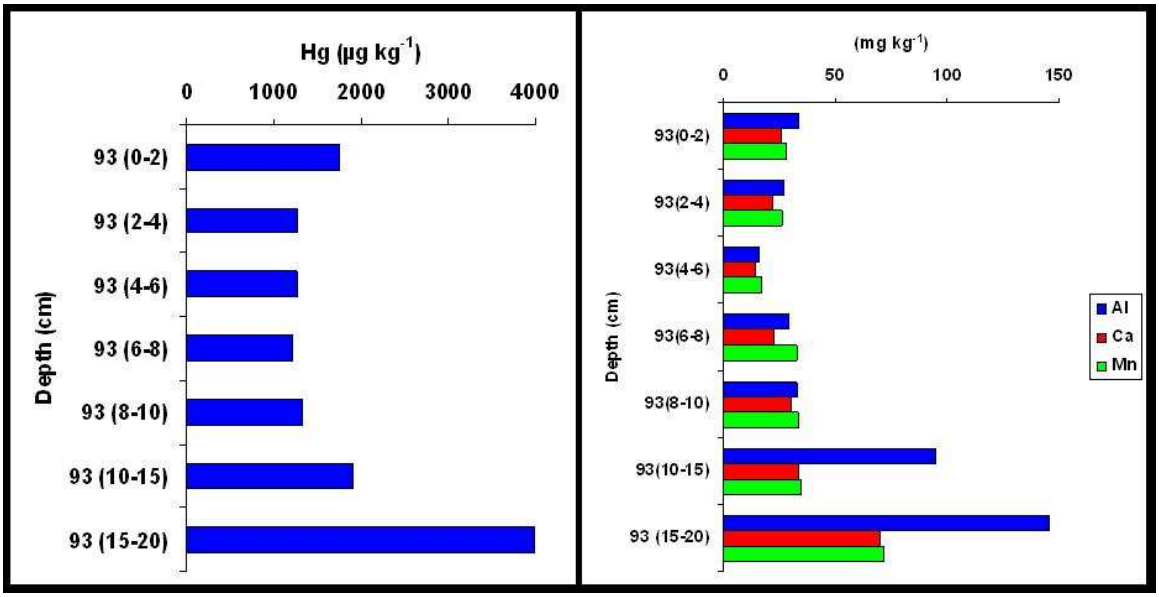

Figure 9.19 Mercury and selected metals patterns in soil profile 93
(Note the metal enrichment 15-20 cm depth)

The general patterns observed in this area may be attributed to downward migration of metals from tailings dumps while the bulk enrichment in the mine soil profile may be caused by the enrichment of organic matter content with depth in the soil (Rosner and van Schalkwyk, 2000). A relatively strong correlation ($R^2 = 0.74$) was found between the organic matter content, expressed here as percentage of carbon, and total mercury in the soil profile 93 (figure 9.20).

Santos-Francés and co-workers (Santos-Francés *et al.*, 2011) have also reported the influential role of the organic matter in mercury distribution in soil profiles.

The mercury enrichment observed at deeper layer in the soil profile 93 may also be an evidence of historical pollution of the site as it was also observed by Yan *et al.* (2008) who reported total mercury concentrations of 15 to 129 times higher than the background concentration in the middle sediment layers of their study site.

Finally, the vertical increase of mercury concentration in soil profile 93 may also be attributed to the volatilization of Hg^0 from the soil surface to the atmosphere, as it was observed by Steinnes (1990).

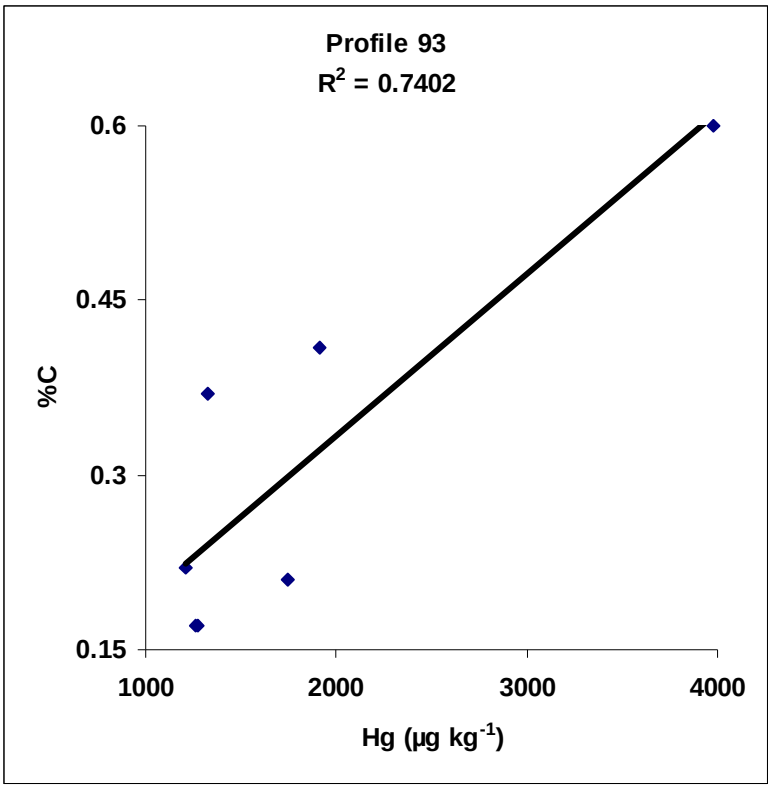

Figure 9.20 Correlation between carbon content and total mercury in the soil profile 93

However, the atmospheric loss of mercury from water and soil surfaces can be a slow process (Lacerda and Salomons, 1998; Schroeder *et al.*, 1992) and much of the mercury lost from sediments as a vapor may be redeposited within the watershed. Thus, the hypothesis of atmospheric loss has to be combined to other mechanisms such as those discussed above to explain the observed pattern in this profile.

In general, most of the metals have exhibited the same pattern as for mercury (table 9.8 and figure 9.21), with an increase of concentrations towards the surface for the majority of the samples.

Table 9.8 Concentrations of selected elements (mg kg^{-1}) in sediment cores from Randfontein

Sample	Al	Ba	Ca	Cs	Cu	Fe	K	Mg	Mn	Ni	Ru
92(0-2)	223.0	3.3	339.6	3.3	6.1	69741.5	2.5	101.1	300.7	1.3	422.6
92(2-4)	5.7	1.1	8.4	1.1	1.3	638.2	0.6	2.3	8.0	0.3	8.4
92(4-6)	191.6	2.4	347.9	2.4	2.8	36355.7	1.3	6.0	418.5	0.8	317.7
92(6-8)	29.7	2.7	25.5	2.7	4.7	2518.9	1.8	8.7	34.5	0.9	38.4
92(8-10)	26.9	1.3	201.1	1.3	5.3	62815.3	2.0	7.3	27.4	1.0	39.1
92(10-15)	30.3	2.0	39.5	2.0	3.1	23284.9	3.1	9.5	23.1	1.2	19.5
92(15-20)	51.9	3.9	23.6	3.8	4.0	1757.9	3.9	12.9	32.5	1.6	26.3
93(0-2)	33.4	1.8	25.5	1.8	4.4	8517.0	1.8	8.4	27.8	2.7	28.1
93(2-4)	26.8	2.7	21.9	2.7	4.5	4113.0	1.6	7.5	26.1	1.3	30.6
93(4-6)	15.7	1.7	13.8	1.7	2.5	2650.5	1.0	4.1	17.0	0.7	17.9
93(6-8)	29.2	3.4	22.3	3.4	4.6	3896.1	1.9	8.4	33.1	1.3	32.2
93(8-10)	32.9	3.1	30.5	3.1	5.3	4598.8	2.1	8.6	33.3	1.2	34.9
93(10-15)	95.1	2.8	33.7	2.8	8.4	4482.9	3.6	12.5	34.7	6.9	37.8
98(0-2)	96.0	3.6	160.6	3.6	2.0	575.0	7.8	8.0	310.8	3.4	4.6
98(2-4)	226.3	7.4	246.4	7.3	3.5	1066.0	11.7	11.7	397.2	7.9	8.5
98(4-6)	83.3	4.6	154.8	4.5	1.7	434.4	5.3	5.2	194.7	3.4	4.0
98(6-10)	188.3	6.0	173.1	6.0	2.8	722.8	6.8	6.9	397.0	5.2	5.8
98(10-15)	111.8	6.2	54.5	6.2	2.6	367.1	6.1	6.2	109.8	3.4	5.4
98(15-20)	67.2	3.6	34.7	3.6	2.4	186.2	3.3	3.5	42.3	3.5	2.5
98(20-25)	69.4	4.0	30.2	4.0	1.4	250.2	3.0	3.1	49.5	2.2	3.2

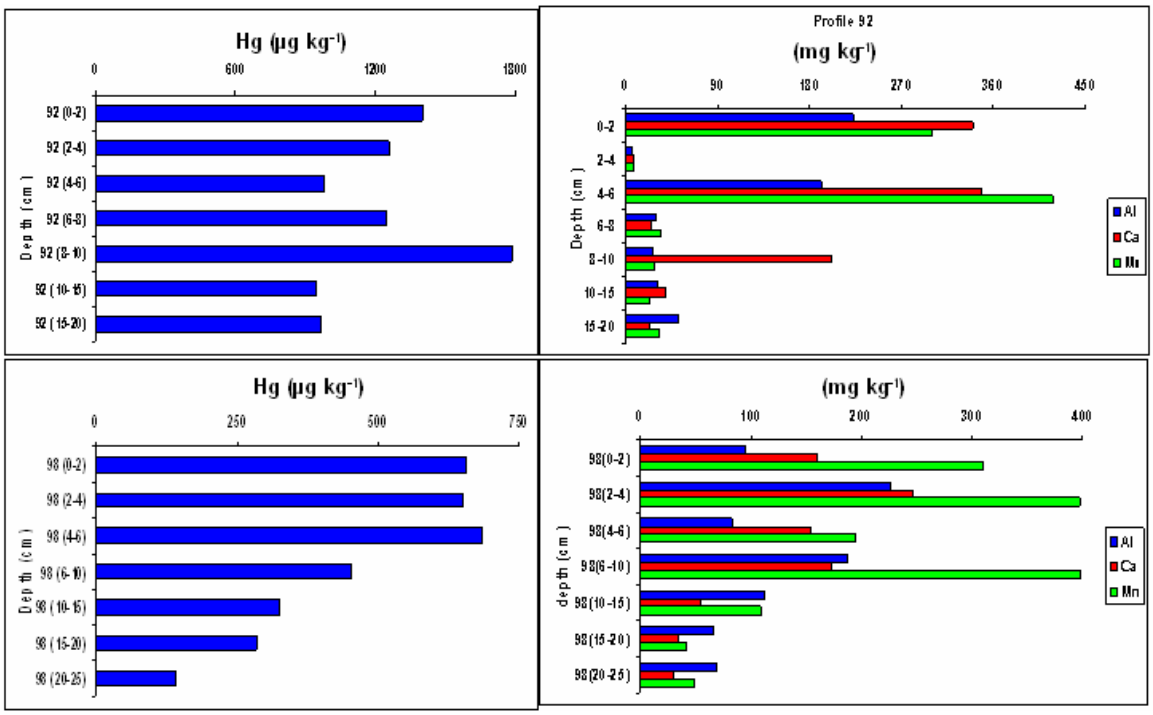

Figure 9.21 Example of mercury and selected metals pattern in soil profiles from the Randfontein site

9.3.6 Factors controlling the mercury methylation in sediments

In order to understand factors that affect the mercury methylation in Randfontein soils, IHg/MHg concentrations of selected soil profiles were compared to factors such as the carbon and sulfate contents. An example of these comparisons is given in figure 9.22.

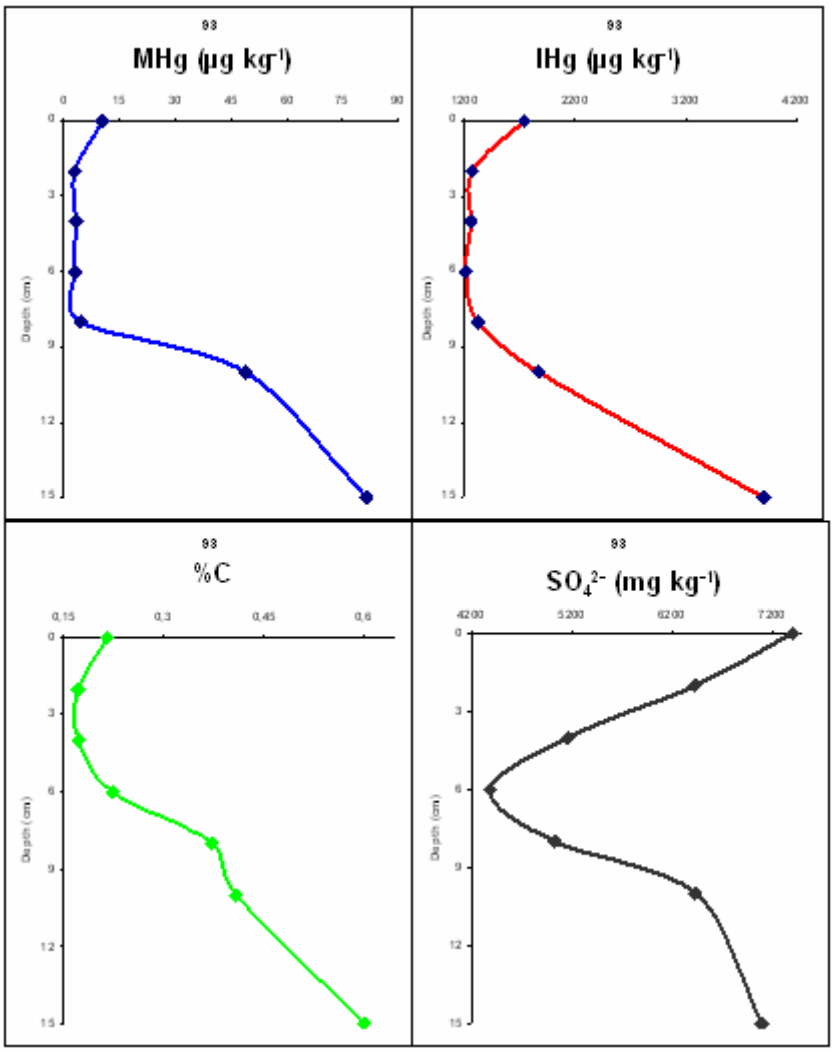

Figure 9.22 Mercury species, organic matter (expressed as %C) and sulfate pattern in the sediment profile “93”

This figure shows an increase of IHg and MHg at about 10 cm depth. The percentage of carbon, as well as the sulfate content of this sediment profile also increased substantially

at the same layer. It is, therefore, believed that organic matters together with bacterial activities (through sulfate reduction) are playing a key role in the mercury methylation in the area. Note that the same observation was made in sediments from the Vaal River site (chapter 8).

Due to the low occurrence of mercury in the Rietfontein site, no particular investigation was made in terms of mercury methylation in the area. However, speciation analysis performed in one of the sediment samples collected from the dry pond revealed the presence of MHg in the analyzed sediment at a concentration of 6.4 µg kg^{-1}, corresponding to 7.6% of Hg_{TOT}. The sediment was marked by a strong rotten egg odor characteristic of the presence of sulfate-reducing bacteria in nature and also by the black colour specific of metal sulfides. The strong reducive conditions in the pond may explain the high MHg proportion observed. It has to be recalled that the water sample from the Rietfontein sump exhibited the lowest Eh value of all the water analyzed in the present study. Although the mercury occurrence is very low at the Rietfontein site, the high percentage of MHg found in the water and sediment from the area is of concern and requires further investigations.

9.3.7 Mercury in plants

Results of total mercury and speciation analyses for Rietfontein and Randfontein plants are presented in tables 9.9 and 9.10, respectively.

Table 9.9 Mercury in Rietfontein plants

Sample (n = 3)	Hg_{TOT} (µg kg^{-1})	IHg (µg kg^{-1})	%RSD	MHg (µg kg^{-1})	%RSD	%MHg
C1	55.9 ± 7.3	46.1	1.5	3.8	3.4	7.6
C2	37.5 ± 4.7	n/a		n/a		
E1	50.8 ± 5.5	n/a		n/a		
E2	81.2 ± 3.8	n/a		n/a		
E3	110.3 ± 8.6	100.8	8.3	0.7	4.7	0.7
Rl1	54.5 ± 6.6	n/a		n/a		
Rl2	74.2 ± 6.4	72.0	6.2	0.7	4.5	1.0
Rp1	23.7 ± 3.7	n/a		n/a		
Rp2	17.0 ± 1.1	n/a		n/a		
Sch1-6	26.6 ± 1.2	n/a		n/a		
Typha 1-6	88.9 ± 8.2	50.8	0.9	10.7	1.3	17.4
T1	50.3 ± 3.5	n/a		n/a		
T2	48.5 ± 5.6	n/a		n/a		

The mercury speciation analysis was performed for selected plants that showed "elevated' Hg_{TOT} concentration or had the highest Hg_{TOT} among samples of same species (please refer to tables 9.1 and 9.2 for samples identity and description).

Total mercury values in Rietfontein plants were between 17 and 110 µg kg^{-1} (mean: 55 µg kg^{-1}) whereas values obtained in Randfontein plants were higher, ranging between 19 and 203 µg kg^{-1} (mean: 112 µg kg^{-1}). This confirms that the mercury content in plants can be a good indicator of the pollution level of a given site since results obtained for sediments and waters from both sites are in good agreement with those obtained with plants analysis. Therefore, while the Rietfontein site can be considered as non (or no longer) affected by mercury pollution due to remediation works, it appears that the impact of historical mining in Randfontein plants is of concern and needs to be investigated on a larger scale.

Table 9.10 Mercury in Randfontein plants

Sample (n =3)	Hg_{TOT} (µg kg^{-1})	IHg (µg kg^{-1})	%RSD	MHg (µg kg^{-1})	%RSD	%MHg
81C	101.4 ± 11.9	84.8	3.3	0.9	8.4	1.1
82B	19.4 ± 3.4	n/a		n/a		
89A	202.6 ± 9.0	198.0	4,6	3.4	4.2	1.7
86A	123.0 ± 7.3	103.6	1.1	7.0	3.7	6.3

The highest mercury concentrations for the different analyzed species (figure 9.23) were found in Randfontein algae with a mean value of 142 µg kg^{-1}. Eucalyptus collected at the Rietfontein landfill also showed relatively high mercury values compared to other plants from the same site with concentrations ranging between 51 to 110 µg kg^{-1} (mean: 81 µg Hg kg^{-1}).

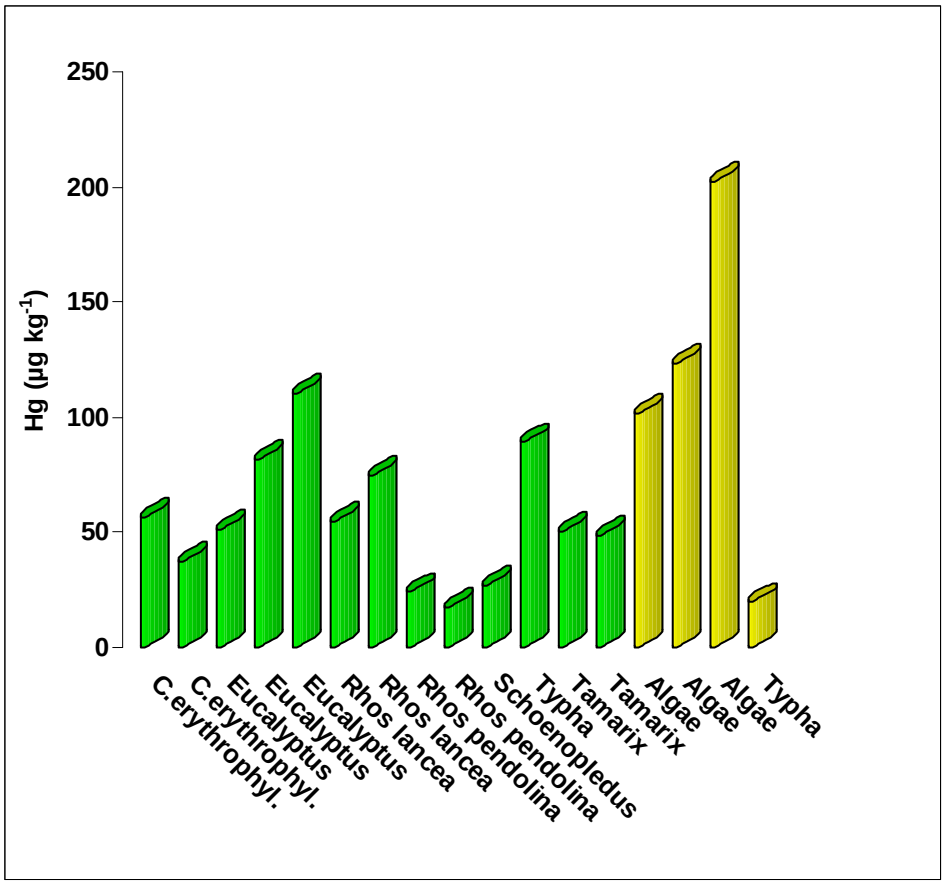

Figure 9.23 Mercury in Rietfontein (green) and Randfontein (yellow) plants

To investigate the mobility and availability of metals from soil to plant, concentrations of mercury in top soils and plants, collected from the Rietfontein landfill near the waste rock pile and from the Randfontein creek in AMD, were used to calculate the transfer coefficients (TC) of mercury from soils to plants, using the following equation (Li *et al.*, 2010):

$$\mathrm{TC} = \frac{P\ (\mathrm{mg\ kg}^{-1}\ \text{fresh weight})}{S\ (\mathrm{mg\ kg}^{-1}\ \text{dry weight})} \qquad (9.1)$$

where P represents the metal concentration in plant tissue and S is the total metal concentration in soil where the plant grows.

Obtained TC values (table 9.11) were of 0.743 and 0.882 for the Rietfontein landfill (mean: 0.813) and of 0.053 and 0.102 (mean: 0.078) for the Ranfontein site. These values were substantially higher than the average of 0.019 (range: 0.003 to 0.025) reported by Li and co-workers (2010) suggesting a great availability of mercury for uptake by plants at both sites.

Table 9.11 Calculated TC values for selected soils and plants

Site	Soil ID	Hg ($\mu g\ kg^{-1}$)	Plant species	Hg ($\mu g\ kg^{-1}$)	TC
Rietfontein	Adit5	68.4	Eucalyptus (E1)	50.8	0.743
	Adit6	125.0	Eucalyptus (E3)	110.3	0.882
Randfontein	87	2316.6	Algae (86A)	123.0	0.053
	92	1982.9	Algae (89A)	202.6	0.102

The TC values obtained for the Rietfontein landfill, where mercury occurred at low values, were very high compared to values obtained for the Randfontein site. This implies a greater mercury uptake by eucalyptus compared to algae, although a comparison of plant species from the same area would provide a better indication of the uptake efficiency.

However, as also mentioned by the above researchers, the TC not only quantifies the relative differences in the availability of metals to plants but also is a function of both soil and plant properties. Therefore, elevated levels of metals in soils may lead to their uptake by plants, which depends not only on metal contents in soils but is also determined by factors such as soil pH, organic matter, clay and phosphate contents, as well as cation exchange capacity. These factors may not change the total amount of metals in soil but they can significantly affect their bioavailability. Other factors, such as plant species as well as growth period, also account for the uptake and translocation of metals (Voutsa *et al.*, 1996; Intawongse and Dean, 2006).

Thus, the TC index, alone, is not sufficient to make reasonable conclusions about metals bioavailability.

Methylmercury values in plants from both sites were low, with almost all concentrations below 10 $\mu g\ kg^{-1}$, except for Typha leaves from the Rietfontein site which showed a MHg value of about 11 $\mu g\ kg^{-1}$ corresponding to 17% of Hg_{TOT} (table 9.9 and figure

9.24). This, again, shows the need of further investigations in order to understand the considerable methylation rate at the Rietfontein site.

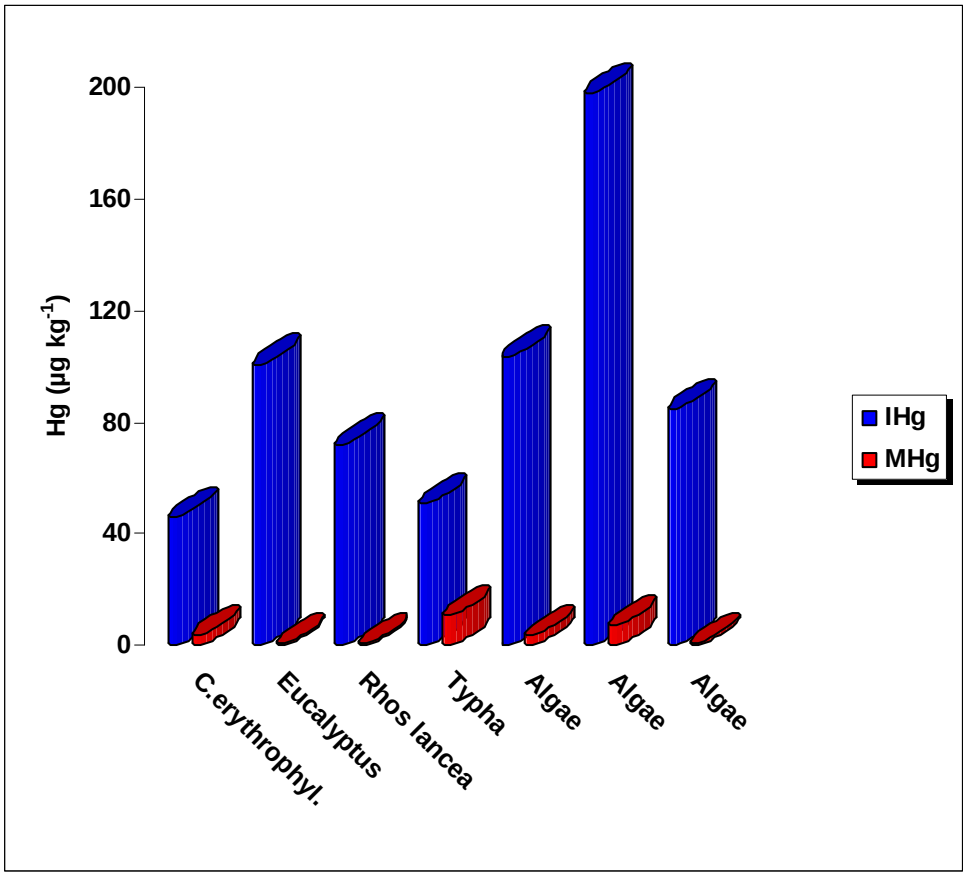

Figure 9.24 Mercury species in selected plants (Algae were from the Randfontein sampling whereas the other plants were from the Rietfontein site)

9.3.8 Mercury fractionation and speciation modeling

In the last years, combined chemical, biological and ecotoxicological studies on contaminated soils have increased importance to predict the mercury fate in the environment. It is generally recognized that mercury toxicity and bioavailability depend largely on the chemical state of the metal rather than on the mere mercury total concentration.

In general, only a small fraction of the total mercury in soils exists in the interstitial waters and the remainder is adsorbed to the soil. The extent of the mercury adsorption by soils is controlled by a number of factors such as the chemical form of mercury, the grain size distribution of the soil, soil mineralogy, humic substance concentrations, soil pH, and the redox potential (Kaplan *et al.*, 2000).

Among these factors, the chemical form of mercury is of primary importance for its sorption (Benes and Havlik. 1979). For example, the hydrolyzed forms of mercury are generally adsorbed more than the chloride complexes and that increasing hydrophobicity of an inorganic mercury species increases its potential to adsorb; thus, $HgCl_2$(aq) will be adsorbed at a less extent than $Hg(OH)_2$(aq), which in turn will be adsorbed lesser than HgS(aq).

Therefore, the Hg-binding forms and speciation can be considered as key factors for conducting bioavailability studies and ecotoxicological hazard assessments. Single and sequential extraction methods have being widely used for discrimination of different solid-phase associations of trace elements in soils or sediments.

In this study, a sequential extraction procedure and equilibrium speciation modeling were applied to determine the concentration of mercury fractions and to predict the type of mercury complexes in selected Randfontein soils and waters.

The determination of mercury speciation in soil samples by means of sequential extraction procedure (SEP) used in this study was based partially on the work of Zagury and co-workers (2006) which proposed the differentiation of mercury compounds into the following four fractions: F1: water-soluble; F2: exchangeable; F3: bound to organic matter, and F4: residual mercury.

Briefly, the water-soluble fraction extractions were carried out using deionized water, the exchangeable fraction was extracted under slightly acidic conditions with 1M $CaCl_2$ (pH=5), and the organic fraction was separated by successive extractions using 0.2 M NaOH and CH_3COOH 4% (v/v). Residual mercury was calculated as the difference between total mercury concentration and the sum of the F1, F2 and F3. The results obtained from the SEP are presented in table 9.12 and figure 9.25.

Table 9.12 Hg concentrations in different leachates of Randfontein soils

Sample	H_2O (µg Hg kg^{-1})	$CaCl_2$ (µg Hg kg^{-1})	NaOH +CH_3COOH (µg Hg kg^{-1})	Residual (µg Hg kg^{-1})	Total (µg Hg kg^{-1})
R92	5,4	8,8	63,2	1322,1	1399,4
R93	2,0	3,6	146,6	1592,5	1744,8
R98	3,0	2,6	29,6	621,0	656,2

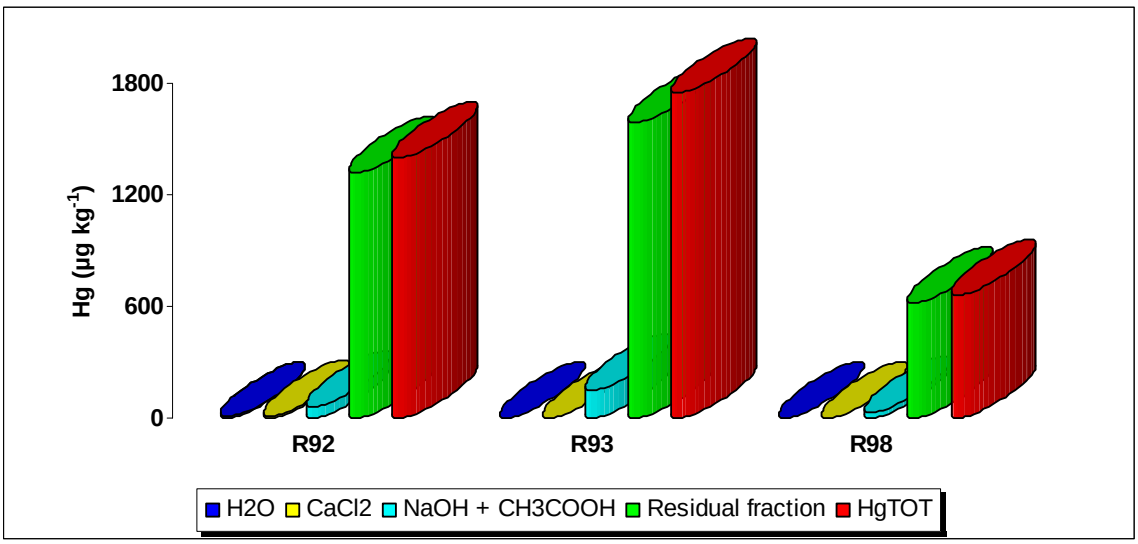

Figure 9.25 Sequential extraction result of selected Randfontein soils

SEP results indicate that the sum of fractions F1, F2 and F3 represented low percentages of total mercury, ranging between 5.4 to 8.7% with an arithmetic mean of 6.5% (table9.13). This mean value was remarkably close to the one of 6.8% (range 2.9 to 13.8%) obtained by Zagury and co-workers (2006) in three contaminated soils from chlor-alkali plants. The most important contribution to the sum was the fraction F3, i.e. the mercury associated to organic matter (table 9.12 and figure 9.26), with results varying between 4.5 % (Soils R92 and R98) and 8.4 % (Soil 93). In contrast, fractions F1 (water soluble Hg) and F2 (Exchangeable Hg) were very low, ranging between 0.1 to 0.5 % and 0.2 to 0.6%, respectively.

Table 9.13 Percentage of Hg leached with different solvents

Sample	%H_2O	%$CaCl_2$	%NaOH +CH_3COOH	%Residual	%Total extract
R92	0,4	0,6	4,5	94,5	5,5
R93	0,1	0,2	8,4	91,3	8,7
R98	0,5	0,4	4,5	94,6	5,4

Results obtained by Zagury *et al.* (2006) were different, with the highest mercury values found in the exchangeable fractions and lowest mercury concentrations in the organically bound fraction (F3). Their results were consistent with the low organic carbon content of chlor-Alkali soils. It has to be recalled that the soils analyzed in the present study were obtained from a wetland and, therefore, it is believed that the organic matter content may explain the high percentage of mercury found in F3.

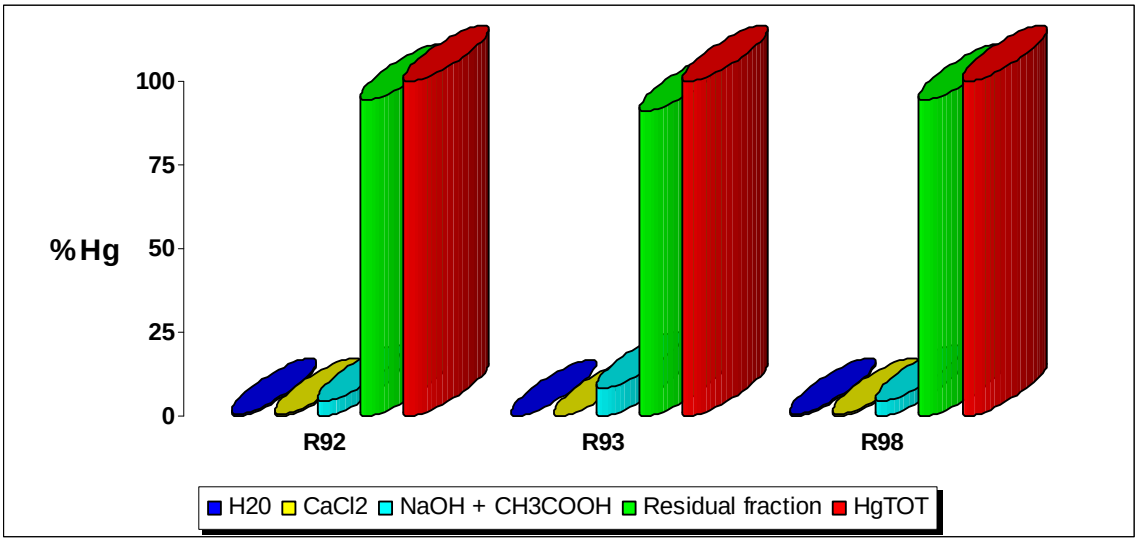

Figure 9.24 Fraction of mercury in different solvents

Blester *et al.* (2002) also observed in their study that mercury was predominately bound, in most of their soils to organic matter. Leachable mercury in their soils occurred as non-reactive, soluble organic mercury complexes such as fulvic acid-bound mercury and reached their highest values (90 µg Hg kg^{-1}) in soils rich in organic matter. These authors also reported that the distribution of mercury in their soil profiles suggested that

migration of mercury to deeper soil layers (about 20 cm) is most effective if mercury is bound to soluble organic complexes, whereas reactive mercury or weak mercury complexes are effectively retained in the uppermost soil layer (5 cm) through sorption on mineral surfaces. The same trend was also observed in the present study with an important migration at deeper layer in the soil profile for samples that have shown a great affinity for organic matters. For example, soil R93 which had the highest concentration of mercury bound to organic matter (147 µg kg^{-1}) exhibited an important migration of mercury in the profile, with a mercury value of 3902 µg kg^{-1} measured at 15 – 20 cm depth whereas soil R98 (Hg in F3 = 30 µg kg^{-1}) had its highest mercury value at the top 5 cm (655 µg kg^{-1} at 4-6 cm depth).

The high mercury content found in F3 was also in agreement with the sulfur content in soils. Soil R93 which had the highest percentage of mercury in F3 also showed the highest percentage of sulfur (table 9.7). This could be indicative of the affinity of mercury for reactive functional groups of the organic matter, especially sulphur groups such as thiol (Yin *et al.,* 1997; Skillberg *et al.,* 2006).

Organic matter may play an important role in the binding of ionic species in soils. The incorporation of Hg^{2+} into soluble or particulate organo-metallic complexes, as previously described for organic carbon rich waters (Santos-Francés *et al.,* 2011 and the reference herein), can be considered as a probable mechanism of mercury mobilization.

Although the water soluble mercury only accounts for about 0.3 % of Hg_{TOT}, this fraction is very important from an environmental risk point of view due to its easy availability in environmental weathering conditions (Zagury *et al.,* 2006 and references therein).

In all soils, the largest mercury proportion was found within the residual fraction, representing 91.3 to 94.6 % of Hg_{TOT}. This fraction is reported to contain the least available form of mercury under naturally occurring conditions, depending on the matrix under study and the source of contamination (Li *et al.,* 2010).

Most of the mercury in this fraction is believed to be Hg^0, as observed by Santos-Francés and colleagues (2011) who reported an estimated Hg^0 content of 87 to 92% to the total mercury in soils of a gold mining region in Venezuela. This chemical form of mercury is very important with regard to environmental risks, since its low reactivity prevents

mobilization in soils and waters but, in contrast, its high vapour pressure provides a high mercury flux (soil-air) in the mining areas (Garcia-Sanchez *et al.*, 2006), which contributes significantly to the local atmospheric pollution and may be to the global mercury cycle.

However, the above discussion need to be considered with caution since it can be misleading due to the fact that it is mostly based on assumptions. Moreover, analytical procedures can be affected by loss and/or contamination occurring during the SEP and also by the efficiency of solvents used to extract mercury, as it is the case in extraction procedures for coal samples.

The relatively low amount of mercury leached from the soil suggests that this element is almost immobile in the study system. However, the average mercury concentration in the creek water (103 ng L^{-1}) is high in relation to the typical natural background range for unpolluted freshwaters (Appleton *et al.*, 2001). This is also of importance, given the low water solubility of Hg^0 and most inorganic mercury compounds.

Equilibrium speciation modeling of mercury in Randfontein waters was performed using the Eh-pH diagram, and the results showed that the dominant inorganic species was Hg^0 for the majority of water samples (figure 9.27), except for samples collected in the creek wetland (samples 88, 90 and 91), which may content significant amounts of mercury soluble compounds such as $HgCl_2$. Thus, in these waters under the measured Eh-pH conditions, the mercury speciation results showed that mercury would mostly exist as Hg^0 which agrees with the results from SEP.

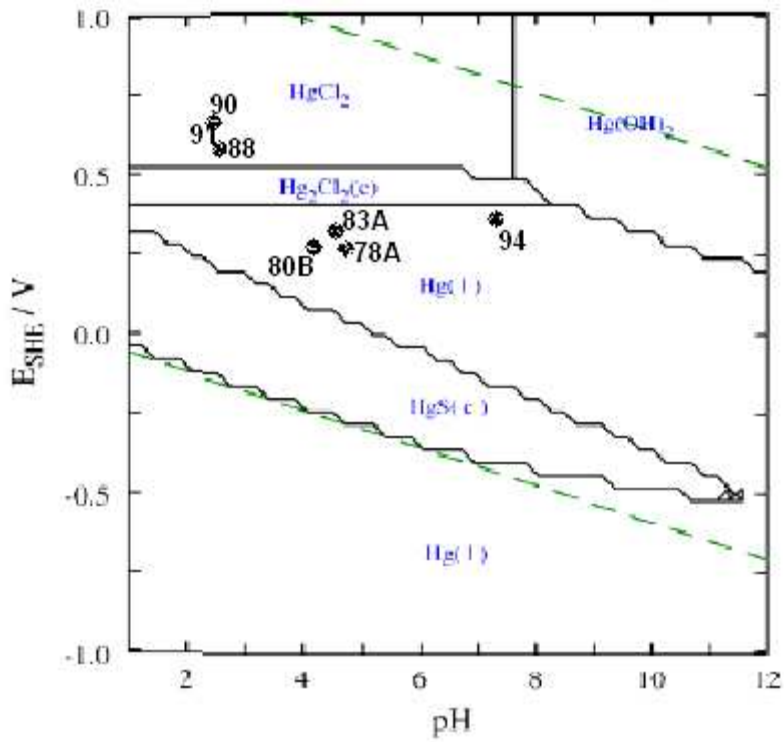

Figure 9.27 Predominant inorganic mercury species in Randfontein waters

The MEDUSA and VISUAL MINTEQ geochemical speciation models were also used to calculate the equilibrium concentrations of dissolved and solid mercury species for the study systems and to obtain more coherent results in the prediction of predominant species. The model runs were conducted using measured Hg, Cl^- and SO_4^{2-} values together with *in situ* pH and Eh measurements.

The results of the geochemical modeling showed a significant variation in the distribution of mercury species. Thus, the dominant species in samples from the mining area were $HgCl_x^{+2-x}$, Hg^{2+} and HgClOH in concordance with the high mercury and chloride concentrations in these samples (figure 9.28 and table 9.14), whereas the dominant species in the game reserve water were $Hg(OH)_2$, HgClOH and $HgCl_x^{+2-x}$, respectively (figure 9.29 and table 9.15). These results are similar to mercury speciation analyses carried out by Navaro *et al.* (Navarro *et al.*, 2009), in mining waste from a mercury mining in Spain.

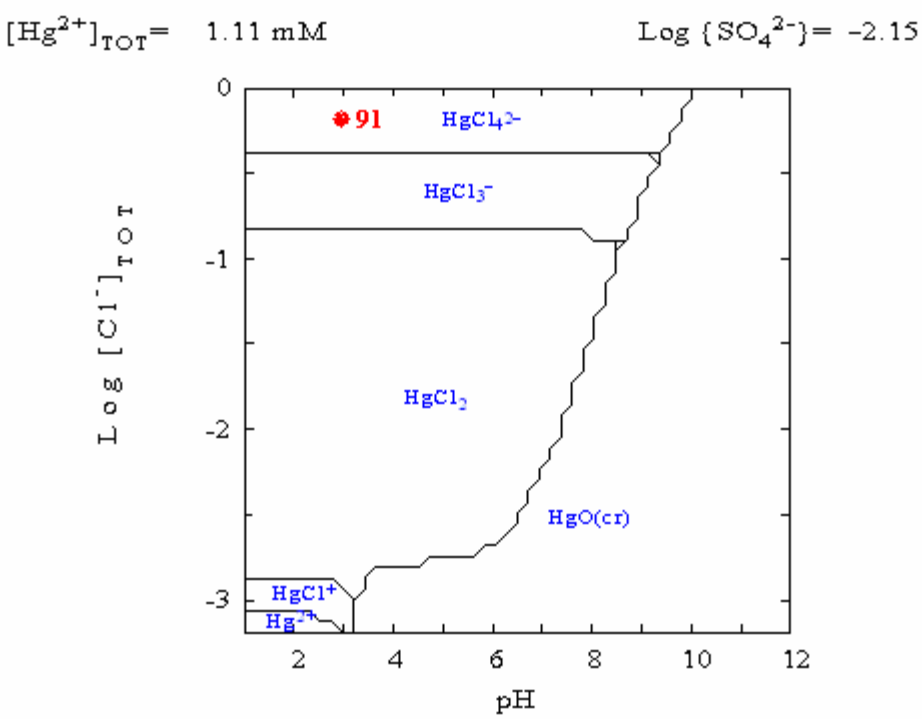

Figure 9.28 pH-Cl diagram of water sample 91from the Randfontein creek in AMD

Table 9.14 Species distribution in water sample 91

Species	Concentration (M)	% of Hg species
Cl^-	7.5226E-08	
H^+	0.00098259	
$Hg(OH)_2$	0.00010397	9.3843
$Hg(SO4)_2^{-2}$	9.3073E-06	0.8400
Hg^{+2}	0.00023253	20.9882
Hg_2OH^{+3}	3.2724E-08	0.0029
$Hg_3(OH)_3^{+3}$	2.8019E-09	0.0002
$HgCl^+$	0.00025666	23.1662
$HgCl_2$ (aq)	0.000089526	8.0806
$HgCl_3^-$	6.7425E-11	6.0858E-06
$HgCl_4^{-2}$	2.6912E-17	2.4291E-12
HgClOH (aq)	0.00021217	19.1505
$HgOH^+$	0.000066488	6.0012
$HgSO_4$ (aq)	0.00013722	12.3855
HSO_4^-	0.00035067	
OH^-	9.6032E-12	
SO_4^{-2}	0.0066064	

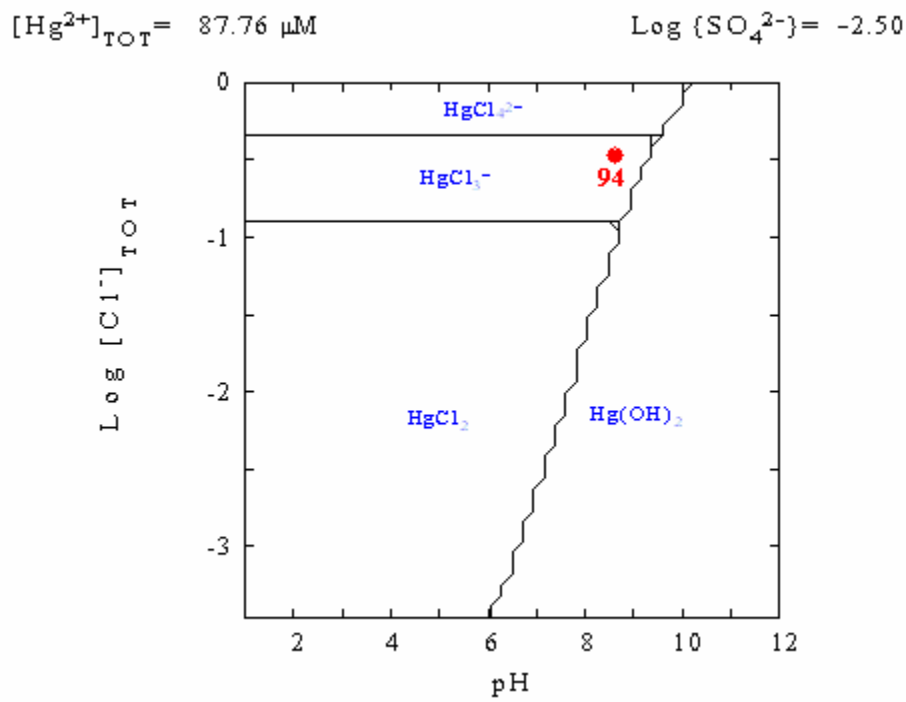

Figure 9.29 pH-Cl diagram of water sample 94 from the game reserve

Table 9.15 Species distribution in water sample 94

Species	Concentration	% Hg species
Cl^-	0,00033	
H^+	1,8905E-08	
$Hg(OH)_2$	0,00007	81,0773
$Hg(SO4)_2^{-2}$	6,6478E-16	7,5543E-10
Hg^{+2}	6,4809E-14	7,3647E-08
Hg_2OH^{+3}	1,1579E-22	1,3158E-16
$Hg_3(OH)_3^{+3}$	5,1555E-24	5,8585E-18
$HgCl^+$	3,9838E-10	0,0004
$HgCl_2$ (aq)	7,5016E-07	0,8524
$HgCl_3^-$	2,4815E-09	0,0028
$HgCl_4^{-2}$	4,2059E-12	4,7794E-06
HgClOH (aq)	0,00002	18,0659
$HgOH^+$	9,4879E-10	0,0011
$HgSO_4$ (aq)	2,0633E-14	2,3447E-08
HSO_4^-	3,4221E-09	
OH^-	3,6686E-07	
SO_4^{-2}	0,00314	

Kaplan *et al.* (Kaplan *et al.*, 2000) predicted that the dominant inorganic mercury species in conditions similar to those encountered in AMD (i.e. pH 4 and 0.002 mg Hg L^{-1}) would be HgS(s), Hg^{2+}, $HgC1_2$, $HgC1_3^-$ and $HgCl_4^{2-}$.

The authors also mentioned that the presence of Cl^- has a significant effect on the mercury speciation, especially at elevated Eh values and observed that Hg^{2+}(aq) would exist in moderate reducing conditions. Several researchers have noted that Hg^{2+} rarely exists in sediment porewater as a free ion due to its propensity to adsorb to solids or form complexes, especially to chloride or organic matter (Schuster, 1991; Wallschlager *et al.*, 1998a and b). From the model system presented in this study, if the system is reduced and/or the pH is increased, then dissolved mercury is expected to be removed from solution as Hg^0 and $Hg(OH)_2$, or under extreme conditions as HgS, making the mercury less mobile and less toxic than in the oxidized environment.

The predominance of the elemental form not only explains the lower mobility, but is also compatible with the range of measured pH and Eh field values downstream of the creek, within the game reserve. Similar observations were made by Pestana *et al.* (Pestana *et al.*, 2000). When Eh values rise, as it was the case within the mining site, the relative importance of Hg^0 declines (figure 9.27).

The model system presented in this work may explain the high level of mercury observed in water samples from the creek wetland since, under the high Eh and low pH conditions, mercury becomes more soluble and, therefore, more available for living organism, confirming the hypothesis discussed in section 9.3.1 which suggested that the high MHg value found in the water sample 91 was mainly due to the important availability of soluble forms of mercury in this water.

9.4 Summary

The present study has demonstrated that mercury released from closed mining operation in the Randfontein area may have significant impact at the neighboring game reserve. The Krugersdorp Game Reserve watersheds are directly downstream from the mine drainage and appear to become impacted by the pollution from historic gold mines.

On the basis of collected data, it can be inferred that the primary source of mercury to the mine creek is the weathering of mine waste materials from the old slimes dam located few hundred meters away and also the point of AMD discharge from the adit at the Rand Uranium. No further surface tributaries to the creek were observed other than AMD along that relatively short transect. The elevated mercury found in a borehole near the creek wetland suggests a groundwater contamination in the area. The contribution of acidic water to the creek at the study site should vary seasonally. Therefore, further samplings are of importance for a better characterization of the impact of historical mining in the area.

The study also showed that mercury transported downstream from the mine site is susceptible to methylation. Methylation of mercury seems to be controlled by factors such as the inorganic mercury content, redox potential, microbial (SRBs) activities and the organic matter content. The sequential extraction procedure together with geochemical modeling have demonstrated the predominance of non soluble mercury species (Hg^0) in study soils and the existence of a variety of mercury species in the mine creek. The presented model also explained remobilization of mercury in water and their availability for methylation. No transport mechanism was found sufficient on its own to explain both vertical and horizontal of mercury in the site.

Finally, the mercury level measured in the Rietfontein water, sediments and plants has shown no significant contamination of the area probably due to remediation works undertaken on the site, although the proportion of methylmercury found in these samples suggests a high methylation rate at the site and requires further investigation.

Chapter 10
Conclusions

The first objective of this study was to develop simple and cost effective analytical procedures for the collection and determination of gaseous mercury (TGM).

Nanostructured gold supported metal oxide materials (i.e. Au/TiO_2, Au/ZnO and Au/Al_2O_3), which contain only 1% wt of gold, were successfully used as adsorbents I in sampling or analytical columns for the trapping, preconcentration and quantification of mercury directly from the gaseous phase.

Analytical performances obtained with the nanogold traps, especially Au/TiO_2, were comparable to those obtained with commercial pure gold wool and gold-coated sand, although mercury retention problems have been observed, in some cases, which are thought to be caused by the inner structure of the materials and may, therefore, be improved during the materials synthesis or during sorbents conditioning prior use. A deeper characterization of the structural properties of these materials is recommended for this purpose. Therefore, the nanogold sorbents, which are synthesized locally, can be considered as an alternative choice to the mostly imported traditional sorbents for a low cost analysis of ultratrace mercury and can also be tested for TGM determination from exhaust gas in coal power stations.

In the present work, the speciation analysis of mercury was carried out in Highveld coals using both developed sample preparation procedures combined with isotope dilution GC-ICP-MS technique, and existing, but modified, sequential extraction procedures. Although no certified reference material of mercury species in coal was available, the closeness of IHg and MHg values obtained using different sample preparation procedures confirms the reliability of the developed methodologies.

Species such as Hg^0, Hg^{2+}, CH_3Hg^+ were identified in all Highveld coals and CH_3Hg^+ occurred at a lower concentration than in some reported China coals. Other unknown species have also been observed and are believed to be organomercurials. Due to the unavailability of specific standards, these unknown species could not be identified but the

use of a theoretical approach has allowed the identification of one of the unknown species as ethylmercury.

This work is, in our knowledge, the very first attempt in identifying monomethylmercury in South African coals.

Although methylmercury concentration was low in Highveld coals, its natural occurrence in the coals may become a concern due to the risk for this toxic species to be continuously released into the environment during coal mining or coal preparation prior to combustion.

Sequential extraction procedures on the other hand have revealed the predominance of organically bound as well as pyritic bound mercury in Highveld coals, and the occurrence, to a lesser extent, of other forms of mercury association such as water-soluble compounds or mercury bound to minerals such as iron oxides, carbonates and silicates.

The variability of leaching efficiency obtained with the different samples was attributed to the variability of the mercury modes of occurrence within the samples. The mercury leaching appeared to be considerably affected by the presence of organic matter. Nevertheless, a caution was made about the above conclusions due to the lack of leaching specificity obtained by the used solvents.

The overall leaching performance obtained with the modified sequential extraction procedure was within the range of standard solvents leaching procedures which shows that this procedure can be used as an alternative technique for mercury removal in coals.

Data presented in this work may be useful for the development of coal cleaning protocols which do not exist in South Africa and also for local environmental pollution assessment of the mercury released during coal mining and beneficiation.

In addition, total mercury determination in both Highveld and Waterberg coals revealed a mean mercury concentration higher than the global average but, still, within the range of reported values by the USGS for South African coals. Therefore, a mean value of 0.2 mg kg^{-1} was recommended to be used for the estimation of the atmospheric emission of mercury from South African power stations, although more coal samples, from different local coalfields, are still needed to improve this average.

The extent of mercury pollution from past and current gold mining operations, which represent the second biggest anthropogenic source of mercury in South Africa, was investigated. Pollution assessment studies of mercury pollution from gold mining performed at 4 different sites, namely Vaal River West, West Wits, West Rand and East Rand regions, all located within the Witwatersrand Basin in South Africa, have generated number of interesting information that could be a useful database for future systematic investigations and also to improve estimations of anthropogenic mercury emission in the country.

In general, results obtained from the analysis of sediment, soil, tailings, water and plant samples have demonstrated a relatively important pollution occurring in almost all the study sites, except for the East Rand site (Rietfontein landfill) which did not show an evidence of pollution, probably due to remediation works that were undertaken in that closed mining site for many years. However, caution was also taken in this partial conclusion because most of the sampling campaigns were performed during the dry season. A later sampling performed after a period of heavy rains at the Vaal River West has shown different trends than what was observed from the dry season sampling, with an important remobilization of mercury in water and its migration several kilometers away from estimated mercury sources. These findings have suggested the need for a continuous monitoring of the study sites for better conclusions.

The impact of the pollution was characterized by high mercury concentrations in sediments as well as in waters with values, in many cases, far beyond US EPA threshold levels. The main sources of pollution appeared to be old TSFs that are known to contain waste from old mining operations when gold used to be extracted by the mercury amalgamation process.

The mercury leached from these tailings through runoff is polluting the adjacent sediments which in turn contaminate the surrounding water systems through drainages or underground seepages. The impact of the water pollution is dependent of the mercury source, the hydrology of the water system, the geochemistry of the study environmental compartment and also of seasonal variations at the site.

The contribution of artisanal mining could not be estimated due to the difficulty of accessing reliable information from local miners and for safety reasons.

This work did not also take into account the contribution of atmospheric mercury emission/deposition at the different sites. Nevertheless, an attempt was made to determine TGM concentrations from few samples collected from an underground source at Vaal River West and the obtained results revealed the urgent need for more extensive samplings and could also suggest that the estimated atmospheric contribution of the mercury emitted from South African gold mines may be underestimated, although the number of analyzed samples were not enough for conclusions that could be trustworthy to be drawn.

Speciation analysis revealed the occurrence of MHg at variable levels in the different study sites. Considerable MHg proportions have been noticed at all sites in different ponds and wetlands including the dry pond at the Rietfontein site (East Rand) which suggest an important methylation rate that has to be monitored with care due to the property of methylmercury to bioaccumulate in the food chain. Fishing activities have been observed at the Vaal River West site whereas the Randfontein site (West Rand) is surrounded by not only the Krugersdorp Game Reserve but also by number of agricultural holdings that are all susceptible to potential pollution occurring at the mining site.

The mercury methylation seems to be controlled by a combination of number of factors mainly the presence of inorganic mercury, redox conditions, pH, bacterial activity, organic matter and sulfur (or sulfate) contents. The competition between inorganic mercury and other metals such as iron for binding sulfur also seems to play an important role in the mercury methylation process.

Plant analysis could not provide much of useful information on the mercury uptake since the sampling of plants was randomly done and triplicate samples of the same species, which is recommended for more conclusive analyses, were scarce. However, from the general trend observed it appeared that plant analysis can be used as a reliable way of monitoring the level of mercury pollution in a given area. In addition, the determination of the transfer coefficient (TC) of mercury from soils to plants at both East Rand and West Rand sites has suggested a substantial mercury uptake by plants, and thus a high bioavailability of mercury, at these sites with TC values much higher than reported elsewhere in the literature.

Further characterization of the mercury speciation was done using, this time, geochemical modeling and sequential extraction procedures (SEP). Obtained models suggested the predominance of elemental mercury as the major inorganic mercury species in both water and soil samples. Other inorganic mercury species such as mercury chlorides ($HgCl_x^{+2-x}$), Hg^{2+} and $Hg(OH)_2$ also occurred at a relatively high level.

It was also shown that elemental mercury mainly from TSFs, enters the water system through drainage during the wet season where it oxidizes, depending on environmental conditions such as AMD, and becomes available for uptake by living organisms. The bioavailable mercury is then susceptible to methylation and subsequent bioaccumulation in the food web. Once mercury enters the water system, it migrates away from the source and becomes a threat for ecosystems such as the Schoonspruit, the Varkenslaagte canal or the Krugersdorp Game Reserve watersheds and other neighboring ecosystems.

Under reducive conditions, mercury species are converted to the elemental form or to insoluble complexes such as $Hg(OH)_2$ or HgS and are removed from the water system through precipitation or adsorption at the surface of the sediment. This may explain the relatively low level of mercury measured in most of the study waters during the dry season. An exception was the Randfontein creek which still showed elevated mercury values even during the dry season. However, mercury concentrations in waters from this site are expected to be considerably higher during wet seasons due to the remobilization of mercury from the bottom sediment.

It has to be emphasized that conclusions presented in this work are partial and require more extensive sampling by a well equipped team and long-term monitoring for a clear understanding of the observed trends.

This study is an important contribution to the assessment of the ecosystem impact of South African mining operations in terms of mercury pollution since it presents, for the very first time, the problem of mercury pollution from gold mining operations in the general context of the Witwatersrand Basin, one of the biggest gold mining areas in the world. It also provides information on the mercury speciation, migration and fate in the region which can be used as a benchmark to understand the unknown transport patterns of mercury in the South(ern) African semi-arid environment.

References

ACAP (2005) Assessment of Mercury Releases from the Russian Federation, Tech. rep., Arctic Council Action Plan to Eliminate Pollution of the Arctic (ACAP), Copenhagen, Denmark.

AGA (2008a) AngloGold Ashanti, Vaal River Country Report 2008, pp61.

AGA (2008b) AngloGold Ashanti, West Wits Country Report 2008, pp55.

AGA (2008c) AngloGold Ashanti, Mineral Resource and Ore Reserve Report 2008, pp165.

AGA (2009a) AngloGold Ashanti West Wits Environmental Management programme, 8 separated chapters, Unpublished.

AGA (2009b) AngloGold Ashanti Vaal River Environmental Management programme, 8 separated chapters, Unpublished.

AGA (2010) AngloGold Ashanti Reportable environmental incidents during 2009, available at wvvw.anglogold.co.za/subwebs/informationforinvestors/.. 7gri-EN23.pdf, accessed on 29/11/2011.

Aguerre, S., Bancon-Montigny, C., Lespes, G. and Potin-Gautier, M. (2000) Solid phase microextraction (SPME): a new procedure forthe control of butyl- and phenyltin pollution in the environment by GC-FPD, Analyst, 125, 263-268.

Ali, I., Gupta, V.K. and Aboul-Enein, H.Y. (2005) Metal ion speciation and capillary electrophoresis: Application in the new millennium, Electrophoresis, 26, 3988- 4002.

Allan, C.J., and Heyes, A. (1998) A preliminary assessment of wet deposition and episodic transport of total and methyl mercury from low order Blue Ridge watersheds, S.E. U.S.A., Water Air Soil Pollut. 105, 573-592.

Allan, C.J., Heyes, A., Roulet, N.T., St. Louis, V.L. and Rudd, J.W.M. (2001) Spatial and temporal dynamics of mercury and organic carbon in Precambrian Shield runoff, Biogeochem. 52, 13-40.

AMAP/UNEP (2008) Technical Background Report to the Global Atmospheric Mercury Assessment, Tech. rep., Arctic Monitoring and Assessment Programme/UNEP Chemicals Branch.

Amouroux, D. (2007) Mercury speciation course Part 1: Mercury speciation overview and sample preparation methods for solid samples, South African Mercury Assessment Programme (SAMA) Seminar, Johannesburg, 15-16 February 2007.

Amouroux, D., Tesaer, E., Pecheyran, C. and Donard, 0.F.X. (1998) Sampling and probing volatile metal(loid) species in natural waters by in-situ purge and cryogenic trapping followed by gas chromatography and inductively coupled plasma mass spectrometry (P-CT-GC-ICP/MS), Analytica Chimica Acta, 377, 241-254.

Amouroux, D., Wasserman, J.C., Tessier, E. and Donard, O.F.X. (1999) Elemental Mercury in the Atmosphere of a Tropical Amazonian Forest (French Guiana), Environ. Sci. Technol., 33 (17), 3044-3048.

Amyot, M., Lean, D. and Mierle, G. (1997) Photochemical formation of volatile mercury in high arctic lakes, Environ. Toxicol. Chem., 16, 2054-2063.

Appleton, J.D., Williams, T., Orbea, H. and Carrasco, M. (2001) Fluvial contamination associated with artisanal gold mining in the Ponce Enríquez, Portovelo-Zaruma and Nambija areas, Ecuador, Water Air Soil Pollut., 131, 19-39.

Armstrong, H.L., Corns, W.T., Stockwell, P.B., O'Connor, G., Ebdon, L. and Evans, E.H. (1999) Comparison of AFS and ICP MS detection coupled with gas chromatography for the determination of methylmercury in marine samples, Analytica Chimica Acta, 390, 245-253.

Ashley, R.P., Rytuba, J.J., Rogers. R., Kotlyar, B.B. and Lawler, D. (2002) Preliminary Report on Mercury Geochemistry of Placer Gold Dredge Tailings, Sediments, Bedrock, and Waters in the Clear Creek Restoration Area, Shasta County, California, U.S. Geological Survey Open-File Report 02–401, pp47.

ASTM (2000) Standard methods D1757, D2361, D2492, D2795, D3174, D3177, D3682, D3761, D4208, D4239, D4326, and D5016, Gaseous Fuels; Coal and Coke, vol. 05.06, American Society for Testing and Materials, Philadelphia, PA, 606 pp.

ASTM (2007a) ASTM Method D2492 – 02 Standard Test Method for Forms of Sulfur in Coal. Available at http://www.astm.org/Standards/D2492.htm.

ASTM (2007b) ASTM Method D3177 – 02 Standard Test Methods for Total Sulfur in the Analysis Sample of Coal and Coke. Available at http://www.astm.org/Standards/D3177.htm.

ATSDR (1999) Toxicological Profile for Mercury, U.S. Department of Health and Human Services, Agency for Toxic Substances and Disease Registry, Atlanta, Georgia.

Babiarz, C.L., Hurley, J.P., Hoffmann, S.R., Andren, A.W., Shafer, M.M. and Armstrong, D.E. (2001) Partitioning of total mercury and methylmercury to the colloidal phase in freshwaters, Environ. Sci. Tech.**,** 35, 4773-4782.

Baeyens, W. (1992) Speciation of mercury in different compartments of the environment, Trends Anal. Chem., 11, 245-254.

Baker, P.G.L., Brunke, E-G., Slerm, F. and Crouch, A.M. (2002) Atmospheric mercury measurements at Cape Point, South Africa, Atmos. Environ., 36, 2459-2465.

Barcelo, D. (1993) Environmental analysis: techniques, applications, and quality assurance, Nature, Elsevier, Amsterdam, p646.

Barkow, L. (1999) Site characterization for abandoned mine/mill sites, modification 1, U.S. Bureau of Land Management, National Applied Resource Sciences Center, Information Bulletin RS-2000-021, November 18, 1999, pp3.

Benes, P., and B. Havlik. (1979) Speciation of Mercury in Natural Waters, In: Biogeochemistry of Mercury in the Environment, Nriagu, J.O. (ed,), The Elsevier, North-Holland Biomedical Press, Amsterdam, pp.176-202.

Benoit, J.M., Mason, R.P. and Gilmour, C.C. (1999a). Estimation of mercury-sulfide speciation and bioavailability in sediment pore waters using octanol-water partitioning, Environ. Toxicol. Chem., 18, 2138-2141.

Benoit, J.M., Gilmour, C.C., Mason, R.P. and Heyes, A. (1999b). Sulfide controls on mercury speciation and bioavailability in sediment pore waters, Environ. Sci. Tech. 33, 951-957.

Benoit, J.M., Mason, R.P., Gilmour, C.C. and Aiken, G.R. (2001) Constants for mercury binding by dissolved organic matter isolates from the Florida Everglades, Geochim. Cosmochim. Acta, *65*, 4445-4451.

Benoit, J., Gilmour, C.C., Heyes, A., Mason, R.P. and Miller, C. (2003) Geochemical and biological controls over methylmercury production and degradation in aquatic ecosystems. In: Biogeochemistry of Environmentally Important Trace Elements, Chai, Y. and Braids, O.C. (eds.), ACS Symposium Series 835, American Chemical Society, Washington, DC., 262-297.

Berman, M. and Bartha, R. (1986) Levels of chemical versus biological methylation of mercury in sediments, Bull Environ Contam Toxicol., 36(3), 401-404.

Berman, M., Chase, T. and Bartha, R. (1990) Carbon flow in mercury biomethylation by *Desulfovibrio desulfuricans*, Appl. Environ. Microbiol., 56, 298-300.

Bettinelli, M., Baroni, U., Pastorelli, N., Bizzarri, G. and Taina, P. (1992) ICP-AES, GFAAS, XRF and NAA coal fly ash analysis: comparison of different analytical techniques, In: Vourvopoulos, G. (Ed.), Elemental Analysis of Coal and Its By-Products, World Scientific Press, Singapore, pp. 372-394.

Biringuccio, V. (1540) The Pirotechnia, Translated from the Italian with an introduction and notes by Smith, C.S. and Gnudi, M.T. (1943), The American Institute of Mining and Metallurgical Engineers (Inc.), New York.

Blester, H., Muller, G. and Scholer, H.F. (2002) Binding and mobility of mercury in soils contaminated by emissions from chlor-alkali plants, Sci Total Environ., 284(1-3),191-203**.**

Bloom, N.S. and Crecelius, E.A. (1983) Determination of mercury in seawater at sub-nanogram per liter levels, Marine Chemistry, 14 (1), 49-59.

Bloom, N.S.,Watras, C.J. (1989) Observations of methylmercury in precipitation, Science of the Total Environment, 87/88, 199.

Bloom, N.S. (1994) Influence of analytical conditions on the observed "reactive mercury" concentrations in natural fresh waters, In: Watras C, Hackabee J, editors. Mercury Pollution Integration and Synthesis, Boca Raton, FL, USA7 Lewis, 541-542.

Bloom, N.S., Colman, J.A. and Barber, L. (1997) Artifact formation of methyl mercury during aqueous distillation and alternative techniques for the extraction of methyl mercury from environmental samples, Fresenius J. Anal. Chem., 358, 371-377.

Bloom, N.S., Gill, G.A., Driscoll, C., Rudd, J. and Mason, R.P. (1999) Speciation and cycling of mercury in Lavaca Bay, Texas, sediments, Environ. Sci. Technol.**,** 33, 7-13.

Bond, G. and Thompson, D. (1999) Catalysis by gold, Cat. Rev.-Sci. Eng., 41, 319.

Boszke, L., Kowalski, A., Głosińska, G., Szarek, R. and Siepak, J. (2003) Selected factors affecting the speciation of mercury in the bottom sediments: an overview, Polish J. Environ. Stud., 12(1), 5-13.

Bothner, M.H. and Robertson D.E. (1975) Mercury contamination of sea water samples stored in polyethylene containers, Anal Chem, 47, 592-595.

Bowers Jr, G.N., Fassett, J. D. and White, E. V. (1993) IDMS and the National Reference System: Accuracy Transfer in Clinical Chemistry, Anal. Chem., 65(12), 475 – 479.

Bredell, J.H. (1987) South African coal resources explained and analysed, Geological Survey of South Africa, 1987–0154.

Bravo-Sanchez, L.R., Ruiz Encinar, J., Fidalgo Martinez, J.I. and Sanz-Medel, A. (2004) Mercury speciation analysis in sea water by solid phase microextraction-gas chromatography-inductively coupled plasma mass spectrometry using ethyl and propyl derivatization. Matrix effects evaluation, Spectrochim. Acta. Part B: At. Spectrosc., 59B, 59–66.

Brosset, C., Lord, E. (1995) Methylmercury in ambient air. Method of determination and some measurement results, Water Air and Soil Pollution, 82, 739–750.

Brown, H.R. and Swaine, D.J. (1964) Inorganic constituents of Australian coals, J. Inst. Fuel, 37, 422-440.

Brumbaugh, W.G., Petty, J.D., May, T.W. and Huckins, J.N. (2000) A passive integrative sampler for mercury vapor in air and neutral mercury species in water, Chemosphere: Global Change Science, 2, 1-9.

Cabanero, A.I., Madrid, Y., and Camara, C. (2002) Evaluation of different simple pre-treatment and extraction procedures for mercury speciation in fish simples, J. Anal. Atom. Spectrom., 17, 1595-1601.

Cai, Y., Jaffe, R. and Jones, R. (1997) Ethylmercury in the soils and sediments of the Florida Everglades, Environ. Sci. Technol., 31, 302-305.

Cai, Y. (2000) Atomic Fluorescence in Environmental Analysis, in: Encyclopedia of Analytical Chemistry, Meyers, R.A. (ed.), John Wiley & Sons Ltd, Chichester, pp. 2270-2292.

Cappon, C.J. (1987) Uptake and speciation of mercury and selenium in vegetable crops grown on compost-treated soil, Water Air Soil Pollut., 34, 353-361.

Caruso, J.A., Ackley, K.L. and Sutton K.L. (2000) Introduction in Elemental Speciation: New approaches for trace element analysis, J.A. Caruso, K.L. Ackley and K.L. Sutton (eds), vol. XXXIII, Elsevier. Amsterdam 1.

CEC (2001) Preliminary Atmospheric Emissions Inventory of Mercury in Mexico, Acosta y Asociados Project, Tech. Rep. 3.2.1.04.

CRC Handbook of Chemistry and Physics (2005) Lide, D.R. (ed.), 86th edition, CRC Press, 2616 pp.

Ceulemans, M. and Adams, F.C. (1996) Integrated sample preparation and speciation analysis for the simultaneous determination of methylated species of tin, lead and mercury in water by purge-and trap injection capillary gas chromatography atomic emission spectrometry, J. Anal. Atom. Spectrom., 11, 201-206.

Chamber of Mines (2004) Facts and Figures, Available online at: www.bullion.org.za.

Choi, S.-C. and Bartha, R. (1993) Cobalamin-mediated mercury methylation by *Desulfovibrio desulfuricans* LS, Appl. Environ. Microbiol., 59, 290-95.

Choi, S.-C., Chase, Jr., T. and Bartha, R. (1994) Metabolic pathways leading to mercury methylation in *Desulfovibrio desulfuricans*, Appl. Environ. Microbiol, 60, 4072-4077.

Choi, S.-C. and Bartha, R. (1994) Environmental factors affecting mercury methylation in estuarine sediments, Bull. Environ. Contam. Toxicol., 53, 805-812.

Churchill, R. (1999) Insights into California mercury production and mercury availability for the gold mining industry for the historical record, Geological Society of America Abstracts with Programs, 31, 45.

Churchill, R.C., Meathrel, C.E. and Suter, P.J. (2004) A retrospective assessment of gold mining in the Reedy Creek sub-catchment, northeast Victoria, Australia: residual mercury contamination 100 years later, Environmental Pollution, 132, 355-363.

Compeau, G. and Bartha, R. (1983) Effects of sea-salt anions on the formation and stability of methyl mercury, Bull. Environ. Contam. Toxicol., 31, 486-493.

Compeau, G.C. and Bartha, R. (1985) Sulfate-reducing bacteria: principal methylators of mercury in anoxic estuarine sediment, Appl. Environ. Microbiol., 50(2), 498-502.

Conrad, V.B. and Krofcheck, D.S. (1992) ICP-MS determination of trace elements in coal and other geological materials, In: Vourvopoulos, G. (Ed.), Elemental Analysis of Coal and Its By-Products, World Scientific Press, Singapore, pp. 97-123.

Cornelis, R., Heumann K.G., Caruso, J.A. and Crews, H. (2003) Introduction in: Handbook of Elemental Speciation, R. Cornelis, K.G. Heumann, .J.A. Caruso and H. Crews (eds).vol. l, Wiley-VCH.

Covelli, S., Faganeli, J., Horvat, M. and Brambati, A. (2001) Mercury contamination of coastal sediments as a result of long-term cinnabar mining activity (Golf of Trieste, northern Adriatic sea), Applied Geochemistry 16(5), 514-558.

Cox, J.A., Przyjazny, A., Schlyter, C. and Saari, R. (1992) Application of ion chromatography to the analysis of coal, In: Vourvopoulos, G. (Ed.), Elemental Analysis of Coal and Its By-Products, World Scientific Press, Singapore, pp. 33-48.

Dabrowski, J.M., Ashton P.J., Murray K., Leaner J.J., Mason R.P. (2008) Anthropogenic mercury emissions in South Africa: Coal combustion in power plants, Atmos Environ, 42, 6620-6626.

Dabrowski, J. (2010) Emissions of Mercury Associated with Coal-Fired Power Stations in South Africa, Report to the Department of Environmental Affairs of South Africa, February 2010.

Dai, Q., Feng, X., Qiu, G. and Jiang, H. (2004) Preliminary study on mercury contamination in gold mining in Tongguan County of Shanxi Province, Environ. Chem., 23, 460–464.

Davidson, R.M. (2000) Modes of Occurrence of Trace Elements in Coal, Report CCC/36, International Energy Agency Coal Research, London 36 pp.

Demuth, N. and Heumann, K.G. (2001) Validation of methylmercury determinations in aquatic systems by alkyl derivatization methods for GC analysis using ICP-IDMS, Analytical Chemistry, 73, 4020-4027.

Dennis, I., Pretorius, J., van Deventer, P. and Steyl, G. (2008) Methods to Assess the Impacts of Tailings Dams on the Groundwater System in South Africa, Journal of Mining and Metallurgy, 44 A (1), 59 – 66.

De Smaele, T., Moens, L. Darns, R., Sandra, P., Van der Eycken, J. and Vandyck, J. (1998) Sodium tetra(n-propyl)borate: a novel aqueous in situ derivatization reagent for the simultaneous determination of organomercury, -lead and -tin compounds with capillary gas chromatography-inductively coupled plasma mass spectrometry, Journal of Chromatography A, 793, 99-106.

De Smaele,T., Moens, L., Sandra, P. and Darns, R. (1999) Determination of organometallic compounds in surface water and sediment samples with SPME-CGC-ICPMS, Mikrochimica Acta, 130, 241-251.

Diederich, H.J., Meyer, S. and Schotz, F. (1994) Automatic adsorptive stripping voltammetrv at thin-mercurv film electrodes (TMFE), Fresenius J. Anal. Chem., 349, 670-675.

Dietz, C., Madrid, Y., and Camara, C. (2001) Mercury speciation using the capillary cold trap coupled with microwave induced plasma atomic emission spectrometry, J. Anal. Atom. Spectrom., 16, 1397-1402.

Dirkx, W., Lobinski, R. and Adams, F.C. (1993) A comparative modelling of gas chromatography with atomic absorption and atomic emission detection for the speciation analysis of organotins, Analytical Sciences, 9, 273-278.

Dixon, K.L. (1997) Background Concentrations of Metals in Wetland Soils On and Near the Savannah River Site, WSRC-MS-97-00692, Rev 1, pp19.

Domagalski, J. (1998) Occurrence and transport of total mercury and methyl mercury in the Sacramento River basin, California, Journal of Geochemical Exploration, 64, 277-291.

Domagalski, J.L., Knifong, D.L., Dileanis, P.D., Brown, L.R., May, J.T., Connor, V. and Alpers, C.N. (2000) Water quality in the Sacramento River Basin, California, 1994–1998, U.S. Geological Survey Circular 1215, pp36.

Donkor, A. K., Nartey, V. K., Bonzongo, J. C. and Adotey, D. K. (2006) Artisanal Mining of Gold with Mercury in Ghana, West Africa Journal of Applied Ecology, 9, ISSN: 0855-4307.

Doughten, M.W. and Gillison, J.R. (1990) Determination of selected elements in whole coal and in coal ash from the eight Argonne premium coal samples by atomic absorption spectroscopy, atomic emission spectroscopy, and ion-selective electrode, Energy Fuels, 4, 426-430.

Driscoll, C.T., Yan, C., Schofield, C.L., Munson, R. and Holsapple, H. (1994) The chemistry and bioavailability of mercury in Adirondack lakes, Environ. Sci. Technol., 28, 136A-I43A.

Dronen L.C, Moore A.E, Kozliak E.I. and Seames W.S. (2004) An assessment of acid wash and bioleaching pre-treating options to remove mercury from coal, Fuel, 83, 181.

Ebinghaus, R., Kock, H.H., Jennings, S.G., Mc Cartin, P. and Orren, M.J. (1995) Measurement of atmospheric mercury concentration in Northwestern and Central Europe – Comparison of experimental data and model results, Atmospheric Environment, 29 (22), 3333-3344.

Ebinghaus, R., Tripathi, R.M., Wallschlager, D. and Lindberg, S.E. (1999) Natural and anthropogenic mercury sources and their impact on the air-surface exchange of mercury on regional and global scales. In *Mercury Contaminate Sites: Characterization, Risk Assessment and Remediation*. Ebinghaus, R., Turner, R.R., de Lacerda, L.D., Vasiliev, O., Salomons, W. Eds., Springer-Verlag, Berlin, 1-50.

Ebinghaus, R., Slemr, F., Brenninkmeijer, C. A. M., van Velthoven, P., Zahn, A., Hermann, M., O'Sullivan, D. A., and Oram, D. E. (2007) Emissions of gaseous mercury from biomass burning in South America in 2005 observed during CARIBIC flights, Geophys. Res. Lett., 34, L08813, doi:10.1029/2006GL028866.

Edner, H., Faris, G.W., Sunesson, A. and Svanberg, S., (1989) Atmospheric atomic mercury monitoring using differential absorption LIDAR technique, Applied Optics, 28, 921.

EIA (2005) Energy Information Administration: National Energy Information Center, 1000 Independence Ave., SW Washington D.C., USA, Also available online at: www.eia.doe.gov.

EIA (2007) Annual Coal Report 2006, Energy Information Administration, DOE/EIA-0584 (2006), November 2007, National Energy Education, Available online at: http://www.eia.doe.gov/cneaf/coal/acr/acr.pdf

EIA (2008) Coal InorCard 2006, Energy Information Administration, January 2008.

EIA (2009) International Energy Outlook, Energy Information Administration, Tech. rep., 4726, Available at: http:30 //www.eia.doe.gov/oiaf/ieo/pdf/coal.pdf.

EMEP (2002) Sampling of mercury in precipitation and air, European Monitoring and Evaluation Programme, EMEP/CCC- Report 1/95.

Encinar, J.R., Alonso, J.I.G.A. and Sanz-Medel, A. (2000) Synthesis and application of isotopically labelled dibntyltin for isotope dilution analysis using gas ehromatography-ICP-MS, Journal of Analytical Atomic Spectrometry, 15, 1233-1239.

Encinar, J.R., Villar, M.I.M., Santamaria, V.G., Alonso J.I.G., and Sanz-Medel, A. (2001) Simultaneous determination of mono-, di-, and tributyltin in sediments by isotope dilution analysis using gas chromatography-ICPMS, Analytical Chemistry, 73, 3174-3180.

Environment Canada (2008) National Pollutant Release Inventory, Environment Canada, Tech. rep., Available online at: http://www.ec.gc.ca.

Evans, J.R., Sellars, G.A. and Johnson, R.G. (1990) Analysis of eight Argonne premium coal samples by X-ray fluorescence spectrometry, Energy Fuels, 4, 440-442.

Fadda, S., Rivoldini, A. and Cau, I. (1995) ICP-MS determination of 45 trace elements in whole coal using microwave oven acid digestion for sample preparation, Geostand. Newsl., 19, 41-54.

Falter, R. and Scholer, H.F. (1994) Interfacing HPLC and CV-AAS with on-line UV irradiation for the determination of organic-mercury compounds, J. chromatogr. A, 675, 253-256.

Fasset, J.D. and Paulsen, P.J. (1989) Isotope Dilution Mass Spectrometry, Anal. Chem., 61(10), 643A-649A.

Feng, X. and Hong, Y. (1999) Modes of occurrence of mercury in coals from Guizhou, People's Republic of China, Fuel, 78, 1181–1188.

Feng, X., Streets, D., Hao, J., Wu, Y., and Li, G. (2009) Mercury emissions from industrial sources in China, In: Mercury fate and transport in the global atmosphere (2009), Pirrone, N. and Mason, R. (eds.), Chap. 3, 67–79, Springer, New York.

Fernandez, R.G., Bayon, M.M., Alonso, J.I.G. and Sanz-Medel, A. (2000) Comparison of different derivatization approaches for mercury speciation in biological tissues by gas chromatography/inductively coupled plasma mass spectrometry, Journal of Mass Spectrometry, 35, 639-646.

Ferrara, R. (1999) Mercury mines in Europe: Assessment of emissions and environmental contamination. *In* Mercury Contaminated Sites (R. Ebinghaus, R.R. Turner, L.D. Lacerda, O. Vasiliev, & W. Salomons, eds.). Springer, Berlin, 51-72.

Ferrara, R., Mazzolai, B., Lanzillotta, E., Nucaro, E., and Pirrone, N. (2000) Volcanoes as emission sources of atmospheric mercury in the Mediterranean basin, Sci. Total Environ., 259, 115–10 121.

Feuilherade, P. (2010) South African Environment Pays Price for Century of Mining, Available at http://www.suite101.com/content/south-african-environment-pays-price-of-century-of-mining-a286577, accessed on 26 January 11.

Filby, R.H., Shah, K.R. and Sautter, C.A. (1977) A study of trace element distribution in the solvent refined coal (SRC) process using neutron activation analysis, J Radioanalyt Chem,37:693–704.

Finkelman, R.B. and Stanton, R.W. (1978) Identification and significance of accessory minerals from a bituminous coal, Fuel, 57, 763-768.

Finkelman, R.B. (1981) Modes of occurrence of trace elements in coal, U.S.G.S. Open-File Rep., 81-99, 312 pp.

Finkelman, R.B. (1982) Modes of occurrence of trace elements and minerals in coal: an analytical approach, In: Filby, R.H., Carpenter, B.S., Ragiani, R.C. (Eds.), Atomic and Nuclear Methods in Fossil Fuel Research, Plenum, New York, NY, pp. 141-149.

Finkelman, R.B. (1988) The inorganic geochemistry of coal: a scanning electron microscopy view, Scanning Microsc, 2, 97-105.

Finkelman, R.B., Palmer, C.A., Krasnow, M.R., Aruscavage, P.J., Sellars, G.A. and Dulong, F.T. (1990) Combustion and leaching behavior of elements in the Argonne premium coal samples, Energy Fuels, 4, 755-766.

Finkelman, R.B. (1994) Mode of occurrence of potentially hazardous elements in coal: levels of confidence, Fuel Process. Technol., 39, 21-34.

Finkelman, R.B., Orem, W., Castranova, V., Tatu, C.A., Belkin, H.E., Zheng, B., Lerch, H.E., Marharaj, S.V. and Bates, A.L. (2002) Health impacts of coal and coal use: Possible solutions, International Journal of Coal Geology, 50, 425-443.

Fish, R.H. (1983) Organometallic Geochemistry Isolation and Identification of Organoarsenic and Inorganic Arsenic Compounds from Green River Formation Oil Shale, In: Geochemistry and Chemistry of Oil Shales, ACS Symposium Series, Vol.230, ISBN 13: 9780841207998, Chapter 23, pp 423-432.

Fitzgerald, W.F. (1986) Cycling of mercury between the atmosphere and oceans, In: Buat-Menard P, editor, The Role of Air–Sea Exchange in Geochemical Cycling, D. Reidel Publishing, p. 363- 408.

Fitzgerald, W.F., Engstrom, D.R., Mason, R.P. and Nater, E.A. (1998) The case for atmospheric mercury contamination in remote areas, Environmental Science & Technology, 32(1), 1-7.

Fitzgerald, W.F., Gill, G.A. and Heurot, A.D. (1984) Air-sea Exchange of Mercury, in C. C. S. Wang, E. Boyle, K.W. Bruland, J.D. Burton and E.D. Goldberg (eds), Trace Metals in Seawater, pp.297–315.

Fitzgerald, W.F. and Lamborg, C.H. (2003) Geochemistry of Mercury in the Environment. In: Lollar, B.S. (ed.), Environmental Geochemistry, Treatise on Geochemistry, Volume 9, Chapter 4, Elsevier Publ.

Fitzgerald, W.F., Mason, R.P. and Vandal, G.M. (1991) Atmospheric cycling and air-water exchange of mercury over mid-continental lacustrine regions, Water Air Soil Pollut., 56, 745-767.

Fogg, T.R. and Fitzgerald, W.F. (1979) Mercury in southern New England rains, J. Geophys. Res., 84, 6987-6988.

Forstner, U. and Wittmann, G.T.W. (1976) Metal Accumulations in Acidic Waters from Gold Mines in South Africa, Geoforum, 7, 41-49.

Forsyth, D.S. and Marshall, W.D. (1985) Performance of an automated gas chromatograph-silica furnace-atomic absorption spectrometer for the determination of alkyllead compounds, Analytical Chemistry, 57, 1299-1305.

Fourie, C.J.S., Du Plessis, S.J., and Henry, G. (2008) New airborne geophysical data from the Waterberg coalfield. South Africa's major future energy source. Science real and relevant: 2nd CSIR Biennial Conference, CSIR International Convention Centre Pretoria, 17 and 18 November 2008, pp 9. Available online at: http://hdl.handle.net/10204/2568.

Friedli, H.R., Radke, L.F., and Lu, J.Y. (2003) Mercury in smoke from biomass fires, Geophys. Res. Lett.**,** 28, 3223-3226.

Fuge, R., Pearce, N.J.G., and Perkins, W.T. (1992) Mercury and gold pollution, Nature, 357, 369.

Fujiki, M. and Tajima, S. (1992) The pollution of Minamata Bay by mercury, Wat. Sci. Technol., 25, 133-140.

Furch, K., Junk, W.J. and Klinge, H. (1982) Unusual chemistry of natural waters from the Amazon region, Acta Cient. Venez., 33, 269-273.

Gabriel, M.C., Williamson, D.G., Brooks, S. and Lindberg, S. (2005) Atmospheric speciation of mercury in two contrasting Southeastern US airsheds, Atmos. Environ.**,** 39, 4947-4958.

Gallus, S.M. and Heumann, K.G. (1996) Development of a gas chromatography inductively coupled plasma isotope dilution mass spectrometry system for accurate determination of volatile element species. Part 1. selenium speciation, Journal of Analytical Atomic Spectrometry, 11, 887-892.

Ganguli, P.M., Mason, R.P., Abu-Saba, K.E., Anderson, R.S. and Flegal, A.R. (2000) Mercury Speciation in Drainage from the New Idria Mercury Mine, California, Environ. Sci. Technol., 34, 4773-4779.

Gao, E., Jiang, G., He, B., Yin, Y. and Shi, J. (2008) Speciation of mercury in coal using HPLC-CV-AFS system: Comparison of different extraction methods, Journal of Analytical Atomic Spectrometry, 23, 1397-1400.

Garcia-Sanchez, A., Contreras, F., Adams, M. and Santos, F. (2006) Atmospheric mercury emissions from polluted gold mining areas (Venezuela), Environ. Geochem. Health, 28, 529-540.

Geerdink, R.B., Breidenbach, R., Epema, O.J. (2007) Optimization of headspace solid-phase microextraction gas chromatography-atomic emission detection analysis of Monomethylmercury, J. Chromatogr., A., 1174, 7–12.

Gill, G.A. and Fitzgerald, W.F. (1985) Mercury sampling of open ocean water at the picomolar level, Deep Sea Res., 32, 287-97.

Gilmour, C.C. and Riedel, G.S. (1995) Measurement of Hg methylation in sediments using high specific-activity ^{203}Hg and ambient incubation, Water Air Soil Pollut., 80, 747–756.

Gilmour, C.C., Riedel, G.S., Ederington, M.C., Bell, J.T., Benoit, J.M., Gill, G.A. and Stordal, M.C. (1998) Methylmercury concentrations and production rates across a trophic gradient in the northern Everglades, Biogeochemistry, 40, 327-345.

Gluskoter, H.J. (1965) Electronic low-temperature ashing of bituminous coal, Fuel, 44, 285-291.

Gluskoter, H.J., Ruch, R.R., Miller, W.G., Cahill, R.A., Dreher, G.B. and Kuhn, J.K. (1977) Trace Elements in Coal: Occurrence and Distribution, Circular, vol. 499, Illinois State Geological Survey, Urbana, IL, 154 pp.

Gong, J.L., Ojifinni, R.A., Kim, T.S., Stiehl, J.D., McClure, S.M., White, J.M. and Mullins, C.B. (2007) Low temperature CO oxidation on Au(111) and the role of adsorbed water, Top. Catal., 44, 57-63.

Gong, J. and Mullins, C.B. (2009) Surface Science Investigations of Oxidative Chemistry on Gold, Accounts of Chemical Research, 42, 8, 1063-1073.

Goodarzi, F., Huggins, F.E., and Sanei, H. (2008) Assessment of elements, speciation of As, Cr, Ni and emitted Hg for a Canadian power plant burning bituminous coal, International Journal of Coal Geology, 74, 1-12.

Gray, J.E., Theodorakos, P.M., Bailey, E.A. and Turner, R.R. (2000) Distribution, speciation, and transport of mercury in streamsediment, stream-water, and fish collected near abandoned mercury mines in southwestern Alaska, USA, The Science of the Total Environment, 260, 21-33.

Grigal, D.F. (2002) Inputs and outputs of mercury from terrestrial watersheds: a review, Environ. Rev., 10, 1-39.

Gustin, M.S., Lindberg, S., Austin, K., Coolbaugh, M., Vetter, A. and Shang, Z. (2000) Assessing the contribution of natural sources to regional atmospheric mercury budgets, Sci. Total Environ.**,** 25, 961-971.

Haas, K., Feldmann, J., Wennrich, R. and Stark, H.J. (2001) Species-specific isotope-ratio measurements of volatile tin and antimony compounds using capillary GC-ICP-time of flight MS, Fresenius Journal of Analytical Chemistry, 310, 587-596.

Hagelskamp, H.H.B., Eriksson, P.G., and Snyman, C.P., (1988) The effect of depositional environment on coal distribution and quality parameters in a portion of the Highveld Coalfield, South Africa, International Journal of Coal Geology, 10, 51-77.

Haitzer, M., Ryan, J. and Aiken, G.R. (2002) Binding of Hg(II) to DOM: the role of Hg (II) to DOM concentration ratio, Environ. Sci. Tech., 36, 3564-3570.

Harris, R., Krabbenhoft, D.P., Mason, R., Murray, M.V., Reash, R. and Saltman, T. (2007) Ecosystem Responses to Mercury Contamination, Indicators of Change, SETAC, New-York.

Hartnady, C.J.H. (2009) South Africa's gold production and reserves, South African Journal of Science, 105, 328-229.

Heisterkamp, M. and Adams, F.C. (2001) Gas chromatography-inductively coupled plasma-time-of-flight mass spectrometry for the speciation analysis of organolead compounds in environmental water samples, Fresenius Journal of Analytical Chemistry, 370, 597-605.

Heller, A.A. and Weber, J.H. (1998) Seasonal study of speciation of mercury(II) and monomethylmercury in *Spartina alterniflora* from the Great Bay estuary, NH, Sci. Total Environ., 221, 181-188.

Heumann, K.G., Gallus, S.M., Radlinger, G. and Vogl, J. (1998) Accurate determination of element species by on-line coupling of chromatographic systems with ICP-MS using

isotope dilution technique, Spectrochimica Acta, Part B-Atomic Spectroscopy, 53, 273-287.

Hines, N.A., Brezonik, P.L. and Engstrom, D.R. (2004) Sediment and Porewater Profiles and Fluxes of Mercury and Methylmercury in a Small Seepage Lake in Northern Minnesota, Environ. Sci. Technol., 38, 6610-6617.

Hintelrnann, H., Evans, R.D. and Villeneuve, J.Y. (1995) Measurement of mercury methylation in sediments by using enriched stable mercury isotopes combined with methylmercury determination by gas chromatography-inductively coupled plasma mass spectrometry, Journal of Analytical Atomic Spectrometry, 10, 619-624.

Hintelmann, H. (1999) Comparison of different extraction techniques used for methylmercury analysis with respect to accidental formation of methylmercury during sample preparation. Chemosphere, 39, 1093–1105.

Hodgson, F.D.I. and Krantz, R.M., (1998) Groundwater quality deterioration in the Olifants River catchment above the Loskop dam with specialised investigations in the Witbank dam sub-catchment, Report to the Water Research Commission by the Institute for Groundwater Studies, University of the Orange Free State, South Africa, WRC Report No. 291/1/98.

Hoenig, M. (2001) Preparation steps in environmental trace element analysis: facts and traps, Talanta, 54, 1021-1038.

Hoffart, A., Seames, W., Kozliak, E., Riedinger, S., Francini, J. and Carlson, C. (2006) A two-step acid mercury removal process for pulverized coal, Fuel, 85, 1166-1173.

Hornberger, M.I., Luoma, S.N., van Geen, A., Fuller, C., and Anima, R. (1999) Historical trends of metals in the sediments of San Francisco Bay, California: Marine Chemistry, 64, 39–55.

Horvat, M., Bloom, N., and Liang, L. (1993) Comparison of distillation with other current isolation methods for the determination of methylmercury compounds in low-level environmental samples, Part I Sediments, Anal. Chim. Acta, 281, 135–152.

Horvat, M., Covelli, S., Faganelli, J., Logar, M., Mandic, V., Rajar, R., Sirca A. and Zagar, D. (1999) Mercury in contaminated coastal environments; a case study: The Gulf of Trieste, Sci Total Environ., 237/238, 43-56.

Huang, J.H. (2005) Artifact formation of methyl and ethylmercury compounds from inorganic mercury during during derivatization using sodium tetra(n-propyl)borate, Anal. Chim. Acta, 532, 113-120.

Huckabee, J.W. and Janzen, S.A. (1975) Mercury in moss: derived from the atmosphere or from the substrate?, Chemosphere 1, 55-60.

Hudson, R.J.M., Gherini, S.A., Watras, C.J., and Porcella, D.B. (1994) Modeling the biogeochemical cycle of mercury in lakes: the mercury cycling model (MCM) and its application to the MTL study lakes. In Mercury Pollution: Integration and Synthesis, Watras, C. and Huckabee, J (eds.), Lewis Publishers, Ann Arbor, MI, chap. V.1, pp. 473-526.

Huerta-Diaz, M.A. and Morse, J.M. (1992) Pyritization of trace metals in anoxic marine sediments, Geochim. Cosmochim. Acta, 56, 2681-2702.

Huggins, F.E. (2002) Overview of analytical methods for inorganic constituents in coal, International Journal of Coal Geology, 50,169-214.

Huggins, F.E., Shah, N. and Huffman, G.P. (1992) Determination of organic sulfur forms in coal by XAFS spectroscopy, In: Vourvopoulos, G. (Ed.), Elemental Analysis of Coal and Its By-Products, World Scientific Press, Singapore, pp. 165-184.

Huggins, F.E., Srikantapura, S., Parekh, B.K., Blanchard, L. and Robertson, J.D. (1997) XANES spectroscopic characterization of selected elements in deep-cleaned fractions of Kentucky #9 coal, Energy Fuels, 11, 691-701.

Hunerlach, M.P. and Alpers, C.N. (2003) Mercury contamination from hydraulic gold mining in the Sierra Nevada, California, in Gray, J.E., ed., Geologic Studies of Mercury by the U.S. Geological Survey, U.S. Geological Survey Circular 1248, p. 23-27.

Huo, D. and Kingston, H. M. (2000) Correction of Species Transformations in the Analysis of Cr(VI) in Solid Environmental Samples Using Speciated Isotope Dilution Mass Spectrometry, Anal. Chem., 72(20), 5047-5054.

Hürkamp, K., Raab, T. and Völkel, J. (2009) Lead pollution of floodplain soils in a historic mining area-age, distribution and binding forms, Water Air Soil Poll., 201(104), 331-345.

Hurley, J.P., Krabbenhoft, D.P., Babiarz, C.L. and Andren, A.W. (1994) Cycling processes of mercury across sediment/water interfaces in seepage lakes. In: Environmental Chemistry of Lakes and Reservoirs, Baker, L.A. (ed.), Advances in Chemistry Series, American Chemical Society, Washington, D.C., 426-449.

IAEA (2003) Development and use of reference materials and quality control materials, International Atomic Energy Agency, IAEA-TECDOC-1350, ISBN 92–0–103303–6, Vienna.

Ikavalko, E., Laitinen, T. and Revitzer, H. (1999) Optimised method of coal digestion for trace metal determination by atomic absorption spectroscopy, Fresenius J. Anal. Chem., 363, 314-316.

IRMM (2010) Certified Reference Materials, Institute for Reference Materials and Measurements (IRMM), Distributed By: Analytical Reference Materials International, USA.

ISO (2003) Natural gas — Determination of mercury — Part 2: Sampling of mercury by amalgamation on gold/platinum alloy, International Organization for Standardization, ISO 6978-2.

Intawongse, M. and Dean, J.R. (2006) Uptake of heavy metals by vegetable plants grown on contaminated soil and their bioavailability in the human gastrointestinal tract, Food Addit. Contam., 23(1), 36-48.

Iverfeldt, A. (1991) Occurrence and turnover of atmospheric mercury over Nordic countries, Water, Air and Soil Pollution, 56, 251-265.

Iwashita, A., Tanamachi, S., Nakajima, T., Takanashi, H. and Ohki, A. (2004) Removal of mercury from coal by mild pyrolysis and leaching behavior of mercury, Fuel, 83, 631-638.

Jackson, T.A. (1988). The mercury problem in recently formed reservoirs of northern Manitoba (Canada): effect of impoundment and other factors on the production of methylmercury by microorganisms in sediments, Can. J. Fish. Aquat. Sci., 45, 97-121.

Jackson, T.A. (1997). Long-range atmospheric transport of mercury to ecosystems, and the importance of anthropogenic emissions — a critical review and evaluation of published evidence, Environ. Rev., 5, 99–120.

Jeffrey, L.S. (2005) Characterization of the coal resources of South Africa, The Journal of The South African Institute of Mining and Metallurgy, 95-102.

Jenkins, R.G. and Walker Jr., P.L. (1978) Analysis of mineral matter in coal, In: Karr, C. (Ed.), Analytical Methods for Coal and Coal Products, vol. II, Academic Press, New York, NY, pp. 265-292, Chap. 26.

Jensen, S. and Jernelov, A. (1969) Biological methylation of mercury in aquatic organisms, Nature, 223, 753-754.

Jia, X.Y., Gong, D.R., Han, Y., Wei, C., Duan, T.C. and Chen, H.T. (2011) Fast speciation of mercury in seawater by short-column high-performance liquid chromatography hyphenated to inductively coupled plasma spectrometry after on-line cation exchange column preconcentration, Talanta, doi:10.1016/j.talanta.2011.10.026.

Jiang, Z., Fan, Y., Chen, M., Liang, A., Liao, X., Wen, G., Shen, X., He, X., Pan, H. and Jiang, H. (2009) Resonance Scattering Spectral Detection of Trace Hg^{2+} Using Aptamer-Modified Nanogold as Probe and Nanocatalyst, Anal. Chem., 81, 5439-5445.

Kannan, K. and Falandysz, J. (1998) Speciation and concentration of mercury in certain coastal marine sediments, Water, Air and Soil Pollut., 103, 129-136.

Kaplan, D.L., Myers, J., Knox, A.C., lverson, G. and Serkiz, S. (2000) Mercury Speciation Modeling Using Site Specific Chemical and Redox Data from the TNXOD OU, a Westinghouse Savannah River Company Report, WSRC-TR-2000-OO058, pp44.
Keeler, G., Glinsorn, G. and Pirrone, N. (1995) Particulate mercury in the atmosphere: its significance, transport, transformation and sources, Water, Air and Soil Pollution, 80, 159-168.

Kelley, K.D. and Hudson, T. (2007) Natural versus anthropogenic dispersion of metals to the environment in the Wulik River area, western Brooks Range, northern Alaska, Geochemistry: Exploration, Environment, Analysis, 7, 87-96.

Kelly, C.A., Rudd, J.W.M., St. Louis, V.L., and Heyes, A. (1995) Is total mercury concentration a good predictor of methyl mercury concentration in aquatic systems?, Water, Air, and Soil Pollution, 80, 715-724.

Kim, A.W., Foulkes, M.E., Ebdon, L., Hill, S.J., Patience, R.L., Barwise, A.G. and Rowland S.J. (1992) Communications. Construction of a capillary gas chromatography inductively coupled plasma mass spectrometry transfer line and application of the technique to the analysis of alkyllead species in fuel, Journal of Analytical Atomic Spectrometry, 7, 1147-1149.

Kim, T. S., Gong, J., Ojifinni, R.A., White, J.M. and Mullins, C.B. (2006) Water activated by atomic oxygen on Au(111) to oxidize CO at low temperatures, J. Am. Chem. Soc., 128, 6282-6283.

Kim, C.S., Rytuba, J.J. and Brown, Jr., G.E. (2004) Geological and Anthropogenic Factors Influencing Mercury Speciation in Mine Wastes: an EXAFS spectroscopy study, Applied Geochemistry, 19, 379-393.

King, J.K., Kostka, J.E. and Frischer, M.E. (2000) Sulfate-reducing bacteria methylate mercury at variable rates in pure culture and in marine sediments, Appl. Environ. Microbiol., 66(6), 2430-2437.

Kingston, H. M. (1995) Method of Speciated Isotope Dilution Mass Spectrometry, US Patent Number: 5, 414, 259.

Kingston, H.M., Huo, D., Lu,Y. and Chalk, S. (1998) Accuracy in Species Analysis Speciated Isotope Dilution Mass Spectrometry (SIDMS) Exemplified by the Evaluation of Chromium Species, Spectrochim. Acta, Part B: Atomic Spectroscopy, 53B(2), 299-309.

Kiss, L.T. (1966) X-ray fluorescence in determination of brown coal inorganics, Anal. Chem., 38, 1713-1715.

Klobes, P., Meyer, K**.** and Ronald G. Munro, R.G. (2006) Porosity and Specific Surface Area Measurements for Solid Materials, National Institute of Standards and Technology, Special Publication 960-17, Washington, pp89.

Kolker, A., Crowley, S., Palmer, C.A., Finkelman, R.B., Huggins, F.E., Shah, N. and Huffman, G.P. (2000) Mode of occurrence of arsenic in four U.S. coals, Fuel Process, Technol., 63, 167-178.

Kolker, A., Mroczkowski, S.J., Palmer, C.A., Dennen, K.O., Finkelman, R.B. and Bullock Jr, J.H. (2002) Toxic substances from coal combustion-a comprehensive assessment phase II: element modes of occurrence for the Ohio 5/6/7, Wyodak, and North Dakota coal samples, Final technical report, DOE interagency Agreement DE-AC22-95PC95145, DOE Contract DE-AC22-95PC95101.

Kolker, A., Tewalt, S.J. and Finkelman, R. (2011) Summary of USGS Coal Quality Data for Mercury and Chlorine in South African Coal, MEC workshop 8, 18-20 May 2011, Kruger, South Africa.

Kortatsi, B.K. (2006) Concentration of Trace Metals in Boreholes in the Ankobra Basin, Ghana, West African Journal of Applied Ecology, ISSN: 08554307, pp16, Available at www.ajol.info/index.php/wajae/article/view/45706/29185, accessed on 29/11/2011.

Korthals, E.T. and Winfrey, M.R. (1987) Seasonal and Spatial Variations in Mercury Methylation and Demethylation in an Oligotrophic Lake, Appl. Environ. Microbiol., 53, 2397-2404.

Kotrebai, M., Birringer, M., Tyson, J.F., Block, E. and Uden, P.C. (1999) Identification of the principal selenium compounds in selenium-enriched natural sample extracts by ion-pair liquid chromatography with inductively coupled plasma- and electrospray ionization-mass spectrometric detection, Analytical Communications, 36, 249-252.

Krabbenhoft, D.P., Wiener, J.G., Brumbaugh, W.G., Olson, M.L., DeWild, J.F., and Sabin, T.J. (1999) A national pilot study of mercury contamination of aquatic ecosystems along multiple gradients, In US Geological Survey Toxic Substances Hydrology Program, Proceeding of the Technical Meeting, Volume 2, Morganwalp, D.W. and Buxton, H. T. (eds), Contamination of Hydrologic Systems and Related Ecosystems: USGS, Water-resources Investigations Report 99-4018B, United States Geological Survey, Reston, VA, 147-160.

Krabbenhoft, D.P., Benoit, J.M., Babiarz, C.L., Hurley, J.P. and Andren, A.W. (1995) Mercury cycling in the Allequash Creek watershed, northern Wisconsin, Water Air Soil Pollut., 80, 425-433.

Krabbenhoft, D.P., Branfireun, B.A. and Heyes, A. (2005) Biogeochemical cycles affecting the speciation, fate and transport of mercury in the environment, Mineralogical Association of Canada, Short Course 34, Chapter 8, Halifax, Nova Scotia, 139-156.

Kroschwitz, J.I. and Grant, M.H. (1993) Chlorocarbons to Combustion, In: Encyclopaedia of Chemical Technology, Separation Science, 4th ed, Technology, John Wiley and Sons, inc, USA, pp 423-539.

Krupp, E.M., Pecheyran, C. Pinaly, H., .Motelica-Heino, M., Koller, D., Young, S.M.M., Brenner, I.B. and Donard, O.F.X. (2001a) Isotopic precision for a lead species (PbEt4) using capillary gas chromatography coupled to inductively coupled plasma-multicollector mass spectrometry, Spectrochimica Acta Part B: Atomic Spectroscopy, 56, 1233-1240.

Krupp, E.M., Pecheyran, C., Meffan-Main,S. And Donard, 0.F.X. (2001b) Precise isotope-ratio measurements of lead species by capillary gas chromatography hyphenated to hexapole Multicollector ICP-MS , Fresenius Journal of Analytical Chemistry, 370(5), 573-580.

Kuban, P., Houserova, P., Kuban, P., Hauser, P.C. and Kuban, V. (2007) Mercury speciation by CE: A review, Electrophoresis, 28, 58-68.

Kuhn, J.T., Harfst, W.F. and Shimp, N.F. (1975) X-ray fluorescence analysis of whole coal, In: Babu, S.P. (Ed.), Trace Elements in Fuel. Adv. Chem. Ser., vol. 141, American Chemical Society, Washington, DC, pp. 66–73, Chap. 6.

Laban, K.L. and Atkin, B.P. (1999) The determination of minor and trace element associations in coal using a sequential microwave digestion procedure, Int. J. Coal Geol., 41, 351-369.

Labatzke, T. and Schlemmer, G. (2004) Anal. Bioanal. Chem., 378, 1075-1082.

Lacerda, L.D., De Paula, F.C.F., Ovalle, A.R.C., Pfeiffer, W.C. and Malm, O. (1990) Trace metals in fluvial sediments of the Madeira River watershed, Amazon, Brazil, The Science of the Total Environment, 97/98, 525-530.

Lacerda, L.D., Salomons, W., Pfeiffer, W.C. and Bastos, W.R. (1991) Mercury distribution in sediment profiles from lakes of the high pantanal, Mato Grosso State, Brazil, Biogeochemistry, 14, 91-97.

Lacerda, L.D (1995) Amazon mercury emissions, Nature, 374,20–21.

Lacerda, L.D. (1997) Global mercury emissions from gold and silver mining, Water Air Soil Pollut., 97, 209-221.

Lacerda, L.D. and Marins, R.V. (1997) Anthropogenic mercury emissions to the atmosphere in Brazil: the impact of gold mining, J Geochem Explor, 58, 223-229.

Lacerda, L.D. and Salomons, W. (1998) Mercury from gold and silver mining: a chemical time bomb?, Springer-Verlag Berlin Heidelberg Publishers, New York.

Lachas, H., Richaud, R., Jarvis, K.E., Herod, A.A., Dugwell, D.R. and Kandiyoti, R. (1999) Determination of 17 trace elements in coal and ash reference materials by ICP-MS applied to milligram sample sizes, Analyst, 124, 177-184.

Lambertsson, L., Lundberg, E., Nilsson, M., and Frech, W. (2001) Application of enriched stable isotope tracers in combination with isotope dilution GC-ICP-MS to study mercury species transformation in sea sediments during in situ ethylation and determination, J. Anal. Atom. Spectrom., 16, 1296-1301.

Lamborg, C.H., Fitzgerald, W.F., O'Donnell, J., and Torgersen, T. (2002) A non-steady-state compartmental model of global-scale mercury biogeochemistry with interhemispheric atmospheric gradients, Geochim. Cosmochim. Acta, 66(7), 1105-1118.

Lang, J. (1995) Coal mining in the life of South Africa: Power base, Jonathan Ball Publishers, Johannesburg, 231.

Lang, S. (2007) Environment-South Africa, Radioactive Water, the Price of Gold, Available at http://ipsnews.net/news.asp?idnews=40325, accessed on 26 January 2011.

Laperdina, T.G. (2002) Estimation of mercury and other heavy metal contamination in traditional gold mining areas of Transbaikalia, Geochemistry: Exploration, Environment, Analysis, 2(3), 219-223.

Laudal, D.L., Heidt, M.K., Galbreath, K.C., Nott, B.R., Brown, T.D., and Roberson, R.L. (1998) A comprehensive evaluation of flue gas mercury speciation methods, Report done for the U.S. DOE/EPRI contract DE-FC21-93MC30098.

Lawrence, S.J. (2003) Mercury in the Carson River Basin, Nevada, in Geologic Studies of Mercury by the U.S. Geological Survey, Gray, J.E. (ed), U.S. Geological Survey Circular 1248, pp29-33.

Lazaga, M.A., Wickham, D.T., Parker, D.H., Kastanas, G.N. and Koel, B.E. (1993) Reactivity of oxygen adatoms on the Au(111) surface, ACS Symp. Ser., 523, 90-109.

Leaner, J. (2006) South African Mercury Assessment Programme (SAMA) Workshop, 7-8 March 2006, CSIR, Pretoria.

Leaner, J. J., Dabrowski, J. M., Mason, R. P., Resane, T., Richardson, M., Ginster, M., Gericke, G., Petersen, C. R., Masekoameng, E., Ashton, P. J., and Murray, K. (2009) Mercury Emissions from Point Sources in South Africa, Springer, New York, Chap. 5, 113–130.

Lechler, J., Miller, J.R., Hsu, L.C. and Desilets, M.O. (1997) Mercury mobility at the Carson River Superfund Site, west-central Nevada, USA: interpretation of mercury speciation data in mill tailings, soils and sediments, J Geochem Exploration, 58, 259-267.

Leermakers, M., Galletti, S., De Galan, S., Brion, N. and Baeyens, W. (2001) Mercury in the southern North Sea and Scheldt Estuary, Mar. Chem., 75, 229–248.

Li, J., Lu, Y., Shim, H., Deng, X., Lian, J., Jiad, Z. and Lid, J. (2010) Use of the BCR sequential extraction procedure for the study of metal availability to plants, J. Environ. Monit., 12, 466–471.

Liang, L., Horvat, M., Feng, X., Shang, L., Li, H. and Pang, P. (2004) Re-evaluation of distillation and comparison with HNO_3 leaching/solvent extraction for isolation of methylmercury compounds from sediment/soil samples, Appl. Organometal. Chem., 18, 264–270.

Lichte, F.E. (1992) Analysis of coal by laser ablation inductively coupled plasma mass spectrometry, In: Vourvopoulos, G. (Ed.), Elemental Analysis of Coal and Its By-Products, World Scientific Press, Singapore, pp. 80-96.

Liebert. C.A., Hall, R.M. and Summers, A.O. (1999) Transposon Tn21, Flagship of the Floating Genome, Microbio. Mol. Biol. Rev., 63, 507-522.

Lindqvist, O., Jernelov, A., Johansson, K. and Rodhe, H. (1984) Mercury in the Swedish environment, global and local sources, SNV PM 1816, Swedish Environmental Protection Agency, S–171 85, Solna, Sweden.

Lindqvist, O. and Rodhe, H. (1985) Atmospheric mercury – A review, Tellus, 37B, 136–159.

Lindqvist, O., Johansson, K., Aastrup, M., Andersson, A., Bringmark, L., Hovsenius, G., Haakanson, L., Iverfeldt, A., Meili, M. and Timm, B. (1991) Mercury in the Swedish environment—recent research on causes, consequences and corrective methods, Water Air Soil Pollut., 55(1-2), 1-261.

Linge, K.L. (2006) Trace Element Determination by ICP-AES and ICP-MS: Developments and Applications Reported During 2004 and 2005, Geostandards and Geoanalytical Research, 157-174.

Liu, W. and Lee, H.K. (1999) Chemical modification of analytes in speciation analysis by capillary electrophoresis, liquid chromatography and gas chromatography, J. Chromatogr. A, 834, 45-63.

Lobinski, R. and Adams, F.C. (l997) Spectrochimica Acta, Part B-Atomic Spectroscopy, 52, 1865-l903.

Lobinski, R., Pereiro, I.R., Chassaigne, H., Wazik, A. and Szpunar J. (1998) Elemental speciation and coupled techniques—towards faster and reliable analyses, Journal of Analytical Atomic Spectrometry, 13, 859-867.

Lobinski, R., Sidelnikov, V., Patrushev, Y., Rodriguez, I. and Wasik, A. (1999) Multicapillary column gas chromatography with element-selective detection, Trac-Trends in Analytical Chemistry, 18, 449-460.

Logar, M., Horvat, M., Akagi, H., Ando, T., Tomiyasu, T., and Fajon, V. (2001) Determination of total mercury and monomethylmercury compounds in water samples from Minamata Bay, Japan: An interlaboratory comparative study of different analytical techniques, Appl. Organomet. Chem., 15, 515-526.

Logar, M., Horvat, M., Akagi, H. And Pihlar, B. (2002) Simultaneous determination of inorganic mercury and methylmercury compounds in natural waters, Anal. Bioanal. Chem., 374, 1015–1021.

Lottermoser, B.G. (2010) Mine Wastes: Characterization, Treatment and Environmental Impacts, Springer-Verlag Berlin Heidelberg, DOI 10.1007/978-3-642-12419-8_I.

Lu, J.Y., Schroeder, W.H., Berg, T., Munthe, J., Schneeberger, D. and Schaedlich, F. (1998) A device for sampling and determination of total particulate mercury in ambient air, Analytical Chemistry, 70, 2403-2408.

Lucotte, M., Mucci, A., Hillaire-Marcel, C., Pichet, P. and Grondin, A. (1995) Anthropogenic mercury enrichment in remote lakes of northern Quebec (Canada), Water Air Soil Poll., 80, 467-476.

Luo, K.L., Wang, W.Y., Yao, G.H., Mi, J.C., Zhang, H.M. and Yang, L.S. (2000) Mercury content and its distribution in Permo-carboniferous coal in Weibei area, Shannxi, Coal Geology and Exploration, 28 (3), 12–14 (In Chinese with English abstract).

Lusilao, J.G.M., (2009) Speciation of mercury in different environmental compartments. Design, development and optimization of analytical methods and procedures, Master dissertation, Wits University.

MacDonald, D.D., Ingersoll, C.G. and Berger, T.A. (2000) Development and Evaluation of Consensus-Based Sediment Quality Guidelines for Freshwater Ecosystems, Arch. Environ. Contam. Toxicol., 39, 20–31.

Mangum, S.J. (2009) Microwave Digestion -EPA Method 3052 on the Multiwave 3000, Perkin Elmer, Inc. (ed.), Waltham, pp3.

Mao. Y., Liu. G., Meichel. G., Cai., Y. and Jiang, G. (2008) Simultaneous Speciation of Monomethylmercury and Monoethylmercury by Aqueous Phenylation and Purge-and-Trap Preconcentration Followed by Atomic Spectrometry Detection, Anal Chem., 80(18), 7163–7168.

Marsden, D.D. (1986) The current limited impact of Witwatersrand gold mine residues on water pollution load in the Vaal River system, J.S. Afr. Inst. Min. Metal., 86, 481-504.

Martinez-Cortizas, A., Pontevedra-Pombal, X., Garcia-Rodeja, E., Novoa-Munoz, J.C. and Shotyk, W. (1999) Mercury in a Spanish peat bog: Archive of climate change and atmospheric metal deposition, Science, 284, 939-942.

Marvin-Dipasquale, M.C. and Oremland, R.S. (1998) Bacterial methylmercury degradation in Florida Everglades peat sediment, Environ. Sci. Technol., 32, 2556-2563.

Marvin-DiPasquale, M., Agee, J., McGowan, C., Oremland, R.S., Thomas, M., Krabbenhoft, D. and Gilmour, C.C. (2000) Methyl-mercury degradation pathways: a comparison among three mercury impacted ecosystems, Environ. Sci.Technol., 34, 4908-4916.

Mason, R.P. and Benoit, J.M. (2003) Organomercury Compounds in the Environment, In: Organometallic Compounds in the Environment, chapter2, Second Edition, Craig, P.J. (ed), John Wiley and Sons Ltd, Chichester, UK, doi: 10.1002/0470867868.

Mason, R.P. and Fitzgerald, W.F. (1991) Mercury speciation in open ocean waters, Water Air Soil Pollut, 56, 779-789.

Mason, R.P., Fitzgerald, W.F. and Morel, F.M.M. (1994) The biogeochemical cycling of elemental mercury: Anthropogenic influences, Geochim. Cosmochim. Acta, 58, 3191-3198**.**

Mason, R.P., Reinfelder, J.R. and Morel, F.M.M. (1995) Bioaccumulation of mercury and methylmercury, Water Air Soil Pollut., 80, 915-921.

Mason, R.P., Reinfelder, J.R. and Morel, F.M.M. (1996) Uptake, toxicity, and trophic transfer of mercury in a coastal diatom, Environ. Sci. Technol., 30, 1835-1845.

Mason, R.P. and Lawrence A.L. (1999) The concentration, distribution and bioavailability of mercury and methylmercury in sediments of Baltimore Harbor and the Chesapeake Bay, Maryland USA, Environ. Toxicol. Chem., 18, 2438-2447.

Mason, R.P. and Sheu, G.-R. (2002) The role of the ocean in the global mercury cycle. Global Biogeo. Cycles, 16(4), 1093, doi:10.1029/2001GB001440.

McCarthy, T.S. and Rubidge, B. (2005) The story of Earth and life: A southern African perspective on a 4.6 billion-year journey, Harvey, L. and Reid, R. (eds), Struik Publishers, Cape Town, pp333.

McCarthy, T.S. and Venter, J.S. (2006) Increasing pollution levels on the Witwatersrand recorded in the peat deposits on the Klip River wetland, SA J. of Sci., 102, 27-34.

Meija, J., Yang, L., Caruso, J.A. and Mester, Z. (2006) Calculations of Double Spike Isotope Dilution Results Revisited, J. Analytical Atomic Spectrometry, 21, 1294-1297. (Referenced on-line Aug. 2006.

Mester, Z., Sturgeon, R. and Pawliszyn J. (2001) Solid phase microextraction as a tool for trace element speciation, Spectrochimica Acta, Part B: Atomic Spectroscopy, 56, 233-260.

Mikac, N., Kwokal, Z., May, K. and Branica, M. (1989) Mercury distribution in the krka river Estuary (Eastern Adriatic Coast), Mar. Chem., 28, 109-126.

Miller, E.K., Panek, J.A., Friedland, A.J., Kadlecek, J. and Mohnen, V.A. (1993) Atmospheric deposition to a high elevation forest at Whiteface Mountain, New York, USA, Tellus, 45B, 209–27.

Miller, C.L. and Mason, R.P. (2001) Factors controlling the production, fate and transport of mercury and methylmercury in sediments, ACS 222nd Meeting, Chicago, August, ACS abstract, 41(2), 514-518.

Miskimmin, B.M. (1991) Effect of natural levels of Dissolved Organic Carbon (DOC) on methvlmercurv formation and sediment-water partitioning, Bull. Environ. Contam. Toxicol., 47, 743-750.

Miskimmin, B.M., Rudd, J.W.M. and Kelly, C.A. (1992) Influence of DOC, pH, and microbial respiration rates on mercury methylation and demethylation in lake water, Can. J. Fish. Aquat. Sci., 49, 17-22.

Moens, L., De Srnaele, T.Dams, R. Van den Broeck, P. and Sandra, P. (1997) Sensitive Simultaneous Determination of Orqanomercury, -lead, and -tin Compounds with Headspace Solid Phase Microextraction Capillary Gas Chromatography Combined with Inductively Coupled Plasma Mass Spectrometry, Analytical Chemistry, 69, 1604-1611.

Monperrus, M., Rodriguez Martin-Doimeadios, R.C., Scancar, J., Amouroux, D., and Donard, O.F.X. (2003) Simultaneous sample preparation and species-specific isotope dilution mass spectrometry analysis of monomethylmercury and tributyltin in a certified oyster tissue. Anal. Chem., 75, 4095-4102.

Monperrus, M., Tessier, E., Veschambre, S., Amouroux, D. and Donard, O. (2005) Simultaneous speciation of mercury and butyltin compounds in natural waters and snow by propylation and species-specific isotope dilution mass spectrometry analysis, Anal. Bioanal. Chem., 381, 854-862.

Montaser, A. (1998) inductively coupled plasma mass spectrometry, Montaser, A. (ed), Wiley-VCH, New-York.

Montgomery, S., Mucci, A., Lucotte, M., and Pichet, P. (1995) Total dissolved Hg in the water column of several natural and artificial systems of Northern Quebec, Canada, Can. J. Fish. Aquat. Sci., 52, 2483-2492.

Moore, T.R., Bubier, J.L.. Heyes, A. and Flelt, R.J. (1995) Methyl and Total Mercury in Boreal Wetland Plants, Experimental Lakes Area, Northwestern Ontario, J. Environ. Qual., 24, 845-850.

Moore, L. J., Kingston, H. M. and Murphy, T. J. (1984) The Use of Isotope Dilution Mass Spectrometry for the Certification of Standard Reference Materials, Environ. Intern., 10(2), 169-173.

Morin, K.A., and Hutt, N.M. (1997) Environmental Geochemistry of Minesite Drainage: Practical Theory and Case Studies, MDAG Publishing, Vancouver, British Columbia, Canada, ISBN 0-9682039-0-6.

Mortensen, J.L. (1963) Complexing of metals by soil organic matter, Proc. Soil Sci. Sot. Am., 27, 179-186.

Mphephu, N.F. (2004) Geotechnical environmental evaluation of mining impacts on the Central Rand, Ph.D.Thesis, University of the Witwatersrand, Johannesburg**.**

Mukherjee, A. B., Bhattacharya, P., Sarkar, A., and Zevenhoven, R. (2009) Mercury Emissions from Industrial Sources in India and its Effects in the Environment, Springer, New York, Chap. 4, 81–112.

Munthe, J., Wängberg, I., Iverfeldt, Å., Lindqvist, O., Strömberg, D., Sommar, J., Gårdfeldt, K., Petersen, G., Ebinghaus, R., Prestbo, E., Larjava, K. and Siemens, V. (2003) Distribution of atmospheric mercury species in Northern Europe: final results from the MOE project, Atmos. Environ., 37, 9-20.

Munthe, J., Wangberg, I., Pirrone, N., Iverfeldt, A., Ferrara, R., Ebinghaus, R., X. Feng, X., Gardfeldt, K., Keeler, G., Lanzillotta, E., Lindberg, S.E., Lu, J., Mamane, Y., Prestbo, E., Schmolke, S., Schroeder, W.H., Sommar, J., Sprovieri, F., Stevens, R.K., Stratton, W., Tuncel, G., Urba, A., (2001) Intercomparison of methods for sampling and analysis of atmospheric mercury species, Atmospheric Environment, 35, 3007–3017.

Naicker, K., Cukrowska, E. and McCarthy, T.S. (2003) Acid mine drainage arising from gold mining activity in Johannesburg, South Africa and environs, Environ. Pollution, 22, 2003, 29-40.

Nand Ram and Raman, K.V (1983) Characterization of metal-humic and metal-fulvic acid complexes -potentiometric, conductometric titrations; Job's plots, Peclologie, 33(2), 137-145, ISSN 0079-0419.

Navarro, A., Cardellach, E. and Corbella, M. (2009) Mercury mobility in mine waste from Hg-mining areas in Almería, Andalusia (Se Spain), Journal of Geochemical Exploration, 101, 236–246.

Nelson, P. F. (2007) Atmospheric emissions of mercury from Australian point sources, Atmos. Environ., 41, 1717-1724.

Nriagu, J. O. (1979) Production and uses of mercury. In: The Biogeochemistry of Mercury in the Environment (ed.J. O. Nriagu). Elsevier/North-Hollan Biomedical Press, Amsterdam, 23–40.

Nriagu, J.G. and Pacyna, J.M. (1988) Quantitative assessment of worldwide contamination of air, water and soils with trace metals, Nature, 333, 134-139.

Nsengimana, H. (2007) Speciation of organometallic of tin, lead and mercury in environmental samples, Ph.D.Thesis, University of the Witwatersrand, Johannesburg.

Ntho, T.A. (2007) Catalytic Oxidation of Carbon Monoxide and Dimethyl Ether Syntheis Over Gold-containing Catalysts, PhD thesis, University of the Witwatersrand, Johannesburg, pp118.

O'Reilly, J.E. and Hicks, D.G. (1979) Slurry injection atomic absorption spectrometry for analysis of whole coal, Anal. Chem., 51, 1905-1915.

Outka, D.A. and Madix, R.J. (1987) Broensted basicity of atomic oxygen on the gold(110) surface: Reactions with methanol, acetylene, water, and ethylene, J. Am. Chem. Soc., 109, 1708-1714.

Ozerova, N.A. (1996) Mercury in geological systems. In: Global and Regional Mercury Cycles: Sources, Fluxes and Mass Balances, NATO ASI: Series 2. Environment, Baeyens, W., Ebinghaus, R. and Vasiliev, O. (eds). Kluwer, Boston, vol. 21, pp. 463–474.

Pacyna, E.G., Pacyna, J.M., Steenhuisen, F.,Wilson, S., (2006) Global anthropogenic mercury emission inventory for 2000, Atmospheric Environment, 40, 4048-4063.

Pacyna, J. M., Pacyna, E. G., and Aas, W. (2009) Changes of emissions and atmospheric deposition of mercury, lead, and cadmium, Atmospheric Environment – Fifty Years of Endeavour, Atmos. Environ., 43, 117–127.

Palmer, C.A., Kolker, A., Finkelman, R.B., Kolb, K.C., Mroczkowski, S.J., Crowley, S.S., Belkin, H.E., Bullock, Jr., J.H. and Motooka, J.M. (1997) Trace Elements in Coal - Modes of Occurrence Analysis, U.S. Geological Survey, Final Technical Report for C.Q.,Inc., DE-AI22-95PC95156, pp99.

Parker, J.L. and Bloom, N.S. (2005) Preservation and storage techniques for low-level aqueous mercury speciation, Science of the Total Environment, 337, 253-263.

Pécheyran, C., Lalère, B. and Donard, O.F.X. (2000) Volatile metal and metalloid species (Pb. Hg. Se) in a European urban atmosphere (Bordeaux, France), Environmental Science and Technology, 34 (1), 27-32.

Pestana, M.H.D., Lechlerb, P., Formosoc, M.L.L. and Millerd, J. (2000) Mercury in sediments from gold and copper exploitation areas in the CamaquaÄ River Basin, Southern Brazil, Journal of South American Earth Sciences, 13, 537-547.

Peter, A., Baia, M., Toderas, F., Lazar, M., Tudoran, L.B. and Danciu, V. (Unpublished) Photo-catalysts based on gold-titania composites, pp11.

Pfeiffer, W.C., Lacerda, L.D., Salomons, W. and Malm, O. (1993) Environmental fate of mercury from gold mining in the Brazilian Amazon, Environ Rev, 1, 26-37.

Piccolo, A. and Stevenson, F.J. (1982) Infrared spectra of Cu^{2+}, Pb^{2+}, and Ca^{2+} complexes of soil humic substances, Geoderma, 27, 195-208.

Pirrone, N., Keeler, G. J., and Nriagu, J. O.(1996) Regional differences in worldwide emissions of mercury to the atmosphere, Atmos. Environ., 30, 2981–2987.

Pirrone, N., Cinnirella, S., Feng, X., Finkelman, R.B., Friedli, H.R., Leaner, J., Mason, R., Mukherjee, A.B., Stracher, G.B., Streets, D.G. and Telmer, K. (2010) Global mercury emissions to the atmosphere from anthropogenic and natural sources, Atmos. Chem. Phys. Discuss., 10, 4719–4752.

Porritt, R.E. and Swaine, D.J. (1976) "Mercury and Selenium in **S**ome Australian Coals and Fly Ash," in proceedings of the Australian Institute of Fuel Conference, Sydney, New South Wales, pp. 18.1-18.9.

Prokopovich, N.P. (1984) Occurrence of mercury in dredge tailings near Folsom South Canal, California, Bulletin of the Association of Engineering Geology, XXI, 531-543.

Puk, R. and Weber, J.H. (1994) Critical review of analytical methods for determination of inorganic mercury and methylmercury compounds, Appl. Organomet. Chem., 8, 293-302.

Pyle, D.M. and Mather, T.A. (2003) The importance of volcanic emissions for the global atmospheric mercury cycle, Atmospheric Environment, 37, 5115-5124.

Querol, X., Klika, Z., Weiss, Z., Finkelman, R.B., Alastuey, A., Juan, R., Lopez-Soler, A., Plana, F., Kolker, A. and Chenery, S.R.N. (2001) Determination of element affinities by density fractionation of bulk coal samples, Fuel, 80, 83–96.

Quevauviller, P. (2001) Metrologie en chimie de l'environment, TEC&DOC (eds), London.

Quiller, R.G., Baker, T.A., Deng, X., Colling, M.E., Min, B.K. and Friend, C.M. (2008) Transient hydroxyl formation from water on oxygen-covered Au(111). J. Chem. Phys., 129, 064702.

Raask, E. (1985) Mineral Impurities in Coal Combustion, Hemisphere Press, Washington, DC.

Ramlal, P.S., Rudd, J.W.M., Furutani, A. and Xun, L. (1985) The effect of pH on methyl mercury production and decomposition in lake sediments, Can. J. Fish. Aquat. Sci., 42, 685-692**.**

Rasmussen, P.E. (1994) Current methods for estimating atmospheric mercury fluxes in remote areas. Environ. Sci. Tech., 28, 2233-2241.

Rasmussen, P.E. (1995) Temporal variation of mercury in vegetation, Water, Air and Soil Pollution, 80, 1039-1042.

Reddy, M.M. and Aiken, G.R. (2000) Fulvic acid-sulfide ion competition for mercury ion binding in the Florida Everglades, Wat. Air Soil Poll., 132, 89-104.

Rimmer, S.M. and Davis, A. (1986) Geologic controls on the inorganic composition of Lower Kittanning coal, In: Vorres, K. (Ed.), Mineral Matter and Ash in Coal, ACS Symp. Ser., vol. 301, American Chemical Society, Washington, DC, pp. 41-52, Chap. 4.

Ripley, E.A., Redman, R.E. and Crowder, A.A. (1996) Environmental effects of mining, St. Luice Press, 2nd ed., Delray Beach.

Robb, L.J. and Robb, V.M. (1998) Gold in the Witwatersrand Basin, In: M.G.C. Wilson and C.R. Anhaeusser (eds), The Mineral Resources of South Africa, Handbook 16, Council for Geoscience, pp. 294–349.

Roberts, D. L. (2008) Chromium Speciation in Coal Combustion Byproducts: Case Study at a Dry Disposal Power Station in Mpumalanga Province, South Africa, PhD Thesis, University of the Witwatersrand, Johannesburg.

Robinson, J.B. and Tuovinen, O.H. (1984) Mechanisms of microbial resistance and detoxification of mercury and organomercury compounds: Physiological, biochemical and genetic analyses, Microbiol. Rev., 48, 95-124.

Rodriguez, I., Schmitt, V.O. and Lobinski, R. (1999) Elemental Speciation Analysis by Multicapillary Gas Chromatography with Microwave-Induced Plasma Atomic Spectrometric Detection, Analytical Chemistry, 71, 4534-4543.

Rodriguez Martin-Doimeadios, R.C., Krupp, E., Amouroux, D., and Donard, O.F.X. (2002) Application of Isotopically Labeled Methylmercury for Isotope Dilution Analysis

of Biological Samples Using Gas Chromatography/ICPMS, Analytical Chemistry, 74, 2505-2512.

Rodriguez Martin-Doimeadios R.C., Monperrus M., Krupp E., Amouroux D. and Donard O.F.X. (2003) Using speciated isotope dilution with GC-inductively coupled plasma MS to determine and unravel the artificial formation of monomethylmercury in certified reference sediments, Analytical Chemistry, 75, 3202-3211.

Rodriguez Martin-Doimeadios, R.C., Tessier, E, Amouroux, D., Guyoneaud, R., Duran, R., Caumette, P., and Donard O.F.X. (2004) Mercury methylation/demethylation and volatilization pathways in estuarine sediment slurries using species-specific enriched stable isotopes, Marine Chemistry, 90, 107-123.

Rodushkin, I., Axelsson, M.D. and Burman, E. (2000) Multielement analysis of coal by ICP techniques using solution nebulization and laser ablation, Talanta, 51, 743-759.

Rood, B.E., Gottgens, J.F., Delfino, J.J., Earle, C.D. and Crisman, T.L. (1995) Mercury accumulation trends in Florida Everglades and Savannas Marsh flooded soils, Water, Air and Soil Pollution, 80, 981-990.

Rosner, T. and van Schalkwyk, A. (2000) The environmental impact of gold mine tailings footprints in the Johannesburg region, South Africa. Bull. Eng. Geol. Env., 59, 137–148.

Ruch, R.R., Gluskoter, H.J. and Kennedy, E.J. (1971) Mercury content of Illinois coals, Illinois State Geological Survey Environment Geology Notes, 43, p15.

Rytuba, J.J. (2005) Geogenic sources of mercury to the environment. *In* Mercury: Sources, Measurements, Cycles, and Effects, Parsons, M.B. and Percival, J.B. (eds.), Mineral. Assoc. Canada, Short Course, 34, 21-41.

Sakulpitakphon, T., Hower, J.C., Schram, W.H. and Ward, C.R. (2004) Tracking mercury from the mine to the power plant: geochemistry of the Manchester coal bed, Clay County, Kentucky, International Journal of Coal Geology, 58, 127-141.

Santos-Francés, F., García-Sánchez, A., Alonso-Rojo, P., Contreras, F. and Adams, M. (2011) Distribution and mobility of mercury in soils of a gold mining region, Cuyuni river basin, Venezuela, Journal of Environmental Management, doi:10.1016/j.jenvman.2010.12.003, 1-9.

SAWQG (1996) South African Water Quality Guidelines, Volume 1, Domestic Water Use, 2nd ed., pp 190.

Schroeder, W. H., Ebinghaus, L., Shoeib, M., Timoschenko, K. and Barrie, L.A. (1995a) Water, Air, and Soil Pollution, 80, 1227–1236.

Schroeder, W. H., Keeler, G., Kock, H., Roussel, P., Schneeberger, D. and Schaedlich, F. (1995b) Water, Air, and Soil Pollution, 80, 611–620.

Schroeder, W.H., Lindqvist, O., Munthe, J. and Xiao, Z. (1992) Volatilization of mercury from lake surfaces. Sci. Total Environ. 125, 47-66.

Schroeder, W.H. and Munthe, J. (1998) Atmospheric Mercury – An Overview, Atmospheric environment, 29, 809-822.

Schubert, P., Rosenberg, E. and Grasserbauer, M. (2000) Comparison of sodium tetraethylborate and sodium tetra(n-propyl)borate as derivatization reagent for the speciation of organotin and organolead compounds in water samples, Fresenius' J. Anal. Chem., 366, 356–360.

Schuster, E. (1991) The Behavior of Mercury in the Soil with Special Emphasis of Complexation and Adsorption Processes – A Review of the Literature, Water Air, and Soil Pollution, 56, 667-680.

Schuster, P.F., Krabbenhoft, D.P., Naftz, D.L., Cecil, L.D., Olson, M.L., Dewild, J.F., Susong, D.D., Green, J.R. and Abbott, M.L. (2002) Atmospheric mercury deposition during the last 270 years: A glacial ice core record of natural and anthropogenic sources, Environ. Sci. Tech., 36, 2303-2310.

Sellers, P., Kelly, C.A., Rudd, J.W.M. and MacHutchon, A.R. (1996) Photodegradation of methymercury in lakes, Nature, 380, 694-697.

Selsbo, P. (1996) Analytical pyrolysis-studies of sulphur in coal and pulp, Doctoral dissertation, Lund University, Sweden.

Shade, C.W. and Hudson, R.J.M. (2005) Determination of MeHg in environmental sample matrices using Hg-thiourea complex ion chromatography with on-line cold vapor generation and atomic fluorescence spectrometric detection, Environ. Sci. Technol., 39, 4974-4982.

Shirazi, A.R. and Lindqvist, O. (1993) An improved method of preserving and extracting mineral matter from coal by very low-temperature ashing (VLTA), Fuel, 72, 125-131.

Sjostrom, S. and Chang, R. (2003) Development and Demonstration of Mercury Control by Adsorption Processes (MerCAP™), Presented at the 2003 EPRI-EPA-NETL-AWMA Combined Power Plant Air Pollutant Control Symposium.

Skillberg, U., Bloom, P.R., Qian, J., Lin, C.M. and Bleam, W.F. (2006) Complexation of mercury (II) in soil organic matter: EXAFS evidence for linear two-coordination with reduced sulphur groups, Environ. Sci. Technol., 40, 4174-4180.

Slaets, S., Adams, F., Pereiro, I.R. and Lobinski, R. (1999) Optimization of the coupling of multicapillary GC with ICP-MS for mercury speciation analysis in biological materials, Journal of Analytical Atomic Spectrometry, 14, 851-857.

Smith, K.S. and Huyck, H.L.O. (1999) An overview of the abundance, relative mobility, bioavailability, and human toxicity of metals, In The Environmental Geochemistry of Mineral Deposits, Part A:Vol. 6A, Chapter 2. Plumlee, G., Logsdon, M. (Volume eds.), Reviews in Economic Geology, Society of Economic Geologists, Inc., Chelsea, MI, 29-70.

Snell, J.P., Stewart, I.I., Sturgeon, R.E. and Frech, W. (2000) Species specific isotope dilution calibration for determination of mercury species by gas chromatography coupled to inductively coupled plasma- or furnace atomisation plasma ionisation-mass spectrometry, Journal of Analytical Atomic Spectrometry, 15, 1540-1545.

Spalding, D. (2003) South African Coal Report, Spalding, D. (ed.), Issue No.14.12.

Stockwell, P.B. and Corns, W.T. (1993) The role of atomic fluorescence spectrometry in the automatic environmental monitoring of trace element analysis, Journal of Automatic Chemistry, 15, 3, 79-84.

Steinnes, E. (1990) Mercury, In: Heavy Metals in Soils, Blackie and Son, Alloway, B.J. (Ed.), Glasgow, pp. 222-236.

Stoichev, T., Amouroux, D., Rodriguez Martin-Doimeadios, R.C., Monperrus, M., Donard, O.F.X. and Tsalev, D.L. (2006) Speciation Analysis of Mercury in Aquatic Environment, Applied Spectroscopy Reviews, 41, 591–619.

Stratton, W.J. and Lindberg, S.E. (1995) Use of a refluxing mist chamber for measurement of gas-phase mercury(II) species in the atmosphere, Water, Air and Soil Pollution, 80, 1269-1278.

Streets, D.G., Hao, J., Wang, S., and Wu, Y. (2009) Mercury emissions from coal combustion in China, Springer, New York, Chap. 2, 51–65.

Stupperich, E., Eisinger, H-J., and Schurr, S. (1990) Corrinoids in anaerobic bacteria, FEMS Microbiol. Rev., 87, 355-360.

Sullivan, J.H. (1995) The geology of the coal-bearing rocks of the Karoo Sequence in the Tshikondeni mine area, northern Transvaal, M.Sc. Thesis, University of Pretoria, Pretoria.

Suzuki, T., Akagi, H., Arimura, K., Ando, T., Sakamoto, M., Satoh, H., Naganuma, A., Futatsuka, M. and Matsuyama, A. (2004) Mercury Analysis Manual, Ministry of the Environment, Japan.

Swaine, D.J. (1975) In Tugarinov, AI, (ed), Rec Contrib Geochem Analyt Chem. Jerusalem, Israel Prog. for Sci. Translations, 539–550.

Swaine, D.J. (1990) Trace Elements in Coal, Butterworths (eds), London.

Swaine, D.J. (2000) Why trace elements are important, Fuel Processing Technology, 65-66, 21-33.

Taysayev, T.T. (1991) Man-made dispersion train of gold and mercury in Golets-Taiga terrain, Dokl. Akad. Nauk SSR. 317(3), 719-722 (translated 1993 by Scripta Technica. Inc.), ISSN 00I2-494X, pp.197-200.

Tekran, (1998) Model 2357A–Principles of Operation, Tekran Inc.

Telmer, K.H. and Veiga, M.M. (2009) World emissions of mercury from artisanal and small scale gold mining. In "Mercury fate and transport in the global atmosphere. Emissions, Measurements and Models", 2009, ISBN; 978-0-387-93957-5, Springer, New York, 131–172.

Templeton, D. M., Ariese, F., Cornelis, R., Danielsson L.G., Muntau, H., Van Leeuwen, H.P. and Lobinski, R. (2000) Guidelines for terms related to chemical speciation and fractionation of elements. Definitions, structural aspects, and methodological approaches (IUPAC Recommendations 2000), Pure and Applied Chemistry, 72, 1453-1470.

Tewalt, S. and Finkelman, L. B. R. (2001) Mercury in U.S. coal: abundance, distribution and modes of occurrence, Geological Society of America, 4726, Available at: http://pubs.usgs.gov/factsheet/fs095-01.

Thornton, I. and Ramsey, M. (1995) Metals in the global environment: facts and misconceptions, Ottawa, International Council on Metals in the Environment, ICME, VIII, ISBN: 1895720095, p103.

Toole- O'Neil, B., Tewalt, S.J., Finkelman, R.B. and Akers, D.J. (1999) Mercury concentration in coal – Unravelling the puzzle, Fuel, 78, 47-54.

Tseng, C.M., De Diego, A., Martin, F.M., and Donard, O.F.X. (1997a) Rapid and quantitative microwave-assisted recovery of methylmercury from standard reference sediments, J. Anal. Atom. Spectrom., 12, 629-635.

Tseng, C.M., de Diego, A., Martin, F.M., Amouroux, D. and Donard, O.F.X. (1997b) Rapid determination of inorganic and methyl mercury in biological reference materials by hydride generation cryofocusing atomic absorption spectrometry after open-focused microwave-assisted alkaline digestion, J. Anal. At. Spectrom., 12, 742-750.

Tseng, C.M., De Diego, A., Pinaly, H., Amouroux, D., and Donard, O.F.X. (1998)

Cryofocusing coupled to atomic absorption spectrometry for rapid and simple mercury speciation in environmental matrices. J. Anal. Atom. Spectrom., 13, 755-764.

Tseng, C. M., Amouroux, D. Brindleb, I. D. and Donard, O. F. X. (2000) Field cryofocussing hydride generation applied to the simultaneous multi-elemental determination of alkyl-metal(loid) species in natural waters using ICP-MS detection, J. Environ. Monit., 2, 603-612.

Tutu, H. (2005) Determination and geochemical modeling of the dispersal of uranium in gold-mine polluted land on the Witwatersrand, PhD Thesis, University of the Witwatersrand, Johannesburg.

U.S. Congress (1990) An act to amend the Clean Air Act to provide for attainment and maintenance of health protective national ambient air quality standards and for other purpose, U.S. Public Law 101-549, Nov. 15, U.S. Government Printing Office, Washington, DC, 314 pp.

USEPA (1992) Water quality standards, Establishment of numeric criteria for priority toxic pollutants, States' compliance, Final rule, Federal Register, 40 CFR Part 131, vol. 246, pp.847-860.

USEPA (1996) Microwave Assisted Acid Digestion of Siliceous and Organically Based Matrices, US Environmental Protection Agency Method 3052, December 1996, pp20.

US EPA (1997a) Mercury Study Report to Congress, EPA 452/R-97-003, Available online at: http://www. epa. gov/oar/mercury.html.

U.S. EPA (1997b) The incidence and severity of sediment contamination in surface waters of the United States, Volume 1–National Sediment Quality Survey: Office of Science and Technology, EPA-823-R-97-006, 6 separately numbered chapters and 9 appendices.

US EPA (2003) Control of mercury emissions from coal-fired electric utility boilers, US Environmental Protection Agency, Air Pollution Prevention and Control Division, Available online at: www.epa.gov/ttnatw01/utility/hgwhitepaperfinal.pdf.

US EPA (2005) National Emission Inventory (NEI), Tech. rep., US EPA, http://www.epa.gov.

USEPA (2007a) Elemental and Speciated Isotope Dilution Mass Spectrometry, United States Environmental protection Agency, SW-846 method 6800, Available online at: www.epa.gov/osw/hazard/testmethods/sw846/pdfs/6800.pdf.

USEPA (2007b) SW-846 Methods, Chapter 3: Inorganic analytes, Rev.4, February 2007, available at www.epa.gov/osw/hazard/testmethods/sw846/pdfs/chap3.pdf.

USEPA (2007c) SW-846 Methods, Determination of inorganic anions by ion chromatography, Method 9056A, Rev.1, February 2007, available at wwv.epa.gov/osw/hazard/testmethods/sw846/pdfs/9056a.pdf.

U.S. EPA (2009) Drinking water contaminants, EPA 81 6-F-09-0004, May 2009, available at http://water.epa.gov/drink/contaminants/index.cfm#Inorganic, accessed on 29/11/2011.

US EPA (2008) Mercury, elemental (CASRN 7439-97-6), Integrated Risk Information System, Available online at: http://www.epa.gov/ncea/iris/subst/0370.htm.

USGS (2001) Mercury in U.S. Coal—Abundance, Distribution, and Modes of Occurrence, USGS Fact Sheet FS–095–01, September 2001, pp4.

USGS (2003) Geologic Studies of Mercury by the U.S. Geological Survey, Gray, J.E. (ed), U.S. Geological Survey Circular 1248.

USGS (2008) Mineral Commodity Summaries, U.S. Geological Survey, U.S. Government Printing Office, Washington, Available online at: http://minerals.usgs.gov/minerals/pubs/mcs/2008mcs.pdf.

USPTO (2006) Mercury sensor using anisotropic gold nanoparticles and related water remediation, US Patent and Trademark Office, Patent Application 20080081376, Available online at: http://www.freshpatents.com/ and accessed on 14 July 2009.

Vanloon, J.C., Alcock, L.R., Pinchin, W.H. and French, JB (1986) Inductively Coupled, Plasma Source Mass Spectrometry - A New Element/Isotope Specific Mass Spectrometry Detector for Chromatography, Spectroscopy Letters, 19, 1125-1135.

Varekamp, J.C., Buchholtz ten Brink, M.R., Mecray, E.L. and Kreulen, B. (2000) Mercury in Long Island Sound sediments, J. Coast. Res., 16, 613-626.

Veiga, M.M. (1997) Mercury in Artisanal Gold Mining in Latin America: Facts, Fantasies and Solutions, UNIDO - Expert Group Meeting - Introducing new technologies for abatement of global mercury pollution deriving from artisanal gold mining, Vienna, 1-3 July 1997.

Veiga, M.M., Maxson, P. A., and Hylander, L. D. (2006) Origin and consumption of mercury in small scale gold mining, J. Clean. Prod., 14, 436–447, Special issue: Improving Environmental, Economic and Ethical Performance in the Mining Industry. Part 1. Environmental Management and Sustainable Development.

Veiga, M.M., Meech, J.A. and Onate, N. (1994) Mercury- pollution from deforestation. Nature (London), 368, 816-817.

Vercauteren, J., Peres, C., Devos, Sandra, P., Vanhaecke, F. and Moens, L. (2001) Stir bar sorptive extraction for the determination of ppq-level traces of organotin compounds in environmental samples with thermal desorption-capillary gas chromatography-ICP mass spectrometry, Analytical Chemistry, 73, 1509-1514.

Voutsa, D., Grimanis, A. and Samara, C. (1996) Trace elements in vegetables grown in an industrial area in relation to soil and air particulate matter, Environ. Pollution, 94 (3), 325-335.

Wagner, N.J. and Hlatshwayo, B. (2005) The occurence of potentially hazardous trace elements in five Highveld coals, South Africa, International Journal of Coal Geology, 63, 228-246.

Waldron, M.C., Colman, J.A. and Breault, R.F. (2000) Distribution, hydrologic transport, and cycling of total mercury and methyl mercury in a contaminated river-reservoir-wetland system (Sudbury River, eastern Massachusetts), Can. J. Fish. Aquat. Sci., 57, 1080–1091.

Wallschlager, D., Desai, M.V.M., Spenger, M. and Wilken, R. (1998a) Mercury Speciation in Floodplain Soils and Sediments along a Contaminated River Transect, J. Environ. Qual., 27, 1034-1044.

Wallschlager, D., Desai, M.V.M., Spenger, M., Windmoler, C.C. and Wilken, R. (1998b) How Hurnic Substances Dominate Mercury Geochemistry in Contaminated Floodplain Soils and Sediments, J. Environ. Qual., 27, 1044-1054.

Wang, Z-W., Chen, Z-S., Duan, N., Zhang, X-S. (2007) Gaseous elemental mercury concentration in atmosphere at urban and remote sites in China, J. Environ. Sci.**,** 19, 176-180.

Wang, J., Sharma, A. and Tomita, A. (2003) Determination of the modes of occurrence of trace elements in coal by leaching coal and coal ashes, Enetgy and Fuels, 17, 29-37

Wang, J.S., Tomlinson, M. J. and Caruso J.A. (1995) Journal of Analytical Atomic Spectrometry, 10, 601-607.

Wang, S., Zhang, L., Li, G., Wu, Y., Hao, J., Pirrone, N., Sprovieri, F., and Ancora, M. P. (2009) Mercury emission and speciation of coal-fired power plants in China, Atmos. Chem. Phys. Discuss., 9, 24051–24083.

Wängberg, I., Munthe, J., Pirrone, N., Iverfeldt, Å., Bahlman, E., Costa, P., Ebinghaus, R., Feng, X., Ferrara, R., Gårdfeldt, K., Kock, H., Lanzillotta, E., Mamane, Y., Mas, F., Melamed, E., Osnat, Y., Prestbo, E., Sommar, J., Schmolke, S., Spain, G., Sprovieri, F. and Tuncel, G. (2001) Atmospheric mercury distribution in Northern Europe and in the Mediterranean region, Atmos. Environ., 35, 3019-3025.

Warhurst, A. (2000) Mining, mineral processing, and extractive metallurgy: an overview of the technologies and their impact on the physical environment, In: Warhurst, A., Noronha, L. (eds), Environmental Policy in Mining: Corporate Strategy and Planning for Closure, Boca Raton, FL: CRC Press LLC.

Wasik, A., Rodriguez-Pereiro, I. and Lobinski, R. (1998) Interface for time-resolved introduction of gaseous analytes for atomic spectrometry by purge-and-trap multicapillary gas chromatography (PTMGC), Spectrochimica Acta Part B, 53, 867-879.

Watling, R.J. and Watling, H.R. (1982) Metal concentrations in some South African coals, South African Journal of Science 78, 166-264.

Watras, C.J., Bloom, N.S., Hudson, R.J.M., Gherini, S., Munson, R., Class, S.A., Morrison, K.A., Hurley, J., Wiener, J.G., Fitzgerald, W.F., Mason, R., Vandel, G., Powell, D., Rada, R., Rislov, L., Winfrey, M., Elder, J., Krabbenhoft, D., Andren, A.W., Babiarz, C., Porcella, D.B., and Huckabee, J.W. (1994) Sources and fates of mercury and methylmercury in Wisconsin Lakes, In: Mercury Pollution: Integration and Synthesis, Watras, C.J. and Huckabee, J.W. (Eds), Lewis Publishers, Boca Raton, 153-177.

WHO (1993) Guidelines for drinking water quality. Revision of the 1984 guidelines. Final task group meeting, Geneva 21–25 September 1992.

Wiener, J.G., Krabbenhoft, D.P., Heinz, G.H.and Scheuhammer, A.M. (2003). Ecotoxicology of mercury. In: Handbook of Ecotoxicology, 2nd edition, Hoffman, D.J., Rattner, B.A., Burton Jr., G.A. and Cairns Jr., J. (eds.), CRC Press, Boca Raton, Florida, USA, 407-461.

Winfrey, M.R. and Rudd, J.W.M. (1990) Environmental factors affecting the formation of methylmercury in low pH lakes: A review, Environ. Toxicol. Chem., 9, 853-869.

Wu, J.C.G. (1991) Interfacing HPLC and cold vapor AA with online preconcentration for mercury speciation, Spectrosc. Lett., 24, 681-697.

Wu, Y., Wang, S., Streets, D. G., Hao, J., Chan, M., and Jiang, J. (2006) Trends in anthropogenic mercury emissions in China from 1995 to 2003, Environ. Sci. Technol., 40, 5312–5318.

Xiao, Z., Sommar, J., Wei, S., Lindqvist, O., (1997) Sampling and determination of divalent mercury in air using KCl coated denuders. Fresenius Journal of Analytical Chemistry, 358, 386–391.

Xun, L., Campbell, N.E.R. and Rudd, J.W.M. (1987) Measurements of specific rates of net methyl mercury production in the water column and surface sediments of acidified and circumneutral lakes, Can. J. Fish. Aquat. Sci., 44, 750-757.

Yan, H., Feng, X., Shang, L., Qiu, G., Dai, Q., Wang, S. and Hou, Y. (2008) The variations of mercury in sediment profiles from a historically mercury-contaminated reservoir, Guizhou province, China, Science of the Total Environment, 407, 497–506.

Yin, Y., Allen, H.E. and Huang, C.P. (1997) Kinetics of mercury (II) adsorption and desorption on soil, Environ. Sci. Technol., 37, 496-503.

Yin, Y.G., Chen, M., Peng, J.F., Liu, J.F. and Jiang, G.B. (2010) Dithizone-functionalized solid phase extraction–displacement elution-high performance liquid chromatography–inductively coupled plasma mass spectrometry for mercury speciation in water samples, Talanta, 81, 1788–1792.

Yu, L.P. and Yan, X.P. (2003) Factors affecting the stability of inorganic and methylmercury during sample storage, Trends Anal. Chem., 22, 245-253.

Zagury, G.J., Neculita, C-M., Bastien, C. and Deschenes, L. (2006) Mercury Fractionation, Bioavailability, and Ecotoxicity in Highly Contaminated Soils from Chlor-alkali Plants, Environmental Toxicology and Chemistry, 25 (4), 1138–1147.

Zejli, H., Sharrock, P., Hidalgo-Hidalgo de Cisneros, J.L., Naranjo- Rodriguez, I. and Temsamani, K.R. (2005) Voltammetric determination of trace mercury at a sonogel-carbon electrode modified with poly-3-methylthiophene, Talanta, 68, 79-85.

Zhang, H. and Lindberg, S. (2001) Sunlight and Iron(III)-Induced Photochemical Production of Dissolved Gaseous Mercury in Freshwater, Environ. Sci. Technol., 35, 928-935.

Zhang, X. and Huang, J. (2010) Functional surface modification of natural cellulose substances for colorimetric detection and adsorption of Hg^{2+} in aqueous media, Chem. Commun., 46, 6042-6044.

Zheng, L., Liu, G. and Chou, C.L.(2008a) Abundance and modes of occurrence of mercury in some low-sulfur coals from China, International Journal of Coal Geology, 73, 19-26.

Zheng, L., Liu, G., Qi, C., Zhang, Y. and Wong, M. (2008b) The use of sequential extraction to determine the distribution and modes of occurrence in Permian Huaibei coal, Anhui Province, China, International Journal of Coal Geology, 73,139-155.

Zhou, B., Hermanans, S. and Sormojai, G.A. (2004) Nanotechnology in Catalysis, vol.1-2, Kluwer Academic press.

Zierhut, A., Leopold, K., Harwardt, L., Worsfoldb, P. and Schustera, M. (2009) Activated gold surfaces for the direct preconcentration of mercury species from natural waters, J. Anal. At. Spectrom., 24, 767-774.

http://www.angloamerican.com/development/case-studies/environment/environment01. Accessed on 21 December2011

http://www.cem.com, Application note for acid digestion, Coal Anthracite, Available at http://cem.com/download19.html, Accessed on 11 January 2009.

http://www.deepbio.princeton.edu, Post Mining Impacts of West Wits Line and Far West Rand Gold Mining, Available at http://deepbio.princeton.edu/samp/reports/Chapter5/3Introduction.doc. Accessed on 21 April 2010.

http://wwwu.edu.uni-klu.ac.at/mmessner/sites/rsa/wits/wits.htm. Accessed on 26 January 2011

http://www.harmony.co.za/im/press/SENS_HAR_uranium_assests_19dec07.pdf (a). Accessed on 21/12/2011

http://www.harmony.co.za/a/history.asp (b). Accessed on 21 December 2011.

http://www.mbendi.com/indy/ming/gold/af/sa/p0005.htm. Accessed on 26 January 2011

http://www.mintek.co.za/. Project Autek, Available at http://www.mintek.co.za/full-pages.php?bus_cat=7fc125319d6e1d8b7b496b8953b77777&guid=60f0c0fee524777d36424aaf3c242914&level=, Accessed on 4 November 2011.

http://www.prf1.com/rand_uranium1.html. Accessed on 21 December 2011.

http://www.randuranium.co.za/oa_overview.php (a), accessed on 21 December 2011.

http://www.sabs.ro/servicii_si_solutii.html. Accessed on 21 July 2011.

http://www.Wikipedia.org, Coal, Available at http://en.wikipedia.org/wiki/Coal. Accessed on 30 October 2008.

Appendix

Appendix 1: SIDMS appeared to be a precise and accurate analytical method for Hg species determination (figure A1).

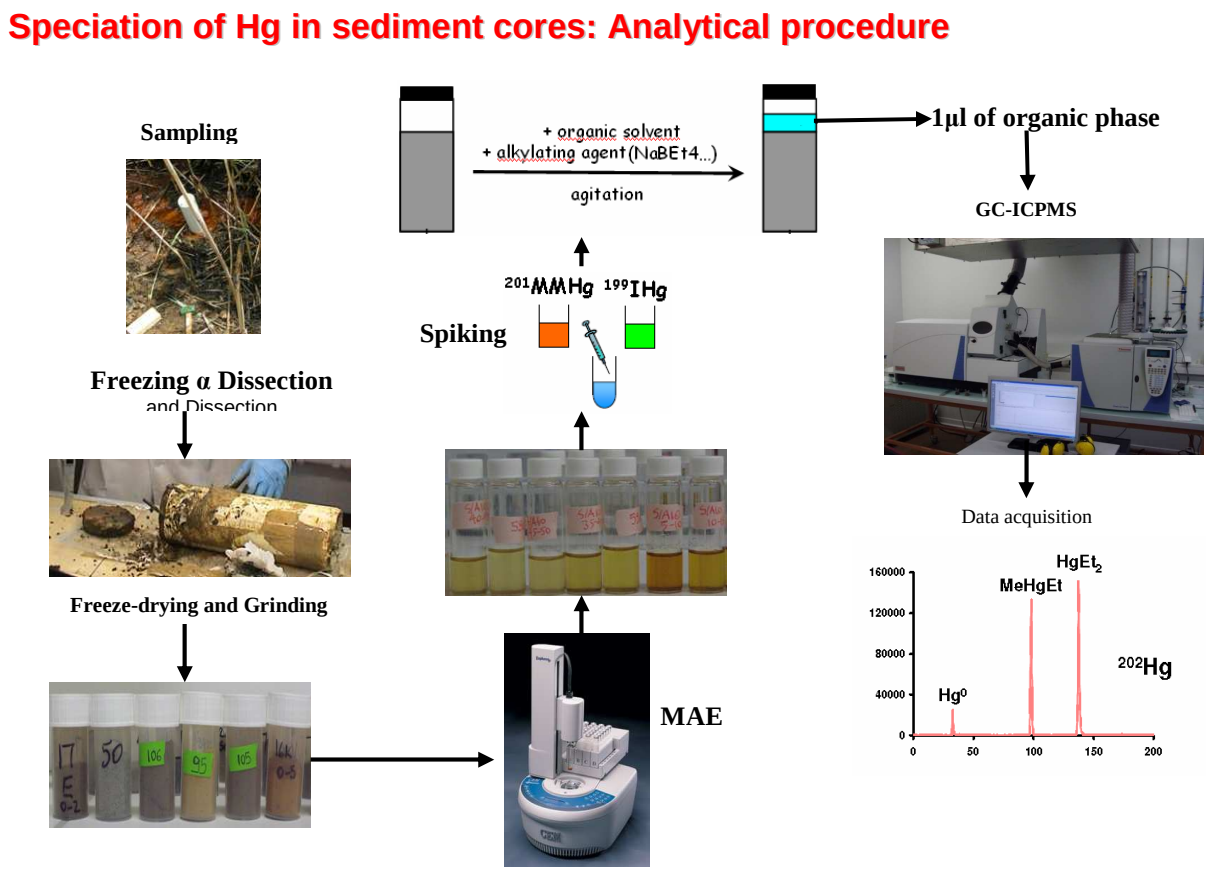

Figure A1 Schematic of different steps of the analytical protocol for the mercury speciation in sediments by ID GC-ICP-MS

Appendix 2: Mercury in the Witwatersrand Basin (Sampling features)

"*The fields are devastated by mining operations ... Further, when the ores are washed, the water which has been used poisons the brooks and streams, and either destroys the fish or drives them away. Therefore the inhabitants of these regions, on account of the devastation of their fields, woods, groves, brooks and rivers, find great difficulty in procuring the necessaries of life, and by reason of the destruction of the timber they are forced to greater expense in erecting buildings. Thus it is said, it is clear to all that there is greater detriment from mining than the value of the metals which the mining produces*". (Reprinted from Agricola (1556) De re metallica, p.8)

The planted trees for phytoremediation at the Rietfontein landfill (figure A2.1A) have demonstrating their efficiency in reducing heavy metals contamination at the site. Decaying plants were also found at the Rietfontein site, as it is shown from the hole in the dry dam (figure A2.1B) after the removal of the PVC core. Note the dark color of the bulk sediment characteristic of reducive conditions at the site. This may explain the relatively high proportion of MHg observed.

AMD was observed at the Savuka mine (figure A2.1C) in the Vaarkenslaagte Canal (West Wits) near TSFs. The important vegetation in the West Wits watersheds (figure A2.1D) may explain the substantial methylation rate at the site.

Figure A2.1 Rietfontein (A, B) and West Wits (C, D) sites

Most of the streams draining in the Witwatesrand Basin, such as the Wonderfontein Spruit (figure A2.2), contain waters that are unsafe for human consumption since they receive discharges from both artisanal and industrial mining operations and also from other industrial activies (figure A2.3).

Figure A2.2 Municipality warning notice at the Wonderfontein Spruit (West Wits)

Figure A2.3 The Kanana township (left) near Schoonspruit (right) where ASGM activities have been reported (VR site)

Number of abandoned or closed shafts from old mining activities could be important sources of TGM in the Witwatersrand Basin (figure A2.4).

Figure A2.4 The closed ventilation shaft (left) near Orkney where elevated TGM concentrations were measured and an example of the mercury trap (right) used during air collection

Flooding at the Bokkamp Dam (figure A2.5), which is built on waste rocks and receives dirty waters from TSFs and metallurgical plants, could be the main cause of the widespread of mercury in the surrounding area.

Figure A2.5 The Bokkamp Dam, one of the most important hot spot of mercury and other heavy metals at the VR site, during the dry (left) and wet (right) season samplings

The following article was published by Inter Press Service (IPS) on the 3 December 2007 and is available at http://ipsnews.net/news.asp?idnews=40325

ENVIRONMENT-SOUTH AFRICA

Radioactive Water, the Price of Gold

By Steven Lang

JOHANNESBURG- Large gold-mining companies operating to the west of South Africa's commercial centre, Johannesburg, stand accused of contaminating a number of water sources with radioactive pollutants.

Acid mine drainage

Gold mines are also finding themselves in the dock over acid mine drainage, another means by which heavy metals are being released into the environment.

Mining operations expose heavy metals and sulphur compounds that have been locked away in the ground. Rising ground water then leaches these compounds out of the exposed earth, resulting in acid mine drainage that can continue to pollute the environment decades after mines have been closed down.

In 2002, acidic water began decanting out of a disused mine on Randfontein Estates about 42 kilometers south-west of Johannesburg. The property belonged at that time to Harmony Gold. In terms of South Africa's National Water Act the owner of land is accountable for the quality of the water flowing out of that ground.

While some of this acidic water was produced by Harmony's own operations, a large proportion was generated by its competitors.

Mining companies extracting ore in the Witwatersrand area, to the east and west of Johannesburg, have created a 300 kilometer labyrinth of interlinking passages, according to the "Water Wheel" magazine (Jan./Feb 2007 issue).

The companies have to work together to make sure their respective operations are not flooded out: this means that in some cases even disused mines have to be pumped dry to ensure the viability of a neighbouring shaft.

Water coming out of the disused mine in Randfontein could not simply be channelled into the nearest river because it was far too acidic and could have had serious consequences for the environment

As an emergency measure, Harmony fed the water into Robinson Lake, at that time a popular recreational area where fishing was a favourite pastime. Today the lake has very high levels of uranium and a pH level of 2.2 which makes it as acidic as lemon juice and completely incapable of sustaining any life forms.

The NNR measured in the water a uranium concentration of 16 milligrammes per litre, obliging it to declare Robinson Lake a radiation area.

Harmony Gold has spent more than 14 million dollars on capital and operational expenses over the last five years to treat the acidic water emerging from disused mines. An additional 200.000 dollars is spent every month to continue with the treatment processes: in its 'Sustainable Development Report 2007' the company claims that it "treats the water to acceptable standards given the current treatment technologies available". What Harmony finds acceptable, however, may be less so to environmentalists. (END)

Water at the Randfontein site is of an extremely poor quality and tends to affect the vegetation within the mining site and even within the Krugersdorp Game Reserve (figure A2.6).

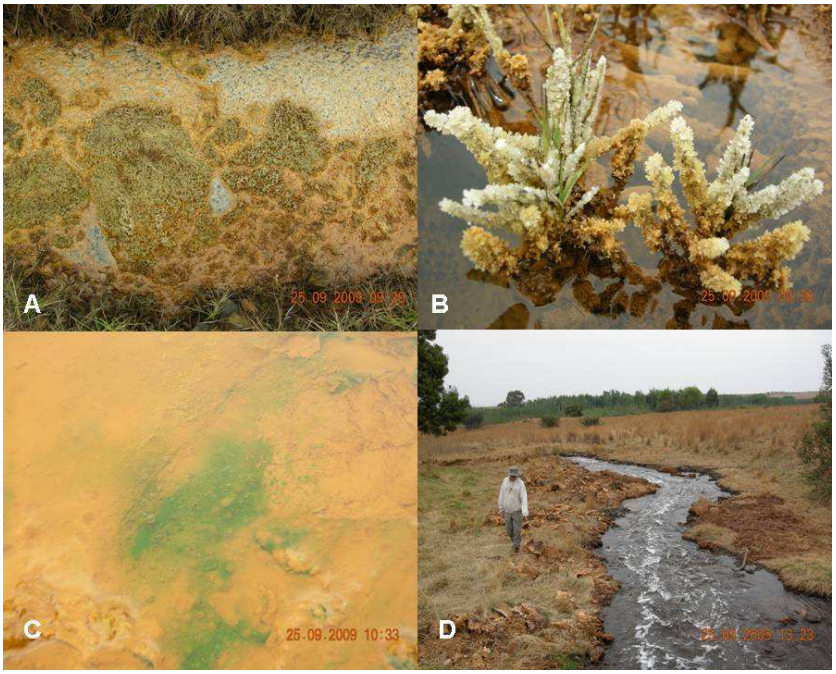

Figure A2.6 Water (A) and vegetation (B) conditions at the Rand Uranium adit, and conditions of the Randfontein creek from the mining site (C) to the Game Reserve (D)

List of publications and conference presentations

Publications

E. M. Cukrowska , H. Nsengimana, J. Lusilao-Makiese, H Tutu, D. Amouroux, E. Tessier. Mercury and tin speciation in the environment affected by old tailings dumps in the Central Rand, Johannesburg, South Africa, Proceedings of the 3rd International Seminar on Mine Closure 14-17 October 2008, Johannesburg, SA, ISBN 978-0-9804185-6-9, pp 673-680.

E.M. Cukrowska, J.L. Makiese, H. Nsengimana, H. Tutu, D. Amouroux and E. Tessier. Speciation of mercury in the environment affected by industrial pollution: determination and modelling. Proceedings of the 3rd AMIREG International Conference, 7-10 September 2009, Athens, Greece, pp 68-70.

E.M. Cukrowska, J. Lusilao-Makiese, E. Tessier, D. Amouroux, I. Weiersbye, Mercury speciation in gold-mining environments – determination and development of predictive models for transformation, transport, immobilisation and retardation, Proceedings of the International Mine Water Association, 5-9 September 2010, Sydney, Nova Scotia, Canada, pp 335-338.

Conference/Seminar presentations and posters

D. Amouroux, E. M. Cukrowska, J. Lusilao-Makiese, H. Nsengimana, H. Tutu, Mercury speciation in the environment : determination and modelling. 35th International Symposium on Environmental Analytical Chemistry, Gdansk (Poland), 22-26 June 2008, Oral presentation.

E. M. Cukrowska , H. Nsengimana, J. Lusilao-Makiese, H Tutu, D. Amouroux, E. Tessier. Mercury and tin speciation in the environment affected by old tailings dumps in the Central Rand, Johannesburg, South Africa, 3rd International Seminar on Mine Closure, 14-17 October 2008, Johannesburg, SA, Oral presentation.

E. M. Cukrowska, J.L. Makiese, H. Nsengimana, H. Tutu, D. Amouroux, E. Tessier: Determination and modeling of mercury speciation in the environment, SACI Convention, 30 November- 5 December 2008, Stellenbosch, South Africa, p.77, no414 Keynote lecture

E. M. Cukrowska, J.L. Makiese, H. Nsengimana, H. Tutu, D. Amouroux, E. Tessier: Mercury Speciation in the Environment Affected by Industrial Pollution: Determination and Modelling, 3rd AMIREG, 7-9 September 2009, Athens, Grece, Oral presentation

J. Lusilao-Makiese, E. Tessier, E. M. Cukrowska, D. Amouroux, Michael Scurrell: Dynamics of adsorption and desorption of mercury from nano-structured gold supported on metal oxides, The 10th International Symposium on ‘Kinetics in Analytical Chemistry’, 2-4 December 2009, Cape Town, South Africa, Oral presentation.

J. Lusilao-Makiese, E. Tessier, E. M. Cukrowska, D. Amouroux, Michael Scurrell: Application of nanogold-metal oxide materials for the trapping and preconcentration of mercury, GOLD 2009: 5th International Conference on Gold Science, Technology and its Applications, 26-29 July 2009, Heidelberg, Germany, Oral presentation.

J. Lusilao-Makiese, E. Tessier, E. M. Cukrowska, D. Amouroux, Michael Scurrell: The use of nano-structured gold supported on metal oxides materials for the preconcentration of mercury , 15th Conference on Heavy Metals in the Environment (ICHMET), 19-23 september 2010, Gdansk, Poland, Presented Poster.

J. Lusilao Makiese, E. Cukrowska, E. Tessier, D. Amouroux, Applications of GC-ICP-MS in the determination of mercury species from different sample matrices, ChromSA Student Seminar, 18 August 2010, Johannesburg, South Africa, Oral presentation.

J. Lusilao-Makiese**,** E. Cukrowska, E. Tessier, I. Weiersbye, D. Amouroux, Characterisation of Mercury Speciation in Some South African Environmental Areas Impacted by Gold Mining, 3rd Cross-Faculty Postgraduate Symposium, Wits University, 12th October 2010, Johannesburg, South Africa, Oral presentation.

E.M. Cukrowska, J. Lusilao-Makiese, E. Tessier, D. Amouroux, I. Weiersbye, Mercury speciation in gold-mining environments – determination and development of predictive models for transformation, transport, immobilisation and retardation, International Mine Water Association, 5-9 September 2010, Sydney, Nova Scotia, Canada, Oral presentation.

J. Lusilao-Makiese, E. Tessier, E. M. Cukrowska, D. Amouroux, Michael Scurrell: The use of nano-structured gold supported on metal oxides materials for the preconcentration of mercury , Analitika 2010, 6-9 December 2010, Stellenbosch, South Africa, Poster.

J.G. Lusilao-Makiese, E.M. Cukrowska, E. Tessier and I. Weiersbye: The Impact of Post Gold Mining on Mercury Pollution in the West Rand Region, SACI Convention 2011, 16-21 January 2011, Johannesburg, South Africa, Oral presentation.

J. Lusilao-Makiese, E.M. Cukrowska, E. Tessier, D. Amouroux: Speciation of mercury in South African coals, 8th MEC Workshop, 18-20 May 2011, Kruger, South Africa, Oral presentation.

J. Lusilao-Makiese, E. Tessier, E.M. Cukrowska, David Amouroux: Use of nano-gold sorbents in the trapping and determination of gaseous mercury, 43rd IUPAC World Chemistry Congress, 31 July-7August 2011, San Juan, Puerto Rico, Oral presentation.

J. Lusilao-Makiese, E.M. Cukrowska, E. Tessier, D. Amouroux: Speciation of mercury in South African coals, SACI Syùposium and NYRS, 14th October 2011, Vereeniging, South Africa, Oral presentation.